UNIVERSITY OF ADELAIDE

FACULTY OF ENGINEERING, COMPUTER AND MATHEMATICAL SCIENCES

Australian School of Petroleum

(Geoscience)

Controls on the geometry, stratigraphic distribution and quality of coals of Middle to Upper Jurassic strata in eastern Australia

By

Carmine Wainman (MSci, FGS)

A thesis submitted for the degree of

Doctor of Philosophy

August 2017

Abstract

The Middle to Upper Jurassic Walloon Coal Measures of eastern Australia host petroleum resources mostly in the form of coal bed methane. The coals accumulated at a high-latitude (>75°S) during a greenhouse epoch and occur in regionally extensive fluviolacustrine successions. Previous studies have described the spatial relationship of facies using a variety of (and sometimes ambiguously defined) stratigraphic frameworks. This was complicated by the absence of marker beds or published radiometric dates. The coal beds are thin and laterally discontinuous and their origin, which has been poorly understood, has implications for consistent stratigraphic correlations. Improved correlation techniques and an understanding of the controls on coal bed geometry should allow better prediction of: 1) the location and architecture of prospective reservoirs, and 2) gas drainage patterns around individual wells. This study aims to address these questions by building upon pre-existing notions on the evolution of eastern Australia during the Middle to Late Jurassic using an integrated approach with new sedimentologic and palynologic data, combined with precise U-Pb dating of volcanic sediments and basin subsidence studies.

Zircon from twenty-eight tuffs in 12 wells across the Surat and Clarence-Moreton Basins were dated using the high-precision chemical abrasion thermal ionization mass spectrometry (CA-TIMS) technique to within an error margin of ±40 ka. In addition, two volcanogenic sandstones from one well that intersected the Birkhead Formation in the Eromanga Basin were dated using the same methodology to within ±50 ka. On a 1237 km transect, five regional datums <420 ka in duration were defined for a chronostratigraphic framework using U-Pb dates. The dated zircons indicate that the Walloon Coal Measures that had previously been considered as Middle Jurassic (Aalenian-Callovian) are largely of Upper Jurassic age (Oxfordian-Tithonian). The new dates also reveal the diachroneity of coal-bearing facies across eastern Australia and inconsistencies in the correlation of lithostratigraphic units. Jurassic spore-pollen units of Price (1997) were also calibrated to the geologic time-scale using the same U-Pb

dates to enable chronostratigraphic horizons to be correlated between basins where volcanic sediments are absent. The first occurrences of key taxa maybe younger than originally estimated, possibly by as much as ~4.2 Ma. These interpretations require further palynological analyses to confirm the age of first occurrences in wells to due to the rarity of key spore-pollen taxa.

A high-resolution investigation on the roles of accommodation creation and climate on coal bed geometry suggest that, although subsidence was important in determining the abundance of coal, the climatic patterns contributed towards their thin, discontinuous character. Although the Walloon Coal Measures were deposited at high latitudes (>75°S), the coals originated from peats that accumulated in mires that experienced a warm temperate climate. Rapid and frequent climate change in the polar region may have limited the window of opportunity for thick, widespread coals to develop.

New sedimentological and palynological data from the Surat Basin substantially revises interpretations of the environments of deposition. Sedimentary facies and spore-pollen assemblages confirm deposition in a predominately fluviolacustrine setting. However, the identification of tidally-influenced facies, acritarchs and dinoflagellate cysts (a first for Jurassic-aged strata in the basin) indicate periods of brackish water conditions. Marine incursions may have come from the north and the east during time of high eustatic sea-level during the Jurassic. Palaeogeographic reconstructions over 13 Ma reveal extensive fluviolacustrine systems draining from an eroding orogenic belt into proximal estuarine complexes. Allocyclic controls revealed by incised valleys and the deposition of transgressive estuarine facies strongly suggests the accumulation of coal (peat) was unlikely to be coeval with clastic sedimentation because of frequent changes in base level.

This study illustrates that a multidisciplinary approach (notably the acquisition of precise U-Pb dates from volcanic sediments and the recognition of subtle indicators of marine influences) can be used to elucidate complex continental successions over large geographic areas. These type of studies will help in the

search for subtle oil and gas reservoirs and better calculation of resource and reserve numbers. They may also be of use in better understanding sedimentary mineral resources and groundwater aquifer systems.

Table of Contents

Declaration of authorship

I certify that this work contains no material which has been accepted for the award of any other degree or diploma in my name, in any university or other tertiary institution and, to the best of my knowledge and belief, contains no material previously published or written by another person, except where due reference has been made in the text. In addition, I certify that no part of this work will, in the future, be used in a submission in my name, for any other degree or diploma in any university or other tertiary institution without the prior approval of the University of Adelaide and where applicable, any partner institution responsible for the joint-award of this degree.

I give consent to this copy of my thesis when deposited in the University Library, being made available for loan and photocopying, subject to the provisions of the Copyright Act 1968.

I acknowledge that copyright of published works contained within this thesis resides with the copyright holder(s) of those works.

I also give permission for the digital version of my thesis to be made available on the web, via the University's digital research repository, the Library Search and through web search engines, unless permission has been granted by the University to restrict access for a period of time.

I acknowledge the support I have received for my research through the provision of an Australian Government Research Training Program Scholarship.

Signed: .....

Date: 26/02/2018

Papers

Chapters 3 to 8 have been written as papers for submission to professional journals. Australian English is used in the thesis and in papers 6, 7 and 8. American English is used in papers 3, 4 and 5. The current status of these papers is as follows:

Paper 1: Wainman, C.C., McCabe, P.J., Crowley, J.L., Nicoll, R.S, 2015. U-Pb zircon age of the Walloon Coal Measures in the Surat Basin, southeast Queensland: implications for paleogeography and basin subsidence. *Australian Journal of Earth Science*, 62, 807-816.

Paper 2: Wainman, C.C., McCabe, P.J., Crowley, J.L, 2017. Solving a tuff problem: defining a new chronostratigraphic framework for Middle to Upper Jurassic strata in eastern Australia using U-Pb zircon dates. *AAPG Bulletin*, 20, 1-28.

Paper 3: Wainman, C.C., McCabe, P.J, In Prep-a. The relative roles of subsidence and climate on coal bed geometry: new insights from the Jurassic Walloon Coal Measures, Surat Basin, Australia. Intend to submit to the *Journal of Sedimentary Research*.

Paper 4: Wainman, C.C., McCabe, P.J, In Prep-b. A reappraisal of the Jurassic Walloon Coal Measures, Surat Basin, Queensland, Australia using a multidisplinary approach. Intend to submit to the journal *Sedimentology*.

Paper 5: Wainman, C.C, Hannaford, C, Mantle, D.J, McCabe, P.J, In Prep. Calibrating the Middle to Late Jurassic spore-pollen palynostratigraphic framework of the Surat Basin, Australia with U-Pb CA-TIMS dates to the geologic time-scale. Intend to submit to the journal *Alcheringa*.

Paper 6: Wainman, C.C, Mantle, D.J., Hannaford, C, McCabe, P.J, In Prep. Dinoflagellate cysts and colonial algae from Tithonian strata of the Surat Basin, Australia: a taxonomic study and their significance. Intend to submit to the journal *Palynology*.

Conferences abstracts and contributions to other papers

During my tenure as a Ph.D. candidate I gave several presentations (with abstracts) based on my research at conferences and co-wrote a number of papers with the following titles:

Wainman, C. C. & McCabe, P. J. 2015. Mires in the dark: high latitude coals in the Jurassic Walloon Subgroup of the Surat Basin, Australia. *AAPG International Conference & Exhibition*. Melbourne, Australia.

Wainman, C. C. & McCabe, P. J. 2016. Tectonic and climatic controls on facies distribution in the Jurassic Walloon Coal Measures, Surat Basin, Australia. *AAPG International Conference and Exhibition*. Barcelona, Spain.

Wainman, C. C. & McCabe, 2016. The correlation of fluviolacustrine strata using volcanic tuffs in the Jurassic Walloon Coal Measures, Surat Basin, Australia: a new technique in the exploration tool box. G*eological Society of London Janet Watson Meeting 2016: The Future of Hydrocarbon Exploration.* London, United Kingdom.

Wainman, C. C. & McCabe, P. J. 2016. Correlation of fluviolacustrine strata using volcanic tuffs: new insights from the Jurassic Walloon Coal Measures, Surat Basin, Australia. *AAPG Annual Convention and Exhibition*. Calgary, Canada.

Wainman, C. C. & McCabe, 2016. The Correlation of fluviolacustrine strata with dated volcanic tuffs: an example from the Jurassic Walloon Coal Measures, Australia. *Australian Earth Sciences Convention*. Adelaide, Australia.

Wainman, C. C. & McCabe, 2016. Climate or subsidence? Geologic controls on the stratigraphic distribution of coal beds in the Jurassic Walloon Coal Measures, Surat Basin, Australia. *Australian Earth Sciences Convention*. Adelaide, Australia.

Wainman, C. C. & McCabe, P. J, 2017. Overcoming challenges in nonmarine stratigraphy using a multidisciplinary approach: an example from Mesozoic basins of eastern Australia. *European Geoscience Union*. Vienna, Austria.

Wainman, C. C. & McCabe. 2017, Using precise CA-TIMS ages of volcanic air-fall tuff beds in correlating the Walloon Coal Measures of the Surat Basin, Australia. *Australian Petroleum Production & Exploration Association* (APPEA) Conference. Perth, Australia.

Hill, R. S., Beer, Y. K., Hill, K. E., Maciunas, E., Tarran, M. A. and **Wainman, C. C,** 2017. Evolution of the eucalypts–an interpretation from the macrofossil record. *Australian Journal of Botany*, 64(8), pp.600-608.

Salmachi, A., **Wainman, C.C**, Rajabi, M. and McCabe, P., 2015. Effect of volcanic intrusions and mineral matters on desorption characteristics of coals (Case Study). *In SPE Asia Pacific Unconventional Resources Conference and Exhibition*. Society of Petroleum Engineers.

Salmachi, A., Rajabi, M., Reynolds, P., Yarmohammadtooski, Z. and **Wainman, C. C**, 2016. The effect of magmatic intrusions on coalbed methane reservoir characteristics: A case study from the Hoskissons coalbed, Gunnedah Basin, Australia. *International Journal of Coal Geology*, 165, pp.278-289.

Appendices

Appendices 1 (p. 324-330): U–Pb zircon age of the Walloon Coal Measures in the Surat Basin, southeast Queensland: implications for paleogeography and basin subsidence.

Text: Analytical techniques and results.

Tables: CA-TIMS results and LA-ICPMS geochronological analyses and trace element concentrations.

Figures: CL images of zircons and grains selected for CA-TIMS and spot analysed by LA-ICPMS.

Appendices 2 (p. 331-361): Solving a tuff problem: a new chronostratigraphic framework for Middle to Upper Jurassic strata in eastern Australia using U-Pb zircon dates.

Text: LA-ICPMS techniques, CA-TIMS techniques and U-Pb geochronology results.

Tables: LA-ICPMS isotopic U-Pb data and trace element concentration data, and U-Pb CA-TIMS isotopic data.

Figures: CL images of zircon from each dated tuff sample

Appendices 3 (p. 362-377): A reappraisal of the depositional environments of the Jurassic Walloon Coal Measures, Surat Basin, Queensland, Australia: a multidisciplinary approach.

Figures: Measured sections and surface, interval and lithology percentage maps from 162.18 to 149.78 Ma.

Appendices 4 (p. 378-382): Calibrating the Middle to Late Jurassic spore-pollen palynostratigraphic framework of the Surat Basin with U-Pb zircon CA-TIMS ages to the geologic time-scale.

Figures: Normalised palynological counts (percent).

Appendices 5 (p. 383-384): Dinoflagellate cysts and colonial algae from Tithonian strata of the Surat Basin, Australia: a taxonomic study and their significance.

Tables: England Finder (EF) coordinates of specimens.

Figures: Common (300 counts) Stratabugs plot for the Indy 3 well.

:

List of figures

Chapter 1: Introduction

Chapter 2: Literature review

Figure 4.4. Cathodoluminescence images (CL) of zircon selected for dating from volcanic air-fall tuff (Wyalla 3 well, 127.40 m (408'14"), Geoscience Australia sample number 2254147) and volcanogenic sandstone beds (Zeus 7 well, 1667.51 m (5470'83"), Geoscience Australia sample number 22550367). Zircon grains dated using laser ablation inductively coupled plasma mass spectrometry (LA-ICPMS) methods are marked with circles and zircon grains dated using CA-TIMS are labelled as z numbers.

Figure 4.5. Probability density plots of LA-ICPMS U-Pb zircon dates from volcanogenic sandstones from Zeus 7 from 1659.03 m (5443'01") to 1659.31 m (5443'93") (2550364) and 1677.31 m (5502'98") to 1677.51 m (5503'64") (2550367). n= number of grains.

Figure 4.6. Plot of CA-TIMS $^{206}Pb/^{238}U$ dates from single grains and fragments of zircon. Samples are grouped by well (from east to west) and in stratigraphic order. Plotted with Isoplot 3.0 (Ludwig, 2003). MSWD = Mean Square of the Weighted Deviates. POF = Probability of Fit. Error bars are at the 2 sigma (2σ) confidence interval. Eleven older dates are not shown.

Figure 4.7. The location of coal bed methane wells correlated for this study in the Surat Basin using wireline logs. The location of the Kalbar 1, Mt Lindesay 1 (Clarnce-Moreton Basin) and Zeus 7 (Eromnaga Basin) wells are not included in this figure.

Figure 4.8. The relationship between coal zone thickness and their lateral continuity in Middle to Upper Jurassic strata, Surat Basin.

Figure 4.9. A chronostratigraphic framework for Middle to Upper Jurassic strata across the Eromanga, Surat and Clarence-Moreton basins based on U-Pb CA-TIMS dates of volcanic air-fall tuff and volcanogenic sandstone beds. Dating errors are shown in Table 4.3. The location of the wells in the cross-section are shown in Figure 4.3.

Figure 4.10. A Wheeler diagram showing the distribution of Eurombah, Walloon, Birkhead and Springbok lithofacies across eastern Australian basins during the

Middle to Late Jurassic. Timescale by Gradstein et al., (2012). The location of wells is shown on Figure 4.3. Dating errors are shown in Table 4.3.

Chapter 5: The relative roles of subsidence and climate on coal bed geometry: new insights from Jurassic coal-bearing strata in the Surat Basin, Australia

Figure 5.1. The lithostratigraphic framework of the Surat Basin adapted from Jell (2013) and Wainman et al. (2017).

Figure 5.2. Geographic extent and structures of the Surat Basin in Queensland. The location of the Stratheden 4 and Stratheden 60 wells are shown in the bottom left. Adapted from Wainman et al. (2015).

Figure 5.3. Simplified measured section of the Stratheden 60 well and tuff beds dated using U-Pb CA-TIMS techniques. Coal beds (in black) are exaggerated for clarity.

Figure 5.4. Total subsidence and tectonic subsidence curves from the Stratheden 60 well extracted from “Backstrip for Mac” to 1 d.p. Dated tuff beds are labelled A to G.

Figure 5.5. A simplified model to explain variations in “subsidence curves” through time. Scenario A shows the classic interpretation of such curves where the shape of the curve is entirely controlled by subsidence. In scenario B the subsidence rate is kept constant but base level changes through time; initially rising at a fast rate but with the rate slowing through time and eventually falling. Note that for a nonmarine basin, base level can be considered as the graded profile of the fluvial system.

Figure 5.6. Cumulative coal and sandstone percentage against stratigraphic depth and the ratio of coal to siliciclastics between dated tuff beds A to G from the Stratheden 60 well.

Figure 6.4c. A measured section (including tuff and palynological sample locations) from Indy 3 spanning the Walloon Coal Measures (390 to 138 m?), the Springbok Sandstone (138 to 124 m?), and the Westbourne Formation (124 to 80 m?).

Figure 6.4d. Legend for measured sections.

Figure 6.5. Raw and annotated core photographs showing double mud drapes, lenticular bedding, tidal bundles and coaly drapes in tidally influenced channel sandstones indicative of sedimentation by tidal processes from the Stratheden 60, Wyalla 3 and Kato 3 wells.

Figure 6.6. Examples of dinoflagellate cysts, acritarchs, and colonial algae from tidally influenced mudflats (1) *Moorodinium crispa*, Indy 3 well, 247.55 m, slide 3, U41/1. (2) *Moorodinium crispa*, Indy 3 well, 247.55 m, slide 3, W47/3. (3) *Skuadinium fusumaster*, Indy 3 well, 247.55 m, slide 3, S44/1. (4) *Skuadinium fusumaster*, Indy 3 well, 247.55 m, slide 3, S44/1. (5) *Micrhystridium* spp., Stratheden 4 well, 452.00 m, slide 1, W34/1. (6) *Micrhystridium* spp, Stratheden 4 well, 444.0 0m, slide 1, W34/1 (7) *Palambages pariunta*, Indy 3 well, 247.55m, slide 3, Q42/3. (8) *Palambages pariunta*, Indy 3 well, 247.55m, slide 3, X15/2.

Figure 6.8. Surface, interval thickness, sandstone percentage and coal percentage maps from the 163.08 Ma to 162.18 Ma interval.

Figure 6.9. Palaeogeographic reconstructions and depositional trends from 163.05 Ma to 149.78 Ma.

Figure 6.10. Regional palaeogeographic interpretation for the Late Jurassic of Australia. Adapted for this study from Struckmeyer and Totterdell (1990) and Bradshaw and Yeung (1992).

Chapter 7: Calibrating the Middle to Late Jurassic spore-pollen palynostratigraphic framework of the Surat Basin with U-Pb zircon CA-TIMS ages to the geologic time-scale.

Moorodinium crispa, L44/0. (13) *Moorodinium crispa*, slide 3, L45/3. (14) *Moorodinium crispa*, slide 3, Q19/0. (15) *Moorodinium crispa*, slide 3, J19/4. (16a/16b) *Moorodinium crispa*, slide 3, F30/3.

Plate 8.2. Dinoflagellate cysts and colonial algae from the Indy 3 well at 247.55 m depth. Scale bar 10 μm throughout. (1) *Skuadinium fusumaster*, slide 3, S44/1. (2a/2b) *Skuadinium fusumaster*, slide 3, Q43/0. (3) *Skuadinium fusumaster*, slide 3, X19/3. (4) *Skuadinium fusumaster*, slide 3, U12/4. (5) *Skuadinium fusumaster*, slide 3, S44/1. (6) *Skuadinium fusumaster*, slide 3, M20/2. (7) *Skuadinium fusumaster*, slide 3, H31/2. (8) *Palambages pariunta*, slide 3, M20/2. (9) *Palambages pariunta*, slide 3, V16/2. (10a/10b) *Palambages pariunta*, slide 3, T17/4. (11a/11b) *Palambages pariunta*, slide 3, Q42/3. (12a/12b) *Palambages pariunta*, slide 3, X15/2. (13a/13b) *Palambages pariunta*, slide 3, X44/2. (14a/14b) *Palambages pariunta*, slide 3, S33/1.

Chapter 9: Thesis conclusions and future work

Not applicable.

List of tables

Chapter 1: Introduction

Not applicable.

Chapter 2: Literature Review

Chapter 3: U–Pb zircon age of the Walloon Coal Measures in the Surat Basin, southeast Queensland: implications for paleogeography and basin subsidence

Not applicable.

Chapter 4: Solving a tuff problem: defining a new chronostratigraphic framework for Middle to Upper Jurassic strata in eastern Australia using U-Pb zircon dates

Chapter 5: The relative roles of subsidence and climate on coal bed geometry: new insights from the Jurassic Walloon Coal Measures, Surat Basin, Australia

Acknowledgements

The work present in this Ph.D. thesis could not have been undertaken without the support from my family, friends, colleagues at the University of Adelaide, and the financial backing of several organisations listed below.

I would like to express my sincere gratitude to my supervisor Peter McCabe for the opportunity to conduct my research in Australia and for all the support you have provided me during my Ph.D. since 2013. I will be forever in your debt.

I would like to thank Kathryn Amos, Robert Hill, Maureen Sutton, Conny Meyer and Ian West at the University of Adelaide for encouragement during my Ph.D., processing countless amounts of university paperwork on my behalf, and for resolving many of my I.T issues.

The project would not have been possible without a scholarship from Australian School of Petroleum that covered most of the travel and analytical costs.

I am also thankful to Geoscience Australia; the University of Queensland; AAPG Grants-in Aid; SEPM; MGPalaeo; Senex Energy; and Arrow Energy who provided financial support for the project. A special mention goes to Bob Nicoll, Joan Esterle, Dan Mantle, Carey Hannaford, Adam Charles, John Lignum, Marty Young, Stephen Scott and Cory MacNeill for their support during my Ph.D.

To Jim Crowley and Debbie Pierce at Boise State University, I thank you for spending hundreds of painstaking hours processing my rock samples and dating zircons grains. Without your analytical skills, my thesis would not have developed in the exciting manner it did.

To Louise Thompson at 22 Joslin Street–thank you for your support during my PhD and the countless lifts to the airport at ungodly hours.

To my friends in Australia, thank you for welcoming me to the city of Adelaide. I thank you for making my time down under so much fun.

To my friends in the UK, I thank you for keeping me at the back of your mind over the past several years. I wish you were all over in Australia with me.

Finally, special thanks go to my Mum, Dad, Sister, and cats for putting up with my ways. Fortune favours the brave as they say and I hope we all reap the benefits of my research in the years to come.

The best-laid schemes o' mice an' men Gang aft agley

From “To a Mouse” by Robert Burns (1785).

No man is an Island

From “Devotions upon Emergent Occasions” by John Donne (1624).

I need to sleep, I can’t get no sleep

Maxi Jazz, singer-songwriter, Faithless (1995).

Chapter 1. Introduction

1.1 Contextual statement

This thesis examines Middle to Upper Jurassic coal-bearing strata in the Eromanga, Surat and Clarence-Moreton basins of eastern Australia. Research conducted over the past 20 years since the onset of commercial coal bed methane (CBM) activities (or coal seam gas, CSG) in eastern Australia has not come to a consensus on a stratigraphic framework, or adequately investigated the character of siliclastic sediments on a regional scale. The work conducted in this thesis intends to fill knowledge gaps in the following areas: the absolute age of coal-bearing strata; to understand the controls on coalbed geometry; reliable correlation of coal-bearing strata within and between basins dominated by continental successions; and the distribution of facies within a robust stratigraphic framework. The goal of this research is to use new methodologies to understand the evolution of resource-rich continental successions across the Middle to Late Jurassic of eastern Australia. This will improve predictions of reservoir geometry in complex, heterolithic successions where easily identifiable marker beds are not present or where biostratigraphic zones cover long time intervals. This study is applicable in heterolithic continental successions with limited or no surface outcrop. The research documented herein incorporates several disciplines including: 1) U-Pb geochronology; 2) subsidence studies; 3) facies analysis; 4) chronostratigraphy, and 5) palynology. The availability of core and wireline log data from Middle to Upper Jurassic coal-bearing strata in eastern Australia (notably in the Surat Basin) provides a rich dataset to test the validity of stratigraphic frameworks and the notion of extensive fluviolacustrine deposition during this timeframe.

These type of studies will help in the search for subtle oil and gas reservoirs and better calculation of resource and reserve numbers. They may also be of use in better understanding sedimentary mineral resources and groundwater aquifer systems.

The thesis is divided into the following chapters: an introduction providing a synopsis of this research (chapter 1); a detailed literature review covering

existing research on the geology of coal and the geology of eastern Australian basins during the Mesozoic (chapter 2); six research papers (chapters 3 to 8) which are formatted for publication in geoscience journals. Finally, chapter 9 concludes the research and provides a direction for future work in these basins.

1.2 Overview of petroleum, gas and coal production in eastern Australia

The Surat, Clarence-Moreton, Mulgildie, Eromanga, and Maryborough basins of eastern Australia contain significant reserves of hydrocarbons (Jell 2013). The extraction of coal-seam gas (better known as CSG or coal-bed methane, CBM) is the main focus of commercial activity in these basins (Department_of_Natural_Resources_and_Mining 2014). Gas is primarily produced from the Jurassic-age Walloon Coal Measures (or Walloon Subgroup) of the Surat Basin in southeast Queensland (Figure 1.1). This formation accounts for 88% of gas production and 64% of proven and probable (2P) reserves in Queensland (Department_of_Natural_Resources_and_Mining 2014; Hamilton et al. 2014a; Towler et al. 2016). Latest estimates of 2P reserves in the Walloon Coal Measures are in the order of 31000 petajoules (PJ) or 28 TCF (trillion cubic feet of gas/year) as of 2016 (Queensland_Government 2016). Gas produced from the Walloon Coal Measures is both thermogenic and biogenic in origin and each can be distinguished by their carbon and hydrogen isotope values (Hamilton et al. 2014a). There are also a series of active coalfields exploiting the Walloon Coal Measures in the Surat Basin (Cambey Downs and Kogan Creek) and Clarence-Moreton Basin (Jeebropilly and New Oakleigh).

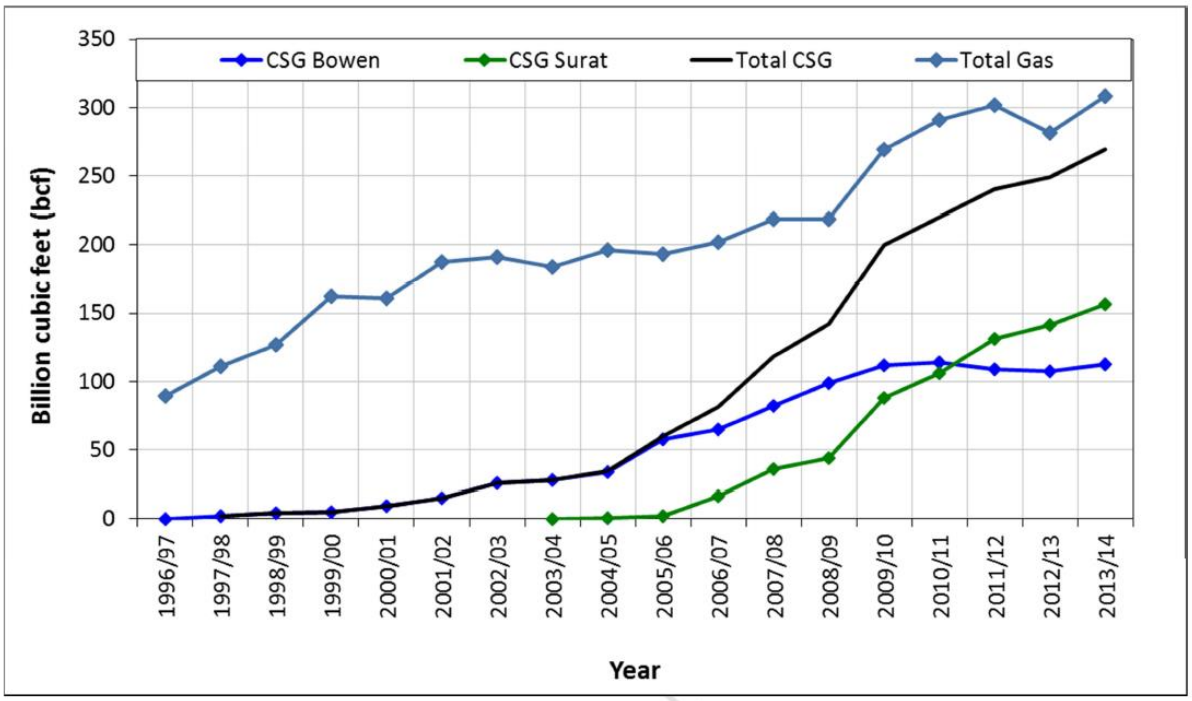

Figure 1.1. Total gas and coal seam gas (CSG) production in Queensland, Australia from 1996 to 2014 taken from Towler et al. (2016).

Conventional gas was first discovered near Roma, Queensland in 1900 (Towler et al. 2016). However, gas production in the Surat Basin and the building of pipelines to commercial markets did not commence until the 1960's (Towler et al. 2016). Production then steadily increased from 10 BCF/yr (billion cubic feet of /year) to 29.5 BCF/yr from 1970 to 1995 (Towler et al. 2016). The production of CSG in the Surat Basin did not commence until the mid-2000's when conventional sources of gas in the basin became depleted (Baker and Skerman 2006; Towler et al. 2016). The process of extracting CSG (Figure 1.2), classified as an unconventional resource, involves dewatering coal beds to reduce the pressure that keeps gas-in-place (Zou 2012). This process releases methane in an adsorbed, dissolved or free state from coal beds (Zou 2012). The lack of initial success in coal seam gas production in eastern Australia, notably the Surat Basin, was attributed to the lack of knowledge in various geological fields including the importance of stress regimes and their influence on coal cleating (Baker and Skerman 2006). Once these obstacles were overcome, the coal-seam gas industry increased fourfold through the 2000's in response to both increased national and international demand for liquid natural

gas or LNG (Baker and Skerman 2006). Gas production is expected to reach in excess of 1400 BCF when LNG trains are in full operation in the 2020's (Towler et al. 2016).

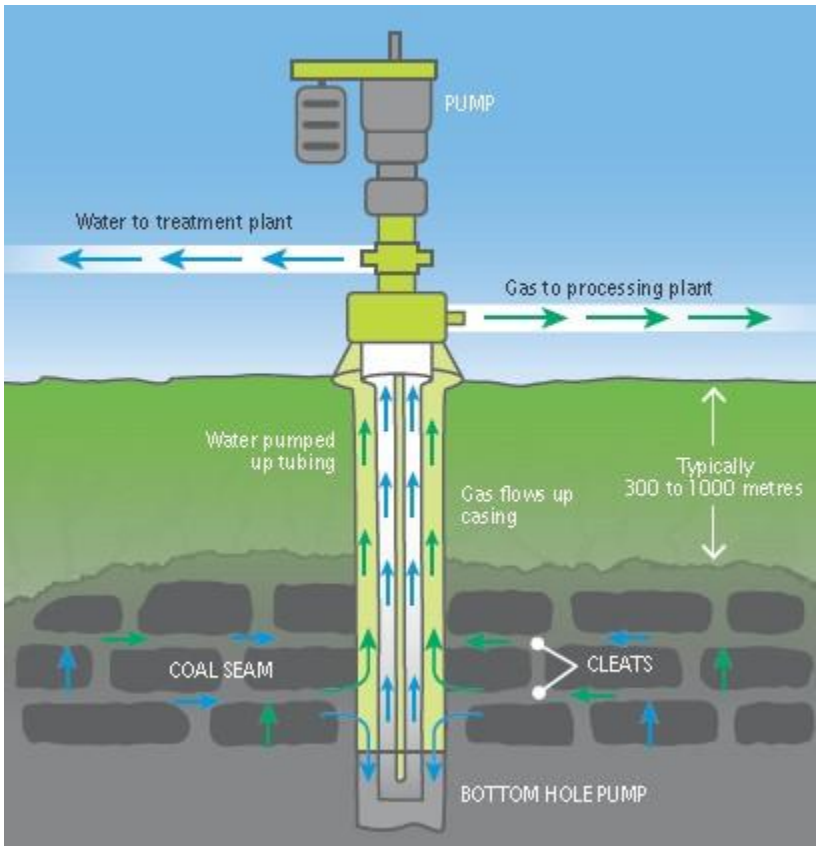

Figure 1.2. Schematic diagram showing the processes involved in the extraction of coal seam gas (CSIRO 2014).

Pilot wells drilled in the early 2000's identified a high degree of variability in the properties (gas content and permeability) (Towler et al. 2016). A consequence of this was well spacing of between 750 m to 1400 m in gas fields across the basin (Towler et al. 2016) because of the thin (0.4 m), laterally discontinuous (<5 km) character of coal beds in the Walloon Coal Measures. This has made it challenging to predict patterns of gas drainage around individual wells (Bradshaw and Bernecker 2016; Morris and Martin 2016). Over 8500 shallow CSG wells have been drilled in the Surat Basin with an additional 31,500 wells expected to become online over the next two decades (Towler et al. 2016).

The Birkhead Formation of the Eromanga Basin hosts major conventional oil and gas resources. These resources are located within structural traps with a

stratigraphic component and a thin oil-net column (Alexander and Hibburt 1996; Department_of_State_Development 2016). Minor coal deposits are also present in the Birkhead Formation (Goscombe and Coxhead 1995). Commercial production from the Eromanga Basin commenced in the late 1970's and peaked in the 1980's (Department_of_State_Development 2016). Latest estimates of potential resources in the basin are in the order 52.8 mmbbl (millions of barrels) (Department_of_State_Development 2016). Unlike in the Surat Basin, there is reduced well density with 1 well per 436 m^2 (Department_of_State_Development 2016). Approximately 2474 wells have been drilled with 1649 designated as development and aspiration wells (Department_of_State_Development 2016). Most wells are located within the perimeter of the underlying Cooper Basin (Department_of_State_Development 2016). Prospects related to the Birkhead Formation lie mostly on the western flank of the Eromanga Basin which are stratigraphically subtle and difficult to delineate (Alexander and Hibburt 1996; Sales et al. 2015).

In comparison to the Surat Basin, the Clarence-Moreton Basin is relatively unexplored with potential for coal seam gas production (Pinder 2004). Little is also known about the Tiaro Coal Measures in the Nambour/Maryborough Basins (Lipski et al. 2001). Igneous intrusions and the structural complexity of the Nambour/Maryborough Basins makes the coal deposits difficult to exploit, despite coal bed thicknesses in excess of 3 m (Jell 2013).

1.3 Overview of coal-bearing strata in the Mesozoic Australian Superbasin

Coal-bearing strata, predominately Jurassic in age, can be found in several basins incorporated by the Mesozoic Australian Superbasin (Figure 1.3). These include the Birkhead Formation of the Eromanga Basin (Bathonian to Kimmeridgian), the Tirao Coal Measures of the Maryborough/Nambour Basin (Sinemurian to Pliensbachian), the Polda Formation of the Polda Basin (Middle Jurassic) and the Dalrymple Sandstone of the Laura Basin (Upper Jurassic) (Shen 1991; Ward 1995; Jell 2013). The Aalenian to Callovian Walloon Coal Measures of the Surat Basin (and to a lesser extent, the Clarence-Moreton Basin) is the most prevalent coal-bearing succession from the Mesozoic (Burger 1994; McKellar 1998). All these basins are considered intracratonic and overlie older Carboniferous to Triassic basins including the Bowen and Copper Basins (Jell 2013). How continental sag ensued in these basins from the Late Triassic and into the Cretaceous remains to be determined (Turner et al. 2009; Jell 2013).

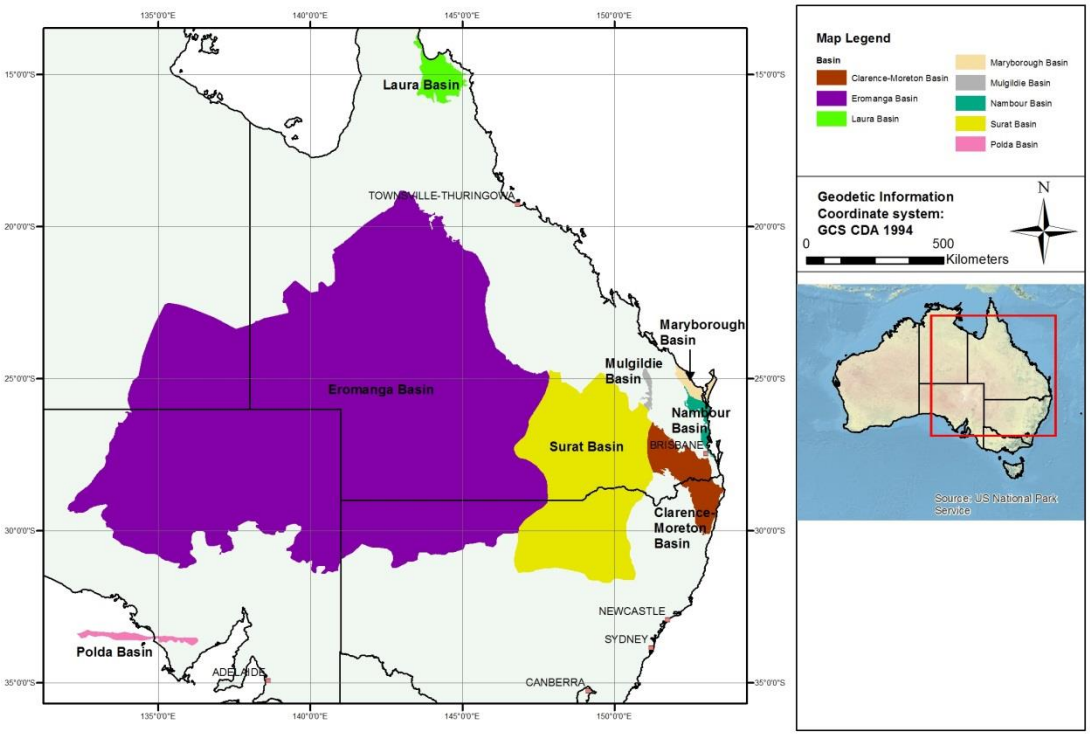

Figure 1.3. The geographic extent of Mesozoic coal-bearing basins in eastern Australia.

During the Mesozoic, eastern Australia was located in the mid to high latitudes (45°S and 80°S) on the southeastern margin of Gondwana (Figure 4.1). (White 1993; Blakey 2011). Extensive fluviolacustrine systems with an abundance of peat-forming mires covered most of eastern Australia during the Middle to Late Jurassic (Bradshaw and Yeung 1992). A defining characteristic of coals from these basins are their thin (<0.4 m), discontinuous (<5 km) character (Ryan et al. 2012; Morris and Martin 2016). This character is in stark contrast to the Permian coal beds in the underlying Bowen Basin which are thick (up to 63 m) and continuous (>30 km) (Ayaz et al. 2015). Despite the high latitudinal setting of the eastern Australia, peat (coal) accumulated when a warm temperate climate prevailed as evidenced by palynofloral assemblages and global climate models (White 1993; Balme et al. 1995; McKellar 1998; Boucot et al. 2013; Martin et al. 2013). New data, however, suggests there were rapid and frequent climatic fluctuations (Brigaud et al. 2008; Dera et al. 2011) as opposed to an equitable and stable climate during the Jurassic (Frakes et al. 2005). Previous studies have also suggested there is a discrepancy between the palaeoclimate and palaeolatitude of eastern Australia during the Jurassic due to the effects of a large landmass at high palaeolatitudes, the Pangean thermal anomaly, and increased orogenic activity (McKellar 1998; McKellar 2004).

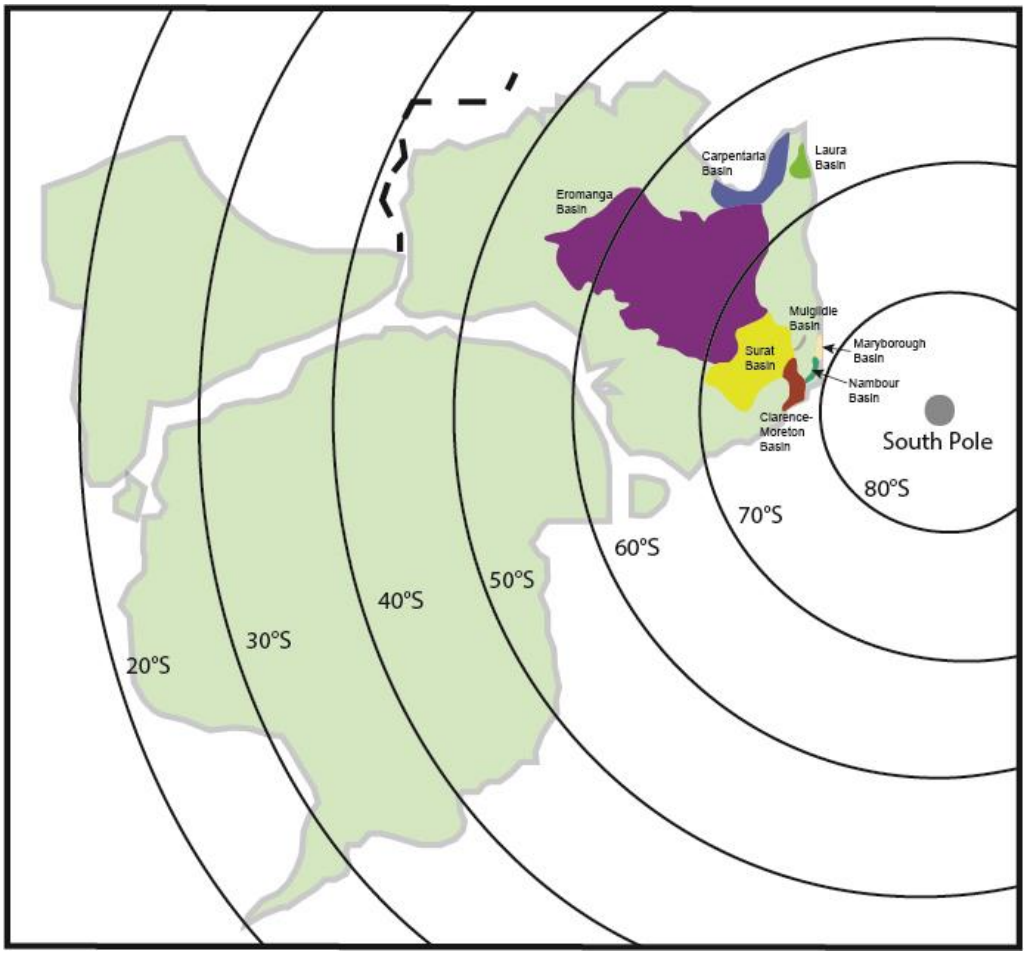

Figure 1.4. The latitudinal position of eastern Gondwana and eastern Australian basins during the Late Jurassic based on palaeomagnetic constraints. Adapted from Klootwijk (2009).

Volcanism was prevalent during the Jurassic leading to the wide distribution of volcanic air-fall tuff (or bentonite) beds in the Walloon Coal Measures (Yago 1996b). Tuffs are also prevalent in the underlying Eurombah Formation and the overlying Springbok Sandstone. These beds are up to 1 m in thickness (Yago 1996b). Temporally equivalent volcanism is thought to be responsible for the deposition of volcanogenic sandstones in the Birkhead Formation of the Eromanga Basin (Boult 1996). The origin and source of the volcanism remain uncertain; from intrabasinal volcanism of the Wellington-Muswellbrook-Narrabri region of northeastern New South Wales; to rift-related bimodal volcanism on the Marion Plateau; to arc volcanism from the Lord Howe Rise (Dulhunty et al. 1987; Jell 2013; Mortimer et al. 2015). These tuff beds had not previously been isotopically dated.

1.4 Geological research in Mesozoic basins of eastern Australia

Research on the Surat Basin has addressed a number a topics including: petroleum potential (Power and Devine 1970; Khorasani 1987; Boreham 1995; Baker and Skerman 2006; Baker and Slater 2008); detailed geochemical analyses of gas and water emanating from coal beds (Papendick et al. 2011; Hamilton et al. 2012; Hamawand et al. 2013; Hamilton et al. 2014a); depositional models (Cameron 1970; Fielding 1993; Yago 1996a; Martin et al. 2013; Shields and Esterle 2015); structure and basin evolution (Exon 1966; Exon 1976; Exon and Burger 1981; Hoffmann et al. 2009; Korsch and Totterdell 2009a; Korsch and Totterdell 2009b; Totterdell et al. 2009; Ryan et al. 2012); palynology (Burger 1976; McKellar 1998; McKellar 2004); coal petrology (Gould 1974; McDonald 2005; Scott et al. 2007; Hentschel et al. 2016); and stratigraphy (Whitehouse 1954; Swarbrick et al. 1973; Jones and Patrick 1981; Green et al. 1997a; Scott et al. 2004; Hamilton et al. 2014b). Detailed geological synopses of the Surat Basin and the Walloon Coal Measures were carried out by Goscombe and Coxhead (1995), Green et al. (1997) and Jell (2013). There is a distinct absence of research on coeval strata in New South Wales which is restricted to the fossils of the Talbragar Fish Beds near Gulgong (White 1981; Bean 2006; Turner et al. 2009; Beattie and Avery 2012; Selden and Beattie 2013), a single article on the Pilliga Sandstone (Arditto 1982); and generic overviews of the Purlawaugh and Ballimore formations (Dulhunty 1973; Stewart and Alder 1995; Ross 1996; Scheibner and Basden 1996).

Research in the Eromanga Basin have addressed a number of topics including basin stratigraphy (Alexander et al. 1996; Lanzilli 2000); palynology (Burger 1982; Sajadi and Playford 2002); structure and basin history (Boult 1996; Mavromatidis 2008); organic geochemistry (Townshend 1993; Michaelsen 2002); and sedimentology (Watts 1987; Alexander et al. 1996). Detailed geological synopses of the Eromanga Basin and the Birkhead Formation were carried out by Goscombe and Coxhead (1995), Alexander and Hibburt (1996) and Jell (2013). These studies had a predominant focus on the South Australian portion of the basin with little research published in the last 20 years.

A limited number of researchers have taken an interest in the Clarence-Moreton Basin. Studies are restricted to several articles which focus on the stratigraphy

(Wells and O'Brien 1994; Pinder 2004); palynology (Burger et al. 1994); structure (O'Brien et al. 1994); organic geochemistry (Martin and Saxby 1982); and sedimentology (Wells 1994) of the basin. Research on coal-bearing strata in other basins including the Maryborough and the Polda Basin are limited to works in theses and books (Shen 1991; Ward 1995; Lipski et al. 2001; Jell 2013).

Despite this research, there remains contention on stratigraphic frameworks utilised in these basins, the geometry of coal bodies and the palaeogeographic evolution of eastern Australia during the Jurassic (most notably the Walloon Coal Measures). This is complicated by the absence of age data and compounded further by thin, discontinuous coal beds that provide datums for reliable subsurface correlation in many other basins around the world (Michaelsen and Henderson 2000; Pinder 2004; Shields and Esterle 2015). The lack of a sound chronostratigraphic framework is evident with the constant revision of stratigraphic nomenclature (Swarbrick, 1973; Scott, 2008; Hamilton et al., 2014b) and widely varying palaeogeographic models notably the palaeocurrent direction with palaeodrainage suggested to the north (Exon 1976), to the west (Fielding 1993; Yago 1996b) and to the south and southeast (Hamilton et al. 2014b; Shields and Esterle 2015; Zhou et al. 2017). Some authors have even suggested marine influences from brackish water acritarchs and ironstones in what has been interpreted as an entirely nonmarine environment (Exon 1976; Burger 1986). Without a reliable stratigraphic framework, there will be uncertainties on reservoir quality, reservoir architecture and the prediction of gas sweet spots across the Surat Basin and beyond. These challenges pose the following questions:

1) What is the true geologic age of the Walloon Coal Measures and coeval strata?

2) Can a high resolution and age-constrained chronostratigraphic scheme be developed for the Walloon Coal Measures (and beyond) for palaeogeographic reconstructions?

3) What factors were responsible for the thin and discontinuous character of coal beds?

4) Does the sedimentology and interpretations of the depositional environment in the Surat Basin require re-evaluation?

5) Can work undertaken in the Surat Basin be applied successfully to other coal-bearing Mesozoic basins?

1.5 Research aims and objectives

The wide distribution of volcanic air fall tuffs and volcanogenic sandstones across Mesozoic basins of eastern Australia provide an opportunity to constrain the age of the Walloon Coal Measures and the Birkhead Formation and overhaul the stratigraphic framework of these coal-bearing successions. In older Permo-Triassic coal bearing basins of eastern Australia including the Bowen Basin, the dating of over 100 zircon-bearing tuff beds using the high precision U-Pb CA-TIMS (chemical abrasion isotope dilution thermal ionisation mass spectrometry) technique has substantially improved interbasinal and intrabasinal stratigraphic frameworks (Nicoll et al. 2015; Laurie et al. 2016). These precise U-Pb dates have changed notions on the evaluation of depositional rates and burial history models for the petroleum industry (Laurie et al. 2015; Nicoll et al. 2015). Mesozoic Basins of the Australian Superbasin would benefit from similar work and would allow for the construction of an age-calibrated stratigraphic framework.

Considering the questions posed in 1.4, the following research aims are put forward:

1) To constrain the age of the Walloon Coal Measures in the Surat Basin using CA-TIMS dates (Chapter 3).

2) To construct a robust chronostratigraphic framework for the complex, heterolithic fluviolacustrine successions across eastern Australia during the Middle to Late Jurassic using CA-TIMS dates (Chapter 4).

3) To examine the interplay of climate and subsidence rates on the thin, discontinuous character of coal beds observed across the Surat Basin (Chapter 5).

4) To reassess the sedimentology and palaeogeography of coal-bearing successions in the Surat Basin within a chronostratigraphic framework (Chapters 6).

5) To utilize the same CA-TIMS dates from tuff beds to recalibrate the palynostratigraphic framework for reliable interbasin correlation across the Middle to Late Jurassic of Australia (Chapter 7 and 8).

To realise these aims, a series of objectives were defined. Each objective matches the corresponding aim above:

1) To sample and separate a series of volcanic ash fall tuffs to see if any yield suitable zircon for CA-TIMS analyses and if successful, obtain the first precise U-Pb age from the Walloon Coal Measures of the Surat Basin.

2). To date several tuff and volcanogenic sandstone beds from a series of well across Mesozoic basins of eastern Australia. These will be used verify correlations within defined time intervals using CA-TIMS dates. These U-Pb ages will form the basis of a new chronostratigraphic framework.

3) To construct a high resolution, high precision subsidence curve using CA-TIMS tuff dates and core data to establish subsidence rates during the time of the Walloon Coal Measures. This can then be compared to climate data from the same time interval to deduce controls on coal preservation and its stratigraphic distribution during the Jurassic

4) To make detailed sedimentologic descriptions of cores and undertake facies analyses incorporating palynological data to reassess the depositional environments of the coal-bearing strata of in the Surat Basin. With the assistance of a chronostratigraphic framework, this will allow for the construction of high-resolution palaeographic maps through the Middle and Late Jurassic.

5) To recalibrate palynostratigraphic schemes for the Surat Basin to the geologic time-scale and correlate chronostratigraphic horizons across the Middle and Late Jurassic of Australia by using the first occurrences of key taxa.

Chapter 2. Literature Review

2.1 Coal geology overview

Coal is defined as a rock containing more than 50% by weight and more than 70% by volume of carbonaceous material (McCabe 1984). Coals are formed by the burial and compaction of altered plants remains, or peat (McCabe 1984) and can either be humic (from plant material) or sapropelic (algal) in origin (Thomas 2012). As peat becomes buried, it transforms into coal of increasing rank (lignite/brown coal to anthracite) as moisture and volatiles are expelled (Thomas 2012). This increases the calorific value and carbon content of coal (Thomas 2012). The organic components of coal are known as macerals and fall into three groups (Table 2.1): vitrinite (woody material); liptinite (derived from lipid rich components of plants/algae including spores, pollen, cuticle and resins); and inertinite (oxidised plant matter) (Teichmuller 1989; Thomas 2012). The proportion of macerals determines the lithotypes and microlithotypes of coal which can reflect the depositional environment of coal (McCabe 1984). Coal also contains inorganic components (or ash) including detrital and authigenic minerals (Stach et al. 1982).

Group maceral	Maceral	Morphology	Origin
Vitrinite	Telinite	Cellular structure	Cell walls of trunks, branches, roots, leaves etc.
	Collinite	Structureless	Reprecipitation of dissolved organic matter in a gel form
	Vitrodetrinite	Fragments of vitrinite	Very early degradation of plant and humic peat particles
Liptinite	Sporinite	Fossil form	Mega and microspores
	Cutinite	Bands which may have appendages	Cuticles – the outer layer of leaves, shoots and thin stems
	Resinite	Cell filling, layers or dispersed	Plant resins, waxes, and other secretions
	Alginite	Fossil form	Algae
	Liptodetrinite	Fragments of liptinite	Degradation residues
Inertinite	Fusinite	Empty or mineral filled cellular structure	Oxidized plant material – mostly charcoal due to burning of vegetation
	Semifusinite	Cellular structure	Partly oxidized plant material
	Macrinite	Amorphous cement	Oxidized gel material
	Inertodetrinite	Small particles of fusinite, semi-fusinite and/or macrininte	Redeposited inertinites
	Micrinite	Granular: rounded grains ~1µm in diameter	Degradation of macerals, especially liptinites, during coalification
	Sclerotinite	Fossil form	Mainly fungal remains

Table 2.1. Macerals and group macerals recognised in hard coals taken from McCabe (1984).

The accumulation of organic matter (mostly peat) occurs in mires - an all-encompassing term covering non-saline wetlands in which peat accumualtes (Gore 1983; McCabe 1984). Mires are created by the terrestrialization of lakes or the paludification of poorly drained areas (Gore 1983; McCabe 1987; Cameron et al. 1989). Extensive mire development can occur in a variety of fluvial, lacustrine, deltaic and paralic environments across a wide range of tectonic and climatic settings (Thomas 2012). Most coals accumulate in palaeolatitudes where on average net precipitation exceeded evaporation and in basins where average subsidence rates approximate peat accumulation rates (McCabe and Parrish 1992). Mires physically and chemically change in similar ways as they evolve from ponds, to grassy marshes and then to forested swamps before culminating in a heath dome irrespective of their geologic setting (Cameron et al. 1989). The quality, shape, and extent of mires depend on a series of factors including humidity, vegetation type, water regimes, the physiographic setting and the tectonic setting (Cameron et al. 1989).

Many of the world's major coal-bearing strata accumulated in foreland basins but few formed in palaeolatitudes between 10° and 40°N/S (McCabe 1984). Allogenic factors including climate and base level change a more considerable role than autogenic factors in determining mire type, rates of vegetation growth, the pace of humification, sediment input, and groundwater levels (McCabe, 1991; McCabe and Parrish, 1992; Bohacs and Suter, 1997). Peat accumulation is controlled by the relative position of the water table which, from a depositional perspective, can be considered as base level (Moore 1995). Basin subsidence is primarily responsible for the rise in the water table and the creation of accommodation for peat accumulation, whilst rates of peat accumulation and the ability of mires to fill the accommodation space created by subsidence is a function of climate (McCabe 1984, 1987). Average peat accumulation rates today range from 0.1 mm/yr in the tundra to 2.3 mm/yr in the tropics (McCabe 1984). Rates of peat accumulation need to match rates of accommodation creation for thousands of years for any coal bed of significant thickness to develop because the coal compaction factor is ~1:10 (McCabe 1984; Bohacs and Suter 1997). If accommodation and peat accumulation rates are not matched, peat can become oxidized or overlain by clastic sediments

(McCabe and Parrish 1992). The link between accommodation and peat accumulation was explored by Bohacs and Suter (1997) who considered primary productivity, the preservation of organic matter, minimal dilution by mineral matter, and subsidence as critical for the preservation of significant volumes of organic matter. Accommodation rates need to be equal to accumulation rates in order for coals to form thick, laterally extensive beds, although this can vary greatly on a local scale (Bohacs and Suter 1997). Varying rates of base level change can affect coal geometries within any given depositional sequence, from lowstand to late transgressive system tracts (Bohacs and Suter 1997). Not all peat deposits are the precursor to coal due to erosion, fire, and decomposition prior to burial (Cameron et al. 1989). The precursor conditions for thick coal include a continually rising water table and minimal clastic influxes prior to burial (Cameron et al. 1989). Domed, ombrotrophic peats are considered the most suitable setting for future economic coal deposits because they accumulate thick, widespread peats with minimal ash and sulphur content (Cameron et al. 1989).

The understanding of the stratigraphy of coal-bearing sequences has been constantly evolving since the late 19th century. Although the dynamics of coal accumulation is well studied, the dynamics of allocyclic controls have been less understood (Holz et al. 2002). One of the most popular ideas to explain cyclical coal deposition stems from the cyclothem concept that remained mainstream amongst stratigraphers until the 1960's (Moore 1964). The cyclothem model relies on a variety of assumptions (including simple transgressive-regressive cycles) with the distribution of facies determined by the prevailing regressive or transgressive conditions (Holz et al. 2002). Changes in coal properties across a basin and the direction of pinch-outs cannot fully be explained by the cyclothem concept or the depositional environment model (Holz et al. 2002). Further discrepancies were revealed by Fassett (1986) when he demonstrated coal seam geometry can extensively vary between coal-bearing formations deposited during the same transgressive cycles in the San Juan Basin, USA. The depositional environment was also assumed to control the geometry of coal beds (McCabe and Shanley 1992). Diessel (1992) made the first attempt to integrate coal accumulation with sequence stratigraphy by studying the

mineralogical and chemical composition of coal in differing depositional system tracts. This provided new insights into the formation of thick coals sequences (e.g. the amalgamation of several mire bodies; (Diessel 1992). Recognition of stacked mires can yield improvements in the predicting coal bed quality and composition (Jerrett et al. 2011a). The application of sequence stratigraphic principles has required the reinterpretation of coal-bearing strata to explain the presence of thick coal beds or amalgamated of thin coal beds, including those of the Bowen Basin of Australia where climate and sea cycles signatures can be identified (Michaelsen and Henderson 2000).

Predicting coal occurrence within a stratigraphic framework is usually tied to relative sea-level change in paralic settings, with parasequence stacking patterns and related coal geometries controlled by the ratio of accommodation to peat production (Bohacs and Suter 1997). The behaviour of groundwater systems (tied to factors including the location of the salt-water wedge, floral assemblages, and topography) controls the initiation, location, and development of mires (Freeze et al. 1979; Holz et al. 2002). Peats will accumulate in areas of non-clastic deposition as long as there is substantial vegetation growth and maintenance of water at or above the peat surface (Hamilton and Tadros 1994). The development of thick peats, whether in abandoned fluvial channels or regionally across a basin, depends on how long mires are isolated from sites of clastic sedimentation (McCabe, 1984; Hamilton and Tadros, 1994). The thickest coals in paralic settings occur in an upper lowstand and basal transgressive systems – these are best conditions for the preservation of organic matter (Bohacs and Suter 1997). In the nonmarine realm, there are more complexities controlling the timing of coal accumulation in a sequence stratigraphic sense (Shanley and McCabe 1994). These include climatic and tectonic factors which control base level, the creation of accommodation space and regional clastic supply (McCabe 1984; Shanley and McCabe 1994). Coal beds in the nonmarine realm, if regionally extensive, can be regarded as sequence boundaries which record the gaps (analogous to condensed sections) in the accumulation of clastic sediment (Hamilton and Tadros 1994). However, they are often associated with sequence boundary surfaces (Jerrett et al. 2011b).

Maceral composition, geophysical signatures, palynofloral assemblages and inorganic content all assist in the correlation of individual coal beds in a chronostratigraphic sense. However, coal beds themselves can sometimes be time transgressive or contain several hiatuses (Fassett and Hinds 1971; Hamilton and Tadros 1994; Nichols 2005; Jerrett et al. 2011a). Petrographic discontinuity surfaces may also be the equivalent of sequence boundaries (Jerrett et al. 2011a). Many coal beds split and amalgamate on a regional scale and this can hinder their interpretation as a regressive or transgressive coal due to their formation over several deposition cycles (Wadsworth et al. 2002). The successful application of sequence stratigraphy to the correlation of strata bearing thin, discontinuous coal seams in the nonmarine realm remains to be tested.

2.2 Overview and evolution of Mesozoic basins in eastern Australia

The geographic distribution of underlying Carboniferous-Triassic basins across eastern Australia are shown in Figure 2.1. These basins are discussed in brief because they strongly influence the structural framework of overlying Late Triassic to mid-Cretaceous basins.

2.2.1 Palaeozoic origins

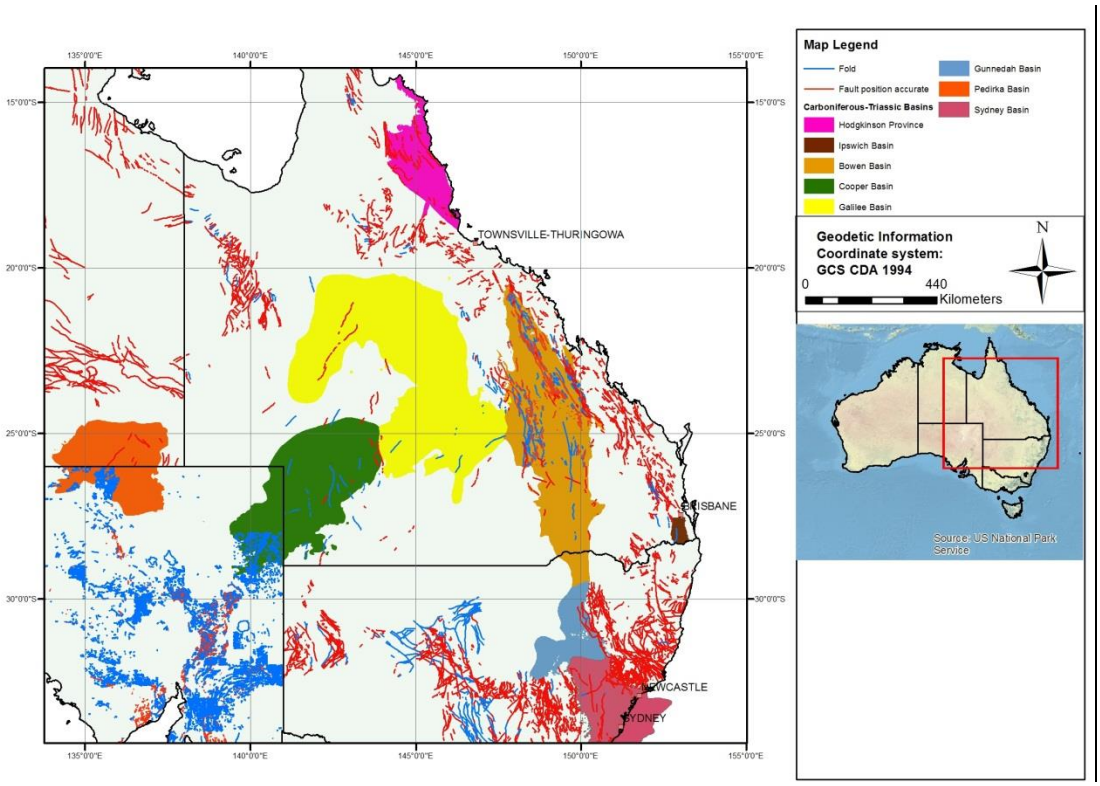

Figure 2.1. Geographic distribution and structural elements within Carboniferous-Triassic basins of eastern Australia.

2.2.1.1 Bowen Basin

Underlying the Surat Basin in Queensland and New South Wales is the north-south trending Permo-Triassic Bowen Basin which forms part of the larger Sydney-Gunnedah-Bowen Superbasin (Mallett et al. 1995). It is considered one of the world's most significant coal-bearing basins (Mallett et al. 1995). The Bowen Basin covers over 160,000 km^2, comprised of up to 10,000 m of infill and overlies Devonian to Carboniferous basement strata including the Drummond Basin and the Connors-Auburn Province (Jell 2013). The Bowen Basin is contiguous with the Gunnedah Basin in the south, bound by the contemporary New England Fold Belt in the east and the stable cratonic

platforms of the Thompson and Lachlan Fold Belts (or the Anakie High) to the west (Mallett et al. 1995; Jell 2013).

The origins of the basin during the Permian remain undefined and complex. This has resulted in numerous interpretations regarding the evolution of the basin; from dextral rotational forces creating a series of en-echelon troughs; a pull apart basin resulting from dextral strike-slip faulting; crustal transpression as a consequence of sinistral strike-slip; and even crustal extension along a passive margin (Yago 1996b; Green et al. 1997a). A minimum of three phases of basin development have been defined by authors including Green (2009), Jell (2013), Mallett et al. (1995) and Yago (1996b) starting with a extensional phase in the early Permian, followed by thermal relaxation in the middle Permian and finally a phase of foreland basin development as a consequence of a major compressional event in the late Permian/Early Triassic. These events contributed towards the development of horsts and grabens and later an asymmetric profile as the foreland phase developed (Yago 1996b). However, the Bowen Basin does not exhibit many characteristics of a foreland basin including difficulty in interpreting a peripheral bulge and the small extent of thrust transport (Jell 2013). An Andean-style subduction zone was present to the east leading to a volcanoclastic-rich infill in the Bowen Basin (Green 2009). Deposition occurred in a variety of environments (fluvial to marine) in topographic lows including the Denison and Taroom Troughs whilst the Comet Ridge and the Collinsville Shelf remained as topographic highs through the Permian (Jell 2013). Late Triassic deformation resulted in the basin spliting into morphotectonics units north of the Taroom Trough (Mallett et al. 1995; Jell 2013). These include the Dawson Fold Zone north of the Blackwater Transfer Zone and the Nebo Synclinorium, north of the Bundarra Transfer Zone (Jell 2013). The Texas Orocline developed in response to back-arc extension (Campbell et al. 2015). A period of erosion and peneplanation led to the demise of the New England Orogen before the onset of the Great Australian Basin in the Late Triassic (Green 2009).

Major coal-beating units in the Bowen Basin include the Reids Dome Beds, the Fort Cooper Coal Measures and the Rangal Coal Measures which host coal

beds that are over 100 m thick and which may extend over 100 km (Jell 2013; Ayaz et al. 2015).

2.2.2.2 Ipswich Basin

Underlying the Clarence-Moreton and Nambour/Maryborough Basins in Southern Queensland is the intermontane, transtensional Late Triassic Ipswich Basin (Staines et al. 1995; Ward 1995). The basin is bound by the D'Agiliar Block to the north, the Beenleigh Block in the east and the West Ipswich Fault to the west. Covering 9000 km^2 with 1200 m of sediment infill, the basin originated as the Middle-Triassic Esk Basin, an asymmetrical transtensional basin formed by series of oblique extensional episodes driven by strike-slip faulting (Korsch et al. 1989; Jell 2013). The origin and controls on sedimentation in the Ipswich Basin are contentious due to the basin lying, in-part, unconformably on Palaeozoic basement with numerous faults (Jell 2013). A thermal relaxation phase and minor compression then followed leading to deposition within the newly formed Ipswich Basin (Wells 1994). Recent research by Babaahmadi et al. (2015) suggests trench advance/retreat and plate boundary migration may be responsible for alternating episodes of extension and contraction in the Triassic leading to the formation of the Esk Trough and subsequently the Ipswich Basin. Structures in the basin include the north to westerly trending Ipswich, Bundamba, South Moreton and Sprigg Mountain Anticlines and a series of north to northwest trending faults (Staines et al. 1995). These structures are believed to have developed during or just after the final phase of deposition in the Ipswich Basin (Staines et al. 1995). The basin hosts predominately fluviolacustrine strata with numerous coal beds within the Ipswich Coal Measures (Staines et al. 1995).

2.2.2.3 Cooper and Galilee basins

Underlying the Eromanga Basin are the Cooper, Galilee and to the far west, the Early Permian Pedirka Basin (Jell 2013). The Cooper Basin is a complex, Carboniferous-Triassic intracratonic basin in eastern central Australia and unconformably overlies the Cambrian-Devonian Warburton Basin (Jell 2013). The basin is separated from the coeval Galilee Basin by the Canaway Ridge in the northwest, bound by the Arunta Block to the north, Proterozoic metamorphics to the south, and the Thompson Orogeny metamorphics to the

east (Gatehouse 1986; Jell 2013). Covering an area of 153,000 km^2, it is regarded as Australia's most prolific onshore petroleum basin (Mavromatidis 2008) having produced 5.29 TCF of gas and 195.4 mmbbll of oil since 1970 (Department_of_State_Development 2017). The inception of the Cooper Basin was influenced by pre-existing basement structures in the early Palaeozoic Warburton and Adavale basins which have their origins in the Precambrian (Beeston 1995). These basins were structurally deformed during the Delamerian and Alice Springs Orogenies (Beeston 1995; Gravestock et al. 1998). Reactivation of strike-slip, high angle reverse, and en-echelon faults during the formation of the Warburton Basin provided the structural framework for the Cooper Basin (Mavromatidis 2008). Compressional events from the Ordovician to middle Carboniferous resulted in the formation of the Gidgealpa-Merrimelia-Innamincka Anticlinal Trend which separates the Copper Basin into its two distinct depocentres: the Patchawarra and Nappamerri Troughs (Apak et al. 1997; Gravestock et al. 1998).

Deposition in the Cooper Basin was initiated during the last phases of the Alice Springs Orogeny during Late Carboniferous which induced crustal thickening and led to the emplacement of granite (Gravestock et al. 1998). Subsequent cooling exponentially reduced heat flow resulted in a period of prolonged downwarping of the glaciated continental crust (Gravestock et al. 1998). This led to the deposition of glacial, fluvial, deltaic, shoreface and lacustrine sediments which was further enhanced by the reactivation of faults in underlying basins (Gravestock et al. 1998). Three significant uplift events (lower Patchawarra, mid-Patchawarra and the Daralingie unconformities) were caused by the plate margin stresses to the east (Strong et al. 2002). These are easily identified in the Cooper Basin (Gravestock et al. 1998). Uplift events were punctuated by periods of thermal relaxation leading to crestal unconformities and the lateral and vertical variations in facies within chronostratigraphic units (Gravestock et al. 1998; Strong et al. 2002). Coal-bearing strata are hosted within the Patchawarra Formation and the Roseneath Shale-Epsilon Formation-Murteree Shale (or better known as the REM) (Alexander et al. 1996). After the last phase of thermal relaxation, an intraplate east-west compressional regime (leading to thin-skinned deformation) commenced in the Early Triassic

(Mavromatidis 2008). This was in response to stress and sediment loading associated with the Hunter-Bowen Orogeny and consequently the cessation of sedimentation in the basin (Mavromatidis 2008). Deposition recommenced in overlying Eromanga Basin in the Early Jurassic during a period of thermal subsidence (Alexander and Hibburt 1996). Structures in the Cooper Basin include the Birdsville Track Ridge, the Arrabury Trough and the Harkaway Anticline (Jell 2013).

The Carboniferous-Triassic Galilee Basin is another intracratonic basin, located to the northeast of the Cooper Basin (Scott et al. 1995; Jell 2013). The basin hosts significant and underdeveloped coal resources (Scott et al. 1995; Jell 2013). The boundaries of the basin are uncertain due to erosion during the Late Permian through to the Middle Triassic (Jell 2013). The basin covers 274,000 km^2 and comprises over 2800 m of sediment infill (Jell 2013). The Galilee Basin overlies the Drummond Basin to the east and north and the Adavale Basin to the south; elsewhere, the basement lies of basement rocks formed during the Thompson Orogeny (Jones and Fielding 2008; Jell 2013). Whether the evolution of the basin was driven by thermal subsidence, foreland subsidence or dextral shear remains uncertain (Jell 2013). With the exception of fault propagation folds induced by thin-skinned tectonics, inversion during the Middle to Late Triassic did little to deform strata in the basin (Jell 2013). Major structures in the basin include the Barcaldine Ridge, Aberfoyle Syncline, Pleasant Creek Arch and the Springsure Shelf which separating the Galilee Basin from the Bowen Basin (Jell 2013). Major depocentres include the Lovelle Depression and the Koburra Trough (Jones and Fielding 2008; Jell 2013). Major coal-bearing units in the Galilee Basin are hosted predominately by the Aramac Coal Measures (Jell 2013)

2.2.2.4 Palaeozoic origins of the Laura Basin

Little is known about the origins of the Laura Basin due to its location within a national park and the absence of data. The Laura Basin is known to overlie Precambrian metamorphics, the Palaeozoic Coen and Yambo inliers and the Hodgkinson Basin to the east of the Palmerville Fault (Jell 2013). In the west, the basin is underlain by the Permo-Triassic Lakefield Basin (Jell 2013).

2.2.2 Surat and Mulgildie basins

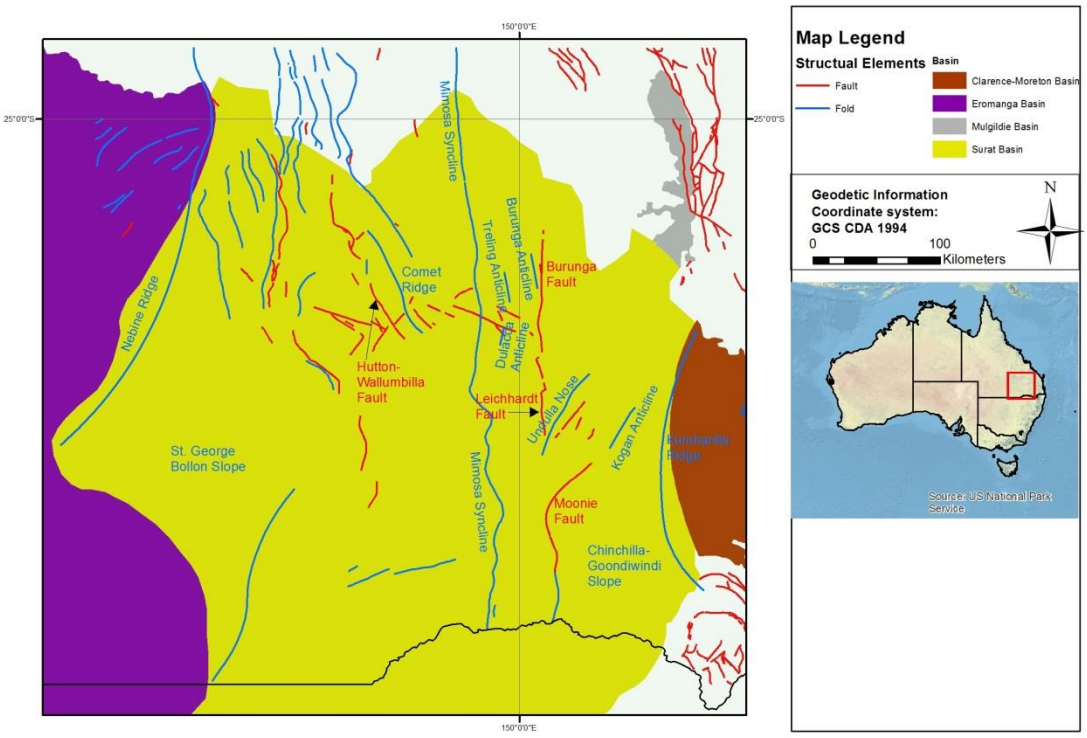

Figure 2.2. Structural elements of the Surat Basin in Queensland.

The Late Triassic to Early Cretaceous intracratonic Surat Basin (Figure 2.2) forms one of a series of depocentres associated with the Mesozoic Great Australian Superbasin (Jell 2013). The Surat Basin comprises ~2300 m of sedimentary infill (Stewart and Alder 1995; Jell 2013). The basin covers over 270,000 km^2 of southern Queensland/northern New South Wales (Goscombe and Coxhead 1995). Approximately 60% of the basin lies within Queensland and 40% in New South Wales (Stewart and Alder 1995). The basin is described as broad and flat with mild folds and several reverse thrust faults (Hamilton et al. 2014b). Strata gently dip to the southwest (Hamilton et al. 2014b). The basin unconformably overlies strata of the Bowen Basin (Stewart and Alder 1995; Raza et al. 2009; Hamilton et al. 2014b). The Surat Basin outcrops in the north and is bound by the Central West Fold Belt/New England Fold Belt to the south (Ryan et al. 2012). To the west, the basin thins out over the Roma Shelf and connects with the Eromanga Basin over the Nebine Ridge (Exon 1976). To the east, the basin is contiguous with the Clarence-Moreton Basin (Jell 2013). The boundary between the basins is contested and may be represented by the

Kumbarilla Ridge (a basement high), the Auburn Arch or the Toowoomba Strait (Pinder 2004; Jell 2013). The western and eastern margins of the basins have been continually modified resulting from several episodes of uplift and erosion (Stewart and Alder 1995). In New South Wales, the southeast portion of the Surat Basin is known as the Oxley Basin and the southwest portion is known as the Coonambie Basin (Stewart and Alder 1995). Many north-south trending structures in the underlying Bowen Basin (including the Taroom Trough and the Roma Shelf) are expressed in the Surat Basin including the Chinchilla-Goondiwindi Slope, Mimosa Syncline and the St. George-Bollon Slope (Scott 2008). Smaller structures including the Undula Syncline, the Kogan Anticline, and the Moonie-Goondiwindi Fault reflect the reactivation of basement faults since the Cretaceous (Ryan et al. 2012; Hamilton et al. 2014b). The Mulgildie Basin is considered a narrow, elongated trough (5200 km^2) off the northeastern sector of the Surat Basin and is thought to be related to a rifting event along north-south faults during the Mesozoic (Goscombe and Coxhead 1995).

Sedimentation on a local scale commenced in the newly formed Surat Basin during the Rhaetian with the Eddystone and Chong beds (Green et al. 1997a; Jell 2013). A short compressional episode in the Triassic known as the Goondiwindi event eroded the majority of these sediments (Stewart and Alder 1995). Deposition recommenced in the Early Jurassic during a phase of thermal sag (Jell 2013). An unconformity between the Walloon Coal Measures and the Springbok Sandstone has been interpreted as the only major hiatus during deposition in the Surat Basin and is thought to be related to the rifting of Argoland *ca*. 155 Ma from Australia in the west (McKellar 1998). Sedimentation ceased in the Surat Basin after deposition of the paralic Griman Creek Formation in the Albian due to the second phase of contraction (a smaller Hunter Bowen deformation event along reactivated faults) during the middle Cretaceous which removed up to 2 km of strata (Fielding 1996; Raza et al. 2009). With the exception of minor fault adjustments during the Cenozoic, the Surat Basin has been relatively quiescent through to the present (Scott 2008).

The tectonic history of the basin during the Jurassic remains enigmatic due to uncertainties on the nature (and position) of the eastern Australian margin and the trigger for large, episodic volcanic eruptions during the Jurassic and

Cretaceous (Bryan et al. 1997; Matthews et al. 2011; Jell 2013; Tucker et al. 2016). Thermal sag related to the cessation of arc volcanism; subduction-related dynamic platform tilting; and rifting resulting from the dissipation of the Pangean Thermal Anomaly have all been suggested as possible mechanisms of basin subsidence from the Jurassic and into the Cretaceous (Korsch et al. 1989; Green et al. 1997; McKellar 2004; Hoffmann et al. 2009; Jell 2013).

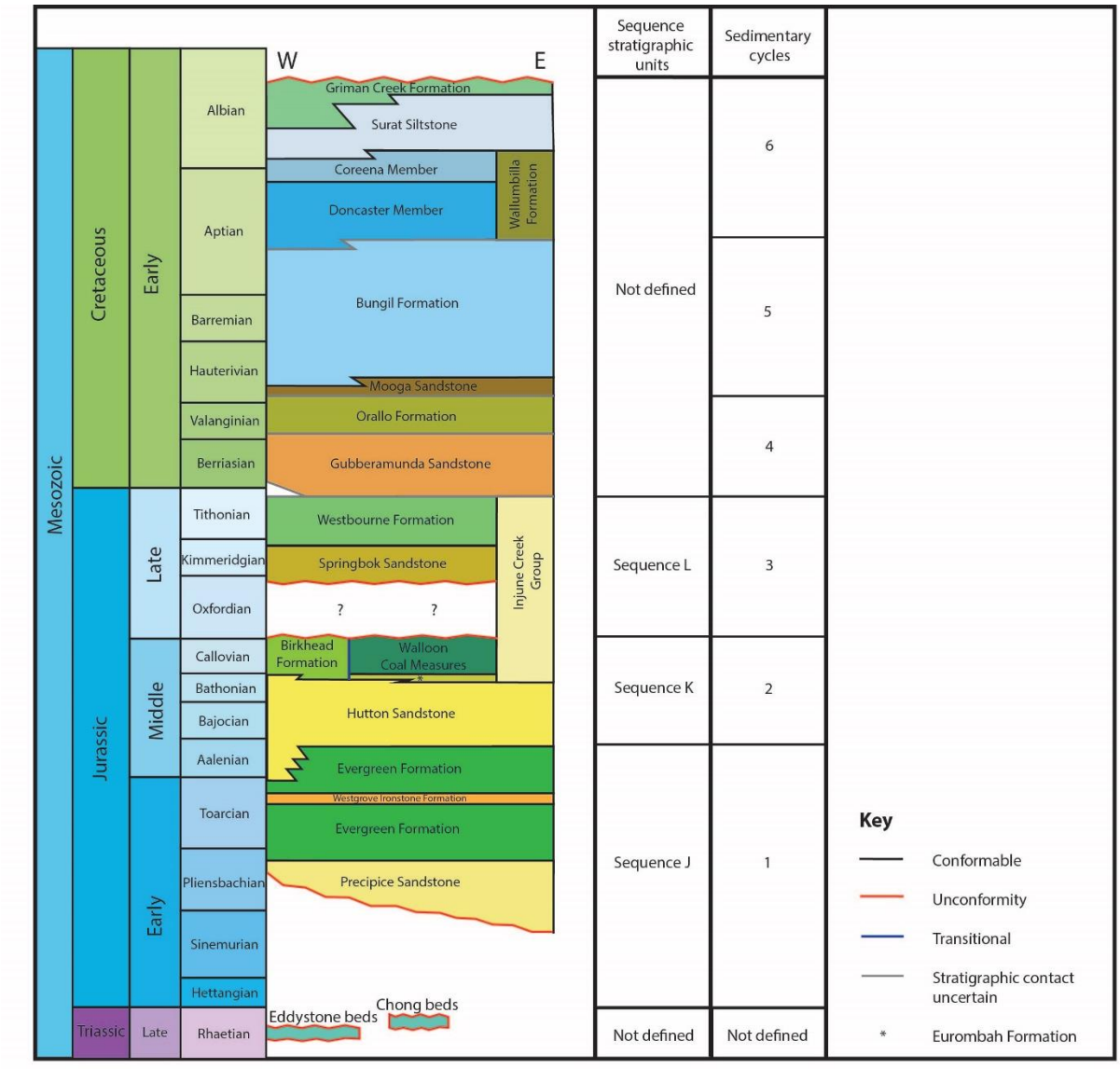

Figure 2.3. Lithostratigraphic units, sequence stratigraphic units and sedimentary cycles of the Surat Basin, Queensland. Adapted from Exon and Burger (1981), Hoffmann et al. (2009) and Jell (2013).

Seventeen lithostratigraphic units and six sedimentary cycles (~20 Ma in duration) are defined in the Surat Basin of Queensland (Figure 2.3) (Exon and

Burger 1981; Jell 2013). The Hutton-Walloon sequence forming the second cycle is the thickest (Exon and Burger 1981). These cycles are up to 600 m in thickness and consist of a series of fining-upward successions commencing with basal sandstones with an erosive base and culminating in labile sandstones, siltstones, mudstones and coals (Exon and Burger 1981). Changes in base level driven by eustatic sea-level change are assumed to have instigated transitions from high-energy braided fluvial to low-energy meandering fluvial deposition culminating with marine, lacustrine or mire deposition (Exon and Burger 1981). The link between eustatic sea-level change and sedimentation is, however, poorly defined (Exon and Burger 1981; Shields and Esterle 2015). Climatic change or recurrent uplifts are considered unlikely factors in influencing these sedimentary cycles (Exon and Burger 1981). Marine deposition did not commence until deposition of the Bungil Formation during the fifth sedimentary cycle in the Early Cretaceous (Exon and Burger 1981; Jell 2013). This was a time when global sea-level rose triggering marine incursions into the basin (Exon and Burger 1981; Jell 2013).

Sequence stratigraphic work by Hoffmann et al. (2009), based on nonmarine sequence stratigraphic principles developed by Shanley and McCabe (1994) defined three Jurassic supersequences in the basin. Each is characterised by a lowstand systems tract, a transgressive systems tract and a highstand systems tract bound by sequence boundaries (J, K, L) defined from seismic sections (Hoffmann et al. 2009). The Walloon Coal Measures form part of supersequence K above horizon S35 (Hoffmann et al. 2009). Supersequence K consists of a series of amalgamated, unconformal basal sandstones (lowstand systems tracts) overlain by fining upward carbonaceous lithologies including coals and laminated mudstones (the transgressive and highstand system tracts) (Hoffmann et al. 2009). Supersequence J (Precipice Sandstone to the Evergreen Formation) and L (Springbok Sandstone to the Westbourne Formation) display similar characteristics with weaker seismic reflectors and more pronounced stratigraphic truncations (Hoffmann et al. 2009). Similar work has yet to be carried out for the Cretaceous successions.

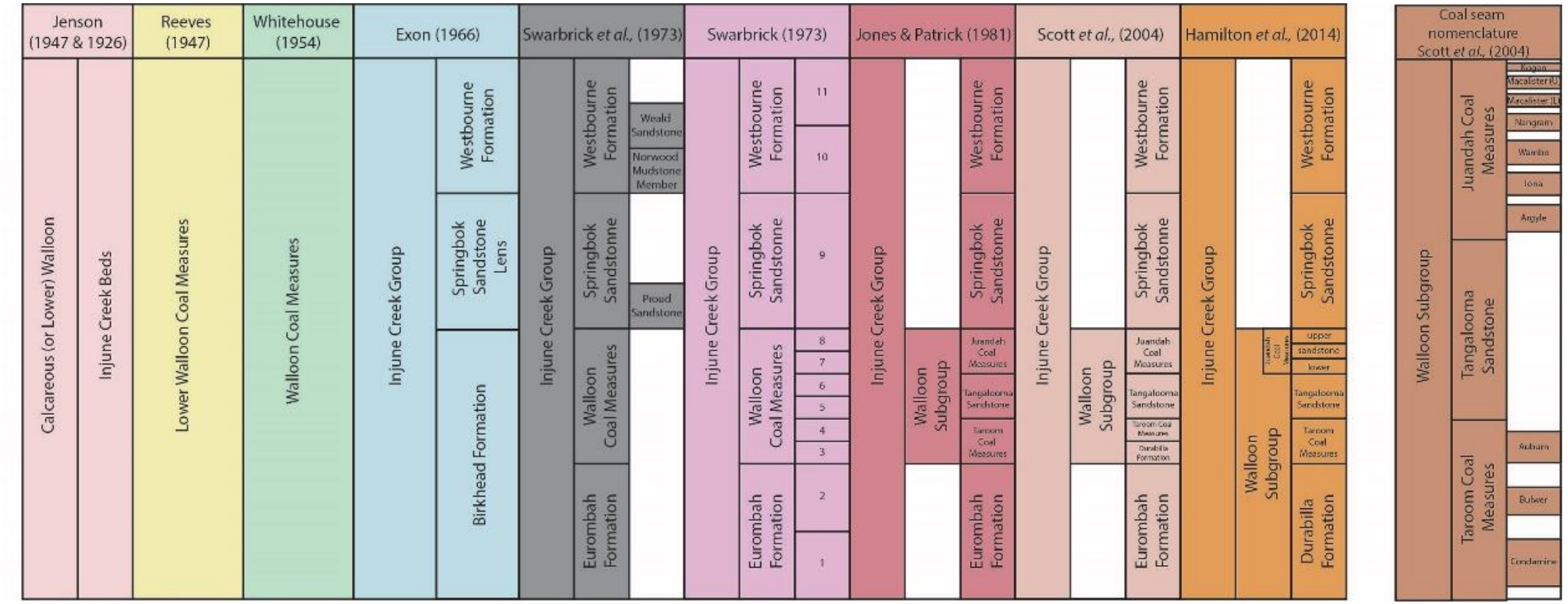

Figure 2.4. Revisions of the lithostratigraphic nomenclature associated with the Walloon Coal Measures/Walloon Subgroup. Adapted from Scott (2008).

The coal-bearing fluviolacustrine Walloon Coal Measures or Subgroup is 350 m to 500 m thick in the Surat Basin comprising labile sandstones, siltstones, mudstones, coal with occasional calcareous sandstones, tuffs, impure limestones and ironstones (Jell 2013). The formation is underlain by the Hutton Sandstone or the Eurombah Formation and overlain unconformably by the Springbok Sandstone (Jell 2013). Formation thickness and coal percentages decrease to the west (Jell 2013). The formation is thickest over the Mimosa Syncline (Ryan et al. 2012). Stratigraphic nomenclature of the Walloon Coal Measures has been under repeated revision (Figure 2.4) since it was first described by Cameron (1907) as the Walloon Beds in the Clarence-Moreton Basin. Numerous redefinitions have split and combined units especially as a result of petroleum exploration activities in the 1960's. The term 'Walloon Coal Measures' was first used in the Surat Basin by Bryan (1946) and developed upon by Reeves (1947) during geological studies in the northern Surat Basin. However, it was Swarbrick (1973) who defined the Walloon Coal Measures in the Surat Basin and differentiated it from the coeval Birkhead Formation on variations in coal content west of Injune, Queensland. Jones and Patrick (1981) redefined the six lithostratigraphic intervals of the Walloon Coal Measures of Swarbrick (1973) and proposed three lithostratigraphic formations comprising the newly named Walloon Subgroup. These units comprise the Taroom Coal Measures, the Tangalooma Sandstone and the Juandah Coal Measures (Scott et al. 2004). An additional formation, the Durabilla Formation, was later defined within the Taroom Coal Measures based on wireline log characteristics (Scott et al. 2004). The Walloon Subgroup is currently the formal stratigraphic name for this unit; however, this is contested due to the localised occurrence of lithostratigraphic subdivisions (Green et al. 1997a; Scott et al. 2004). Coal bed terminology varies between exploration companies, mines, and geographic districts and no attempt has been made to collate the diverse coal bed nomenclature. Lithostratigraphic, coal bed and even biostratigraphic frameworks are regarded as flawed leading to variable interpretations of depositional system architecture as each may incorrectly reveal the thinning or thickening of stratigraphic sections between wells (Martin et al. 2013).

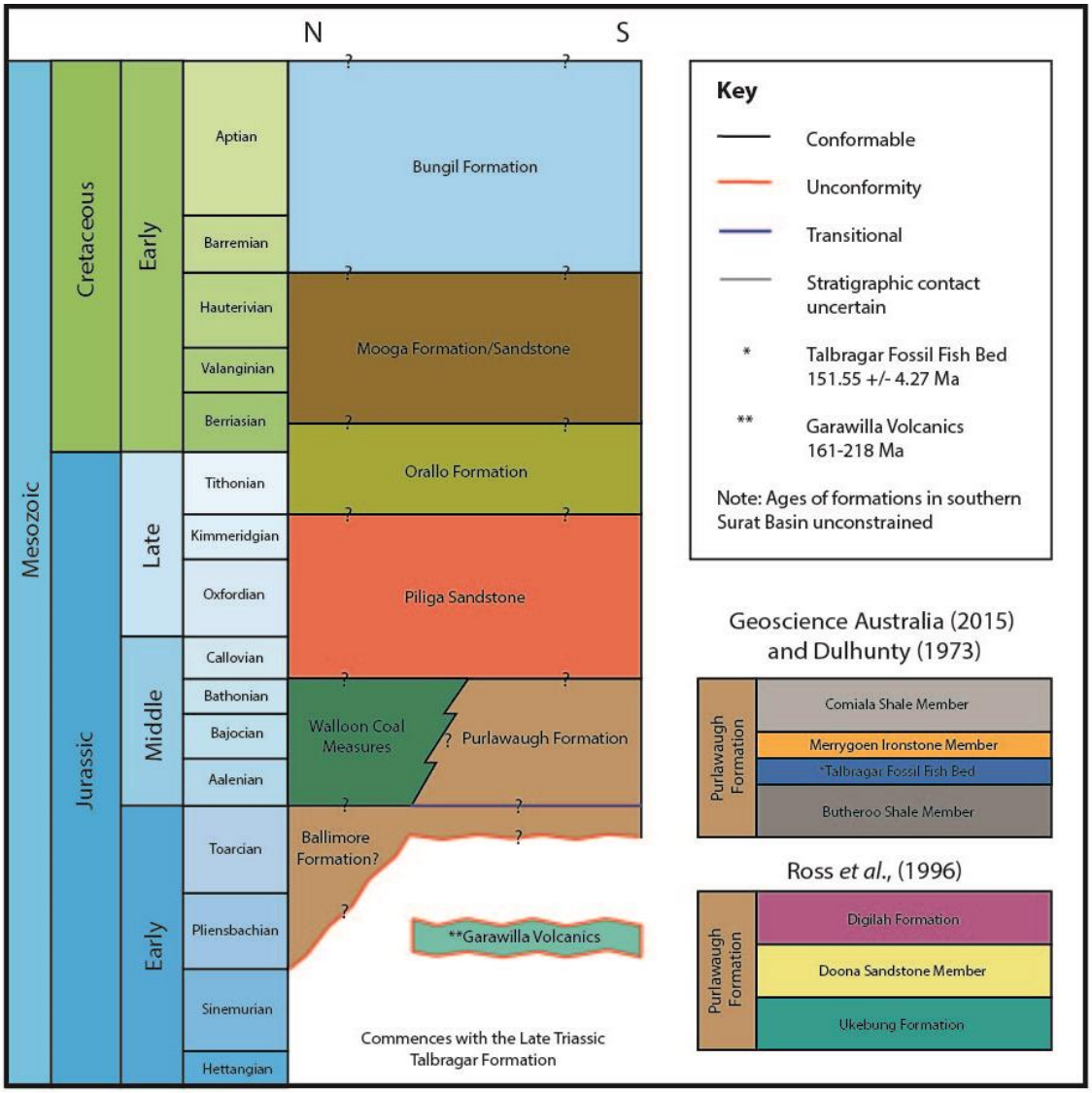

Figure 2.5. The lithostratigraphic units of the Surat Basin, New South Wales. Adapted from Dulhunty (1973) and Stewart and Alder (1995), Ross (1996) and Geoscience_Australia (2016).

The New South Wales portion of the Surat Basin is relatively poorly understood due to the lack of acreage availability for coal seam gas development. To date, fewer than 100 wells have been drilled with limited acquisition of seismic data (Stewart and Alder 1995). Only three studies have attempted to elucidate the Mesozoic stratigraphy in New South Wales and summarised in Figure 2.5. Dulhunty (1973) was the first to define Mesozoic stratigraphy using K-Ar dates from the Garrawilla Volcanics and palynofloral assemblages from other formations for age control. Arditto (1982) is the only author to describe the fluvial Pilliga Sandstone. Stewart and Alder (1995) provides the latest summary of stratigraphic units in New South Wales and their petroleum potential. Five formations have been identified in the Jurassic of New South Wales and are part of a continuum with coeval formations in Queensland (Stewart and Alder 1995). The Walloon Coal Measures are considered transitional with the Purlawaugh Formation before the onset of the Coonamble Basin (Stewart and Alder 1995). There have been numerous revisions of the Purlawaugh Formation, however, these are poorly defined and lack robust age controls (Stewart and Alder 1995; Ross 1996; Geoscience_Australia 2016). One ‘Sensitive High Mass Resolution Ion MicroProbe’ (SHRIMP) age of 155 ± 4.27 Ma (Kimmeridgian) from the Talbragar Fish Bed within the Purlawaugh Formation reveals the need for a comprehensive review the stratigraphy of the Mesozoic in New South Wales (Bean 2006). A summary of Middle to Late Jurassic coal-bearing lithostratigraphic units in Queensland and their equivalents in New South Wales are described in Table 2.2.

Formation	Biostratigraphic age	Stratigraphic relationship with underlying formation	Lithology	Thickness	Depositional setting	Other
Eurombah Formation	Bajocian to Bathonian	Conformable	Coarse to fine clayey sandstones. Minor siltstones, carbonaceous mudstone, and coals	Up to 95 m	Low energy, fluviatile, swamps	Difficulty in differentiating it from the Walloon Coal Measures. Not regionally extensive. Higher volcanic detrital content to the Hutton Sandstone
Walloon Coal Measures	Aalenian to Callovian	Conformable	Medium to fine-grained sub-lithic to feldspathic arenites. Siltstones, mudstones, carbonaceous mudstones, tuffs, and coals. Rare oolitic ironstone	Up to 500 m (919 m in the Clarence-Moreton Basin)	Low energy, fluviolacustrine with swamps	Difficult to distinguish subunits, especially in the Clarence-Moreton Basin. Sandstones predominantly volcanic lithic in composition (andesitic)
Ballimore Formation	Upper Triassic to Lower Jurassic	Unconformable	Lithic to tuffaceous sandstones, highly ferruginous, carbonaceous red-brown and black mudstone, coaly shale, thin coal seams	Uncertain	Low energy, fluviolacustrine with swamps?	Not recognised by Geoscience Australia

Formation	Biostratigraphic age	Stratigraphic relationship with underlying formation	Lithology	Thickness	Depositional setting	Other
Purlawaugh Formation	Pliensbachian to Bathonian	Conformable	Fine to medium grained lithic to labile sandstone thinly interbedded with siltstone, mudstone, and thin coal seams. Abundant carbonaceous fragments. Occasional thin beds of flint clay. Can comprise a 10-15 m package of massive claystone with grey to brown-red pigmented lithic fragments with carbonised plant fragments	100 m	Fluvial (meandering)	Superseded Ukebung and Digilah formations. Time equivalent to the Walloon Coal Measures
Taroom Coal Measures	Early to Middle Jurassic	Conformable	Fine grained sandstones, mudstones, siltstones and coals	Up to 180 m	Low energy, fluviolacustrine with swamps	The lower boundary defined by Condamine seam, the upper boundary defined by the Auburn seam. Contains 3 coal intervals. An additional member, the Condamine Sandstone sometimes used
Tangalooma Sandstone	Middle Jurassic	Conformable	Fine to medium grained argillaceous sandstones with siltstones, mudstones and rare coals	Up to 100 m	Low energy, fluviolacustrine with swamps	Thickness as low as 10 m. Lower base defined by the Auburn seam and top defined by Argyle seam

Formation	Biostratigraphic age	Stratigraphic relationship with underlying formation	Lithology	Thickness	Depositional setting	Other
Juandah Coal Measures	Early to Middle Jurassic	Conformable	Fine grained sandstones, mudstones, siltstones and coals with a high ash content	Up to 270 m	Low energy, fluviolacustrine with swamps	Very similar to the Taroom Coal Measures. Defined at the base by the Argyle Seam and contains 6 coal intervals. Can be split into the lower Juandahs, Juandah sandstone, and upper Juandahs
Birkhead Formation	Bathonian to Kimmeridgian	Conformable	Fine grained lithic sandstones, siltstones and carbonaceous mudstone with rare coals	Up to 110 m	Low energy fluviolacustrine, rare swamps	Contiguous with the Walloon Coal Measures in the west, brackish-marginal marine influences, diachronous
Butheroo Shale Member	Lower Jurassic	Conformable	Blue-white fire clay shale and mudstone with imbedded fusain plant material interbedded with coal, carbonaceous shales, and coaly shales	Uncertain	Low energy, fluviolacustrine with swamps?	Informal stratigraphic name
Talbragar Fossil Fish Bed	Early to Middle Jurassic	Conformable	Thin tuffaceous siltstones and sandstones with clay, cherts and fossil fish	1.5 m	Shallow freshwater lake/shoreface	Inundated by volcanic ash fall. One SHRIMP age of 151.55 Ma

Formation	Biostratigraphic age	Stratigraphic relationship with underlying formation	Lithology	Thickness	Depositional setting	Other
Merrygoen Ironstone Member	Early to Middle Jurassic	Conformable	Grey-blue shale and mudstone, numerous sideritic chert bands up to 25cm in thickness. Can be abundant in siderite, haematite, limonite and ferruginous gravels	Uncertain	Shallow freshwater lake /shoreface	Contains fossil fish
Comiala Shale Member	Middle Jurassic	Conformable	Non-ferruginous blue-grey shale, mudstone, minor lithic sand and thin coaly shale beds	Uncertain	Low energy, fluviolacustrine with swamps?	Informal stratigraphic name
Ukebung Formation	Early to Middle Jurassic	Conformable	Kaolinite clay, carbonaceous, pelletal and massive flint clay, quartz litharenites, ironstone and minor coal	50 m	Low energy, fluviolacustrine with swamps	Superseded by the Purlawaugh Formation

Formation	Biostratigraphic age	Stratigraphic relationship with underlying formation	Lithology	Thickness	Depositional setting	Other
Donna Sandstone Member	Middle to Late Jurassic	Conformable	Dull grey to white, fine to medium grained arenites with fragments of flint clay in a kaolinite matrix. Cubic jointing, worm trails, and plant remains observed	3 m	Low energy, fluviolacustrine with swamps	Formal stratigraphic name
Digilah Formation	Middle to Early Jurassic	Conformable	Monotonous succession of thinly bedded mudstone and siltstone, lenticular ironstone beds with minor white flint clay	30 m	Low energy, fluviolacustrine	Superseded by the Purlawaugh Formation
Springbok Sandstone	Bathonian to Callovian	Unconformable	Coarse to fine grained volcanic, feldspathic and quartzose sandstones. Minor pebbly quartzose sandstones, siltstones, mudstones and thin coals	275 m	High energy fluvial with increasing overbank and swamp deposits up strata	Contemporary volcanism during deposition. Lower interval is known as the Proud Sandstone

Formation	Biostratigraphic age	Stratigraphic relationship with underlying formation	Lithology	Thickness	Depositional setting	Other
Pilliga Sandstone	Callovian to Kimmeridgian	Conformable?	Massive medium to very coarse quartzose sandstones and conglomerates. Minor mudstone, siltstone, fine-grained sandstone, and coal. Carbonaceous fragments and iron staining	300 m	High energy, braided	None
Westbourne Formation	Kimmeridgian-Tithonian	Conformable	Interbedded fine grained quartzose sandstones, siltstones, and shales	250 m	Lacustrine/lacustrine delta	Low-energy back swamps and meandering streams in the Norwood Mudstone Member. Increasing proportion of sandstone to the west and south. Widespread in the Eromanga Basin.
Norwood Mudstone Member	Jurassic?	Conformable?	Sandstone, siltstone, mudstone, coal and tuffs	?	Low energy meandering channels and swamps	None

Table 2.2. The lithostratigraphic breakdown of Middle to Upper Jurassic coal-bearing units in the Surat Basin and their equivalents in New South Wales (Exon 1976; Jones and Patrick 1981; Scott et al. 2004; Jell 2013; Geoscience_Australia 2016).

2.2.3 Eromanga Basin

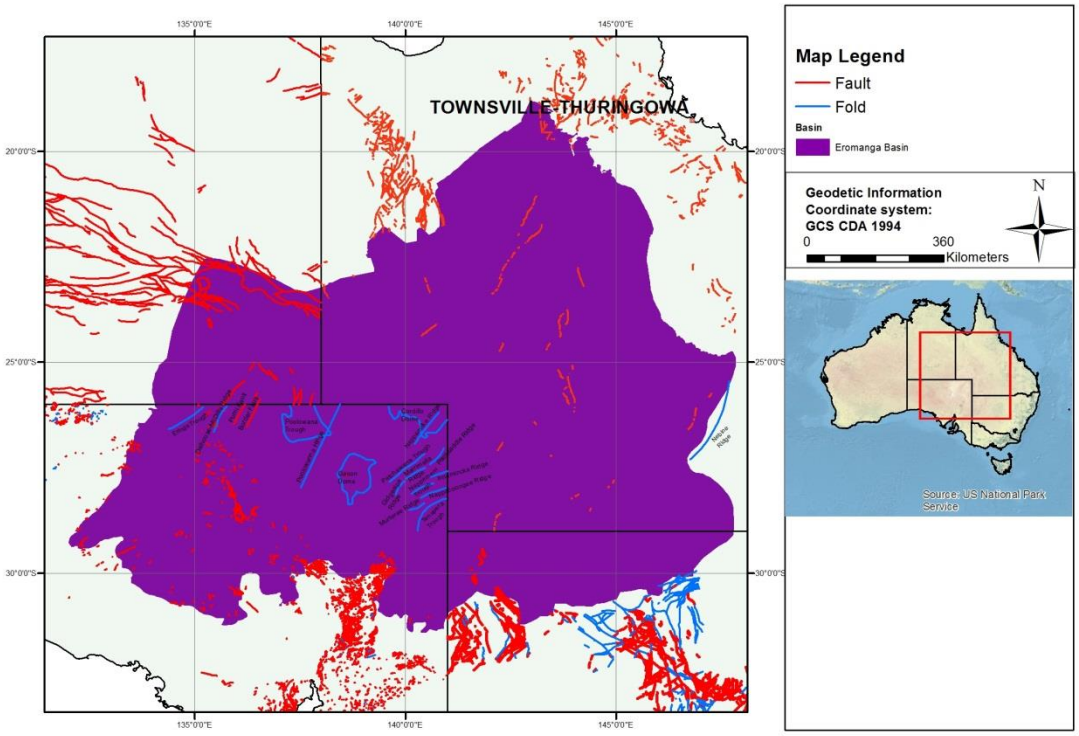

Figure 2.6. Structural elements of the Eromanga Basin.

The Late Triassic to Late Cretaceous Eromanga Basin (Figure 2.6) is a contemporary intracratonic downwarp to the east of the Surat Basin and overlies strata of the Permo-Triassic Cooper Basin (Alexander and Jensen-Schmidt 1996). The Eromanga Basin is the largest of the Mesozoic Australian Super basins covering over 1,000,000 km^2 of Queensland, South Australia, New South Wales and the Northern Territory (Goscombe and Coxhead 1995). The Eromanga Basin has ~2500 m of sedimentary infill (Goscombe and Coxhead 1995; Jell 2013). Strata gently dip at a shallow angle forming a broad synclinal structure spanning most of the basin (Goscombe and Coxhead 1995). Structures in the Eromanga Basin reflect those in the underlying Cooper and Galilee Basins (Jell 2013). It is described as being part of the larger Great Artesian Basin, extending from the Nebine Ridge and Eulo ridges in the east to the Euroka Arch in the northeast (Wiltshire 1982). To the north and west, the basin laps onto Palaeozoic rocks of the Amadeus, Simpson, and Warburton basins and is bound to the south by the Lachlan Fold Belt and the Flinders Ranges (Boult et al. 1998). Structures in the basin follow the pre-existing north

to the northeast fabric in the basement including the Maneroo Platform, the Canaway Fault, the Beryl Anticline and the Tara Monocline (Jell 2013). Many of these structures were reactivated during the Cenozoic (Jell 2013).

The evolution of Eromanga Basin begins with the termination of sedimentation in the Cooper Basin during the Triassic as a consequence of an east-west regional compressional event (Apak et al. 1997). This resulted in basin-wide uplift and the creation of the Nappamerri unconformity (Mavromatidis 2008). Basin-wide deposition was initiated by tectonic downwarping in the Early Jurassic (Alexander and Jensen-Schmidt 1996). During the Early to mid Cretaceous, the rate of basin subsidence more than quadrupled due to a combination of changing stress fields on the margins of the Australian plate, lithospheric rebound and sediment loading from the deposition of volcaniclastics (Gallagher and Lambeck 1989). This allowed for marine incursions into the Eromanga Basin (Gallagher et al. 1994; Waschbusch et al. 2009). Sedimentation was fairly continuous from the Jurassic and into the Cretaceous with the exception of a hiatus between the Birkhead Formation and the Adori/Namour Sandstones (Alexander and Jensen-Schmidt 1996). Uplift and erosion ended deposition in the basin during the Late Cretaceous and is marked by an unconformity (Alexander and Jensen-Schmidt 1996). Deposition re-commenced in the overlying Lake Eyre Basin during the late Palaeocene (Alexander et al. 1996).

A number of authors have considered the tectonic setting of the Eromanga Basin including Gallagher (1988), Gallagher and Lambeck (1989), Gallagher et al. (1994) and Waschbusch et al. (2009). The proposed mechanism driving subsidence in the basin varies from prolonged thermal relaxation to sub-lithospheric convection, to sediment loading (Gallagher 1988; Gallagher and Lambeck 1989; Gallagher et al. 1994). More recently, the role of dynamic platform tilting resulting from viscous mantle corner flow above a subducting plate has been suggested (Waschbusch et al. 2009). The role of near- and far-field deflection of the retrolithosphere (driven by pressure gradients at the base of the lithosphere above a subduction zone) is thought to have influence beyond the limits of the Surat Basin (Waschbusch et al. 2009). This is

suggested by the fourfold increase in sediment accumulation and the doubling of subsidence rates between the Eromanga and Surat basins during the Middle to Late Jurassic (Gallagher et al. 1994; Waschbusch et al. 2009).

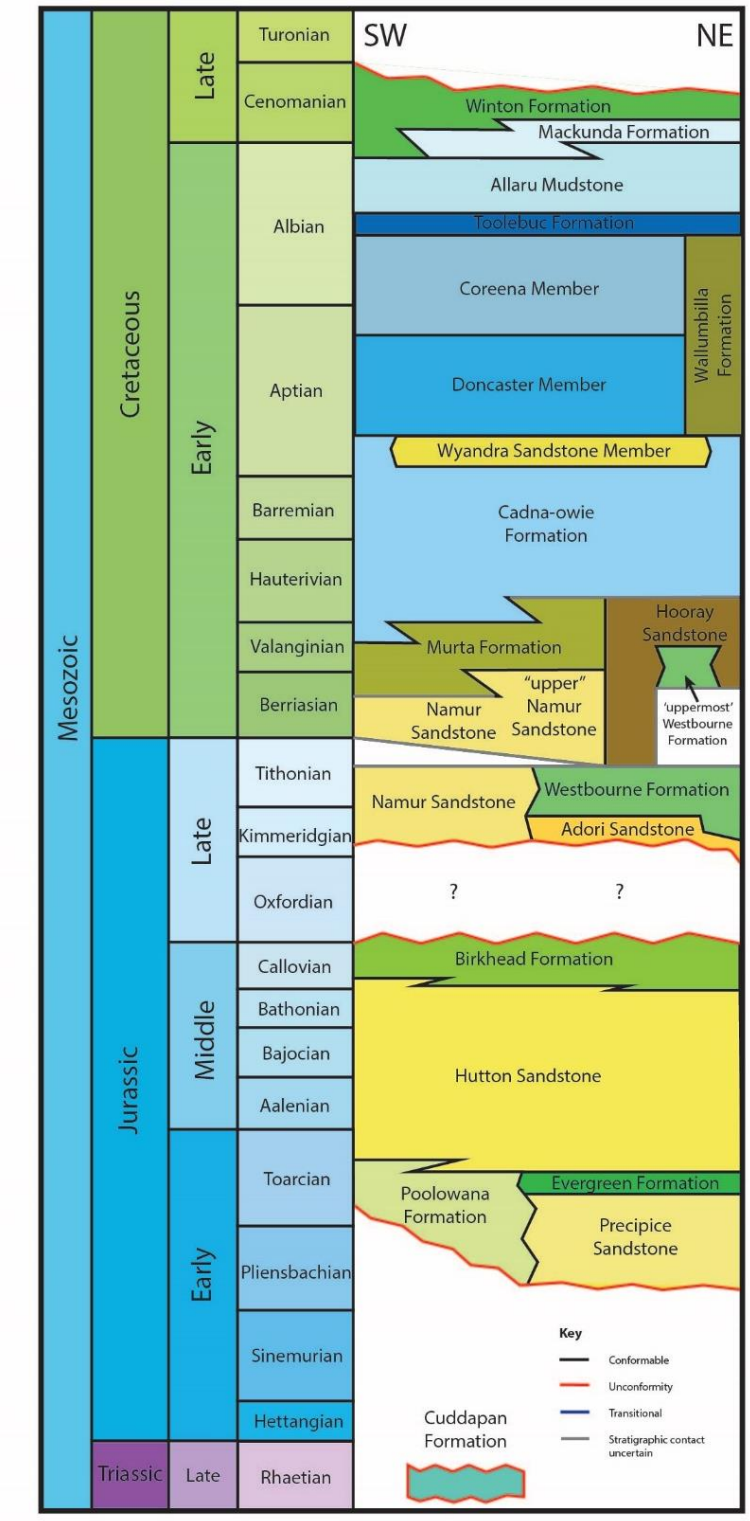

Figure 2.6. Lithostratigraphic units of the Eromanga Basin. Adapted from Jell (2013).

Deposition in the Eromanga Basin occurred in four distinct phases: 1) localised deposition in the Late Triassic; 2) extensive fluviolacustrine deposition through the Jurassic and into the Early Cretaceous; 3) marine incursions initiating paralic deposition in the Early Cretaceous; and 4) terminal paralic, fluvial and lacustrine deposition into the early Late Cretaceous (Figure 2.6) (Jell 2013). Cyclical sedimentation related to eustatic sea-level change is suggested in the Eromanga Basin. However, local tectonic events and sediment oversupply by large volume silicic volcanism overprints such signatures in the basin (Jell 2013). Deposition shifted west through the Mesozoic with deposition beyond the Birdsville Ridge some 500 km to the west of the Eringa Trough (Alexander and Jensen-Schmidt 1996). Variable sediment provenance is a major characteristic of many formations in the basin. In the case of the Birkhead Formation, sandstones were derived from sediments eroded from cratonic crust to the southeast (1600-1900 Ma) and from a volcanic arc to the northeast (1000-950 Ma) (Whitford et al. 1994). The causes for the rapid transition between cratonic and volcaniclastic derived sediments vary from climate change, rising base level and blockage of the fluvial system from the increased input of volcanic material into the basin (Burger 1986; Wiltshire 1989). In addition to a lithostratigraphic framework (Figure 2.6), a chronostratigraphic framework based on the first occurrence of key spore-pollen taxa is the main tool for high resolution correlation across the Eromanga Basin (Gallagher et al. 2008).

The coal-bearing fluviolacustrine Birkhead Formation is Callovian to Kimmeridgian in age and is regional in extent and up to 110 m in thickness (Jell 2013). The formation was first described by Woolley (1941) in the near the town of Tambo in Queensland. The Birkhead Formation was initially called the ‘Lower Intermediate Series’ during early petroleum exploration efforts in the Basin (Woolley 1941). The stratigraphy was refined by Exon (1966) by splitting the Lower Intermediate Series into the Hutton Sandstone and the Birkhead Formation and incorporating it within the Injune Creek Group. The Birkhead Formation has not been subsequently sub-divided into members or beds since its differentiation from the coeval Walloon Coal Measures in the Surat Basin (Swarbrick et al. 1973; Krieg et al. 1995; Alexander et al. 1996; Draper 2002).

In Queensland, the Birkhead Formation and the Walloon Coal Measures are used to describe rocks with similar characteristics, with some authors recommending the discontinuation of the term ‘Birkhead Formation’ in this area (Reeves 1947; Power and Devine 1970). The geographic extent of the Birkhead Formation has been redefined several times in response to seismic surveys and drilling (Alexander et al. 1996).

The Birkhead Formation interfingers with the underlying Hutton Sandstone and is unconformably overlain by the Adori Sandstone. It is considered coeval with the Walloon Coal Measures to the east (Jell 2013). The formation is comprised of fine to coarse grained sandstones, siltstones, mudstones and lenticular coal seams with occasional red palaeosols (Alexander et al. 1996; Gallagher et al. 2008).

2.2.4 Clarence-Moreton Basin

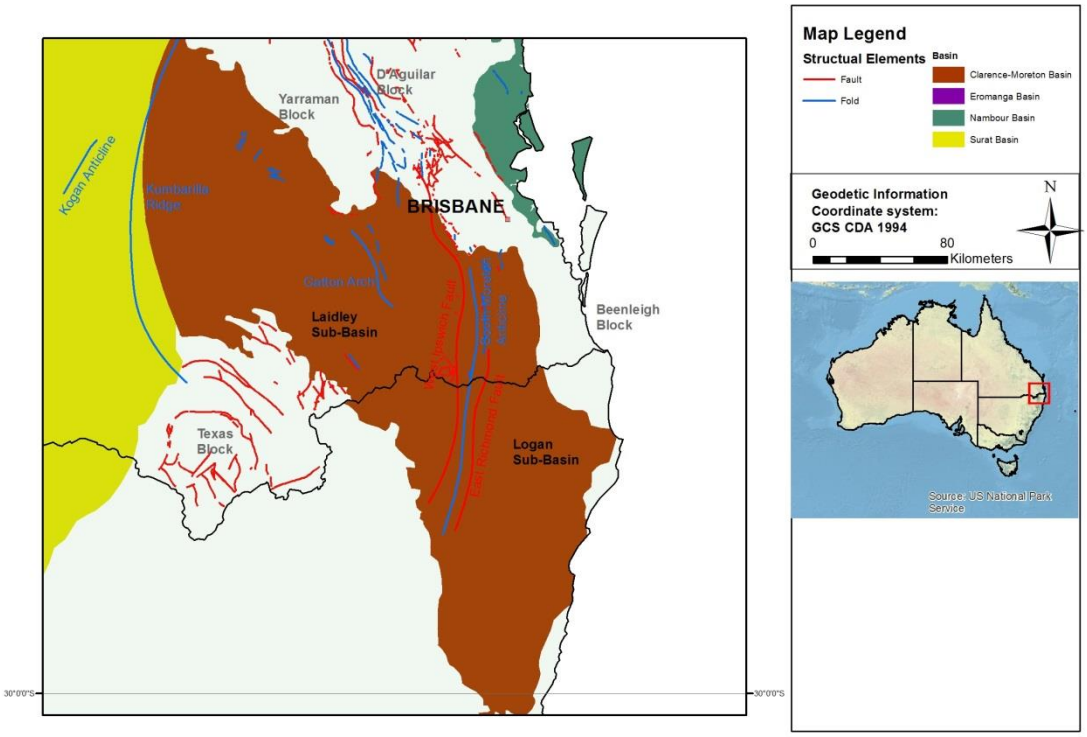

Figure 2.7. Structural elements of the Clarence-Moreton Basin.

The Late Triassic to Middle Jurassic intracratonic Clarence-Moreton Basin (Figure 2.7) covers an area of 43,000 km^2 of southeastern Queensland and northern New South Wales (Goscombe and Coxhead 1995). Some 10,000 km^2 of the Clarence-Moreton Basin lies offshore (Jell 2013).The basin is one of the thickest depocentres of the Mesozoic in eastern Australia (Goscombe and Coxhead 1995). The basin overlies two earlier Mesozoic depocentres; the Early Triassic Esk Trough and the Middle Triassic Ipswich Basin (Korsch et al. 1989; Powell et al. 1993; Jansson et al. 2008). The basin is bound by the Beenleigh Subprovince, the Yarraman and D'Aguillar blocks to the north (Jell 2013). The Texas, the Silverwood and Coffs Harbour Blocks bound the basin in the south and it is separated from the Surat Basin by the Toowoomba Straight and the Kumbarilla Ridge in the west (Pinder 2005; Jell 2013). The Clarence-Moreton Basin also interfingers with the Nambour Basin through the Brisbane Straight in the north (Goscombe and Coxhead 1995). Unlike in the Surat Basin, basaltic intrusions are common throughout the Clarence-Moreton Basin (Martin and Saxby 1982). Structures within the basin reflect those in the underlying basins.

The South Moreton Anticline, the West Ipswich Fault and the East Richmond Fault split the basin into the westerly Ladley Sub-Basin (or the Warrill Creek Sub-Basin) and the easterly Logan Sub-Basin (Korsch et al. 1989). The Cecil Plains Sub-Basin to the west of the Gatton Arch may belong to the Surat Basin, but the relationship of the Clarence-Moreton to the Surat Basin is unknown (Jell 2013). Little is known about the basement of the Clarence-Moreton Basin and it is thought to comprise exotic terranes which accreted during the New England Orogeny (O'Brien et al. 1994; Jell 2013).

The basin has a highly complex structural origin, but only experienced a prolonged period of thermal subsidence and sediment loading after the Middle Triassic (Korsch et al. 1989). The rate of subsidence is half of that of the underlying Ipswich Basin (Korsch et al. 1989; Babaahmadi et al. 2015). The subsidence history of the basin is not well understood because of the lack of precise dates through the Jurassic, but it is believed to be an epicratonic basin (Wells and O'Brien 1994). Deposition ceased during the Early Cretaceous due to compressional events resulting from lithospheric rebound when subduction ceased to the east (Martin and Saxby 1982).

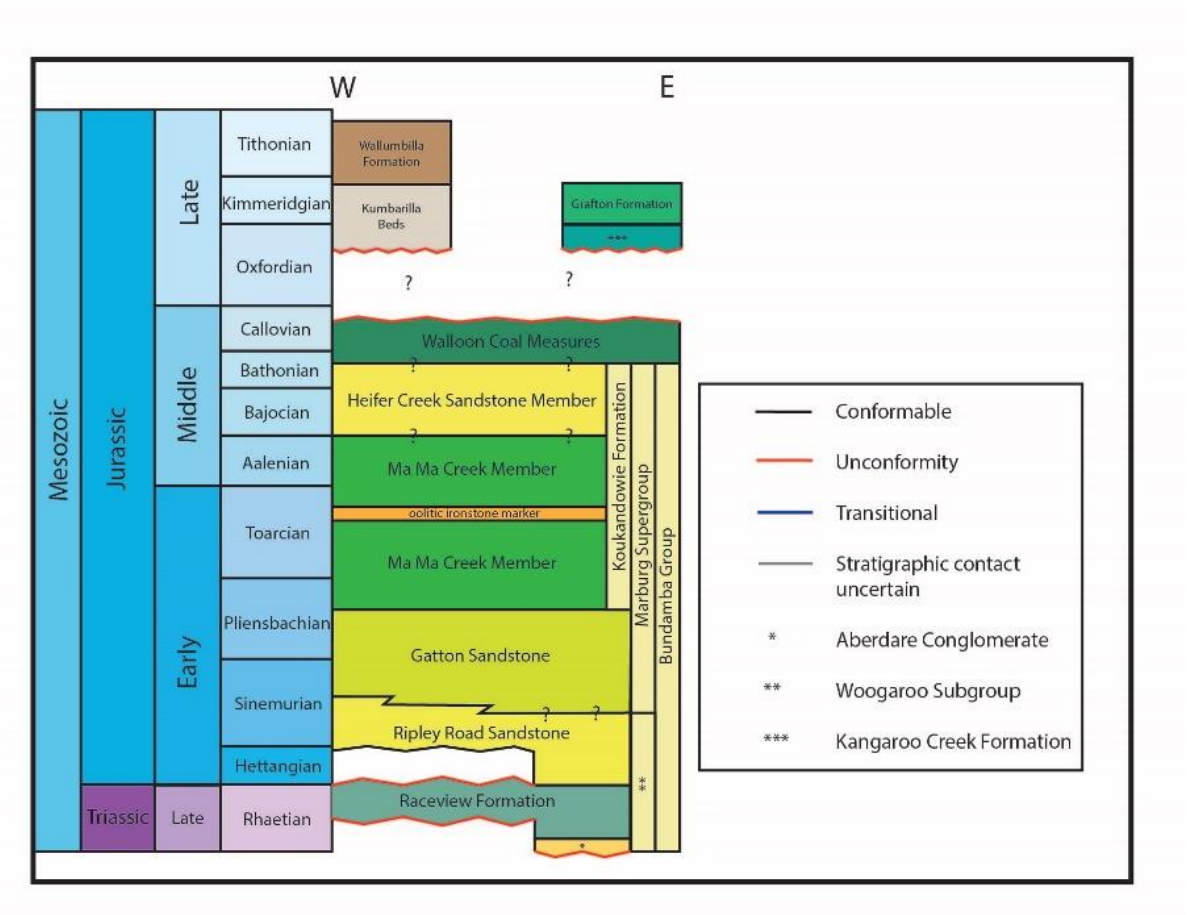

Figure 2.8. Lithostratigraphic units of the Clarence-Moreton Basin. Adapted from Pinder (2004) and Jell (2013).

Fluviolacustrine sedimentation was prevalent in the Clarence-Moreton Basin during the Mesozoic (Jell 2013). The 3000 m succession is divided into a variety of groups, subgroups, and formations including the Woogaroo Subgroup, the Marburg Subgroup and the Koukandowie Formation (Figure 2.8): (Wells and O'Brien 1994). These lithostratigraphic groups are difficult to distinguish on seismic reflection profiles (Wells and O'Brien 1994) but an attempt to determine a seismic stratigraphic framework was devised by O'Brien et al. (1994). Four seismic sequences were defined: crystalline basement; steeply dipping rift sediments lying unconformably over basement rocks; sediments of the Toogoolawah Group (volcanics, volcaniclastic conglomerates; andesitic lava, tuffs, sandstones and shales) comprising the fill material of the Esk Trough and Ipswich Basin; and sediments of the Clarence-Moreton Basin (O'Brien et al. 1994). Intrusive and extrusive rocks from the Cenozoic are

concentrated in the north and are associated with the Mount Warming Complex, the Main Range and Lamington Volcanics (Jell 2013).

The coal-bearing Walloon Coal Measures, up to 919 m thick in the Clarence-Moreton Basin, are considered similar in character to the Walloon Coal Measures of the Surat Basin (Goscombe and Coxhead 1995). The formation is underlain by the Heifer Creek Sandstone Member of the Koukandowie Formation and overlain unconformably by Cenozoic sediments (Jell 2013). The type section of the Walloon Coal Measures is located in the Rosewood-Walloon coalfield near Ipswich (Cameron 1970; Fielding 1993). The Walloon Coal Measures are not stratigraphically divided to the same extent as in the Surat Basin with only basal, middle and upper subdivisions proposed (Fielding 1993). Palynological investigations suggest a degree of diachroneity between the Walloon Coal Measures between the two basins (Burger 1994; Jell 2013).

2.2.5 Maryborough and Nambour basins

In comparison to the Eromanga, Surat, and Clarence-Moreton basins, little is known about the Maryborough and Nambour Basins. The two basins are now considered contiguous from studies of the Duckinwilla Group (Jell 2013). The Nambour Basin is regarded as an intracratonic basin but the Maryborough Basin evolved in a different and uncertain setting with back-arc, epicratonic, foreland and extensional environments all proposed (Hill 1994; Lipski et al. 2001).

The Nambour Basin, located to the north of the Clarence-Moreton Basin covers an area of 4100 km^2, comprises ~800 m of sedimentary infill and overlies the Ipswich Basin (Goscombe and Coxhead 1995). The basin is fault-bound in the west and south against rocks of the D'Aguillar and Beenleigh Blocks (Goscombe and Coxhead 1995). The Gympie province in the north and Bunker Ridge define the northern and eastern limits of the basin (Goscombe and Coxhead 1995; Jell 2013). The Nambour Basin is also connected to the Clarence-Moreton Basin by the Brisbane Straight to the southwest (Goscombe and Coxhead 1995). From the north to the south, open folds transition into tight, isoclinal and drape style folds (Hill 1994).

The tectonic history of these basins began in the Triassic resulting from oblique extension and a period of thermal relaxation through the Jurassic (Lipski et al. 2001). Subsidence was increased by sediment loading (Lipski et al. 2001). In the Cretaceous, basin inversion occurred related to island arc volcanism off the Queensland Coast in the Whitsunday Islands and the Bundaberg Volcanic Province when the Tasman Sea opened (Robertson 1993; Bryan et al. 1997; Lipski et al. 2001). The tectonic history after the Cretaceous is beyond the scope of the thesis and is outlined in Robertson (1993) Bryan et al. (1997) and Lipski et al. (2001).

Cyclical sedimentation was suggested by Hill (1994) from a series of fining-up cycles ending in coal deposition – this is regarded to have been driven by episodes of subduction and the emplacement of plutonic and volcanic rocks (Hill 1994). Sedimentary infill is predominantly comprised of fluvial sediments

(Goscombe and Coxhead 1995). No sequence stratigraphic frameworks are defined for this basin.

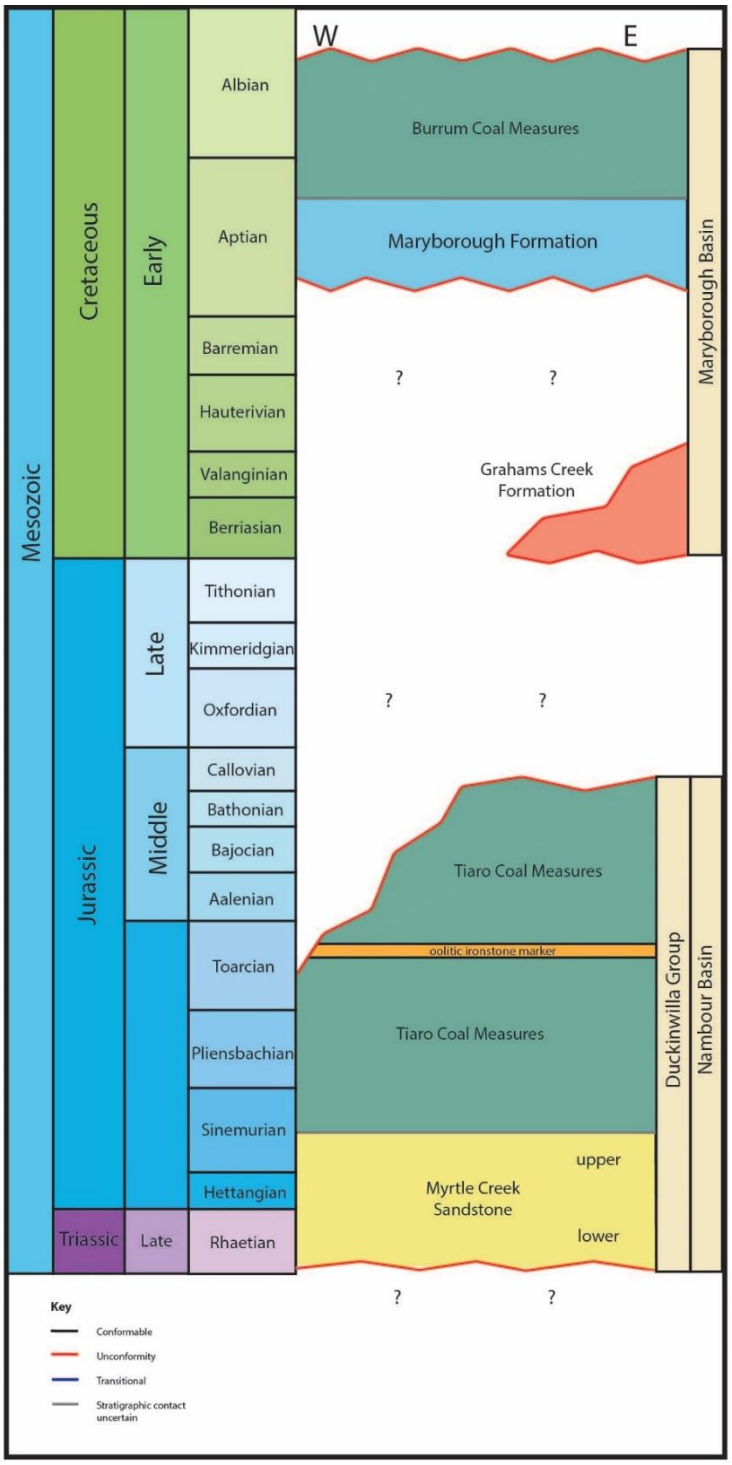

Figure 2.9. Lithostratigraphic units of the Nambour/Maryborough Basin. Adapted from McKellar (1993), Lipski et al. (2001) and Jell (2013).

The Tiaro Coal Measures, Sinemurian to Bathonian in age, conformably overlie the Myrtle Creek Sandstone and overlain by the Grahams Creek Formation (Jell 2013). The formation is up to 850 m thick and is composed of sandstones, siltstones, shales, ferruginous clay oolites and coals (Jell 2013). The Tiaro Coal Measures is extensively folded and intruded by dykes and sills (Hill 1994). The lithostratigraphic framework of the Maryborough/Nambour Basin is shown in Figure 2.9.

2.2.6 Other Jurassic coal bearing basins of eastern Australia

In addition to the basins discussed above, coals of Jurassic age are also found in the Dalrymple Sandstone of the Laura Basin in northwest Queensland, and in the Polda Formation of the Polda Basin in South Australia (Shen 1991; Jell 2013).

The intracratonic Laura Basin, off Queensland's Cape York, is the least studied Jurassic coal-bearing unit in Australia due to its proximity to the Great Barrier Reef which restricts exploration in the region. The basin covers ~18,000 km^2 comprising up to 2000 m of sedimentary infill (Jell 2013). The Laura Basin is contiguous with the Carpentaria Basin over the Kimba Arch in the southwest (Jell 2013). The limits of the basin are poorly defined (Jell 2013). The basin overlies Precambrian metamorphics; Palaeozoic granitoids of the Coen and Yambo Inliers; the Palaeozoic Hodgkison Province; and the Permo-Triassic Lakefield Basin (Jell 2013). Sedimentation and basin subsidence were controlled by the Palmerville Fault with sediments deposited as drapes over basement highs (Jell 2013). After sedimentation ceased in the Early Cretaceous, deposition reoccurred in the overlying Kalpowar Basin in the Cenozoic (Jell 2013). The 540 m thick marine-influenced fluviolacustrine Late Jurassic Dalrymple Sandstone forms the basal unit of the Laura Basin and is conformably overlain by the Early Cretaceous Gilbert River Formation (Jell 2013). The Dalrymple Sandstone forms the principal coal-bearing unit in the basin (Jell 2013).

The elongate, east-west oriented Polda Basin in South Australia covers over 8,300 km^2 with up to 5000 m of infill (Shen 1991). The transtensional basin originated from tectonic regimes which gave rise to the Amadeus and Officer basins (Shen 1991). The basin developed over several phrases during the Phanerozoic (Shen 1991). There is sharp structural contrast across the basin: the western Polda Basin features a simple graben structure which is fault-bounded and intersected by faults following the structural trend in the Eyre Sub-Basin (Shen 1991). The central part of the basin, by contrast, is normally and symmetrically faulted (Shen 1991). The coal-bearing Late Jurassic Polda Formation is 282 m thick, with coal beds between 0.5-6 m thick (Shen 1991). The Polda Formation unconformably overlies the Permo-Carboniferous

Coolardie Formation and is overlain unconformably by the Middle Eocene Polepna Formation (Shen 1991)

.

2.3 Age control and stratigraphic correlation

In the Great Australian Superbasin, the age of nonmarine strata is determined by spore-pollen palynostratigraphy whilst lithostratigraphy is the principle correlation technique (Gallagher et al. 2008; Jell 2013; Hamilton et al. 2014b). Correlations using lithostratigraphic principles work well when lithological changes are associated with major hiatuses or parallel with chronostratigraphic horizons, nevertheless, there can be major lateral variations in lithology or coal character over very short distances in nonmarine settings (Laurie et al. 2016). This often leads to questionable correlations within and between basins (Laurie et al. 2016). This is most evident for the heterogeneous Walloon Coal Measures in the Surat Basin. The use of higher resolution (and often poorly defined) lithostratigraphic frameworks are unable to assist in regionally propagating correlations across the basin in the absence of basin-wide marker beds (Shields and Esterle 2015).

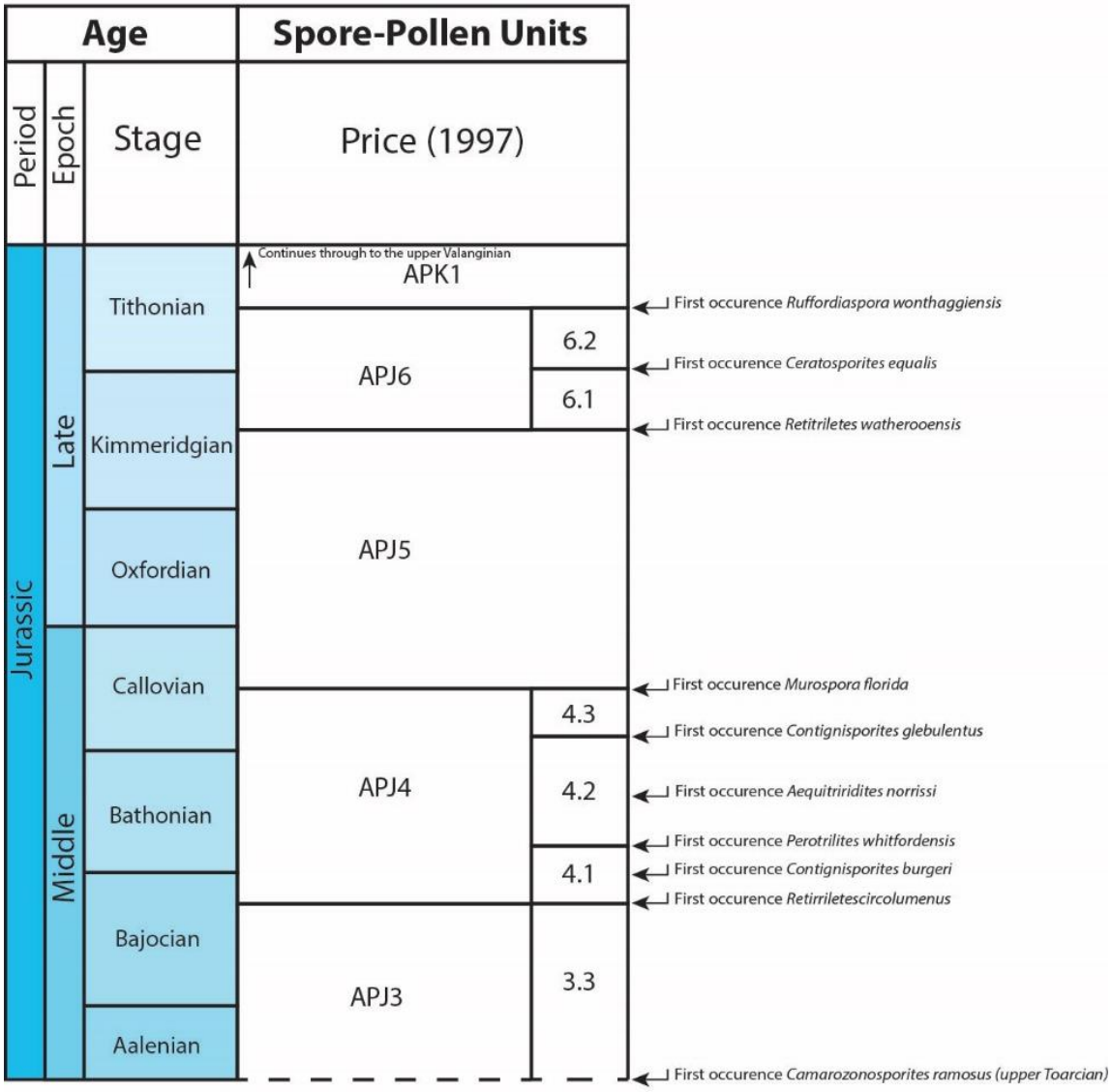

Figure 2.10. Jurassic spore-pollen palynostratigraphic units APJ3.3 to APJ6.2 encompassing key coal-bearing stratigraphic units of eastern Australia in accordance with Price (1997)

Biostratigraphy has traditionally been seen as the most successful technique for intra- and interbasinal correlation in the Mesozoic basins of eastern Australia (Gallagher et al. 2008). Palynostratigraphic frameworks stem from early works by Balme (1964) and Balme (1966) devised in western Australia with subsequent modifications in eastern Australian basins by Burger (1968), Burger (1982), Burger (1986), Burger et al. (1994), Burger and Senior (1979), McKellar (1982) and McKellar (1993). More recent taxonomic and palynostratigraphic schemes were devised by McKellar (1998) for the Jurassic of the Surat Basin

and by Sajadi and Playford (2002) for the Jurassic and Early Cretaceous of the Eromanga Basin. The most widely used biostratigraphic framework utilized by exploration companies is the alpha-numeric scheme of Price (1997) (Figure 2.10) although many petroleum companies have devised their own high resolution internal zonations (Gallagher et al. 2008). Jurassic coal-bearing strata in eastern Australia basins span palynostratigraphic zones APJ3.3 to APJ6 (Price 1997). Price (1997) suggests these zones span the Early Jurassic Toarcian through to the Late Jurassic Tithonian. These zones are defined by the first occurrence of a single, morphologically distinct spore or pollen species (e.g. *Murospora florida*) which is ubiquitous within the zone (Gallagher et al. 2008). The success of biostratigraphy varies between individual basins, palaeolatitude and depositional environments. Challenges with the biostratigraphy include: 1) fluctuations and longevity of mire (coal-forming) plants in response to base level changes; 2) highly localised sourcing of palynofloras; 3) rarity (and absence) of key taxa and the reliable determination of their first occurrence; 4) unfavourable habitats for the parent plants of key biostratigraphic taxa; 5) the longevity of palynostratigraphic zones and their associated taxa; and 6) the high variation in palynomorphs between adjacent samples (Martin et al. 2013).

Precise age calibration to the geologic time-scale is one of the biggest challenges faced by biostratigraphic schemes utilized in Australia. Tentative geologic ages are assigned by studying coeval strata with similar floral assemblages and marine fauna (including ammonites) in Asia or Western Australia which then can be tied back to age-constrained biostratigraphic schemes in Europe or America (Riding and Mantle 2010). This is hampered by climatic-oceanic provincialism and differing floral assemblages across Australia (Helby et al. 1987; Turner et al. 2009). Only three published studies have attempted to calibrate Mesozoic biostratigraphic frameworks of the southern hemisphere to the geologic time-scale International Stratigraphic nonsense. These studies are of the Jurassic Botany Bay Group (Antarctica), the Jurassic Casterton Formation (Australia) and the Cretaceous Cerro Negro Formation (Antarctica) and use low resolution fission track, $^{40}Ar/^{39}Ar$ and ^{238}U-^{206}Pb dating techniques (Mitchell et al. 1997; Hathway et al. 1999; Hunter et al. 2005).

Without adequate age constraints on palynostratigraphic zones, reliable correlations (and subsequently the timing of key tectonic events and rates of sedimentation) cannot be deduced with any precision (Nicoll et al. 2015).

Other techniques including sequence stratigraphy using seismic and core data (Hoffmann et al. 2009), nonmarine sequence stratigraphy using gamma peaks from well logs (Shields and Esterle 2015) and chemostratigraphy using ICP-MS data (Martin et al. 2013) have yielded mixed results or are only useful for correlation purposes at a local-scale.

2.4 Jurassic coals

Coals are recorded from the Jurassic on all continents except Antarctica (Figure 2.10) (Boucot et al. 2013). The Jurassic and the Cretaceous are considered to be one of the main episodes of coal accumulation in the Phanerozoic (Thomas 2012). In spite of this, the Middle Jurassic is considered one of the most unfavourable times for the formation of organic-rich source rocks, in contrast to the Late Jurassic which was one of the best (Klemme and Ulmishek 1991; McCabe 2012). A combination of climatic and tectonic conditions allowed coal accumulation to become widespread in the high latitudes during the Jurassic. Related global tectonic events include the breakup of Pangea (and associated volcanism) and major orogenic events in Asia. Climatically there was an absence of arid belts in the northern hemisphere, a low equator to pole climate gradient, and an increased cloud cover over the high latitudes with the migration of humid climatic belts towards the poles (Sellwood and Valdes 1997; Thomas 2012; Boucot et al. 2013). The presence of a large land mass over the equatorial regions and subsequent heating of the continental interior may have deflected the intertropical convergence zone (ICTZ) away from the palaeoequator lead to the establishment of a mega-monsoonal atmospheric circulation system (Hallam 1982; Scotese et al. 1999). This would have restricted coal accumulation to the high latitudes or the edge of continental landmasses where climates were less seasonal (Hallam 1982; Scotese et al. 1999). Global warming and increasing rates of precipitation during the Jurassic triggered coal-forming mires to evolve from narrow riparian, lake-fringing swamps and marshes, to extensive conifer-dominated swamps with an increasing variability of floral associations in the understory (Parrish and Barron 1986; Greb et al. 2006). Northern hemisphere mires were dominated by taxodiaceous conifers, while in the southern hemisphere, mires were dominated by podocarpaceous and araucarian conifers (Greb et al. 2006). This is reflected in a high liptinite content of coals in the southern hemisphere (Retallack et al. 1996). Whether the climate remained warm and equitable for the entire Jurassic remains debatable (Dera et al. 2011).

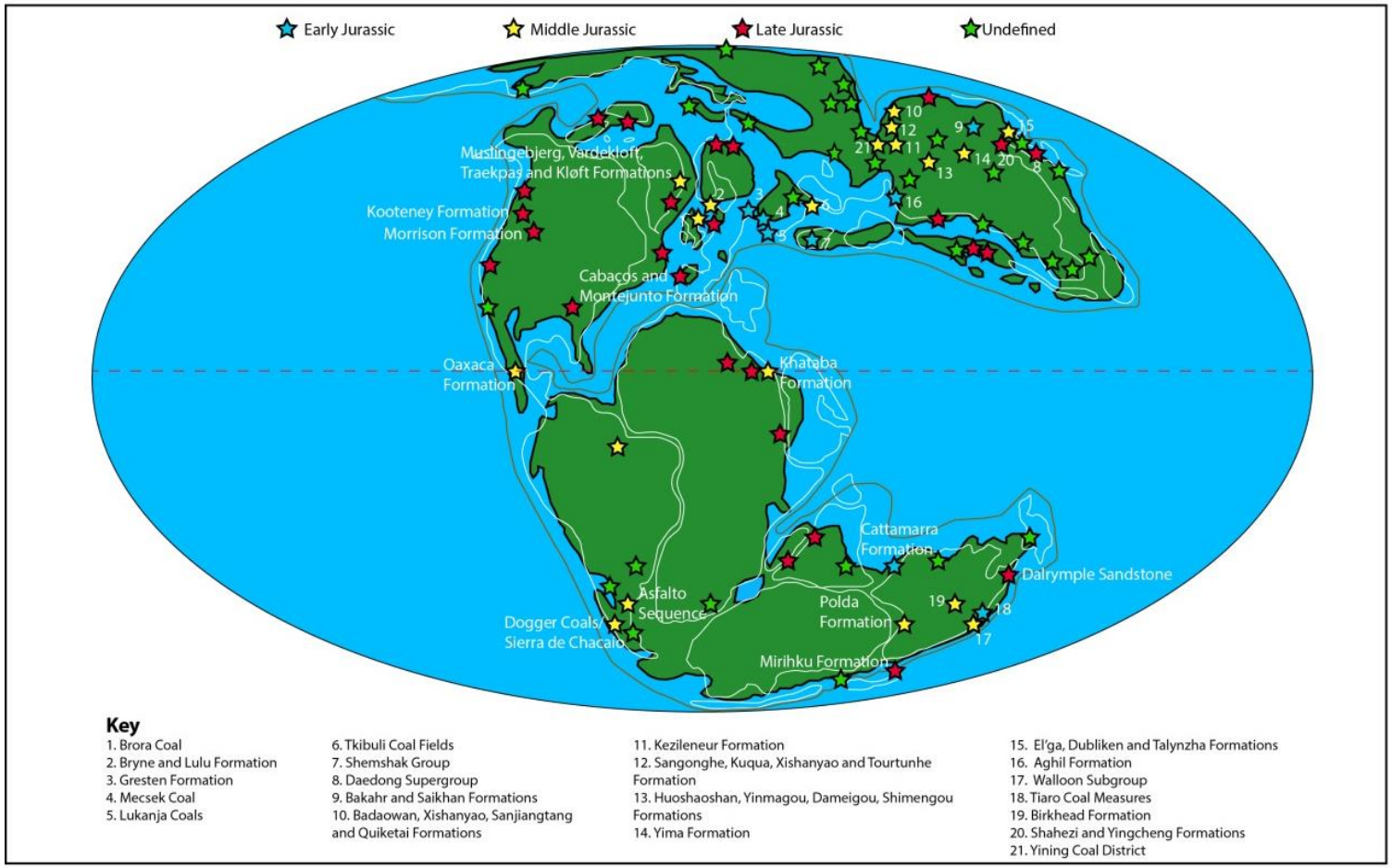

Figure 2.11. Global distribution of Jurassic coal-bearing strata (adapted from Scotese (2001) and Boucot et al. (2013)). Some sites are omitted for clarity.

In Europe and the America's, coal accumulations were restricted to rift settings related to the opening of the Atlantic or the Seiver fold and thrust belt (Flores 2002) . In Asia, coal accumulated in foreland and intermontane settings related to the accretion of cratons to the Eurasian plate and the beginnings of the Alpine-Himalayan Orogeny (Hendrix et al. 1995). In Africa, coal accumulation was constrained to tropical wet belts in alluvial and fluvial systems (Keeley 1994). Palaeoclimate and palaeolatitude were the main controls in South America resulting in their limited lateral extent across the continent (Thomas 2012). Coal deposits may have developed in these regions because subsidence rates would have matched peat accumulation rates due to the prevailing climate regime, notably in Asia where there were many foreland and intermontane basins (McCabe 1991). Jurassic coal deposits are also recorded in north-western China, Canada, India, Kyrgyzstan, Turkmenistan, Spitzbergen, Pakistan, Burma, Thailand, Laos, the Korean Peninsula, Japan, Paraguay, and Chile; these basins are relatively unexplored with little information available from the literature (Hallam 1982; Weaver et al. 1994; Thomas 2012). The highest concentrations of Jurassic coals are found in Asiatic Russia or China; information on these basins (Kansk-Achinsk, South-Yakutia, and the Ulugkhem basins) is limited and mainly restricted to journals published in Russian or Chinese.

An outline of Jurassic coal-bearing strata and their characteristics are outlined in Tables 2.3 to 2.7.

Table 2.3. Jurassic coal-bearing strata in Europe.

Name of coal-bearing strata and age	Basin	Tectonic setting	Bed thickness	Lateral continuity	Interpreted controls on coal accumulation	Environment of deposition	Reference
Bryne and Lulu formations (Bathonian-Callovian, Middle Jurassic)	Søgne Basin	Intracratonic rift	0.14-2 m	Extensive over basin	Sea-level change	Paralic	Petersen and Andsbjerg (1996)
Brora Coal Formation (Bathonian, Middle Jurassic)	Moray Basin	Rift Basin	Unknown	Unknown	Sea-level change	Paralic to coastal lagoon/estuarine	Hudson (1964)
Muslingebjerg Formation (Middle Jurassic)	Wollaston Forland rift basin	Rift Basin	0.15 to 3.45 m	Not determined due to faulting	Sea-level change	Fluvial to marginal marine	Petersen et al. (1998)

Name of coal-bearing strata and age	Basin	Tectonic setting	Bed thickness	Lateral continuity	Interpreted controls on coal accumulation	Environment of deposition	Reference
Cabaços and Montejunto Formation (Oxfordian-Kimmeridgian, Late Jurassic)	Lusitanian Basin	Marginal rift basin	Interbedded, no thickness recorded	Unknown	Subsidence and sea-level change	Lacustrine-to shallow marine	Costa et al. (2010)
Rønne Formation (Pliensbachian , Early Jurassic)	Rønne Graben	Complex fault-bounded horst, rift	Up to 2.5 m thick,	Varied, structurally controlled (extensive to localised)	Subsidence and sea-level change	Deltaic	Nielsen et al. (2010)

Name of coal-bearing strata and age	Basin	Tectonic setting	Bed thickness	Lateral continuity	Interpreted controls on coal accumulation	Environment of deposition	Reference
Gresten Formation (Hettanginian, Early Jurassic)	Vienna Basin	Rift Basin	mm's to cm's	Widespread	Subsidence	Fluvial and deltaic	Sachsenhofer et al. (2006)
Mecsek Coal Formation (Hettangian, Early Jurassic)	Bohemian Massif and Vindelician High	Rift Basin	0.5 m – 5 m	Varied, structurally controlled (extensive to localised)	Relative sea-level change (Milankovitch)	Fluvial to paralic	Götz et al. (2011)
Lukanja Coal Beds and Tuden Formation (Early Jurassic)	Unknown	Unknown	Unknown	Unknown	Unknown	Continental?	Tchoumatchenco et al. (2006)

Name of coal-bearing strata and age	Basin	Tectonic setting	Bed thickness	Lateral continuity	Interpreted controls on coal accumulation	Environment of deposition	Reference
Vardekløft Formation, Traekpas Formation, Kløft Formation (Bathonian-Kimmeridgian, Middle to Late Jurassic)	Hochstetter Forland	Foreland	2-3 m	Unknown	Subsidence and sea-level change	Paralic	Clemmensen and Surlyk (1976)

Table 2.4. Jurassic coal-bearing strata in the Americas.

Name of coal-bearing strata and age	Basin	Tectonic setting	Bed thickness	Lateral continuity	Interpreted controls on coal accumulation	Environment of deposition	Reference
Kootenay Formation (Tithonian, Late Jurassic)	Fernie Basin	Foreland in front of Sevier thrust belt	2 -18.3 m	Unknown	Depositional environment	Paralic, deltaic and fluvial	Gibson (1985)
Sierra de Chacaico (Early to Middle Jurassic)	Neuquén	Extensional	Thin seams, <1 m	Unknown	Climate	Paralic	Volkheimer et al. (2008)
Asfalto Sequence (Middle Jurassic)	Cañadón Asfalto basin	Extensional	Thin seams, <1 m	Unknown	Climate	Lacustrine	Volkheimer et al. (2008)

Name of coal-bearing strata and age	Basin	Tectonic setting	Bed thickness	Lateral continuity	Interpreted controls on coal accumulation	Environment of deposition	Reference
Dogger Coals (Callovian Middle Jurassic)	Neuquén	Extensional	51-76 cm	Limited	Climate	Paralic	Flores-Williams (1978)
Oaxaca Formation (Early to Middle Jurassic)	Simon-Rosario and Zorrillo	N/A	cm's to 3 m	Limited	Structural	Continental?	Ojeda-Rivera (1978)
Morrison Formation (Kimmeridgian, Late Jurassic)	Bighorn, Powder River, Wind River and East Green River basins	Marginal cratonic/ foreland basin	Unknown	Unknown	Unknown	Fluvial	

Table 2.5. Jurassic coal-bearing strata in Africa.

Name of coal-bearing strata and age	Basin	Tectonic setting	Bed thickness	Lateral continuity	Interpreted controls on coal accumulation	Environment of deposition	Reference
Khataba Formation (Middle Jurassic)	Gebel Rissu Basin	Rift basin with strike-slip tectonism	1.3-1.9 m	Unknown	Sea-level change	Fluvial	Keeley (1994)

Table 2.6. Jurassic coal-bearing strata in Oceania.

Name of coal-bearing strata and age	Basin	Tectonic setting	Bed thickness	Lateral continuity	Interpreted controls on coal accumulation	Environment of deposition	Reference
Murihiku Supergroup (Late Jurassic)	Reinga Basin	Rift (back-arc extension)	Unknown	Widespread?	Unknown	Fluvial	Campbell et al. (2003)
Cattamarra Coal Measures (Early Jurassic)	Perth Basin	Rift	5-11 m	Laterally discontinuous	Sea-level change	Fluvio-deltaic	

Table 2.7. Jurassic coal-bearing strata in Asia.

Name of coal-bearing sequence and strata	Basin	Tectonic setting	Bed thickness	Lateral continuity	Interpreted controls on coal accumulation	Environment of deposition	Reference
Badaowan, Xishanyao, Sanjiangtang and Quiketai formations (Early to Middle Jurassic)	Junggar	Foreland. Tectonic accretion on the southern Asian continental margin	Up to 70.3 m, average 9.3 m	Laterally continuous in lacustrine facies in the southern basin, sheet-like	Subsidence	Fluvial and lacustrine deltaic	Hendrix et al. (1995)
Kezilenuer Formation (Early to Middle Jurassic)	Tarim	Foreland. Tectonic accretion on the southern Asian continental margin	>20 m	Laterally continuous in the northern basin, sheet-like	Subsidence	Fluvial and lacustrine deltaic	Hendrix et al. (1995)

Name of coal-bearing strata and age	Basin	Tectonic setting	Bed thickness	Lateral continuity	Interpreted controls on coal accumulation	Environment of deposition	Reference
Sangonghe, Kuqua, Xishanyao and Toutunhe formations (Early to Middle Jurassic)	Turpan	Foreland. Tectonic accretion on the southern Asian continental margin	Unknown	Unknown	Subsidence	Fluvial and lacustrine deltaic	Hendrix et al. (1995)
Huoshaoshan, Yinmagou, Dameigou, Shimengou formations (Toarcian-Callovian, Middle Jurassic)	Qaidam	Intermontane basin small scale foreland style basin, Tectonic accretion on the southern Asian margin	Unknown	Unknown	Subsidence	Base of fold-thrust belt of Qilian Mountains Fluvial-lacustrine	Wang et al. (2005)

Name of coal-bearing strata and age	Basin	Tectonic setting	Bed thickness	Lateral continuity	Interpreted controls on coal accumulation	Environment of deposition	Reference
Yima Formation, (Middle Jurassic)	Yima	Intermontane Basin	0-26.8m	Unknown	Subsidence climate, syndepositional tectonics	Alluvial/pluvial setting	Miao et al. (1989)
El'ga, Dubliken and Talynzha formations (Tithonian, Middle Jurassic)	Bureya	Foreland, Collisional , oblique subduction offshore	2-30 cm	Unknown	Subsidence and climate	Unknown	Kirillova (2005)
Aghil Formation, (Early Jurassic)	N/A	Collisional and later sutured	0.1-2 m	Up to 6 km lateral extent along strike, generally discontinuous, structurally controlled	Unknown	Carbonate hosted	Donnelly (2004)

Name of coal-bearing strata and age	Basin	Tectonic setting	Bed thickness	Lateral continuity	Interpreted controls on coal accumulation	Environment of deposition	Reference
Tkibuli Coal Field (Bajocian-Bathonian, Middle Jurassic)	Part of the super basin comprising the Kerman-Tabas and Elburz basins across the Alpine-Himalayan Fold Belt Tabas	Submontane to intermontane	1-4 m	Unknown	Unknown	Unknown	Polyansky (1983)
Shemshak Group (Early Jurassic)	Block Basin	Foreland, within the Alpine-Himalayan Fold Belt	>0.4 m	Inter-Regional and structurally controlled	Subsidence	Fluvial-Lacustrine	Stasiuk et al. (2006); (Wilmsen et al. 2009)

Name of coal-bearing strata and age	Basin	Tectonic setting	Bed thickness	Lateral continuity	Interpreted controls on coal accumulation	Environment of deposition	Reference
Daedong Supergroup (Late Jurassic)	Bansong half-graben	Intermontane	Unknown	Unknown	Subsidence	Continental?	Cluzel (1992)
Bakhar Formation, Saikhan Formation (Early to Middle Jurassic)	Mongolia Coal basins (Southern Khangi, Ikh Bodg and Ongi to the Eastern Mongolian Province)	Flexural Basin?	5-49.7 m	Structurally controlled	Subsidence	Lacustrine, fluvial and deltaic	Erdenetsogt et al. (2009)
Shahezi and Yingcheng formations (Late Jurassic)	Songliao	Intracratonic rift	Unknown	Unknown	Subsidence	Alluvial fan, braided fluvial	(Zhao et al. 2008)

2.5 Analogues

Modern and ancient analogues can be used to predict aerial geometries, depositional trends and three-dimensional stacking patterns in the subsurface. Perfect depositional analogues are extremely unlikely due to the differing tectonic and climatic conditions in the geologic past, but when the scale and nature of processes are compared, they can be useful in interpreting palaeoenvironments especially if there is limited well control.

Comparison of the Walloon Coal Measures to modern and ancient analogues have been made based on the following characteristics: 1) peat mires growing in a highly seasonal sub-polar to temperate climate; 2) meandering river channels up 400 m wide on a wide and waterlogged alluvial plain; 3) an endorheic drainage basin; 4) broad floodplains and discontinuous swamp environments frequently affected by overbank sand deposition and reworking by channel migration; and 5) located within an intracratonic basin affected by persistent volcanic air-fall deposits; and situated at high latitude (Yago 1996b; Day et al. 2006; Ryan et al. 2012; Shields and Esterle 2015). The need for an exact analogue for the Walloon Coal Measures has been deemed unnecessary by Martin et al. (2013) due to the rich dataset available (thousands of closely spaced wells) for reservoir modelling, whereas Fielding (1993) has used outcrops in opencast mines to understand spatial relationships and the architecture of depositional elements (Fielding 1993; Martin et al. 2013).

Previous analogues of the Walloon Coal Measures include the Maastrichtian–Danian Fort Union Formation of the Powder River Basin, river systems on the western flank of Hudson Bay in Canada, the River Ob in Siberia and Cumberland Lake in Saskatchewan. Comparisons to the Fort Union Formation were made due to the fluviolacustrine system draining uplands into a lacustrine dominated depocentre to the northwest, while outcrops allow for the connectivity of coal beds to be conceptualised (Yago 1996b; Day et al. 2006; Martin et al. 2013). Coal beds of the Walloon Coal Measures are much thinner and less laterally continuous compared to those in the Powder River Basin which are up to 30 m thick and extend laterally for up to 20 km (Ryan et al. 2012). Modern analogues including the River Ob, river systems on the flanks of Hudson Bay and Cumberland Lake are used based on their large area, high

latitude and the expanse of waterlogged alluvial plains (Ryan et al. 2012). Cumberland Lake, Saskatchewan has been suggested as a perfect analogue for the geometry and size of depositional elements including lacustrine bodies, mires, and channels (Ryan et al. 2012; Shields and Esterle 2015). Many issues which needs to be addressed when comparing the Walloon Coal Measures to other modern and ancient analogues include: 1) the lack of extant or modern plants able to endure winter darkness at high latitude in a greenhouse world (Francis 1990); 2) finding an analogue where peats have low ash content and are thick enough to form significant coal beds if preserved in the stratigraphic record, and 3) a fluviolacustrine system with abundant peat mires close to an active volcanic system. Modern analogues not addressed in the existing literature which may be analogues to the Walloon Coal Measures include 1) the Magdalena River in Colombia (wetland environments covering up to 80 to 90% of the basin floor) (Smith 1986); 2) Kamchatka Peninsula in the Russian Far East (high latitude with large seasonal fluctuations in temperature and rainfall) (Dirksen et al. 2013), and 3) the mires of Hokkaido in Japan (frequent burial by air-fall volcanic ash) (Hotes et al. 2006).

Comparisons of the Birkhead Formation to modern and ancient analogues have been based on the following characteristics: a fluvial system with large aerial extent; endorheic drainage into the centre of the continent; cyclical wet and dry periods modifying where sediments are deposited; geographically short lateral distances between areas of floodplain and lacustrine deposition; seasonal water flow; a system exhibiting both high and low sinuous meandering river channel systems; and rivers sourced by sediment from different provinces. Suggested analogues of the Birkhead Formation include the Volga Delta where it drains into the Caspian Sea and the Okavango Delta. Comparisons are made to the Volga Delta where braided streams flow into the Caspian Sea (Boult 1996). Similarities with the Okavango Delta include: two fluvial styles controlled by a faulted graben; channels of similar dimensions (~100 m); numerous crevasses splays which form in response to seasonal flooding; and sediments of similar grain size (Smith et al. 1997; McCarthy and Tooth 2004; Tooth and McCarthy 2004). Any future research attempting to find a suitable analogue for

the Birkhead Formation needs to consider peat accumulation, the presence of calcretes and findings from zircon provenance studies.

There are many descriptions of ancient coal-bearing strata. Table 2.8 lists major coal-bearing units that may be analogous in some form to those of the Middle to Late Jurassic of eastern Australia.

Table 2.8. Ancient coal-bearing strata analogous to Middle to Late Jurassic strata of eastern Australian basins.

Coal-bearing strata and locality	Age	Basin	Tectonic setting of basin	Environment of depositional	Bed thickness	Reference
Dunkard Group (Eastern USA)	Late Pennsylvanian /Early Permian	Appalachian	Foreland, related to the Alleghanian orogeny. In an equatorial setting	Fluvial-deltaic	0.17-0.97 m, thin and discontinuous	Cecil (2013), Cecil et al. (2011)
Fruitland Formation (Western USA)	Late Cretaceous	San Juan	Asymmetrical Laramide structural Basin	Coastal plain,	0.1-20 m	Ambrose and Ayers Jr (2007)
Loa Kulu Formation (Indonesia)	Miocene	Kutei Basin	Back-arc to cratonic, within the SE, directed subduction zone of NW Borneo	Delatic	Numerous thin coal seams <1 m, can be up to 3.25 m	Allen and Chambers (1998), Land and Jones (1987)

Coal-bearing strata and locality	Age	Basin	Tectonic setting of basin	Environment of depositional	Bed thickness	Reference
Neslen Formation (Western USA)	Late Cretaceous	Uinta	Foreland	Fluvial/tidal flats/marshes	0.3-1 m, thin and discontinuous	Pitman et al. (1987), Willis (2000)
Blackhawk Formation, Mesaverde Group (Western USA)	Late Cretaceous (Campanian-Maastrichtian)	Paradox	Foreland	Coastal plain to alluvial plain	Rare – thin and lenticular	Yoshida (2000)
Dakota Sandstone (Western USA)	Late Cretaceous (Cenomanian)	Present in all basins on the Colorado Plateau	Foreland	Fluvial to nearshore marine	Mainly 0.6 m and up to 2.7 m, in SW and SE, lenticular and variable in thickness over short distances	Kirschbaum et al. (2000)

Coal-bearing strata and locality	Age	Basin	Tectonic setting of basin	Environment of depositional	Bed thickness	Reference
Toreva Formation (Western USA)	Late Cretaceous (Turonian)	Black Mesa, Kaiparowits Plateau, Wasatch basins	Foreland	Fluvial, nearshore marine, coastal plain	Discontinuous	Kirschbaum et al. (2000)
Smoky Hollow Member (Western USA)	Late Cretaceous (Turonian)	Black Mesa, Kaiparowits Plateau, Wasatch basins	Foreland	Fluvial/coastal plain	Thin and lenticular	Kirschbaum et al. (2000)
Ferron Sandstone (Western USA)	Late Cretaceous (Turonian)	Wasatch and Henry Mountains Basins	Foreland	Coastal plain	Up to 2.6 m, laterally extensive	Kirschbaum et al. (2000)
Crevasse Canyon Sandstone (Western USA)	Late Cretaceous (Turonian)	Black Mesa, Kaiparowits Plateau, Wasatch basins	Foreland	Coastal plain, alluvial plain	Thin seams, can be up to 1.1 m	Kirschbaum et al. (2000)

Coal-bearing strata and locality	Age	Basin	Tectonic setting of basin	Environment of depositional	Bed thickness	Reference
Wepo Formation (Western USA)	Late Cretaceous (Coniacian-Santonian)	Black Mesa, Kaiparowits Plateau, Wasatch basins	Foreland	Coastal Plain	1.2 m to 2.4 m, up to 6 m more numerous, widespread, thin seams discontinuous	Kirschbaum et al. (2000)
John Henry Member (Western USA)	Late Cretaceous (Coniacian-Santonian)	Black Mesa, Kaiparowits Plateau, Wasatch basins	Foreland	Coastal plain	Up to 18 m	Kirschbaum et al. (2000)

Coal-bearing strata and locality	Age	Basin	Tectonic setting of basin	Environment of depositional	Bed thickness	Reference
Blackhawk Formation (Western USA)	Late Cretaceous (Campanian)	Wasatch Basin	Foreland	Coastal plain,	0.6 m to 3 m, laterally extensive	(Kirschbaum et al. 2000)
Masuk Formation (Western USA)	Late Cretaceous (Campanian)	Henry Mountains Basin	Foreland	Marine?	Up to 4.1 m	Kirschbaum et al. (2000)
Mount Garfield Formation (Western USA)	Late Cretaceous (Campanian)	South Piceance Basin	Foreland/structural	Nearshore marine, coastal plain	Up to 7 m	Kirschbaum et al. (2000)
Williams Fork Formation (Western USA)	Late Cretaceous (Campanian-Maastrichtian)	Danforth Hills and Yampa basins	Foreland	Alluvial plain, marine-coastal plain	Up to 7.6 m	Kirschbaum et al. (2000)

Coal-bearing strata and locality	Age	Basin	Tectonic setting of basin	Environment of depositional	Bed thickness	Reference
Iles Formation (Western USA)	Late Cretaceous (Campanian)	Danforth Hills and Yampa basins	Foreland	Nearshore marine, coastal plain	Up to 4.2 m	Kirschbaum et al. (2000)
Menefee Formation (Western USA)	Late Cretaceous (Campanian)	San Juan Basin	Foreland/structural basin	Coastal plain	Up to 5.9 m	Kirschbaum et al. (2000)
Raccoon Group, McLeansboro Group and Carbondale Formation (Central USA)	Pennsylvanian	Illinois Basin	Cratonic (failed rift)	Deltaic	15 to 45 cm, thin, lenticular coals.	Hatch and Affolter (2002), Edwards et al. (2005)
Nanushuk Group and Colville Group (Alaska, USA)	Albian to Maastrichtian (Early to Late Cretaceous)	Colville Basin	Foreland	Fluvial dominated fluvial system	8 cm to 5 m	Spicer et al. (1992)

Coal-bearing strata and locality	Age	Basin	Tectonic setting of basin	Environment of depositional	Bed thickness	Reference
Mungaroo Formation (NW Australia)	Triassic (Ladinian)	North Carnarvon Basin	Cratonic, rift to passive margin	Fluvio-Deltaic	Thin coals	Chongzhi et al. (2013), Stuart (2015)
Žacléř Formation (Czech Republic)	Carboniferous	Intra-Sudetic Basin	Continental?	Fluvial	Variable, up to 4 m	Opluštil et al. (2013)
Fossil Bluff Group (Antarctica)	Cretaceous	Larsen Basin	Passive margin/bac	Fluviolacustrine? Deltaic?	2-43 cm	Macdonald and Francis (1992)
Buchanan Lake Formation (Axel Heiberg Island)	Eocene	Sverdrup Basin	Pericratonic	Fluviolacustrine	40-60 cm and up to 1 m	Greenwood and Basinger (1994), Kojima et al. (1998)
Bagå Formation (Denmark	Middle Jurassic	Rønne Graben	Rift	Fluviolacustrine	10-40 cm	Nielsen et al. (2010)

The coals of the Walloon Coal Measures are generally thin (<0.4 m) and laterally discontinuous (rarely correlatable in the subsurface more than 5 km). Controls on the formation of thin, discontinuous coal beds are is quite variable between basins. Climate change, whether driven by tectonic uplift or Milankovitch cyclicity, is thought to have inhibited the duration of peat accumulation. This notion is developed for the Colville Group of the Colville Basin where climatic cooling is thought to have reduced peat accumulation, leading to thinner coal beds despite constant subsidence rates (Spicer et al. 1992). High frequency sea-level change, by contrast, is thought to be the primary control for coal accumulation the Blackhawk Formation (Kirschbaum et al. 2000), the Fruitland Formation (Kirschbaum et al. 2000), and the Loa Kulu Group (Land and Jones 1987). For the majority of coal-bearing formations in the Cretaceous North American foreland basins, tectonic subsidence is considered have been the main control on coal accumulation (Kirschbaum et al. 2000). This is related to the development of thrust sheets and consequent times of sediment starvation with reorganisation of rivers systems (Kirschbaum et al. 2000). Many authors consider the interplay of two or more controls on coal accumulation including McCabe and Parrish (1992). Opluštil et al. (2013) suggest that tectonics created the accommodation space while climate influenced vegetation cover and clastic input to explain the nature of coals in the Žacléř Formation in the Intra-Sudetic Basin.

Statement of Authorship

Title of Paper	U-Pb zircon age of the Walloon Coal Measures in the Surat Basin, southeast Queensland: implications for paleogeography and basin subsidence
Publication Status	X Published ☐ Accepted for Publication ☐ Submitted for Publication ☐ Unpublished and unsubmitted work written in manuscript style
Publication Details	Wainman, C.C., McCabe, P.J., Crowley, J.L. and Nicoll, R.S., 2015. U–Pb zircon age of the Walloon Coal Measures in the Surat Basin, southeast Queensland: implications for paleogeography and basin subsidence. Australian Journal of Earth Sciences, 62(7), pp.807-816. DOI: http://dx.doi.org/10.1080/08120099.2015.1106975

Principal Author

Name of Principal Author (Candidate)	Carmine C. Wainman		
Contribution to the Paper	Majority of the data collection and interpretation. Wrote the greater majority of the paper with exceptions noted in the co-authorship contributions. Produced final version of the paper using editorial suggestions of the co-authors.		
Overall percentage (%)	80		
Certification:	This paper reports on original research I conducted during the period of my Higher Degree by Research candidature and is not subject to any obligations or contractual agreements with a third party that would constrain its inclusion in this thesis. I am the primary author of this paper.		
Signature		Date	10/08/2017

Co-Author Contributions

By signing the Statement of Authorship, each author certifies that:

i. the candidate's stated contribution to the publication is accurate (as detailed above);
ii. permission is granted for the candidate in include the publication in the thesis; and
iii. the sum of all co-author contributions is equal to 100% less the candidate's stated contribution.

Name of Co-Author	Peter J. McCabe		
Contribution to the Paper	Supervisor of Ph.D. – Extensive critical advice and guidance on research project and editorial comments for the paper. Made contributions to the section titled "Zircon dates and implications".		
Signature		Date	10/8/2017

Name of Co-Author	James L. Crowley		
Contribution to the Paper	Carried out CA-TIMS and LA-ICPMS. Provided guidance on research project and editorial comments for the paper. Wrote the first two paragraphs in the section titled "zircon dates and implications and drafted figures 3.4 and 3.5. Wrote the appendices (appendices 1).		
Signature		Date	August 10, 2017

Name of Co-Author	Robert S. Nicoll
Contribution to the Paper	Advice and guidance on research project and editorial comments for the paper.
Signature	Date 31/8/2017

Chapter 3. U-Pb zircon age of the Walloon Coal Measures in the Surat Basin, southeast Queensland: implications for paleogeography and basin subsidence

This chapter is an exact copy of the article published in the *Australian Journal of Earth Science.* A statement of authorship is provided on the previous page.

Citation: Wainman, C.C., McCabe, P.J., Crowley, J.L. and Nicoll, R.S., 2015. U–Pb zircon age of the Walloon Coal Measures in the Surat Basin, southeast Queensland: implications for paleogeography and basin subsidence. *Australian Journal of Earth Sciences*, 62(7), p.807-816.

Abstract

The Jurassic Walloon Coal Measures of the Surat Basin were previously estimated to be of Middle Jurassic age, ranging from Aalenian to Callovian, based on an uncalibrated eastern Australian biostratigraphic framework. New U–Pb dates of 162.55 ± 0.05 Ma and 158.86 ± 0.04 Ma obtained from zircons in ash-fall volcanic tuffs now place the Walloon Coal Measures of the Surat Basin in the Upper Jurassic Oxfordian. The new dates have several implications for the interpretation of the Jurassic strata in the Surat Basin. First order subsidence rates of 61 m/Myr for the Walloon Coal Measures are more akin to those of foreland basins than the previously assumed intracratonic setting. The dates also imply deposition of the Walloon coals in substantially higher latitudes than previously assumed and that they accumulated as peats in mires that experienced more than three months continual darkness each winter. Zircon dating of tuffs and associated geochemistry should assist with the correlation of the laterally impersistent coals, fluvial sandstone and mudstone of the Walloon Coal Measures, which are currently difficult to correlate over distances of more than a few kilometres. Dating of the palynostratigraphic zones APJ4.2 to APJ5 (*Aequitriradites norrisii* Zone to *Murospora florida* Association Zone) will also need to be recalibrated.

3.1 Introduction

The Walloon Coal Measures (also formally known as the Walloon Subgroup) of the Surat Basin in southeast Queensland and northeast New South Wales contain the majority of Australia's coal seam gas (CSG) resources, accounting for 64% of the continent's proven and probable (2P) estimates (Hamilton et al. 2014a). Several studies have provided insight into the geological evolution and characteristics of the Surat Basin in light of recent CSG exploration including studies of the stratigraphy and sedimentology (Ryan et al. 2012; Martin et al. 2013; Hamilton et al. 2014b), coal petrology (Scott et al. 2007; Hentschel et al. 2016), palynology (McKellar 1998), and regional stress regimes (Baker and Skerman 2006). Despite these studies, there remains considerable uncertainty on the basic stratigraphic framework for the Walloon Coal Measures due to the geological heterogeneity of the strata and the thin, discontinuous nature of the coal seams and sandstones. This is evident from several attempts to define and redefine the lithostratigraphic units of the Walloon Coal Measures (Cameron 1970; Scott et al. 2004; Scott 2008; Hamilton et al. 2014b). Consequently, there are numerous inconsistencies in the understanding of the formation and the basin in the literature (Martin et al. 2013; Hamilton et al. 2014b).

The primary method of age determination for the Walloon Coal Measures has been using biostratigraphy within an Australian framework constructed on spore-pollen zones that have not been previously calibrated against the international geological timescale by isotopic dating of associated tuffs (Price 1997; McKellar 1998; Jell 2013). The age ascribed to the Walloon Coal Measures, both in the Surat and neighbouring Clarence-Moreton Basin to the east, varies from Aalenian to Callovian (Gleadow 1990; Burger 1994; Jell 2013), with the consensus being late Bathonian to Callovian from palynological studies (Exon and Burger 1981; Wells 1994; Price 1997; McKellar 1998; Jell 2013). This is a wide range in absolute time from 163.5 Ma to 174.1 Ma (Cohen et al. 2013; updated). The use of biostratigraphy has been limited because of the wide age range of spore-pollen taxa, with zonal index species being rare or even absent (Martin et al. 2013). This paper presents new age dates acquired by U–Pb chemical abrasion isotope dilution thermal ionisation mass spectrometry (CA-TIMS) of zircons obtained from tuff layers within coals of the

Walloon Coal Measures. These ash fall tuffs have been chosen for dating as once deposited on a mire, such tuffs remain *in situ* through to diagenesis (Triplehorn and Bohor 1986). The dating of the numerous, widely distributed tuff beds, offers the promise of a new understanding of the stratigraphy and event history of the basin.

3.2 Geologic setting

The Surat Basin is widely regarded as an intracratonic basin with marine and nonmarine strata (Green et al. 1997a; Martin et al. 2013) covering over 300 000 km^2 of southeast Queensland and northeast New South Wales (Goscombe and Coxhead 1995). It overlies the Permo-Triassic Bowen and Gunnedah basins and forms part of the Great Australian Superbasin (Goscombe and Coxhead 1995; Jell 2013). The Walloon Coal Measures crop out in an arcuate belt between the towns of Morven and Dalby in the north of the basin and are widespread in the subsurface, gently dipping to the southwest (Hamilton et al. 2014b). Structures in the Surat Basin include the Mimosa Syncline, the Burunga Fault, and the St George-Bollon Slope, which are expressions of structures in the underlying Bowen Basin (Scott 2008; Ryan et al. 2012). The Kogan Nose and the Undulla Nose likely were structurally active during the deposition of the Walloon Coal Measures and further tightened due to reactivation of basement structures in the Late Cretaceous to Cenozoic (Hamilton et al. 2014b). Tectonic activity during the deposition of the Surat Basin, however, remains poorly understood (Hamilton et al. 2014b). The Central West Fold Belt and the New England Fold Belt bound the basin to the south. The Clarence-Moreton Basin and New England Orogen lie to the east with the Kumbarilla Ridge (or Gatton Arch) marking the boundary between the Clarence-Moreton and Surat basins (Goscombe and Coxhead 1995; Holcombe et al. 1997; Pinder 2004). The basin passes into the Eromanga Basin to the west of the Nebine Ridge and Cunnamulla Shelf (Goscombe and Coxhead 1995; Jell 2013).

The Surat Basin originated in the Rhaetian (latest Triassic) after a period of folding, uplift and peneplanation across eastern Australia (Jell 2013). Accommodation space in the Surat Basin is interpreted to have been created by two episodes of thermal relaxation and a period of lithospheric flexure through the Jurassic and into the Cretaceous, allowing 1800 m of strata to be deposited (Exon 1976; Goscombe and Coxhead 1995; Green et al. 1997a; Korsch and Totterdell 2009a). Controls on the rate of subsidence in the Surat Basin remain enigmatic with multiple interpretations ranging from rifting, to thermal sag after the cessation of volcanic-arc activity, to viscous corner flow in

the mantle wedge above a subducting plate (Korsch et al. 1989; McKellar 2004; Hoffmann et al. 2009; Korsch and Totterdell 2009a). Six sedimentary cycles, consisting of a series of fining-upward cycles have been recognised in the Surat Basin (Exon and Burger 1981). Each cycle consists of an upward succession of strata deposited by (a) braided streams, (b) meandering streams and (c) swamps, lakes, deltas and shallow seas (Exon 1976; Exon and Burger 1981; Jell 2013). These cycles were interpreted by Exon & Burger (1981) to be created by changes in base level driven by eustatic sea-level change. The Walloon Coal Measures form the upper part of the second sedimentary cycle of Exon & Burger (1981), with deposition in swamp, lacustrine and fluvial environments (Ryan et al. 2012; Martin et al. 2013; Hamilton et al. 2014b). Volcanism was pervasive during the deposition of the Walloon Coal Measures and overlying formations; whether this was intrabasinal or extrabasinal remains a topic of debate (Yago 1996b; Boult et al. 1998; Turner et al. 2009). Sedimentation continued in a similar fashion until the Early Cretaceous when eustatic sea-level fluctuations allowed for marine incursions into the basin with the deposition of marine and paralic formations (Jell 2013). Basin inversion in the middle to late Cretaceous led to the erosion of ~2 km of strata resulting from rebound of the lithosphere after the cessation of subduction off the east coast of Australia (Hoffmann et al. 2009; Waschbusch et al. 2009). Subsequently, the Surat Basin has been relatively quiescent, except for some minor post-Mesozoic adjustment of faults (Scott 2008).

3.3 Stratigraphy

The Walloon Coal Measures, the formal lithostratigraphic name currently for the stratigraphic unit recognised by Geoscience_Australia (2014) and the Geological Survey of Queensland (Jell 2013), was first referenced by Bryan (1946) with the official type section described by Cameron (1970). A basic outline of the lithostratigraphic units of the Surat Basin is shown in Figure 3.1.

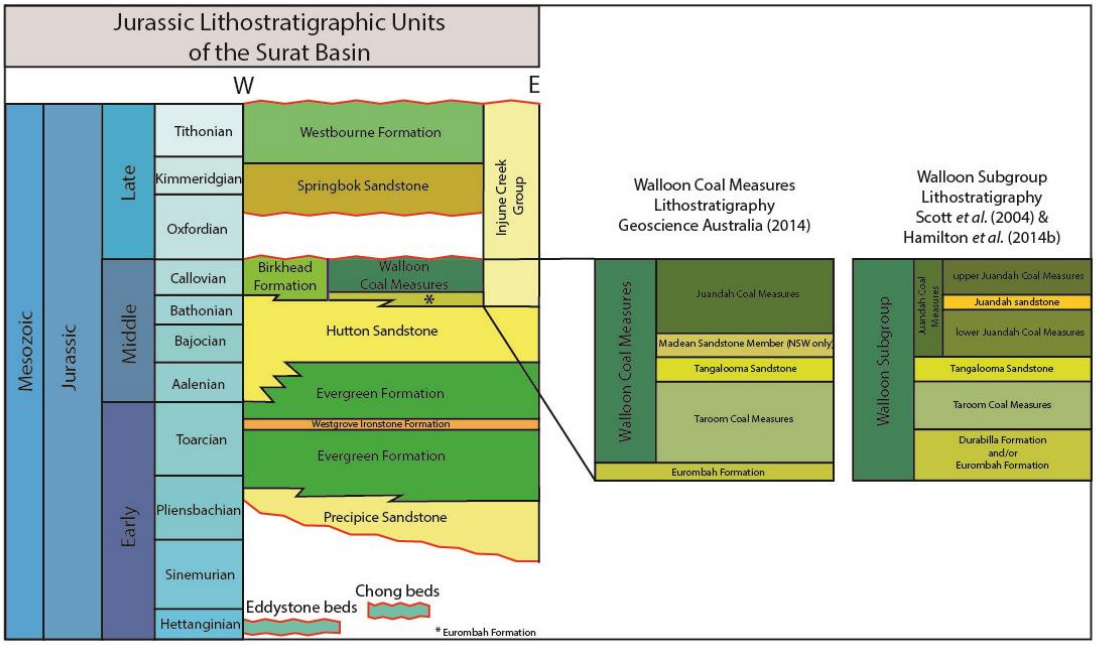

Figure 3.1. Jurassic lithostratigraphic framework for the Surat Basin including a breakdown of the Walloon Coal Measures/Walloon Subgroup lithostratigraphic framework not including new information (McKellar 1998; Scott et al. 2004; Jell 2013; Hamilton et al. 2014a).

The Walloon Coal Measures are regionally extensive, thin to the west, and are between 350 m to 450 m thick (Goscombe and Coxhead 1995; Jell 2013). The formation forms the lower part of the coal-bearing Injune Creek Group, underlain conformably by the Hutton Sandstone or Eurombah Formation and overlain unconformably by the Springbok Sandstone, also part of the Injune Creek Group (Exon 1966).

The Springbok Sandstone unconformably overlies the Walloon Coal Measures, with incision being greater in the eastern part of the basin (Hamilton et al. 2014b). However, the length of time represented by this hiatus in sedimentation

is not known. The Walloon Coal Measures incorporates four members: Taroom Coal Measures, Tangalooma Sandstone, the Maclean Sandstone Member (found only in NSW and Taroom Coal Measures (Geoscience_Australia 2014). Although the Walloon Coal Measures are formally ranked as a formation (Geoscience_Australia 2014), a number of workers informally assign the Walloons subgroup status including the transitional Durabilla/Eurombah Formation between the underlying Hutton Sandstone and the overlying Taroom Coal Measures (Jones and Patrick 1981; Scott et al. 2004; Hamilton et al. 2014b). The definition of the Walloon Coal Measures has been revised several times since the unit was first recognised as the Walloon beds by Cameron (1907), in his effort to describe the Mesozoic succession in the Walloon-Rosewood Coalfield, to the west of Ipswich (Queensland). It was further described by Jensen (1921) as the Calcareous (or Lower) Walloon and as part of the Injune Creek Beds by Reeves (1947) before being designated as the Walloon Coal Measures by Whitehouse (1954) during hydrological investigation in the Great Artesian Basin. After petroleum discoveries in the Surat Basin, numerous attempts have been made to divide and amalgamate coal-bearing units of the Injune Creek Group and the Walloon Coal Measures (Scott et al. 2004; Scott 2008). Debate continues on the stratigraphic status of the Walloon Coal Measures (*versus* the Walloon Subgroup terminology; (Jell 2013) due to the localised occurrence of the members in the Surat Basin and the recognition and geological separation of the Eurombah and Durabilla formations (lability, coal content and porosity contrasts) from both the Walloon Coal Measures and the Hutton Sandstone (Swarbrick et al. 1973; Green et al. 1997a; Scott et al. 2004; Scott 2008). More recent work by Hamilton et al. (2014b) has broken down the Walloon Coal Measures (Subgroup) further in an informal fashion by incorporating less extensive, erosionally truncated units including the lower Juandah Coal Measures, the Juandah sandstone or Wambo sandstone, and the upper Juandah Coal Measures. The Durabilla Formation is amalgamated with the Eurombah Formation due to difficulties differentiating between the two using wireline responses (Hamilton et al. 2014b). Importantly, the lateral stratigraphic relationships of subunits of the Walloon Coal Measures in the Surat Basin with the incomplete section of the formation in the Clarence-Moreton Basin by Cameron (1970) (where the type section of the formation has

been formally defined) remains unknown. Comprehension of these relationships is integral to the resolution of the present nomenclatural debacle.

No attempt has been made to collate the diverse coal-bed nomenclature associated with the Walloon Coal Measures, with coal-bed names varying between exploration companies, mines and geographic districts (Scott 2008). Current lithostratigraphic and coal-bed lithostratigraphic frameworks are discredited, as other correlation methods change the interpretation of depositional-basin architecture (Martin et al. 2013).

The Walloon Coal Measures in the Surat Basin were considered to have been Middle Jurassic and no younger than Callovian, using spore-pollen biostratigraphy (Price 1997; McKellar 1998; Geoscience_Australia 2014), with some estimates of the formation, in the Clarence-Moreton Basin, to the east, being as old as Aalenian (Burger 1994). The previously estimated age of the underlying Hutton Sandstone ranges from Aalenian to Bathonian, whilst the overlying Springbok Sandstone has been considered to be Late Jurassic/Oxfordian from biostratigraphy (Price 1997; McKellar 1998; Geoscience_Australia 2014). However, these ages now need to be revised, based on the radiometric dates obtained herein from the Walloon Coal Measures.

3.4 Methodology

Stratheden 4 (Geoscience Australia well code GA ENO 554973, Geological Survey of Queensland well code ARM Stratheden 4), a coal seam gas well on the eastern edge of the Surat Basin, near the town of Dalby on the eastern flank of the Kumbarilla Ridge (27°11'58"S, 151°01'04"E) (Figure 3.2) was selected for this study. It was drilled to a total depth of 531.16 m in April 2008, permitting extraction of 380 m of continuous core from the Walloon Coal Measures (Oberhardt 2008). The Walloon Coal Measures intersected between 122 and 489 m, however, the interval was not fully cored (Oberhardt 2008). This core is stored at the Exploration Data Centre, Zillmere by the Geological Survey of Queensland (Department_of_Natural_Resources_and_Mines). The core was logged at a scale of 1:100 with tuff beds greater than 5 cm interbedded between coals sampled (Figure 3.3). The bottom of the core is ~19 m above the base of the Taroom Coal Measures (determined from wireline logs) and the top is in the upper Juandah Coal Measures, 11 m below the unconformity with the Springbok Sandstone. Alluvium (0–69 m), Springbok Sandstone (69–122 m), Eurombah Formation (489–519 m) and the Hutton Sandstone (>519.48 m) were also intersected in the well.

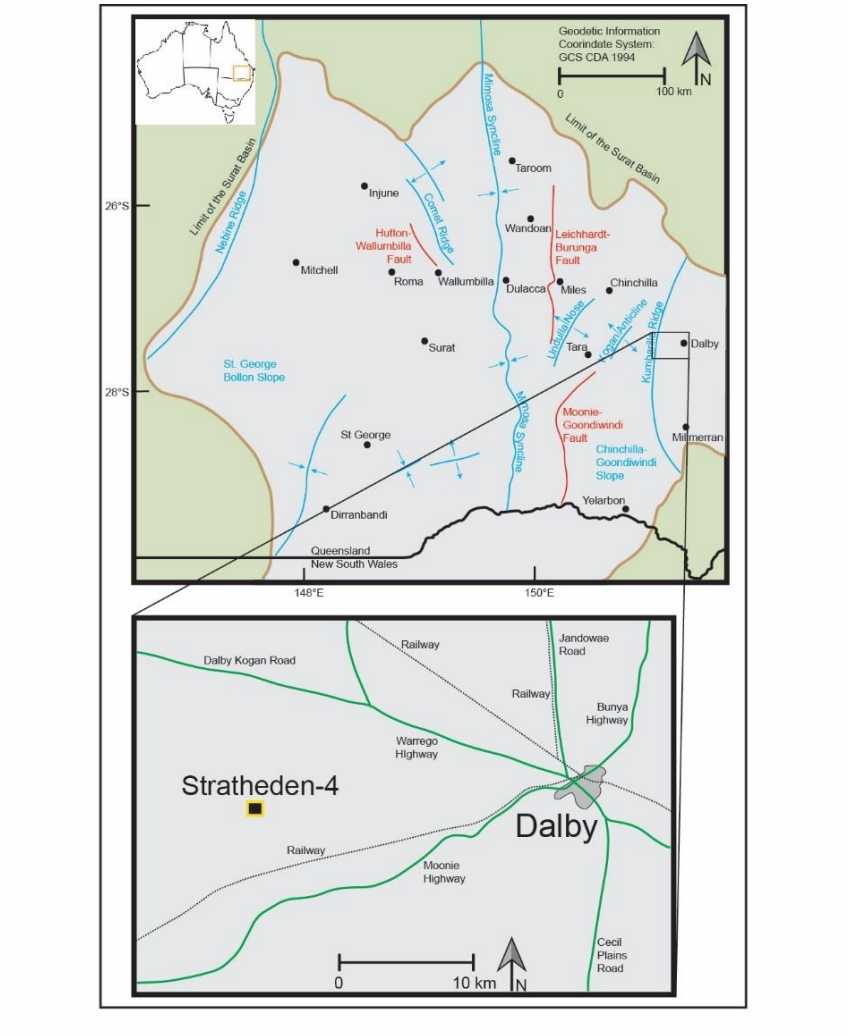

Figure 3.2. Location of the Stratheden 4 well in the Surat Basin and the geological context of the basin.

Two tuffs were selected and dated. Sample GA2180600 (Geoscience Australia sample code) is from the Taroom Coal Measures at depth of 396.41 to 396.46 m and sample GA2180601 is from the Juandah Coal Measures at depth of 182.84 to 183.04 m. Zircon separation by standard methods was performed at the Australian National University. Zircons were analysed at Boise State University by U–Pb chemical abrasion isotope dilution thermal ionisation mass spectrometry (CA-TIMS) and laser ablation inductively coupled plasma (LA-ICPMS) methods (see appendices 1 for details). Cathodoluminescence (CL) images of zircons, CA-TIMS and LA-ICPMS results are given in the Supplementary Papers. U–Pb dates are plotted in Figure 3.4 with errors given at 2σ.

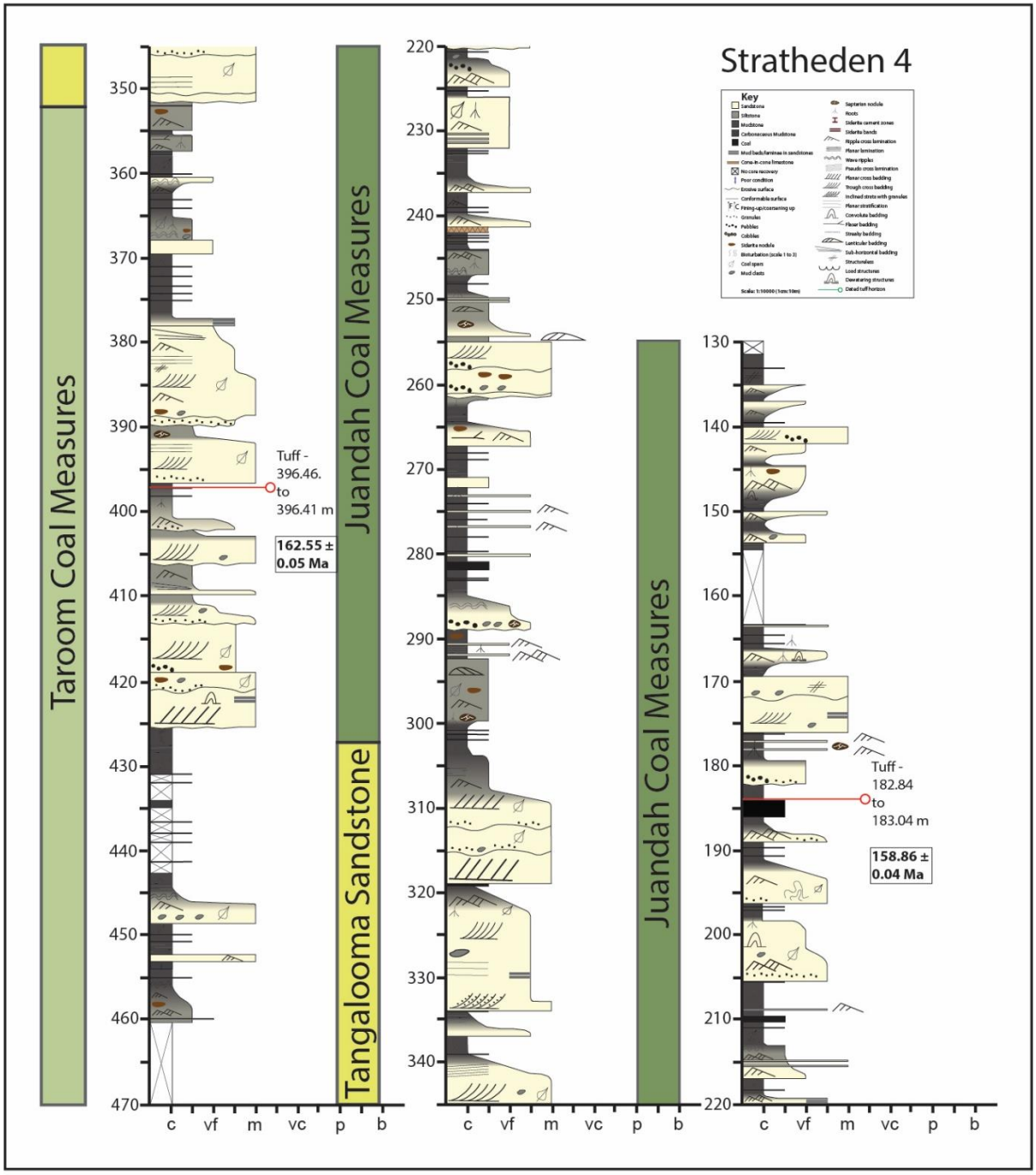

Figure 3.3. Graphic log for the Stratheden 4 well, and the intervals from where tuffs were sampled (396.46-41 and 183.04-182.84m) for U-Pb CA-TIMS dating and analysed by LA-ICPMS.

3.5 Zircon dates and implications

CL images show the zircon grains from both samples are elongate, prismatic, and have simple oscillatory zoning. Six zircon grains from GA2180601 yielded equivalent $^{206}Pb/^{238}U$ dates with a weighted mean of 158.86 ± 0.04 Ma (MSWD = 1.5, probability of fit = 0.18; Figure 3.4). Chemistry of the zircons from LA-ICMPS suggests a mafic magma from (1) relatively high and variable Th/U and (2) variable Eu anomalies, including some that are very small (Figure 3.5). Seven zircon grains from GA2180600 yielded equivalent $^{206}Pb/^{238}U$ dates with a weighted mean of 162.55 ± 0.05 Ma (MSWD = 0.6, probability of fit = 0.74; Figure 3.4). Three other grains from GA2180600 yielded older dates of 162.8 ± 0.1, 169.9 ± 0.2 and 171.2 ± 0.2 Ma imply they contain inherited components. Chemistry of the zircons from LA-ICPMS suggests a granitic magma demonstrated by low Th/U and Eu/Eu* ratios (Figure 3.5).

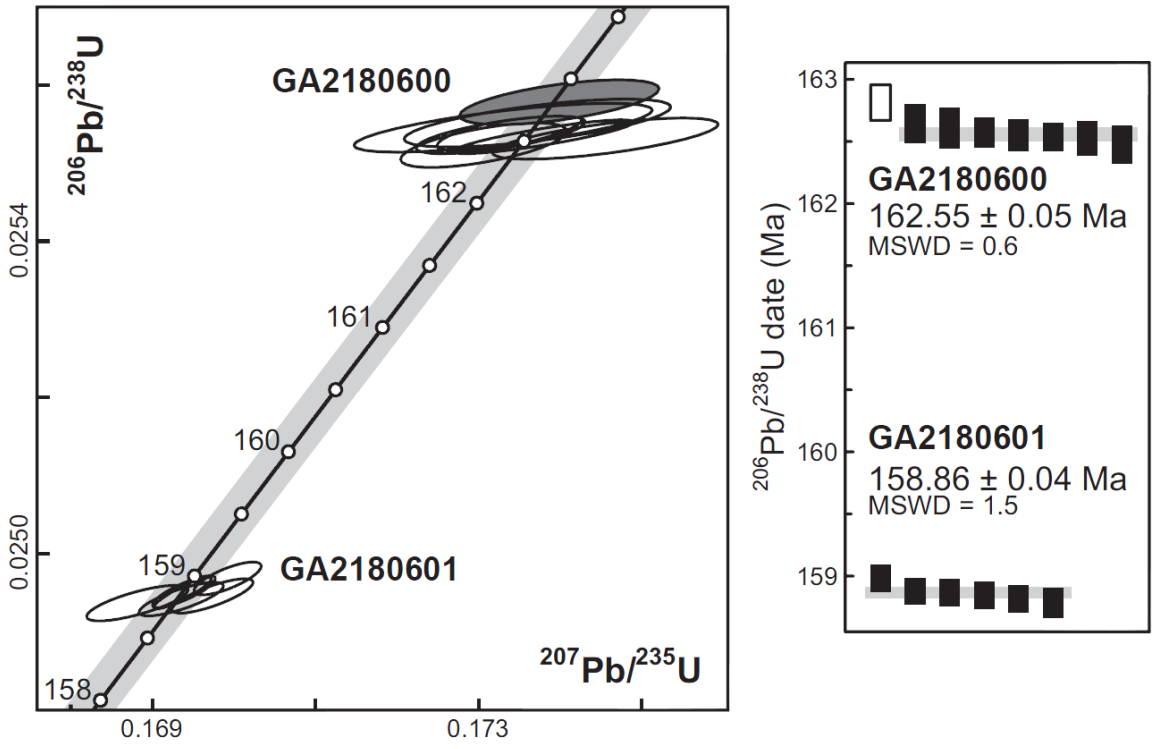

Figure 3.4. Plots of CA-TIMS U-Pb dates from zircon, using Isoplot 3.0(Ludwig 2003). For the concordia plot, the grey ellipse in the sample of GA2180600 is not included in the weighted mean calculation, and two older analyses from this tuff are not shown. The grey rectangle behind concordia line represents the 2σ uncertainty on concordia. For the $^{206}Pb^{238}U$ plot, error bars are at 2σ. Weighted mean dates are shown and represented by the grey boxes behind the error

bars. Three older dates, of which two (169.9 ± 0.2 and 171.2 ± 0.2 Ma) are omitted for being detrital in origin and being substantially older than other dated zircons.

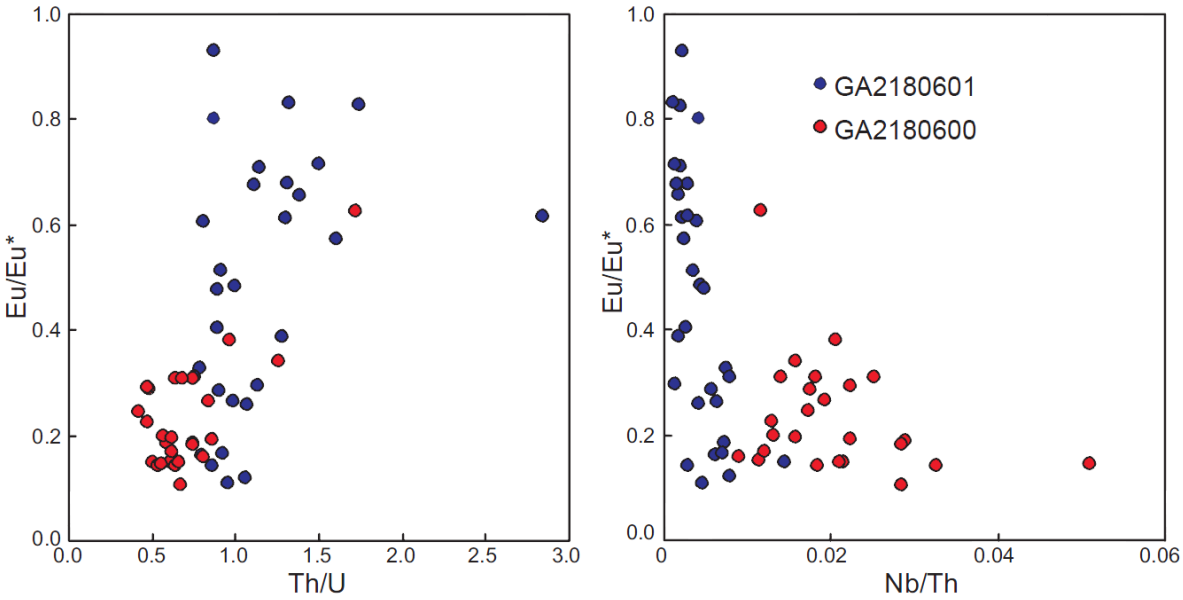

Figure 3.5. Plots of Th/U vs Eu/Eu* and Nb/Th vs Eu/Eu* concentrations for GA2180600 and GA2180601, illustrating the different source magmas of the zircons of the two tuffs.

The weighted mean CA-TIMS U–Pb dates are the interpreted ages of ash deposition based on the high probability of fit (0.6 to 1.5), large numbers of grains dated, and morphology and zoning that are consistent with volcanic zircon. The source of the volcanism remains uncertain. Possible volcanic sources are: (1) rift-related bi-modal volcanism on the Marion Plateau (162.0–154.3 Ma) (Jell 2013); (2) intraplate volcanism of the Wellington–Muswellbrook–Narrabri region of northeastern NSW (217–148 Ma) (Dulhunty 1967); and (3) volcanic centres to the northeast of the Clarence-Moreton Basin (Yago 1996b).

The dates reported here, which are the first radiometric dates recorded from the Walloon Coal Measures, have significant implications for our understanding of the Surat Basin and its formation. The most important are reassignment of the Walloon Coal Measures, from the Middle Jurassic to the Upper Jurassic Oxfordian Stage. Taking into account the 2σ confidence of ±1 Ma for the lower and upper limits of the Oxfordian (163.5–157.3 Ma), determined by the

International Commission on Stratigraphy (Gradstein et al. 2012; Cohen et al. 2013; updated), the Walloon Coal Measures lie entirely within the Oxfordian (Figure 3.6).

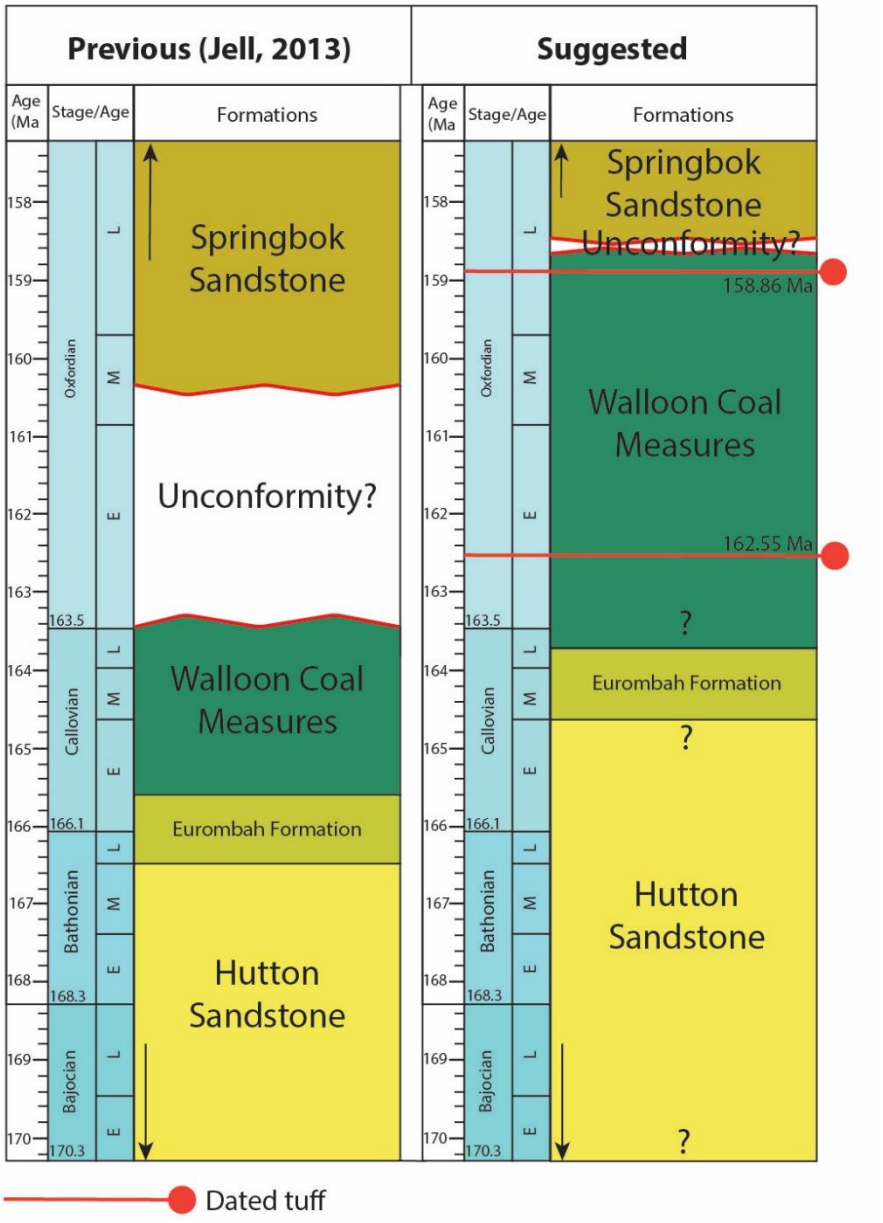

Figure 3.6. Previous lithostratigraphic framework for the Middle to Upper Jurassic of the Surat Basin based on biostratigraphic correlation and a suggested lithostratigraphic based on isotopic dating of two tuff samples in accordance with geological timescales defined by Gradstein et al. (2012) and Ogg et al. (2012).

Current time-stratigraphic interpretations associated with the palynostratigraphic units defined by authors including Helby et al. (1987) and Price (1997) will need to be revised, to take into account not only the age assigned here to the Walloon Coal Measures (in the Surat Basin), but also the more constrained time interval for deposition of the unit. The oldest section is either 1) unlikely to fall into the *Aequitriradites norrisii* Association Zone of APJ4.2 and *Contignisporites glebulentus* Interval Zone of APJ4.3 that covers the Bathonian–Callovian transition, or 2) the first appearance datums need to be recalibrated in the Surat Basin (Price 1997). Biostratigraphic work needs to focus on finding the base of *the Murospora florida* Association Zone of APJ5 in the Surat Basin. This may be challenging in light of the near absence of *Murospora florida* in the Walloon Coal Measures as a consequence of the ecological niche of its parent plant, a pteridophyte tree fern and the diachronous nature of the basal Walloon Coal Measures from the Surat into the Clarence-Moreton Basin (McKellar 1998; Martin et al. 2013).

The extent of erosion before deposition of the overlying Springbok Sandstone can now be more accurately defined. The hiatus was likely much shorter than previously assumed (McKellar 1998; Hamilton et al. 2014b) and occurred in the late Oxfordian as opposed to across the late Callovian/early Oxfordian boundary. Until a tuff horizon is dated in the Springbok Sandstone or the base of the Westbourne Formation, the duration of the hiatus will remain uncertain.

The new dates have interesting implications for paleogeography and paleoecology because, according to current plate tectonic reconstructions, they indicate that the coals of the Surat Basin accumulated as peats in paleolatitudes higher than 75°S (Klootwijk 1996; Blakey 2011; Boucot et al. 2013) compared to the 55°S–65°S previously assumed based on a Middle Jurassic age (Veevers et al. 1991; Balme et al. 1995). A position that was well within the polar zone (66°S and higher) would have experienced extreme seasonality, with winter darkness lasting at least three months and continuous daylight for three months during the summer. The climate, despite being in high latitudes, is interpreted as temperate (up to 10°C), humid and with high rainfall (>1000 mm/yr) based on palynofloral assemblages and global climate models, suitable for peat accumulation (Balme et al. 1995; McKellar 1998; Martin et al.

2013). It is well documented that similar climatic conditions existed in the Late Cretaceous and from the late Paleocene–Early Eocene allowing for warm, mid-latitude flora to migrate poleward as climatic belts expanded globally, irrespective of limitations of existing at high latitudes (Spicer and Chapman 1990; Wing et al. 2005). The winter darkness would have restricted primary productivity to the spring to autumn months, even if conditions for coal accumulation and its subsequent preservation were otherwise suitable. Models of peat growth rates in the high latitudes range from approximately 0.01–0.05 mm/yr and can be exceeded by basin subsidence, causing mires to be inundated by clastics or drowned by flooding with the creation of lakes (McCabe 1991; Bohacs and Suter 1997; Loisel et al. 2012). This may explain the thin nature of the Walloon coal beds. Other high latitude coals, such as those from the Cretaceous of Antarctica and Alaska, also have thin, discontinuous seams (Spicer and Parrish 1986; Macdonald and Francis 1992).

A first order estimate of subsidence rates can be defined using the equations and methodologies of Allen and Allen (2013). Using the new U–Pb dates and stratal thicknesses from core, a basin subsidence/backstripped rate of ~61 m/Myr is calculated. This is similar, although slightly higher, to subsidence rates calculated for the late Mesozoic foreland basins of the western United States that on average, range from ~51 m/Myr to ~35 m/Myr over the lifetime of a basin (Cross 1986). By comparison, the calculated rate of subsidence of ~25 to 5 m/Myr for the cratonic Williston Basin in the northern United States (DeRito et al. 1983) is considerably lower. Despite the complex prehistory of the Surat Basin (rifting and foreland loading) influencing depositional architecture, theories of continental, intracratonic sag for the Surat Basin, including subduction-related dynamic platform tilting and intracratonic sag (Green et al. 1997; Waschbusch et al. 2009; Jell 2013) are now questionable.

3.6 Summary

U–Pb zircon dating of *ca.* 159 Ma and 162 Ma tuffs place the Walloon Coal Measures in the Oxfordian, which is substantially younger than previous estimates based on eastern Australian biostratigraphic frameworks. These dates also place the Surat Basin at higher latitudes (>75°S) during the deposition of the Walloon Coal Measures than previously assumed. The coals accumulated as peats in mires that experienced at least three months of continuous darkness per year. The new dates allow for precision in measuring basin subsidence rates, which may help determine the tectonic setting of the basin: subsidence rates were more similar to those of foreland rather than intracratonic basins. The dates will also provide the basis for a new, more precise biostratigraphic framework for the Jurassic of Australia.

Lithostratigraphic correlation of strata of the Walloon Coal Measures within the Surat Basin has long been difficult due to the heterolithic, laterally impersistent coals and sandstones. Dating of zircons (and associated geochemistry) from additional volcanic tuffs offers the possibility of more precise correlations across the Surat Basin and further afield that may allow for the development of better nonmarine sequence-stratigraphic models.

3.7 Supplementary papers

See appendices 1 (p. 312-318).

Statement of Authorship

Title of Paper	Solving a tuff problem: defining a new chronostratigraphic framework for Middle to Upper Jurassic strata in eastern Australia using U-Pb zircon dates
Publication Status	☐ Published ☒ Accepted for Publication ☐ Submitted for Publication ☐ Unpublished and unsubmitted work written in manuscript style
Publication Details	Wainman, C.C., McCabe, P.J. and Crowley, J.L. in press. U Solving a tuff problem: defining a new chronostratigraphic framework for Middle to Upper Jurassic strata in eastern Australia using U-Pb zircon dates. American Association of Petroleum Geologists (AAPG) Bulletin. pp. 1-29. Accepted on 26th July 2017.

Principal Author

Name of Principal Author (Candidate)	Carmine C. Wainman		
Contribution to the Paper	Majority of the data collection and interpretation. Wrote the greater majority of the paper with exceptions noted in the co-authorship contributions. Produced final version of the paper using editorial suggestions of the co-authors.		
Overall percentage (%)	80		
Certification:	This paper reports on original research I conducted during the period of my Higher Degree by Research candidature and is not subject to any obligations or contractual agreements with a third party that would constrain its inclusion in this thesis. I am the primary author of this paper.		
Signature		Date	10/08/2017

Co-Author Contributions

By signing the Statement of Authorship, each author certifies that:

i. the candidate's stated contribution to the publication is accurate (as detailed above);
ii. permission is granted for the candidate in include the publication in the thesis; and
iii. the sum of all co-author contributions is equal to 100% less the candidate's stated contribution.

Name of Co-Author	Peter J. McCabe		
Contribution to the Paper	Supervisor of Ph.D. – Extensive critical advice and guidance on research project and editorial comments for the paper.		
Signature		Date	10/8/2017

Name of Co-Author	James L. Crowley		
Contribution to the Paper	Carried out CA-TIMS and LA-ICPMS. Provided guidance on research project and editorial comments for the paper. Wrote the third paragraph in the section titled "Methodology" and wrote the section titled "U-Pb CA-TIMS results". Drafted figures 4.5 and 4.6. Wrote the appendices (appendices 2).		
Signature		Date	August 10, 2017

Chapter 4. Solving a tuff problem: a new chronostratigraphic framework for Middle to Upper Jurassic strata in eastern Australia using U-Pb zircon dates

This chapter is an exact copy of the article published in the *AAPG Bulletin.* A statement of authorship is provided on the previous page.

Citation: Wainman, C.C., McCabe, P.J., Crowley, J.L, 2017. Solving a tuff problem: defining a new chronostratigraphic framework for Middle to Upper Jurassic strata in eastern Australia using U-Pb zircon dates. *AAPG Bulletin*, 20, 1-28.

Abstract

To better predict the architecture of reservoirs and the location of undiscovered resources in fluvial-dominated strata a sound chronostratigraphic framework is needed. This study reassesses the stratigraphic framework of petroleum-bearing Jurassic fluviolacustrine successions in the Eromanga, Surat and Clarence Moreton basins of eastern Australia. Correlation of the strata is challenging owing to the heterolithic facies, the absence of conventional stratigraphic marker beds and the longevity of palynostratigraphic zones. The abundance of laterally discontinuous volcanic air-fall tuffs and volcanogenic sandstones across the Jurassic of eastern Australia allows for the construction of a new, regional chronostratigraphic framework. High-precision U-Pb zircon CA-TIMS dates ranging from 168.07 ± 0.07 to 149.08 ± 0.06 Ma were obtained from 30 samples from 13 wells across 3 basins. Five chronostratigraphic datums were defined and extrapolated to 677 wells within a time interval 420 ka or less over hundreds of kilometers across eastern Australia. The new chronostratigraphic framework reveals inaccuracies in picking lithostratigraphic units based on lithology and wireline log characteristics and shows coal-bearing facies of the Walloon Coal Measures to be diachronous. The study also demonstrates the feasibility of extending chronostratigraphic datums to neighboring basins without tuff beds by dating the youngest zircon in volcanogenic sandstones by U-Pb CA-TIMS following LA-ICPMS analysis. The dates provide a substantial revision to the Middle to Late Jurassic stratigraphy of eastern Australia. The use of precise U-Pb CA-TIMS dates should help

elucidate the lithofacies architecture of nonmarine successions in other basins and assist in petroleum development

4.1 Introduction

The construction of a stratigraphic framework in fluvial-dominated strata is challenging because of the discontinuous nature of the lithofacies (Shanley and McCabe 1994). In most of these successions, the absence of marker beds, poor biostratigraphic recovery, and biozones of long time duration also make correlation difficult. Characterization and modelling of fluvial strata requires precise correlation of surfaces that is challenging in the absence of 3D seismic surveys or where the stratigraphic intervals are below seismic resolution (Shepherd 2009a). Correlation of core and wireline log data can be difficult because of the laterally discontinuous nature of channel sandstones and associated lithofacies such as crevasse splays, floodplain deposits, lacustrine sediments and coals. The construction and application of a robust chronostratigraphic framework in such strata can significantly reduce uncertainties about the location, geometry and connectivity of prospective reservoirs especially those located in subtle stratigraphic traps. This paper examines the gas- and oil-rich Middle to Upper Jurassic strata of eastern Australia and suggests a new stratigraphic framework for correlation based on the dating of volcanic tuff beds.

The Walloon Coal Measures of the Surat Basin host Australia's largest source of coal bed methane (CBM) comprising ~31,000 petajoules (PJ) of proven and probable reserves (2P) (Queensland_Government 2016) or ~28,200 billion cubic feet (BCF) of gas (1.1PJ = 1 BCF). In the adjacent Eromanga Basin, the Hutton Sandstone, Birkhead Formation and the Namur Sandstone host Australia's largest onshore conventional oil and gas accumulations with approximately 52.8 million barrels (MMbbl) of estimated undiscovered resources (Department_of_State_Development 2016). These strata have been the subject of numerous studies since the mid-1980s e.g. (Paton 1986; McKellar 1998; Lanzilli 2000; Baker and Slater 2008; Gallagher et al. 2008; Chaffee et al. 2010; Ryan et al. 2012; Martin et al. 2013; Hamilton et al. 2014b; Shields and Esterle 2015; Hentschel et al. 2016; Morris and Martin 2016), however, there is little consensus on the basic stratigraphic framework due to the complex, heterolithic succession of fluvial-lacustrine strata with thin, discontinuous lithofacies (Jell 2013; Martin et al. 2013; Shields and Esterle

2015; Morris and Martin 2016). The correlation of stratigraphic units within and across eastern Australian basins is relatively poor due to limited exposures on the surface, low well density and little seismic coverage outside of major petroleum fields. The lack of a reliable stratigraphic framework has major implications for exploration and production efforts including 1) predicting the distribution of coal deposits across the basin; 2) determining patterns of gas drainage around production wells; and 3) the discovery of new subtle stratigraphic traps (Sales et al. 2015; Bradshaw and Bernecker 2016).

In recent years, there have been steps to rectify these issues by dating the numerous volcanic air-fall tuffs in the Walloon Coal Measures. The first U-Pb chemical abrasion thermal ionization mass spectrometry (CA-TIMS) dates of zircon from tuffs in the Walloon Coal Measures from the Surat Basin showed that the Walloon Coal Measures are Late Jurassic Oxfordian age, rather than Middle Jurassic as had previously been believed, which has significant implications for understanding the paleogeographic setting and subsidence history of the Surat Basin (Wainman et al. 2015).

This study also suggests that the maximum depositional ages of volcanogenic sandstones can be determined using the same U-Pb CA-TIMS methodology. The sandstones in the Birkhead Formation of the Eromanga Basin were derived from a concurrent volcanic arc system to the east (Boult 1996; Gallagher et al. 2008). These beds, therefore, should contain volcanic zircon grains of a similar age to those sourced from tuff beds of the Surat Basin allowing for correlation between the two basins. This has never been attempted before in any stratigraphic study in Australia.

Newly acquired U-Pb CA-TIMS dates (including those derived from volcanogenic sandstones) obtained from wells across the Eromanga, Surat and the Clarence-Moreton basins are used to test the validity of previous stratigraphic models of Middle to Upper Jurassic strata of eastern Australia.

4.2 Geological context of the Eromanga, Surat and Clarence-Moreton basins

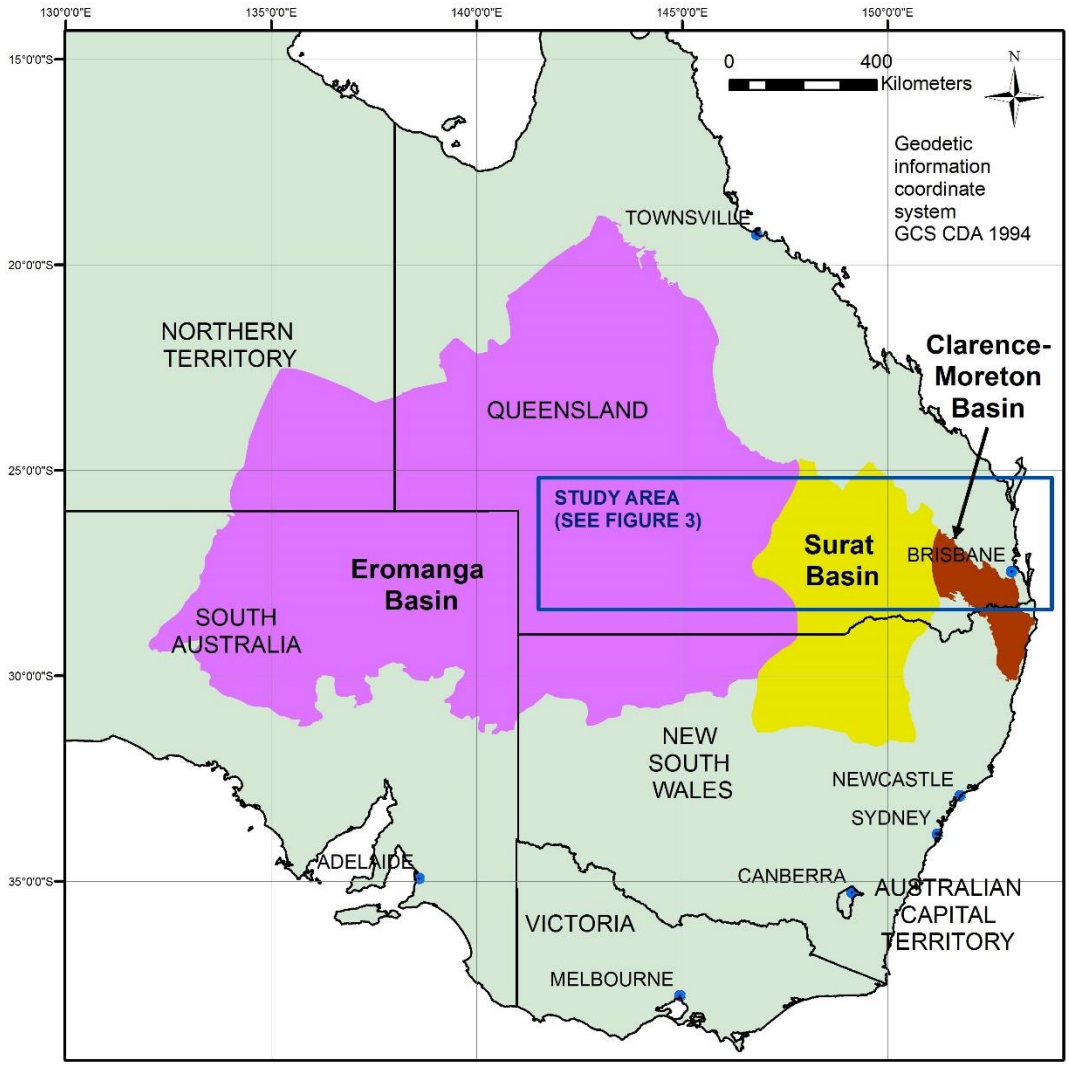

Figure 4.1. The location of the Eromanga, Surat and Clarence-Moreton basins in eastern Australia. The study area is outlined in blue.

4.2.1 Eromanga Basin

The Late Triassic to Late Cretaceous Eromanga Basin (Figure 4.1) forms one of a series of depocentres associated with the Mesozoic Great Australian Superbasin (Jell 2013). The basin covers over 1,000,000 km^2 (386,102 sq mi) of Queensland, South Australia, New South Wales and the Northern Territory with up to 2.5 km (1.6 mi) of infill (Goscombe and Coxhead 1995; Jell 2013). Strata dip at a low angle forming a broad synclinal structure spanning most of the basin (Alexander and Jensen-Schmidt 1996). The Eromanga Basin overlies

the Carboniferous-Permian Cooper Basin (Alexander and Jensen-Schmidt 1996).

Cessation of sedimentation in the underlying Cooper Basin was associated with a widespread east-west compressional event in the Late Triassic (Apak et al. 1997) that resulted in basin-wide uplift (Mavromatidis 2008). Subsequently, the Eromanga Basin was initiated by tectonic downwarping during the Early Jurassic (Alexander and Jensen-Schmidt 1996). According to Alexander and Jensen-Schmidt (1996), sedimentation was continuous throughout the Jurassic and Cretaceous with no major depositional breaks except for an unconformity between the Birkhead Formation and overlying the Adori and Namour Sandstones (Figure 4.2). A combination of changing stress fields on the Australian plate margin, lithospheric flexure and sediment loading from the increased rate of deposition of volcanogenic rocks more than quadrupled the rate of subsidence during the Early to middle Cretaceous and allowed for marine incursions into the Eromanga Basin (Gallagher et al. 1994; Waschbusch et al. 2009). Uplift and erosion brought an end to deposition in the Late Cretaceous (Alexander and Jensen-Schmidt 1996). Deposition recommenced in the overlying Lake Eyre Basin in the late Paleocene (Alexander et al. 1996).

The intracratonic origin of the Eromanga Basin has been the topic of some speculation. The subsidence history of the basin is thought to be similar to that of foreland basins (Draper 2002) whilst others consider it comparable to rift-related basins (Jell 2013). The proposed mechanism of basin subsidence varies from the prolonged thermal relaxation of the lithosphere, sub-lithospheric convection to sediment loading (Gallagher 1988; Gallagher and Lambeck 1989; Gallagher et al. 1994). More recently, the role of dynamic platform tilting resulting from viscous mantle corner flow above a subducting plate has been discussed by Waschbusch et al. (2009). They suggest that near- and far-field deflection of the retrolithosphere (driven by pressure gradients at the base of the lithosphere above a subduction zone) contributed to accommodation space creation in the basin.

4.2.2 Surat Basin

The Late Triassic to Early Cretaceous Surat Basin comprises up to 2.3 km (1.4 mi) of sedimentary infill and spans 270,000 km^2 (104,247 mi sq) of southern Queensland and adjacent northern New South Wales (Figure 4.1) (Stewart and Alder 1995; Jell 2013). The basin is up to 800 km (497 mi) long and 450 km (280 mi) wide (Goscombe and Coxhead 1995) with strata gently dip to the southwest (Stewart and Alder 1995; Raza et al. 2009; Hamilton et al. 2014b). The Surat Basin lies unconformably over the Bowen Basin (Jell 2013)

The depositional history of the Surat Basin is intrinsically tied to the evolution of basement structures in the underlying Bowen and Gunnedah basins (Korsch and Totterdell 2009b). Deposition in these basins ceased in the Middle Triassic when up to 2.5 km of sediment was removed during a phase of crustal shortening and uplift known as the Hunter-Bowen Orogeny (Green et al. 1997). Deposition recommenced in the newly formed Surat Basin in the Rhaetian (Green et al. 1997; Jell 2013). A short compressional episode in the Late Triassic, known as the Goondiwindi Event, led to the erosion of Rhaetian sediments and the formation of thrust and back thrust faults (Green et al. 1997; Korsch and Totterdell 2009b) (Figure 4.2). Sedimentation restarted in the Early Jurassic and continued uninterrupted into the Early Cretaceous (Stewart and Alder 1995). Syntectonism during deposition occurred on reactivated Triassic fault systems and induced regional folding during the Jurassic (Hamilton et al. 2014b). Some authors have suggested the presence of an unconformity in the Late Jurassic between the Walloon Coal Measures and the Springbok Sandstone but the cause and duration of the hiatus are uncertain (Jell 2013; Hamilton et al. 2014b) (Figure 4.2). Exon and Burger (1981) recognized six cycles of sedimentation in the Surat Basin and interpreted them as being driven by eustasy with several marine incursions during the Cretaceous. A major contractional episode in the middle Cretaceous terminated deposition in the Surat Basin and subsequently led to the erosion of 2 km (1.2 mi) of strata (Fielding 1996; Raza et al. 2009). Structures such as the Hutton-Wallumbilla Fault reactivated in response to short-lived compressional events in the Cenozoic (Stewart and Alder 1995; Hamilton et al. 2014b).

Sedimentation and subsidence rates in the Surat Basin were more than double those in the Eromanga Basin (Waschbusch et al. 2009), however, the tectonic origin of the Surat Basin is poorly understood with continued debated as to whether the creation of accommodation was driven by foreland loading, rifting, back-arc extension or dynamic platform tilting (Exon 1976; Fielding 1993; Bryan et al. 1997; Waschbusch et al. 2009; Jell 2013; Tucker et al. 2016).

Pervasive volcanic activity during deposition during the Late Jurassic influenced sedimentation in the basin with volcanic fallout frequently blanketing lakes and mires in ash (Yago and Fielding 2015). Where exactly the volcanoes were located and whether the volcanism was driven by subduction or incipient rifting (or both) remains unknown because the precise location and character of the eastern Australian Margin during the Jurassic is poorly constrained (Fielding 1996; Korsch and Totterdell 2009b; Jell 2013; Babaahmadi et al. 2015). However, they were presumably to the north and east as indicated by the fluvial paleocurrents e.g. (Hamilton et al. 2014b). On a regional perspective, (Bryan et al. 1997) and (Jell 2013) speculate the pervasive volcanism was related to rifting and the break-up of eastern continental Gondwana and the formation of the modern eastern Australian passive margin since the Middle Jurassic. This is reinforced by seismic profiles of eastern margin of Australia together with geochronological, geochemical and petrological data from the Whitsunday Volcanic Province and the Marion Plateau. In contrast, it has been recently suggested from detrital zircon U-Pb geochronology and Lu-Hf isotope analysis from Winton and Mackunda formations of the Eromanga Basin that a long lived magmatic arc existed until the Late Cretaceous on the eastern margin of Australia (Tucker et al. 2016).

4.2.3 Clarence-Moreton Basin

The smaller intracratonic Late Triassic to Early Cretaceous Clarence-Moreton Basin (Figure 4.1) comprises 3 km (1.9 mi) of sedimentary infill and covers 43,000 km^2 (16,602 sq mi) of northern New South Wales and southeastern Queensland with an additional 10,000 km^2 (3861 sq mi) located offshore (Goscombe and Coxhead 1995; Jell 2013). The basin overlies the Early Triassic Esk Trough and the Middle Triassic Ipswich Basin (Korsch et al. 1989; Powell et al. 1993). The basin is widely regarded to have experienced a

prolonged period of thermal subsidence and sediment loading starting in the Middle Triassic despite having a complex structural origin associated with crustal transtension (Korsch et al. 1989). After a depositional hiatus in the Late Triassic, deposition in the Clarence-Moreton Basin was relatively continuous through to the Early Cretaceous before lithospheric rebound induced by compression events brought an end to sedimentation in the basin (Martin and Saxby 1982).

4.3 Defining Middle to Upper Jurassic Strata in eastern Australia

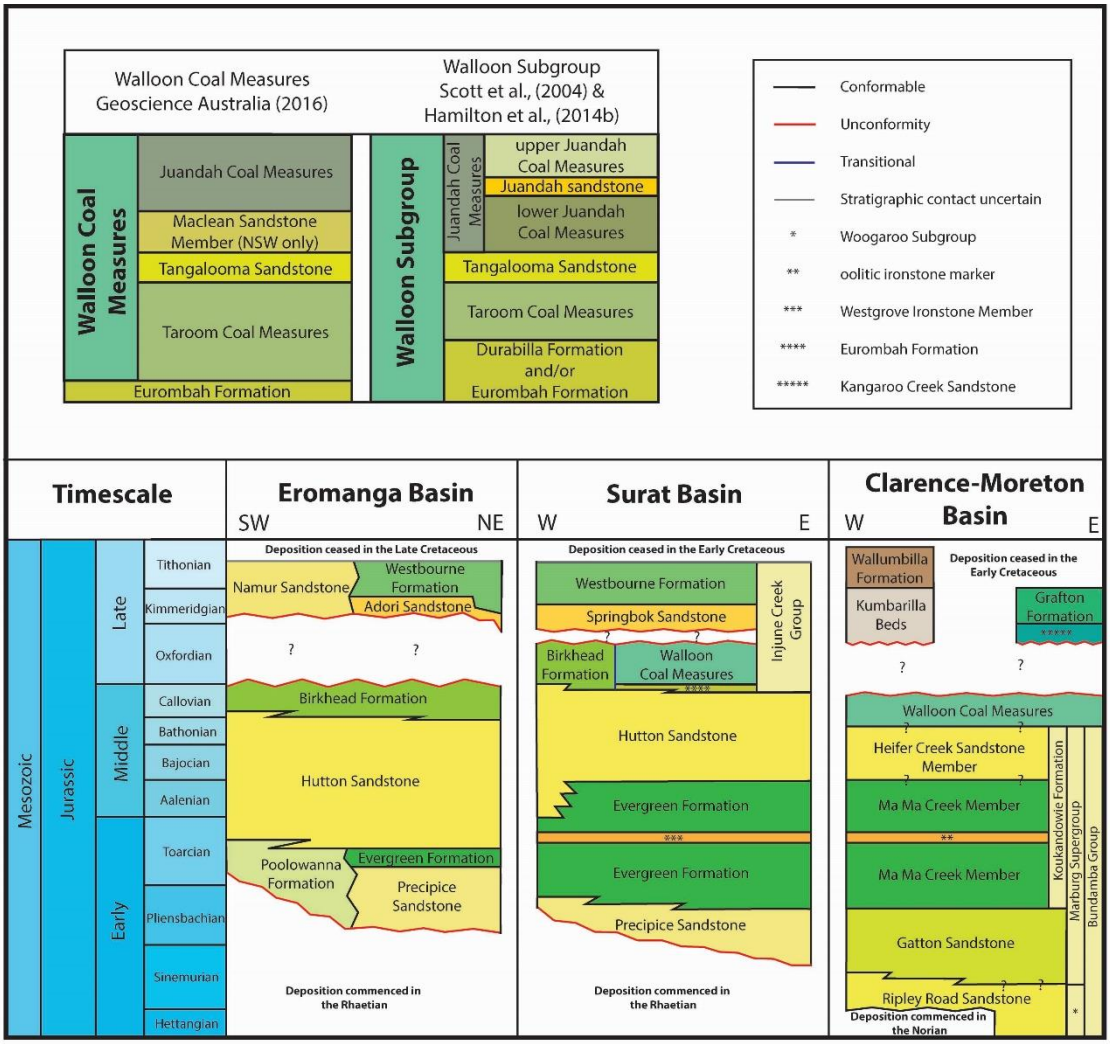

Figure 4.2. Jurassic lithostratigraphic framework of the Eromanga, Surat and Clarence-Moreton basins and the stratigraphic breakdown of the Walloon Coal Measures in Queensland, adapted from Alexander et al. (1996), Pinder (2004), Jell (2013), Hamilton et al. (2014b), Wainman et al. (2015) and Geoscience_Australia (2016).

Even though more than 10,000 wells have been drilled in the Eromanga, Surat and Clarence-Moreton basins, the stratigraphic framework is still a matter of contention (Alexander et al. 1996; Martin et al. 2013; Towler et al. 2016) and arguably some of the nomenclature has become more of a hindrance than a help as evidenced by frequent renaming and redefinition of stratigraphic units over the last 50 years e.g. (Scott 2008). The major lithostratigraphic units from the Jurassic defined for the Eromanga, Surat, and Clarence-Moreton basins are

shown in Figure 4.2. The Walloon Coal Measures are the principal coal-bearing formation in the Surat and Clarence-Moreton basins, whereas the Birkhead Formation hosts one of the principal petroleum reservoir units in the Eromanga Basin (Gallagher et al. 2008; Geoscience_Australia 2016). The Springbok Sandstone and the Westbourne Formation also host minor coal deposits (Jell 2013).These formations are the focus for this study. Descriptions of these Middle to Upper Jurassic stratigraphic units, their wireline log characteristics and equivalents in eastern Australia basins are shown in Table 4. 1. For this paper, siltstones are defined as rocks comprising >66% of silt-sized particles (2–62 µm) and mudstones for all other fine-grained siliciclastic rocks comprising >66% of particles <62 µm in size.

Table 4.1. Descriptions of key Middle to Upper Jurassic lithostratigraphic units and their equivalents in the Eromanga, Surat and Clarence-Moreton basins from the literature (Exon 1976; Jones and Patrick 1981; Alexander et al. 1996; Scott et al. 2004; Geoscience_Australia 2016).

Formation	Biostratigraphic age	Stratigraphic relationship with underlying formation	Lithology	Wireline log characteristics	Thickness (m and ft)	Depositional setting	Other
Eurombah Formation	Bajocian to Bathonian	Conformable	Coarse to fine clayey sandstones. Minor siltstones, carbonaceous mudstones and coals	Low resistivity, increased spontaneous potential and higher gamma values to the underlying Hutton Sandstone. Rare density kicks to low values	Up to 95 m (312 ft)	Low energy, fluviatile, swamps	Difficulty in differentiating the formation from the Walloon Coal Measures. Not regionally extensive. Higher volcanic detrital content compared to the Hutton Sandstone
Durabilla Formation	Middle Jurassic	Conformable	Medium to fine grained interbedded sandstone, siltstone and mudstone and rare thin coal beds	High peaks on the resistivity log and increasing gamma values up-strata. Difficult to differentiate on wireline logs from the Eurombah Formation and the Taroom Coal Measures	Up to 120 m (394 ft)	Low energy, fluviatile, swamps	Defined as occurring between the Hutton Sandstone or the Eurombah Formation. Widespread and lithologically distinct in comparison to the Hutton Sandstone, Eurombah Formation and the Taroom Coal Measures
Walloon Coal Measures	Aalenian to Callovian	Conformable	Medium to fine-grained sub lithic to feldspathic arenites. Siltstones, mudstones, carbonaceous mudstones, tuffs and coals. Rare oolitic ironstones	Base defined as the highest resistivity peak at the top of the Hutton Sandstone. Exhibits Low resistivity values and noisy sonic with slow velocities. High gamma values throughout with bell shaped and serrated responses. Regular kicks to low density values	Up to 919 m (3015 ft)	Low energy, fluviolacustrine with swamps	Difficult to distinguish subunits and/or members. Sandstones predominantly volcanilithic in composition (andesitic)

Formation	Biostratigraphic age	Stratigraphic relationship with underlying formation	Lithology	Wireline log characteristics	Thickness	Depositional setting	Other
Taroom Coal Measures	Early to Middle Jurassic	Conformable	Fine grained sandstones, mudstones, siltstones and coals	Not defined in the literature	Up to 180 m (590 ft)	Low energy, fluviolacustrine with swamps	The lower boundary defined by Condamine seam and the upper boundary defined by the Auburn seam. Contains 3 coal intervals. An additional member, the Condamine Sandstone, is sometimes used
Tangalooma Sandstone	Middle Jurassic	Conformable	Fine to medium grained argillaceous sandstones with siltstones, mudstones and rare coals	Not defined in the literature	Up to 100 m (328 ft)	Low energy, fluviolacustrine with swamps	Thickness as low as 10 m (33 ft). Lower base defined by the Auburn seam and the top defined by Argyle seam
Juandah Coal Measures	Early to Middle Jurassic	Conformable	Fine grained sandstones, mudstones, siltstones and coals with a high ash content	Not defined in the literature	Up to 270 m (886 ft)	Low energy, fluviolacustrine with swamps	Similar to the Taroom Coal Measures. Defined at the base by the Argyle Seam and contains 6 coal intervals. Can be split into the lower Juandah Coal Measures, Juandah sandstone, Wealden sandstone, and upper Juandah Coal Measures
Purlawaugh Formation	Pliensbachian to Bathonian	Conformable	Fine to medium grained lithic to labile sandstone thinly interbedded with siltstone, mudstone, and thin coals. Abundant carbonaceous fragments. Occasional thin beds of flint clay	Not defined in the literature	100 m (328 ft)	Fluvial (meandering)	Superseded Ukebung and Digilah formations. Time-equivalent to the Walloon Coal Measures
Springbok Sandstone	Bathonian to Callovian	Unconformable	Fine to Coarse grained volcanic, feldspathic and quartzose sandstones. Minor pebbly quartzose sandstones, siltstones, mudstones and thin coals	High average resistivity and low gamma values. Top of the formation can be difficult to recognise in gamma logs due to an increase in the K feldspar content of sandstones	275 m (902 ft)	High energy fluvial with increasing overbank and swamp deposits up strata	Contemporary volcanism during deposition. Lower interval is known as the Proud Sandstone. Transitions into the Pilliga Sandstone to the south

Formation	Biostratigraphic age	Stratigraphic relationship with underlying formation	Lithology	Wireline log characteristics	Thickness	Depositional setting	Other
Westbourne Formation	Kimmeridgian to Tithonian	Conformable	Interbedded fine grained quartzose sandstones, siltstones, and shales	Low average resistivity and increasing gamma values up-strata	250 m (820 ft)	Lacustrine and/or lacustrine delta	Low energy back swamps and meandering streams in the Norwood Mudstone Member. Increasing proportion of sandstone to the west and south. Widespread in the Eromanga Basin.
Birkhead Formation	Bathonian to Kimmeridgian	Conformable	Fine grained lithic sandstones, siltstones and carbonaceous mudstones with some rare coals	Base defined by a shift in the baseline of the sonic log to the Hutton Sandstone. Top defined by a kick in the gamma log to high values	Up to 110 m (361 ft)	Low energy fluviolacustrine, rare swamps	Contiguous with the Walloon Coal Measures across the Nebine Ridge, brackish-marginal marine influences, diachronous

4.3.1 Birkhead Formation

Strata now referred to as the Birkhead Formation (up to 110 m (360 ft) thick and shown in Figure 4.2), were first described by Woolley (1941) in the Eromanga Basin near the town of Tambo in Queensland and was initially called the Lower Intermediate Series during the early phases of petroleum exploration. The stratigraphy was further refined by Exon (1966) who split the Lower Intermediate Series into the Hutton Sandstone and the Birkhead Formation. The Birkhead Formation comprises fine to coarse-grained sandstones with common pebble beds, siltstones, mudstones and lenticular coal beds with rare red paleosols (Swarbrick et al. 1973; Krieg et al. 1995; Alexander et al. 1996; Draper 2002).

The geographic extent of the Birkhead Formation has been redefined several times in response to seismic surveys and drilling (Alexander et al. 1996). More recent efforts have subdivided the Birkhead Formation using sequence stratigraphic concepts (e.g. transgressive surfaces) and subdividing the palynostratigraphy into six zones based on increases or high abundances of spore species within an existing palynostratigraphic framework (Price 1997; Lanzilli 2000; Gallagher et al. 2008).

The terms Birkhead Formation and the Walloon Coal Measures were used to describe rocks with similar characteristics in the Eromanga Basin and Surat Basin (Swarbrick 1973; Swarbrick et al. 1973). However, some authors recommended the term Birkhead Formation be discontinued in the Surat Basin and be replaced by the term Walloon Coal Measures because the strata contain numerous coal beds (Reeves 1947; Power and Devine 1970; Swarbrick et al. 1973).

Petrographic studies reveal that the buff colored volcanogenic sandstones of the Birkhead Formation (up to 3.7 m (12 ft) in thickness) are lithic arenites which are poorly sorted, coarse to fine grained and comprised of angular to sub-rounded grains of quartz (30 to 91%), volcanic lithics (2 to 11%) and feldspar (5 to 47 %) (Gravestock 1982; Boult 1996). Calcite, siderite and dolomite cement are present with diagenetic sericite and kaolinite filling pore spaces (Alexander et al. 1996). Tourmaline, pyroxene, biotite and zircon are

present in trace amounts (Alexander et al. 1996). Grains with a poikilitic texture are used to infer the sediments were derived from felsic volcanoes (Boult 1996).

4.3.2 Walloon Coal Measures

The Walloon Coal Measures (Figure 4.2) consist of up to 919 m (3015 ft) of sandstone, siltstones, mudstone, coal and tuffs with minor calcareous sandstone, impure limestone and ironstone (Goscombe and Coxhead 1995; Jell 2013). The strata were first studied by Cameron (1907) who described Jurassic coal-bearing strata in the Ipswich-Rosewood coalfield of the Clarence-Moreton Basin as the “Walloon Beds”. The term “Walloon” was also used by Jensen (1921) and Reeves (1947) who briefly described coal-bearing strata around Roma in the Surat Basin (Figure 4.3). Whitehouse (1954) designated a type section for the Walloon Coal Measures near the township of Walloon in the Clarence-Moreton Basin but it was not fully described until investigations by and Fielding (1993).

The stratigraphic subdivision of the Surat Basin was formalized by Exon (1966) and later by Swarbrick et al. (1973) who subdivided the Injune Creek Group into the Walloon Coal Measures, the Springbok Sandstone, and the Westbourne Formation (Figure 4.2). Based on coring programs, Swarbrick (1973) and Swarbrick et al. (1973) suggested that the Walloon Coal Measures extend across the Surat Basin. A new transitional sandstone unit termed the Eurombah Formation (Figure 4.2) was defined between the Walloon Coal Measures and the underlying Hutton Sandstone based on lability differences of the sandstones which can be picked up on wireline logs (Swarbrick 1973; Exon 1976). Exon and Burger (1981) later incorporated the Walloon Coal Measures within their second sedimentary cycle of the Surat Basin.

Jones and Patrick (1981) renamed the Walloon Coal Measures the “Walloon Subgroup” by dividing the formation into the Taroom Coal Measures, the Tangalooma Sandstone and the Juandah Coal Measures (from oldest to youngest) based upon the distribution of coal beds and the mineralogical composition of sandstones. Terminology associated with these subunits were thought not to be appropriate by Green et al. (1997a) and recommended the

stratigraphic breakdown be discontinued as they were only a local occurrence in the northeast of the Surat Basin. Scott et al. (2004) later suggested that the subunits are identifiable based on the maceral composition of coals and overall lithological characteristics. The lateral discontinuity and variable thickness of coal beds, however, make their correlation challenging on a basin scale (Hamilton et al. 2014b). Subsequent investigations have used the subdivisions and have introduced additional, informally named subunits including the "Durabilla Formation", the "Juandah sandstone" and the "Condamine sandstone" (Scott et al. 2007; Ryan et al. 2012; Hamilton et al. 2014b).

Petrographic studies reveal the sandstones of the Walloon Coal Measures are lith-arenites derived from a volcanic terrane. These are poorly sorted, medium to fine grained and comprised of quartz and feldspar (40%) with some lithics (mostly intermediate volcanic lithics), muscovite, biotite, chlorite, and montmorillonite clay cements derived from altered feldspar grains (Exon 1976). Up to 10 tuff beds of thicknesses no greater than 1 m in thickness are present in core within this stratigraphic interval. They are commonly interbedded with coals or lacustrine mudstones in the Surat Basin and not within the fluvial channel and crevasse splay sandstones. This relationship suggests that these tuffs have remained *in-situ* from deposition through to diagenesis and are therefore not of a detrital origin. Tuffs are typically buff in colour, massive, very fine grained and commonly altered to bentonite or smectite. The lower contacts of these beds are generally sharp whilst the upper contacts are gradational or sharp. Several tuffs are partially incorporated into the matrix of the coal giving them a mottled appearance. Petrographic studies were not attempted due to the clay-rich and altered character of the tuff beds, however, Th/U vs Eu/Eu* and Nb/Th vs Eu/Eu* data obtained by Wainman et al. (2015) demonstrate that the source magmas of the zircon were both mafic and felsic and possibly sourced from bi-modal volcanics of the Marion Plateau to the east.

4.3.3 Springbok Sandstone and Westbourne Formation

The Springbok Sandstone and the overlying Westbourne Formation (Figure 4.2) have a combined thickness of up to 525 m. Little research has been done on them since they were originally defined (Exon 1966; Power and Devine 1970; Exon 1976; Green et al. 1997a). The relationship of the Walloon Coal

Measures to the Springbok Sandstone is poorly understood but is thought to mark the boundary between major sedimentary cycles (Exon 1976; Exon and Burger 1981). Many authors, including McKellar (1998) and Hamilton et al. (2014b), consider the contact to be a significant regional unconformity with erosional truncation into the underlying Walloon Coal Measures. They suggest the unconformity was created by uplift associated with a rifting event when Argoland separated from northwestern Australia *ca.* 155 Ma. Others, including Exon (1976), consider the relationship to be conformable albeit with some localized scouring. The Springbok Sandstone shares many lithological similarities with the Walloon Coal Measures including feldspathic sandstone, significant amounts of volcanic detritus and interbedded siltstone and mudstone (Exon 1966; Exon 1976; Scott et al. 2007; Jell 2013). However, coal beds have a higher inertinite content of up to 46% compared with those in the Walloon Coal Measures (Scott et al. 2007). The Westbourne Formation conformably overlies the Springbok Sandstone and comprises interbedded shale, siltstone and fine-grained quartzose sandstone with glauconitic material (Exon 1966; Jell 2013). The coal-bearing member of the Westbourne Formation in the Surat Basin is known by some authors as the Norwood Mudstone Member (Exon 1976).

4.3.4 Other stratigraphic methods and notions

Hoffmann et al. (2009) used seismic sections and well data to define three supersequences named J (for Sinemurian to Toarcian aged sequences), K (for Aalenian to Callovian aged sequences), and L (for Oxfordian to Tithonian aged sequences) which are based on nonmarine sequence stratigraphic principles developed by Shanley and McCabe (1994). In the Hoffmann et al. (2009) nomenclature, the Walloon Coal Measures form the upper part of supersequence K above seismic horizon S35 which is weak and discontinuous-to-strong. Supersequence K comprises a series of amalgamated basal sandstones of the Hutton Sandstone (interpreted as the lowstand systems tract) overlain by fining-upward sandstones with coal and laminated mudstone (transgressive and highstand system tracts) of the Walloon Coal Measures and recognised on seismic sections by strong parallel-bifurcating reflections which undulate and have no terminations. The Springbok Sandstone and overlying

Westbourne Formation of supersequence L (with similar lithological characteristics to supersequence K albeit fewer coal beds) form the base of seismic horizon S40 characterized by discontinuous reflections with rare truncation and rare onlaps. Strong horizontal and continuous reflections define the Springbok Sandstone and the Westbourne Formation in seismic sections.

The stratigraphy of the Surat Basin in New South Wales is not well defined because of the paucity of outcrops and subsurface data and is not described in detail for this study. Here the Purlawaugh Formation (and its constituent members) are thought to be transitional with the Walloon Coal Measures of Queensland close to the Coonamble Embayment in the southern part of the basin Stewart and Alder (1995). The Springbok Sandstone and the Westbourne Formation are thought to intertongue with the Pilliga Sandstone to the south (Exon 1976).

Up until now, the ages of Jurassic strata in eastern Australia and regional stratigraphic correlations were based on spore-pollen palynostratigraphy (not shown). The Walloon Coal Measures, the Birkhead Formation, the Springbok Sandstone and the Westbourne Formation span Australian spore–pollen zones APJ3.3 to APJ6.2.2 (Price 1997). This alpha-numerical scheme is based on the first appearance of a spore or pollen taxon that are ubiquitous within a zone for Carboniferous to Cretaceous strata of eastern Australia (Price 1997; Jell 2013). Detailed spore-pollen palynostratigraphic work was carried out by Burger (1994) in the Clarence-Moreton Basin, McKellar (1998) in the Surat Basin and by Sajadi and Playford (2002) in the Eromanga Basin. Challenges arising from using spore-pollen palynostratigraphy include 1) variable and changing plant communities in mires in response to base level changes; 2) the paucity of key taxa makes reliable determination of their first occurrence difficult; 3) unfavourable habitats for key biostratigraphic taxa; 4) the longevity of palynostratigraphic zones, and 5) the high variation in palynomorph species between adjacent samples (Martin et al. 2013). Precise age calibration to the international geologic time-scale is also a major challenge faced by Australian biostratigraphic schemes. Geologic ages have been assigned by studying strata with similar floral assemblages and marine fauna (including ammonites) in Asia or Western Australia which then can be tied back to age-constrained

biostratigraphic schemes in Europe or America (McKellar 1998; Riding and Mantle 2010).

4.4 Constructing a chronostratigraphic framework using air-fall tuffs and volcanogenic sandstones

4.4.1 Current challenges and solutions

The lack of basin-wide marker beds and the heterolithic character of the fluviolacustrine lithofacies pose many challenges in correlating Middle to Upper Jurassic strata in eastern Australia (Hamilton et al. 2014b; Shields and Esterle 2015). A variety of correlation techniques (Table 4.2) have been employed including chemostratigraphy, biostratigraphy, and lithostratigraphy, yet many of these schemes are poorly defined or only are useful on a local-scale (McKellar 1998; Scott 2008; Martin et al. 2013; Hamilton et al. 2014b; Shields and Esterle 2015). We introduce the correlation of age-equivalent volcanic tuff beds and volcanogenic sandstones using high-precision U-Pb zircon CA-TIMS geochronology and builds upon earlier work by Wainman et al. (2015). CA-TIMS has a 95% confidence interval better than 0.1% (e.g., an error of ± 0.16 Ma on a 160 Ma U-Pb date) and can accurately record the crystallization age of volcanic zircon selected with the assistance of cathodoluminescence (CL) images (Crowley et al. 2007). This method takes advantage of the widespread geographical distribution of tuff and volcanogenic sandstone beds across the Eromanga, Surat and Clarence-Moreton basins (Boult 1996; Yago 1996b).

Table 4.2. Stratigraphic correlation techniques utilized in correlating Middle to Upper Jurassic strata of eastern Australia from the literature (McKellar, 1998[1]; Hoffmann et al., 2009[2]; Martin et al., 2013[3]; Hamilton et al., 2014b[4]; Shields and Esterle, 2015[5]).

Correlation technique utilized in the Surat and Clarence-Moreton basins	Benefits	Drawbacks
Lithostratigraphy[4,5]	Thousands of open access wireline logs available at <1 km spacing Low cost and fast	Complex facies architecture (thin and discontinuous strata) makes correlations challenging and open to interpretation Lack of reliable datums to hang correlations on Disagreement between many authors on distinguishing subunits of the Walloon Coal Measures and the Springbok Sandstone
Biostratigraphy[1,3]	Distinctive palynological assemblages of coal seams One accepted scheme (Price 1997) utilized by the majority of petroleum companies Higher resolution scheme defined by McKellar (1998) available Allows for inter-basinal correlation Provides reliable datums in nonmarine settings	Low turnover of spore-pollen taxa does not allow does not allow for a high resolution stratigraphic breakdown in comparison to dinocysts Only 4 palynostratigraphic units defined between the Bathonian and the Tithonian in the literature Uncalibrated to the international geologic timescale Rarity of key taxa Time consuming Facies controlled
Chemostratigraphy[3]	Characterisation based upon the inorganic geochemistry of strata Geochemical changes should be coeval between units Overcomes issues of barren intervals encountered in biostratigraphy Low cost and fast	Geochemical changes may only occur on a local scale May require complex analytical methods to deduce trends Results open to interpretation No chemostratigraphy undertaken in the Clarence-Moreton Basin

Correlation technique utilized in the Surat and Clarence-Moreton basins	Benefits	Drawbacks
Sequence Stratigraphy[2]	Relies on correlating regional chronostratigraphic surfaces. More reliable than lithostratigraphy Many accepted models can be applied in the Surat Basin	May require seismic sections, of which many are 2D, vintage or limited in extent across the Surat Basin Supersequence K covers the Hutton Sandstone to the Walloon Coal Measures The lack of reliable datums to hang cross-sections on Utilization of HST, SB, LST and TST may be unsuitable in the nonmarine realm (depositional changes may not be driven by eustatic sea-level change on a regional scale) The current scheme mirrors the lithostratigraphic framework

4.4.2 Methodology

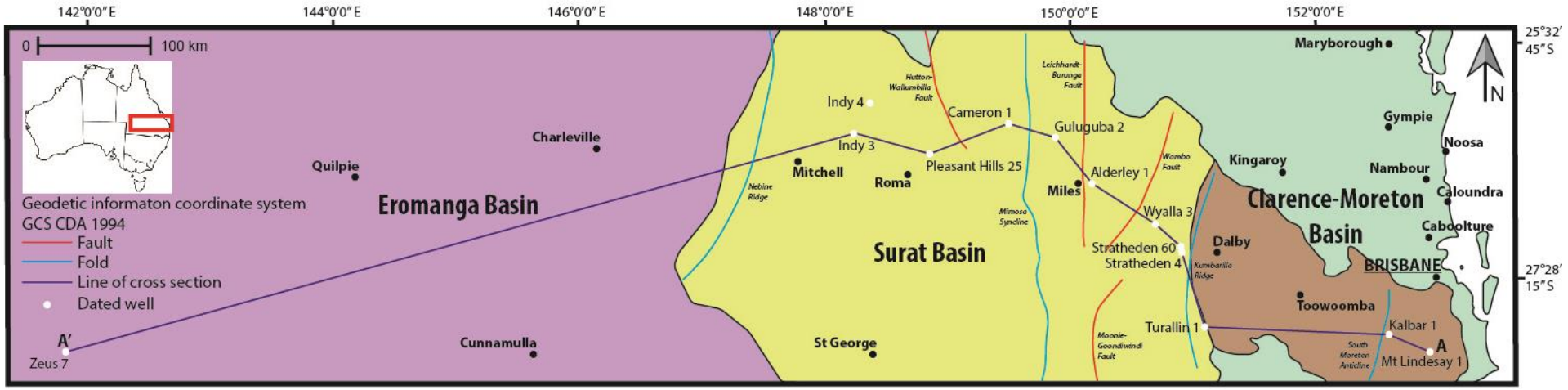

Figure 4.3. Map of the study area showing the location of geologic structures and the line of cross-section for this study showing the 13 wells from which samples were collected for dating. Partially adapted from Ryan et al. (2012).

To develop a chronostratigraphic framework for the Middle and Upper Jurassic of eastern Australia, thirteen wells (Figure 4.3) were investigated across the three basins. One hundred and nine tuffs and six volcanogenic sandstones were sampled from lithostratigraphic units interpreted as the Eurombah Formation, Walloon Coal Measures, Birkhead Formation, Springbok Sandstone and the Westbourne Formation from well completion reports for age dating. Well site geologists who initially picked these formations in the thirteen wells during drilling campaigns used stratigraphic frameworks devised by McKellar (1998) or Scott et al. (2004) and based their stratigraphic interpretations on notable changes in lithology (clean quartzitic sandstones of the Springbok Sandstone to clay-rich sandstones and interbedded siltstones, mudstones and coals of the Walloon Coal Measures), drilling rate (generally slower for the Eurombah Formation) and a sharp SP break and/or a reduced gamma signature (from the Eurombah Formation into the Hutton Sandstone) e.g. Oberhardt (2008).

Fifty-seven tuff and two volcanogenic sandstone beds were subsequently selected for heavy mineral separation using standard techniques at Boise State University. Thirty-two samples, including the two volcanogenic sandstones and two tuffs dated by Wainman et al. (2015), yielded zircon suitable for CA-TIMS dating. For the tuffs, this was based on their morphology (sharply faceted) and internal zoning (homogeneous and lacking inherited cores) from CL images (Figure 4.4), both of which suggest a volcanic origin and deposition by air-fall owing to the lack of abrasion and the lack of transport. For the volcanogenic sandstones, this was based on morphology (a sizable portion of the grains are sharply faceted) and LA-ICPMS dates (discussed below) that show a large population of young Jurassic grains. These characteristics and the immaturity of the sandstones suggest that deposition was proximal to the volcanic source area or the location of volcanic fallout.

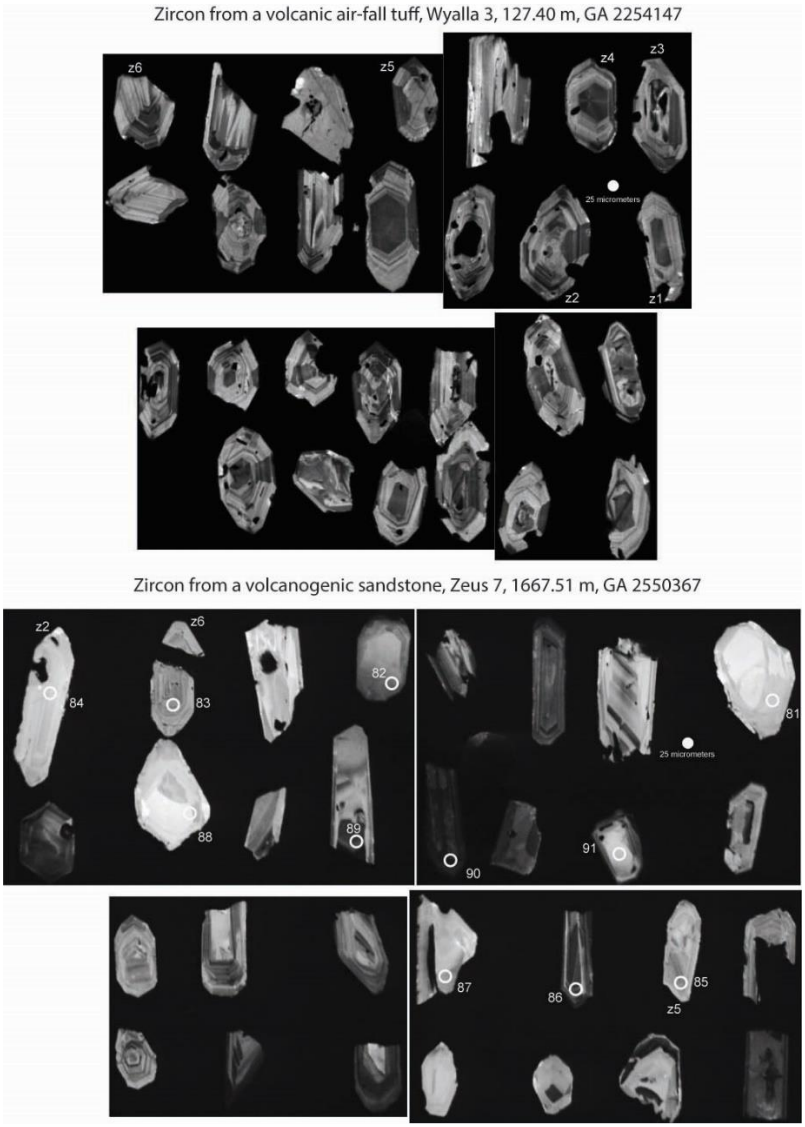

Figure 4.4. Cathodoluminescence images (CL) of zircon selected for dating from volcanic air-fall tuff (Wyalla 3 well, 127.40 m (408’14”), Geoscience Australia sample number 2254147) and volcanogenic sandstone beds (Zeus 7 well, 1667.51 m (5470’83”), Geoscience Australia sample number 22550367). Zircon grains dated using laser ablation inductively coupled plasma mass spectrometry (LA-ICPMS) methods are marked with circles and zircon grains dated using CA-TIMS are labelled as z numbers.

Ten samples (including the two tuffs from Wainman et al. (2015) and both sandstone samples) required U-Pb dating by laser ablation inductively coupled plasma mass spectrometry (LA-ICPMS) to discriminate between young volcanic zircon, and older zircon that were inherited in the magma chamber or detrital grains thereby increasing the probability of dating young grains by CA-TIMS.

LA-ICPMS was done at Boise State University using methods outlined in appendices 1 and the results are in Table 1, supplementary material as AAPG Datashare 79. Two of the tuff samples were deemed unsuitable for CA-TIMS because zircon was found to substantially predate deposition. The two volcanogenic sandstones were considered suitable for CA-TIMS because LA-ICPMS dates that overlapped with the assumed depositional age were obtained from ~20% the grains (Figure 4.5).

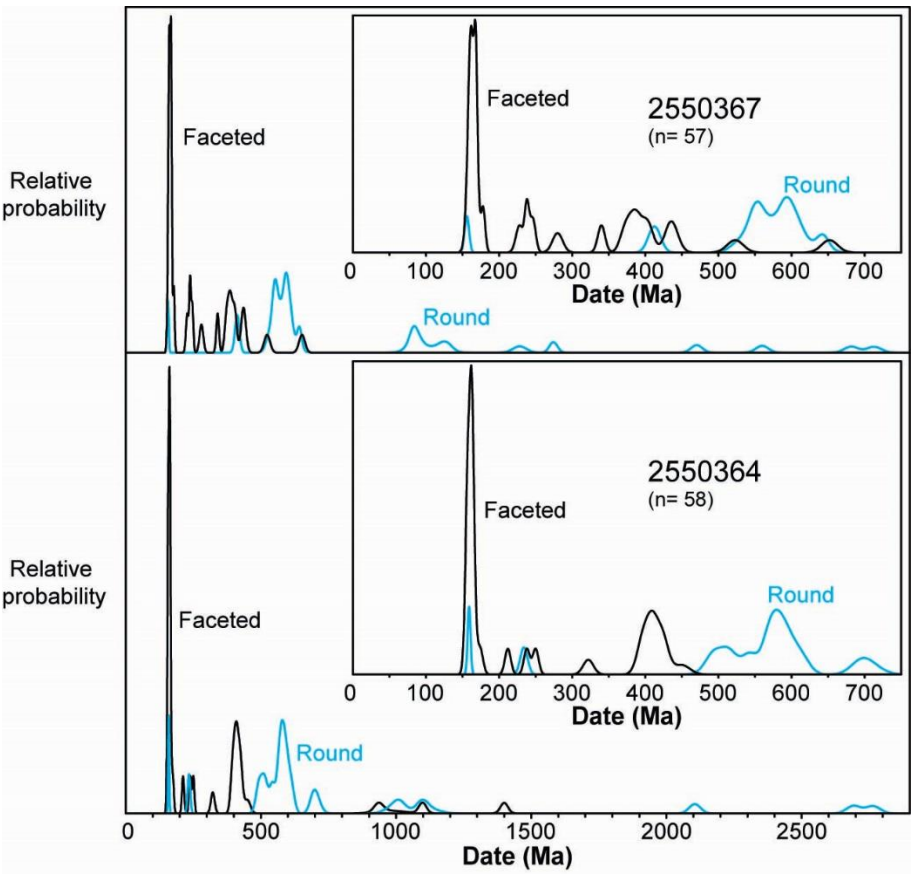

Figure 4.5. Probability density plots of LA-ICPMS U-Pb zircon dates from volcanogenic sandstones from Zeus 7 from 1659.03 m (5443’01”) to 1659.31 m (5443’93”) (2550364) and 1677.31 m (5502’98”) to 1677.51 m (5503’64”) (2550367). n= number of grains.

4.4.3 U-Pb CA-TIMS results

CA-TIMS of thirty samples was done at Boise State University, including two obtained by Wainman et al. (2015). Dates from the Stratheden 4 well were altered slightly since the publication of Wainman et al. (2015) owing to an improved understanding of the U blank (contamination). The data, CL images,

and a sample-by-sample description of the results and methods are available in appendices 2 and in the supplementary material as AAPG Datashare 78. Weighted mean $^{206}Pb/^{238}U$ dates are summarized in Table 4.3 and Figure 4.6 with errors given at 2σ. An average of 8 grains per tuff or volcanogenic sandstone were analyzed, with the age of deposition being interpreted from an average of 5 grains per sample. In eight of the tuff samples, all analyzed grains yielded age-equivalent dates (i.e., probability of fit >0.05). For these samples, weighted mean $^{206}Pb/^{238}U$ dates were calculated from all dates using Isoplot 3.0 (Ludwig 2003) and interpreted as the ages of tuff deposition. For 21 of the remaining 22 tuff and volcanogenic sandstone samples, weighted mean $^{206}Pb/^{238}U$ dates were calculated from age-equivalent dates (i.e., probability of fit >0.05) that are at the young end of the age spectra and interpreted as the ages of tuff deposition, or for the case of the volcanogenic sandstones, interpreted as the maximum age of deposition. The older dates are interpreted as being from detrital grains, grains that had extended residence histories in the magma chamber, or grains that were inherited into the magma chamber. For one sample in which there are no age-equivalent dates (GA 2390012), the youngest analysis is considered the maximum age of deposition. The fact that weighted mean U-Pb dates from each well obey the laws of superposition demonstrates that this approach to interpreting complex zircon populations is valid.

Table 4.3. U-Pb CA-TIMS dates from 13 wells utilized for stratigraphic correlation in the Eromanga, Surat and Clarence-Moreton basins including CA-TIMS dates from Wainman et al. (2015) which are labelled with a star. Each dated tuff and volcanogenic sandstone bed is assigned a Geoscience Australia (GA) sample number.

GA sample number	Well	Depth from (m)	Depth to (m)	Depth from (ft)	Depth to (ft)	Age (Ma)	Age Error (+/- Ma)	Number of dates in weighted mean	Number of dates	Mean Square of Weighted Deviates	Probability of fit	Comment
2389974	Mt. Lindesay 1	151.30	151.23	496'39"	496'16"	**155.38**	0.07	5	6	1.4	0.23	From the Clarence-Moreton Basin. Older date at 155.9 Ma
2233282	Kalbar 1	400.67	400.50	1314'53"	1313'97"	**167.56**	0.06	4	10	2.2	0.08	From the Clarence-Moreton Basin. 6 older dates are up to 168.3 Ma
2254136	Turallin 1	185.66	185.37	609'12"	608'17"	**164.74**	0.04	6	6	0.3	0.91	All 6 dates are age equivalent
2180600	Stratheden 4*	396.46	396.41	1212'14"	1211'97"	**162.54**	0.05	7	10	0.6	0.74	3 older dates at 162.8, 169.9 and 171.2 Ma
2231585	Stratheden 4	209.87	209.62	688'55"	687'73"	**159.69**	0.04	6	6	1.0	0.41	All 6 dates are age equivalent
2180601	Stratheden 4*	183.04	182.84	600'52"	599'57"	**158.86**	0.04	6	6	1.5	0.18	All 6 dates are age equivalent
2231590	Stratheden 60	477.70	477.64	1567'26"	1567'10"	**168.07**	0.07	3	12	1.7	0.18	Other dates are slightly older (168.3-169.3 Ma) and 1 is much older (173.0 Ma)
2231589	Stratheden 60	342.31	342.24	1064'00"	1063'78"	**162.18**	0.06	5	9	1.1	0.37	Older dates are up to 162.7 Ma
2231588	Stratheden 60	247.66	247.61	812'53"	812'37"	**160.54**	0.12	2	9	1.3	0.25	3 dates are slightly older (161.0, 161.2 and 162.1 Ma), 2 are ~171 Ma, 1 is 197 Ma, and 1 is 343 Ma
2254143	Stratheden 60	212.55	212.50	397'34	697'18"	**160.45**	0.05	7	9	1.5	0.18	7 youngest of 9 grains. 2 others are slightly older up to 160.9 Ma
2254141	Stratheden 60	136.11	135.86	446'56"	455'73"	**159.02**	0.04	6	6	1.8	0.10	All 6 dates are age equivalent
2254151	Wyalla 3	345.60	345.54	1163'85	1133'66"	**163.16**	0.06	4	10	0.5	0.72	6 older dates at 163.4 to 166.1 Ma
2254147	Wyalla 3	127.40	127.30	417'98"	417'65"	**159.67**	0.04	6	6	2.2	0.05	All 6 dates are age equivalent

GA sample number	Well	Depth from (m)	Depth to (m)	Depth from (ft)	Depth to (ft)	Age (Ma)	Age Error (+/- Ma)	Number of dates in weighted mean	Number of dates	Mean Square of Weighted Deviates	Probability of fit	Comment
2254165	Alderley 1	402.76	402.68	1321’39	1321’13”	**163.08**	0.05	6	9	0.5	0.78	3 other dates are equivalent at 163.4- 163.5 Ma
2254160	Alderley 1	156.17	156.13	512’36”	512’24”	**157.55**	0.05	5	10	1.8	0.13	5 older dates at 157.7 to 160.0 Ma.
2254159	Alderley 1	135.29	135.24	443’86”	433’70”	**152.99**	0.06	3	10	0.6	0.55	Older dates are 154.0, 154.1, 156.4, 162.8, 162.8, 164.6, and 181.4 Ma
2233310	Guluguba 2	509.43	509.40	1671’36”	1671’25”	**165.93**	0.05	6	9	1.6	0.17	Older dates between 169.4 and 519.2 Ma
2233308	Guluguba 2	428.57	428.51	1406’07”	1405’67”	**163.05**	0.05	5	6	0.9	0.46	Older date at 163.4 Ma
2233302	Guluguba 2	404.23	404.16	1326’21”	1325’98”	**162.40**	0.04	6	8	1.5	0.19	2 older dates at 162.7 and 162.9 Ma
2233298	Guluguba 2	279.15	279.11	915’84”	915’72”	**159.92**	0.06	4	7	1.5	0.23	3 older dates are age equivalent at 160.2 Ma
2233290	Guluguba 2	162.10	162.03	531’84”	531’59”	**157.97**	0.08	4	13	2.1	0.10	6 older dates agree at 159.0 Ma and 1 at 163.2 Ma. 1 grain with a Proterozoic core (678.6 Ma)
2389991	Cameron 1	221.40	221.30	726’38”	726’00”	**157.70**	0.05	5	5	0.3	0.88	5 dates are age equivalent
2390012	Pleasant Hills 25	512.20	512.07	1680’45”	1680’02”	**<151.39**	0.12	N/A	N/A	N/A	N/A	No dates are equivalent. 4 older dates at 162.1, 164.6, 166.5, and 197.9 Ma
2390007	Pleasant Hills 25	335.08	335.00	1099’34	1099’08”	**150.77**	0.06	7	8	2.0	0.06	1 older date at 151.1 Ma
2233272	Indy 4	202.00	201.59	662’73”	661’38”	**152.90**	0.07	4	6	1.8	0.14	2 older dates at 157.4 and 188.1 Ma
2254172	Indy 3	159.76	159.57	525’52”	524’15”	**150.11**	0.04	5	5	1.2	0.31	5 dates are age equivalent
2254170	Indy 3	140.38	139.97	460’57”	459’22”	**149.78**	0.06	6	8	1.0	0.41	2 older dates at 160.8 and 190.1 Ma
2254169	Indy 3	104.62	104.40	343’24”	342’52”	**149.08**	0.06	6	6	1.1	0.36	6 dates are age equivalent
2550367	Zeus 7	1677 .51	1677 .31	5503’64”	5502’98”	**162.39**	0.06	3	7	2.5	0.08	4 older dates up to 169.8 Ma
2550364	Zeus 7	1659. 31	1659. 03	5443’93”	5443’00”	**161.11**	0.05	4	8	0.8	0.47	4 dates are age equivalent

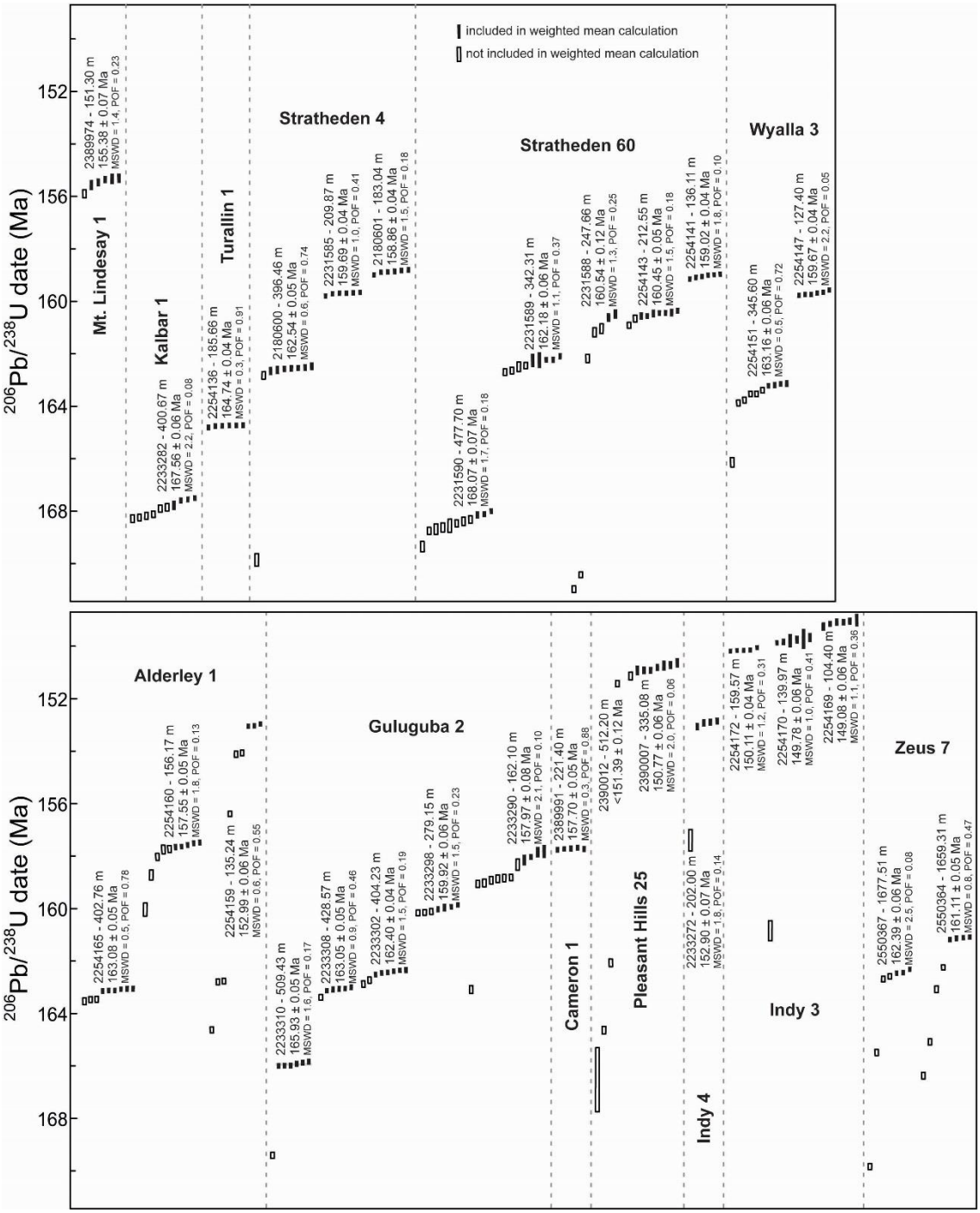

Figure 4.6. Plot of CA-TIMS $^{206}Pb/^{238}U$ dates from single grains and fragments of zircon. Samples are grouped by well (from east to west) and in stratigraphic order. Plotted with Isoplot 3.0 (Ludwig 2003). MSWD = Mean Square of the Weighted Deviates. POF = Probability of Fit. Error bars are at the 2 sigma (2σ) confidence interval. Eleven older dates are not shown.

4.4.4 The chronostratigraphic framework

To develop a stratigraphic framework, chronostratigraphic datums on a cross-section were defined consisting of strata that are approximately coeval: that is, within between 90 and 420 ka as defined by zircon dating (Table 4.4, Figure 4.3). The 13 wells with zircon age control are spaced at intervals of between 3 km (1.9 mi) and 680 km (423 mi) across the three basins. Using Schlumberger's Petrel stratigraphy module, wireline logs (gamma, density, and neutron) from 677 additional wells (Figure 4.7) were used to correlate chronostratigraphic datums and their correlative surfaces across the basins. Except for Kalbar 1, Mt Lindesay 1 and Zeus 7, the remaining 674 wells are in the Surat Basin. To enable correlations of these datums to undated wells, the optimal spacing between wells for the successful correlation of coal beds was determined. Density logs, which easily highlight the unusually low density of coal beds, were particularly useful for local stratigraphic correlation. Coal zones (several closely spaced coal beds) were identified from density logs and correlated to other wells in all directions from three wells for the correlation exercise: Stratheden 4 in the eastern Surat Basin, Berwyndale South 10 in the northern Surat Basin, and Combabula 1 in the western Surat Basin. If the coal zone could not be identified, the correlation was discontinued in that orientation. The maximum distance of any given correlation along any given azimuth was recorded and plotted on a chart of coal zone thickness against lateral extent (Figure 4.8). Where possible, well spacing was kept to <5 km (3.1 mi) to ensure confidence in well correlation as 70% of coal zones cannot be successfully correlated beyond this distance. Correlations into the Eromanga and Clarence-Moreton basins, however, were based solely on the age of tuff beds and volcanogenic sandstones. It should be noted that the position of chronostratigraphic datums these wells are estimated due to the distance between dated wells which is commonly >5 km and typically greater than the distance a coal zone can be correlated for with confidence in the subsurface.

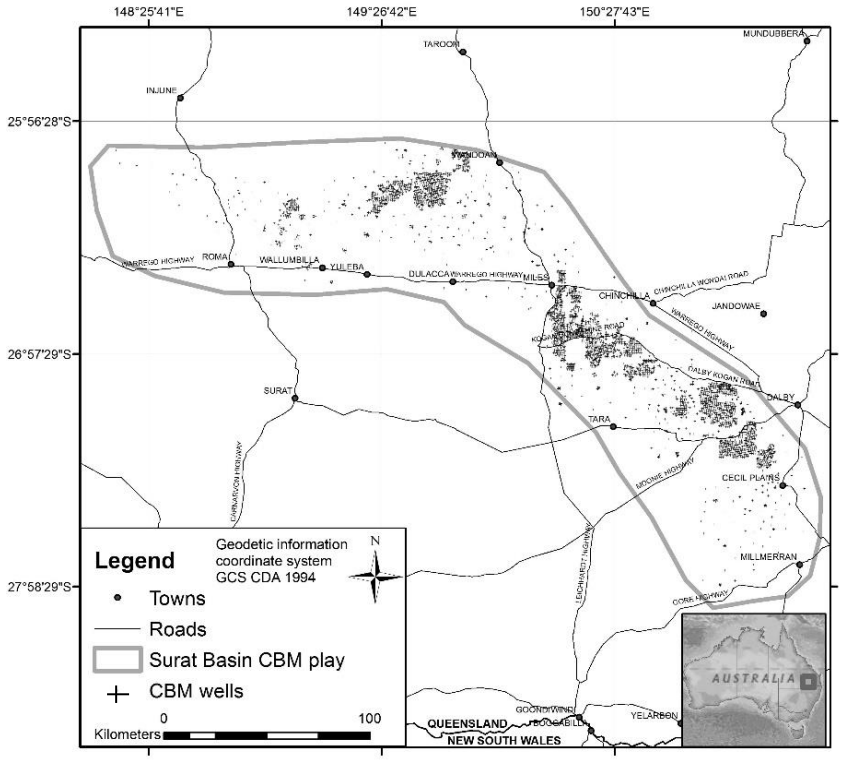

Figure 4.7. The location of coal bed methane wells correlated for this study in the Surat Basin using wireline logs. The location of the Kalbar 1, Mt Lindesay 1 (Clarence-Moreton Basin) and Zeus 7 (Eromanga Basin) wells are not included in this figure.

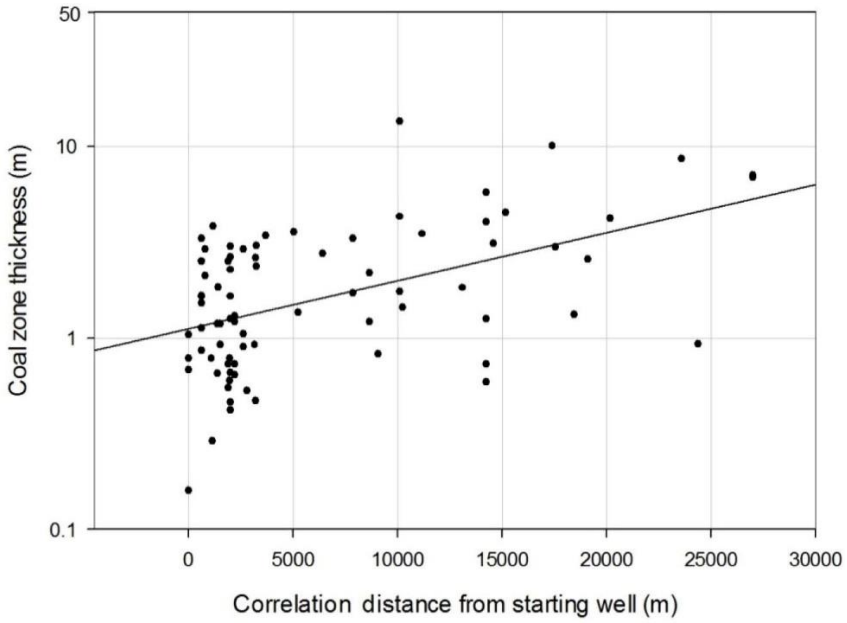

Figure 4.8. The relationship between coal zone thickness and their lateral continuity in Middle to Upper Jurassic strata, Surat Basin.

Table 4.4. Regional chronostratigraphic datums defined using CA-TIMS dates in the Middle to Upper Jurassic strata of eastern Australia.

Regional chronostratigraphic datums	Wells with age equivalent tuff and volcanogenic sandstone beds	Time interval
163.05 -163.16 Ma	Wyalla 3, Alderley 1 and Guluguba 2	110 ka
162.18 -162.54 Ma	Stratheden 4, Stratheden 60, Guluguba 2 and Zeus 7	360 ka
159.67 -159.92 Ma	Stratheden 4, Wyalla 3 and Guluguba 2	250 ka
157.55 -157.97 Ma	Alderley 1, Guluguba 2 and Cameron 1	420 ka
152.90 -152.99 Ma	Alderley 1 and Indy 4	90 ka

Five of the chronostratigraphic datums extend for hundreds of kilometers across eastern Australia as shown in Figure 4.9. Eight other chronostratigraphic datums were extrapolated and constrained where possible by age controls. In the southern and western Surat Basin, the shortage of tuff dates and reduced well density increased the uncertainty of correlations in these regions based on wireline log signatures. To the southeast, Upper Jurassic strata are absent due to post-Cretaceous uplift, incision and erosion. The correlation of strata younger than 158.86 Ma in the eastern Surat Basin was not possible due to the casing of wells or erosion above the interval termed the Walloon Coal Measures. Many wells did not penetrate strata younger than ~163 Ma in the Surat Basin.

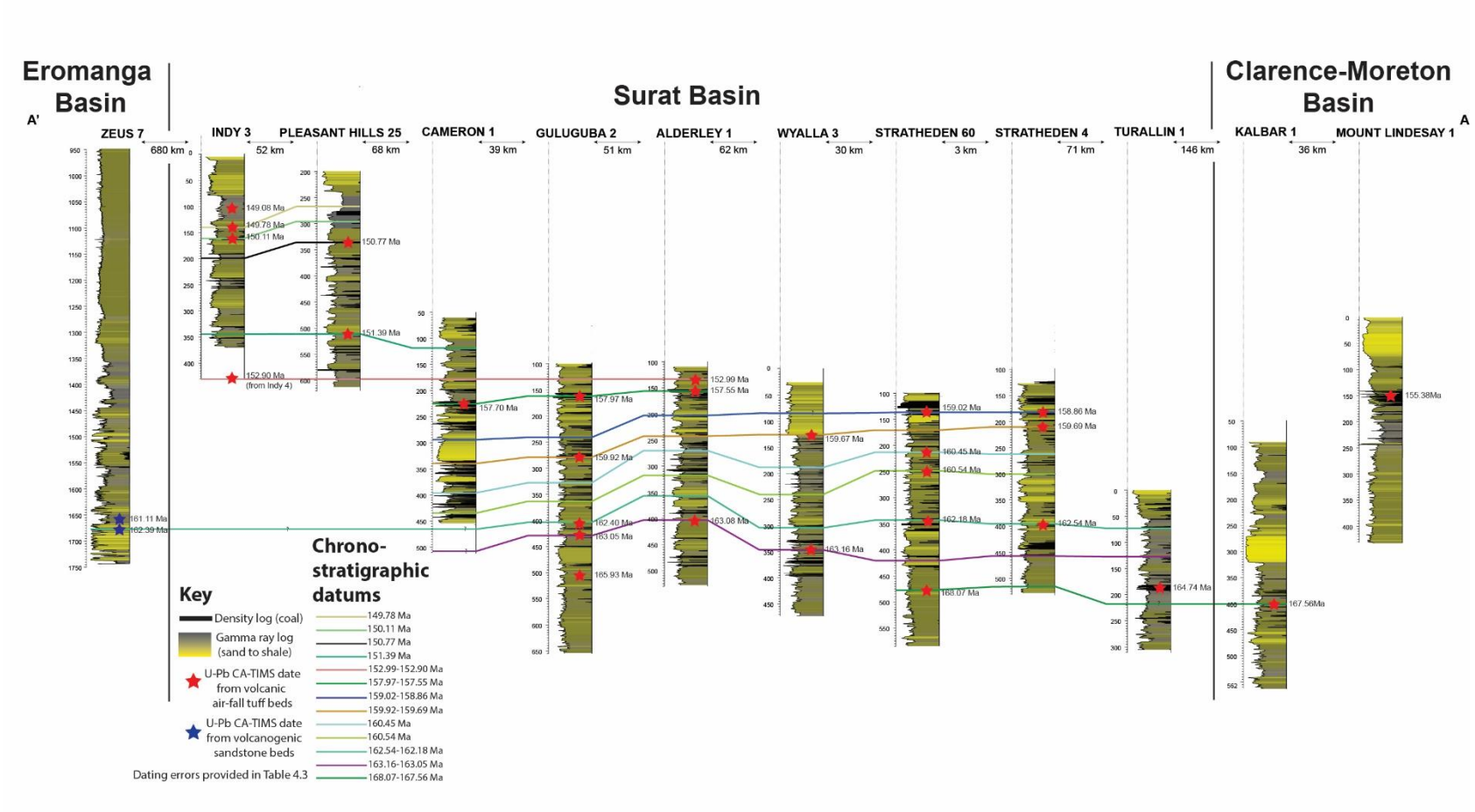

Figure 4.9. A chronostratigraphic framework for Middle to Upper Jurassic strata across the Eromanga, Surat and Clarence-Moreton basins based on U-Pb CA-TIMS dates of volcanic air-fall tuff and volcanogenic sandstone beds. Dating errors are shown in Table 4.3. The location of the wells in the cross-section are shown in Figure 4.3.

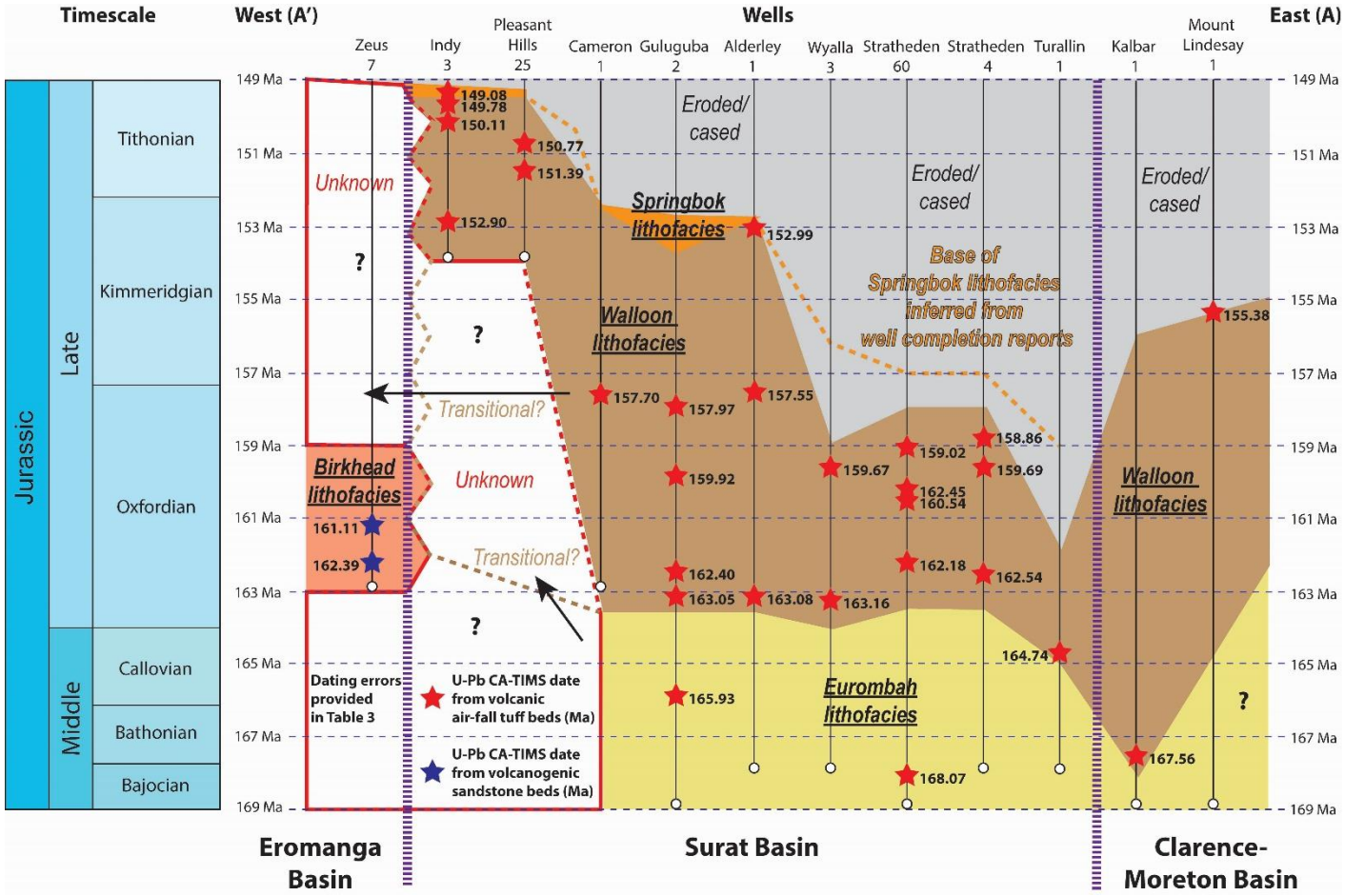

Figure 4.10. A Wheeler diagram showing the distribution of Eurombah, Walloon, Birkhead and Springbok lithofacies across eastern Australian basins during the Middle to Late Jurassic. Timescale by Gradstein et al., (2012). The location of wells is shown on Figure 4.3. Dating errors are shown in Table 4.3.

4.5 New stratigraphic interpretations

The newly defined chronostratigraphic framework as defined by zircon dates provides insights into the Middle to Upper Jurassic coal-bearing strata on a regional scale (Figures 4.9 to 4.10) which have not been elucidated by traditional correlation techniques. We use the terms “Eurombah lithofacies”, “Walloon lithofacies”, “Birkhead lithofacies” and “Springbok lithofacies” to describe lithological associations commonly ascribed to the respective formations.

The first is the variation in age of the coal-bearing “Walloon lithofacies” between the Clarence-Moreton and the Surat basins and its subsequent transition into sandier “Birkhead lithofacies” of the Eromanga Basin from the Wheeler Diagram in Figure 4.10. Previous studies by Yago (1996b) and Pinder (2004) had assumed “Walloon lithofacies” were coeval. CA-TIMS dates from the Kalbar 1 (167.56 ± 0.06 Ma) and Mount Lindesay 1 (155.38 ± 0.07 Ma) wells in the Clarence-Moreton Basin and the Turallin 1 (164.74 ± 0.04 Ma) and Stratheden 60 (168.07 ±0.07 Ma) wells in the Surat Basin indicate that coal accumulation did not begin simultaneously on a regional scale and that the duration of coal (peat) accumulation between the two basins was different. CA-TIMS dates from Zeus 7 well (162.39 ± 0.06 and 161.11 ± 0.05 Ma) support the lateral transition of coal-bearing “Walloon lithofacies” into the sandier “Birkhead lithofacies” in the western Surat Basin and Eromanga Basin (Swarbrick et al. 1973). Coal-bearing lithofacies in the Queensland sector of the Surat Basin are similar in age to the Talbragar Fish Bed (151 ± 4.27 Ma) in the Surat Basin of New South Wales near Gulgong (Turner et al. 2009). This age from the sensitive high mass-resolution ion microprobe (SHRIMP) raises the interesting possibility for long distance correlation of strata between different areas of the Surat Basin where there is a paucity of wireline logs.

Secondly, in the Pleasant Hills 25, Indy 3 and Indy 4 wells of the western Surat Basin, no dates older than 152.90 Ma were determined despite the abundance of coal-bearing lithofacies in these wells (Figures 4.9 and 4.10). In the northern and eastern Surat Basin, by contrast, dates range from 168.07 ± 0.07 to 152.99 ± 0.06 Ma. This demonstrates disparities in the age in what has been termed the “Walloon lithofacies” and the “Springbok lithofacies” across the basin

despite hosting similar lithofacies. Although 200 m (656 ft) of coal-bearing Walloon lithofacies are present in the western Surat Basin (similar to the Walloon lithofacies in the classic areas of the eastern Surat Basin), there may be older coal resources that have yet to be discovered in this part of the basin.

Thirdly, previous workers have suggested a major unconformity (the “Springbok unconformity”) between the Walloon Coal Measures and the Springbok Sandstone (Figure 4.2). The Springbok unconformity in the Surat Basin is inferred from a break between the Birkhead Formation and the Adori Sandstone in the Eromanga Basin and incision of the Walloon Coal Measures in the eastern Surat Basin by the overlying Springbok Sandstone (Green et al. 1997a; Scott 2008). Zircon dates from the Indy 3 well do not indicate a major time break between “Walloon lithofacies” and the “Springbok lithofacies” at 138 m – there is < 700 ka between dates in the two facies. The “Springbok lithofacies” lies closely above the “Walloon lithofacies” in all the wells, as indicated by well completion reports and geologic maps, and we consider it likely that the transition between the two facies is diachronous as suggested in Figure 4.10. However, there is a notable ~4.5 Ma difference in ages in the Alderley 1 well between 156 m (512 ft) and 135 m (443 ft). This 21 m (69 ft) thick interval is entirely comprised of “Walloon lithofacies” and exhibits no indicators of an unconformity such as paleosol development, juxtaposed lithofacies, pebble lags or lithological indicators suggesting a fall in base-level. The interval was clearly deposited under a relatively low rate of creation of accommodation and it is possible that elsewhere in the basin there was a fall in base level during the Late Jurassic. If that were the case the “Springbok unconformity” may be a compound feature created by two or more base level drops over time. The diachronous nature of the lithofacies is also evident with the inconsistent picking of “Eurombah lithofacies” (168.07 ± 0.07 Ma in the Stratheden 60 well to >152.90 ± 0.07 Ma in the Indy 3 well) from wireline logs in comparison to chronostratigraphic principles.

Fourthly, there is a noticeable thinning of strata (~90 m or ~295 ft) between the 163.16-163.05 Ma and 159.02-158.86 Ma chronostratigraphic datums from the Stratheden 4 well in the east to Guluguba 2 well in the west (Figure 4.9). This demonstrates that there was a significantly higher rate of subsidence east of

the Leichhardt-Burunga, Wambo, and Goondiwindi-Moonie Faults (Figure 4.3). Waschbusch et al. (2009) also noted stratigraphic thinning to the west of these faults and into the Eromanga Basin but their subsidence model was constructed without robust age controls.

Finally, this study also demonstrates the feasibility of determining the maximum depositional age of volcanogenic sandstones in the Birkhead Formation of the Eromanga Basin with a high degree of precision. Using several methods to discriminate between grains including petrography, CL imaging and LA-ICPMS dating are shown to improve the possibility of dating young zircon with CA-TIMS. If there is a high probability of fit (>0.05) and several grains yield equivalent CA-TIMS dates for any given volcanogenic sandstone sample, the maximum deposition age can be interpreted with a degree of confidence. This is novel for applications in stratigraphic correlations in Australian strata without tuffs. Zircon extracted from sandstones are usually sourced from several provenances and derived from rocks of different ages. Zircon grains from the Birkhead Formation are very fine to fine-grained and angular to rounded (see Appendices Figures 22a to 23b). The grain shapes show that some of the zircon were proximately sourced from the very small size of the grains as supported by petrography and implies that they were likely to have been transported by intermittent suspension in rivers in a low energy river system. Probability density plots (see Figure 4.5) reveal that most of the sharply faceted grains were derived from a young source area. It is probable that zircon and other rock fragments were sourced from volcanic source area to the east or deposited directly onto fluvial channels by air-fall. The maximum ages of deposition derived by CA-TIMS derived from sharply faceted zircon (euhedral) grains (162.39 ± 0.06 and 161.11 ± 0.05 Ma) in the Zeus 7 well are similar in age to tuffs in the Stratheden 4 (162.54 ± 0.05 Ma), Stratheden 60 (162.18 ± 0.06 Ma) and Guluguba 2 (162.40 Ma ± 0.04 Ma) wells. This strongly demonstrates the tuffs and the volcanogenic sandstones were deposited at around the same time.

4.6 Conclusion

The complex, heterolithic character of the fluvial sequence and channel geometries makes correlation based on fining-upward successions or individual coal beds uncertain without employing region-wide chronostratigraphic datums in the subsurface. Our results show how robust chronostratigraphic datums within time intervals of <420 ka can be constructed using precise U-Pb CA-TIMS zircon dates derived from tuffs and volcanogenic sandstones. This technique has allowed complex and heterolithic fluvial-dominated strata of the Middle to Late Jurassic in eastern Australia be correlated with confidence over thousands of kilometers across multiple basins in the absence of regional marker beds. We demonstrate coal-bearing lithofacies of the Walloon Coal Measures to be highly diachronous and transition into sandier lithofacies of the Birkhead Formation to the west. The same chronostratigraphic datums demonstrate the difficulty of identifying the sequence boundaries without chronostratigraphic data.

We also show that precise zircon dates obtained from volcanogenic sandstones can be used to ascertain the maximum age of deposition. This requires identification of zircon that did not reside for extended periods within the source area. We demonstrate that volcanogenic sandstones of the Birkhead Formation were deposited coevally with tuffs in the Walloon Coal Measures as shown by zircon dating. This highlights the possibility of extending chronostratigraphic datums into non coal-bearing nonmarine strata where tuff beds are absent and when young zircon are identified.

Better understanding of the stratigraphy of nonmarine strata can lead to new concepts for exploration. The new chronostratigraphic framework for the Walloon Coal Measures suggests, for example, that there may be deeper coals in the west of the Surat Basin that are age equivalent to those of the central and eastern Surat Basin. These could be a new target for exploration for coal seam gas resources. This study also emphasizes the notion that a stratigraphic subdivision that may be useful in a local petroleum lease area may lead to significant misconceptions if applied on a basinal scale. A better understanding of nonmarine strata can also help in the search for subtle conventional traps. The new dates for the Birkhead Formation, for example, allow construction of

paleogeographic maps that may allow better prediction of reservoirs and seals in underexplored regions. It is likely that improved chronostratigraphic frameworks for nonmarine strata in other parts of the world will help better elucidate the petroleum potential of basins.

4.7 Acknowledgements

This research was funded through several research grants and scholarships. Carmine Wainman has a Ph.D. scholarship from the University of Adelaide that has covered most of the travel and analytical costs. We are thankful to Geoscience Australia and Bob Nicoll; Cory MacNeill and Stephen Scott from Senex Energy, and Joan Esterle from the University of Queensland who provided funds that defrayed some of the costs of CA-TIMS dating. Arrow Energy, Senex Energy and the Geological Survey of Queensland's Exploration Data Centre kindly provided access to core material. ESRI provided a free academic license for ArcGIS to produce Figures 4.1 and 4.7. Schlumberger provided a free academic license for Petrel allowing for stratigraphic correlation and the production of Figure 4.9. We would also like to thank Renate Sliwa and Daren Shields from the University of Queensland who kindly who kindly provided normalized wirleline logs from eastern Australian basins. Debra Pierce and Alexandra Edwards from Boise State University assisted with mineral separation and preparation. The authors would like to thank the AAPG Editor Barry Katz as well as Rhodri Jerrett (University of Manchester), Stephen Sheppard (Curtin University) and Eugene Szymanski (Chevron) for their comments which improved the clarity and quality of the manuscript.

4.8 Supplementary papers

See appendices 2 (p. 319-349).

Statement of Authorship

Title of Paper	The relative roles of subsidence and climate on coal bed geometry: new insights from Jurassic coal-bearing strata in the Surat Basin, Australia
Publication Status	☐ Published ☐ Accepted for Publication ☐ Submitted for Publication X Unpublished and unsubmitted work written in manuscript style
Publication Details	Wainman, C.C., McCabe, P.J. In Prep-a. The relative roles of subsidence and climate on coal bed geometry: new insights from Jurassic coal-bearing strata in the Surat Basin, Australia. Intend to submit to Journal of Sedimentary Research.

Principal Author

Name of Principal Author (Candidate)	Carmine C. Wainman		
Contribution to the Paper	Majority of the data collection and interpretation. Wrote the greater majority of the paper with exceptions noted in the co-authorship contributions. Produced final version of the paper using editorial suggestions of the co-author.		
Overall percentage (%)	90		
Certification:	Majority of the data collection and interpretation. Wrote all of the paper. Produced final version of the paper using editorial suggestions of the co-author.		
Signature		Date	10/08/2017

Co-Author Contributions

By signing the Statement of Authorship, each author certifies that:

i. the candidate's stated contribution to the publication is accurate (as detailed above);
ii. permission is granted for the candidate in include the publication in the thesis; and
iii. the sum of all co-author contributions is equal to 100% less the candidate's stated contribution.

Name of Co-Author	Peter J. McCabe		
Contribution to the Paper	Supervisor of Ph.D. – Extensive critical advice and guidance on research project and editorial comments for the paper. Contributed to paragraphs 1-3 in the section titled "Scenario B: Variations due to changes in base level".		
Signature		Date	10/8/2017

Chapter 5. The relative roles of subsidence and climate on coal bed geometry: new insights from Jurassic coal-bearing strata in the Surat Basin, Australia

To be submitted to the *Journal of Sedimentary Research*. A statement of authorship is provided on the previous page.

Co-authors: Peter McCabe

Abstract

In any formation, the abundance and three-dimensional geometry of coal beds are influenced by several factors that influenced the mires in which the original peat accumulated. This includes basin tectonics and climate as well as the depositional environment. Dating of air-fall tuff beds allows a high-resolution investigation (on timescales <1 Ma) of changes to the rate of creation of accommodation through 345 m of strata of the Jurassic Eurombah Formation and Walloon Coal Measures of the Surat Basin in eastern Australia. The percentage of coal is highest at times of faster subsidence. Peat accumulation should have been able to keep pace with all the calculated rates of subsidence but the coal beds are thin (< 0.4 m) and laterally discontinuous across the basin. The nature of the coal beds appears to be a function of climatic conditions during deposition. The coals originated as peats that accumulated in mires at high latitude (>75°S) during greenhouse conditions. Despite the high latitude, the climate appears to have been warm temperate. Long winter darkness, lasting more than three months, combined with mild temperatures and minor fluctuations in climate would have been stressful on plants. High latitudes are particularly susceptible to climate change and it seems likely that relatively small changes in climate may have been enough to pass thresholds for extensive plant growth and hence mire development.

5.1 Introduction

The economic viability of coal bed methane (CBM) plays and coal mines are determined, in large part, by the thickness and lateral continuity of coal beds. An understanding of coal-bed geometries can also be important for correlation of strata in the subsurface. Relatively little is known, however, about the geologic controls on the three-dimensional geometry of coal beds. In this paper we present newly acquired, high-precision dates for volcanic air-fall tuff beds in the Jurassic of the Surat Basin in eastern Australia that provide a unique opportunity to evaluate the relative roles of accommodation creation on coal accumulation. These dates are from the Walloon Coal Measures and the upper part of the underlying Eurombah Formation (Wainman et al. 2017). We will also examine the paleolatitude at which the coal accumulated and discuss the role of paleoclimate on coal bed geometry.

The role of paleoclimate has long been recognized as the major controlling factor in determining the distribution of global coal resources (Parrish et al. 1982).The vast majority of coals formed in either the tropics (0-15° paleolatitude) or temperate zones (35-70°) which are similar to the latitudinal distribution of modern peat deposits (Gore 1983; Moore 1995). These are the latitudes where, on average, precipitation exceeds evaporation which is essential for the maintenance of an elevated peat-forming surface (Gore 1983; Moore 1995). Tectonism also appears to be an important factor in determining the preservation of coal as many major coal-bearing stratigraphic units occur in foreland basins. McCabe (1991) suggested that this was because the subsidence rates in these basins are favourable for the build-up of thick peat accumulations.

Coals are derived from peats that accumulate in mires. Mires are created by the terrestrialization of lakes or the paludification of poorly drained areas (Gore 1983; McCabe 1987; Cameron et al. 1989). However, there have been relatively few studies examining the role of allocyclic controls on coal-bed geometry. The thickness and lateral extent of a coal bed are determined by the areal extent of the original mire in which the peat (coal) accumulated, the thickness of peat accumulation and any subsequent erosion. A combination of allocyclic (processes external to the basin including climate and eustasy) and

autocyclic factors (processes internal to the basin such as channel avulsion) determine the geometry of the original peat accumulation (McCabe and Parrish 1992). For a peat to accumulate, groundwater flow and precipitation into mires must be equal to outflow, evapotranspiration and retention (Diessel 1992). The rate of peat accumulation is a function of both climate and the rate at which accommodation is created. Average peat accumulation rates today are clearly correlatable to the annual temperate and length of the growing season: rates range from 0.1 mm/yr in the high latitudes to 2.3 mm/yr in the tropics (McCabe 1984). Although raised mires may build up a few meters above the surrounding topography, thick peat (coal) accumulation requires a rise in the regional groundwater tables. The accommodation space for peat accumulation is therefore controlled by the water table which, from a depositional perspective, can be considered as base level (Moore 1995). In the short term, seasonal fluctuations in the water table control the position of the acrotelm (the upper aerobic layer with high hydraulic conductivity where growth occurs) and the catotelm (the lower anaerobic layer with low hydraulic conductivity where humification of organic matter into peat occur). Over thousands or millions of years, for example in a coastal setting, long-term rises in water table are associated with rises in relative sea-level – a function of basin subsidence and eustasy – whereas in a completely nonmarine setting long-term rises in water table are due solely to basin subsidence.

Peat accumulation must keep pace with the creation of accommodation, otherwise, the mire will drown and the peat would be overlain by lacustrine sediments in nonmarine basins and lagoonal or marine strata if in a coastal setting (McCabe 1991; Bohacs and Suter 1997). Any fall in base level would cause the peat to be lost through oxidation, possibly by wildfires (Cameron et al. 1989). Bohacs and Suter (1997) suggested that, if peat production rates exceed accommodation rates, mires would be exposed, eroded and reworked but as the former is a function of the latter this is not a realistic scenario. However, as McCabe (1991) and McCabe and Parrish (1992) noted, slow rates of creation of accommodation would require that accumulation of thick peat take place over extended periods of time and that climatic changes are more

likely to be a limiting factor to peat thickness: a change to a drier climate ending peat growth and causing degradation of earlier peat accumulations.

The ratio between the rate of organic accumulation and the rate of clastic input in a mire determines the percentage of inorganics within a peat (ash content) and whether it will eventually be preserved as a coal or a carbonaceous mudstone. The accumulation of coal will only occur in a mire that is isolated from clastic deposition for thousands of years (McCabe 1984) due to relatively infrequent inundation of sediment from flooding. Assuming a peat-to-coal compaction ratio of about 10:1 (McCabe 1984), a 1 m thick coal bed may represent the accumulation of peat over a period of between 4,000 and 100,000 years depending on the climatic regime and assuming adequate accommodation space was being created.

The relative roles of allocyclic and autocyclic controls on coal beds has long been debated. Fielding (1987), for example, suggested that factors controlling the continuity and thickness of coal beds that accumulated in deltaic and alluvial settings include regional and local variations in subsidence rates and the nature of contemporaneous siliciclastic sedimentation. Opluštil et al. (2013), by contrast, interpreted a complex interplay of tectonics and climate to explain coal bed thickness patterns in the Carboniferous of the Czech Republic and suggests that tectonic movements controlled the distribution of sedimentary environments and regional variations in accommodation whereas changes in precipitation, driven by glacial cycles, influenced coal-bed thickness and lateral continuity (Opluštil et al. 2013). This paper will attempt to determine the relative role of subsidence and climate in the accumulation of a major coal-bearing succession in the Jurassic of eastern Australia.

5.2 The Walloon Coal Measures and the tectonic setting of the Surat Basin

The Walloon Coal Measures were deposited in the Surat Basin of southeast Queensland and northeast New South Wales, Australia between the Bathonian to the Tithonian (Wainman et al. 2017). The formation (Figure 5.1) is between 350 and 500 m thick and consists of fluvial sandstones, lacustrine and overbank mudstones and coals (Jell 2013; Martin et al. 2013). The coal beds are relatively thin (mostly <0.4 m) and laterally discontinuous and in the subsurface, most coal beds are only laterally correlatable in the subsurface for less than 5 km (Wainman et al. 2017).

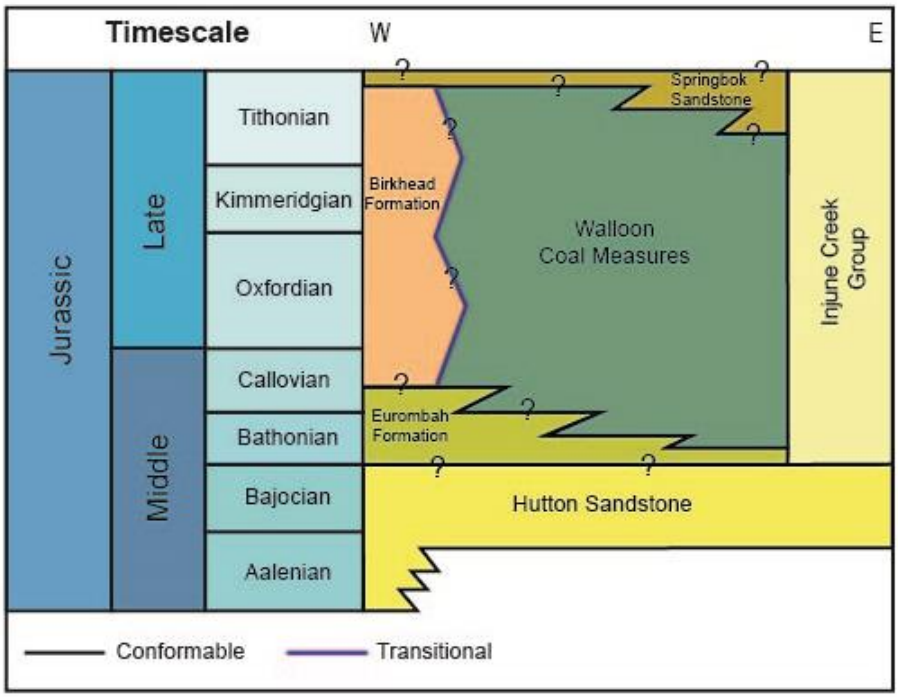

Figure 5.1. The lithostratigraphic framework of the Surat Basin adapted from Jell (2013) and Wainman et al. (2017). Deposition in the basin commenced in the Rhaetian with the Chong and Eddystone beds and ceased after deposition of the Griman Creek Formation in the Albian.

Sedimentation in the Surat Basin commenced after peneplanation in the Middle Triassic (Exon 1976; Hamilton et al. 2014b). Continental sag and lithospheric flexure ensued before basin inversion in the middle to Late Cretaceous terminated deposition in the basin (Exon 1976; Goscombe and Coxhead 1995;

Hoffmann et al. 2009; Hamilton et al. 2014b). The Surat Basin is considered to be intracratonic in origin (Fielding 1996; Martin et al. 2013), however, the driving mechanism for continental sag remains uncertain (Korsch et al. 1989; Gallagher et al. 1994; Green et al. 1997a; Korsch and Totterdell 2009b). There is debate as to whether incipient rifting or subduction off the eastern margin of Gondwanaland were controlling subsidence rates (Fielding 1996; McKellar 1998; Waschbusch et al. 2009). The Surat Basin was located in high latitudes (>75°S) during deposition of the Walloon Coal Measures, but it was a time when warm temperate conditions apparently prevailed near the South Pole (Boucot et al. 2013; Wainman et al. 2015).

5.3 Dating of volcanic tuffs

Volcanic air-fall tuff beds are common within coal beds of the Walloon Coal Measures (Yago 1996a): in any single core through the formation, there are up to ten tuff beds. Wainman et al. (2015) showed the feasibility of dating zircons in these tuffs to within +/- 40,000 years using the U-Pb CA-TIMS (chemical abrasion isotope dilution thermal ionization mass spectrometry) technique. The abundant volcanic tuff beds in the Walloon Coal Measures provide a special opportunity to investigate depositional rates in coal-bearing strata.

Two exploration wells were chosen for this study: Stratheden 4 (27°11'58"S, 151°01'04"E) and Stratheden 60 (27°10'28"S, 151°00'52"E). These two wells are located near the town of Dalby in the eastern Surat Basin (Figure 5.2). Together the wells provide a continuous cored stratigraphic section; from the underlying Hutton Sandstone and into the Eurombah Formation, through the Walloon Coal Measures and up to the unconformity with the overlying Springbok Sandstone. The two wells are only 2.79 km apart and coal beds can be correlated between the two wells with a high degree of confidence (see Figure 4.9). The geographic extent of the basin and the location of the two wells chosen for this study are shown in Figure 5.2.

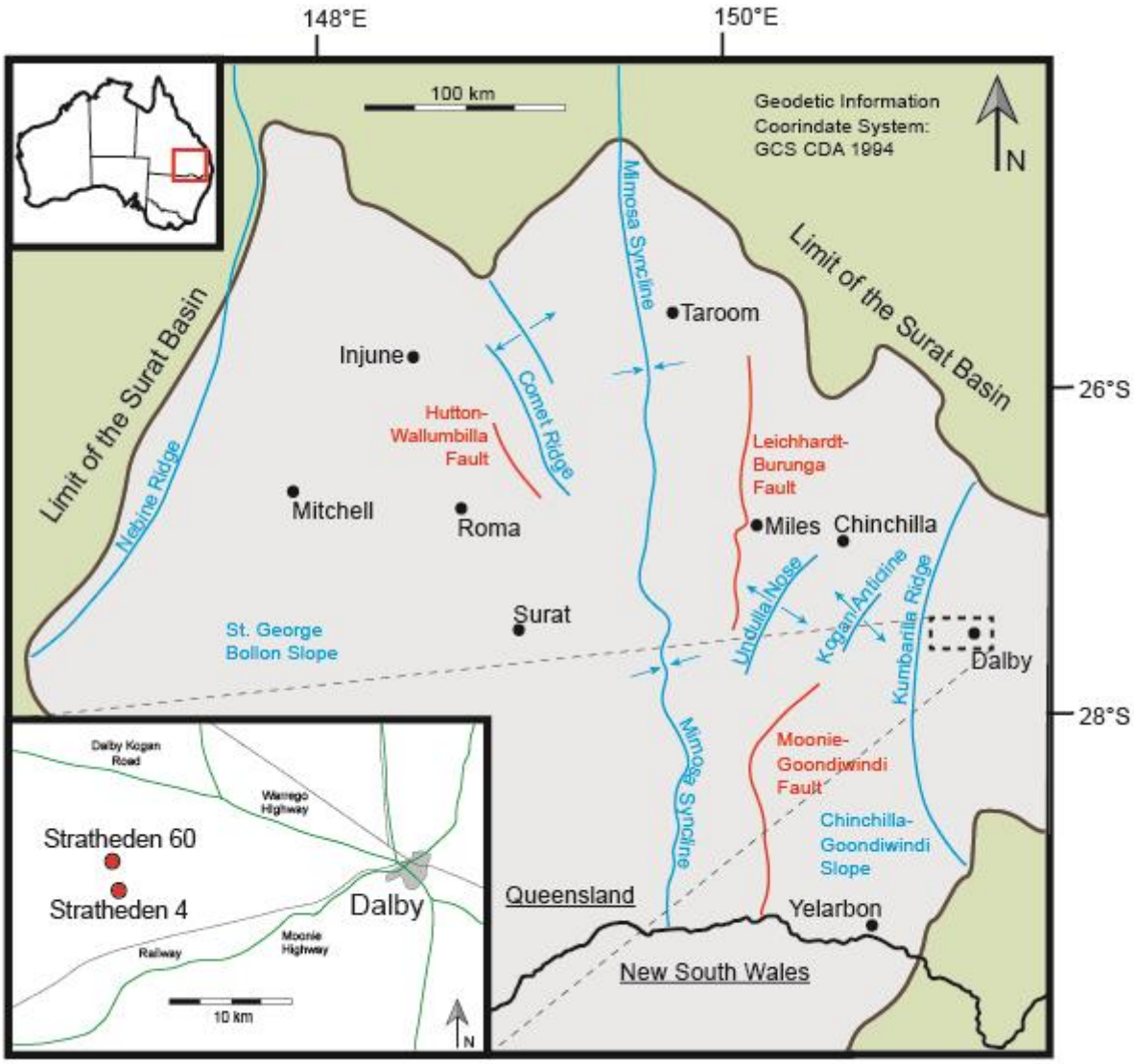

Figure 5.2. Geographic extent and structures of the Surat Basin in Queensland. The location of the Stratheden 4 and Stratheden 60 wells are shown in the bottom left. Adapted from Wainman et al. (2015) and Figure 3.2.

A total of 830 m of drillcore from the Stratheden 4 and Stratheden 60 wells was logged at a scale of 1:100 including notes on the location of tuff beds within the Walloon Coal Measures and the underlying Eurombah Formation. Tuffs from these formations are beige to grey in colour. They are massive due to intense alteration to clay minerals and have sharp basal top contacts. The base of some beds appear bioturbated with highly sinuous tubular structures. Beds are up to 2.13 m in thickness but on average are only 0.4 m. Tuff beds greater than 5 cm were sampled if they were interbedded with coals or from laminated

mudstones. The location of tuffs within these facies makes it likely that they were deposited directly by air-fall with little or no detrital component. Previous work by Wainman et al. (2015) and Wainman et al. (2017) successfully obtained precise U-Pb zircon dates using CA-TIMS from the Walloon Coal Measures of the Surat Basin. Dates from seven tuff beds in the Stratheden 4 and 60 wells (ranging in age from the Middle Jurassic Bathonian to the Late Jurassic Oxfordian) were selected for this investigation are shown in Table 5.1. Methodologies outlining CA-TIMS and LA-ICPMS techniques employed in this investigation are described in Wainman et al. (2015) and Wainman et al. (2017). Well correlation, using the stratigraphy module within Schlumberger's Petrel suite, was undertaken between the wells to ensure the same stratigraphic horizon was picked in each well. A simplified measured section from the Stratheden 60 well with the position of dated tuff beds and equivalents in the Stratheden 4 well is shown in Figure 5.3. Tuff dates utilised for the tectonic subsidence plot are shown in Figure 5.4 and labelled A to G

Well	Depth (m)	Tuff	Geoscience Australia sample code	Equivalent horizon in the Stratheden 60 well	Number of crystals dated	Date (Ma)	Error (+/- Ma)
**Stratheden 60	477.70 to 477.64	A	2231590	N/A	12 with 3 crystals of equivalent age	168.07	0.04
*Stratheden 4	396.46-396.41	B	2180600	350.80	8 crystals with 7 crystals of equivalent age	162.54	0.05
**Stratheden 60	342.31-342.24	C	2231589	N/A	9 with 5 crystals of equivalent age	162.18	0.06
**Stratheden 60	247.66-247.61	D	2231588	N/A	7 with 2 crystals of equivalent age	160.54	0.14
**Stratheden 60	212.55-212.5	E	2254143	N/A	6 with 3 crystals of equivalent age	160.45	0.07
**Stratheden 4	209.87-209.62	F	2231585	170.67	6 crystals, all of equivalent age	159.69	0.05
**Stratheden 60	136.11-135.86	G	2254141	N/A	6 crystals, all of equivalent age	159.02	0.04

*From Wainman et al. (2015) ** From Wainman et al. (2017)

Table 5.1. U-Pb CA-TIMS dates and depths utilized in subsidence modelling.

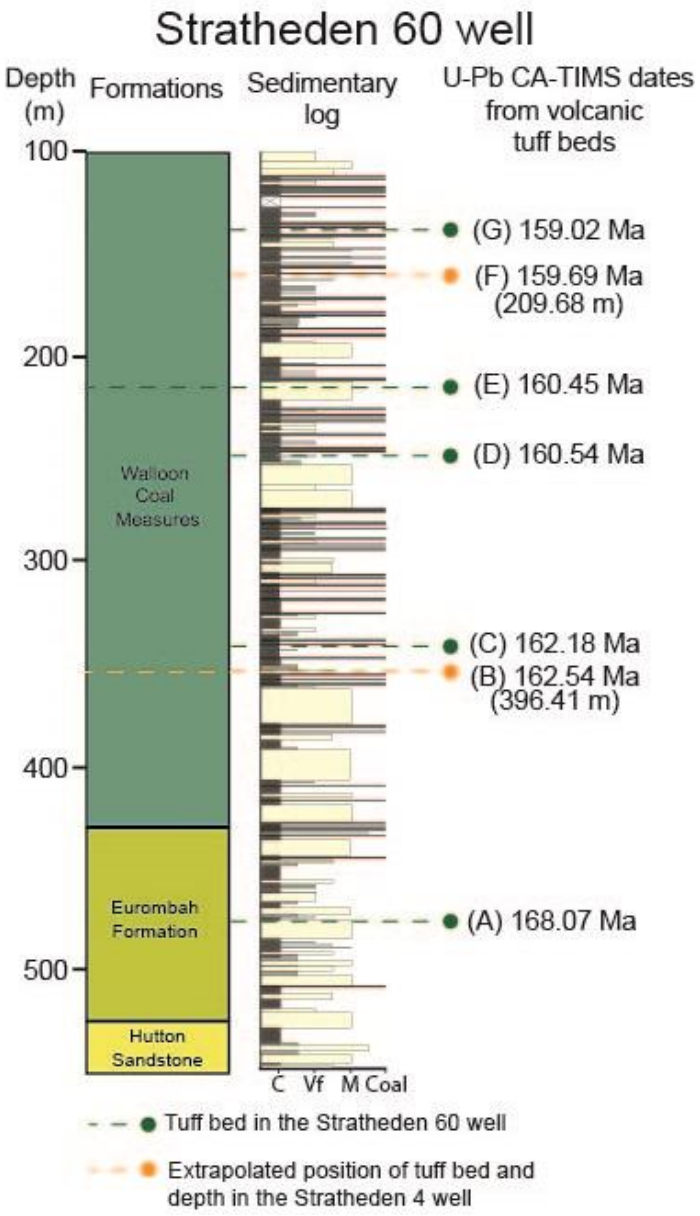

Figure 5.3. Simplified measured section of the Stratheden 60 well and tuff beds dated using U-Pb CA-TIMS techniques. Coal beds (in black) are exaggerated for clarity.

5.4 Estimating depositional rates

Assuming an adequate sediment supply, the long-term sedimentation rates in continental strata are determined by the rate of creation of accommodation space that, in turn, is controlled by basin subsidence rates (tectonic subsidence plus subsidence related to compaction of underlying strata and isostatic adjustments due to sediment loading) and changes in base level. In a continental environment, base level equates to the graded profile of rivers and associated terrestrial environments, such as floodplains and mires (Shanley and McCabe 1994). This base level may change over time due to uplift in the source area, with related increases in sediment supply, or because of downstream changes, such as fluctuations in relative sea-level or lake level.

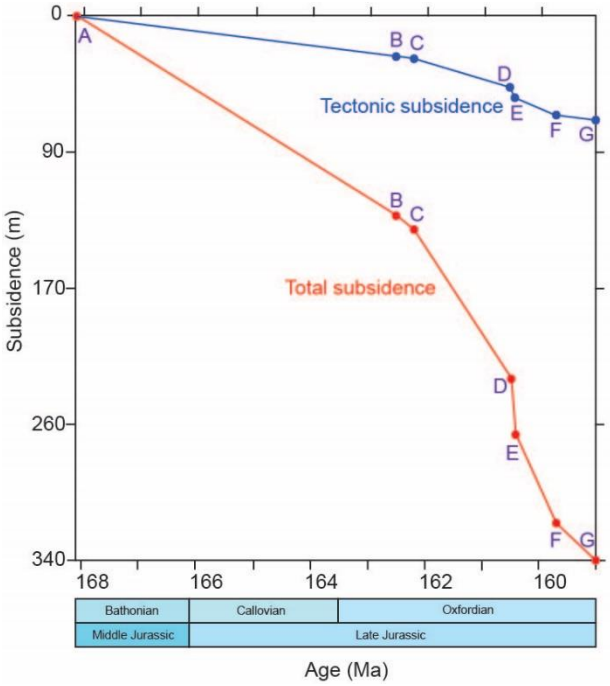

Tuff	Age (Ma)	Total subsidence (m)	Tectonic subsidence (m)
A	168.07	0	0
B	162.54	126	25
C	162.18	135	27
D	160.54	230	45
E	160.45	265	52
F	159.69	322	62
G	159.02	345	67

Figure 5.4. Total subsidence and tectonic subsidence curves from the Stratheden 60 well extracted from “Backstrip for Mac” to 1 d.p. Dated tuff beds are labelled A to G.

A back-stripping analysis was carried out on the stratigraphic section of the Stratheden 60 well using the program ‘Backstrip for Mac’ (Figure 5.4). This program calculates total subsidence over time and, by removing the effect of sediment compaction, water depth, and sediment loading through time, produces a curve that represents tectonic subsidence. The 1D back-strip

undertaken assumes water and sediment loads are compensated locally by the displaced weight of the asthenosphere, and sediment porosity exponentially decreases with depth. Stratigraphic data (depth and age), water depths, paleowater depth and changes in porosity with depth (incorporating sediment grain density, porosity depth coefficient, and surface porosity values) are used to determine both total and tectonic subsidence rates. Formulas for the 1D back-strip were extrapolated from Watts (2001) and Allen and Allen (2013) are listed in Table 5.2. Sediment grain density, porosity depth coefficient, and surface porosity values were chosen on the dominant lithology in each interval under investigation. These were based on the generic composition of sandstone, shaly sandstone or shale. These values were determined from porosity and sonic logs from studies by Sclater and Christie (1980) and Allen and Allen (2013). These values are shown in Table 5.3. Assumptions made during back-stripping include: 1) the absence of major depositional hiatuses within the Eurombah Formation and Walloon Coal Measures; 2) a continental setting for the Eurombah Formation and the Walloon Coal Measures; and 3) the compaction factor of peat into coal was not incorporated into calculations as coal comprises only 5.67 % of strata in the stratigraphic interval under investigation. Subsidence curves produced are generic and reflect overall subsidence trends for this heterogeneous, nonmarine formation.

Table 5.2. Formulas for the backstripping procedure taken from Watts (2001) and Allen and Allen (2013).

Name of back-strip procedure	Formula	Notes
Exponential decrease of porosity with depth	$\Phi = \Phi_o e^{-cy}$	c = porosity coefficient, Φ_o = surface porosity Φ = the porosity at depth y.
General decompaction	$y'_2 - y'_1 = y_2 - y_1 - (\Phi_o/c) * \{\exp(-cy_1) - \exp(-cy_2)\} + (\Phi_o/c) * \{\exp(-cy'_1) - \exp(-cy'_2)\}$	y'_1 and y'_2 = base and top a stratigraphic unit before compaction, y_1 and y_2 = present base and top of the unit after compaction.
Sediment loading correction	Marine basin: $Y = S\{(\rho_m - \rho_s) / (\rho_m - \rho_w)\}$ Continental basin: $Y = S\{(\rho_m - \rho_s) / (\rho_m)\}$	Y i= depth to the basement corrected for sediment load, S = total thickness of the column corrected for compaction, ρ_m = mantle, ρ_s = mean sediment column , ρ_w = water density In a marine basin, any depression is filled with water. Therefore the density of the fluid that supports the loads is $(\rho_m - \rho_w)$. In a continental basin, any depression is filled with air which has a density near zero. Therefore the density of the fluid that supports the loads is (ρ_m).
Water loading correction	Marine basin: $Y_t = Y - \Delta_{SL}\{\rho_m / (\rho_m - \rho_w)\} + WD$ Continental basin: $Y_t = Y - \Delta_{SL}$	In a marine basin, Δ_{SL} = change of sea level relative to the present, and WD is water depth. In a continental basin, Δ_{SL} = paleoelevation of the top of the basin with respect to the present sea level. In a continental basin, the depression is filled with air, not water.

Table 5.3. Surface porosity, porosity depth coefficient and sediment grain density values utilized in subsidence modelling extrapolated from Sclater and Christie (1980) and Allen and Allen (2013).

Lithology	Surface porosity (f_o)	Porosity-depth coefficient (c, x 10^{-5} cm)	Sediment grain density (ρ_{sg}, g/cm^3)	Water density (kg/m^3)	Mantle density (kg/m^3)
Shaly sandstone	0.56	0.39	2680	1000	3300
Sandstone	0.49	0.27	2650	1000	3300
Shale	0.63	0.51	2720	1000	3300

In most back-stripping studies the intervals between data points are measured in 10's of millions of years and the resulting curves are assumed to be entirely due to basin subsidence (and/or uplift) as the effects of any base-level fluctuations are trivial on such long-term time scales. However, with the significantly higher time resolution in this study, with seven data points over ~9 million years, it is worth considering possible effects of base-level changes. In the case of fluvial strata, base level is considered to be the graded profile of the river system (Shanley and McCabe 1994). Two end-member scenarios can be considered: (a) variations in the gradient of the back-strip curve are solely due to changes in subsidence rates over time and any base-level fluctuations were so minor as not to influence the curve, and (b) basin subsidence rates were constant and variations in the gradient of the curve are due to changes in base level over time. While the curve could be a result of variations in both subsidence and base level over time, the implications of the end-member scenarios are worth considering.

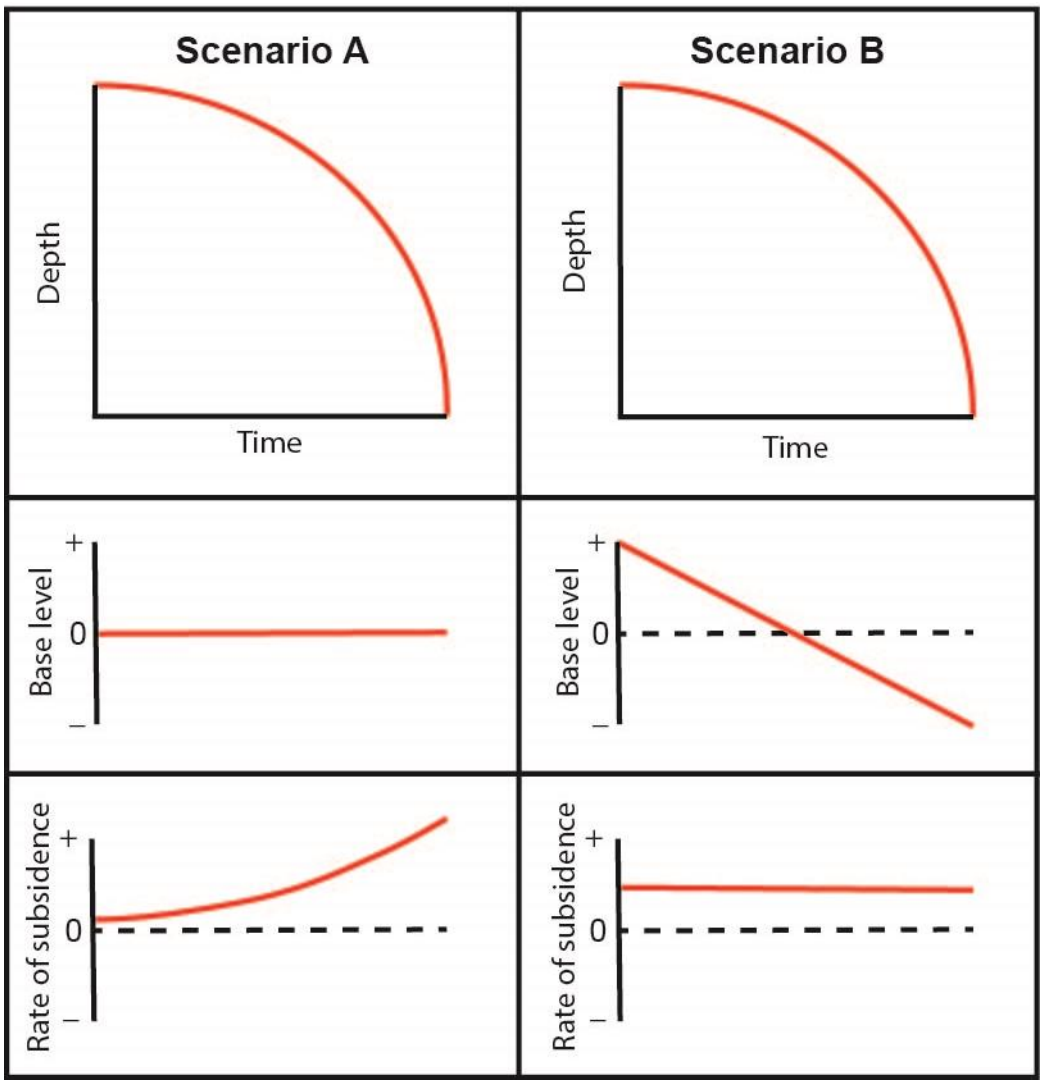

Figure 5.5. A simplified model to explain variations in “subsidence curves” through time. Scenario A shows the classic interpretation of such curves where the shape of the curve is entirely controlled by subsidence. In scenario B the subsidence rate is kept constant but base level changes through time; initially rising at a fast rate but with the rate slowing through time and eventually falling. Note that for a nonmarine basin, base level can be considered as the graded profile of the fluvial system.

5.4.1 Scenario A: Variation due to changes in basin subsidence

This scenario, assumes a classic back-stripping approach in estimating total and tectonic subsidence. In this case a subsidence curve is entirely a function of variations in the rate of subsidence (Figure 5.5). The subsidence curve for the Stratheden 60 well calculated from the back-strip model (Figure 5.4) suggests varying subsidence rates during deposition of the Walloon Coal Measures. The shape of the curves in suggest marked changes in subsidence rates occurred at the data points (dated tuff beds) but this is an artefact of the plotting and in reality, the inflexion points may well have been different. For example, the figure suggests a marked increase in subsidence took place at 162.18 Ma (tuff C) but the increase in subsidence rate may have taken place up to a million years later. It is also important to remember that the more data points available the more complex the subsidence curve may be: the subsidence rate between tuff A and tuff B, for example, may have been much more variable through time than the straight line suggests. For this study, however, the curve gives a good indication of relative rates of subsidence over time.

Total subsidence rates calculated for the stratigraphic section between the dated tuffs (A to G) are shown in Table 5.4. Total subsidence rates increased from 22.5 m/Ma to 350 m/Ma) between tuff A and tuff E. Subsidence rates then decrease from tuff E to tuff G to 32.9 m/Ma. There is a notable sixfold increase in total subsidence rates from tuff A to tuff E. Subsidence rates before tuff A and after tuff G remain unknown due to the absence of tuffs beds suitable for dating. Through the entire stratigraphic interval, total subsidence rates were on average 37.67 m/Ma. From tuff C, however, total subsidence rates were on average 61.42 m/Ma. Subsidence rates during the time of the Walloon Coal Measures are comparable to those of foreland basins (McCabe 1991; Allen and Allen 2013).

Time Interval (Ma)	Lithology	Depth between dated tuff beds (m)	Cumulative total subsidence (m)	Cumulative tectonic subsidence (m)	Total subsidence rate in interval (m/Ma)	Tectonic subsidence rate in interval (m/Ma)
168.1-162.6	Sandstone	(A to B) 126.8	126	25	22.5	4.5
162.6-162.2	Shale	(B to C) 8.6	135	27	30.0	6.7
162.2-160.5	Shaly sandstone	(C to D) 94.6	230	45	55.9	10.6
160.5-160.4	Shaly sandstone	(D to E) 35.1	265	52	350.0	70.0
160.4-159.7	Shaly sandstone	(E to F) 42.0	322	62	81.4	14.3
159.7-159.0	Shale	(F to G) 34.4	345	67	32.9	7.1

Table 5.4. Total and tectonic subsidence rates through the Stratheden 60 well.

Subsidence rates during the lifespan of the Surat Basin also need to be taken into consideration. The weight of overlying strata will affect porosity with depth, sediment loading, and water loading. This will affect subsidence rates through time. After the Walloon Coal Measures, deposition continued until the Albian before uplift and erosion of 2 km of strata from the middle to Late Cretaceous to the present day (Scott 2008). Total subsidence rates during deposition of the Walloon Coal Measures are more than twice the basin average. This is revealed from the backstripping of a well in the northern Surat Basin (Carinya 6) a well which penetrates many of formations comprising the Surat Basin infill. The average subsidence rate from this well from the Middle Jurassic to the Early Cretaceous was 26.9 m/Ma. The reason for the rapid subsidence rate is currently unclear: subsidence rates at the time have been linked to thermal sag after the cessation of a volcanic arc activity (Korsch et al. 1989), flexure/loading as a response to extension occuring at the plate margin to the east (Hoffmann et al. 2009), and dynamically induced platform tilting (Korsch and Totterdell 2009b).

5.4.2 Scenario B: Variations due to changes in base level

In this scenario, the back-strip plot of thickness versus depth is taken as a plot of rates of creation of accommodation over time. Assuming a constant rate of subsidence variations from a straight line plot is a function of rises or falls in base level (Figure 5.5). For the Stratheden 60 well an average rate of basin subsidence was estimated as 37.7 m/Ma by dividing the 345 m of strata between the oldest and the youngest date by the length of time represented: 9.05 Ma. The total amount and average rates of base level fluctuation were then calculated by subtracting the plotted rate of sediment accumulation from the average rate for the formation. This suggests a base level rise of almost 135 m at a rate of 0.014 mm/yr from tuff A to tuff C, followed by a base level fall of about 187 m at a rate of 0.038 mm/yr from tuff C to tuff F.

The estimated amount of base level shift would be difficult to explain by an upstream control: the fluvial systems and associated mires (coals) of the Walloon Coal Measures suggest a very low gradient environment. Any base level shift of the magnitude calculated is, therefore, more likely controlled by a downstream factor, presumably relative sea-level. Although total base level shift

is substantial, the estimated rates of change are a couple of orders slower than rates of eustatic rise and fall during the Pleistocene and more in line with rates expected during a greenhouse epoch.

Interestingly the maximum base level rise in this scenario coincides with a period of transgression from the Middle Callovian and into the Early Oxfordian that a number of other authors have suggested was the most significant transgression event during the Jurassic (Vail et al. 1984; Hallam 2001). This transgressive event was apparently in response to the opening of the Atlantic Ocean and the reorganisation of global tectonic plates (Hallam 2001). Haq (2018) has recently suggested sea-level in the long term rose by more than 50 m from the early Oxfordian to the early Tithonian with superimposed short term (<1 Ma) variations in excess of 100 m. This may explain the magnitude of base level shifts calculated but the cause of short term sea-levels variations are uncertain and likely to be linked to 405 ka eccentricity cycles and associated climate trends (Haq 2018). Marine transgressions, observed with increased acritarch abundances in Mesozoic basins of Australia, indicate brief episodes of brackish-marine conditions in continental settings (Exon and Burger 1981). These events are thought to control the six sedimentary cycles in the Surat Basin (Exon and Burger 1981). From tuff A to tuff C, the calculated base level shift of 135 m is larger than one might anticipate for a eustatic cycle during a greenhouse epoch. From tuff F to tuff G, a decline in the rise of base level is contrary to notions of a marine transgression during the Late Oxfordian (Hallam 2001; Colombié et al. 2014). It would be expected that base level would have continued to rise through this interval. It could be suggested tectonic uplift, as opposed to changes in eustatic sea-level, may have influenced base level changes in the Surat Basin during this timeframe. This would be similar to the interpretation of the Middle Oxfordian to Tithonian strata of the Neuquén Basin in western Argentina, adjacent to the Andes (Hallam 2001).

If Scenario B is supported by subsequent high-resolution chronostratigraphic studies in strata of similar age in the Walloon Coal Measures elsewhere, it offers the possibility of measuring the amount and rate of change during a single eustatic cycle of the Late Jurassic.

5.5 Coal preservation and rates of creation of accommodation

No matter whether caused by tectonic subsidence or sea-level fluctuations, the calculated rates of the creation of accommodation provide insights on controls on coal accumulation. In the Stratheden 60 well, there is 19.36 m of coal in the 341.56 m interval between dated tuff beds A and G. Coal beds represent 5.67 % of lithologies within the interval. There are 163 coal beds ranging in thickness from less than 1 cm to a maximum of 46 cm. On average, coal beds are ~12 cm thick. Through the stratigraphic interval, there are only minor variations in the percentage of coal, sandstone, and the ratio of coal to siliciclastics between dated tuff beds (Figure 5.6). It is important to remember that some of the peat (coal) that acccumulated in the Surat Basin between the deposition of tuffs A and B (168.07 and 162.54 Ma), but was subsequently cut out by channels now represented by sandstones.

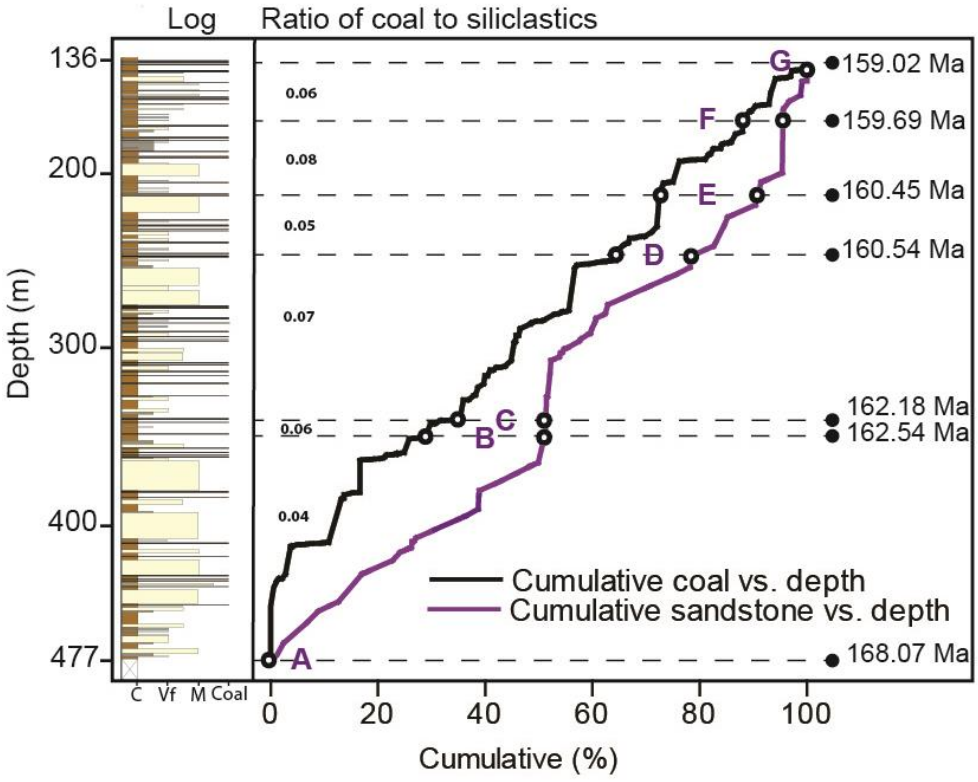

Figure 5.6. Cumulative coal and sandstone percentage against stratigraphic depth and the ratio of coal to siliciclastics between dated tuff beds A to G for the Stratheden 60 well.

When cumulative coal bed thickness is plotted against geologic time (Figure 5.6), there are two distinct breaks in the percentage of coal: at 342.24 m (tuff C) and 212.50 m (tuff E). ~27% of coal occurs in the interval from tuff A to tuff C, ~45% of coal is present from tuff C to tuff E, and ~10% of coal occurs from tuff E to tuff G. From 477.64 to 136.11 m core depth, the ratio of coal to siliciclastic (between inflection points A and G) is relatively constant (0.04-0.08) despite variations in subsidence rates. When time is considered, coal beds become more prolific when subsidence rates double and base level rises after tuff C. From tuff E to tuff G, coal beds are less prolific when subsidence rates declined. The percentages of coal and sandstone vary with time but remains uniform through the Walloon Coal Measures interval after tuff C irrespective of varying rates in the creation of accommodation. Table 5.4a and 5.4b outlines the relationship between time, stratigraphic depth, cumulative coal bed thickness, cumulative sandstone bed thickness and variations in subsidence rates through time.

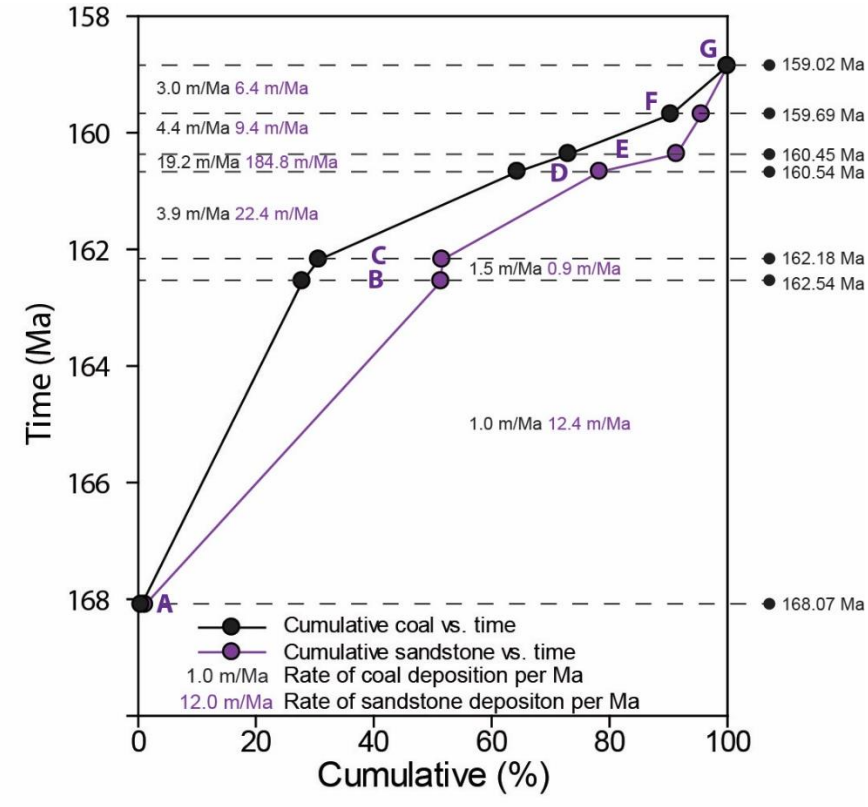

Figure 5.7. Cumulative coal and sandstone percentage versus geologic time. Rates of coal preservation and sandstone deposition are calculated between dated tuff beds A to G for the Stratheden 60 well.

Table 5.5a. The relationship between time, coal thickness and changes in subsidence rates through different stratigraphic intervals of the Eurombah Formation and the Walloon Coal Measures in the Stratheden 60 well.

Depth interval (m)	Depth between dated tuff beds (m)	Time represented in interval (Ma)	Cumulative net coal in interval (m)	Cumulative net coal in interval (%)	Coal in interval (m)	Coal in interval (%)	Total subsidence rate within the interval (m/Ma)	Tectonic subsidence rate within interval (m/Ma)
477.64-350.80	(A to B) 126.84	5.53	5.28	27.27	5.28	4.16	22.5	4.5
350.80-342.24	(B to C) 8.56	0.36	5.86	30.11	0.55	6.43	30.0	6.7
342.24-247.61	(C to D) 94.63	1.64	12.28	63.43	6.45	6.82	55.9	10.6
247.61-212.50	(D to E) 35.11	0.09	14.01	72.37	1.73	4.93	350.0	70.0
212.50-170.48	(E to F) 42.02	0.76	17.34	89.57	3.33	7.92	81.4	14.3
170.48-136.11	(F to G) 34.37	0.67	19.36	100	2.02	5.88	32.9	7.1

Table 5.5b. The relationship between time, sandstone thickness and changes in subsidence rates through different stratigraphic intervals of the Eurombah Formation and the Walloon Coal Measures in the Stratheden 60 well.

Depth interval (m)	Depth between dated tuff layers (m)	Time represented in interval (Ma)	Cumulative net sandstone in interval (m)	Cumulative net sandstone in interval (%)	Sandstone in interval (m)	Sandstone in interval (%)	Total subsidence rate within the interval (m/Ma)	Tectonic subsidence rate within interval (m/Ma)
477.64-350.80	(A to B) 126.84	5.53	68.75	50.97	68.75	54.20	22.5	4.5
350.80-342.24	(B to C) 8.56	0.36	69.09	51.22	0.34	3.97	30.0	6.7
342.24-247.61	(C to D) 94.63	1.64	105.83	78.46	36.74	38.82	55.9	10.6
247.61-212.50	(D to E) 35.11	0.09	122.46	90.79	16.63	47.37	350.0	70.0
212.50-170.48	(E to F) 42.02	0.76	129.59	96.08	7.13	16.97	81.4	14.3
170.48-136.11	(F to G) 34.37	0.67	134.88	100	5.29	15.39	32.9	7.1

To match total subsidence rates, average peat accumulation rates would have had to be equal or greater than 0.35 mm/yr during the period of the fastest calculated rates of accommodation creation: tuff D to tuff E. At other times during deposition of the Walloon Coal Measures, minimum rates of peat accumulation to keep pace with accommodation would have varied between 0.02-0.08 mm/yr. By comparison to Holocene rates of peat accumulation, these are very slow rates. The rate of peat accumulation on the Yukon Delta in Alaska, for example, is about 0.1 mm/yr but rates are several times faster in the cool temperate climates of Western Europe and British Columbia and are an order of magnitude faster in warm temperate and equatorial regions (McCabe 1984). As peat accumulation should have been able to keep up with the rise in water table due to the creation of accommodation, it raises the question as to why the coals are relatively thin and discontinuous even though they comprise 5.67% of the succession under investigation. In the Carboniferous Springville Coal Member of the intracratonic Illinois Basin, which also developed in an intracratonic setting but where peat accumulation occurred on the equator, maximum coal bed thickness is over eight times greater (up to 4 m) (Willard et al. 1995; Willard et al. 2007) than in the Walloon Coal Measures.

Between tuff A and tuff B, an interval spanning ~5.5 Ma, subsidence may have been more variable with episodes of uplift. Key inflection points in the subsidence model or in the timing of coal preservation may have occurred earlier or later than shown due to nature of tuff sampling. One possibility is that rates of creation of accommodation were more intermittent than shown by the calculated curves (Figure 5.4). It seems unlikely that this could be due to variations in tectonic subsidence rates given that the geographical extent of the Surat Basin is over 250,000 km^2 and there are no observable changes in the overall pattern of coal thickness characteristics over the basin or relative to the few basement faults. Minor fluctuations in sea-level (and thus accommodation creation) may have occurred that are not detectable with the resolution of the calculated rates of accommodation creation. While frequent minor variations in relative sea-level could create thin coal beds, this seems unlikely for the Walloon Coal Measures given that the distance from a coeval shoreline was great (no fully marine strata interfinger with the Walloon Coal Measures) and

that paleogeographic reconstructions suggest any shoreline was hundreds of kilometers from the centre of the basin (Exon 1976; Bradshaw and Yeung 1992; Martin et al. 2013).

Frequent avulsion of the river systems that deposited the clastic sediments of the Walloon Coal Measures could also be invoked as a mechanism to explain the thin coals. However many other coal basins that are dominated by fluvial strata, such as the Fort Union Formation of the Powder River Basin of Wyoming and the Fort Cooper Coal Measures of the Bowen Basin of Queensland have thick coals (up to ~60 m in both cases) that span the majority of the basin (Flores et al. 1999; Ayaz et al. 2015).

It seems more likely that climate during deposition of the Walloons Coal Measures was the critical factor and that peat accumulation was intermittent due to fluctuations in the climate over time.

5.6 Coal preservation and climate

Given the size of the coal resource, conditions were clearly favourable for peat accumulation to occur in the Surat Basin during the Oxfordian. The Surat Basin was located in high latitudes (>75°S) on the eastern margin of the Gondwanan supercontinent during the Middle and Late Jurassic (Figure 5.8) (Blakey 2011; Wainman et al. 2015) based on paleomagnetic records that record plate movement changes as pole path features—loops, bends and overprints (Klootwijk 2009). Palaeogeographic reconstructions by Li and Powell (2001) show eastern Australia at a lower latitude (>65°S), however, they are based on a review of the literature prior to 2001. Such polar latitudes today are cool and arid with no large plants and no mires in which peat could accumulate. However, the Late Jurassic was a time when greenhouse conditions prevailed (Hallam 1985) with high levels of atmospheric carbon dioxide (up to four times greater than today) driven by increased volcanic activity as Pangea began to break apart (Sellwood and Valdes 1997).

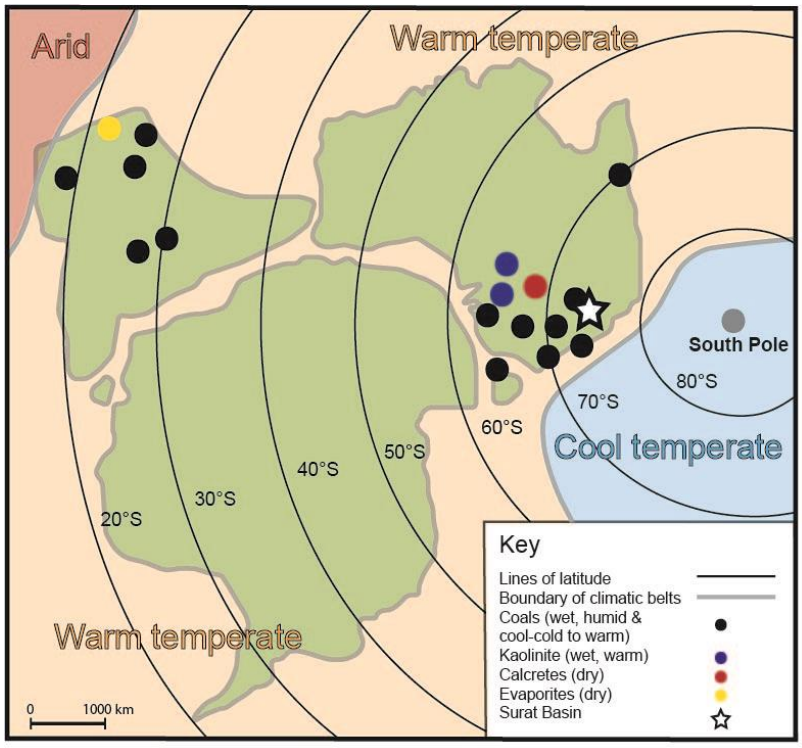

Figure 5.8. A tectonic plate reconstruction showing the location of the Surat Basin in the Late Jurassic from Klootwijk (1996). Superimposed on the map are climatic indicators from lithologies and suggested boundaries for climate zones from Boucot et al. (2013).

5.6.1 Climatic change and climatic cyclicity during the Late Jurassic

Hallam (1982) originally suggested tropical warmth and equability on a global scale through the Late Jurassic. Subsequent studies of oxygen ($\delta^{18}O$ ‰ PDB), carbon ($\delta^{13}C$ ‰ PDB) and strontium ($^{87}Sr/^{86}Sr$) isotope records, however, have provided new perspectives on the climate during the Late Jurassic (Jones and Jenkyns 2001; Weissert and Erba 2004; Dera et al. 2011). These studies suggest a number of long and short-term climatic trends (Figure 5.9) with rapid temperatures variations greater than 8°C on million year timescales. Brigaud et al. (2008), also suggested a mid-Oxfordian warming pulse from oxygen (δ18O ‰) analyses of oyster shells of the Paris Basin in France.

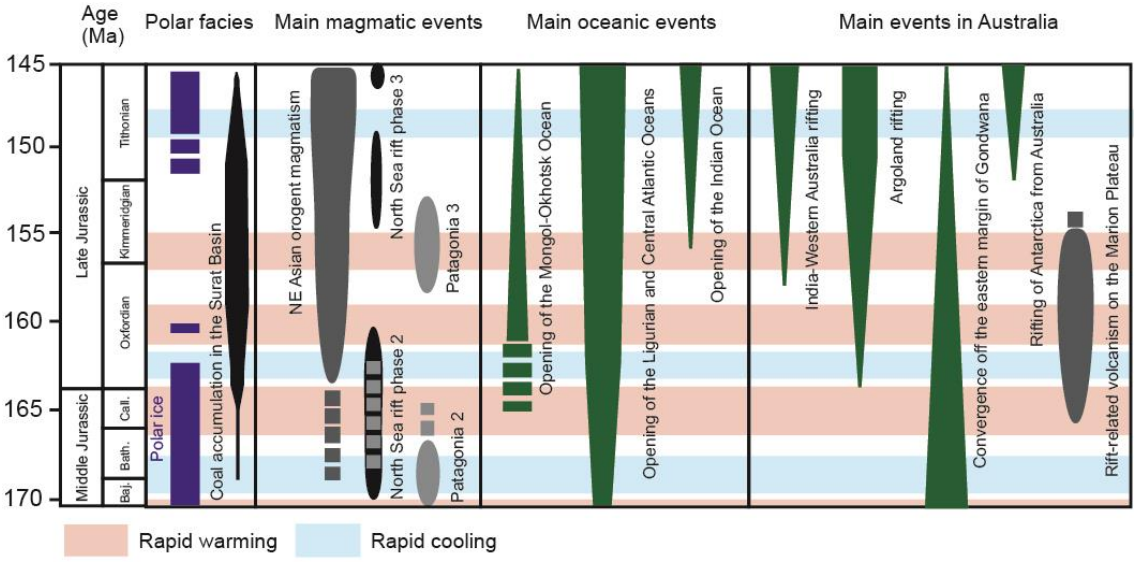

Figure 5.9. Major geologic and climate events during the Middle to Late Jurassic. Adapted from Dera et al. (2011) with additional interpretations from Jell (2013).

Throughout the Oxfordian, there were at least three episodes of rapid climate change on timescales of less than 1 Ma (Dera et al. 2011). Polar climates may be particularly dynamic during greenhouse intervals (Price and Passey 2013). The high latitudes are generally more sensitive to climate change in greenhouse epochs as a consequence of: 1) perturbations to the hydrological cycle; 2) a decline in sea ice and a slowing of global thermohaline circulation; 3) wider latitudinal excursions by the Intertropical Convergence Zone during the year as a consequence of weaker polar fronts; and 4) variations in stratospheric

cloud cover in the polar regions (Ziegler et al. 1987; Anisimov et al. 2007; Zachos et al. 2008). At lower latitudes, the associated monsoonal rainfall pattern coinciding with a changing climate would have increased silicate weathering, a freshening of oceanic waters and elevated organic carbon burial (Weissert and Mohr 1996; Sellwood and Valdes 1997). Consequences of these changes during the Late Jurassic included drought-prone continental interiors and an increased coverage of wetlands in the high latitudes with implications for carbon storage and methane production (Perlmutter and Matthews 1992; Sellwood and Valdes 1997; Walter and Heimann 2000). This is supported by IPCC SRES climate scenarios for 2080 predicting that high latitudes will become wetter (up to 28% more rainfall) and warmer (up to 16°C higher) due to increased atmospheric carbon (Anisimov et al. 2007). This is likely to lead to increased methane production (up by 37%) when soil temperatures increase by >1°C with increased peat decomposition - this is further amplified by their aerial extent and the melting of permafrost (Walter and Heimann 2000). Such a scenario may have increased the sensitivity of the high latitudes to climate change during the Late Jurassic and consequently influenced peat accumulation.

Many geologic studies have shown the influence of Milankovitch cycles on global circulation models. Shifts in the position of the Hadley, Ferrel, and Polar cells are known to have implications for changes in rainfall patterns, the strength of monsoons and the build-up of ice at the poles (and consequently eustatic sea-level) (Perlmutter and Matthews 1992; Valdes et al. 1995; Fielding and Webb 1996). This can impact sediment supply and depositional architecture as rainfall becomes more seasonal on an annual basis (Fielding and Webb 1996). Greater vegetation cover during wetter periods is thought to reduce fluvial discharge and clastic deposition, increasing the likelihood of widespread peat accumulation in contrast to drier periods (Opluštil et al. 2013). Fielding and Webb (1996) suggested Milankovitch cycles (notably 19 Ka precessional cycles) influenced the timing of peat accumulation in the high-latitude Late Permian Bainmedart Coal Measures of Antarctica (60°S) which hosts thick coal beds >1 m in a fluviolacustrine setting.

Frequent changes in climate during deposition of the Walloon Coal Measures may well explain the thin laterally discontinuous nature of the coal beds. Favourable climatic conditions for peat accumulation may not have lasted long enough for thick peat accumulations to develop. Peat accumulation in present-day warm temperate climates such as the Okefenokee Swamp and Everglades varies between 0.3 to 1 mm/yr (McCabe 1984). Assuming a peat to coal compaction ratio and an average accumulation rate of 0.6 mm/yr it would have taken close to 17 ka to accumulate a 1 m thick coal in the Walloon Coal Measures – this compares to 19 ka for a precessional cycle.

Thin (<1 m), laterally discontinuous coal beds are a common characteristic of other coal-bearing formations which develop at high latitude during greenhouse times irrespective of their tectonic setting. For example, in the Mesozoic foreland Coleville Basin (75°N during the Late Cretaceous), total subsidence rates were averaged 27 m/Ma (7 m/Ma tectonic) (Cole et al. 1997). These are comparable to overall rates observed in the Surat Basin, but lower in comparison to rates observed in the Walloon Coal Measures. Despite the Coleville Basin steadily subsiding during the Late Cretaceous, coal bed thickness declines from 96 to 23 cm in response to climate cooling (Spicer et al. 1992). This is revealed by frost damage and a decline in annual growth rates revealed by fossil tree rings (Spicer et al. 1992). In the Cretaceous Fossil Bluff Group of Antarctica (80°S), located in a forearc basin, coal beds are less than 50 cm and are laterally discontinuous (Macdonald and Francis 1992). The high latitude coals of the Upper Cretaceous Paparoa Coal Measures of New Zealand have some thick coal beds (>10 m) but these are thought to have accumulated in localized areas controlled by differential subsidence during a major rifting event (Newman and Newman 1992).

5.6.2 Climate during deposition of the Walloon Coal Measures

Using the global climate models of Moore et al. (1992), Martin et al. (2013) suggested that the annual temperature range during deposition of the Walloon Coal Measures was from -22°C to +10°C with precipitation greater than 1000 mm/yr. This suggests temperatures similar to Fairbanks, Alaska today (a daily mean temperature in January of -22°C and in July +17°C) and an annual precipitation comparable to Vancouver, Canada (1150 mm/year). By contrast, Boucot et al. (2013) suggest that there was a low global climatic gradient in the Late Jurassic and that, based on paleoclimate indicators, the warm temperate belt extended into high latitudes, including the Surat Basin (see Figure 5.8). This interpretation is based on the presence of the coals in the Upper Jurassic of eastern Australia and the presence of kaolinites and calcretes in central Australia, which at that time, lay further towards the equator (Figure 5.8).

Palynological and paleobotanical data from the Walloon Coal Mesures coals suggest a high degree of floral diversity (McKellar 1998). Podocarp and araucarian conifers were the dominant flora on mires with an understory of liverworts, lycopods, equisetaleans, ferns, pteridosperms and bennettitaleans/cycadeoids (Balme et al. 1995). Diverse floral assemblages have also been described from high latitude coal deposits in the Eocene of Axel Heiberg Island in the Canadian High Arctic (79°N) and in the Cretaceous of Antarctica (80°S) (Macdonald and Francis 1992; Greenwood and Basinger 1994). The maceral composition of the Walloon Coal Measures coals may also reflect the diverse flora with vitrinite content varying between 62.4% and 90.6% and liptinite content varying between 7.6% and 19.5% (Scott et al. 2007). Today araucarian conifers are present at latitudes between the equator and about 30°S that would be compatible with Boucot et al. (2013) interpretation of a warm temperate climate. Podocarps have a wider latitudinal distribution growing today as far south as New Zealand. Ginkgo’s, which are a cooler climate tree, are notably absent in the Walloon flora (McKellar 1998). Although the Walloon Coal Measures accumulated in a polar region, they may have had more affinity to mires that are such as the Okefenokee or Everglades that are in a warm temperate climate than mires in Alaska, Siberia or northwest Europe.

This would be especially the case in the size of the large trees and rates of organic degradation.

Scott et al. (2007) showed that there is an upward increase in the inertinite content of the coals in the Walloon Coal Measures and overlying Springbok Sandstone (averaging 10% volume and as high as 46% volume in coals within the Springbok Sandstone): this suggests an increased frequency of oxidation or combustion events over time. Pacey (2011) and Hentschel et al. (2016) observed a positive $\delta^{13}C$ excursion in coals at the same stratigraphic interval which indicates higher water stress – this is thought to reflect lower water tables in peat mires or the oxidation of plant matter. This may also reflect a positive $\delta^{13}C$ excursion during the Oxfordian in response to increasing levels of CO_2 in the atmosphere (Hentschel et al. 2016). Evidence of dry conditions in mires and the presence of caliches in the coeval Birkhead Formation of the Eromanga Basin to the west indicates drier and warmer climatic conditions prevailed during the Oxfordian. This may have disrupted the maintenance of an elevated peat-forming surface and limited the thickness of peat accumulations.

5.6.3 Stresses on plants growing in Polar Regions

At a latitude of 75°S, there would have been approximately 3 months total darkness and 1.5 months of limited daylight in the winter months and 3 months of continuous daylight in the summer. There is no a similar ecological niche today where plants take advantage of high latitude warmth and a polar light regime (Francis and Poole 2002). Warm temperate conditions with prolonged winter darkness would have had major implications for plant physiology (Francis 1990; Spicer 1990; Boucot et al. 2013) and subsequent peat accumulation. The ability of plants to cope with sharp transitions from summer into winter and to rapidly grow in the summer months would have been critical (Spicer 1990; Read and Francis 1992). Plants would also need to overwinter effectively during warm winters without exhausting key metabolites built up during summer photosynthesis (Francis 1990; Read and Francis 1992; Francis and Poole 2002). Failure to adapt to these conditions would have restricted plant growth, induced tissue damage or death (Read and Francis 1992). Of importance would be high summer productivity and minimal loss of winter biomass to enable high net organic accumulation and allow for the formation of

thick coal deposits (Spicer 1990). Although Araucaria and Podocarps are evergreen trees today, it has been suggested that when these plants grew at high latitudes they may have had a deciduous habit, allowing them to tolerate the high-latitude light regime (Macdonald and Francis 1992). The production of large quantities of leaf litter has been demonstrated as a potential mechanism for the formation of thick coals at high latitude in the Cretaceous of Alaska and the Tertiary of Arctic Canada (Spicer and Parrish 1986; Macdonald and Francis 1992). In contrast, peat accumulation in modern high-latitude peat bogs is facilitated by decreased levels of bacterial decay during the cold winters (Ziegler et al. 1987).

5.7 Conclusion

The interplay of climate and tectonics is essential for controlling the geometrical attributes of coal beds. The Walloon Coal Measures were deposited with a foreland basin whose subsidence rates are particularly favourable for coal accumulation (McCabe 1991) but, despite comprising ~6% of the formation, the coals are thin and discontinuous. Climatic factors rather than variable subsidence rates or short-term changes in base level appear to have been the critical factor in determining the thin, laterally discontinuous character of coal beds. Rapid fluctuations in climate during the Oxfordian within the polar region may have restricted the duration of peat accumulation in mires across the Surat Basin. The high latitude in which the peats accumulated would have induced enormous stresses on plants as they experienced >3 months darkness per year with mild winter temperatures. Relatively small changes in climate may have been enough to pass thresholds for extensive plant growth and hence mire development. This may have included the frequency of hard winter frosts or changes in precipitation. The notion of frequent climate change in high latitudes during greenhouse times being a critical factor in determining the nature of the coal beds is supported by other examples of high latitude coal-bearing formation in the Cretaceous.

5.8 Acknowledgements

Carmine Wainman has a Ph.D. scholarship from the University of Adelaide that has covered most of the travel and analytical costs. We are thankful to Dr. Jim Crowley of Boise State University, Idaho, USA who performed CA-TIMS on zircon extracted from tuff beds – without his encouragement and support this study would not have been possible. We would like to thank Joan Esterle and the Centre for Coal Seam Gas at the University of Queensland in providing a grant to cover the costs of four of the zircon analyses. Schlumberger also kindly provided academic licenses for Petrel 2016.

Statement of Authorship

Title of Paper	A reappraisal of the depositional environments of the Jurassic Walloon Coal Measures, Surat Basin, Queensland, Australia using a multidisciplinary approach
Publication Status	☐ Published ☐ Accepted for Publication ☐ Submitted for Publication X Unpublished and unsubmitted work written in manuscript style
Publication Details	Wainman, C.C., McCabe, P.J, In Prep-b. A reappraisal of the depositional environments of the Jurassic Walloon Coal Measures, Surat Basin, Queensland, Australia using a multidisciplinary approach. Intend to submit to Sedimentology.

Principal Author

Name of Principal Author (Candidate)	Carmine C. Wainman		
Contribution to the Paper	Majority of the data collection and interpretation. Wrote the greater majority of the paper with exceptions noted in the co-authorship contributions. Produced final version of the paper using editorial suggestions of the co-author.		
Overall percentage (%)	80		
Certification:	Majority of the data collection and interpretation. Wrote all of the paper. Produced final version of the paper using editorial suggestions of the co-author.		
Signature		Date	10/08/2017

Co-Author Contributions

By signing the Statement of Authorship, each author certifies that:

i. the candidate's stated contribution to the publication is accurate (as detailed above);
ii. permission is granted for the candidate in include the publication in the thesis; and
iii. the sum of all co-author contributions is equal to 100% less the candidate's stated contribution.

Name of Co-Author	Peter J. McCabe		
Contribution to the Paper	Supervisor of Ph.D. – Extensive critical advice and guidance on research project and editorial comments for the paper. Made contributions in the section titled "Depositional environments - holistic perspective.		
Signature		Date	10/8/2017

Chapter 6. A reappraisal of the depositional environments of the Jurassic Walloon Coal Measures, Surat Basin, Queensland, Australia using a multidisciplinary approach

To be submitted to *Sedimentology*. A statement of authorship is provided on the previous page.

Co-authors: Peter McCabe

Abstract

The Jurassic Walloon Coal Measures of the Surat Basin in eastern Australia hosts one of the continent's most significant sources of coalbed methane. Previous studies have interpreted the Walloon Coal Measures within a single depositional facies model that was deposited in a wholly terrestrial setting. We take a multidisciplinary approach using facies analysis, palynology and wireline logs to describe the evolution of the Walloon Coal Measures within a new chronostratigraphic framework defined by precise U-Pb tuff dates. Analysis of facies indicates that the majority of the Walloon Coal Measures were deposited by small (<300 m wide), low gradient rivers on a poorly-drained floodplain with numerous small lakes and mires. However, this study also identified some tidally-influenced facies. These facies appear to have been deposited within incised valleys during transgressions. The evidence of base level shifts also suggests that the coals were not coevally deposited with at least some of the thicker sandstones. Palaeogeographic maps for 11 time slices suggest that rivers drained towards to the south/southwest and southeast, presumably into proximal estuarine complexes. Marine incursions likely came from the north and the east during times of high eustatic sea-level. A similar multidisciplinary approach should help elucidate the evolution of other fluviolacustrine systems in other basins and aid in resource prediction.

6.1 Introduction

Many fluvial-dominated strata host major petroleum, groundwater and mineral resources (Owen et al. 2017). Unlike in the marine realm, the complex interplay of tectonics, climate and topography play a greater role in controlling stacking patterns and lateral facies distributions rather than eustatic sea-level variations which can vary markedly across continental basins (Shanley and McCabe 1994; Shanley and McCabe 1998). This often results in a labyrinth reservoir style made up of a complex arrangement of sand pods, lenses, and channels over short distances which are difficult to infer in the subsurface (Shepherd 2009b). Even with extensive exposures, the availability of 3D seismic surveys, prominent marker beds, or closely spaced wells, it is often challenging to create palaeogeographic maps or predict the distribution of resources in the subsurface hosted in fluvial successions (Bridge 2009; Shepherd 2009b).

The high latitude (75°S) Jurassic Walloon Coal Measures of the Surat Basin in Queensland, Australia provides a classic case study where thin, discontinuous nonmarine facies make stratigraphic correlations difficult on a regional scale (Wainman et al. 2015). The Walloon Coal Measures is an important source of coal bed methane (CBM) hosted within fluvial-dominated strata (Martin et al. 2013). The formation is a world-class gas resource, with a cumulative thickness of coal of >30 m (Towler et al. 2016), and has current proven and probable (2P) reserves of approximately 31,000 petajoules (28,200 billion cubic feet of gas) (Queensland_Government 2016). Reservoir models are important for resource exploration and effective gas production. In the Walloon Coal Measures, such models have been developed from the study of drill core, wireline logs and a limited number of seismic surveys described within a poorly defined lithostratigraphic framework (Shields and Esterle 2015; Bradshaw and Bernecker 2016). In this study, we re-evaluate the evolution of depositional environments and the palaeogeography of the Walloon Coal Measures by integrating sedimentary facies analysis, wireline logs and palynology in conjunction with a newly defined chronostratigraphic framework using high-precision U-Pb chemical abrasion thermal ionization mass spectrometry dates (CA-TIMS).

6.2 Geologic setting of the Walloon Coal Measures in the Surat Basin

The Walloon Coal Measures is a 350 to 500 m thick formation that crops out on the northern and eastern flanks of the Surat Basin in Queensland, Australia and is laterally extensive in the subsurface throughout the basin (Yago 1996b; Jell 2013; Towler et al. 2016). The economic significance of CBM in the Walloon Coal Measures has led to a great deal of interest from exploration companies and government agencies (Scott et al. 2007). The formation was long thought to be entirely Middle Jurassic (Callovian) in the Surat Basin, but recent dating of tuffs, using U-Pb CA-TIMS undertaken by Wainman et al. (2015) and Wainman et al. (2017) demonstrate that they were deposited over a substantially longer time period (Middle Jurassic Callovian to Late Jurassic Tithonian) and the facies are diachronous with younger strata in the west.

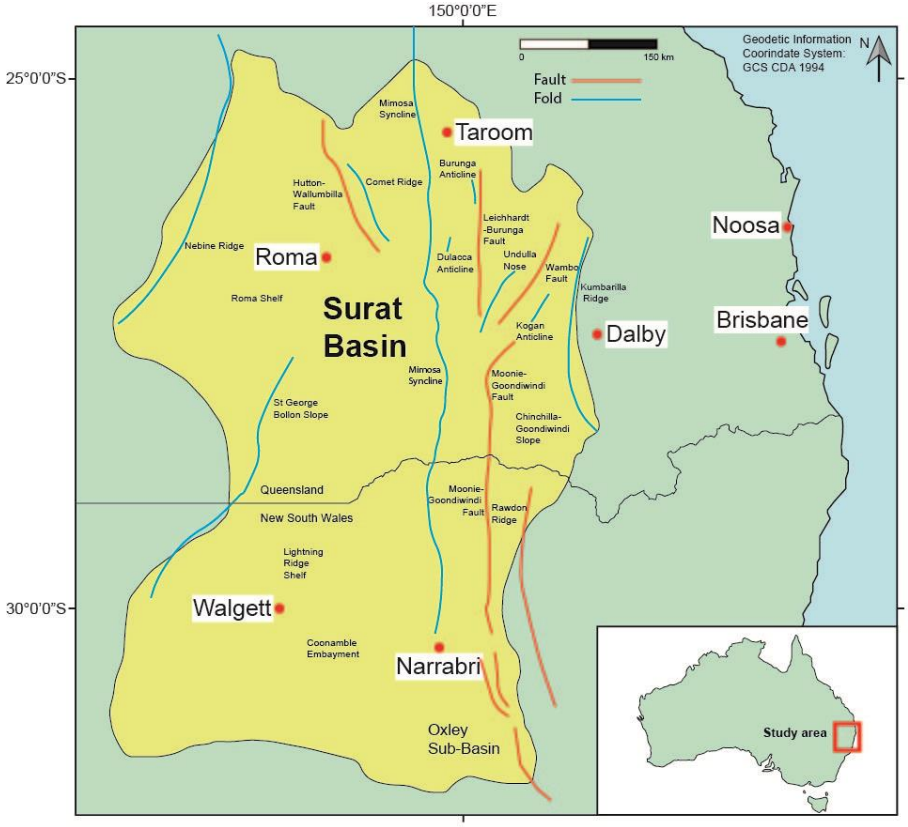

Figure 6.1. The structural and geographic extent of the Surat Basin in eastern Australia adapted from Arditto (1982) and Hamilton et al. (2014b).

The Late Triassic to Early Cretaceous intracratonic Surat Basin (Figure 6.1) covers approximately 270,000 km^2 of southern Queensland and northern New South Wales (Goscombe and Coxhead 1995). The main depocentre unconformably overlies the Permo-Triassic Bowen and Gunnedah basins whereas the margins of the basin overlie crystalline basement of the Early Devonian to Late Triassic orogenic complexes known as the Central West and New England Fold Belts (Ryan et al. 2012). The basin is contiguous with the Clarence-Moreton Basin over the Kumbarilla Ridge in the east and to the west, connects with the Eromanga Basin over the Nebine Ridge (Exon 1976; Goscombe and Coxhead 1995). Overall, the basin is broad, flat lying with a number anticlines, synclines and faults (Raza et al. 2009). In the centre of the basin, the Mimosa Syncline mirrors the Taroom Trough of the underlying Bowen Basin (Jell 2013). The margins of the Surat Basin are characterised by a several anticlinal and synclinal structures (e.g. the Kogan Anticline) controlled for the greater part by the reactivation of Triassic and basement faults including the Hutton-Wallumbilla Fault (Ryan et al. 2012). The tectonic setting of the basin remains a matter of debate: intracratonic, retro-arc and foreland settings have all been suggested with readers referred to the works of Green et al. (1997), Waschbusch et al. (2009), Shields and Esterle (2015) for more details on the geologic setting of the Surat Basin.

Localized deposition commenced in the Late Triassic after the Hunter-Bowen Orogeny and an episode of peneplanation (Green et al. 1997; Jell 2013). The Goondiwindi Event, a short-lived compressional event, eroded the majority of Late Triassic sediments in the Surat Basin (Ryan et al. 2012). The same event also led to the creation of thrust and back thrust faults including the Leichhardt-Burunga Fault (Green et al. 1997; Ryan et al. 2012). Six cycles of sedimentation then occurred from the Early Jurassic depositing a series of alternating fluviolacustrine and, in the Cretaceous, paralic and marine successions (Exon and Burger 1981; Jell 2013). An episode of compression and uplift in the middle Cretaceous (~95 Ma) known as the Moonie Event led to the erosion of 2 km of Mesozoic sediments (Raza et al. 2009). This is thought to tie in with the end of convergent tectonism and the onset of seafloor

spreading in the Tasman Sea (Ryan et al. 2012). The basin has remained relatively dormant through the Cenozoic (Fielding 1996; Raza et al. 2009).

Jurassic lithostratigraphic units of the Surat Basin are shown in Figure 6.2. The Walloon Coal Measures consist of sandstones with a high percentage of volcanic rock fragments, mudrocks and coal that have been interpreted as the deposits of a fluviolacustrine system with numerous peat-forming mires in the interfluves (Exon 1976; Ryan et al. 2012; Shields and Esterle 2015; Shields et al. 2017). Several lines of evidence have been used to infer this including the abundance of plant macrofossils (Yago 1996b); the amount of organic material in channel bodies suggesting vegetated riverbanks (Goscombe and Coxhead 1995); the presence of dinosaur footprints (Yago 1996b); strata interpreted as crevasses splays into shallow lakes (Shields and Esterle 2015); the scarcity of wavy bedding (Fielding 1993; Yago 1996b); and the absence of fully marine strata (Martin et al. 2013). Most of the studies have focused primarily on the eastern Surat Basin (Martin et al. 2013; Shields and Esterle 2015) rather than on a regional geologic setting. Some studies (Scott et al. 2007; Hentschel et al. 2016) entirely focus on the organic-rich facies rather than the siliciclastic sediments. Previous studies have also described the formation within a poorly defined lithostratigraphic framework defined by Jones and Patrick (1981), Hamilton et al. (2014b) and Zhou et al. (2017).

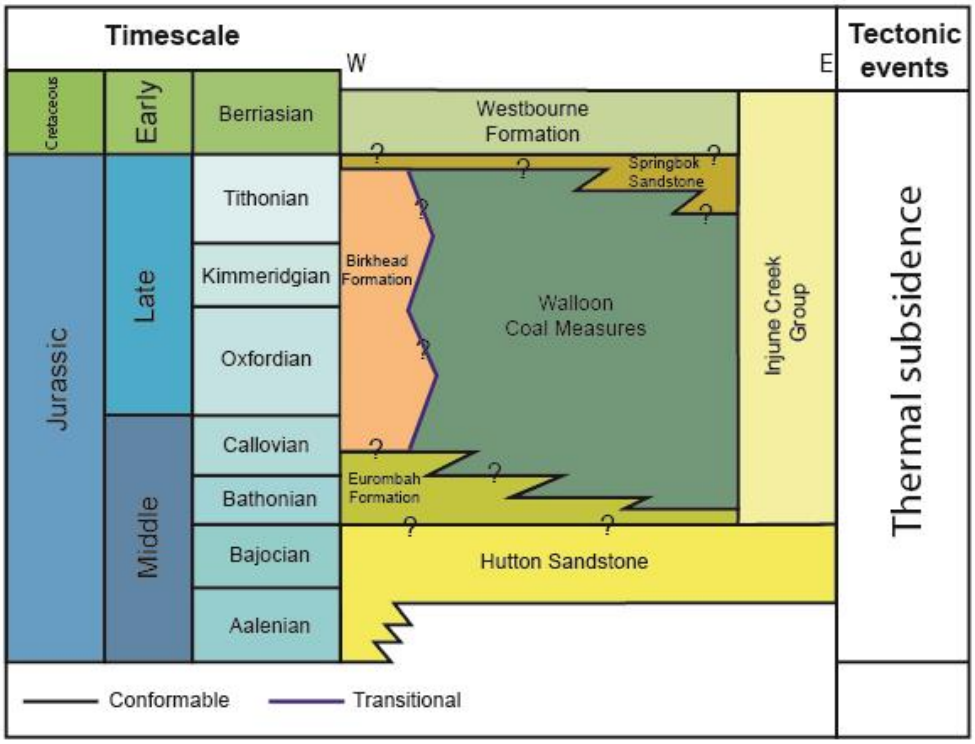

Figure 6.2. Coal-bearing lithostratigraphic units and tectonic events in the Surat Basin adapted from Jell (2013), Ryan et al. (2012) and Wainman et al. (2017). Deposition in the basin commenced in the Rhaetian with the Chong and Eddystone beds and ceased after deposition of the Griman Creek Formation in the Albian. The contact between the Walloon Coal Measures and the Springbok Sandstone maybe unconformable.

The predominant palaeocurrent direction is disputed. Exon (1976) interpreted palaeodrainage to the north while Fielding (1993) and Yago (1996b) suggested, from outcrop studies in the adjoining Clarence-Moreton Basin, that rivers flowed towards the Eromanga Basin in the west. In contrast, more recent studies by Hamilton et al. (2014b), Shields and Esterle (2015) and Zhou et al. (2017) advocate palaeodrainage in the Surat Basin to the south and southeast based on sandstone isopach maps and image logs. Boult et al. (1998) palaeogeographic reconstruction suggests that the rivers of the Walloon Coal Measures drained into a large endorheic lake (Lake Birkhead) in what is now northeast South Australia and southeast Queensland. However, the possibility of marine influences in the Surat Basin during the Late Jurassic and in coeval

strata in neighbouring basins has been suggested from clay mineralogy, the presence of brackish water acritarchs, ironstones and glauconite (Exon 1976; Burger 1986; Boult 1996; Martin et al. 2013) from a few locations.

There have been relatively few studies of other Upper Jurassic coal-bearing units including the Springbok Sandstone and the Westbourne Formation in the Surat Basin (Exon 1976; Exon and Burger 1981; Green et al. 1997a; Jell 2013). These formations share many characteristics with the Walloon Coal Measures including thin coal beds interbedded with sandstones, siltstones, and mudstones with significant amounts of volcanilithic detritus. These were deposited in a range of fluvial and lacustrine environments (Jell 2013).

6.3. Facies analysis

6.4.1 Methodology

Sections were measured from nine wells across the Surat Basin through the upper Hutton Sandstone, Eurombah Formation, Walloon Coal Measures, Springbok Sandstone and the Westbourne Formation (Figure 6.3). Features including lithology, grain size, bed thickness, lithological trends and sedimentary structures were measured and recorded. For this paper, siltstones are defined as rocks comprising >66% of silt-sized particles (2–62 µm) and mudstones for all other fine-grained siliciclastic rocks comprising >66% of particles <62 µm in size. Measured sections were divided into facies based on grain size and sedimentary structures that reflect a depositional process. Facies found in close association to one another were grouped into facies associations and their depositional environment interpreted. A palynological study was undertaken primarily to understand the biostratigraphic framework but the results also throw light on the depositional environments. Samples were taken from mudstones, siltstones, carbonaceous shales, and coals. These were processed using standard palynological techniques (Traverse 2007; Brown 2008) with residues mounted on glass slides for investigation under the microscope. Detailed palynological results from the Walloon Coal Measures are described in section 7.6. Measured sections and sampling locations for palynology from a selection of wells including Stratheden 60, Guluguba 2 and Indy 3 are shown in Figures 6.4a to 6.4c. A legend for the measured section is provided in Figure 6.4d. Other measured sections and sampling locations from the Turallin 1, Stratheden 4 from Wainman et al. (2015), Wyalla 3, Alderley 1, Pleasant Hills 25 and Kato 3 wells are included in appendices 5 (Figures 1 to 6).

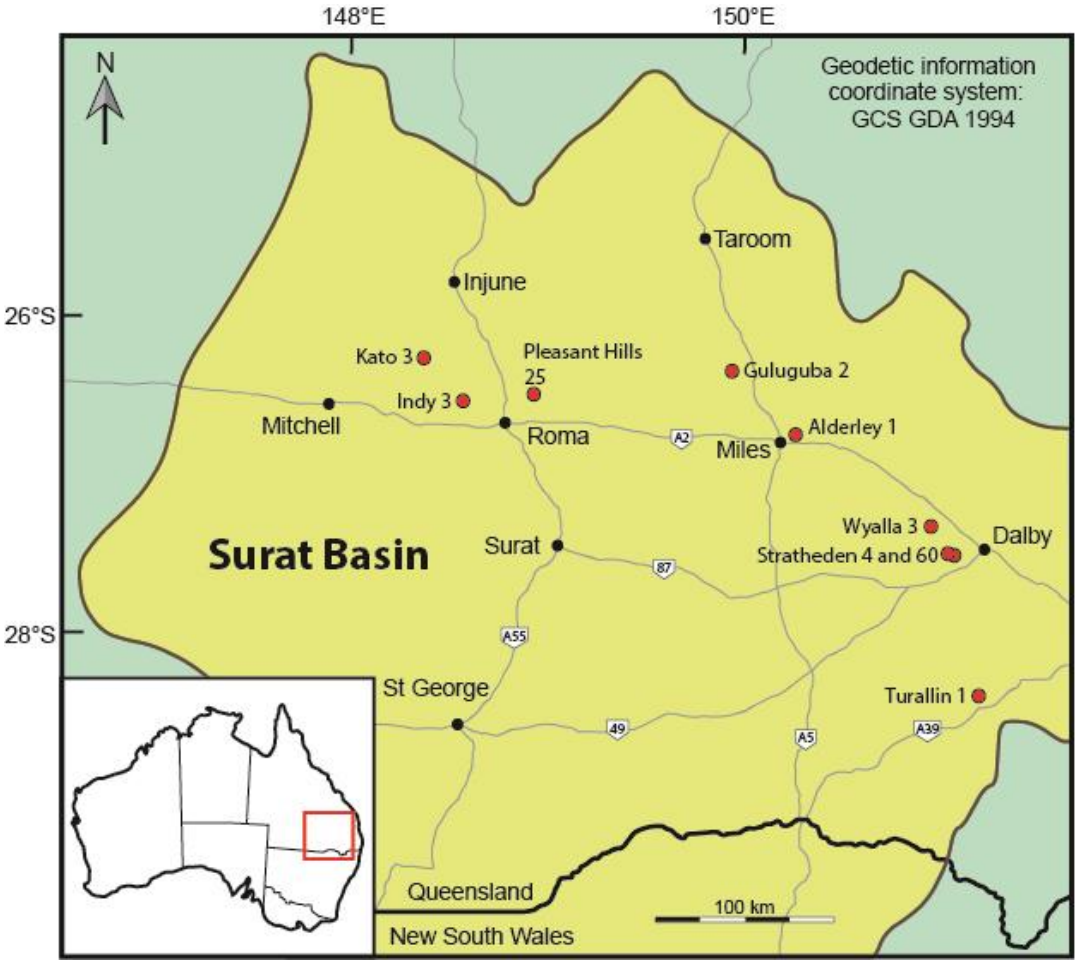

Figure 6.3. The location of measured sections derived from drill core in the Surat Basin, Queensland.

6.4.2 Facies, facies associations descriptions and interpretations

Ten facies were defined (Table 6.1): facies are assigned a number and a colour for ease of identification on the measured sections (Figures 6.4a to 6.4c and supplementary paper Figures 1 to 6). An eleventh facies (marked in light brown) consisting of bioturbated hummocky cross-beds is also defined, however, it belongs to the Westbourne Formation and beyond the remit of this study. The sandstones of the Walloon Coal Measures are buff to grey in colour, medium to fine-grained, poorly sorted with a high matrix/cement content consisting of expanding authigenic clays which fill pore spaces (Jones and Patrick 1981; Ryan et al. 2012). These sandstones are composed of clastic fragments of a volcanic origin while the medium to fine-grained material is composed of quartz, feldspars, mica with varying amounts of carbonaceous material (Jones and Patrick 1981; Martin et al. 2013). Petrographically, they are classified as lithic

and feldspathic labile sandstones (Goscombe and Coxhead 1995; Martin et al. 2013).

A total of eight facies associations were then identified: these are assigned a letter for identification (A to H) on each of the measured sections (Figures 6.4a to 6.4c and in the supplementary paper Figures 1 to 6). A ninth facies association (labelled I and interpreted as a deep lake or paralic?) is also identified but is beyond the remit of this study because it belongs to the Westbourne Formation. The facies associations are briefly described below with interpreted depositional environments. Facies assigned to each association are indicated by their respective number in parentheses – note that some facies are present in more than one association. In later sections of this paper, the relationships between the facies associations in time and space are explored in depth: these relationships allow a significantly more detailed interpretation of the depositional environments.

.

Table 6.1. Facies of Middle to Upper Jurassic strata of the Surat Basin.

#	Colour on measures sections	Facies	Sub-facies	Typical thickness	Composition, organic material and palynomorphs	Sedimentary structures	Depositional process
1		Horizontal to low angle stratified sandstone.	N/A	1 - 3 m.	Very fine to medium-grained, moderately sorted. May contain mud clasts, sideritic clasts, and organic debris. Granule lags at the base of a few beds.	Horizontal lamination, low angle cross-beds (<10^{o}).	High energy, upper flow regime.
2		Cross-bedded sandstone.	N/A	1 - 6 m.	Very fine to medium-grained, moderately sorted. May contain mud clasts, sideritic clasts, and organic debris. Granule lags at the base of some beds.	Planar-tabular cross-beds, trough cross-beds.	Lower flow regime, downstream migration of 2D and 3D dunes due to unidirectional flow.
3		Massive and convoluted sandstones.	N/A	<0.5 - 3 m.	Very fine to medium grained, rare interlaminations of siltstone and mudstone. May contain mud clasts.	Massive, convoluted beds.	Soft sediment deformation due to liquefaction and/or rapid deposition.
4		Cross-laminated sandstones.	Sub-facies A: Cross-laminated.	<0.5 m - 4 m.	Very fine to fine-grained. Some beds are heterolithic with thin interlaminations of siltstone and mudstone. Can be bioturbated. Rare mud clasts and a few basal lags.	Cross-lamination – unidirectional and symmetrical ripples.	Lower flow regime, downstream migration of ripples due to unidirectional flow. Rare periods of oscillatory flow.
			Sub facies B: Climbing ripples.			Cross-lamination – climbing, unidirectional ripples.	Lower flow regime, high rates of sedimentation relative to ripple migration rates.
5		Sandstone with mudstone.	Sub-facies A: Sandstone with mud drapes.	<10 m. Mostly 2 - 4 m.	Interbeds of very fine to fine-grained sandstones and mudstone (cm to m in	Random mud drapes in sands, some cross-beds.	Unidirectional flow with occasional periods of deposition from suspension.

			Sub-facies B: Wavy and lenticular bedding.		scale) with small organic particles (coffee grinds).	Lenticular bedding, flaser bedding, streaky bedding, symmetrical ripples, bundles, double mud drapes.	Frequent variations in current strength. Bidirectional and/or oscillatory flow. Tidal influence?
6		Laminated siltstones and mudstones.	Sub-facies A: With pollen and spores (where analysed).	<0.5 m - 4 m.	Silt to mud with a few thin interbeds of very fine-grained sandstones (mm to cm scale). Contain tuff beds. Rare roots. Usually dominated by terrestrial palynomorphs. May have dinoflagellate cysts, acritarchs, and chlorophyte algae.	Symmetrical ripples, lenticular bedding, ripple cross-laminated, climbing ripples. May be bioturbated and convoluted.	Unidirectional - lower flow regime and slow-moving water with periods of oscillatory and bidirectional flow. Subaqueous to subaerially exposed.
			Sub-facies B: With dinoflagellate cysts, acritarchs and colonial algae (where analysed).			Symmetrical ripples, lenticular bedding, ripple cross-laminated. Some bioturbation.	Unidirectional - lower flow regime and slow-moving water with periods of oscillatory and bidirectional flow. Subaqueous – brackish?
7		Massive siltstones and mudstones.	Sub-facies A: With pollen and spores (where analysed).	<0.5 - 7 m.	Silt to mud with diffuse thin interbeds of very fine-grained sandstones (mm to cm scale). Rare laminations. Some beds contain roots. Usually dominated by terrestrial palynomorphs. May have dinoflagellate cysts, acritarchs, and chlorophyte algae.	Structureless, convoluted, desiccation cracks. Some beds are bioturbated. Slickensides commonly associated with roots.	Sub-aerial exposure with periods of standing water. Palaeosol development in some beds.
			Sub-facies B: With dinoflagellate cysts, acritarchs and chlorophyte algae (where analysed).			Structureless, convoluted. Some beds are bioturbated.	Standing water – brackish?
8		Heterolithic strata.	N/A	<0.5 - 6 m.	Centimeter to decimeter beds of medium-grained to very fine-grained sandstone, siltstone, and mudstone. Common roots. Usually dominated by terrestrial palynomorphs.	Most sandstones are cross-laminated. Beds may be bioturbated or contain convolute bedding.	Overbank deposition and subaerial exposure.
9		Coal.	N/A	<0.85 m mostly 0.05 m -0.4 m.	mm-scale bands of vitrain with common bands of durain. Rare clarain and	Banded.	Peat accumulation.

					fusain. Has both dulling-up and brightening-up profiles. Cleats are common. Tuffs and carbonaceous mudstones up to 0.85 cm interbedded between coals. Usually dominated by terrestrial palynomorphs.		
10		Carbonaceous mudstone.	N/A	<0.1 m - 1.5 m.	A mix of mudstone, coaly shale, and carbonaceous mudstone. Some roots.	Massive to laminated.	Peat accumulation with frequent inundation of siliciclastic sediment.

Facies Association A – Fluvial channel

Description: This facies association consists of sandstones up to 18 m thick but is generally between 3 to 10 m thick. The sandstones have sharp, scoured bases, commonly with mud clasts or granule clasts, and fine upward. The lower parts consist of horizontal bedding (1), cross-beds (2) or may be massive or have contorted bedding (3). Several erosional surfaces may be present within the lower part of the thicker sandstones. The upper, finer part of the sandstone units consists of cross-laminated sandstones and mudstones (4a and/or 5b). Examples of fluvial channel facies associations are found in the Stratheden 60 well from 380 to 360 m (Figure 6.4a), in the Guluguba 2 well from 405 to 392 m (Figure 6.4b) and in the Indy 3 well from 185 to 175m (Figure 6.4c).

Interpretation: This facies association is interpreted as the deposits of fluvial channels. On average, the rivers were probably less than 5 m deep with the thicker sandstones representing vertical aggradation or amalgamation of several channel deposits. The morphology of the rivers is difficult to determine based on vertical profiles (cores) but the absence of evidence for flashy discharge and extensive planar-tabular cross-beds produced by bars suggests that the rivers were most likely meandering or anastomosed rather than braided.

Facies association B – Crevasse splay complex/Crevasse delta

Description: This association consists predominantly of sandstones in units up to 2 m thick. The most common facies in the association are cross-laminated sandstones (4) but there may also be sandstone beds with horizontal stratification (1), cross-bedding (2), massive or convoluted bedding (3). There are minor interbeds of siltstones and mudstones (6 and 8). Units may either fine-upward or coarsen-upward. This association is commonly interbedded with overbank or lacustrine mudstones (facies associations C and D). Examples of crevasse splay complex/crevasse delta facies associations are found in the Stratheden 60 well from 282 to 278 m (Figure 6.4a), the Guluguba 2 well from 176 to 171m (Figure 6.4b) and the Indy 3 well from 344 to 338 m (Figure 6.4c).

Interpretation: These sandstones are interpreted as overbank crevasse splay deposits. Units that coarsen-upward are interpreted as prograding complexes that were either crevasse-splay lobes built out onto a vegetated floodplain or as small deltas into lakes. Fining-upward units are interpreted as small channels that fed such crevasse splays.

Facies association C – Floodplain

Description: Siltstones and mudstones (7a and 8), that are generally structureless, sparsely bioturbated and rooted, comprise this association. Units are mostly between 0.3 and 4 m thick but can be up to 7 m thick. Some have thin (<1 cm) beds of fine and very fine-grained sandstones. A few beds have desiccation cracks and burrows. Randomly oriented slickensides are common in beds with roots. Palynological residues of samples from this facies association are abundant in spores and pollen (90 to 100% of the assemblage). Examples of floodplain facies associations are found in the Stratheden 60 well from 325 to 320 m (Figure 6.4a) and the Guluguba 2 well from 434 to 428 m (Figure 6.4b).

Interpretation: This facies association is interpreted as the deposits of an emergent vegetated floodplain with pedogenic activity.

Facies Association D – Shallow lacustrine or abandoned channel

Description: This association consists of siltstones and mudstones (6a and 7a) with parallel laminations, symmetrical ripples, cross-lamination, and small-scale contorted structures. Some beds are burrowed. Beds are between 0.5 and 4 m thick but are generally <2.5 m. Palynological residues from analysed from this facies association are abundant in spores and pollen (> 90% of the assemblage) with rare freshwater algae from the genera *Leiosphaerida* and *Tetraporina*. This association is commonly interbedded with facies association C. Examples of shallow lacustrine or abandoned channel facies associations are found in the Guluguba 2 well from 407 to 405 m (Figure 6.4b) and the Indy 3 well from 305 to 300 m (Figure 6.4c).

Interpretation: This facies association is interpreted as having been deposited in shallow lakes. Given the relationship with facies association C, these lakes may have been abandoned channels or other floodplain lakes.

Facies association E – Mire

Description: Coal beds (9) comprise this facies association. Beds have a maximum thickness of 0.85 m but are typically between 0.2 and 0.4 m. There are thinner beds – some <0.01 m. Interbeds of tuff and carbonaceous mudstone are common. Palynological assemblages derived from the coal are typically dominated by one or two species of spore or pollen (e.g. *Retitriletes circolumensis*, *Gleicheniidities senonicus,* and *Camarozonosporites ramosus)*. Examples of mire facies associations are found in the Stratheden 60 well from 141 to 135 m (Figure 6.4a), the Guluguba 2 well from 280 to 275 m (Figure 6.4b) and the Indy 3 well from 163 to 157 m (Figure 6.4c).

Interpretation: This facies association is indicative of the accumulation of peat in mires which were regularly inundated by volcanic air-fall ash. The low palynological diversity suggests limited sediment and palynomorph transport in the mire.

Facies association F – Wetland

Description: Facies association F comprises a mix of carbonaceous mudstone and coaly shales (10) with some thin coal stringers. These are laminated to massive, with roots. Most beds are between 0.2 and 0.6 m with a maximum thickness of 0.8 m. Examples of wetland facies associations are found in the Stratheden 60 well from 385 to 381 m (Figure 6.4a), the Guluguba 2 well from 335 to 333 m (Figure 6.4b) and the Indy 3 well from 163 to 161 m (Figure 6.4c).

Interpretation: This facies association is interpreted as the deposits of vegetated wetlands which were inundated by clastic sediments on a regular basis perhaps occupying low lying areas on the floodplain in close proximity to fluvial channels.

Facies association G – Tidally-influenced channel

Description: Facies association H consists of very fine to medium grained sandstones with interbeds of siltstone or mudstone. Generally between 3 to 8 m thick, units of the association are up to 10 m thick. Units of the association have a sharp base overlain by sandstones with horizontal lamination, cross-bedding, convolute bedding, and massive bedding with some mud drapes (1, 2, 3 and 5a) that pass upward to finer-grained cross-laminated sandstones and wavy and lenticular bedding (4a and 5b) (Figure 6.5). Examples of tidally influenced channel facies associations are found in the Stratheden 60 well from 265 to 260 m (Figure 6.4a) and the Indy 3 well from 265 to 260 m and 220 to 216 m (Figure 6.4c).

Interpretation: The erosional base of the units and their fining-upward nature is typical of channel deposits. However, the abundant mud drapes and wavy and lenticular bedding suggest that these units were deposited in channels quite different from those in which facies association A were deposited. The different sedimentary structures may indicate that these channels were influenced by tides. Frequent slack water conditions would explain the abundant mud drapes and a tidal cyclicity would favour the formation of wave ripples and lenticular bedding. The notion of a tidal influence on the Walloon Coal Measures in the Surat Basin will be explored fully later in the paper.

Facies association H – Tidally-influenced mudflat

Description: This facies association is similar to facies associations C and D in that it consists of very fine sandstones, siltstones, and mudstones with cross laminations, symmetrical ripples, lenticular bedding and massive mudstones, but is distinguished by the presence of acritarchs (*Micrhystridium)*, colonial algae (*Palambages*) and dinoflagellate cysts (*Moorodinium and Skuadinium*) (6a, 7a). Palynoflora are composed of up to 10% acritarchs and up to 70% algae and dinoflagellate cysts (Figure 6.6), with the remainder consisting of spores, pollen, and freshwater algae. Beds are typically < 1 m thick. The association occurs in conjunction with facies association G. Some beds have a few burrows of unknown type (possibly escape burrows from the presence of spreite). Examples of tidally influenced mudflat facies associations are found in

the Stratheden 4 well from 460 to 450 m (supplementary paper Figure 2) and the Indy 3 well from 255 to 240 m (Figure 6.4c).

Interpretation: This facies association is interpreted as the deposit of mudflats. The sedimentary structures are typical of tidal mudflats and the unique palynological assemblages suggest that these sediments may have been deposited in brackish conditions. This will be discussed fully later in the paper.

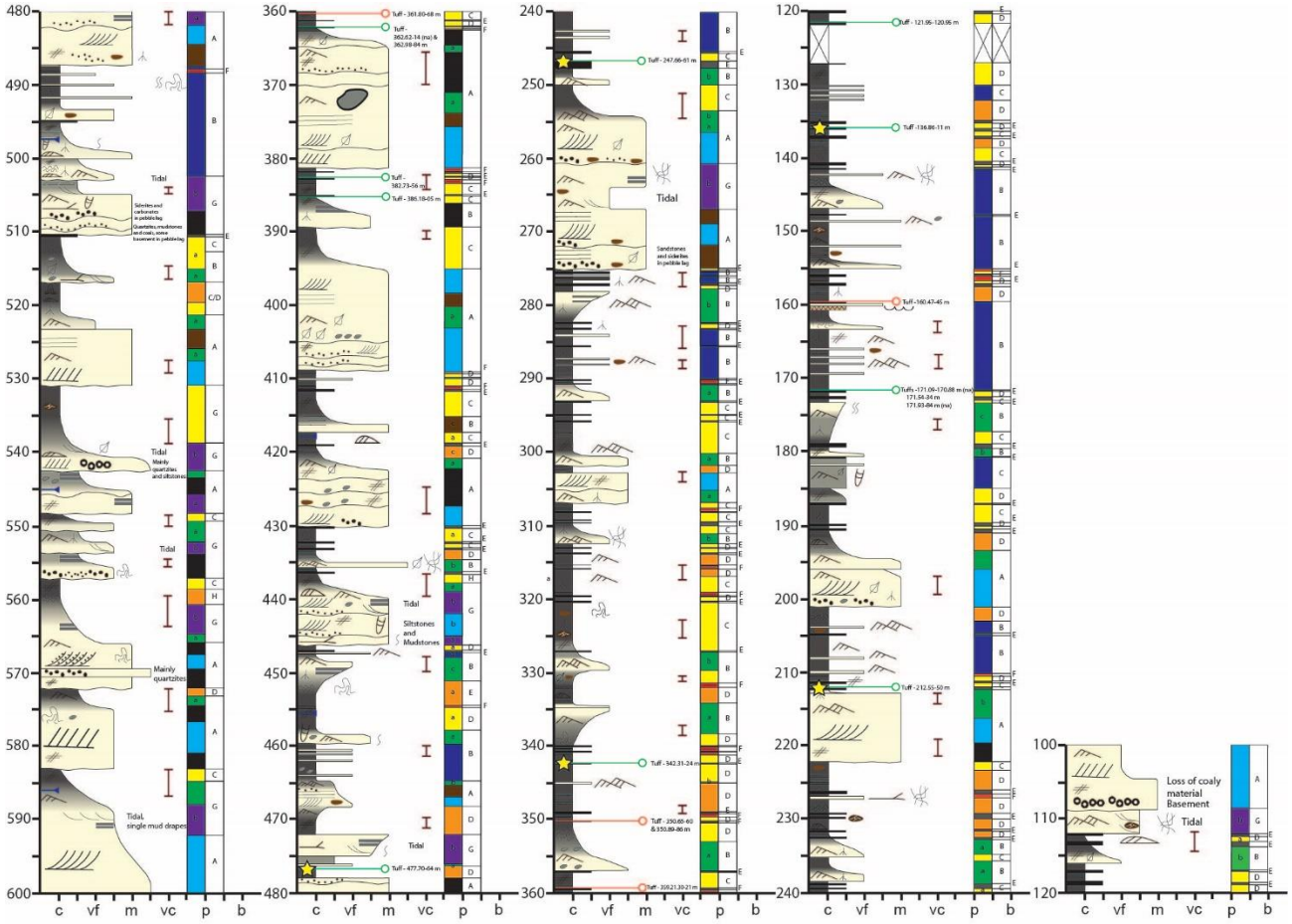

Figure 6.4a. A measured section (including tuff and palynological sample locations) from the Stratheden 60 well spanning the upper Hutton Sandstone (600 to 439 m), the Eurombah Formation (439 to 314 m) , and the Walloon Coal Measures (314 to 100 m) to the unconformity with the Springbok Sandstone.

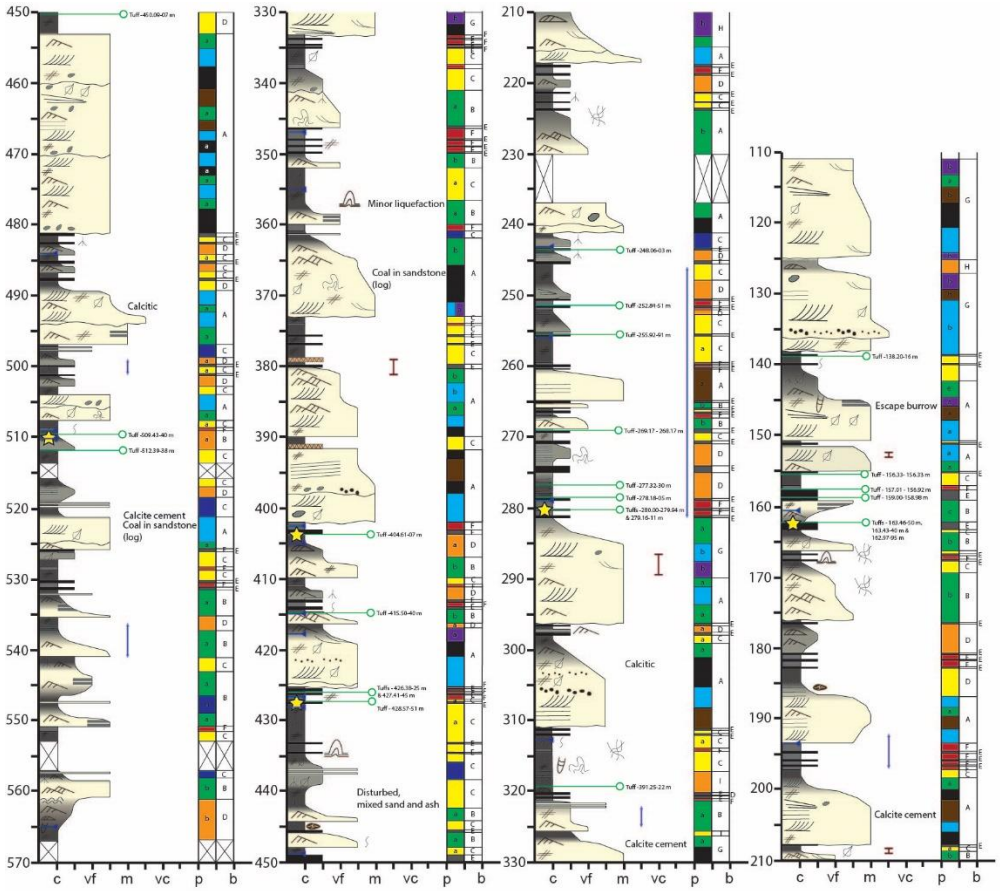

Figure 6.4b. A measured section (including tuff and palynological sample locations) from the Guluguba 2 well spanning the Eurombah Formation (570 to 552 m), the Walloon Coal Measures (552 to 138 m), and the Springbok Sandstone (138 to 110 m).

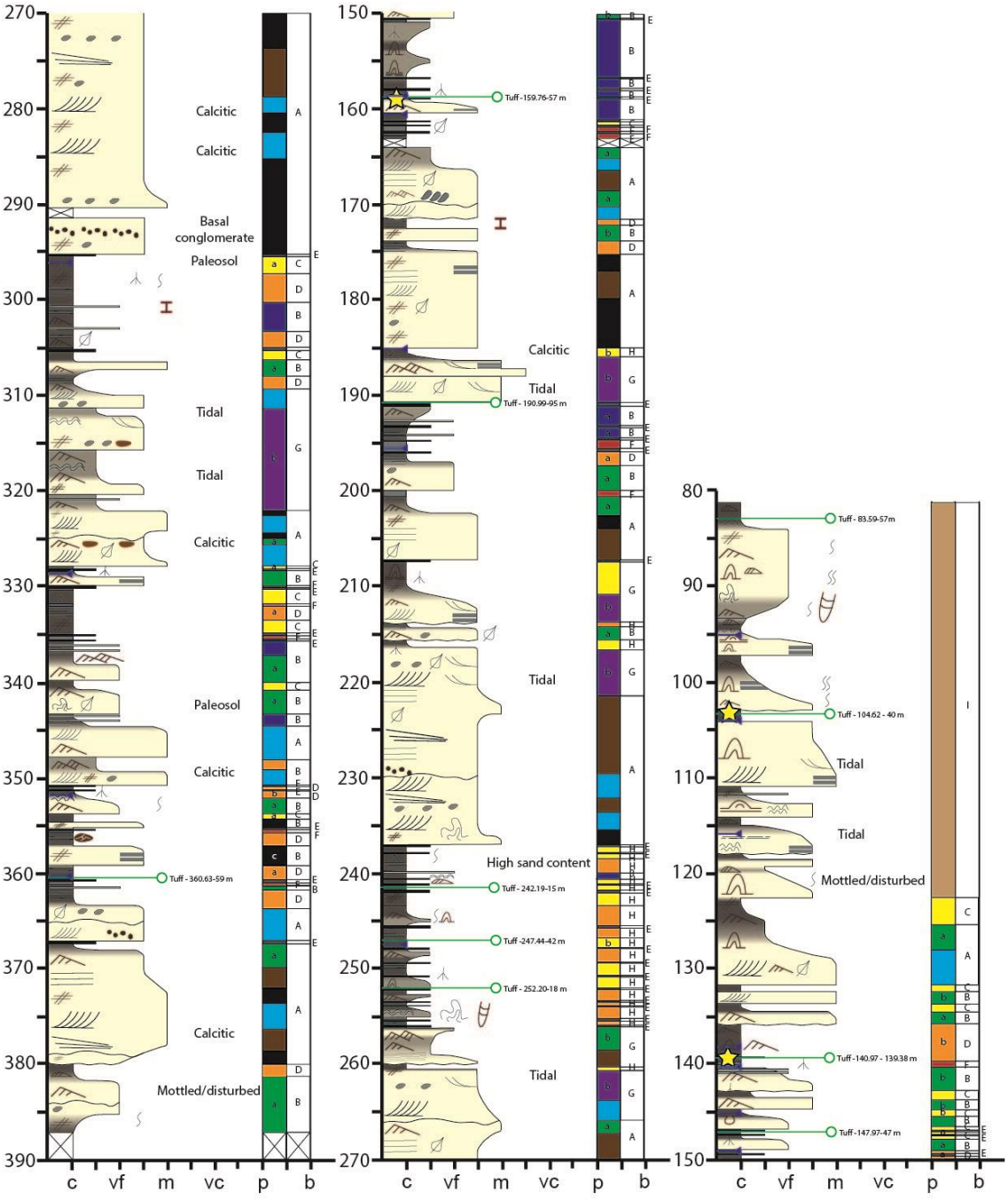

Figure 6.4c. A measured section (including tuff and palynological sample locations) from the Indy 3 well spanning the Walloon Coal Measures (390 to 138 m?), the Springbok Sandstone (138 to 124 m?), and the Westbourne Formation (124 to 80 m?).

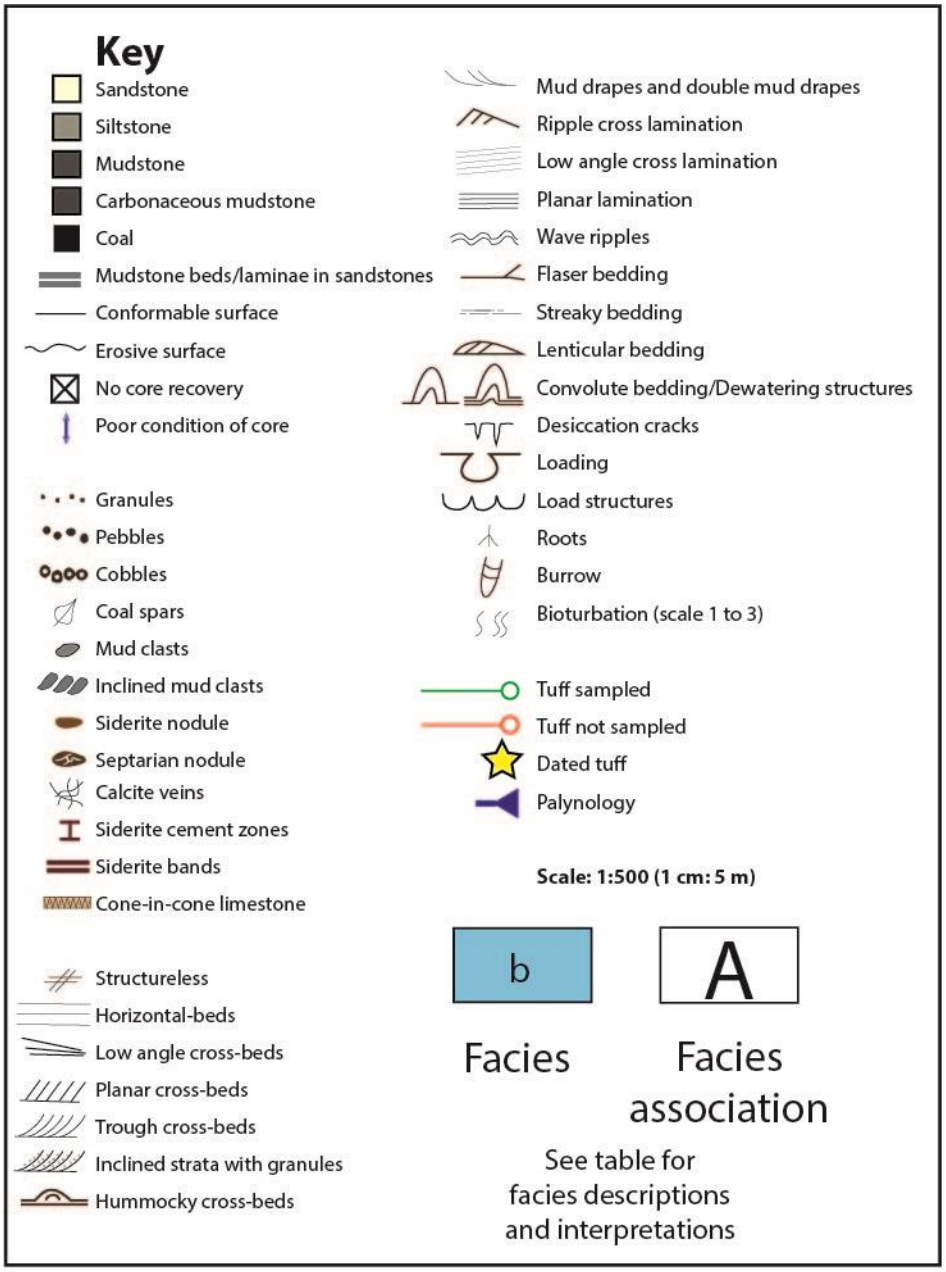

Figure 6.4d. Legend for measured sections.

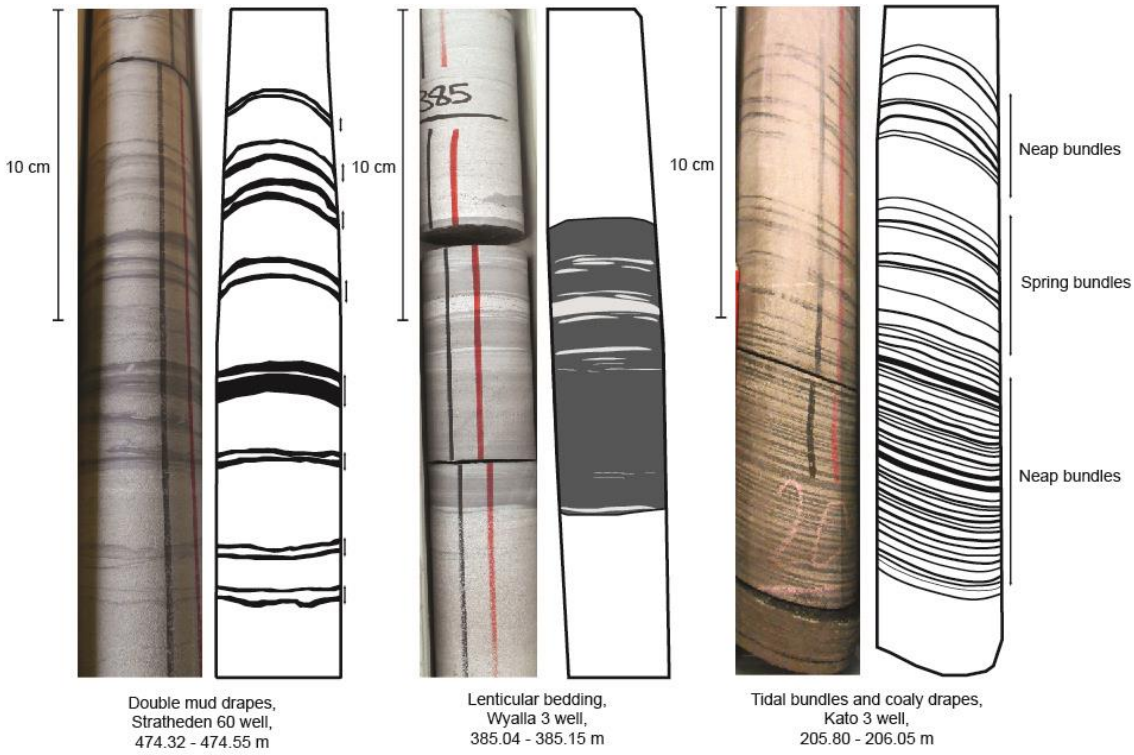

Figure 6.5. Raw and annotated core photographs showing double mud drapes, lenticular bedding, tidal bundles and coaly drapes in tidally influenced channel sandstones indicative of deposition by tidal processes from the Stratheden 60, Wyalla 3 and Kato 3 wells.

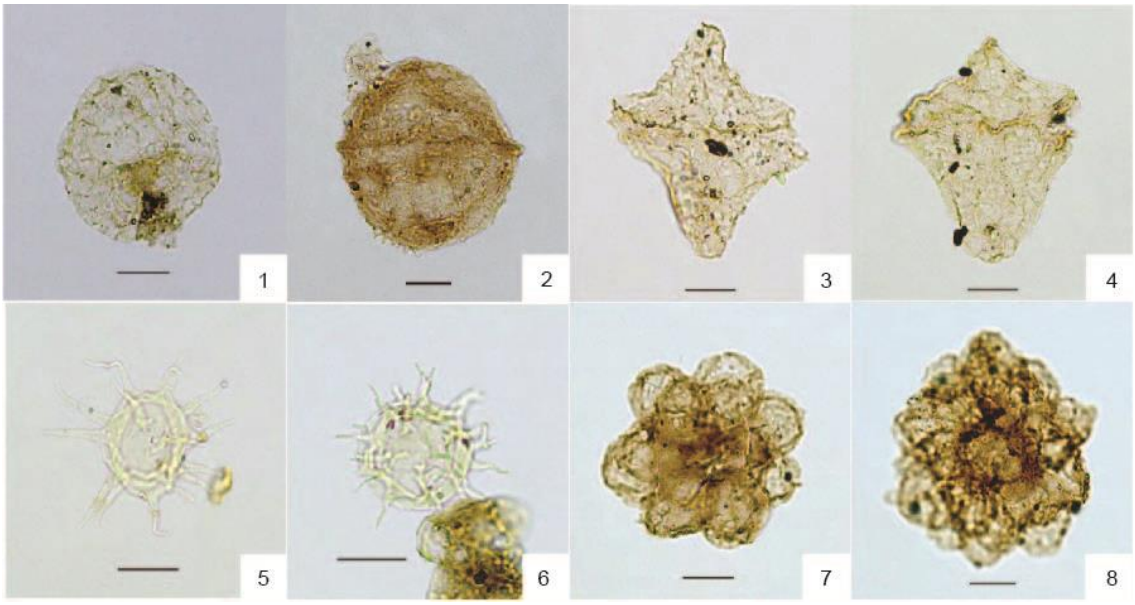

Figure 6.6. Examples of dinoflagellate cysts, acritarchs, and colonial algae from tidally influenced mudflats: (1) *Moorodinium crispa*, Indy 3 well, 247.55 m, slide 3, U41/1. (2) *Moorodinium crispa*, Indy 3 well, 247.55 m, slide 3, W47/3. (3) *Skuadinium fusumaster*, Indy 3 well, 247.55 m, slide 3, S44/1. (4) *Skuadinium fusumaster*, Indy 3 well, 247.55 m, slide 3, S44/1. (5) *Micrhystridium* spp, Stratheden 4 well, 452.00 m, slide 1, W34/1. (6) *Micrhystridium* spp, Stratheden 4 well, 444.0 0m, slide 1, W34/1 (7) *Palambages pariunta*, Indy 3 well, 247.55m, slide 3, Q42/3. (8) *Palambages pariunta*, Indy 3 well, 247.55m, slide 3, X15/2.

6.5 Palaeogeographic maps

6.5.1 Methodology

A series of palaeogeographic maps (Figures 6.7 and 6.8) were constructed showing the evolution of the Walloon Coal Measures in the area of the CBM play in the Surat Basin based on our interpretation of the overall depositional systems. The maps are based on analyses of measured sections of cores from 9 wells (Figures 6.4a to 6.4c and supplementary paper Figures 1 to 6) and wireline logs from 674 wells (Table 6.2) including those with measured sections. Palaeogeographic maps were constructed for eleven chronostratigraphic intervals over a time span of ~13 Ma using the new chronostratigraphic framework of Wainman et al. (2017) (see Section 4.4.4). The time represented by each palaeogeographic map varies from between 0.09 and 4.56 Ma. No single stratigraphic interval spans the entire CBM play (Wainman et al. 2017) (see Section 4.4.4) and lateral equivalents are either undrilled or have been removed by erosion. The geographic extent of the maps was limited by a paucity of wells and limited age control to the south and to the east in the Clarence-Moreton Basin. Likewise, it was not possible to construct meaningful maps of the Middle Jurassic.

Facies	Density value (g/cm^3)	Gamma value (API)
Organic-rich assemblage (facies associations E and F)	<1.8	N/A
Fine-grained assemblage (facies associations C, D and H)	≥2.0	≥90
Channel assemblage (facies association A, B and G)	≥2.0	≤90

Table 6.2. Gamma and density cut-off values for assemblages determined for palaeogeographic maps in Middle to Upper Jurassic Strata of the Surat Basin. Adapted from Hamilton et al. (2014b).

To generate palaeogeographic maps, strata were divided into three assemblages based on the facies analysis of drill core and interpretation of wireline logs. A “channel assemblage” was mapped where the percentage of sandstone was greater than 50% - these sandstones are interpreted as the deposits of fluvial channels, crevasse splays and tidal channels (facies associations A, B, and G). An “organic-rich assemblage” was mapped where more than 5% of the time slice is composed of facies associations E and F (coal and carbonaceous mudstone) and less than 30% sandstone. Although Facies E and F rarely comprise more than 40% of a section through a time slice it is important to remember that these facies have undergone substantially more compaction than other facies – the peat-to-coal compaction ratio may well have been >10:1. This assemblage is interpreted as areas where peat-forming mires and wetlands prevailed for long periods of time. All other strata were assigned to a “fine-grained assemblage” that consists predominantly of strata deposited in floodplain, shallow lacustrine and tidal flats environments (facies associations C, D and H).

A series of maps were created in Schlumberger’s Petrel stratigraphy module and exported via Petrosys into ESRI’s ArcGIS for analysis to show the thickness, composition and interpreted depositional environments. Isopach maps were not corrected for dip owing to the shallow dip of strata in the Surat Basin. Figure 6.7 shows the suite of maps for time interval 163.05 to 162.18 Ma (early Oxfordian). Ten other interval thickness and environments of deposition maps are included in the supplementary papers (Figures 7 to 16).

Depositional trends and the distribution of assemblages in these palaeogeographic maps are generic and were likely much more variable than those depicted in the maps but hopefully, they portray general trends and the relatively short time periods represented by each map throws new light on the evolution of the entire system.

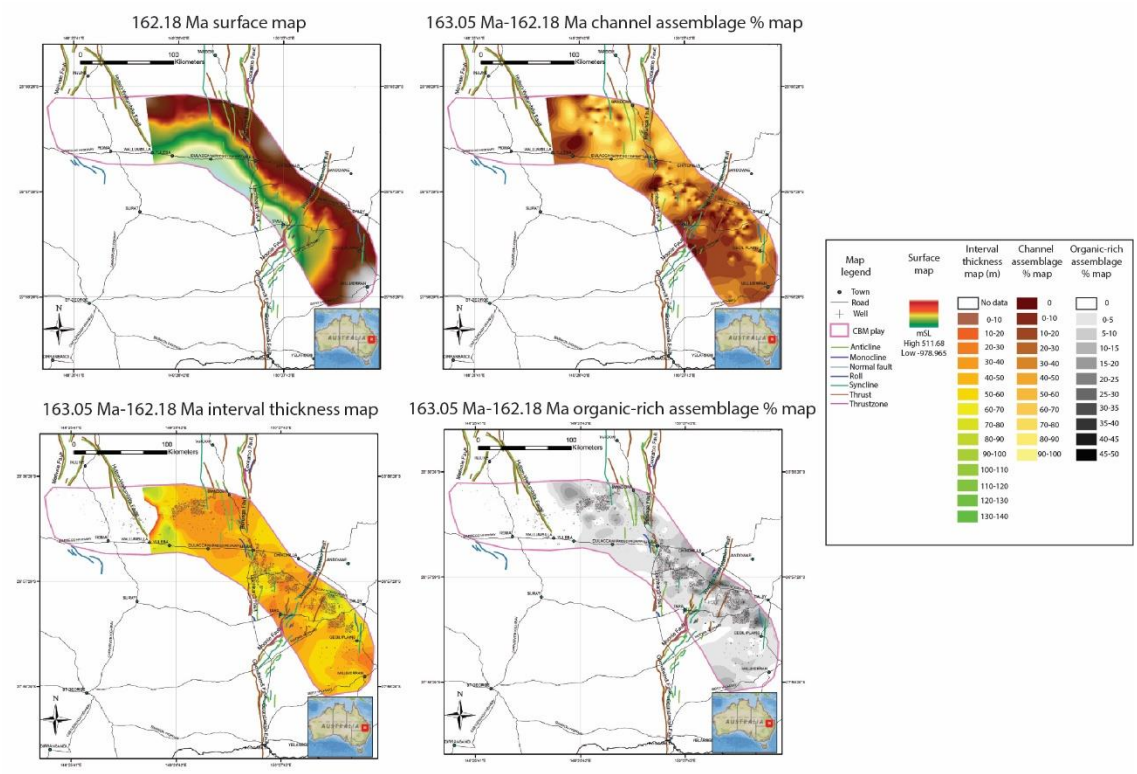

Figure 6.7. Surface, interval thickness, channel assemblage percentage and organic-rich assemblage percentage maps from the 163.08 Ma to 162.18 Ma time slice.

6.5.2 Palaeogeographic evolution

The palaeogeographic maps reveal a fluviolacustrine system that drained to the south/southwest and southeast. Rivers flowed from several entry points in highlands comprising the New England Orogenic Belt and were orientated for the greater part towards the axial trend of the Mimosa Syncline to the south. In the eastern Surat Basin, some rivers flowed towards the Clarence-Moreton Basin to the southeast. The role of faults and differential subsidence on sediment pathways is revealed with rivers confined to channel belts in areas of low subsidence to the west. This is most apparent adjacent to the Leichhardt-Burunga Fault (Figure 6.8) and near the Wambo Fault and Moonie-Goondiwindi Faults with stacked channel fills (e.g. Guluguba 2 well from 480 to 455 m, Figure 6.4b) and the increased percentage of channel assemblages (Figure 6.8). In the eastern Surat Basin, there was a greater prevalence of smaller, isolated fluvial channels revealed by low percentages of sandstones facies associations (Figure 6.8) and single story channel fills (e.g. Stratheden 60 well

from 222 to 215 m, Figure 6.4a). There was a marked increase in channel assemblages in the middle Oxfordian from 159.92 to 158.86 Ma (Figure 6.8). During this time interval, there was a reorganisation of the fluviolacustrine system in the eastern Surat Basin with drainage towards the southeast. At 157.55 Ma (late Oxfordian), the system orientated back to the south and southwest. Fine-grained assemblages including floodplains and shallow lakes prevailed in the interfluves or were isolated from avulsion events.

Organic-rich assemblages have pod and lensoidal geometries of limited lateral extent (<10 km) with no preferential orientation (Figure 6.8). The organic-rich assemblage tends to occur in areas where intervals are thicker and may be adjacent to channel belts or isolated from clastic deposition on the floodplain or close to tidal mudflats. On a regional scale, organic-rich assemblages were more widespread between 163.16 (early Oxfordian) and 151.39 Ma (early Tithonian) to the east of the Leichhardt-Burunga Fault and absent in the western Surat Basin after 150.11 Ma.

On a regional scale, it is likely that rivers drained into proximal estuarine complexes in incised valleys to the south and southeast with the intrusion of brackish conditions at times of high eustatic sea-level during the Callovian and Tithonian. This is supported by Callovian and Tithonian U-Pb CA-TIMS zircon dates from tuff beds in the Walloon Coal Measures (Wainman et al. 2017) that are in close association with tidally-influenced facies. The palaeodrainage patterns on our maps suggest that these marine transgressions into the continental interior may have originated from both the Carpentaria Basin in the north and from the east via the Clarence-Moreton Basin (Figure 6.9). These marine incursions onto the continent may have been precursors to those of the Early Cretaceous mapped by Struckmeyer and Totterdell (1990) and Bradshaw and Yeung (1992). Previous palaeogeographic interpretations from the Late Jurassic previously suggested a vast lowland comprising meandering rivers, swamps and shallow lakes with no marine influences in the continental interior of eastern Australia (Struckmeyer and Totterdell 1990; Bradshaw and Yeung 1992).

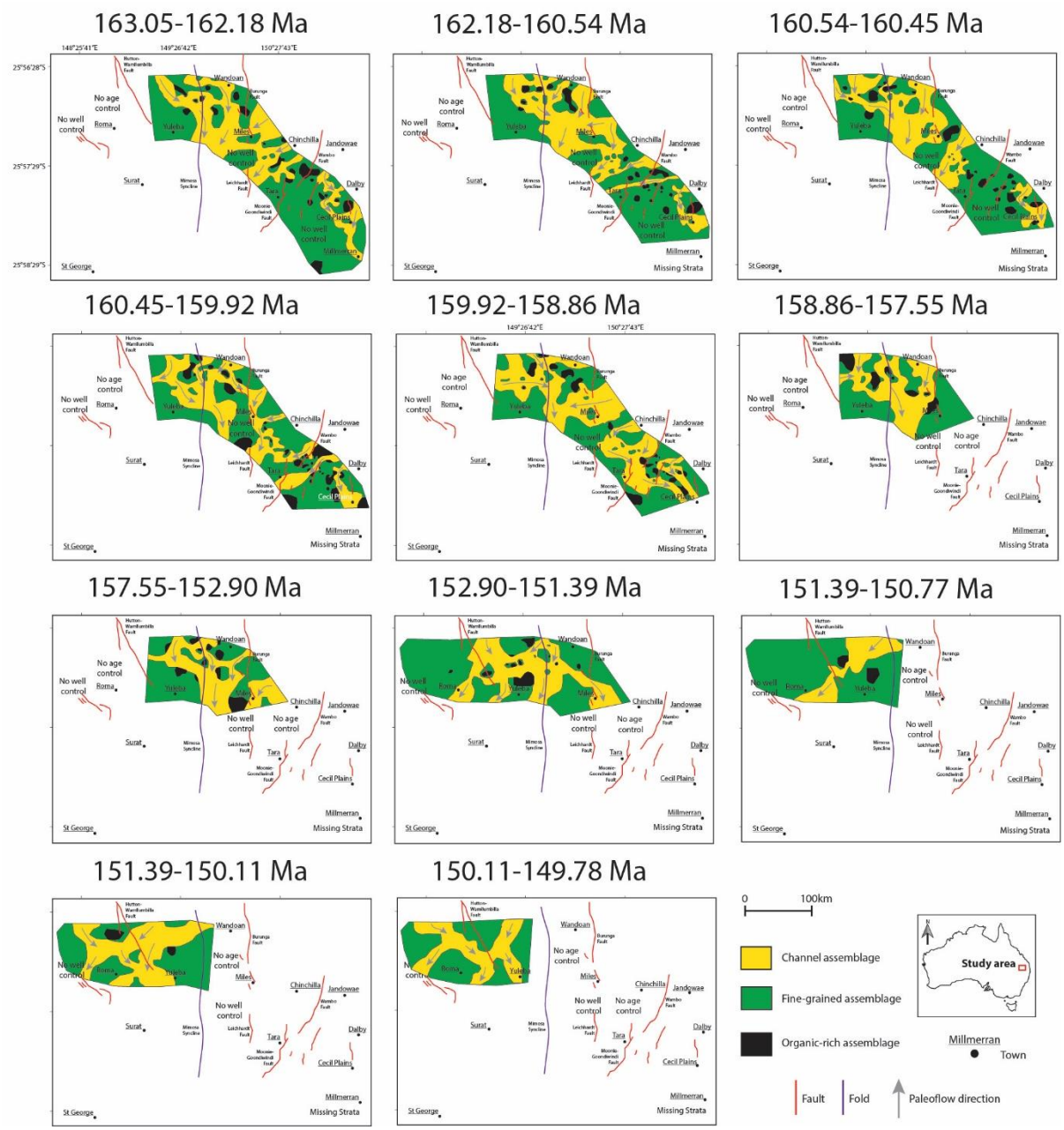

Figure 6.8. Palaeogeographic reconstructions and depositional trends from 163.05 Ma to 149.78 Ma.

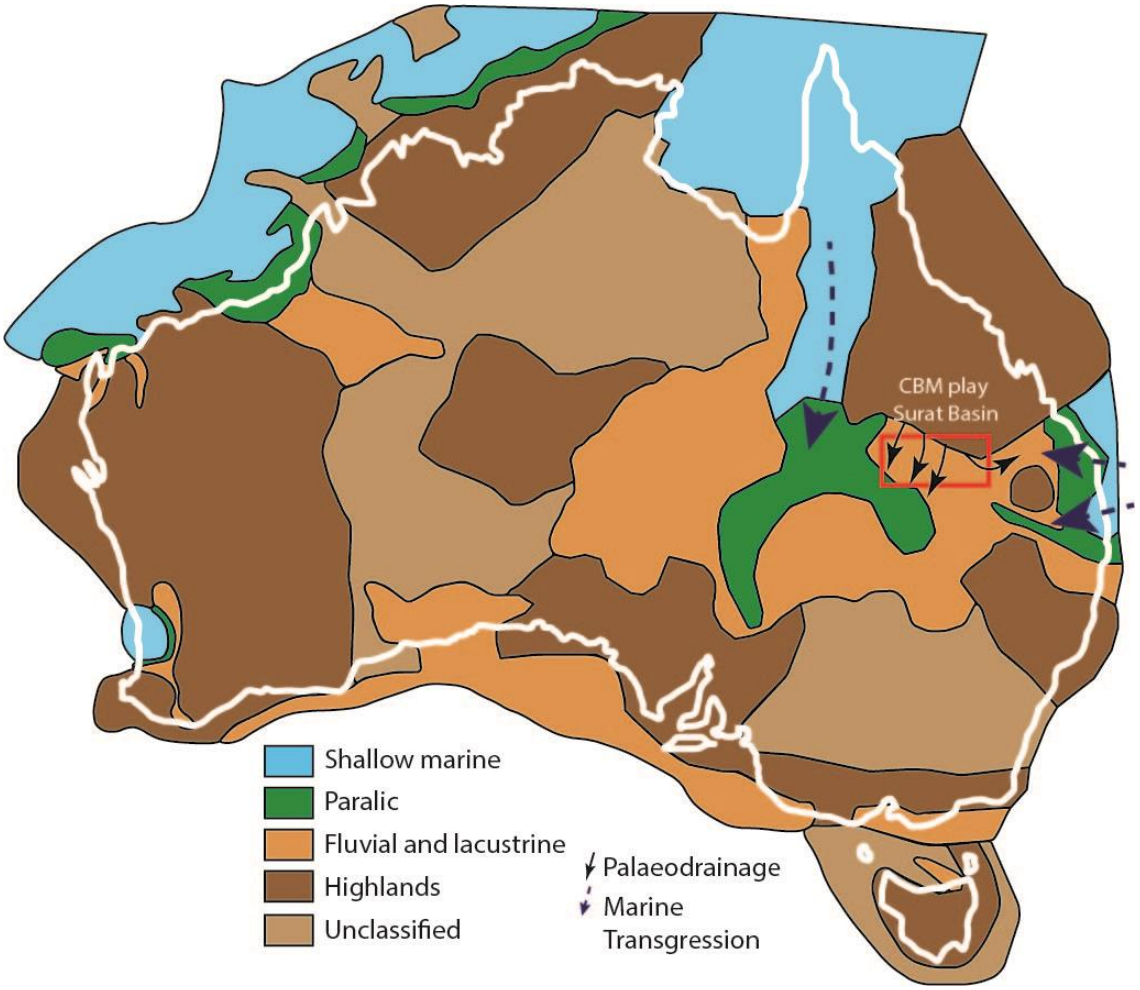

Figure 6.9. Regional palaeogeographic interpretation for the Late Jurassic of Australia. Adapted for this study from Struckmeyer and Totterdell (1990) and Bradshaw and Yeung (1992).

6.6 Depositional environments – a holistic perspective

There have been numerous interpretations of the depositional environments of the Walloon Coal Measures, however Exon (1976), Exon and Burger (1981), (Yago 1996b); Martin et al. (2013), Hamilton et al. (2014b), Shields and Esterle (2015) or Zhou et al. (2017) did not address fundamental questions about the evolution of the depositional systems over time. Typically, previous authors have attempted to develop a single depositional facies model for the entire formation. On a regional basis, the formation represents deposition over 19 million years and any one vertical section through the formation represents deposition over at least 4 million years (Wainman et al. 2017). If one considers how dramatically any terrestrial environment today has changed over the last

million years, and even more so since the Miocene, it seems highly unlikely that the environment of deposition remained relatively constant in the Surat Basin from the late Middle Jurassic through much of the Late Jurassic. Allocyclic controls must have shifted many times over that time period – these may have included climatic shifts, the gradient of river systems created by uplift or denudation in the source area, downstream changes in lake or sea-level, and temporal variations in subsidence rates within the basin. We will now discuss such fundamental questions in light of our new data.

6.6.1 Indications of base level shifts

The Walloon Coal Measures have previously been considered entirely terrestrial in nature. Yago (1996b) and Martin et al. (2013), for example, consider the Walloon Coal Measures as entirely nonmarine with the Surat Basin hundreds of kilometres from the palaeocoastline with endorheic drainage to the west towards a lacustrine body known as Lake Birkhead on the Queensland/South Australia border (Boult 1996). Facies Associations G and H, however, provide evidence of brackish water conditions with some tidal influence. Whereas none of the sedimentary structures (such as double mud drapes) or microfossils (such as dinoflagellate cysts) are unequivocal evidence of such marine influence, the unique association of several of these features at discrete levels within the formation is a powerful indicator that such conditions existed. Similar sedimentary structures, including double mud drapes, are preserved in the tidal channels of the Holocene Oosterschelde tidal basin in the Rhine Estuary of southwest Netherlands (Nio and Yang 1991). Dinoflagellate cyst assemblages similar to those of the Walloon Coal Measures are present in the marginal marine to lacustrine depositional environments of the Jurassic Plover Formation in the Bonaparte Basin of Australia (Riding and Helby 2001). The reach of tidal processes upstream in rivers and incised valleys have also been documented for a number of other ancient fluvial systems, including the on Miocene-late Pleistocene southern Java Sea Shelf (Posamentier 2001), Upper Carboniferous fluvio–deltaic strata of the southern North Sea (Hampson et al. 1999), and the Late Cretaceous Hollin and Napo formations of the Oriente Basin in Ecuador (Shanmugam et al. 2000). No fully marine strata have been

documented from the Surat Basin and the position of the coastline at times of maximum transgression is not known.

The marine-influenced facies provide evidence of times of base level rise while strata interpreted as incised valleys suggest periods of base level fall. The multistorey channel successions that appear fluvial in the lower part and more tidally-influenced in the upper part are similar to many incised valley deposits including the Quaternary Trinity/Sabine incised valley in Texas (Thomas and Anderson 1994) and the Turonian Ferron Sandstone of the Cretaceous Western Interior Seaway Basin in Utah (Garrison Jr and Van den Bergh 2006). McCabe and Shanley (1992) and Shanley and McCabe (1993) described similar incised valleys from the Cretaceous of the Western Interior of the USA which could clearly be linked to a fall and rise in relative sea-level in coeval shoreface and open marine strata several tens of kilometres seaward. The fluvial-tidal transition in an estuarine complex is dominated by mud (Kvale and Barnhill 1994) and such a setting may explain the mud-rich character of the tidally-influenced facies in the Walloon Coal Measures. On this evidence, it seems likely that the tidally-influenced strata of the Walloon Coal Measures were deposited many kilometres inland from coeval shorelines to the south and southeast and it is possible that any shoreface deposits of the highstands were eroded during subsequent lowstands.

Previous workers have attempted to apply sequence stratigraphic nomenclature to the Walloon Coal Measures. Shields and Esterle (2015) suggest there is parasequence-scale cyclicity in the formation (fining-upwards successions of channel sandstones overlain by heterolithics and coal), however, they note that without robust chronostratigraphic datums, it was not possible to correlate to extra-basinal events. They also suggest that a zone within the formation with more abundant coals and fewer channel sandstones represent a maximum flooding surface. Others including Zhou et al. (2017) make comparisons to sequence stratigraphic models in paralic settings of Bohacs and Suter (1997) where coal thickness directly relates to changes in base level mainly caused by changes in eustatic sea-level (e.g. thicker coal packages during the early transgressive and highstand systems tracts). These interpretation(s) of the Walloon Coal Measures do not identify any marine or brackish facies

associated with the supposed maximum flooding surface. Furthermore, recent stratigraphic correlations based on high resolution dating of tuffs by Wainman et al. (2017) suggest that there is no basin-wide zone of coal enrichment (Figure 6.9). Development of a meaningful sequence stratigraphic interpretation of the Walloon Coal Measures will require considerably more detailed studies with the correlation of candidate sequence boundaries (bases of sandstones interpreted as incised valleys) and transgressive deposits as indicated by tidal sedimentary structures with associated brackish palynomorphs.

If some of the channels represent the infill of incised valleys, as indicated by the stacked channels and an upward transition from fluvial to tidally-influenced strata, it is also possible that some of the stacked channel sandstones that are entirely fluvial in character are also the infill of valleys cut during lowstands of base level. It is important to remember that base level in a river system is not necessarily driven by downstream controls (rise and falls of downstream sea or lake levels) but can also be driven by variations in subsidence across a basin or by changes in the elevation of the source terrain. As some of the channel units of facies association A are multistorey in nature, as in the Guluguba 2 well between 482 and 454 m (Figure 6.4b), it is possible that these also represent a fall and rise in base level (Shields and Esterle 2015).

6.6.2 Which facies were coeval?

Recognition that base level falls and rises took place during the accumulation of the Walloon Coal Measures raises the question as to which facies were coeval. Clearly, it is unlikely that there were widespread mires and lakes during the cut and fill of the incised valleys with their associated brackish water/tidally-influenced facies as valley incision would leave laterally equivalent interfluve surfaces well-drained, prone to subaerial exposure and the development of palaeosols (Flint et al. 1995). It is possible that mires and lakes were only extensive at certain times when climate and groundwater levels were favourable (see Section 5.6). Jerrett et al. (2011b) for example suggested that some coals in the Appalachian Basin resulted from paludification of interfluves between incised valleys and may mark the transition of a transgressive to highstand systems tract (Flint et al, 1995). However, although coals are common and represent up to 6% of the total thickness of the formation, our

stratigraphic correlations based on 674 wells do not show convincing evidence of any regionally extensive coal beds or lacustrine intervaMartin et al. (2013)ls. This is contrary to the interpretation of Jones and Patrick (1981) who suggested that the coals are laterally persistent.

McCabe (1984) and Bohacs and Suter (1997) argue that coal (peat) accumulation is unlikely to take place in close association with active clastic environments unless there are raised mires. This is because low-lying mires would easily be inundated by floodwaters that introduce sediment significantly diluting the organic content of the peat: in such cases, the final sediment would likely be a carbonaceous mudstone (as in facies association F) rather than a true coal. Although coal beds in the Walloon Coal Measures are relatively thin (<0.46 m) the original peats were thicker (up to 4.6 m assuming a 10 to 1 compaction ratio) and they may have been deposited by raised mires. Martin et al. (2013), Shields and Esterle (2015) and Shields et al. (2017) who describe some of the mires as ‘channel hugging’ or in close proximity to active channels with their position controlled by the palaeorivers. This seems unlikely if the mires were low-lying whereas a raised mire can control the geometry of a river (McCabe and Shanley 1992). Without further evidence, it is unclear whether coal (peat) accumulation took place coevally and in close association with the deposition of much of the fluviolacustrine strata. Although it is a natural inclination to regard adjoining facies in continental strata as having been deposited coevally and in close association, lessons from the marine realm suggest that may well not be the case. The new evidence from the Walloon Coal Measures suggests that deposition of at least some of the facies were driven by allocyclic controls.

6.6.3 The nature of the fluviolacustrine system

Previous workers have interpreted the siliciclastic strata of the Walloon Coal Measures as the deposits of meandering and/or anastomosed rivers (Jones and Patrick 1981; Green et al. 1997a; Shields and Esterle 2015; Zhou et al. 2017) based on the correlation of similar sedimentary facies. Given the length of time represented by the formation and its geographic extent, it is most likely that there were several river types over time and space. Consequently, it is dangerous to over interpret the morphology of the rivers that deposited the

sandstones. The abundance of cross-lamination and maximum grain size of medium sand in most fining-upward successions suggests relatively low-gradient rivers were present during deposition of the Walloon Coal Measures. The paucity of planar-tabular cross-beds suggest that sand bars were not common: as these are signature features of sandy braided rivers including the Tana River in Norway (Collinson 1970), the Platte River in Nebraska (Smith 1971) and the South Saskatchewan River in Canada (Cant and Walker 1978; Sambrook Smith et al. 2006). This suggests that there were few, if any such systems within the Surat Basin during deposition of the Walloon Coal Measures. Anastomosed and meandering rivers are not mutually exclusive – in fact, the larger rivers within an anastomosed system are often meandering including the Magdalena River in Columbia (Smith 1986; Morón-Polanco 2016) and the Murray River in southeastern Australia (Nanson and Knighton 1996). The avulsion of meandering rivers may result in an anastomosed river complex that eventually reverts to a meandering system over time as one channel becomes dominant as evident in the Saskatchewan River of Cumberland House (Smith and Perez-Arlucea 1994; Morozova and Smith 2000). The depth of meandering channels at bankfull discharge can be estimated by the vertical distance between the basal scour surface of a fining-upward succession and the transition to mudrocks (Leeder 1973). It is not always easy, however, to determine the “basal” scour of a channel in thick sandstones in core where it is impossible to know whether multiple scour surfaces were produced within a single fluvial channel or whether the thick sandstones represent stacking of several channel units. In most cases, the uppermost fining-upward succession is of a similar magnitude to fining-upward sandstones without multiple scour surfaces – indicating that the thick sandstones are likely stacked channel deposits. Given that assumption, our estimates of bankfull depth of the rivers are up to a maximum of 14.6 m but many are in the range of 2.3 to 7.8 m. This suggests that the rivers may have been no larger than the meandering Wabash River of Illinois and Indiana (Jackson 1975) that has a channel width of ~300 m and a meander-belt width of ~5 km. Shields and Esterle (2015) suggest that some of the rivers were meandering based on the presence of inclined heterolithic strata produced by lateral migration of a channel. However, it is unclear how this type of stratal pattern was identified in core and, if indeed

inclined heterolithic strata are present it is more likely an indicator of tidally-influenced channels rather than purely fluvial meandering systems (Thomas et al. 1987; Choi et al. 2004; Sisulak and Dashtgard 2012).

Shields and Esterle (2015) have suggested that the Walloons Coal Measures were deposited by a single fluvial system that flowed parallel to the New England orogenic belt which changed in the central Surat Basin from a meandering tributary system, in its more proximal reaches, to a distributive fluvial system (Nichols and Fisher 2007; Weissmann et al. 2010) downstream towards the south. According to the definition of Weissmann et al. (2010), a distributive fluvial system is one that radiates "outward from an apex that is located where the river enters the sedimentary basin" – this is clearly not the case in Shields and Esterle (2015). However, the suggestion that the river transformed from a tributary system to a distributary system downstream is an interesting one. Distributary systems are obviously important in fluvial and tide-dominated deltas but such a setting is not the case for the Surat Basin. A distributive fluvial system should have smaller channels in a downstream direction as the flow is split between progressively more channels. Our observations do suggest that the channel sandstones (facies association A) tend to be thinner (6 m) in the southeast and that agrees with Shields & Esterle's model, but our palaeogeographic maps (see previous section) do not support the notion of a trunk system running through the entire Surat Basin.

The Okavango Delta is an example of a distributive fluvial system with extensive wetlands. The Okavango river transforms into a distributive system when it crosses the Gumare Fault and forms an "inland delta" that covers an area of approximately 12,000 km^2 (McCarthy and Ellery 1998; Gumbricht et al. 2001) – an area equivalent to about one-quarter of the present-day Surat Basin in Queensland. The gradient of the fluvial system in the Okavango Delta is low: about 25 cm per kilometre. Although the tectonic and climatic setting of the Okavango Delta is quite different from that of the Walloon Coal Measures, some interesting comparisons can be made. The first question is whether the Surat Basin strata was fed by a single large river that split up as it entered the basin or whether there were many smaller rivers entering the basin – our palaeogeographic maps suggest the latter was the case (Figure 6.8). The

second question is whether the Surat Basin had an inland drainage pattern forming an “inland delta”. Our interpretation of marine-influence in parts of the Walloon Coal Measures suggests that was not the case contrary to previous interpretations including by Boult (1996).

The petrographic immaturity of sandstones (medium-grained litharenites) (Martin et al. 2013) suggests that the fluvial systems were proximal to the source area. Isopachs of sandstone percentage suggest that there were several systems emanating from the northern flank of the basin and that the loci of these systems remained constant for extended periods of time. Thick, stacked channel-fills in the Guluguba 2 well appear to have formed within one of these proximal locations. Of particular interest is that within the northern part of the Surat Basin, amalgamated channel fills are found in areas of low subsidence with low interval thickness. This is contrary to models of channel belt stacking by Bridge and Leeder (1979) who suggested that fault-induced topography will cause rivers (and channel belts) to shift towards the zone of maximum subsidence. For the Walloon Coal Measures, channel stacking patterns appear to be more similar to those observed in the intermontane Pleistocene fluvial successions in the Körös Basin in Hungary where an increase in sediment supply or tectonic activity trap rivers along the basin margins which compensates for subsidence (Nádor and Sztanó 2010). Many axial river systems in foreland basins also bypass the area of highest subsidence near the thrust front (Nádor and Sztanó 2010). The Burunga-Leichardt and Hutton Wallumbilla Faults may have acted in an equivalent manner during the Late Jurassic leading to low sand body connectiveness, shallow channel incision and high percentages of mudstone and siltstone facies in the eastern Surat Basin where subsidence rates were higher. Similar interpretations are made by Hamilton et al. (2014b) and Shields and Esterle (2015) who also suggest that local tectonism on the Leichhardt-Burunga Fault may have produced amalgamated fluvial channel sandstones in the northern Surat Basin.

6.6.4 Floodplain lakes and overbank facies

Fine-grained sediments (facies associations C, D and F) comprise a substantial part of the strata of the Walloon Coal Measures with increasing percentages in

the east in comparison to the western part of the Surat Basin (approximately 13% in the Indy 3 well and 30% in the Stratheden 60 well). These strata suggest extensive flat, vegetated areas and shallow lakes between river channels. The lakes were probably no more than 2.5 m deep (the thickest unit of facies association D is 4 m) and may have covered up to a few tens of square kilometres in area. Lacustrine sediments make up about 50% of the overbank strata and their abundance suggests that lakes were commonly formed by either rapid rises of groundwater tables, controlled by base level or climatic variations over time, or by river avulsion. The environment envisaged may have been similar (though in a much cooler climate) to the Sudd swamp of Southern Sudan where rivers flow across floodplains with shallow lakes and poorly drained swamps (Rzóska 1974). The Saskatchewan River avulsion area is also characterised by extensive lakes and crevasse splay complexes that prograde into peatlands and shallow lakes adjacent to active river channels (Morozova and Smith 2000).

6.7 Conclusion

This multidisciplinary study sheds new light on the character and evolution of the Jurassic Walloon Coal Measures. Detailed facies analyses indicate that, for the most part, deposition of the Walloon Coal Measures was characterised by a fluviolacustrine system with small (<300 m wide) low-gradient rivers on a poorly drained floodplain with numerous small lakes.

At a few intervals facies have sedimentary structures (such as double mud-drapes) and a palynoflora (including dinoflagellate cysts and acritarchs) that indicate a brackish and tidal influence. These facies are associated with thick amalgamated sandstones that are interpreted as the fill of incised valleys cut during lowstands and filled during subsequent transgressive episodes.

Evidence of base level shifts suggests that it would be simplistic to apply a single sedimentary facies model to the entire Walloon Coal Measures. The formation was deposited over a 19 million-year interval and that allocyclic controls may have allowed the preferential development of certain facies at different times. For example, many coals may have formed during times of higher precipitation or when water tables rose along with base level rise.

Palaeogeographic reconstructions suggest that rivers entered the basin from several loci from the New England Orogenic Belt to the north and east. Amalgamation of fluvial channel sandstones appear to form in some areas due to differential local subsidence. The rivers drained to the south/southwest and southeast, presumably into proximal estuarine complexes. This drainage pattern is compatible with the notion that marine transgressions into the Australian continent came from the north and the east as has been suggested for the Early Cretaceous).

This study emphasizes the need for an interdisciplinary approach to identify candidate sequence boundaries and transgressive deposits in predominantly nonmarine settings. The same approach should also help elucidate the evolution of other fluviolacustrine systems.

6.8 Acknowledgements

This research was funded through several research grants and scholarships. Carmine Wainman has a Ph.D. scholarship from the University of Adelaide that has covered most of the travel and analytical costs. We are thankful to Geoscience Australia, Arrow Energy, Senex Energy and Joan Esterle from the University of Queensland for providing research funds and access to drill core. MGPalaeo Ltd kindly provided palynological slides for this study. ESRI, Schlumberger, and Petrosys kindly provided free ArcGIS, Petrel and Petrosys licenses. We would like to thank Renate Silwa, Daren Shields and Abbas Babaahmadi from the University of Queensland who kindly who kindly provided normalised well logs and the latest structural framework data from eastern Australian basins. We also thank Sandra Mann at the University of Adelaide for providing feedback prior to submission.

6.9 Supplementary papers

See appendices 3 (p. 350-365).

Statement of Authorship

Title of Paper	Calibrating the Middle to Late Jurassic spore-pollen palynostratigraphic framework of the Surat Basin, Australia with U-Pb CA-TIMS dates to the geologic time-scale
Publication Status	☐ Published ☐ Accepted for Publication ☐ Submitted for Publication X Unpublished and unsubmitted work written in manuscript style
Publication Details	Wainman, C. C., Hannaford, C., Mantle, D. J., McCabe, P. J. and Wood G. R. in prep-c. Calibrating the Middle to Late Jurassic spore-pollen palynostratigraphic framework of the Surat Basin, Australia with U-Pb CA-TIMS dates to the geologic time-scale. Intend to submit to Gondwana Research.

Principal Author

Name of Principal Author (Candidate)	Carmine C. Wainman		
Contribution to the Paper	Majority of the data collection and interpretation. Wrote the greater majority of the paper with exceptions noted in the co-authorship contributions. Produced final version of the paper using editorial suggestions of the co-authors.		
Overall percentage (%)	85		
Certification:	This paper reports on original research I conducted during the period of my Higher Degree by Research candidature and is not subject to any obligations or contractual agreements with a third party that would constrain its inclusion in this thesis. I am the primary author of this paper.		
Signature		Date	10/08/2017

Co-Author Contributions

By signing the Statement of Authorship, each author certifies that:

i. the candidate's stated contribution to the publication is accurate (as detailed above);
ii. permission is granted for the candidate in include the publication in the thesis; and
iii. the sum of all co-author contributions is equal to 100% less the candidate's stated contribution.

Name of Co-Author	Carey Hannaford		
Contribution to the Paper	Advice and guidance on research project and editorial comments for the paper. Produced all the Stratabugs figures in the appendices.		
Signature		Date	8/8/2017

Name of Co-Author	Daniel J. Mantle		
Contribution to the Paper	Advice and guidance on research project and editorial comments for the paper. Contributed to the section titled "Palynological processing and analysis" and produced Plate 7.1.		
Signature		Date	10/8/2017

Name of Co-Author	Peter J. McCabe		
Contribution to the Paper	Supervisor of Ph.D. – Extensive critical advice and guidance on research project and editorial comments for the paper.		
Signature		Date	10/8/2017

Chapter 7. Calibrating the Middle to Late Jurassic spore-pollen palynostratigraphic framework of the Surat Basin, Australia with U-Pb zircon CA-TIMS dates to the geologic time-scale

To be submitted to *Alcheringa*. A statement of authorship is provided on the previous page.

Co-authors: Carey Hannaford, Daniel Mantle and Peter McCabe.

Abstract

Spore-pollen palynostratigraphy is commonly used to subdivide and correlate Jurassic continental successions in eastern Australia and thus aid the construction of geological models for the petroleum and coal industries. However, the current spore-pollen framework has only been tenuously calibrated to the geologic time-scale. Age determinations are reliant on indirect correlations of ammonite and dinoflagellate assemblages from New Zealand, the North West Shelf of Australia and Southeast Asia to the standard European stages. New U-Pb CA-TIMS dates from 19 tuff beds in the Middle–Upper Jurassic Injune Creek Group of the Surat Basin enables regional spore-pollen palynostratigraphic zones to be precisely dated for the first time. These results show the base of the APJ4.2 and APJ4.3 subzones are similar in age to previous estimates (Middle Jurassic, Bathonian) from indirect palynostratigraphic correlation. However, the base of the APJ5 Zone and the APJ6.1 Subzone may be younger than previously estimated, possibly as much as ~2.5 and ~4.2 Ma, respectively. The continued utilization of U-Pb CA-TIMS dates will further refine the absolute ages of these zones, improve the inter- and intrabasinal correlation of Middle–Upper Jurassic strata in eastern Australian basins and greatly enhance intercontinental correlations.

7.1 Introduction

Palynostratigraphic frameworks play a key role in coal and petroleum exploration in Australia. In Upper Triassic–Upper Cretaceous strata of eastern Australia, the first and last occurrences of key spore and pollen taxa provide hypothetical chronostratigraphic surfaces within and between basins (Gallagher et al. 2008). This can help where there are lateral variations in nonmarine facies that can make lithostratigraphic correlations difficult (Laurie et al. 2016). However, some care is required as the spore-pollen assemblages may also be facies dependent and key marker taxa may be missing due to the local scarcity of parent plants, hydrodynamic properties limiting spore-pollen transport, or broader palaeoclimatological factors. As a consequence, it cannot be assumed that the first and last occurrence of a particular species is coeval between different localities (Bowring and Schmitz 2003). This, along with the difficulty in accurately tying the eastern Australia spore-pollen zones to the geologic time-scale of Ogg et al. (2016) creates a series of challenges to the broad application of palynostratigraphic frameworks in the region. Recently acquired U-Pb dates from Surat Basin tuff beds provide the first absolute age constraints on the duration of eastern Australian Jurassic spore-pollen zones. Better age dating of these spore-pollen zones will also allow the construction of more accurate geologic and burial history models where datable tuff beds are absent (Nicoll et al. 2015).

The standard practice to determine the age and duration of Mesozoic spore-pollen zones in eastern Australian basins has required making tenuous correlations to marine successions with ammonites and dinoflagellate cysts, in New Zealand, Southeast Asia and the North West Shelf of Australia (Helby et al. 1987; McKellar 1998; Stevens 2004; Riding and Mantle 2010; Riding et al. 2010). This allows for indirect calibration to the geological time-scale using the standard European ammonite zones. These zones are used to define all the stages of the Jurassic and they allow calibration to other physical, biological and geochemical stratigraphic frameworks (Ogg et al. 2016). Correlating to these European zones is not without its challenges including the rarity of key ammonite marker taxa outside of Europe and that many ammonites in Australia and New Zealand are endemic or comprise only a rare element in European

assemblages (Hall 1989; Stevens 2004). There is also uncertainty whether the ammonite marker taxa are themselves coeval in the northern and southern hemispheres (Hall 1989; Stevens 2004). In addition to the above, many of the Australian spore-pollen marker taxa are rare in marine strata (McKellar, 1998). In the absence of shared ammonite faunas, dinoflagellate cyst assemblages have also been commonly used to correlate to the European biozones, but these have many of the same issues, such as a high degree of endemism in Australian assemblages and a lack of certainty that all marker taxa are coeval in both hemispheres (Riding and Mantle 2010). The near absence of Jurassic marine strata from onshore eastern Australia further negates the utility of either ammonites or dinoflagellate cysts for global correlations. This lack of reliable faunal correlations to the standard European stages and the moderate palynofloral provincialism in Australia result in a considerable degree of uncertainty in the ages assigned to all Australian Jurassic spore-pollen zones, not just those in eastern Australian basins (Helby et al. 1987; McKellar 1998; Zeiss 2003; Riding and Mantle 2010).

U-Pb zircon ion probe dates from Jurassic Botany Bay Group in Antarctica (Hunter et al. 2005), $^{40}Ar/^{39}Ar$ dates from the Cretaceous Cerro Negro Formation of the South Shetland Islands (Hathway et al. 1999), and K-Ar and fission track dates from the Jurassic Casterton Formation of the Otway Basin in Australia (Mitchell et al. 1997) are currently the only published studies where Mesozoic spore-pollen zones in the southern hemisphere have been directly calibrated to the geologic time-scale using radiometric dates. Barham et al. (2016) have also recently calibrated the Early Cretaceous *Endoceratium ludbrookiae* Dinoflagellate Cyst Zone (107.50 to 104.00 Ma) using detrital U-Pb zircon dates from fine- to medium-grained micaceous glauconitic sandstone in the Bight Basin, Australia. These dates are, however, imprecise (up to ±10 Ma) and greater than the duration of most geologic stages in the Phanerozoic. U-Pb Chemical abrasion thermal ionization mass spectrometry (CA-TIMS) enables the dating of zircon crystals with far greater precision from a variety of rock types including air-fall tuffs (Mattinson 2005). This is achieved by chemical abrasion which removes parts of the zircon affected by Pb loss due to corrosion or radiation damage (Mattinson 2005). U-Pb zircon ages obtained using CA-

TIMS may have precisions of 0.1% or better (Mattinson 2005; Laurie et al. 2016). The value of U-Pb CA-TIMS dates in recalibrating spore-pollen palynostratigraphic frameworks has already been demonstrated in the older Permo-Triassic basins of eastern Australia where correlations to the geologic time-scale were previously restricted by the high degree of endemic biota and provincialism (Metcalfe et al. 2011; Laurie et al. 2016). U-Pb CA-TIMS dates from over 100 volcanic air-fall tuff beds have improved interbasinal correlation and recalibrated the age of spore-pollen palynostratigraphic zones by as much as 16 Ma (Laurie et al. 2015; Metcalfe et al. 2015; Nicoll et al. 2015; Laurie et al. 2016).

High-precision U-Pb dates have recently been obtained from the Jurassic Injune Creek Group of the Surat Basin in Queensland (168.07 ± 0.07 to 149.08 ± 0.06 Ma) (Wainman et al. 2015; Wainman et al. 2017) and provide an initial opportunity to directly calibrate existing Jurassic spore-pollen frameworks of eastern Australia to the geologic time-scale.

7.2 Geology of the Surat Basin

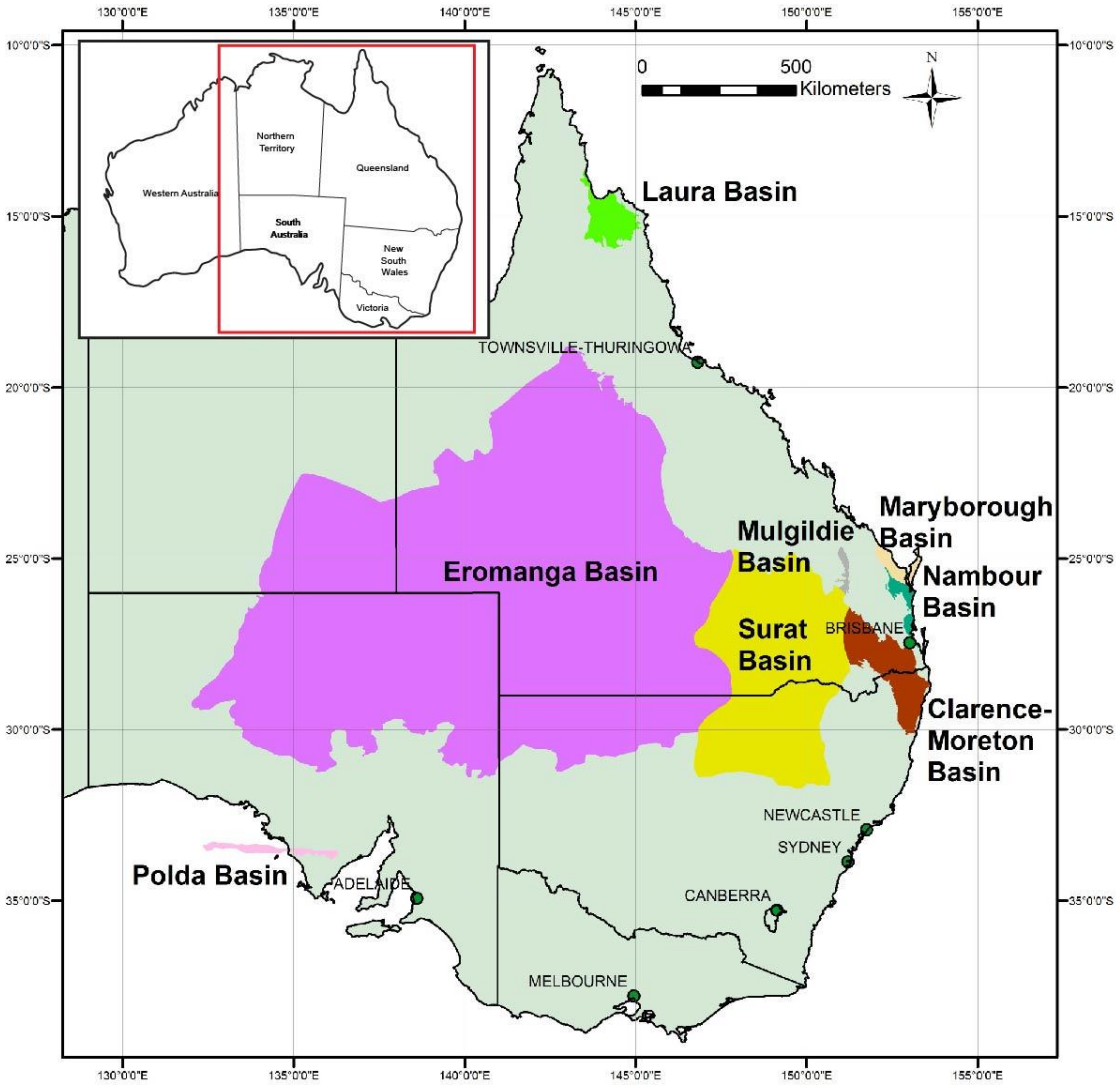

Figure 7.1. The geographic extent of Mesozoic basins across eastern Australia including the Surat Basin.

The Late Triassic to Early Cretaceous intracratonic Surat Basin (Figure 7.1) is part of the greater Australian Superbasin covering over 300,000 km^2 in southeast Queensland and northeast New South Wales with strata gently dipping to the southwest (Raza et al. 2009; Jell 2013). Basin architecture is controlled either by a series of pre-existing faults and folds in the underlying Permo–Triassic Bowen Basin (e.g. the Taroom Trough) or by the crystalline basement of the Early Devonian–Late Triassic orogenic complexes (e.g. the Leichhardt-Burunga Fault) (Ryan et al. 2012; Hamilton et al. 2014b). Deposition in the basin occurred over six sedimentary cycles from the Early Jurassic and

into the Cretaceous depositing terrestrial, paralic and later marine successions in response to eustatic sea-level change (Exon 1976; Exon and Burger 1981; Green et al. 1997a). The basin has been relatively inactive since the uplift and erosion of two kilometres of strata during the mid-Cretaceous (Scott 2008; Raza et al. 2009). The Injune Creek Group of the Surat Basin (the focus of this study) comprises the Eurombah Formation, the Walloon Coal Measures, the Springbok Sandstone and the Westbourne Formation (Figure 7.3)Opluštil et al. (2013) (Jell 2013). These formations were deposited predominantly in a fluviolacustrine environment with some brackish water influences (see Section 6.6.1).The basin hosts significant coal and coal seam gas reserves which are predominately located in the Walloon Coal Measures (Martin et al. 2013). Abundant tuff beds in the Injune Creek Group resulted from periodic volcanic eruptions that deposited ash onto mires, floodplains and lakes, but their source and associated tectonic environment (intraplate, rift or a subduction zone) remain uncertain (Fielding 1993; Yago 1996a; Jell 2013). The Surat Basin wells selected for this study are shown in Figure 7.2.

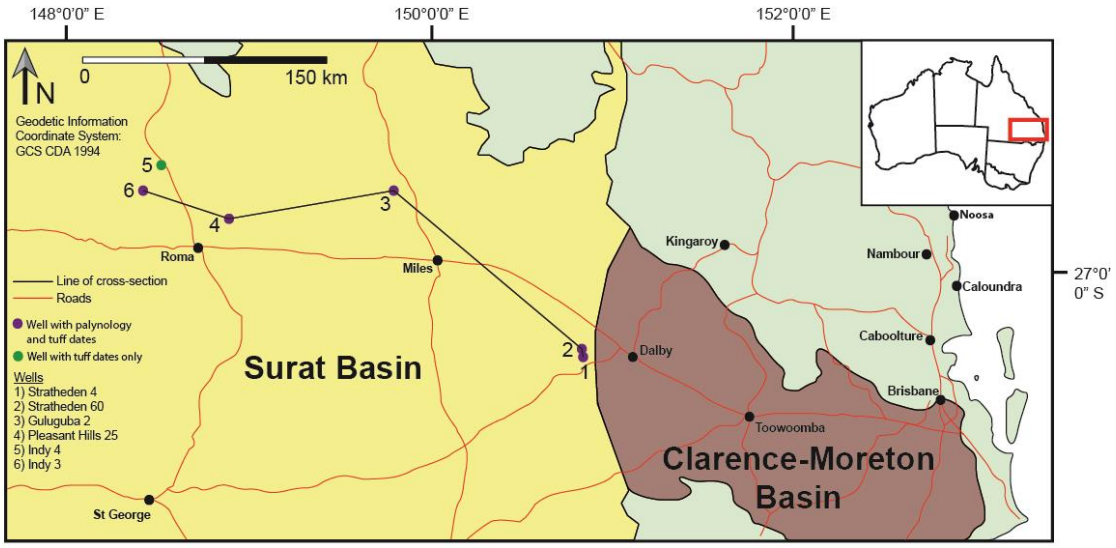

Figure 7.2. Location of wells with tuff beds dated using CA-TIMS in the Surat Basin of Queensland and subsequently selected for palynological investigations. Adapted from Wainman et al. (2017).

7.3 Jurassic palynostratigraphic schemes from eastern Australian basins

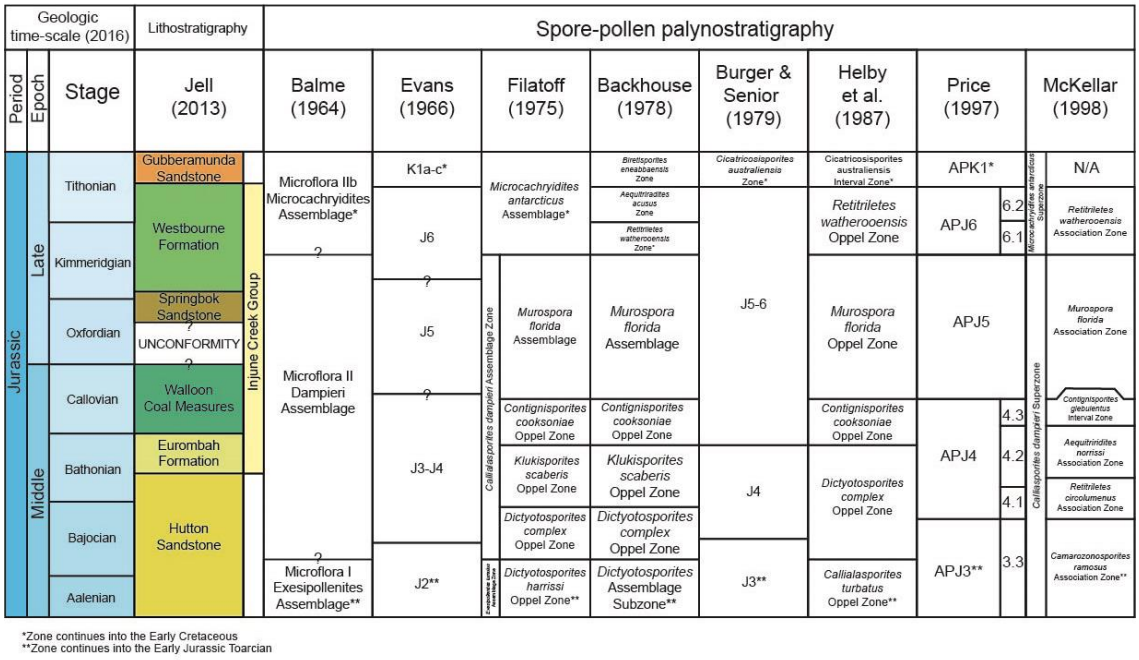

Figure 7.3. The evolution of the spore-pollen palynostratigraphic framework of Mesozoic Australian basins from the Middle to Late Jurassic tied to lithostratigraphic units from the Surat Basin. Adapted from McKellar (1998) and Sajadi and Playford (2002).

Australian Jurassic spore-pollen zonations have evolved considerably over the last 50 years (Figure 7.3). The early frameworks stemmed from low-resolution schemes constructed by Balme (1957, 1964) at the University of Western Australia, prior to Evans (1966) developing the first alphanumeric scheme whilst working at the Australian Bureau of Mineral Resources. This alphanumeric structure was conceived to help overcome problems associated with local palynological nomenclature and to unify the various stratigraphic terminologies and subdivisions already in use. This zonation would become the cornerstone for eastern Australian palynostratigraphy for the next two decades. Subsequent Jurassic spore-pollen zonations were constructed by Filatoff (1975) and Backhouse (1978) for the Perth Basin, Burger and Senior (1979) for the Eromanga Basin, and Reiser and Williams (1969) and De Jersey (1975) for the Surat Basin. Much of this data was synthesized in Price et al. (1985) and

shortly after in the ground-breaking pan-Australian scheme collated by Helby et al. (1987). However, as coal exploration continued apace in eastern Australia, the finer resolution provided by regional schemes and their relationship to local lithostratigraphic units led to the refined, hierarchical zonation published by Price (1997) for the Surat and Bowen basins, and subsequently applied to most of the eastern Australian coal-bearing basins. This zonation is largely based on the first appearances of single spore or pollen marker taxa and can be difficult to use in wells where only cuttings are available (cavings issues) or where these single marker taxa are locally rare due to unfavourable ecological, depositional or hydrodynamic factors.

In the Surat Basin of Queensland, six spore-pollen zones encompass the Injune Creek Group (Price 1997). Detailed palynological investigations (including taxonomic descriptions) from the Evergreen to Westbourne Formations of the Surat Basin were also undertaken by McKellar (1974, 1998) . Earlier schemes were either low-resolution, used the spore-pollen subdivisions in Western Australia to infer the ages of eastern Australian spore-pollen assemblages, or focused on the interval below the Injune Creek Group (De Jersey and Paten 1964; Burger 1968; Burger 1984). McKellar (1998) designated eight spore-pollen zones (*Corollina torosa* Abundance Zone to the *Retitriletes watherooensis* Association Zone) to this interval and assigned tentative ages to them based on correlations to coeval marine strata in New Zealand and New Caledonia (McKellar 1998). With the exception of the APJ4.2 Subzone that spans a marginally longer interval than the *Aequitriradites norrisii* Association Zone in the Surat Basin, the schemes of Price (1997) and McKellar (1998) present palynological units of identical duration. This paper will focus on attaching absolute ages to the more widely utilised Price scheme (1997).

7.4 Palynological processing and analysis

Sixty-six core samples from the Stratheden 4, Stratheden 60, Guluguba 2 and Indy 3 wells (Figure 7.2) comprising mudstones, siltstones and coals were processed at the MGPalaeo laboratory in Malaga, Perth. Samples were derived from the underlying Hutton Sandstone and the Injune Creek Group. Where possible, between two and four core samples adjacent to each of the dated tuff beds were processed for palynology (Figure 7.4). The fine-grained siliceous samples were processed using standard palynological techniques (Traverse 2007; Brown 2008). Hydrofluoric (48%) and hydrochloric (32%) acid digestion steps were used to extract the organic matter, prior to sieving the kerogen through 10 µm polycarbonate filters to remove unwanted palynodebris. A final oxidation step, using nitric (69%) acid, was applied before mounting the palynomorph assemblages on glass slides for microscopy. The coal samples were either subjected to a single nitric (69%) acid digestion or simply crushed and sieved. Palynological counts were undertaken by I (Carmine Wainman) in accordance with a taxonomic scheme devised by McKellar (1998) for the Jurassic spore-pollen rich assemblages of the Surat Basin: ‘standard’ three hundred specimen counts (counting all palynomorphs) and ‘normalised’ one hundred specimen counts (excluding commonly observed taxa) were conducted on an Olympus CX31 light microscope. Further scans of the slides were undertaken to locate rare marker taxa not recorded within the count limits. The coordinates of key biostratigraphic taxa were recorded using an England Finder Slide. Microfossil yield and preservation were good for most of the core samples. Three samples from 253.60, 415.00 and 417.00 m in the Guluguba 2 well were barren. Geoff Wood of Santos Limited also kindly provided existing palynological datasets from the Pleasant Hills 25 well.

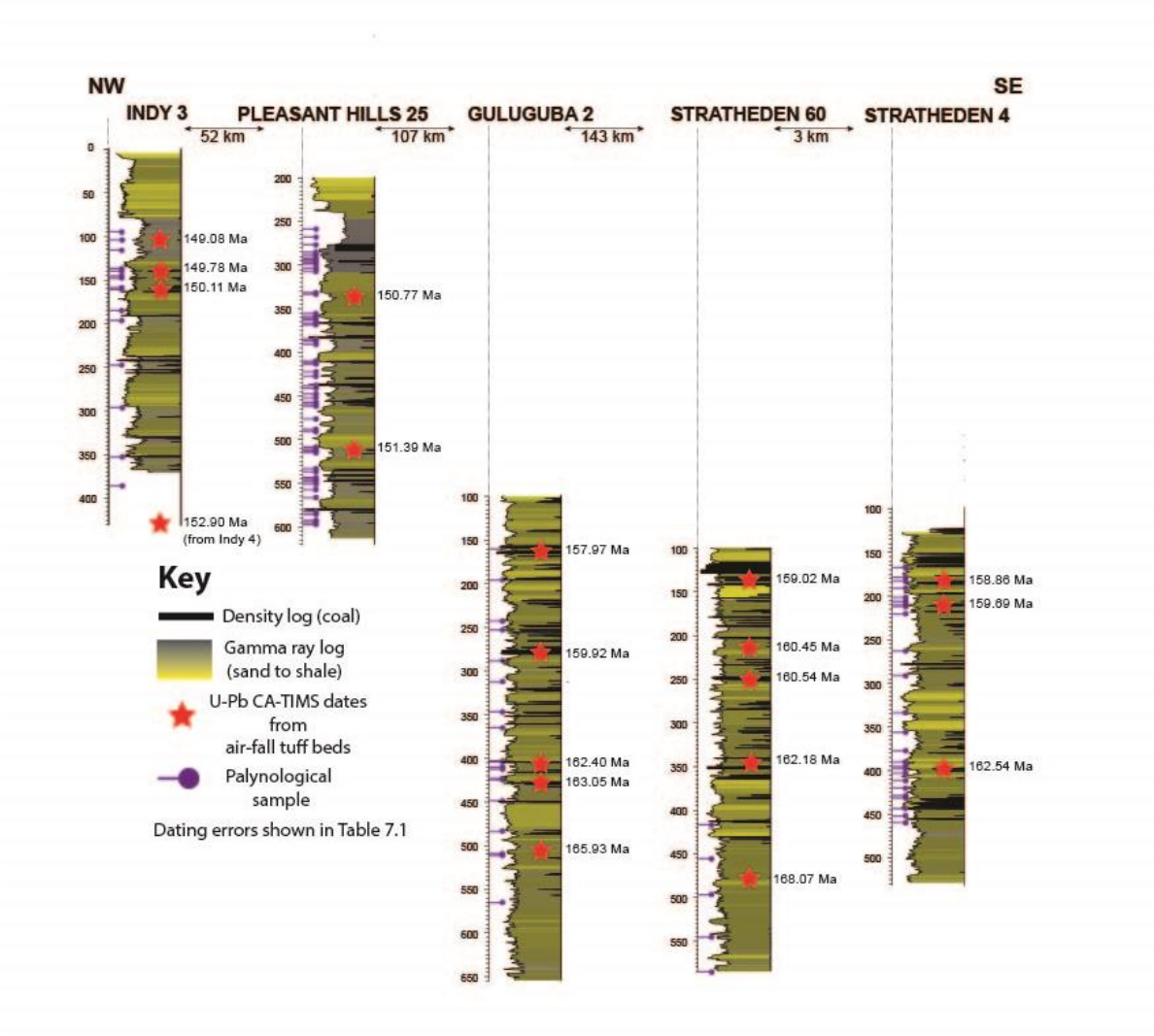

Figure 7.4. Gamma and density logs (northwest to southeast) from the Indy 3, Pleasant Hills 25, Guluguba 2, Stratheden 60 and Stratheden 4 wells showing the location of dated tuff beds and palynological samples. The line of the cross-section is shown in Figure 7.3.

7.5 Tuffs and U-Pb CA-TIMS zircon dates

Tuff beds have a wide geographic distribution across the Surat Basin within the Injune Creek Group. Dating of zircons from these tuffs allows the calibration of spore-pollen zones across the basin to the geologic time-scale. Cathodoluminescence (CL) images and laser ablation inductively coupled plasma mass spectrometry (LA-ICPMS) were used to pick zircons that crystallised shortly prior to eruption (thus excluding crystals with long magma residence times) (Crowley et al. 2007; Wainman et al. 2015; Laurie et al. 2016). These zircons were then dated using the CA-TIMS methodology outlined by Jim Crowley at Boise State University, USA; see Wainman et al. (2015) and Wainman et al. (2017) for a fuller account of the procedures undertaken to date these samples. This resulted in U-Pb CA-TIMS dates for 19 tuff beds (each designated a Geoscience Australia sample number) from the Stratheden 4, Stratheden 60, Guluguba 2, Pleasant Hills 25, Indy 3 and Indy 4 wells (Wainman et al. 2015; Wainman et al. 2017). These zircon dates ranged from 168.07 Ma ± 0.07 Ma to 149.08 ± 0.06 Ma spanning the Middle Jurassic Bathonian to the Late Jurassic Tithonian and are listed in full in Table 7.1. Three U-Pb CA-TIMS dates from the Stratheden 60 and Pleasant Hills 25 wells (GA 2231588, GA 2231590 and GA 2390007) contained a mixture of volcanic and detrital zircons. As a consequence, weighted mean $^{206}Pb/^{238}U$ dates were calculated from age-equivalent dates (i.e. probability of fit >0.05) or from the youngest analysis (Wainman et al. 2017).

GA sample number	Well	Depth from (m)	Depth to (m)	U-Pb CA-TIMS date	Error +/- (Ma)
**2231590	Stratheden 60	477.70	477.64	168.07	0.07
**2233310	Guluguba 2	509.43	509.40	165.93	0.05
**2233308	Guluguba 2	428.57	428.51	163.05	0.05
* 2180600	Stratheden 4	396.46	396.41	162.54	0.05
**2233302	Guluguba 2	404.23	404.16	162.40	0.04
** 2231589	Stratheden 60	342.31	342.24	162.18	0.06
** 2231588	Stratheden 60	247.66	247.61	<160.54	0.12
** 2254143	Stratheden 60	212.55	212.50	160.45	0.05
**2233298	Guluguba 2	279.15	279.11	159.92	0.06
** 2231585	Stratheden 4	209.87	209.62	159.69	0.05
**2254141	Stratheden 60	136.11	135.86	159.02	0.04
* 2180601	Stratheden 4	183.04	182.84	158.86	0.04
**2233290	Guluguba 2	162.10	162.03	157.97	0.08
**2233272	Indy 4	202.00	201.59	152.90	0.07
**2390012	Pleasant Hill 25	512.20	512.07	<151.39	0.12
**2390007	Pleasant Hill 25	335.08	335.00	150.77	0.06
**2254172	Indy 3	159.76	159.57	150.11	10.04
**2254170	Indy 3	140.38	139.97	149.78	0.06
**2254169	Indy 3	104.62	104.40	149.08	0.06

* From Wainman et al. (2015) **From (Wainman et al. 2017)

Table 7.1. U-Pb CA-TIMS dates and errors from the Stratheden 4, Stratheden 60, Guluguba 2, Pleasant Hills 25, Indy 3 and Indy 4 wells in chronological order.

7.6 Palynological results and remarks

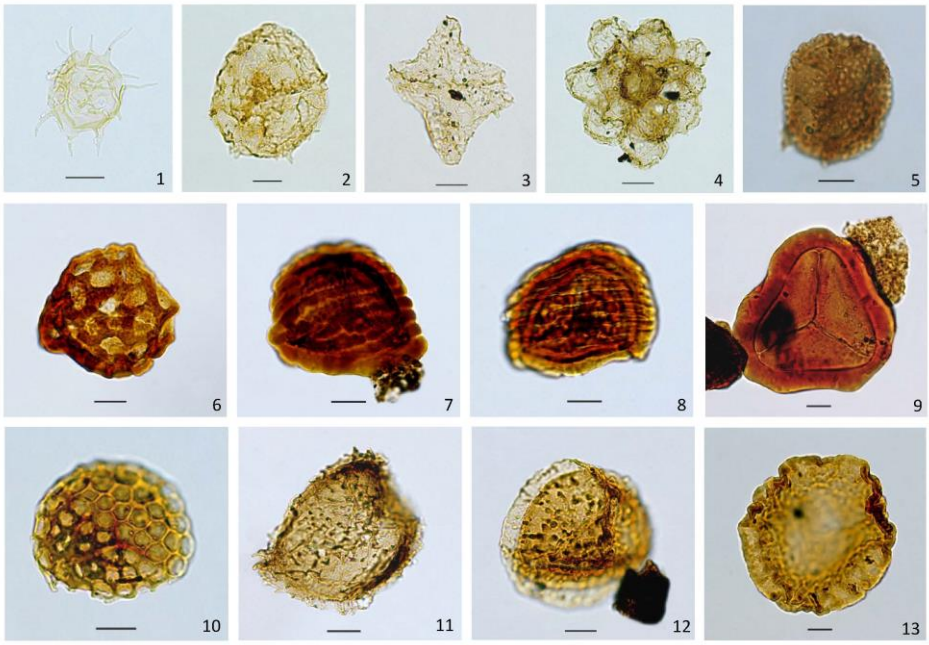

Plate 7.1. Key spore-pollen taxa utilized in the main eastern Australian palynostratigraphic frameworks along with the rare brackish to marine microplankton found in some wells. (1) *Micrhystridium* spp. Sarjeant (1967). Stratheden 4 well, 444.00 m, slide 1 V39/1. (2) *Moorodinium crispa* (See Section 8.3). Indy 3 well, 247.55 m, slide 3, F30/3. (3) *Skuadinium fusumaster* (See Section 8.3). Indy 3 well, 247.55 m, slide 3, U12/4. (4) *Palambages pariunta* (See Section 8.3), Indy 3 well, 247.55 m, slide 3, S33/1. (5) *Retitriletes watherooensis* Backhouse (1978), Indy 3 well, 166.50 m, slide 1, M29. (6) *Klukisporites variegatus* Couper (1957). Guluguba 2 well, slide 1, 346.00 m, P31/2. (7) *Contignisporites cooksoniae/burgeri* (Dettmann 1963) emend. In Backhouse (pars). Guluguba 2 well, slide 1, 160.50 m, P40/2. (8). *Contignisporites glebulentus* (Dettmann 1963) emend. Filatoff and Price (1988). Stratheden 4 well, 292.00 m, slide 1, N16/0. (9) *Murospora florida* (Balme 1957) emend. Pocock (1961). Indy 3 well, 159.20 m, slide 1, P14/0. (10) *Retitriletes circolumenus* (Cookson and Dettmann 1958) emend. Backhouse (1978). Stratheden 4 well, 183.06 m, slide 1, S41/4. (11) *Perotrilites whitfordensis* Backhouse (1978). Stratheden 60 well, 498.71 m, slide 1, V40/3. (12) *Aequitriradites norrisii* Backhouse (1978). Stratheden 60 well, slide 1, 418.45 m, W21/0. (13) *Callialasporites dampieri* Balme (1957). Stratheden 4 well, 418.00 m, slide 1, R26/0. Scale bars are 10 µm throughout.

7.6.1 Spores and pollen

The majority of mudstone and siltstone samples yielded assemblages dominated by osmundaceous fern spores and araucarian conifer pollen (often up to 75%). However, these common spore-pollen groups provide no useful quantitative trends or correlative palynological events, as noted in previous regional studies (Gallagher et al. 2008). Thus, 'normalised' counts (excluding these dominant spore-pollen groups) were conducted on the remaining spore-pollen fraction to identify any valuable biostratigraphic events.

Many of these normalised palynological counts are dominated by *Camarozonosporites ramosus* (up to 59%) and *Retitriletes austroclavatidites* (up to 27%), along with frequent *Annulispora* spp., *Neoraistrickia* spp., *Retitriletes* spp. and *Sculptisporis* spp. There are also noticeable spikes of *Leptolepidites major*, *Leptolepidites verrucatus*, *Sellaspora asperata*, *Corollina* spp., *Perotriletes* spp. and *Klukisporites* spp. The palynological preparations from coals were typically dominated by one or two species (e.g. *Retitriletes circolumensus*, *Gleicheniidities senonicus,* and *Camarozonosporites ramosus*), thus indicating locally sourced palynomorphs from plants growing close to the mire where the peat (coal) formed. For the greater part only broad palynological correlation could be inferred in the Surat Basin (see appendices 4). Palynological assemblages also support continental deposition (see appendices 4) with the majority of taxa indicating warm, wet and swampy conditions (Martin et al. 2013).

As with previous biostratigraphic studies of the Surat Basin, including McKellar (1998) and Martin et al. (2013), key spore taxa (Plate 7.1, Figures 5-12) have been found to be rare or absent in many of the palynological preparations. Many of the prevailing terrestrial depositional environments (floodplains, mires, and shallow lakes) across the Surat Basin may have been unsuitable for the parent plants of the key spore-pollen taxa for much of the Middle–Late Jurassic (Martin et al. 2013). Thus it must also be noted that the absence of these key spore-pollen marker taxa from a sample does not always provide reliable evidence that a particular zone is not represented by that sample (Martin et al. 2013).

7.6.2 Acritarchs, algae and dinoflagellate cysts

Increased abundances of acritarchs, algal cysts, and dinoflagellate cysts are also present in several of the palynological preparations (Plate 7.1, Figures 1 to 4). In the Stratheden 4 well between 452.00 and 411.90 m, up to 10% of the palynofloral assemblage comprises spinose acritarchs, mostly *Micrhystridium* spp. These have been recorded in Jurassic strata across eastern Australian basins (Evans 1966; McKellar 1974; Exon 1976; Burger 1986; Hannaford and MacPhail 2011) and are often considered to indicate marine or brackish strata. Such *Micrhystridium*-rich units are commonly associated with marine transgressive events through the Mesozoic (Sarjeant 1967; Stancliffe 1990; Sarjeant and Stancliffe 1994; Dalseg et al. 2016) and it is tantalising to do so herein. However, there is also some evidence that *Micrhystridium* spp. may also be present in large, saline lakes rather than true epeiric systems (Chahud et al. 2012). Of further interest, the 247.55 m sample in the Indy 3 well contained a palynoflora dominated by dinoflagellate cysts (55%); these represent the first records of dinoflagellate cysts from the Jurassic of the Surat Basin and include common *Moorodinium* spp. and *Skuadinum* spp. Both of these genera are strongly associated with brackish to marginal marine palaeoenvironments in the Perth and Carnarvon basins respectively, where they were first described (Backhouse 1988; Riding and Helby 2001). The significance of an abundant dinoflagellate cyst assemblage in the Jurassic of the Surat Basin will be discussed in more detail in a future paper.

7.7 Recalibrating spore-pollen zones to the geologic time-scale

These U-Pb CA-TIMS dates for the Surat Basin allow for an initial check on the ages currently assigned to the Middle to Late Jurassic spore-pollen zones of Price (1997) and McKellar (1998) and allows tentative recalibration of these zones to the geologic time-scale as defined by Ogg et al. (2016). Table 7.2 and Figure 7.5 summarise the key results and interpretations. Suggested modifications from previous correlations are discussed below:

APJ4.2 Subzone (Price 1997)

Definition of the zonal base: first occurrence of *Perotrilites whitfordensis*.

Definition of the zonal top: first occurrence of *Contignisporites glebulentus*.

Typical palynological assemblages: characterised by *Antulsporites saevus*, *Leptolepidites verrucatus*, *Dictyotosporites complex* and the first appearance of herpatician spores including *Aequitriradites norrissi* and *Perotrilites cameronii*.

Lithostratigraphic distribution in the Surat Basin: Ranges from the uppermost Hutton Sandstone to the Eurombah Formation.

Previous age range: Bathonian to basal Callovian.

New U-Pb CA-TIMS ages: The first occurrence of *Perotrilites whitfordensis* in the Stratheden 60 well occurs 68.21 m below the 477.64–477.70 m tuff bed that yielded an early Bathonian age (168.07 ± 0.07 Ma).

Remarks: The new date suggests the first occurrence of *Perotrilites whitfordensis* (and thus the base of the APJ4.3 Subzone) is very similar to previous estimates from indirect calibrations to the standard European biozones.

APJ4.3 Subzone (Price 1997)

Definition of the zonal base: the first occurrence of *Contignisporites glebulentus*.

Definition of the zonal top: the first occurrence of *Murospora florida*.

Typical palynological assemblages: characterised by the prominence of *Leptolepidites verrucatus*, *Camarozonosporites ramosus* and decreasing *Klukisporites scaberis*.

Lithostratigraphic distribution in the Surat Basin: from the Eurombah Formation and into the Lower Walloon Coal Measures.

Previous age range: early Callovian.

New U-Pb CA-TIMS ages: an early Callovian age is suggested for the base of the zone as assemblages with abundant *Leptolepidites verrucatus* and *Camarozonosporites ramosus* along with the near absence of *Klukisporites scaberis* occur between 510.00 m and 405.00 m in the Guluguba 2 well. There is also a noticeable spike in *Annulispora* spp. (often associated with the APJ4.3 Subzone) at 405.00 m in the same well. These assemblages are present between dated tuff beds at 428.51–428.57 m (163.05 ± 0.05 Ma) and 509.40–509.43 m (165.93 ± 0.05 Ma) in the well.

Remarks: the formal marker taxa for the base of the zone, *Contignisporites glebulentus*, was not observed in the upper Hutton Sandstone, Eurombah Formation or lower Walloon Coal Measures of the Surat Basin, in either the Stratheden 60 or Guluguba 2 wells. This is not unexpected as all *Contignisporites* spp. are less prominent in the Surat Basin than in the Eromanga Basin to the west, due to less favourable conditions for the parent plants and dilution by plant detritus (Martin et al. 2013). Thus, the base of the subzone can only be approximated from other trends in the spore-pollen assemblages (as noted above). This inferred subzonal base is similar in age to previous estimates.

APJ5 Zone (Price 1997)

Definition of the zonal base: the first occurrence of *Murospora florida*.

Definition of the zonal top: the first occurrence of *Retitriletes watherooensis.*

Typical palynological assemblages: characterised by prevalent *Matonisporites* spp. and frequent *Impardecispora* spp. and *Concavissimisporites* spp.

Lithostratigraphic distribution in the Surat Basin: Ranges from the lower Walloon Coal Measures to the middle Springbok Sandstone.

Previous age range: early Callovian to late Kimmeridgian.

New U-Pb CA-TIMS ages: an early Oxfordian age (162.54 ± 0.05 Ma) is suggested by the first occurrence of *Murospora florida* at 444.00 m in the Stratheden 4 well. This occurrence is 47.54 m below the dated tuff at 396.41-396.46 m.

Remarks: Although this age (162.54 ± 0.05 Ma) is ~2.5 Ma younger than previous estimates for the base of the zone, the first occurrence of *Murospora florida* in the well was nearly 50 m below the tuff and thus the base of the zone may be older than 162.54 Ma. It should also be noted that *Murospora florida* was only a rare constituent of many of the samples and thus further U-Pb CA-TIMS dates (with associated APJ5 assemblages) are required before such major changes to the base of the zone are confirmed.

APJ6.1 Subzone (Price 1997)

Definition of the zonal base: the first occurrence *Retitriletes watherooensis*.

Definition of the zonal top: the first occurrence of *Ceratosporites equalis*.

Typical palynological assemblages: characterised by an increased abundance and diversity of lycopod spores (e.g. *Dictyotosporites* spp.), *Foraminisporis dailyi*, *Ruffordiaspora* spp. and *Gleicheniidities* spp. within the zone. There is also a marked increase in *Podosporites variabilis* at the base of this zone. The zone also represents the transition interval from the Jurassic inaperturate pollen associations (*Callialasporites* palynoflora) to the Cretaceous trisaccate pollen associations (*Microcachryidites* palynoflora).

Lithostratigraphic distribution in the Surat Basin: Upper Walloon Coal Measures/Middle Springbok Sandstone to the lower Gubberamanuda Sandstone (beyond the limit of this investigation).

Previous age range: Late Kimmeridgian to late Tithonian.

New CA-TIMS ages: an early Tithonian age (150.77 ± 0.06 Ma) was calculated from a tuff bed 30.42 m below the first occurrence of *Retitriletes watherooensis* (304.58 m) in the Pleasant Hills 25 well. *Retitriletes watherooensis* also first occurs in the early Tithonian in the Indy 3 well at 116.80 m, only 12.18 m above a tuff bed (104.40–104.62 m) that yielded a 149.08 ± 0.06 Ma age.

Remarks: The age base of the APJ6 Subzone is likely to be ~4.2 Ma younger than previous estimates from the presence of *Retitriletes watherooensis* in two wells that are located in close proximity to dated tuff beds. As for the underlying APJ5 Zone, further U-Pb CA-TIMS dates are required before major changes are confirmed for the basal age of the subzone.

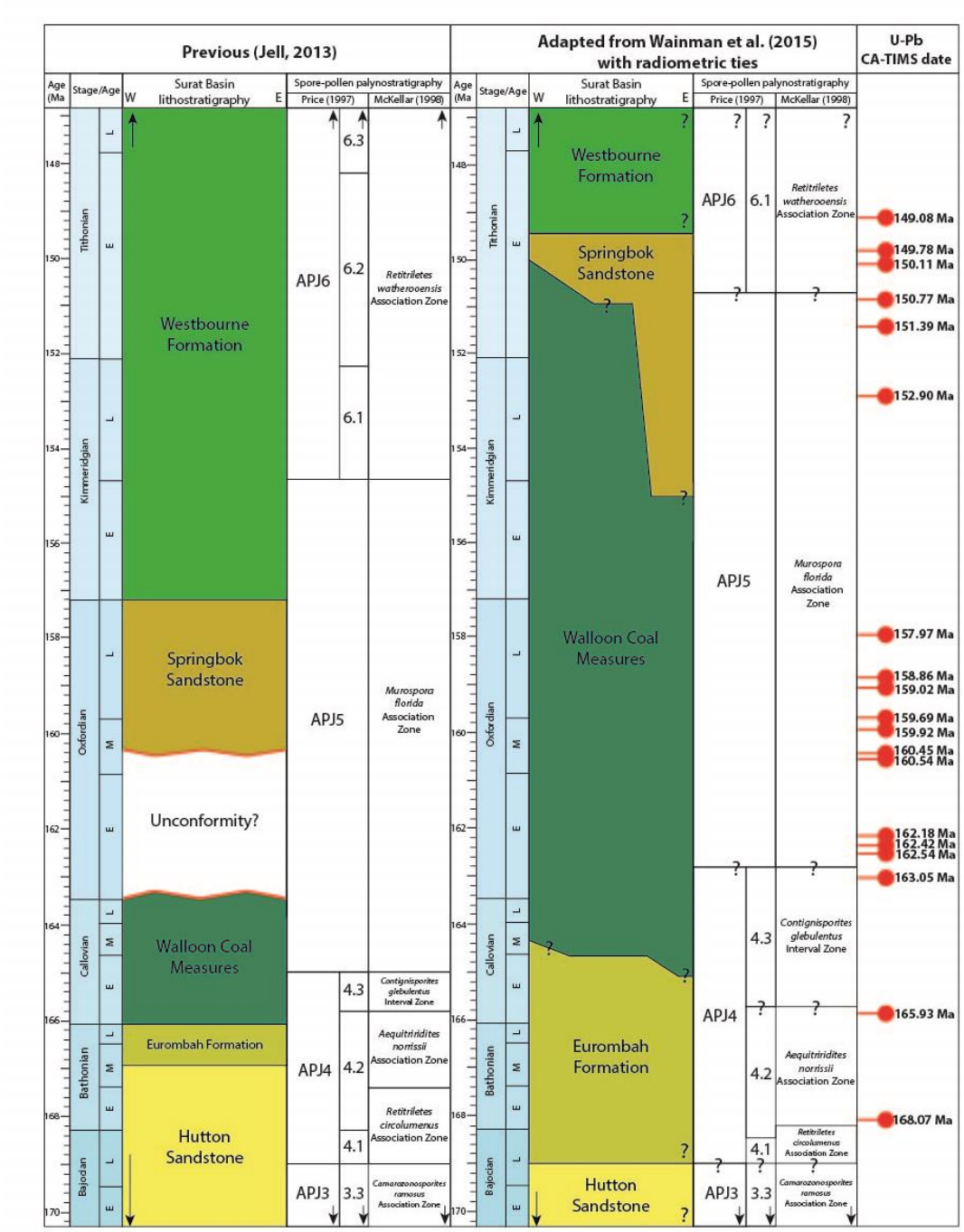

Figure 7.5. Recalibration of palynostratigraphic schemes b by Price (1997) and McKellar (1998) to the international geologic timescale (Gradstein et al. 2012; Ogg et al. 2012; Cohen et al. 2013; updated; Ogg et al. 2016). Surat Basin formation names and ages adapted from Jell (2013), Wainman et al. (2015) and Wainman et al. (2017).

Sample type	Well	Depth (m)	Spore-pollen Zone/Subzone	Tuff date (Ma)	Position of the first occurrence to a dated tuff bed (m)
Core	Stratheden 60	545.85	APJ 4.2	>168.07	-68.25
Core	Stratheden 60	498.71	*Aequitriradites norrisii* Association Zone	<168.07	-20.01
Core	Guluguba 2	509.43	APJ4.3 (inferred)/ *Contignisporites glebulentus* Interval Zone (inferred)	~165.93	+0.57
Core	Stratheden 4	444.00	APJ5/ *Murospora florida* Association Zone	162.54	-47.54
Core	Pleasant Hills 25	304.58	APJ6.1/ *Retitriletes watherooensis* Association Zone	150.77	+30.42
Core	Indy 3	159.20	APJ6.1/ *Retitriletes watherooensis* Association Zone	149.08	+12.18

Table 7.2. A summary of key palynological results and interpretations.

7.8 Conclusion

Dates from zircons from air-fall tuff beds using the U-Pb CA-TIMS methodology substantially improves the calibration of established eastern Australian Middle to Late Jurassic spore-pollen zones to the geologic time-scale. Previous correlations relied on tenuous indirect correlations that utilised ammonite or dinoflagellate assemblages to obtain an imprecise geologic age for the spore-pollen zones. The new calibration will enable better correlation of the palynofloras to areas outside of Australia and will enhance the accuracy of geological and burial history models.

The ages of the bases of the APJ4.2 and APJ4.3 subzones of Price (1997) are confirmed to be close to previous estimates (Figure 7.5). In contrast, the bases of the APJ5 and APJ6 zones may be substantially younger than previously thought by as much as 4.2 Ma (Figure 7.5). These changes are only suggested because the marker taxa (e.g. *Murospora florida*) are locally scarce. Dating of tuff-bearing lithostratigraphic units including the Early Jurassic Evergreen Formation and the Early Cretaceous Orallo Formation in eastern Australia would further help constrain the age and duration of the spore-pollen zones.

On a regional level, the longevity of the APJ5 spore-pollen zone (~11 Ma) also means it has limited value for intrabasinal correlations between formations of the Surat Basin and adjacent basins. The first appearance of *Murospora florida* also acts as the basal marker taxum for the pan-Australian *Murospora florida* Zone (Helby et al. 1987). This and other spore-pollen zones of western Australia are not easily correlated with those of eastern Australia due to deposition at significantly lower palaeolatitudes and in different palaeoenvironments (Helby et al. 1987). Future dates from western Australia basins may give insights into the calibration of spore-pollen zones with the geologic time-scale.

This study has shown the need for a substantial revision of the Middle–Late Jurassic APJ zones in the Surat Basin. Further investigations to tie in radiometric dates with the pollen zones will allow improvements on tentative zonal ages suggested by the current study.

7.9 Acknowledgements

Carmine Wainman has a Ph.D. scholarship from the University of Adelaide that has covered most of the travel and analytical costs. We thank Jim Crowley, Debra Pierce and Alexandra Edwards from Boise State University who assisted with mineral separation, preparation and the dating of zircon grains using CA-TIMS. Geoff Wood from Santos Limited kindly provided palynological summaries and range charts for the Pleasant Hills 25 well. We thank Robert Nicoll of Geoscience Australia for reviewing the manuscript prior to submission and John Backhouse for insightful discussions regarding the identification of thin-walled brackish-marginal marine dinoflagellate cysts. Jesse Vitacca from MGPalaeo kindly assisted with palynological processing. Stratabugs was used under license to produce palynological plots in the appendices.

7.10 Supplementary papers

See appendices 5 (p. 366-370).

Statement of Authorship

Title of Paper	Dinoflagellate cysts and colonial algae in Tithonian strata of the Surat Basin, Australia: a taxonomic study and their significance.
Publication Status	☐ Published ☐ Accepted for Publication ☐ Submitted for Publication X Unpublished and unsubmitted work written in manuscript style
Publication Details	Wainman, C.C., Mantle, D.J., Hannaford, C. and McCabe, P. J. in prep-d. Dinoflagellate cysts and colonial algae in Tithonian strata of the Surat Basin, Australia: a taxonomic study and their significance. Intend to submit to Palynology

Principal Author

Name of Principal Author (Candidate)	Carmine C. Wainman
Contribution to the Paper	Majority of the data collection and interpretation. Wrote the greater majority of the paper with exceptions noted in the co-authorship contributions. Produced final version of the paper using editorial suggestions of the co-authors.
Overall percentage (%)	80
Certification:	This paper reports on original research I conducted during the period of my Higher Degree by Research candidature and is not subject to any obligations or contractual agreements with a third party that would constrain its inclusion in this thesis. I am the primary author of this paper.
Signature	Date 10/08/2017

Co-Author Contributions

By signing the Statement of Authorship, each author certifies that:

i. the candidate's stated contribution to the publication is accurate (as detailed above);
ii. permission is granted for the candidate in include the publication in the thesis; and
iii. the sum of all co-author contributions is equal to 100% less the candidate's stated contribution.

Name of Co-Author	Daniel J. Mantle
Contribution to the Paper	Advice and guidance on research project and editorial comments for the paper. Made contributions to the first paragraph in the section titled "Palynology of the Indy 3 well" and wrote the taxonomic description of *Moorodinium crispa* in the section "Systematic palynology". Drafted plates 8.1 and 8.2.
Signature	Date 10/8/2017

Name of Co-Author	Carey Hannaford
Contribution to the Paper	Advice and guidance on research project and editorial comments for the paper. Drafted the Stratabugs plot in the appendices.
Signature	Date 8/8/2017

Name of Co-Author	Peter J. McCabe
Contribution to the Paper	Supervisor of Ph.D. – Extensive critical advice and guidance on research project and editorial comments for the paper.
Signature	Date 10/8/2017

Chapter 8. Dinoflagellate cysts and colonial algae from Tithonian strata of the Surat Basin, Australia: a taxonomic study and their significance

To be submitted to *Palynology*. A statement of authorship is provided on the previous page.

Co-authors: Daniel Mantle, Carey Hannaford and Peter McCabe

Abstract

Jurassic sedimentary successions in eastern Australia are widely thought to have been deposited in nonmarine environments. Thus, the discovery of a low diversity dinoflagellate cyst assemblage with associated colonial algae in the Walloon Coal Measures of the western Surat Basin either provides new evidence of a short-lived marine transgression or of the very rare occurrence of nonmarine dinoflagellate cysts in pre-Cretaceous strata. Their small size, thin walls and simple proximate shapes are typical of freshwater to brackish dinoflagellate cysts, as is the low diversity, high dominance nature of the assemblage. Two new species of dinoflagellate cysts (*Moorodinium crispa* sp. nov. and *Skuadinium fusumaster* sp. nov.) and a new species of colonial algae (*Palambages pariunta* sp. nov.) are described from these assemblages.

Tidal channel and tidal mudflat facies associated with these assemblages provide evidence of a possible upper estuarine setting. Support for a marine incursion is provided by U-Pb dating. This yielded a 150.11 ± 0.04 Ma age (~100 m above the dinoflagellate cyst assemblage in the Indy 3 well) that ties to an episode of high eustatic sea level during the Tithonian. Thus, a marine transgressive event during the Tithonian may have allowed dinoflagellates to migrate into the interior of the Australian continent. If found not to be a local occurrence, these dinoflagellate cysts assemblages may provide a useful correlative tool for tracing distinctive brackish to marginal marine flooding surfaces in continental successions in eastern Australia.

8.1 Introduction and geologic setting

Middle to Upper Jurassic sedimentary strata of eastern Australia are widely believed to have deposited in nonmarine settings (Green et al. 1997a; McKellar 1998; Jell 2013). The absence of indisputable marine fossils and the dominance of terrestrially derived palynomorphs from these successions have supported this interpretation (Fielding 1989; McKellar 1998; Martin et al. 2013). However, some authors (Exon 1976; Exon and Burger 1981; Burger 1986; Browne and Hart 1990; Wells and O'Brien 1994) have used the sporadic presence of spinose acritarchs, hummocky cross-stratification, barite nodules and glauconite to infer short-lived marine incursions across the continental interior during the Jurassic. New data reported in Sections 6.6 and 7.6 suggests that there are tidally influenced sedimentary strata within the Late Jurassic Walloon Coal Measures and the Springbok Sandstone of the Surat Basin. This new interpretation is largely based on the analysis of sedimentary facies but also the presence of spinose acritarchs (notably *Micrhystridium* spp.), colonial algae and dinoflagellate cysts. These dinoflagellate cysts are present in the Late Jurassic APJ5 Spore-Pollen Zone of Price (1997) and represent the first record of this group from the Jurassic of the Surat Basin. In this paper, we provide systematic descriptions for these new palynomorphs and consider the significance of the assemblage in conjunction with sedimentological and geochronological data, and published eustatic sea-level curves.

The Late Triassic to mid-Cretaceous intracratonic Surat Basin (part of the Greater Australian Superbasin) spans much of southeastern Queensland and northeast New South Wales and comprises a 2.3 km thick sedimentary succession (Jell 2013). The basin fill contains a mix of fluviolacustrine, paralic and shallow marine successions that were deposited during six sedimentary cycles corresponding to changes in eustatic sea-level during the Jurassic and Cretaceous (Exon and Burger 1981). Deposition ended in the basin after a major contractional event in the mid-Cretaceous before seafloor spreading commenced in the Tasman Sea (Ryan et al. 2012).

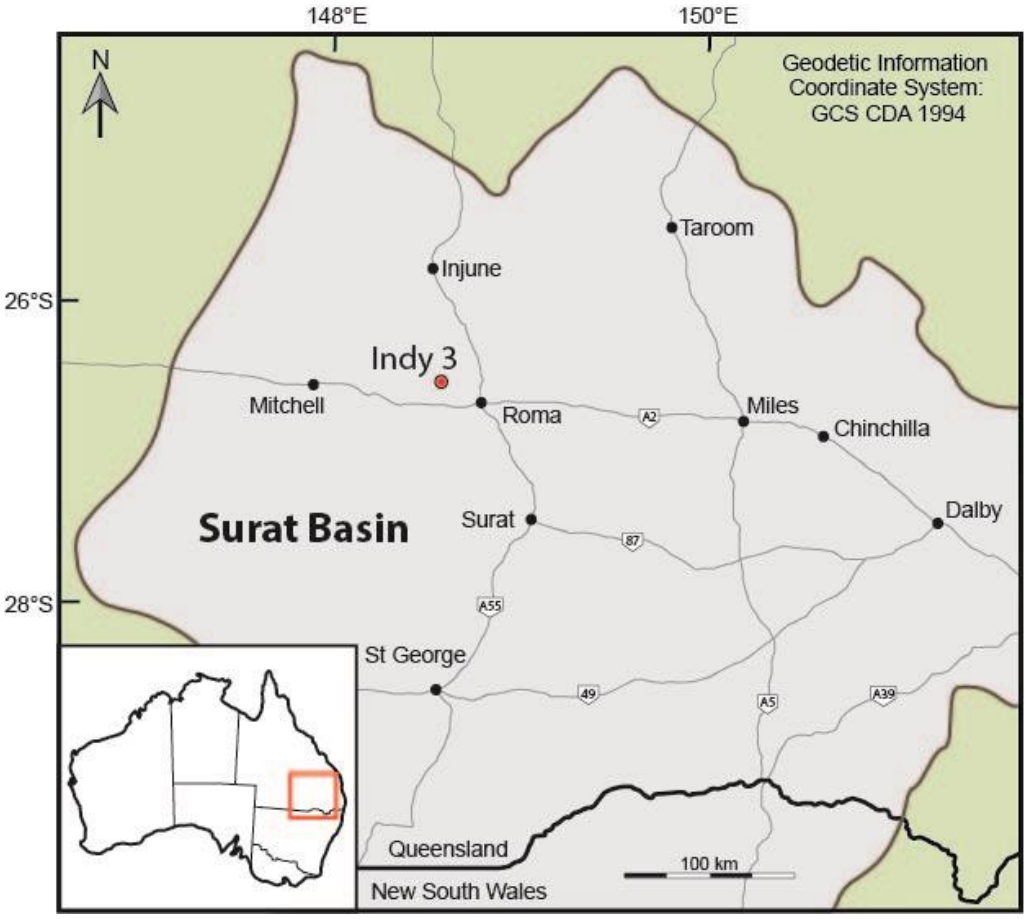

Figure 8.1. Location map showing the position of the Indy 3 well in the Surat Basin of Queensland, Australia.

The Late Jurassic Walloon Coal Measures, in the Indy 3 well in the western Surat Basin (Figure 8.1), are the predominant focus of this study. These strata are comprised of a mix of sandstones, siltstones, mudstones, coals, and tuffs which were deposited during the latter part of the second sedimentary cycle in the Surat Basin, as defined by Exon and Burger (1981) and Jell (2013). Nine distinct facies associations across this interval. These are groups of facies based on grain size, lithology, sedimentary structures and where present their palynomorph assemblages (Section 6.3 and Figure 8.2). Most of these facies associations are interpreted as the deposits of fluviolacustrine depositional environments or nonmarine wetlands. However, tidally-influenced facies were also noted and a brackish upper estuarine setting was suggested for the G and H facies associations (Section 6.3). These are of particular relevance, as the dinoflagellate cyst assemblage described herein (sample 247.55 m, Indy 3 well) was recovered from a dark grey mudstone interpreted as a tidal mudflat

(association H). This assemblage overlies facies interpreted as tidally influenced channels (association G) and is interbedded between coals that accumulated as peats in mires (association E). In addition, facies association G and H in the Indy 3 well are thought to have been deposited in an incised valley because the architecture of the sedimentary deposits reflects a progressive rise in base level—transitioning from fluvial to estuarine environments (Section 6.6).

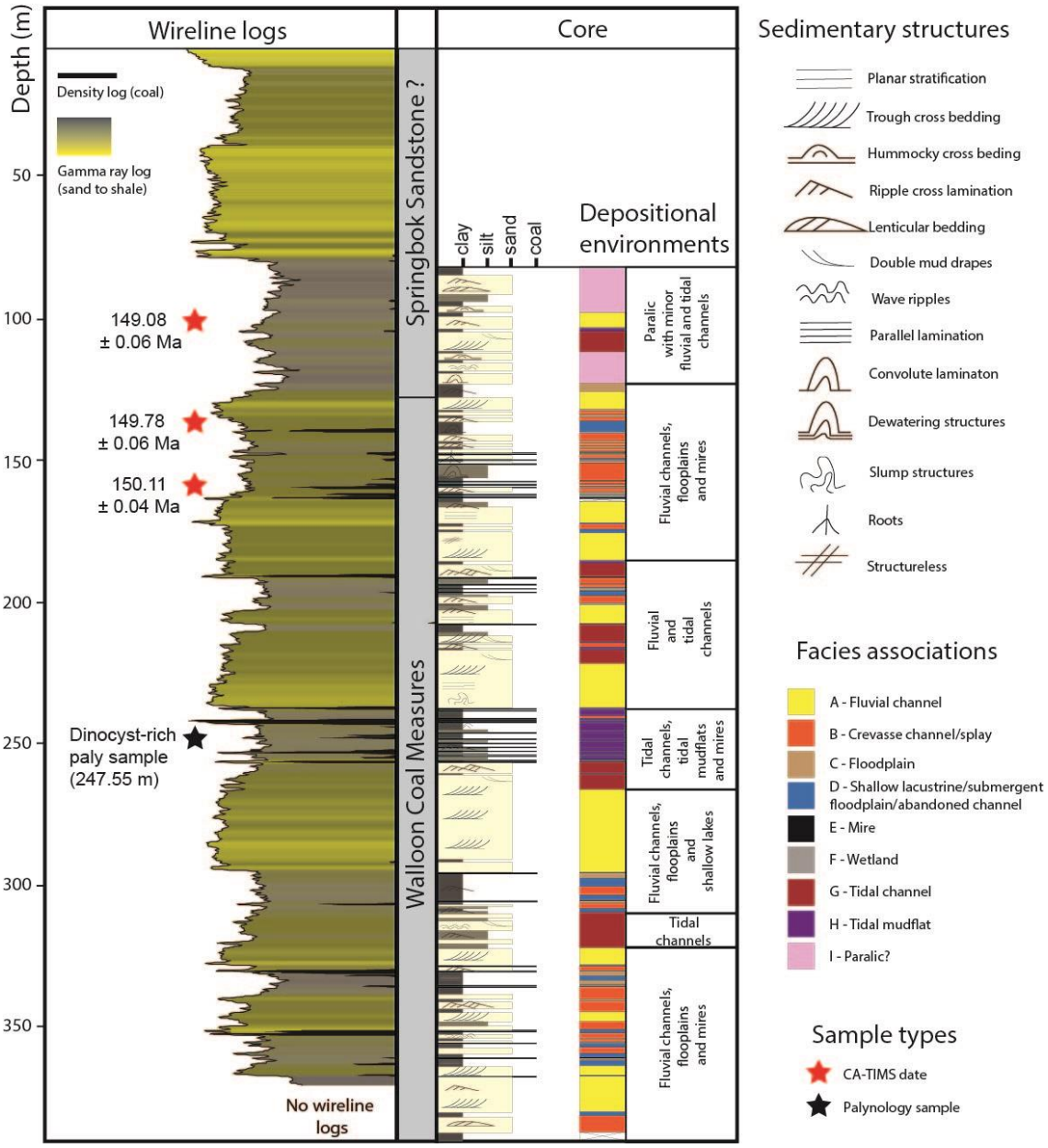

Figure 8.2. Wireline logs (gamma ray and density), stratigraphic column, core data and interpreted facies associations for the Indy 3 well. The approximate position of the U-Pb CA-TIMS dated tuffs and the dinoflagellate cyst-rich assemblage are shown with red and black stars respectively. Adapted from Section 6.3.

Three volcanic air-fall tuff beds from the Indy 3 well were dated by Wainman et al. (2017) using the U-Pb high precision chemical abrasion thermal ionization (CA-TIMS) methodology. These dates (150.11 ± 0.04 Ma at 159.57 m; 149.78 ± 0.06 Ma at 139.97 m; and 149.08 ± 0.06 Ma at 104.40 m) confirm a Tithonian depositional age for the upper Walloon Coal Measures and lowermost Springbok Sandstone. The dinoflagellate cyst-rich sample is located approximately 100 m lower than the oldest dated tuff in the Walloon Coal Measures in the Indy 3 well. A tuff from the nearby Indy 4 well (201.59 m) correlates to a point approximately 182 m below the dinoflagellate cyst assemblage and was dated by Wainman et al. (2017) as late Kimmeridgian (152.90 ± 0.07 Ma). The dinoflagellate assemblage is therefore of late Kimmeridgian or early Tithonian age.

8.2 Palynology of the Indy 3 well

Seventeen core samples from the Indy 3 well were selected for palynological analysis and processed at the MGPalaeo laboratory in Malaga, Perth. Standard palynological preparatory techniques, as outlined by Phipps and Playford (1984), Wood et al. (1996) and Brown (2008) were used. The samples, weighing between 20 and 60 g, were scrubbed and washed to remove any drilling additives or modern spore-pollen contaminants. They were then crushed to a 2–5 mm diameter grit and immersed in 100 ml of hydrochloric acid (32%) for 2 hours to breakdown any calcareous minerals. The remaining residue was then left in 100 ml of cold hydrofluoric acid (48%) for 24 hours to digest the majority of the siliciclastic minerals. Following neutralisation, the samples were washed with hydrochloric acid to eliminate any fluorides that may have formed, prior to heavy mineral separation using zinc bromide (specific gravity 2.1). The resulting float was again neutralised before filtering through 10 µm and 100 µm nylon sieves to remove fine organic particles and coarser woody fragments, respectively. The kerogen fraction was subjected to a moderately short oxidation (30 sec) in nitric acid (69%), followed by a final neutralisation and mounting of the residue on glass slides for microscopic analysis.

Palynomorph counts (300 specimens) were then conducted in accordance with a taxonomic scheme derived by McKellar (1998) for each sample and this data is illustrated in the Stratabugs chart (appendices 5). The relative abundance of the main palynomorph groups in the Indy 3 well is shown in Figure 8.3. These data show that most assemblages are composed, almost entirely, of terrestrial palynomorphs, particularly spores and pollen (96 to 100%) along with occasional freshwater algal cysts (up to 4%, mostly leiospheres). The pollen fraction consists of common Araucariaceae types (*Araucariacites* spp. and *Callialasporites* spp.) whilst the spore component is dominated by common fern taxa (*Camarozonosporites* spp., *Cyathidites* spp*., Osmundacidites* spp. and *Retitriletes* spp.) In contrast, the 247.55 m sample contains an abundant but low diversity dinoflagellate cyst suite comprising *Moorodinium* sp. (47%), *Skuadinium* sp. (5%) and the colonial alga *Palambages* sp. (18%).

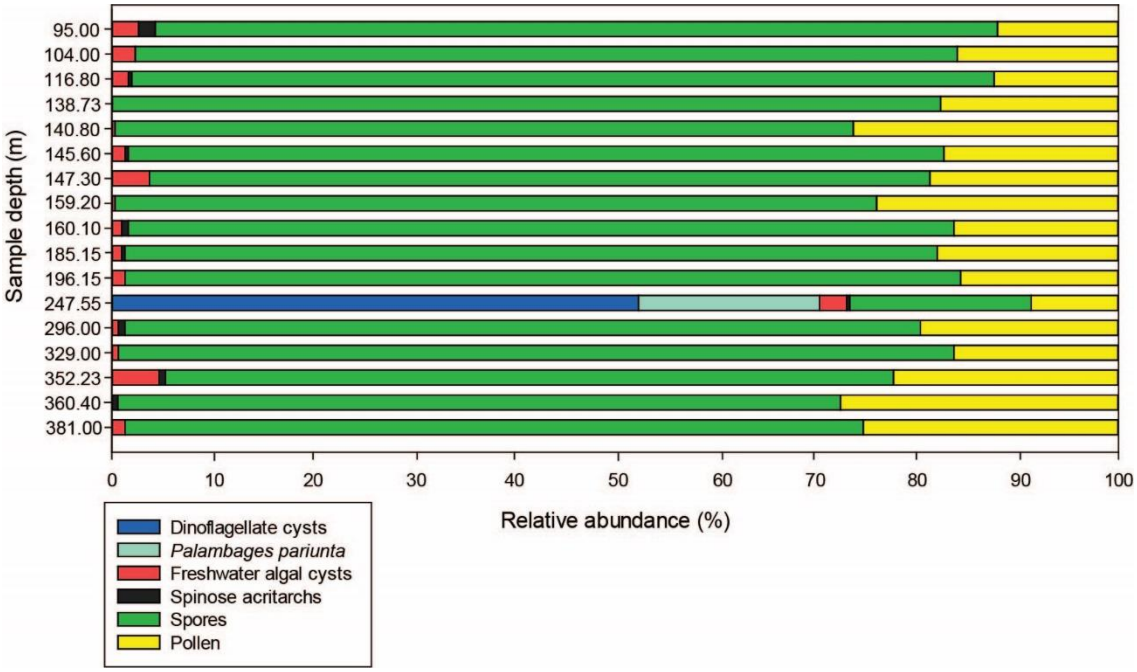

Figure 8.3. Relative abundances of major palynomorph groups in the Indy 3 well. Note that the dinoflagellate cyst rich assemblage was unique to a single sample in an otherwise terrestrially dominated sequence.

Two main palynozonations are used in the Surat Basin: the alphanumeric zonation of Price (1997) and the Roma Shelf zonation of McKellar (1998). The palynomorph assemblages from 116.80 to 381.00 m in the Indy 3 well are assigned to the APJ5 Spore-Pollen Zone (Price 1997) and the *Murospora florida* Association Zone (McKellar 1998) based on the rare occurrences of *Murospora florida* and the lack of younger marker taxa. It should also be noted that the marker species, *Retitriletes watherooensis,* for the overlying APJ6 Spore-Pollen Zone is extremely rare in the Surat Basin and some of the upper samples could be time-equivalent to this zone. However, as *Retitriletes watherooensis* is first recorded 130 m above the dinoflagellate cyst assemblage, it seems most likely that this assemblage belongs in the APJ5 Spore-Pollen Zone. Certainly, a late APJ5 or even early APJ6 zonal assignment would both fit well with the overlying Tithonian U-Pb CA-TIMS dates (150.11 ± 0.04 Ma to 149.08 ± 0.06 Ma).

8.3 Systematic palynology

Two new dinoflagellate cysts and a new colonial algal species are described from the Late Jurassic Walloon Coal Measures of the Surat Basin, southern Queensland. The dinoflagellate cyst classification of Fensome et al. (1993) is not followed herein, largely due to the unknown affinities of these relatively thin-walled and largely non-tabulate dinoflagellate cysts. All figured specimens, including holo- and paratypes, are housed in the Commonwealth Palaeontological Collection (CPC) maintained by Geoscience Australia in Canberra, ACT, Australia. All digital images were taken with an Olympus LC20 camera and an Olympus CX31 microscope and standard England Finder (EF) coordinates for each figured specimen are given in the plates and Table 1 in the appendices. Minor palynodebris surrounding the figured specimens have been digitally removed, but any organic particles overlapping the figured specimens are left in place to ensure they are not digitally altered.

Division: **Dinoflagellata** (Bütschli 1885) emend. Fensome *et al.* 1993

Genus: ***Moorodinium*** Backhouse 1988

Type: *Moorodinium spinatum* Backhouse 1988

Synopsis: small ovoid to trilobate dinoflagellate cysts with an epicystal archaeopyle, adnate or free, and largely lacking paratabulation other than the paracingulum or rare parasutural folds. Full paratabulation formula unknown; indications of six postcingular plates on the type species. The surface ornament between the low membranous septa or folds varies from smooth to granulate. The antapex may be lobate or bearing low rounded spines.

Remarks: The Late Jurassic *Moorodinium* taxon described herein from the Surat Basin is likely older than the largely ?Tithonian-Berriasian *Moorodinium* suite originally described by Backhouse (1988) from the Perth Basin, Western Australia. Although Backhouse (1988) noted that all four *Moorodinium* that he described had dorso-ventral structures, usually non-tabular membranous septa passing over the apex of the cyst, similar structures are not readily apparent on the Surat Basin species. However, the generic diagnosis is not expanded to include forms without these dorso-ventral structures as the low relief nature of these septa means they could easily be masked by the pervasive folds covering the new species.

***Moorodinium crispa* sp. nov.** (Plate 8.1, Figures 1-16)

Etymology: Latin, *crispa*, wrinkled, referring to the pervasive fine folds covering the surface of the cyst.

Diagnosis: a subcircular to ovoidal *Moorodinium* with a thin to moderately thick, smooth to microrugulate or microreticulate wall layer or layers, covered in numerous fine folds or membranous septa, with or without short hypocystal spines.

Holotype: Indy 3 well, conventional core sample at 247.55 m, slide number 3, EF coordinates F30/3 (Plate 8.1, Figures 16a & 16b), CPC number 43730.

Paratypes: both from the Indy 3 well, conventional core sample at 247.55 m, slide number 3. Paratype 1, EF coordinates J42/1 (Plate 8.1, Figures 11a & 11b), CPC number 43725. Paratype 2, EF coordinates L45/3 (Plate 8.1, Figure 13), CPC number 43727.

Description: a small proximate to proximochorate dinoflagellate cyst with a subcircular to ovoidal ambitus. The hypocyst is hemispherical, whilst the epicyst may be similarly rounded or broadly conical. The wall may be composed of a single layer or formed by several closely appressed layers that are only evident at the paracingular margins of broken or excysted specimens. The comprehensively wrinkled or finely folded surface ornament also suggests minor separation of two wall layers with only the periphragm forming these folds or low crests (1–3 µm high). The folds delimit an irregular surface reticulum with broadly equant lumina ranging from 3 to 20 µm in diameter. Low conical, hollow spines with rounded or rarely sharp tips, are largely confined to the hypocyst and longest around the antapex where they may surmount the low septa or crests. The paratabulation is only clearly indicated by the paracingulum, however, the coarser folds may, in part, represent parasutural septa but the numerous accessory folds mask the recognition of any individual paraplates. The paracingulum (5–12 µm wide) exhibits moderately well-spaced cross-striae that are most easily seen on isolated hypocysts. A small dark, diffuse subcircular accumulation body is also often located close to the paracingulum. The archaeopyle is epicystal, type [tAtP], and the operculum is typically adnate or only partly detached. Fully detached opercula are rare.

Dimensions: 40 specimens were measured.

	Holotype	Range: min. (mean) max.
Overall length:	47 µm	30 (40) 57 µm
Overall width:	39 µm	31 (37) 52 µm
Length of spines:	2 (3) 4 µm	1 (2) 4 µm

Stratigraphic range: the Callovian to Tithonian APJ5 Spore-Pollen Zone of Price (1997) in the Indy 3 well.

Remarks: There is a strong suggestion that there is a periphragm forming the crests and spines of the *Moorodinium* observed in the Surat Basin. As such, the original diagnosis pertaining to an autophragm would need to be broadened to include the possibility of two or more wall layers. Indeed, it is noted that *Moorodinium simplex* Backhouse (1988) may also comprise two wall layers separated only by minor antapical cavation. However, until further specimens have been recovered that show this beyond doubt, or until better preserved specimens are available for SEM analysis, these changes are not formalised. The thinner walled Surat Basin specimens were also noted to have less well-developed surface ornament, including lower septa or folds, a smoother surface and were much less likely to develop antapical spines; for now, these are considered within the variation of the species, rather than splitting a morphologically simple dinoflagellate cyst into two new species.

Comparisons: *Moorodinium spinatum* Backhouse (1988) bears similar antapical spines but exhibits obvious hypocystal paratabulation and lacks the pervasive folds of *Moorodinium crispa*. *Moorodinium peregrinum* Backhouse (1988) and *Moorodinium quindalupense* Backhouse (1988) are both noticeably larger, with distinct dorso-ventral septa running across the apex. The former taxon also has a more strongly lobate antapex, whilst the latter has a single, long, fine antapical spine. *Moorodinium simplex* Backhouse (1988) is most similar to the non-spinose forms of *Moorodinium crispa* but also lacks the comprehensive folding diagnostic of the latter taxon. The non-spinose forms of *Moorodinium crispa* are also superficially very similar to small *Mendicodinium* Morgenroth 1970 emend. Palliani et al. 1997. The lack of well-defined dorso-ventral septa across the apex of *Moorodinium crispa* makes separation from *Mendicodinium* particularly difficult. However, very few *Mendicodinium* bear spines and those that do, the spines are typically solid and sharp and are distributed evenly across the whole cyst rather than concentrated antapically.

Genus: ***Skuadinium*** Riding and Helby 2001

Type: *Skuadinium biturbinatum* Riding and Helby 2001

Synopsis: small to intermediate fusiform cysts with an unknown archaeopyle, possibly epicystal, and lacking paratabulation other than the paracingulum and rare parasulcal folds. The surface ornamentation is smooth to scrabrate or finely reticulate and nontabular. One or two dark accumulation bodies are generally present in the paracingular region. Apical and antapical horns relatively short, blunt and conical. Some species may bear hypocystal protuberances at or below the paracingulum.

Remarks: The Late Jurassic *Skuadinium* taxon described herein from the Surat Basin is considerably younger than the Toarcian (Early Jurassic) *Skuadinium* suite described by Riding and Helby (2001) from the Bonaparte Basin on the North West Shelf of Australia. The three species described by Riding and Helby (2001) share many characteristics with those from the Surat Basin including low relief ornamentation, a conical to biconical form, and lacking obvious paratabulation other than the laevorotatory paracingulum and possible epicystal archaeopyles.

***Skuadinium fusumaster* sp. nov.** (Plate 8.2, Figures 1-7)

Etymology: Latin, *fusum*, bears some resemblance to a spindle top.

Diagnosis: a fusiform to cruciform *Skuadinium* with a thin, finely reticulate to scrabrate wall covered in fine folds and with a strongly laevorotatory paracingulum. Moderately elongate hypocyst with a broad, conical antapex and a shorter epicyst that may be pyramidal with a sharp point or narrow to a short rounded apical horn.

Holotype: Indy 3 well, conventional core sample at 247.55 m, slide 3, EF coordinates M20/2 (Plate 8.2, Figure 6), CPC number 43736.

Paratypes: both from the Indy 3 well, conventional core sample from 247.55 m, slide number 3. Paratype 1, EF coordinates U12/4 (Plate 8.2, Figure 4), CPC

number 43734. Paratype 2, EF coordinates S44/1 (Plate 8.2, Figure 5), CPC number 43731.

Description: a small proximate cyst with a fusiform to cruciform ambitus. Longitudinally elongate. The epicyst may be broadly triangular with a sharp apical point or a short-rounded horn whilst the hypocyst is conical with a broad, blunt or rounded antapex. Only a single thin wall layer with many fine folds and low surface ornament is evident on most specimens, however, minor apical cavation, on some specimens, indicates two or more closely appressed layers may be present. The surface ornamentation is scrabrate to finely reticulate (lumina 3–8 µm in diameter). Paratabulation is only clearly indicated by the strongly laevorotatory paracingulum that is marked by coarse, low, partly granulate ridges; the paracingulum is offset by its full width. Further parasutural ridges are largely masked by the numerous accessory folds and reticulation. The archaeopyle is not readily apparent but may be epicystal, type [tAtP], with the operculum typically adnate. Rare accumulation bodies may be present as dark, spherical to subspherical patches located close to the paracingulum.

Dimensions: 20 specimens were measured.

	Holotype	Range: min. (mean) max.
Overall length:	46 µm	34 (43) 55 µm
Overall width:	41 µm	27 (36) 48 µm

Stratigraphic range: the Callovian to Tithonian APJ5 Spore-Pollen Zone of Price (1997) in the Indy 3 well.

Remarks: The Surat Basin species show some minor variation in cyst size and the degree to which the paracingulum is offset. However, these differences are considered well within reasonable limits for intraspecific variation.

Comparisons: *Skuadinium fusumaster* is a lot smaller and squatter with a less pointed or elongate antapical horn than the Toarcian *Skuadinium* species described from the Timor Sea, northern Australia (Riding and Helby 2001). In contrast to some of these *Skuadinium* species, paracingular proturberances are also distinctly absent or poorly developed on *Skuadinium fusumaster*. It does

however, share many characteristics with these taxa—the relatively simple fusiform amb, the largely acavate structure, very thin walls, and the uncertain (though likely epicystal) archaeopyle type. It also exhibits similar, though not as pervasive or well-developed, reticulation, as for *Skuadinium asymmetricum* Riding and Helby 2001 and *Skuadinium reticulatum* Riding and Helby 2001. Both of these Toarcian taxa are much larger whilst the former also exhibits a strongly asymmetrical outline formed by swollen ventral paraplates, whilst the latter bears much longer and narrower apical and antapical horns. Both taxa also have much larger, darker and more clearly defined accumulation bodies. *Skuadinium biturbinatum* Riding and Helby 2001 has thin, largely smooth walls, longer apical and antapical horns with blunt or rounded apices and is again considerably larger than *Skuadinium fusumaster*.

Chapter 8

Division: **Chlorophyta** Pascher 1914

Genus: ***Palambages*** Wetzel 1961

Type: *Palambages morulosa* Wetzel 1961

Synopsis: small colonial, bacciform algal cysts with spheroidal to oblate cells. Membranous, psilate to microgranulate and finely folded. Colonies can consist of up to 100 cells.

Remarks: *Palambages* are relatively simple groupings of small spheroidal cells (typically 10–30 µm) which are often inadequately described in the literature. Their origins remain enigmatic, and whilst for now considered to be Chlorophyta, their initial classification as *incertae sedis* is not totally defunct (Wetzel 1961). They were described as “egglike” as their morphology is similar to the egg-balls of planktonic crustaceans and the coenobia of the alga *Coelastrum* (Wetzel 1961). Srivastava (1968) suggests that these structures may represent green algal colonies or balls of fungal spores. The *Palambages* species described by Wetzel (1961), Srivastava (1968), Jameossanaie (1987) and Firth (1993) are all colonial and constructed of tight bunches of thin-walled oval to spherical cells. Firth (1993) noted two types of connections between individual cells: trilete structures connecting adjacent cells in the equatorial region, and bar and ring structures present on the dorsal side of each cell. However, most *Palambages* do not exhibit obvious connections between the individual cells.

The oldest known occurrence of *Palambages* are reported from the Late Jurassic (Oxfordian) to Early Cretaceous (Albian) Pemba Formation in the Rovuma Basin, Northern Mozambique (Smelror et al. 2008). *Palambages* have also been recorded from Cretaceous flintstones in the Baltic Sea (Wetzel 1961); the Coniacian to Santonian Menefee Formation in the San Juan Basin, USA (Jameossanaie 1987); the Maastrichtian Alpha Ridge in Arctic Canada (Firth and Clark 1998); the Maastrichtian Edmonton Formation of Alberta, Canada (Srivastava 1968); and in the Maastrichtian Providence Formation of southwest Georgia, USA (Firth 1993). There are no published records of *Palambages* from

the Mesozoic basins of eastern Australia, but these rare colonial cysts may be easily overlooked or ignored.

***Palambages pariunta* sp. nov.** (Plate 8.2, Figures 8-14)

Etymology: Latin, *pariunt*, comparable to the gelatinous mass of frog eggs or “frogspawn”.

Diagnosis: Bacciform colonial algae. Individual cells oval to spheroidal with membranous, granulate to micropunctate and often pervasively folded walls. Colony clustered around a thicker walled central cell.

Holotype: Indy 3 well, conventional core sample at 247.55 m, slide number 3, EF coordinates S33/1 (Plate 8.2, Figures 14a and 14b), CPC number 43744.

Paratypes: both from the Indy 3 well, conventional core sample at 247.55 m, slide number 3. Paratype 1, EF coordinates T17/4, (Plate 8.2, Figures 10a and 10b), CPC number 43740. Paratype 2, EF coordinates Q42/3 (Plate 8.2, Figures 11a and 11b), CPC Number 43741.

Description: a small, bacciform colonial alga with 10–30 cells forming most colonies. The colony is clustered around a spherical, thick walled central cell. Individual cells are oval to spheroidal and granulate to micropunctate, composed of a single layer and often covered in fine folds. No apertures or rods are noted to join the individual cells.

Dimensions: 22 specimens were measured.

	Holotype	Range: min. (mean) max
Overall colony length:	43 µm	31 (42) 52 µm
Overall colony width:	40 µm	30 (39) 44 µm
Individual cell diameter:	13 (13) 14 µm	5 (9) 16 µm
Cell wall thickness:	0.3 (0.5) 0.8 µm	0.2 (0.5) 1.2 µm

Stratigraphic range: the Callovian to Tithonian APJ5 Spore-Pollen Zone of Price (1997) in the Indy 3 well.

Remarks: *Palambages pariunta* is unique within the genus in possessing a noticeably thicker central cell and thus is superficially very similar to a foraminiferal test lining. However, the consistent size of the individual cells (not increasing in size from an innermost to outermost ‘chamber’), the shape of the cells, the lack of obvious coiling or connection between cells and overall small size are all inconsistent with their identification as foraminifera. The rather petaloid outline (with each cell protruding outwards) is also different to the more smoothly spherical ambitus of most *Palambages*, but overall the collection of thin-walled, apparently inaperturate spherical cells is broadly consistent for this genus. *Palambages pariunta* is also notably older than the majority of previous records; most *Palambages* spp. described in the literature are Turonian or younger. There is a single record of Late Jurassic to Early Cretaceous *Palambages* from the Pemba Formation in the Rovuma Basin, Mozambique (Smelror et al. 2008), but these specimens are not figured. *Palambages pariunta* also represents the first published account of this genus from eastern Australian Mesozoic basins.

Comparisons: *Palambages pariunta* is most similar to the *Palambages* sp. of Jameossanaie (1987) and *Palambages* sp. 1 of Gies (1972)—all three taxa consist of a similar number of small spheroidal cells with thin, psilate to finely granulate walls. However, only *Palambages pariunta* has a noticeably thicker central cell and also lacks the small spines and larger overall diameter of *Palambages* sp. 1 of Gies (1972). All other *Palambages* spp. also lack the diagnostic thicker and darker central cell of *Palambages pariunta* and most are also considerably larger and composed of a larger number of individual cells.

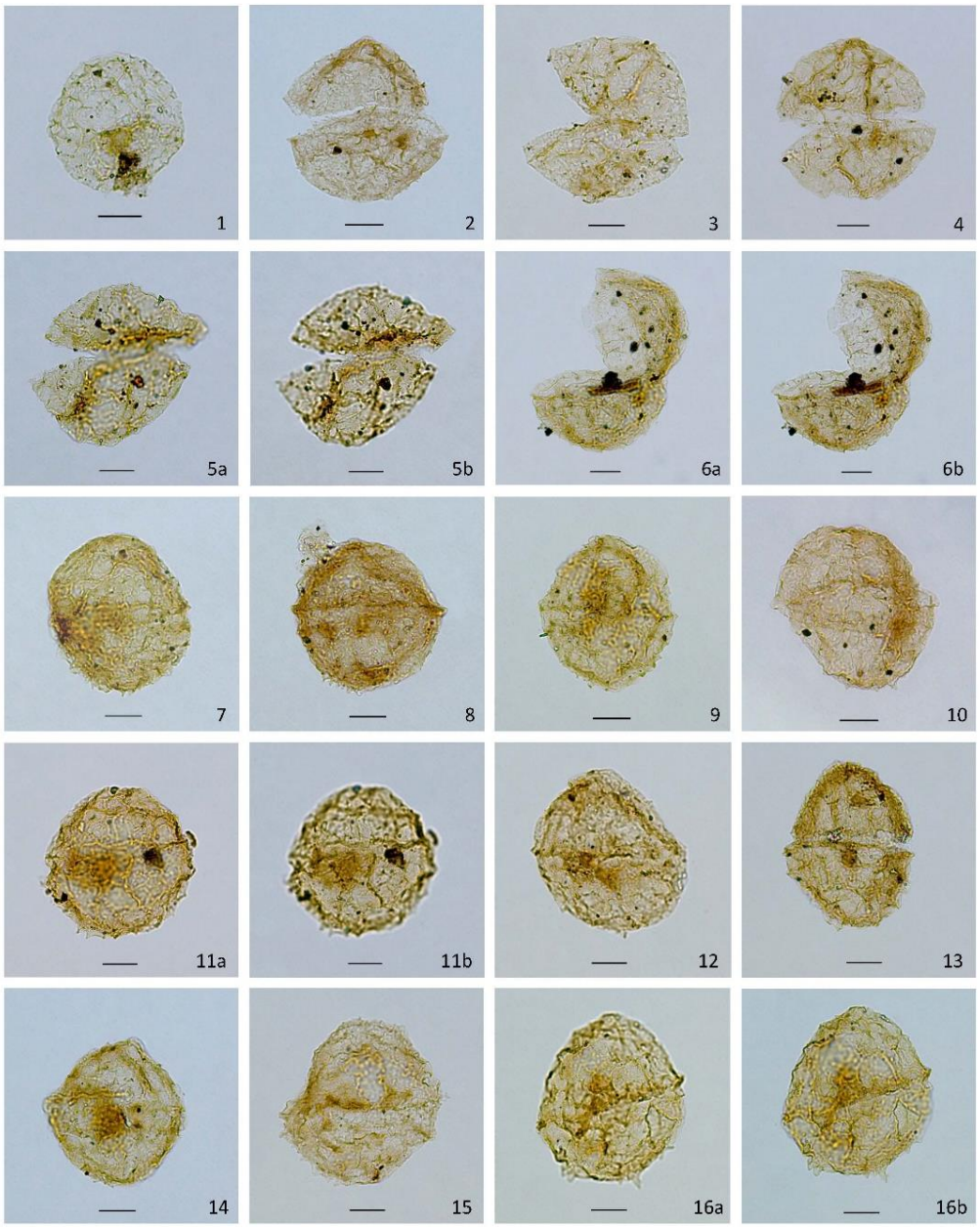

Plate 8.1. Dinoflagellate cysts from the Indy 3 well at 247.55 m depth. Scale bar 10 µm throughout. (1) *Moorodinium crispa*, slide 3, U41/1. (2) *Moorodinium crispa*, slide 3, W47/3. (3) *Moorodinium crispa*, U23/0. (4) *Moorodinium crispa,* slide 3, C41/4. (5a/5b) *Moorodinium crispa,* slide 3, S40/4. (6a/6b) *Moorodinium crispa*, slide 3, U41/2. (7) *Moorodinium crispa*, slide 3, S40/4. (8) *Moorodinium crispa*, slide 3, C38/2. (9) *Moorodinium crispa*, slide 3, R26/3. (10) *Moorodinium crispa*, slide 3, N19/2. (11a/11b) *Moorodinium crispa*, slide 3, J42/1. (12 *Moorodinium crispa*, L44/0. (13) *Moorodinium crispa*, slide 3, L45/3. (14) *Moorodinium crispa*, slide 3, Q19/0. (15) *Moorodinium crispa*, slide 3, J19/4. (16a/16b) *Moorodinium crispa*, slide 3, F30/3.

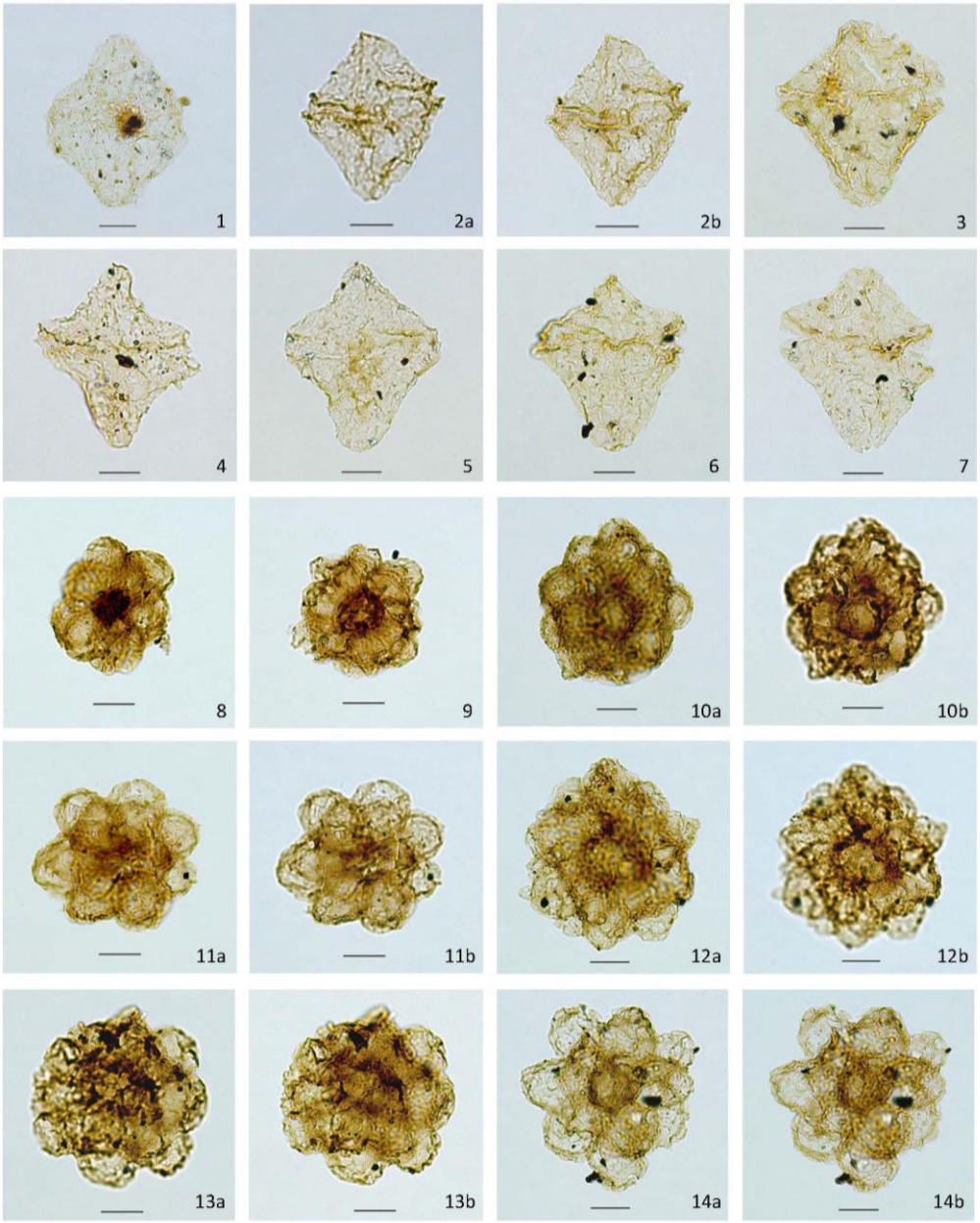

Plate 8.2. Dinoflagellate cysts and colonial algae from the Indy 3 well at 247.55 m depth. Scale bar 10 µm throughout. (1) *Skuadinium fusumaster*, slide 3, S44/1. (2a/2b) *Skuadinium fusumaster*, slide 3, Q43/0. (3) *Skuadinium fusumaster*, slide 3, X19/3. (4) *Skuadinium fusumaster*, slide 3, U12/4. (5) *Skuadinium fusumaster*, slide 3, S44/1. (6) *Skuadinium fusumaster*, slide 3, M20/2. (7) *Skuadinium fusumaster*, slide 3, H31/2. (8) *Palambages pariunta*, slide 3, M20/2. (9) *Palambages pariunta*, slide 3, V16/2. (10a/10b) *Palambages pariunta*, slide 3, T17/4. (11a/11b) *Palambages pariunta*, slide 3, Q42/3. (12a/12b) *Palambages pariunta*, slide 3, X15/2. (13a/13b) *Palambages pariunta*, slide 3, X44/2. (14a/14b) *Palambages pariunta*, slide 3, S33/1.

8.4 Discussion

The presence of dinoflagellate cysts and *Palambages* from Upper Jurassic strata of the Surat Basin raises questions about the palaeoenvironment and palaeoecology of the largely nonmarine successions from which they were derived. Dinoflagellates are dominantly marine organisms and are only sporadically recorded from fully freshwater habitats from the Early Cretaceous onwards (Harding and Allen 1995); they are more widespread in nonmarine settings in the Cenozoic (Batten 1989). Mesozoic freshwater to brackish dinoflagellate cysts have been recorded from: the ?Tithonian–Berriasian Parmelia Formation of the Perth Basin in Western Australia (Backhouse 1988); the Early Cretaceous of the Great Australian Basin (Morgan 1975); the Valanginian to Barremian Wealden Group of the Wessex Basin in England (Batten and Lister 1988); the Lower Cretaceous Jydegård Formation in Denmark (Piasecki 1984); the Hauterivian to Maastrichtian intracontinental basins in northeast China (Mao et al. 1999); the Albian Mattagami Formation of the Moose River Basin in Canada (Zippi 1998); and from the Turonian-lower Santonian Latrobe Group of the Gippsland Basin in Australia (Marshall 1989).

With differences in osmotic pressures and ionic concentrations, the transition from marine to freshwater habitats is a strong environmental and ecological barrier for most aquatic organisms. This would certainly apply to marine microplankton and the construction of rDNA dinoflagellate phylogenies demonstrates that relatively few dinoflagellate lineages have made this transition (Logares et al. 2007). Their study also confirmed that many of these transitions are not recent, albeit without assigning ages to these evolutionary shifts. They also suggest that major sea-level changes during the Mesozoic and Cenozoic allowed marine waters to flood large continental areas, introducing dinoflagellates into the nonmarine realm. The temporary nutrient availability in these newly flooded and salinity stressed environments may have driven several episodes of rapid ecological diversification (Harding and Allen 1995). Indeed, many of the Cretaceous nonmarine to brackish dinoflagellate cyst assemblages share very few of the same taxa, thus suggesting independent evolutionary events.

The key question for the Surat Basin dinoflagellate cyst assemblage is whether it represents evidence of marine incursions into the basin or is rather one of the oldest occurrences of nonmarine or brackish dinoflagellate cysts. Palynological assemblages above and below the dinoflagellate-rich sample (247.55 m) contain exclusively terrestrial palynofloras (Figure 8.3) as is typical of all other palynological studies of this age in the Surat Basin. This dinoflagellate cyst assemblage contains none of the common Australian Jurassic marine genera and the low diversity, high abundance and high dominance of a small number of species is also typical of nonmarine to brackish assemblages (Backhouse 1988). Furthermore, the small size, thin walls, and simple, proximate morphologies are also all typical of nonmarine to brackish dinoflagellate cysts, as is the lack of paratabulation (other than the paracingulum) and the poorly defined archaeopyle. Along with the absence of any marine macrofossils or other marine microfossil groups (foraminifera etc.), it seems that a fully marine depositional environment can be easily ruled out, but eliminating all marginal marine or brackish influences is more challenging.

The Surat Basin dinoflagellate cyst assemblage share compositional similarities with the Toarcian Plover Formation assemblages in the Bonaparte Basin and the ?Tithonian–Berriasian Parmelia Formation of the Perth Basin; all three suites contain simple thin-walled *Moorodinium*, whilst the fusiform *Skuadiniu*m are only present in first two basins. The Bonaparte Basin assemblages are considered to reflect marginal marine to lacustrine depositional environments (Osborne 1990; Riding and Helby 2001), whereas the Perth Basin suites are considered to represent brackish to freshwater lacustrine deposition (Backhouse 1988). However, the latter assemblage occurred in a pre-breakup rift valley (India rifting from Greater Australia) where short-lived marine incursions may have sporadically inundated coastal lakes.

Acritarchs associated with marine to brackish environments, including *Micrhystridium*, are not as common in the Indy 3 well compared to other localities across the Surat Basin, where some samples contain up to 10% spinose acritarchs (See Section 7.6). Although spinose acritarchs may be abundant in shallow marine environments, they are reported in moderate numbers in marginal marine settings (Dixon et al. 2012) and are also

associated with brackish episodes during short-lived transgressive events in intracontinental basins as suggested for the Surat Basin (Burger 1986) and the Dwyka Group of the Karoo Basin (Césari 2007).

The presence of common *Palambages* is also not considered a significant palaeoenvironmental indicator, as these supposed chlorophyte green algae have been recorded from a wide range of depositional environments. Srivastava (1968), Jameossanaie (1987) and Firth (1993) all reported *Palambages* from coal-bearing facies associated with shoreface strata from the Maastrichtian of Alberta, the Santonian of New Mexico, and the Maastrichtian of southwest Georgia, but the various *Palambages* species they recorded were all uncommon. Furthermore, *Palambages* are also recorded from a variety of marine settings, including shelf to upper slope environments in Maastrichtian organic-rich mudstones in the Arctic (Firth and Clark 1998), offshore cherts and flints of the Upper Cretaceous to Cenozoic of the Baltics (Wetzel 1961), and the marine Upper Cretaceous Mancos Shale of Colorado (Gies 1972).

Three lines of evidence from the Walloon Coal Measures support deposition in a brackish to upper estuarine as opposed to a fully nonmarine setting. The first is the presence of lenticular bedding and double mud drapes in the Walloon Coal Measures—these are generally indicative of tidal processes (see Section 6.6). Secondly, sedimentary successions in the Indy 3 well are also associated with the infilling of an incised valley (fluvial to estuarine facies) during a progressive rise in base level (see Section 6.6). Thirdly, analysis of eustatic sea-level curves suggest the Tithonian marked a peak in sea-level before declining into the Early Cretaceous (Haq et al. 1987, 1988; Hallam 2001) and is supported by the dating of tuffs beds in the Indy 3 well. High sea-level during this timeframe may have initiated marine transgressions and provided a corridor for dinoflagellates to migrate into the interior of the Australian continent from the north (via the Carpentaria and Eromanga basins) or from the east (via the Clarence-Moreton Basin) (see Section 6.6).

8.5 Conclusion

Two new species of dinoflagellate cyst (*Moorodinium crispa* and *Skuadinium fusumaster*) and one species of colonial alga (*Palambages pariunta*) are described from the Late Jurassic Walloon Coal Measures of the Surat Basin. The case for a freshwater to brackish dinoflagellate cyst suite seems compelling, based on their morphological traits (small, thin-walled, simple proximate cysts), the assemblage composition (low diversity, high dominance), and the lack of any other marine micro- or macro-faunas. The Surat Basin suite may represent one of the oldest occurrences of nonmarine dinoflagellate cysts, however, it is also noted that this assemblage is uniquely associated with sedimentary structures indicative of tidal deposition (double mud drapes and lenticular bedding) that suggest an upper estuarine setting. This possibility is supported by U-Pb CA-TIMS dates that tie the succession to high eustatic sea-level in the Tithonian and the prospect for marine incursions into the continental interior.

Both *Moorodinium* and *Skuadinium* are also associated with freshwater to brackish or even marginal marine settings in the Toarcian of the Bonaparte Basin and the ?Tithonian-Berriasian of the Perth Basin. If similar dinoflagellate cysts are discovered within the same stratigraphic interval and found to be widespread across eastern Australian basins during the Tithonian, they may provide a useful correlative tool in the complex brackish to lacustrine and fluvial successions of eastern Australia.

8.6 Acknowledgements

Carmine Wainman has a Ph.D. scholarship from the University of Adelaide that has covered most of the travel and analytical costs. We thank Senex Energy for making the Indy 3 well available for analysis. We are grateful to John Backhouse for this assistance in the taxonomic identification of dinoflagellate cysts for this study. We also thank Jim Crowley, Debra Pierce and Alexandra Edwards from Boise State University who assisted with mineral separation, preparation and the dating of zircon grains using CA-TIMS.

8.7 Supplementary papers

See appendices 5 (p. 371-372).

Chapter 9. Conclusions and future work

9.1 Conclusions

The evolution and character of Middle to Upper Jurassic coal-bearing strata in eastern Australia has been studied using a multidisciplinary approach integrating sedimentology, palynology, stratigraphy, and basin analysis. A key element of this study was the first application of high precision U-Pb CA-TIMS dates derived from volcanic zircons that gave new insights to the age of the strata and allowed the construction of a new chronostratigraphic framework. Major conclusions from this study are:

- New U-Pb CA-TIMS dates show that deposition of the Walloon Coal Measures occurred from 168 Ma (Middle Jurassic Bathonian) to 149 Ma (Late Jurassic Tithonian). This is distinctly younger than had previously been supposed as the formation had been assumed to be entirely Middle Jurassic in age.

- A robust chronostratigraphic framework for eastern Australian basins has been defined using new U-Pb CA-TIMS dates from tuffs and volcanogenic sandstones. This shows that coal facies are highly diachronous and young from the Clarence-Moreton Basin (168 Ma) into the western Surat Basin (149 Ma). Volcanogenic sandstones of the Birkhead Formation of the Eromanga Basin to the west were dated as Oxfordian showing their deposition to be coeval with the lower part of the Walloon Coal Measures in the Surat Basin. The new dates also demonstrate the difficulty of identifying sequence boundaries within these nonmarine strata without chronostratigraphic data.

- The coal-bearing strata accumulated at high latitude (>75°S) during a greenhouse epoch. Coal comprises ~6% of the Walloon Coal Measures but, although the subsidence rates of the basin appear to have been favourable for peat (coal) accumulation, coal beds are thin (<0.4 m), and laterally discontinuous (< 5 km). Frequent and rapid changes in climate

at such high latitudes may have limited the duration of periods when conditions were favourable for peat development

- Most of the Walloon Coal Measures were deposited in a fluviolacustrine setting with drainage to the south and southwest. The recognition of sedimentary structures indicative of tidal processes, including double mud drapes, in association with dinoflagellate cysts suggests periods of deposition in proximal estuarine complexes. These periods appear to have been ones of high eustatic sea-level in the Callovian and Tithonian.

- Allocyclic controls, including sea-level change, likely controlled the deposition of some facies with the formation of incised valleys and associated transgressive estuarine deposits.

- Using the new U-Pb CA-TIMS dates, spore-pollen zones of Price (1997) in eastern Australia can now be calibrated to the geologic time-scale of Ogg et al. (2016) without the need for more tenuous correlations to ammonite or dinoflagellate assemblages. Some zones (e.g. APJ6.1 Zone) may be up to 4.2 Ma younger than previously suggested but precise correlation is difficult because marker taxa are locally scarce.

- Two new species of dinoflagellate cyst (*Moorodinium cris*pa and *Skuadinium fusumaster*) and one species of colonial algae (*Palambages pariunta*) have been identified from the Late Jurassic Walloon Coal Measures of the Surat Basin. The dinoflagellate cysts may provide a useful correlative tool for tracing distinctive brackish to marginal marine flooding surfaces in continental successions in eastern Australia.

9.2 Future work

- Precise dating of volcanogenic sandstones offers the opportunity to improve the age constraints of other nonmarine strata worldwide. This should help overcome issues in stratigraphic correlation in basins hosting such strata.

- Further work is required to improve our understanding of dinoflagellate cysts in nonmarine and marginal marine successions prior to the Cretaceous. Although the assemblage in the Walloon Coal Measures may document one of the earliest evolutionary episodes where they evolved in fresh to brackish water settings, they are associated with sedimentary structures that suggest tidal influence. Additional research will be required to better understand their ecological niche.

- High resolution dating of strata, as has been carried out in this study, offers the possibility of measuring the amount and rate of change during a single eustatic cycle. It would be particularly interesting to test the estimated 187 m drop in sea-level calculated for the early Oxfordian in Scenario B in Chapter 5.

- The notion of rapid climate shifts at high latitude in the Late Jurassic could be tested in other areas and in other facies including marine strata.

- Further studies are need to confirm the nature and timing of marine incursions onto the Australian continent during the Jurassic that may have been precursors to those of the Early Cretaceous. This may be possible with more detailed studies of the Jurassic marginal marine Dalrymple Sandstone in the Laura Basin in northern Queensland.

- The Middle to Late Jurassic chronostratigraphic framework of eastern Australia could be further refined. With additional tuff dates from wells spaced >5 km apart, better correlations will be possible in the complex, heterolithic character of the coal-bearing sequences.

- Dating of three to four tuffs beds in several wells, including areas of the Talinga Field near Chinchilla, the Lacerta Field near Roma, and the Laidley Sub-Basin (Clarence-Moreton Basin) close to Toowoomba, could confirm regional chronostratigraphic correlations. Dating of tuffs near major fault lines (especially near the Hutton-Wallumbilla Fault in the northern Surat Basin) would also significantly improve correlations.

- The potential of precisely correlating the Birkhead Formation to the Walloon Coal Measures has been shown to be feasible by dating zircon from volcanogenic sandstones. Further dates from the Birkhead Formation will allow a much better understanding of the regional palaeogeographic evolution.

- Further research will be required to identify strata hosting dinoflagellate cysts. If they are present across eastern Australia, they may provide a useful correlative tool in the complex brackish to lacustrine and fluvial successions of eastern Australia. In particular, they may help identify subtle stratigraphic traps in the Eromanga Basin.

References

Kristensen et al. (1995)Alexander, E., and Hibburt, J., 1996, The Petroleum Geology of South Australia. Vol. 2: Eromanga Basin: South Australia. Department of Mines and Energy. Report Book, v. 96, p. 20.

Alexander, E. M., and Jensen-Schmidt, B., 1996, Structural and Tectonic Setting in "the Petroleum Geology of South Australia. Vol. 2: Eromanga Basin": South Australia. Department of Mines and Energy. Report Book, v. 96, p. 1-27.

Alexander, E. M., Sansome, A., and Cotton, T. B., 1996, Lithostratigraphy and Environments of Deposition in "the Petroleum Geology of South Australia. Vol. 2: Eromanga Basin": South Australia. Department of Mines and Energy. Report Book, v. 96, p. 1-129.

Allen, G. P., and Chambers, J. L., 1998, Regional Geology and Stratigraphy of the Kutei Basin, *in* G. P. Allen and J. L. Chambers, eds., Sedimentation in the Modern and Miocene Mahakam Delta, v. 1, Indonesian Petroleum Association, p. 159-171.

Allen, P. A., and Allen, J. R., 2013, Basin Analysis: Principles and Application to Petroleum Play Assessment: London, John Wiley & Sons, pp. 451.

Ambrose, W. A., and Ayers Jr, W. B., 2007, Geologic Controls on Transgressive-Regressive Cycles in the Upper Pictured Cliffs Sandstone and Coal Geometry in the Lower Fruitland Formation, Northern San Juan Basin, New Mexico and Colorado: AAPG Bulletin, v. 91, p. 1099-1122.

Anisimov, O. A., Vaughan, D. G., Callaghan, T. V., Furgal, C., Marchant, H., Prowse, T. D., Vilhjálmsson, H., and Walsh, J. E., 2007, Polar Regions (Arctic and Antarctic): Climate Change, v. 15, p. 653-685.

Apak, S. N., Stuart, W. J., Lemon, N. M., and Wood, G., 1997, Structural Evolution of the Permian-Triassic Cooper Basin, Australia: Relation to Hydrocarbon Trap Styles: AAPG Bulletin, v. 81, p. 533-555.

Arditto, P. A., 1982, Deposition and Diagenesis of the Jurassic Pilliga Sandstone in the Southeastern Surat Basin, New South Wales: Journal of the Geological Society of Australia, v. 29, p. 191-203.

Ayaz, S., Esterle, J., and Martin, M., 2015, Spatial Variation in the Stratigraphic Architecture of the Fort Cooper and Equivalent Coal Measures, Bowen Basin, Queensland: Australian Journal of Earth Sciences, v. 62, p. 547-562.

References

Babaahmadi, A., Rosenbaum, G., and Esterle, J., 2015, Alternating Episodes of Extension and Contraction During the Triassic: Evidence from Mesozoic Sedimentary Basins in Eastern Australia: Australian Journal of Earth Sciences, v. 62, p. 563-579.

Backhouse, J., 1978, Palynological Zonation of the Late Jurassic and Early Cretaceous Sediments of the Yarragadee Formation, Central Perth Basin, Western Australia, v. 53: Perth, Geological Survey of Western Australia, pp. 54.

Backhouse, J., 1988, Late Jurassic and Early Cretaceous Palynology of the Perth Basin, Western Australia: Geological Survey of Western Australia Bulltein, v. 135, p. 1-233.

Baker, G., and Slater, S., 2008, The Increasing Significance of Coal Seam Gas in Eastern Australia: Proceedings of the PESA Eastern Australasian Basins Symposium III, p. 14-17

Baker, G. L., and Skerman, W. R., 2006, The Significance of Coal Seam Gas in Eastern Queensland: APPEA Journal, v. 46, p. 329-341.

Balme, B., Kershaw, A., and Webb, J., 1995, Floras of Australian Coal Measures, with Notes on Their Associated Mesozoic Faunas: Geology of Australian Coal Basins, v. 1, p. 41-32.

Balme, B. E., 1957, Spores and Pollen Grains from the Mesozoic of Western Australia. : Commonwealth Scientific and Industrial Research Organization, Australia, Coal Research Section, Technical Communication, v. 25: Perth, Australia, Commonwealth Scientific and Industrial Research Organization (Australia), pp. 48.

Balme, B. E., 1964, The Palynological Record of Australian Pre-Tertiary Floras, *in* L. M. Cranwell, ed., Ancient Pacific Floras. The Pollen Story, v. 1: Honolulu, Hawaii, University of Hawaii Press, p. 48-80.

Balme, B. E., 1966, Spores and Pollen Grains from the Mesozoic of Western Australia, v. 25, Division of Coal Research, Commonwealth Scientific and Industrial Research Organization, pp. 48.

Barham, M., Kirkland, C., Reynolds, S., O'Leary, M., Evans, N., Allen, H., Haines, P., Hocking, R., McDonald, B., and Belousova, E., 2016, The Answers Are Blowin'in the Wind: Ultra-Distal Ashfall Zircons, Indicators of Cretaceous Super-Eruptions in Eastern Gondwana: Geology, v. 44, p. 643-646.

Batten, D., 1989, Cretaceous Freshwater Dinoflagellates: Cretaceous Research, v. 10, p. 271-273.

Batten, D., and Lister, J., 1988, Evidence of Freshwater Dinoflagellates and Other Algae in the English Wealden (Early Cretaceous): Cretaceous Research, v. 9, p. 171-179.

Bean, L., 2006, The Leptolepid Fish Cavenderichthys Talbragarensis (Woodward, 1895) from the Talbragar Fish Bed (Late Jurassic) near Gulgong, New South Wales: Records-Western Australian Museum v. 23, p. 43-76.

Beattie, R. G., and Avery, S., 2012, Palaeoecology and Palaeoenvironment of the Jurassic Talbragar Fossil Fish Bed, Gulgong, New South Wales, Australia: Alcheringa: An Australasian Journal of Palaeontology, v. 36, p. 453-468.

Beeston, J., 1995, Cooper Basin: Geology of Australian Coal Basins, Ward, CR, Harrington, HJ, Mallett, CW, Beeston, JW (eds). Geological Society of Australia Incorporated, Coal Geology Group, Special Publication, v. 1, p. 353-359.

Blakey, R., 2011, Global Paleogeography: http://www2.nau.edu/rcb7/globaltext2.html Date accessed 06/05/2016.

Bohacs, K. M., and Suter, J., 1997, Sequence Stratigraphic Distribution of Coaly Rocks; Fundamental Controls and Paralic Examples: AAPG Bulletin, v. 81, p. 1612-1639.

Boreham, C., 1995, Origin of Petroleum in the Bowen and Surat Basins: Geochemistry Revisited: APEA Journal, v. 35, p. 579-579.

Boucot, A. J., Chen, X., and Scotese, C. R., 2013, Phanerozoic Paleoclimate: An Atlas of Lithologic Indicators of Climate, *in* G. Nichols and B. Ricketts, eds., Sepm Concepts in Sedimentology and Paleontology, v. 11: Tulsa, Oklahoma, Society of Economic Paleontologists and Mineralogists, p. 1-484.

Boult, P., Lanzilli, E., Michaelsen, B., McKirdy, D. M., and Ryan, M., 1998, A New Model for the Hutton/Birkhead Reservoir/Seal Couplet and the Associated Birkhead-Hutton Petroleum System: APEA Journal, v. 38, p. 724-745.

Boult, P. J., 1996, An Investigation of Reservoir/Seal Couplets in the Eromanga Basin; Implications for Petroleum Entrapment and Production: Development of

Secondary Migration and Seal Potential Theory and Investigation Techniques, University of South Australia, Adelaide, Australia, pp. 255.

Bowring, S. A., and Schmitz, M. D., 2003, High-Precision U-Pb Zircon Geochronology and the Stratigraphic Record: Reviews in Mineralogy and Geochemistry, v. 53, p. 305-326.

Bradshaw, M., and Bernecker, T., 2016, Science Capabilities Unlock Australia's Oil and Gas Potential: The Leading Edge, v. 35, p. 15-21.

Bradshaw, M. T., and Yeung, M., 1992, Jurassic, *in* M. T. Bradshaw and M. Yeung, eds., Palaeogeographic Atlas of Australia, v. 8: Canberra, Australia, Bureau of Mineral Resources, p. 1-60.

Bridge, J., 2009, Numerical Modelling of Alluvial Deposits: Recent Developments, *in* P. de Boer, G. Postma, K. van der Zwan, P. M. Burgess and P. Kukla, eds., Analogue and Numerical Modelling of Sedimentary Systems: From Understanding to Prediction (Special Publication of the Ias), v. 40, p. 97-138.

Bridge, J. S., and Leeder, M. R., 1979, A Simulation Model of Alluvial Stratigraphy: Sedimentology, v. 26, p. 617-644.

Brigaud, B., Pucéat, E., Pellenard, P., Vincent, B., and Joachimski, M. M., 2008, Climatic Fluctuations and Seasonality During the Late Jurassic (Oxfordian–Early Kimmeridgian) Inferred from Δ^{18}o of Paris Basin Oyster Shells: Earth and Planetary Science Letters, v. 273, p. 58-67.

Brown, C., 2008, Palynological Techniques Aasp Special Publications, v. 1: College Station, USA, Association of Stratigraphic Palynologists Foundation, pp. 137.

Browne, G. H., and Hart, B. S., 1990, Discussion: Hummocky Cross-Stratification from the Boxvale Sandstone Member in the Northern Surat Basin, Queensland: Australian Journal of Earth Sciences, v. 37, p. 377-978.

Bryan, S., Constantine, A., Stephens, C., Ewart, A., Schön, R., and Parianos, J., 1997, Early Cretaceous Volcano-Sedimentary Successions Along the Eastern Australian Continental Margin: Implications for the Break-up of Eastern Gondwana: Earth and Planetary Science Letters, v. 153, p. 85-102.

References

Bryan, W. H., 1946, The Geological History of Queensland: A Stratigraphic Outline: University of Queensland, Department of Geology Papers, v. 2, p. 1-110.

Burger, D., 1968, Stratigraphy and Palynology of Upper Mesozoic Sections in Some Deep Wells in the Surat Basin, Queensland: Bureau of Mineral Resources, Australia, Record, v. 24, p. 1-35.

Burger, D., 1976, Palynological Observations in the Surat Basin. Appendix 5: A Guide to the Geology of the Bowen and Surat Basins in Queensland, v. 1, pp. 51-54.

Burger, D., 1982, Palynology of the Eromanga Basin and Its Applications, *in* M. P. S and T. J. Mount, eds., Eromanga Basin Symposium Summary Papers, v. 1: Adelaide, SA, Australia, Geological Society of Australia and the Petrolem Exploration Society of Australia, p. 83-174.

Burger, D., 1984, A Palynological Review of the Jurassic Below the Injune Creek Group in the Eromanga Basin, Queensland, Bureau of Mineral Resources, Geology and Geophysics, p. 23.

Burger, D., 1986, Palynology, Cyclic Sedimentation, and Palaeoenvironments in the Late Mesozoic of the Eromanga Basin: Contributions to the geology and hydrocarbon potential of the Eromanga Basin. Geological Society of Australia, Special Publication, v. 12, p. 53-70.

Burger, D., 1994, Palynological Studies of the Bundamba Group and Walloon Coal Measures in the Clarence-Moreton Basin: Geology and petroleum potential of the Clarence-Moreton basin, New South Wales and Queensland, v. 241, p. 164-180.

Burger, D., and Senior, B. R., 1979, A Revision of the Sedimentary and Palynological History of the Northeastern Eromanga Basin, Queensland: Journal of the Geological Society of Australia, v. 26, p. 121-133.

Burger, D., Wells, A. T., and O'Brien, P. E., 1994, Palynology of the Uppermost Walloon Coal Measures, Kangaroo Creek Sandstone, and Grafton Formation, Clarence-Moreton Basin: Geology and Petroleum potential of the Clarence-Moreton basin, New South Wales and Queensland. Australian Geological Survey Organisation, Bulletin, v. 241, p. 181-188.

Bütschli, O., 1885, Dinoflagellata. Bronn's Klass. U. Ordn. D: Tier. Reichs. Protozoa. Leipzig y Heidelberg, v. 1, p. 906-1029.

Cameron, C. C., Esterle, J. S., and Palmer, C. A., 1989, The Geology, Botany and Chemistry of Selected Peat-Forming Environments from Temperate and Tropical Latitudes: International Journal of Coal Geology, v. 12, p. 105-156.

Cameron, J. B., 1970, The Rosewood-Walloon Coalfield: Geological Survey of Queensland Publication, v. 344, p. 1-42.

Cameron, W. E., 1907, The West Moreton Coal-Fields, Queensland: Geological Survey of Queensland Publication, v. 204, p. 37-45.

Campbell, H., Mortimer, N., and Turnbull, I., 2003, Murihiku Supergroup, New Zealand: Redefined: Journal of the Royal Society of New Zealand, v. 33, p. 85-95.

Campbell, M., Rosenbaum, G., Shaanan, U., Fielding, C., and Allen, C., 2015, The Tectonic Significance of Lower Permian Successions in the Texas Orocline (Eastern Australia): Australian Journal of Earth Sciences, v. 62, p. 789-806.

Cant, D. J., and Walker, R. G., 1978, Fluvial Processes and Facies Sequences in the Sandy Braided South Saskatchewan River, Canada: Sedimentology, v. 25, p. 625-648.

Cecil, C. B., 2013, An Overview and Interpretation of Autocyclic and Allocyclic Processes and the Accumulation of Strata During the Pennsylvanian-Permian Transition in the Central Appalachian Basin, USA: International Journal of Coal Geology, v. 119, p. 21-31.

Cecil, C. B., DiMichele, W. A., Fedorko, N., and Skema, V., 2011, Autocyclic and Allocyclic Controls on the Origin of the Dunkard Group: Geology of the Pennsylvanian–Permian in the Dunkard Basin, v. 1.

Césari, S. N., 2007, Palynological Biozones and Radiometric Data at the Carboniferous–Permian Boundary in Western Gondwana: Gondwana Research, v. 11, p. 529-536.

Chaffee, A. L., Lay, G., Marshall, M., Jackson, W. R., Fei, Y., Verheyen, T. V., Cassidy, P. J., and Scott, S. G., 2010, Structural Characterisation of Middle Jurassic, High-Volatile Bituminous Walloon Subgroup Coals and Correlation with the Coal Seam Gas Content: Fuel, v. 89, p. 3241-3249.

Chahud, A., Pacheco, M. L. A. F., van Enck Meira, F., Romero, G. R., and Petri, S., 2012, Paleontology and Depositional Environments of the Tatuí and

Irati Formations (Permian) in the Ponte Nova Farm, Ipeúna, State of São Paulo: Brazilian Journal of Geology, v. 42, p. 198-212.

Choi, K. S., Dalrymple, R. W., Chun, S. S., and Kim, S.-P., 2004, Sedimentology of Modern, Inclined Heterolithic Stratification (Ihs) in the Macrotidal Han River Delta, Korea: Journal of Sedimentary Research, v. 74, p. 677-689.

Chongzhi, T., Guoping, B., Junlan, L., Chao, D., Xiaoxin, L., Houwu, L., and Dapeng, W., 2013, Mesozoic Lithofacies Palaeogeography and Petroleum Prospectivity in North Carnarvon Basin, Australia: Journal of Palaeogeography, v. 1, p. 007.

Clemmensen, L. B., and Surlyk, F., 1976, Upper Jurassic Coal-Bearing Shoreline Deposits, Hochstetter Forland, East Greenland: Sedimentary Geology, v. 15, p. 193-211.

Cluzel, D., 1992, Late Palaeozoic to Early Mesozoic Geodynamic Evolution of the Circum-Pacific Orogenic Belt in South Korea and Southwest Japan: Earth and Planetary Science Letters, v. 108, p. 289-305.

Cohen, K., Finney, S., Gibbard, P., and Fan, J., 2013; updated, The Ics International Chronostratigraphic Chart: Episodes, v. 36, p. 199-204.

Cole, F., Bird, K. J., Toro, J., Roure, F., O'Sullivan, P. B., Pawlewicz, M., and Howelll, D. G., 1997, An Integrated Model for the Tectonic Development of the Frontal Brooks Range and Colville Basin 250 Km West of the Trans-Alaska Crustal Transect: Journal of Geophysical Research: Solid Earth (1978–2012), v. 102, p. 20685-20708.

Collinson, J. D., 1970, Bedforms of the Tana River, Norway: Geografiska Annaler. Series A. Physical Geography, v. 52, p. 31-56.

Colombié, C., Giraud, F., Schnyder, J., Götz, A., Boussaha, M., Aurell, M., and Bádenas, B., 2014, Timing of Sea Level, Tectonics and Climate Events During the Uppermost Oxfordian (Planula Zone) on the Iberian Ramp (Northeast Spain): Palaeogeography, Palaeoclimatology, Palaeoecology, v. 412, p. 17-31.

Condon, D. J., Schoene, R. B., McLean, N. M., Bowring, S. A., Parrish, R., and Noble, S. R., 2015, Calibration of the Earthtime 235u-233u-205pb-(202pb) Tracer for High-Precision U/Pb Geochronology: Part I, Metrology and Traceability: Geochimica et Cosmochimica Acta v. 164, p. 444-463.

References

Cookson, I. C., and Dettmann, M. E., 1958, Some Trilete Spores from Upper Mesozoic Deposits in the Eastern Australian Region: Proceedings of the Royal Society of Victoria, v. 70, p. 95-128.

Costa, A., Flores, D., Suárez-Ruiz, I., Pevida, C., Rubiera, F., and Iglesias, M., 2010, The Importance of Thermal Behaviour and Petrographic Composition for Understanding the Characteristics of a Portuguese Perhydrous Jurassic Coal: International Journal of Coal Geology, v. 84, p. 237-247.

Couper, R., 1957, British Mesozoic Microspores and Pollen Grains. A Systematic and Stratigraphic Study: Palaeontographica Abteilung B, v. 103, p. 75-179.

Cross, T., 1986, Tectonic Controls of Foreland Basin Subsidence and Laramide Style Deformation, Western United States: Special publication of the International Association of Sedimentologists, p. 15-39.

Crowley, J., Schoene, B., and Bowring, S., 2007, U-Pb Dating of Zircon in the Bishop Tuff at the Millennial Scale: Geology, v. 35, p. 1123-1126.

CSIRO, 2014, What Is Coal Seam Gas?: http://www.csiro.au/Outcomes/Energy/Energy-from-oil-and-gas/UnconventionalGas/Learn-more/What-is-coal-seam-gas.aspx. Date accessed 02/02/2014.

Dalseg, T. S., Nakrem, H. A., and Smelror, M., 2016, Dinoflagellate Cyst Biostratigraphy, Palynofacies, Depositional Environment and Sequence Stratigraphy of the Agardhfjellet Formation (Upper Jurassic–Lower Cretaceous) in Central Spitsbergen (Arctic Norway): Norwegian Journal of Geology, v. 96, p. 119-133.

Day, R. W., Prefontaine, R. F., Bubendorfer, P. A. J., Oberhardt, M. H., Pinder, B. J., Holden, D. J., and Gunness, R. A., 2006, Discovery and Development of the Kogan North and Tipton West Coal Seam Gas (Csg) Fields, Surat Basin, Southeast Queensland: APPEA Journal, v. 46, p. 191-199.

De Jersey, N., 1975, Miospore Zones in the Lower Mesozoic of Southeastern Queensland, *in* K. Campbell, ed., Gondwana Geology, v. 1: Canberra, Australia, Australian National University Press Canberra, p. 159-172.

De Jersey, N. J., and Paten, R. J., 1964, Jurassic Spores and Pollen Grains from the Surat Basin: Geological Survey of Queensland Publication v. 322, p. 1-18.

Department_of_Natural_Resources_and_Mines, 2013, Queensland's Coal Seam Gas Overview (January 2014): http://www.qca.org.au/getattachment/aaaeab4b-519f-4a95-8a65-911bc46cc1d3/CSG-investigation.aspx. Date accessed 02/05/2014.

Department_of_Natural_Resources_and_Mining, 2014, Queensland's Coal Seam Gas Overview: http://mines.industry.qld.gov.au/assets/coal-pdf/csg-update-2014.pdf. Date accessed 03/05/2015.

Department_of_State_Development, 2016, Prospectivity of the Eromanga Basin: http://petroleum.statedevelopment.sa.gov.au/prospectivity/eromanga_basin. Date accessed 03/02/2016.

Department_of_State_Development, 2017, Prospectivity of the Cooper Basin: http://petroleum.statedevelopment.sa.gov.au/prospectivity/cooper_basin. Date accessed 03/08/2016.

Dera, G., Brigaud, B., Monna, F., Laffont, R., Pucéat, E., Deconinck, J.-F., Pellenard, P., Joachimski, M. M., and Durlet, C., 2011, Climatic Ups and Downs in a Disturbed Jurassic World: Geology, v. 39, p. 215-218.

DeRito, R. F., Cozzarelli, F. A., and Hodge, D. S., 1983, Mechanism of Subsidence of Ancient Cratonic Rift Basins: Tectonophysics, v. 94, p. 141-168.

Dettmann, M. E., 1963, Upper Mesozoic Microfloras from South-Eastern Australia, v. 77: Melbourne, Australia, Royal Society of Victoria, pp. 149.

Diessel, C. F. K., 1992, The Conditions of Peat Formation, *in* C. F. K. Diessel, ed., Coal-Bearing Depositional Systems: Berlin, Germany, Springer, p. 5-39.

Dirksen, V., Dirksen, O., and Diekmann, B., 2013, Holocene Vegetation Dynamics and Climate Change in Kamchatka Peninsula, Russian Far East: Review of Palaeobotany and Palynology, v. 190, p. 48-65.

Dixon, M., Morgan, R., Goodall, J., and Van Den Berg, M., 2012, Higher-Resolution Palynostratigraphy of the Norian-Carnian (Triassic) Upper Mungaroo Formation, Offshore Carnarvon Basin: The APPEA Journal, v. 52, p. 683-683.

Donnelly, L. J., 2004, Geological Investigations at a High Altitude, Remote Coal Mine on the Northwest Pakistan and Afghanistan Frontier, Karakoram Himalaya: International Journal of Coal Geology, v. 60, p. 117-150.

References

Draper, J., 2002, Geology of the Cooper and Eromanga Basins, Queensland, v. 1, Department of Natural Resources and Mines, pp. 92.

Dulhunty, J., 1967, Mesozoic Alkaline Volcanism and Garrawilla Lavas near Mullaley, New South Wales: Journal of the Geological Society of Australia, v. 14, p. 133-138.

Dulhunty, J., 1973, Mesozoic Stratigraphy in Central Western New South Wales: Journal of the Geological Society of Australia, v. 20, p. 319-328.

Dulhunty, J., Middlemost, E., and Beck, R., 1987, Potassium–Argon Ages, Petrology and Geochemistry of Some Mesozoic Igneous Rocks in Northeastern New South Wales: Journal and Proceedings of the Royal Society of NSW, v. 120, p. 71-90.

Edwards, C. M., Howell, J. A., and Flint, S. S., 2005, Depositional and Stratigraphic Architecture of the Santonian Emery Sandstone of the Mancos Shale: Implications for Late Cretaceous Evolution of the Western Interior Foreland Basin of Central Utah, USA: Journal of Sedimentary Research, v. 75, p. 280-299.

Erdenetsogt, B.-O., Lee, I., Bat-Erdene, D., and Jargal, L., 2009, Mongolian Coal-Bearing Basins: Geological Settings, Coal Characteristics, Distribution, and Resources: International Journal of Coal Geology

v. 80, p. 87-104.

Evans, P., 1966, Mesozoic Stratigraphic Palynology in Australia: Australasian Oil and Gas Journal, v. 12, p. 58-63.

Exon, N., 1966, Revised Jurassic to Lower Cretaceous Stratigraphy in the South-East Eromanga Basin, Queensland: Queensland Government Mining Journal, v. 67, p. 232-238.

Exon, N. F., 1976, Geology of the Surat Basin in Queensland: Bulletin of the Bureau of Mineral Resources and Geophysics, Australia, v. 166, p. 57-69.

Exon, N. F., and Burger, D., 1981, Sedimentary Cycles in the Surat Basin and Global Changes of Sea Level: BMR Journal of Australian Geology & Geophysics, v. 6, p. 153-159.

References

Fassett, J. E., 1986, The Non-Transferability of a Cretaceous Coal Model in the San Juan Basin of New Mexico and Colorado: Geological Society of America Special Papers, v. 210, p. 155-172.

Fassett, J. E., and Hinds, J. S., 1971, Geology and Fuel Resources of the Fruitland Formation and Kirtland Shale of the San Juan Basin, New Mexico and Colorado: US Geological Survery, Professional Paper, v. 676, p. 76.

Fensome, R. A., Taylor, F. J. R., Norris, G., Sarjeant, W. A. S., Wharton, D. I., and Williams, G. L., 1993, A Classification of Living and Fossil Dinoflagellates: Micropaleontology Special Publication, v. 7, p. 351.

Fielding, C. R., 1987, Coal Depositional Models for Deltaic and Alluvial Plain Sequences: Geology, v. 15, p. 661-664.

Fielding, C. R., 1989, Geological Note: Hummocky Cross-Stratification from the Boxvale Sandstone Member in the Northern Surat Basin, Queensland: Australian Journal of Earth Sciences, v. 36, p. 469-471.

Fielding, C. R., 1993, The Middle Jurassic Walloon Coal Measures in the Type Area, the Rosewood-Walloon Coalfield, Se Queensland: Australian Coal Geology, v. 9, p. 1-16.

Fielding, C. R., 1996, Mesozoic Sedimentary Basins and Resources in Eastern Australia: Geological Society of Australia Abstracts, p. 180-185

Fielding, C. R., and Webb, J. A., 1996, Facies and Cyclicity of the Late Permian Bainmedart Coal Measures in the Northern Prince Charles Mountains, Macrobertson Land, Antarctica: Sedimentology, v. 43, p. 295-322.

Filatoff, J., 1975, Jurassic Palynology of the Perth Basin, Western Australia: Palaeontographica Abteilung B, v. 154, p. 1-113.

Filatoff, J., and Price, P., 1988, A Pteridacean Spore Lineage in the Australian Mesozoic, *in* J. Filatoff and P. Price, eds., Palynological and Palaeobotanical Studies in Honour of Basil E. Balme., v. 5, p. 89-124.

Firth, J. V., 1993, Dinoflagellate Assemblages and Sea-Level Fluctuations in the Maastrichtian of Southwest Georgia: Review of Palaeobotany and Palynology, v. 79, p. 179-204.

References

Firth, J. V., and Clark, D. L., 1998, An Early Maastrichtian Organic-Walled Phytoplankton Cyst Assemblage from an Organic-Rich Black Mud in Core Fl-533, Alpha Ridge: Evidence for Upwelling Conditions in the Cretaceous Arctic Ocean: Marine Micropaleontology, v. 34, p. 1-27.

Flint, S., Aitken, J., and Hampson, G., 1995, The Application of Sequence Stratigraphy to Coal-Bearing Coastal Plain Successions: Implications for the Uk Coal Measures, *in* M. Whateley and D. Spears, eds., European Coal Geology, v. 82: London, UK, Geological Society, London, Special Publications, p. 1-16.

Flores-Williams, H., 1978, Chilean, Argentine, and Bolivian Coals: Geological Society of America Special Papers, v. 179, p. 1-14.

Flores, D., 2002, Organic Facies and Depositional Palaeoenvironment of Lignites from Rio Maior Basin (Portugal): International Journal of Coal Geology, v. 48, p. 181-195.

Flores, R., Ochs, A., Bader, L., Johnson, R., and Vogler, D., 1999, Framework Geology of the Fort Union Coal in the Powder River Basin: US Geological Survey Professional Paper, v. 1625-A, p. 1-37.

Frakes, L. A., Francis, J. E., and Syktus, J. I., 2005, Climate Modes of the Phanerozoic: Cambridge, UK, Cambridge University Press, pp. 275.

Francis, J. E., 1990, Polar Fossil Forests: Geology Today, v. 6, p. 92-95.

Francis, J. E., and Poole, I., 2002, Cretaceous and Early Tertiary Climates of Antarctica: Evidence from Fossil Wood: Palaeogeography, Palaeoclimatology, Palaeoecology, v. 182, p. 47-64.

Freeze, R. A., Cherry, J. A., and JA, C., 1979, Groundwater, v. 629: Englewood Cliffs, USA, Prentice Hall Inc., pp. 617.

Gallagher, K., 1988, The Subsidence History and Thermal State of the Eromanga and Cooper Basins: PhD thesis, Australian National University, Canberra, Australia, pp. 392.

Gallagher, K., Dumitru, T. A., and Gleadow, A. J. W., 1994, Constraints on the Vertical Motion of Eastern Australia During the Mesozoic: Basin Research, v. 6, p. 77-94.

References

Gallagher, K., and Lambeck, K., 1989, Subsidence, Sedimentation and Sea-Level Changes in the Eromanga Basin, Australia: Basin Research, v. 2, p. 115-131.

Gallagher, S., Wood, G., and Lemon, N., 2008, Birkhead Formation Chronostratigraphy on the Murteree Horst, South Australia: Identifying and Correlating Reservoirs and Seals: PESA Eastern Australasian Basins Symposium III, Sydney, p. 14-17

Garrison Jr, J. R., and Van den Bergh, T., 2006, Effects of Sedimentation Rate, Rate of Relative Rise in Sea Level, and Duration of Sea-Level Cycle on the Filling of Incised Valleys: Examples of Filled and Overfilled Incised Valleys from the Upper Ferron Sandstone, Last Chance Delta, East-Central Utah, *in* R. W. Dalrymple, D. Leckie and R. Tillman, eds., Incised Valleys in Time and Space: Sepm Special Publication, v. 85: Tulsa, Oklahoma, SEPM, p. 239-279.

Gatehouse, C. G., 1986, The Geology of the Warburton Basin in South Australia: Australian Journal of Earth Sciences, v. 33, p. 161-180.

Geoscience_Australia, 2014, Australian Stratigraphic Units Database: http://dbforms.ga.gov.au/pls/www/geodx.strat_units.sch_full?wher=stratno=19303. Date.

Geoscience_Australia, 2016, Australian Stratigraphic Units Database: http://dbforms.ga.gov.au/pls/www/geodx.strat_units.sch_full?wher=stratno=19303. Date accessed 05/07/2016.

Gerstenberger, H., and Haase, G., 1997, A Highly Effective Emitter Substance for Mass Spectrometric Pb Isotope Ratio Determinations: Chemical Geology, v. 136, p. 309-312.

Gibson, D. W., 1985, Stratigraphy, Sedimentology, and Depositional Environments of the Coal-Bearing Jurassic-Cretaceous Kootenay Group, Alberta and British Columbia, v. 357, Geological Survey of Canada Bulletin, pp. 108.

Gies, T. F., 1972, Palynology of Sediments Bordering Some Upper Cretaceous Strand Lines in Northwestern Colorado: PhD thesis, Michigan State University, East Lansing, Michigan, pp. 355.

Gleadow, A. W., 1990, Apatite Fission Track Thermochronology and Tectonics in the Clarence-Moreton Basin of Eastern Australia: International Journal of Radiation Applications and Instrumentation. Part D. Nuclear Tracks and Radiation Measurements, v. 17, p. 413-414.

Gore, A. J. P., 1983, Ecosystems of the World 4b. Mire: Swamp, Bog, Fen, and Moor. Regional Studies.: Amsterdam, The Netherlands, Elsevier Scientific Publishing Company., pp. 478.

Goscombe, P., and Coxhead, B., 1995, Clarence-Moreton, Surat, Eromanga, Nambour, and Mulgildie Basins: Geology of Australian Coal Basins, v. 1, p. 489-511.

Götz, A. E., Ruckwied, K., and Barbacka, M., 2011, Palaeoenvironment of the Late Triassic (Rhaetian) and Early Jurassic (Hettangian) Mecsek Coal Formation (South Hungary): Implications from Macro-and Microfloral Assemblages: Palaeobiodiversity and Palaeoenvironments, v. 91, p. 75-88.

Gould, R. E., 1974, The Fossil Flora of the Walloon Coal Measures: A Survey: Proceedings of the Royal Society of Queensland, v. 85, p. 33-4.

Gradstein, F. M., Ogg, J. G., Schmitz, M., and Ogg, G., 2012, The Geologic Time Scale 2012 v. 2: Stuttgart, Germany, Elsevier, pp. 1176.

Gravestock, D., 1982, Jurassic to Lower Cretaceous Stratigraphy of the Eromanga Basin, South Australia–Problems and Progress in Subsurface Correlation: Eromanga Basin Symposium p. 79-91

Gravestock, D., Hibburt, J., and Drexel, J., 1998, The Petroleum Geology of South Australia. Vol. 4: Cooper Basin: South Australia. Department of Primary Industries and Resources. Report Book, 98, v. 9: Adelaide, Australia, PIRSA, pp. 98.

Greb, S. F., DiMichele, W. A., and Gastaldo, R. A., 2006, Evolution and Importance of Wetlands in Earth History: Geological Society of America Special Papers, v. 399, p. 1-40.

Green, P., 2009, The Surat and Bowen Basin, South-East Queensland: Brisbane, Australia, Queensland Department of Mines and Energy, pp. 238.

Green, P., Carmichael, D., Brain, T., Murray, C., McKellar, J., Beeston, J., Gray, A., and Green, P., 1997a, Lithostratigraphic Units in the Bowen and Surat Basins, Queensland: In Green, P.M. (ed) The Surat and Bowen Basins, southeast Queensland. Queensland Minerals and Energy Review Series, Queensland Department of Mines and Energy, p. 41-108.

References

Green, P., Hoffmann, K., Brian, T., Gray, A., Murray, C., Carmichael, D., McKeller, J., Beeston, J., Price, P., and Smith, M., 1997, The Surat and Bowen Basins, South-East Queensland: Queensland Minerals and Energy Review Series, Queensland Department of Mines and Energy, p. 238.

Greenwood, D. R., and Basinger, J. F., 1994, The Paleoecology of High-Latitude Eocene Swamp Forests from Axel Heiberg Island, Canadian High Arctic: Review of Palaeobotany and Palynology, v. 81, p. 83-97.

Gumbricht, T., McCarthy, T., and Merry, C. L., 2001, The Topography of the Okavango Delta, Botswana, and Its Tectonic and Sedimentological Implications: South African Journal of Geology, v. 104, p. 243-264.

Hall, R. L., 1989, Lower Bajocian Ammonites (Middle Jurassic; Soninniidae) from the Newmarracarra Limestone, Western Australia: Alcheringa, v. 13, p. 1-20.

Hallam, A., 1982, The Jurassic Climate, Climate in Earth History. Studies in Geophysics, National Academy Press Oxford, p. 159-163.

Hallam, A., 1985, A Review of Mesozoic Climates: Journal of the Geological Society, v. 142, p. 433-445.

Hallam, A., 2001, A Review of the Broad Pattern of Jurassic Sea-Level Changes and Their Possible Causes in the Light of Current Knowledge: Palaeogeography, Palaeoclimatology, Palaeoecology, v. 167, p. 23-37.

Hamawand, I., Yusaf, T., and Hamawand, S. G., 2013, Coal Seam Gas and Associated Water: A Review Paper: Renewable and Sustainable Energy Reviews, v. 22, p. 550-560.

Hamilton, D. S., and Tadros, N., 1994, Utility of Coal Seams as Genetic Stratigraphic Sequence Boundaries in Nonmarine Basins: An Example from the Gunnedah Basin, Australia: AAPG Bulletin, v. 78, p. 267-286.

Hamilton, S., Esterle, J., and Sliwa, R., 2014b, Stratigraphic and Depositional Framework of the Walloon Subgroup, Eastern Surat Basin, Queensland: Australian Journal of Earth Sciences, v. 8, p. 1061-1080.

Hamilton, S. K., Esterle, J. S., and Golding, S. D., 2012, Geological Interpretation of Gas Content Trends, Walloon Subgroup, Eastern Surat Basin, Queensland, Australia: International Journal of Coal Geology, v. 101, p. 21-35.

Hamilton, S. K., Golding, S. D., Baublys, K. A., and Esterle, J. S., 2014a, Stable Isotopic and Molecular Composition of Desorbed Coal Seam Gases from the Walloon Subgroup, Eastern Surat Basin, Australia: International Journal of Coal Geology, v. 122, p. 21-36.

Hampson, G., Davies, S., Elliott, T., Flint, S., and Stollhofen, H., 1999, Incised Valley Fill Sandstone Bodies in Upper Carboniferous Fluvio–Deltaic Strata: Recognition and Reservoir Characterization of Southern North Sea Analogues, Geological Society, London, Petroleum Geology Conference Series, v. 5: London, UK, Geological Society of London, p. 771-788.

Hannaford, C., and MacPhail, M., 2011, Palynology of Bellevue 1/1r, Berwyndale 2/2r, Berwyndale South 10, Codie 1a, Jen 1 and Jordan 3, Perth, Morgan Goodall Palaeo p. 1-26.

Haq, B. U., 2018, Jurassic Sea-Level Variations: A Reappraisal: GSA Today, v. 28.

Haq, B. U., Hardenbol, J., and Vail, P. R., 1987, Chronology of Fluctuating Sea Levels since the Triassic: Science, v. 235, p. 1156-1167.

Haq, B. U., Hardenbol, J., and Vail, P. R., 1988, Mesozoic and Cenozoic Chronostratigraphy and Cycles of Sea-Level Change, *in* C. Wilgis, B. Hastings, C. Kendal, H. W. Posamentier, A. Ross and J. Van Wagoner, eds., Sepm Speical Publication, v. 42, p. 71-108.

Harding, I., and Allen, R., 1995, Dinocysts and the Palaeoenvironmental Interpretation of Non-Marine Sediments: An Example from the Wealden of the Isle of Wight (Lower Cretaceous, Southern England): Cretaceous Research, v. 16, p. 727-743.

Hatch, J. R., and Affolter, R. H., 2002, Resource Assessment of the Springfield, Herrin, Danville, and Baker Coals in the Illinois Basin: U.S. Geological Survey Professional Paper, v. 1625-D, p. 425.

Hathway, B., Duane, A., Cantrill, D., and Kelley, S., 1999, 40ar/39ar Geochronology and Palynology of the Cerro Negro Formation, South Shetland Islands, Antarctica: A New Radiometric Tie for Cretaceous Terrestrial Biostratigraphy in the Southern Hemisphere: Australian Journal of Earth Sciences, v. 46, p. 593-606.

References

Helby, R., Morgan, R., and Partridge, A., 1987, A Palynological Zonation of the Australian Mesozoic: Memoir of the Association of Australasian Palaeontologists, v. 4, p. 1-94.

Hendrix, M. S., Brassell, S. C., Carroll, A. R., and Graham, S. A., 1995, Sedimentology, Organic Geochemistry, and Petroleum Potential of Jurassic Coal Measures: Tarim, Junggar, and Turpan Basins, Northwest China: AAPG Bulletin, v. 79, p. 929-958.

Hentschel, A., Esterle, J., Golding, S., and Pacey, D., 2016, Petrologic and Stable Isotopic Study of the Walloon Coal Measures, Surat Basin, Queensland: Peat Accumulation under Changing Climate and Base Level: International Journal of Coal Geology, v. 160-161, p. 11-27.

Hill, P. J., 1994, Geology and Geophysics of the Offshore Maryborough, Capricorn and Northern Tasman Basins: Results of Agso Survey 91, v. 1, Australian Geological Survey Organisation.

Hoffmann, K. L., Totterdell, J. M., Dixon, O., Simpson, G. A., Brakel, A. T., Wells, A. T., and McKellar, J. L., 2009, Sequence Stratigraphy of Jurassic Strata in the Lower Surat Basin Succession, Queensland: Australian Journal of Earth Sciences, v. 56, p. 461-476.

Holcombe, R., Stephens, C., Fielding, C., Gust, D., Little, T., Sliwa, R., Kassan, J., McPhie, J., and Ewart, A., 1997, Tectonic Evolution of the Northern New England Fold Belt: The Permian–Triassic Hunter–Bowen Event: Tectonics and Metallogenesis of the New England Orogen, v. 19, p. 52-65.

Holz, M., Kalkreuth, W., and Banerjee, I., 2002, Sequence Stratigraphy of Paralic Coal-Bearing Strata: An Overview: International Journal of Coal Geology, v. 48, p. 147-179.

Hotes, S., Poschlod, P., and Takahashi, H., 2006, Effects of Volcanic Activity on Mire Development: Case Studies from Hokkaido, Northern Japan: The Holocene, v. 16, p. 561-573.

Hudson, J., 1964, The Petrology of the Sandstones of the Great Estuarine Series, and the Jurassic Palaeogeography of Scotland: Proceedings of the Geologists' Association, v. 75, p. 499-IN2.

Hunter, M. A., Cantrill, D. J., Flowerdew, M. J., and Millar, I. L., 2005, Mid-Jurassic Age for the Botany Bay Group: Implications for Weddell Sea Basin Creation and Southern Hemisphere Biostratigraphy: Journal of the Geological Society, v. 162, p. 745-748.

Jackson, R. G., 1975, Velocity–Bed-Form–Texture Patterns of Meander Bends in the Lower Wabash River of Illinois and Indiana: Geological Society of America Bulletin, v. 86, p. 1511-1522.

Jaffey, A., Flynn, K., Glendenin, L., Bentley, W., and Essling, A., 1971, Precision Measurement of Half-Lives and Specific Activities of U 235 and U 238: Physical Review C, v. 4, p. 1889.

Jameossanaie, A., 1987, Palynology and Age of South Hospah Coal-Bearing Deposits, Mckinley County, New Mexico: New Mexico Bureau of Mines & Mineral Resources Bulletin, v. 112, p. 1-64.

Jansson, I., McLoughlin, S., Vajda, V., and Pole, M., 2008, An Early Jurassic Flora from the Clarence-Moreton Basin, Australia: Review of Palaeobotany and Palynology, v. 150, p. 5-21.

Jell, P. A., 2013, Geology of Queensland / Edited by Peter a Jell: Brisbane, Geological Survey of Queensland, pp. 599.

Jensen, H., 1921, The Geology of the Country North of Roma: Queensland Government Mining Journal, v. 22, p. 92-93.

Jerrett, R., Davies, R., Hodgson, D., Flint, S., and Chiverrell, R., 2011a, The Significance of Hiatal Surfaces in Coal Seams: Journal of the Geological Society, v. 168, p. 629-632.

Jerrett, R. M., Flint, S. S., Davies, R. C., and Hodgson, D. M., 2011b, Sequence Stratigraphic Interpretation of a Pennsylvanian (Upper Carboniferous) Coal from the Central Appalachian Basin, USA: Sedimentology, v. 58, p. 1180-1207.

Jones, A. T., and Fielding, C. R., 2008, Sedimentary Facies of a Glacially Influenced Continental Succession in the Pennsylvanian Jericho Formation, Galilee Basin, Australia: Sedimentology, v. 55, p. 531-556.

Jones, C. E., and Jenkyns, H. C., 2001, Seawater Strontium Isotopes, Oceanic Anoxic Events, and Seafloor Hydrothermal Activity in the Jurassic and Cretaceous: American Journal of Science, v. 301, p. 112-149.

Jones, G., and Patrick, R., 1981, Stratigraphy and Coal Exploration Geology of the Northeastern Surat Basin: Coal Geology, v. 1, p. 153-163.

References

Keeley, M., 1994, Phanerozoic Evolution of the Basins of Northern Egypt and Adjacent Areas: Geologische Rundschau, v. 83, p. 728-742.

Khorasani, G. K., 1987, Oil-Prone Coals of the Walloon Coal Measures, Surat Basin, Australia, *in* A. C. Scott, ed., Coal and Coal-Bearing Strata: Recent Advances, v. 32: London, UK, Geological Society, London, Special Publications, p. 303-310.

Kirillova, G., 2005, The Late Mesozoic-Cenozoic Sedimentary Basins at the Continental Margin of Southeastern Russia: Geodynamic Evolution and Coal and Petroleum Potential: Geotectonics, v. 39, p. 389-407.

Kirschbaum, M. A., Roberts, L. N. R., and Biewick, L. H., 2000, Geologic Assessment of Coal in the Colorado Plateau: Arizona, Colorado, New Mexico, and Utah: U.S. Geological Survey Professional Paper, v. 1625-B, p. 321.

Klemme, H., and Ulmishek, G. F., 1991, Effective Petroleum Source Rocks of the World: Stratigraphic Distribution and Controlling Depositional Factors (1): AAPG Bulletin, v. 75, p. 1809-1851.

Klootwijk, C., 1996, Phanerozoic Configurations of Greater Australia: Evolution of the North West Shelf, v. 53: Canberra, Australian Geological Survey Organisation, pp. 148.

Klootwijk, C., 2009, Sedimentary Basins of Eastern Australia: Paleomagnetic Constraints on Geodynamic Evolution in a Global Context: Australian Journal of Earth Sciences, v. 56, p. 273-308.

Kojima, S., Sweda, T., LePage, B. A., and Basinger, J. F., 1998, A New Method to Estimate Accumulation Rates of Lignites in the Eocene Buchanan Lake Formation, Canadian Arctic: Palaeogeography, Palaeoclimatology, Palaeoecology, v. 141, p. 115-122.

Korsch, R., O'Brien, P., Sexton, M., Wake-Dyster, K., and Wells, A., 1989, Development of Mesozoic Transtensional Basins in Easternmost Australia: Journal of the Geological Society of Australia, v. 36, p. 13-28.

Korsch, R. J., and Totterdell, J. M., 2009a, Evolution of the Bowen, Gunnedah and Surat Basins, Eastern Australia: Australian Journal of Earth Sciences, v. 56, p. 271-272.

Korsch, R. J., and Totterdell, J. M., 2009b, Subsidence History and Basin Phases of the Bowen, Gunnedah and Surat Basins, Eastern Australia: Australian Journal of Earth Sciences, v. 56, p. 335-353.

Krieg, G., Alexander, E., and Rogers, P., 1995, Eromanga Basin: The Geology of South Australia, v. 2, p. 101-127.

Kristensen, S., Ward, C., Harrington, H., Mallett, C., and Beeston, J., 1995, Perth Basin: Geology of Australian Coal Basins, p. 387-394.

Krogh, T., 1973, A Low-Contamination Method for Hydrothermal Decomposition of Zircon and Extraction of U and Pb for Isotopic Age Determinations: Geochimica et Cosmochimica Acta, v. 37, p. 485-494.

Kvale, E. P., and Barnhill, M. L., 1994, Evolution of Lower Pennsylvanian Estuarine Facies within Two Adjacent Paleovalleys, Illinois Basin, Indiana, *in* R. Boyd, R. W. Dalrymple and B. A. Zaitlin, eds., Incised-Valley Systems: Origin and Sedimentary Sequences. Sepm, v. 51, p. 191-207.

Land, D. H., and Jones, C. M., 1987, Coal Geology and Exploration of Part of the Tertiary Kutei Basin in East Kalimantan, Indonesia, *in* A. C. Scott, ed., Oal and Coal Bearing Strata: Recent Advances, v. 32: London, UK, Geological Society, London, Special Publications, p. 235-255.

Lanzilli, E., 2000, A Sequence Stratigraphic Approach to Reservoir Characterisation of the Birkhead Formation, Gidgealpa South Dome, Eromanga Basin, Australia: 2000 AAPG International Conference & Exhibition

Laurie, J. R., Bodorkos, S., Smith, T. E., Crowley, J., and Nicoll, R. S., 2015, The Ca-Idtims Method and the Calibration of Endemic Australian Palynostratigraphy to the Geological Timescale: International Conference & Exhibition. http://www.searchanddiscovery.com/pdfz/documents/2015/51207laurie/ndx_laurie.pdf.html.

Laurie, J. R., Bordorkos, S., Nicoll, B., Crowley, J., Mantle, D., Mory, A. J., Wood, G., Backhouse, J., Holmes, E. K., Smith, T. E., and Champion, D. C., 2016, Calibrating the Middle and Late Permian Palynostratigraphy of Australia to the Geologic Time-Scale Via U-Pb Zircon Ca-Idtims Dating: Australian Journal of Earth Sciences, v. 64, p. 1-30.

Leeder, M., 1973, Fluviatile Fining-Upwards Cycles and the Magnitude of Palaeochannels: Geological Magazine, v. 110, p. 265-276.

Li, Z., and Powell, C. M., 2001, An Outline of the Palaeogeographic Evolution of the Australasian Region since the Beginning of the Neoproterozoic: Earth-Science Reviews, v. 53, p. 237-277.

Lipski, P., Hill, K., and Bernecker, T., 2001, Geology and Hydrocarbon Potential of the Jurassic–Cretaceous Maryborough Basin: Eastern Australasian Basins Symposium: a refocussed energy perspective for the future, Hill, KC and Bernecker, T., eds. Petroleum Exploration Society of Australia Special Publication, p. 263-268

Logares, R., Shalchian-Tabrizi, K., Boltovskoy, A., and Rengefors, K., 2007, Extensive Dinoflagellate Phylogenies Indicate Infrequent Marine–Freshwater Transitions: Molecular phylogenetics and evolution, v. 45, p. 887-903.

Loisel, J., Gallego-Sala, A., and Yu, Z., 2012, Global-Scale Pattern of Peatland Sphagnum Growth Driven by Photosynthetically Active Radiation and Growing Season Length: Biogeosciences, v. 9, p. 2737-2746.

Ludwig, K. R., 2003, User's Manual for Isoplot 3.00: A Geochronological Toolkit for Microsoft Excel: Berkeley Geochronology Center Special Publication No. 1a, p. 1-53.

Macdonald, D. I., and Francis, J. E., 1992, The Potential for Cretaceous Coal in Antarctica: Geological Society of America Special Papers, v. 267, p. 385-396.

Mallett, C., Pattison, C., McLennan, T., Balfe, P., and Sullivan, D., 1995, Bowen Basin: Geology of Australian Coal Basins, v. 1, p. 299-339.

Mao, S.-z., Wan, C.-b., and Qiao, X.-y., 1999, Cretaceous Nonmarine Dinoflagellates from Northeast China: Grana, v. 38, p. 144-161.

Marshall, N. G., 1989, An Unusual Assemblage of Algal Cysts from the Late Cretaceous of the Gippsland Basin, Southeastern Australia: Palynology, v. 13, p. 21-56.

Martin, A., and Saxby, J., 1982, Geology, Source Rocks and Hydrocarbon Generation in the Clarence-Moreton Basin: APEA Journal, v. 22, p. 5-16.

Martin, M. A., Wakefield, M., MacPhail, M. K., Pearce, T., and Edwards, H. E., 2013, Sedimentology and Stratigraphy of an Intra-Cratonic Basin Coal Seam Gas Play: Walloon Subgroup of the Surat Basin, Eastern Australia: Petroleum Geoscience, v. 19, p. 21-38.

Matthews, K. J., Hale, A. J., Gurnis, M., Müller, R. D., and DiCaprio, L., 2011, Dynamic Subsidence of Eastern Australia During the Cretaceous: Gondwana Research, v. 19, p. 372-383.

Mattinson, J. M., 2005, Zircon U–Pb Chemical Abrasion ("Ca-Tims") Method: Combined Annealing and Multi-Step Partial Dissolution Analysis for Improved Precision and Accuracy of Zircon Ages: Chemical Geology, v. 220, p. 47-66.

Mavromatidis, A., 2008, Two Layer Model of Lithospheric Compression and Uplift/Exhumation in an Intracratonic Setting: An Example from the Cooper-Eromanga Basins, Australia: International Journal of Earth Sciences, v. 97, p. 623-634.

McCabe, P., 2012, Distribution of Organic-Rich Sediments through the Phanerozoic, AAPG ICE & Exhibition, Singapore.

McCabe, P. J., 1984, Depositional Environments of Coal and Coal Bearing Strata, *in* R. Rahmani and R. Flores, eds., Sedimentology of Coal and Coal-Bearing Sequences, v. 7: Hoboken, New Jersey, International Association of Sedimentologists, p. 13-42.

McCabe, P. J., 1987, Facies Studies of Coal and Coal-Bearing Strata, *in* A. C. Scott, ed., Coal and Coal-Bearing Strata: Recent Advances, v. 32: London, UK, Geological Society of London, p. 51-66.

McCabe, P. J., 1991, Tectonic Controls on Coal Accumulation: Bulletin de la Société Géologique de France, v. 162, p. 277-282.

McCabe, P. J., and Parrish, J. T., 1992, Tectonic and Climatic Controls on the Distribution and Quality of Cretaceous Coals: Controls on the Distribution and Quality of Cretaceous Coals: Geological Society of America, Special Paper, v. 267, p. 1-15.

McCabe, P. J., and Shanley, K. W., 1992, Organic Control on Shoreface Stacking Patterns: Bogged Down in the Mire: Geology, v. 20, p. 741-744.

McCarthy, T., and Ellery, W., 1998, The Okavango Delta: Transactions of the Royal Society of South Africa, v. 53, p. 157-182.

McCarthy, T., and Tooth, S., 2004, Controls on the Transition from Meandering to Straight Channels in the Wetlands of the Okavango Delta, Botswana: Earth

Surface Processes and Landforms: The Journal of the British Geomorphological Research Group, p. 1627-1650.

McDonald, A., 2005, Effects of Coal Maceral Composition on Gas Content of the Walloon Coal Measures, Tipton West Area, Surat Basin, Queensland: Honours thesis, University of Queensland, Brisbane, Australia, pp. 215.

McKellar, J., 1974, Jurassic Miospores from the Upper Evergreen Formation, Hutton Sandstone, and Basal Injune Creek Group, North-Eastern Surat Basin. Geological Survey of Queensland. Publication 361: Palaeontological Paper, v. 35, p. 89.

McKellar, J., 1982, Late Triassic ('Rhaetian') and the Jurassic Palynostratigraphy of the Surat Basin: Eromanga Basin Symposium Summary Papers, p. 172-173.

McKellar, J., 1993, Stratigraphic Relationships in the Nambour Basin, Southeastern Queensland: Queensland Government Mining Journal, v. 5, p. 2-17.

McKellar, J., 2004, Geophysical Controls on Late Palaeozoic-Early Mesozoic Geological History and Floral Succession: Eastern Australia in Perspective: Memoir-Association of Australian Palaeotologists v. 29, p. 47-84.

McKellar, J. L., 1998, Late Early to Late Jurassic Palynology, Biostratigraphy and Palaeogeography of the Roma Shelf Area, Northwest Surat Basin, Queensland, Australia: PhD thesis, University of Queensland, Brisbane, Australia, pp. 620.

McLean, N. M., Condon, D. J., Schoene, R. B., and Bowring, S. A., 2015, Calibration of the Earthtime 235u-233u-205pb-(202pb) Tracer for High-Precision U/Pb Geochronology: Part Ii, Evaluating Analytical and Systematic Uncertainties: Geochimica et Cosmochimica Acta, v. 164, p. 481-501.

Metcalfe, I., Crowley, J., Nicoll, R., and Schmitz, M., 2015, High-Precision U-Pb Ca-Tims Calibration of Middle Permian to Lower Triassic Sequences, Mass Extinction and Extreme Climate-Change in Eastern Australian Gondwana: Gondwana Research, v. 28, p. 61-81.

Metcalfe, I., Nicoll, R., Crowley, J., Ives, M., Mantle, D., Ruming, K., Huyskens, M., and Foster, C., 2011, New Middle Permian-Early Triassic U-Pb Zircon Ca-Idtims Isotopic Ages of Tuffs in the Sydney Basin, Australia: International Calibration of Stratigraphy and Biostratigraphy: Programme & Abstracts. The

XVII International Congress on the Carboniferous and Permian, Perth, 3–8 July 2011, p. 92

Miao, F., Qian, L., and Zhang, X., 1989, Peat-Forming Materials and Evolution of Swamp Sequences—Case Analysis of a Jurassic Inland Coal Basin in China: International Journal of Coal Geology, v. 12, p. 733-765.

Michaelsen, B. H., 2002, Geochemical Perspectives on the Petroleum Habitat of the Cooper and Eromanga Basins, Central Australia: PhD thesis, The University of Adelaide, Adelaide, Australia, pp. 58.

Michaelsen, P., and Henderson, R. A., 2000, Facies Relationships and Cyclicity of High-Latitude, Late Permian Coal Measures, Bowen Basin, Australia: International Journal of Coal Geology, v. 44, p. 19-48.

Mitchell, M., Duddy, I., and O'sullivan, P., 1997, Reappraisal of the Age and Origin of the Casterton Formation, Western Otway Basin, Victoria: Australian Journal of Earth Sciences, v. 44, p. 819-830.

Moore, G. T., Hayashida, D. N., Ross, C. A., and Jacobson, S. R., 1992, Paleoclimate of the Kimmeridgian/Tithonian (Late Jurassic) World: I. Results Using a General Circulation Model: Palaeogeography, Palaeoclimatology, Palaeoecology, v. 93, p. 113-150.

Moore, P. D., 1995, Biological Processes Controlling the Development of Modern Peat-Forming Ecosystems: International Journal of Coal Geology, v. 28, p. 99-110.

Moore, R. C., 1964, Paleoecological Aspects of Kansas Pennsylvanian and Permian Cyclothems: Symposium on Cyclic Sedimentation: Kansas Geological Survey Bulletin, p. 287-380

Morgan, R., 1975, Some Early Cretaceous Organic-Walled Microplankton from the Great Australian Basin, Australia: Journal and Proceedings of the Royal Society of NSW, p. 157-167

Morón-Polanco, S. E., 2016, Understanding the Origin and Controls on the Development of Anabranching Rivers: PhD thesis, The University of Adelaide, Adelaide, Australia, pp. 256.

Morozova, G. S., and Smith, N. D., 2000, Holocene Avulsion Styles and Sedimentation Patterns of the Saskatchewan River, Cumberland Marshes, Canada: Sedimentary Geology, v. 130, p. 81-105.

Morris, J. R., and Martin, M. A., 2016, Coal Architecture, High-Resolution Correlation and Connectivity: New Insights from the Walloon Subgroup in the Surat Basin of Se Queensland, Australia: Petroleum Geoscience, v. 23, p. 251-261.

Mortimer, N., Turnbull, R., Palin, J., Tulloch, A., Rollet, N., and Hashimoto, T., 2015, Triassic–Jurassic Granites on the Lord Howe Rise, Northern Zealandia: Australian Journal of Earth Sciences, v. 62, p. 735-742.

Nádor, A., and Sztanó, O., 2010, Lateral and Vertical Variability of Channel Belt Stacking Density as a Function of Subsidence and Sediment Supply: Field Evidence from the Intramountaine Körös Basin, Hungary, *in* S. Davidson, S. Leleu and C. North, eds., From River to Rock Record, Sepm Special Publication, v. 97: Tulsa, Oklahoma, SEPM, p. 375-392.

Nanson, G. C., and Knighton, A. D., 1996, Anabranching Rivers: Their Cause, Character and Classification: Earth Surface Processes and Landforms, v. 21, p. 217-239.

Newman, J., and Newman, N., 1992, Tectonic and Paleoenvironmental Controls on the Distribution and Properties of Upper Cretaceous Coals on the West Coast of the South Island, New Zealand: Geological Society of America Special Papers, v. 267, p. 347-368.

Nichols, D. J., 2005, Palynology in Coal Systems Analysis—the Key to Floras, Climate, and Stratigraphy of Coal-Forming Environments: Geological Society of America Special Papers, v. 387, p. 51-58.

Nichols, G. J., and Fisher, J. A., 2007, Processes, Facies and Architecture of Fluvial Distributary System Deposits: Sedimentary Geology, v. 195, p. 75-90.

Nicoll, R. S., Laurie, J. R., Bodorkos, S., Crowley, J., and Smith, T. E., 2015, The Impact of Ca-Idtims on the Understanding of Permian and Triassic Lithostratigraphy and Correlation in Eastern Australian Coal Basins: International Conference & Exhibition. http://www.searchanddiscovery.com/pdfz/documents/2015/51209nicoll/ndx_nicoll.pdf.html.

Nielsen, L. H., Petersen, H. I., Dybkjær, K., and Surlyk, F., 2010, Lake-Mire Deposition, Earthquakes and Wildfires Along a Basin Margin Fault; Rønne Graben, Middle Jurassic, Denmark: Palaeogeography, Palaeoclimatology, Palaeoecology, v. 292, p. 103-126.

Nio, S.-D., and Yang, C.-S., 1991, Diagnostic Attributes of Clastic Tidal Deposits: A Review, *in* D. Smith, B. Reinson, B. A. Zaitlin and R. Rahmani, eds., Clastic Tidal Sedimentology, v. 16, p. 3-28.

O'Brien, P., Korsch, R., Wells, A., Sexton, M., and Wake-Dyster, K., 1994, Structure and Tectonics of the Clarence-Moreton Basin, *in* A. T. Wells and P. O'Brian, eds., Geology and Petroleum Potential of the Clarence-Moreton Basin, New South Wales and Queensland, v. 241, AGSO, p. 195-216.

Oberhardt, M. H., 2008, Well Completion Report Stratheden 4 Atp790p, Brisbane, Arrow Energy Ltd, p. 1-53.

Ogg, J., Hinnov, L., and Huang, C., 2012, Chapter 26—Jurassic, *in* F. Gradstein, J. G. Ogg, M. Schmitz and G. Ogg, eds., The Geologic Time Scale, v. 2 volume-set: Amsterdam, Netherlands, Elsevier, p. 731-791.

Ogg, J. G., Ogg, G., and Gradstein, F. M., 2016, A Concise Geologic Time Scale: 2016: Amsterdam, Netherlands, Elsevier, pp. 234.

Ojeda-Rivera, J., 1978, Main Coal Regions of Mexico: Geological Society of America Special Papers, v. 179, p. 73-84.

Opluštil, S., Edress, N. A., and Sýkorová, I., 2013, Climatic Vs. Tectonic Controls on Peat Accretion in Non-Marine Setting; an Example from the Žacléř Formation (Yeadonian–Bolsovian) in the Intra-Sudetic Basin (Czech Republic): International Journal of Coal Geology, v. 116, p. 135-157.

Osborne, M., 1990, The Exploration and Appraisal History of the Skua Field: AC/P2-Timor Sea: APPEA Journal (Australian Petroleum Production and Exploration Association), v. 30, p. 197-211.

Owen, A., Ebinghaus, A., Hartley, A. J., Santos, M. G., and Weissmann, G. S., 2017, Multi-Scale Classification of Fluvial Architecture: An Example from the Palaeocene–Eocene Bighorn Basin, Wyoming: Sedimentology, v. 64, p. 1572-1596.

Pacey, D., 2011, An Investigation of the Macroscopic and Microscopic Vertical Trends, Characteristics and Cyclicity in the Jurassic Age Walloon Coals, Surat Basin, Queensland: Bachelors thesis, University of Queensland, Brisbane, pp. 100.

Papendick, S. L., Downs, K. R., Vo, K. D., Hamilton, S. K., Dawson, G. K. W., Golding, S. D., and Gilcrease, P. C., 2011, Biogenic Methane Potential for

Surat Basin, Queensland Coal Seams: International Journal of Coal Geology, v. 88, p. 123-134.

Parrish, J. T., and Barron, E. J., 1986, Paleoclimates and Economic Geology, Tulsa, Oklahoma, SEPM Short Course, p. 1-162.

Parrish, J. T., Ziegler, A., and Scotese, C. R., 1982, Rainfall Patterns and the Distribution of Coals and Evaporites in the Mesozoic and Cenozoic: Palaeogeography, Palaeoclimatology, Palaeoecology, v. 40, p. 67-101.

Pascher, A., 1914, Über Flagellaten Und Algen: Deutsche Botanische Gesellschaft, v. 32, p. 60-136.

Paton, I., 1986, The Birkhead Formation-a Jurassic Petroleum Reservoir, *in* P. S. Moore and T. J. Mount, eds., Contributions to the Geology and Hydrocarbon Potential of the Eromanga Basin: Geological Society of Australia Special Publication: Adelaide, Australia, Geological Society of Australia and Petroleum Exploration Society of Australia, p. 195-201.

Perlmutter, M. A., and Matthews, M. D., 1992, Global Cyclostratigraphy: A Model, *in* T. A. Cross, ed., Quantitative Dynamic Straitgraphy: Englewood Cliffs, Prentice Hall, p. 102-155.

Petersen, H., and Andsbjerg, J., 1996, Organic Facies Development within Middle Jurassic Coal Seams, Danish Central Graben, and Evidence for Relative Sea-Level Control on Peat Accumulation in a Coastal Plain Environment: Sedimentary Geology, v. 106, p. 259-277.

Petersen, H., Bojesen-Koefoed, J., Nytoft, H., Surlyk, F., Therkelsen, J., and Vosgerau, H., 1998, Relative Sea-Level Changes Recorded by Paralic Liptinite-Enriched Coal Facies Cycles, Middle Jurassic Muslingebjerg Formation, Hochstetter Forland, Northeast Greenland: International journal of coal geology, v. 36, p. 1-30.

Phipps, D., and Playford, G., 1984, Laboratory Techniques for Extraction of Palynomorphs from Sediments: Papers of the Department of Geology, University of Queensland, v. 11, p. 23.

Piasecki, S., 1984, Dinoflagellate Cyst Stratigraphy of the Lower Cretaceous Jydegård Formation, Bornholm, Denmark: Bulletin of the Geological Society of Denmark, v. 32, p. 145-161.

References

Pinder, B. J., 2004, Coal Seam Gas Prospectivity of the Ipswich and Clarence-Moreton Basins: In Boult, P.J., Johns, P.R., & Lang, S.C. (eds) PESA Eastern Australian Basins Symposium II, p. 339-344.

Pinder, B. J., 2005, Well Completion Report: Kalbar-1 (Atp 641p), Arrow Energy N.L., p. 1-29.

Pitman, J. K., Franczyk, K. J., and Anders, D. E., 1987, Marine and Nonmarine Gas-Bearing Rocks in Upper Cretaceous Blackhawk and Neslen Formations, Eastern Uinta Basin, Utah: Sedimentology, Diagenesis, and Source Rock Potential: AAPG Bulletin, v. 71, p. 76-94.

Pocock, S. A., 1961, Microspores of the Genus Murospora Somers from Mesozoic Strata of Western Canada and Australia: Journal of Paleontology, v. 35, p. 1231-1234.

Polyansky, B. V., 1983, Early Mesozoic Landscapes in the Cacasus-Pamir Coal Bearing Formations of the Mediterranean Belt: Compte rendu: 10. Congrès Internat. de Stratigr. et de Geologie du Carbonifère, p. 71

Posamentier, H. W., 2001, Lowstand Alluvial Bypass Systems: Incised Vs. Unincised: AAPG Bulletin, v. 85, p. 1771-1793.

Powell, T., O'Brien, P., and Wells, A., 1993, Petroleum Prospectivity of the Clarence-Moreton Basin, Eastern Australia: A Geochemical Perspective: Australian Journal of Earth Sciences, v. 40, p. 31-44.

Power, P., and Devine, S., 1970, Surat Basin, Australia-Subsurface Stratigraphy, History, and Petroleum: AAPG Bulletin, v. 54, p. 2410-2437.

Price, G. D., and Passey, B. H., 2013, Dynamic Polar Climates in a Greenhouse World: Evidence from Clumped Isotope Thermometry of Early Cretaceous Belemnites: Geology, v. 41, p. 923-926.

Price, P., 1997, Permian to Jurassic Palynostratigraphic Nomenclature of the Bowen and Surat Basins *in* P. M. Green, ed., The Surat and Bowen Basins, South-East Queensland, v. 1: Brisbane, Queensland Department of Mines and Energy

p. 137-178.

References

Price, P., Filatoff, J., Williams, A., Pickering, S., and Wood, G., 1985, Late Palaeozoic and Mesozoic Palynostratigraphical Units: CSR Oil & Gas Division, Palynology Facility, Report, v. 274, p. 25.

Queensland_Government, 2016, Queensland Petroleum and Coal Seam Gas 2016-2017: http://www.australiaminerals.gov.au/__data/assets/pdf_file/0003/47622/Queenslands-petroleum-and-coal-seam-gas-2017.pdf. Date accessed 02/04/2016.

Raza, A., Hill, K., and Korsch, R., 2009, Mid-Cretaceous Uplift and Denudation of the Bowen and Surat Basins, Eastern Australia: Relationship to Tasman Sea Rifting from Apatite Fission-Track and Vitrinite-Reflectance Data: Australian Journal of Earth Sciences, v. 56, p. 501-531.

Read, J., and Francis, J., 1992, Responses of Some Southern Hemisphere Tree Species to a Prolonged Dark Period and Their Implications for High-Latitude Cretaceous and Tertiary Floras: Palaeogeography, Palaeoclimatology, Palaeoecology, v. 99, p. 271-290.

Reeves, F., 1947, Geology of Roma District, Queensland, Australia: AAPG Bulletin, v. 31, p. 1341-1371.

Reiser, R., and Williams, A., 1969, Palynology of the Lower Jurassic Sediments of the Northern Surat Basin, Queensland, v. 339: Brisbane, Queensland, SG Reid, Government Printer, pp. 1-24.

Retallack, G. J., Veevers, J. J., and Morante, R., 1996, Global Coal Gap between Permian-Triassic Extinction and Middle Triassic Recovery of Peat-Forming Plants: Geological Society of America Bulletin, v. 108, p. 195-207.

Riding, J., and Helby, R., 2001, Early Jurassic (Toarcian) Dinoflagellate Cysts from the Timor Sea, Australia: Memoir-Association of Australasian Palaeontologists, v. 24, p. 1-32.

Riding, J., and Mantle, D., 2010, Age Really Is an Issue: Earthwise, v. 26, p. 58-59.

Riding, J. B., Mantle, D. J., and Backhouse, J., 2010, A Review of the Chronostratigraphical Ages of Middle Triassic to Late Jurassic Dinoflagellate Cyst Biozones of the North West Shelf of Australia: Review of Palaeobotany and Palynology, v. 162, p. 543-575.

Robertson, A., 1993, Bundaberg Volcanic Province: Queensland Geology, v. 5, p. 44-87.

Ross, P. K. R., 1996, Coal Geology of the Walloon Coal Measures: PhD thesis, Queensland University of Geology, Brisbane, Australia, pp. 255.

Ryan, D. J., Hall, A., Erriah, L., and Wilson, P. B., 2012, The Walloon Coal Seam Gas Play, Surat Basin: APPEA Journal, v. 52, p. 273-290.

Rzóska, J., 1974, The Upper Nile Swamps, a Tropical Wetland Study: Freshwater Biology, v. 4, p. 1-30.

Sachsenhofer, R., Bechtel, A., Kuffner, T., Rainer, T., Gratzer, R., Sauer, R., and Sperl, H., 2006, Depositional Environment and Source Potential of Jurassic Coal-Bearing Sediments (Gresten Formation, Höflein Gas/Condensate Field, Austria): Petroleum Geoscience, v. 12, p. 99-114.

Sajadi, F., and Playford, G., 2002, Systematic and Stratigraphic Palynology of Late Jurassic-Earliest Cretaceous Strata of the Eromanga Basin, Queensland, Australia: Part One: Palaeontographica Abteilung B-Palyaophytologie, v. 261, p. 1-112.

Sales, M., Altmann, M., Buick, G., Dowling, C., Bourne, J., and Bennett, A., 2015, Subtle Oil Fields Along the Western Flank of the Cooper/Eromanga Petroleum System, APPEA Conference, Melbourne, CSIRO, p. 440-440.

Sambrook Smith, G., Ashworth, P., Best, J., Woodward, J., and Simpson, C., 2006, The Sedimentology and Alluvial Architecture of the Sandy Braided South Saskatchewan River, Canada: Sedimentology, v. 53, p. 413-434.

Sarjeant, W., 1967, Observations on the Acritarch Genus Micrhystridium (Deflandre): Revue de micropaléontologie, v. 9, p. 201-208.

Sarjeant, W., and Stancliffe, R., 1994, The Micrhystridium and Veryhachium Complexes (Acritarcha: Acanthomorphitae and Polygonomorphitae): A Taxonomic Reconsideration: Micropaleontology, p. 1-77.

Scheibner, E., and Basden, H., 1996, Geology of New South Wales-Synthesis, v. 2: Sydney, Australia, NSW Department of Mineral Resources.

Schmitz, M. D., and Schoene, B., 2007, Derivation of Isotope Ratios, Errors, and Error Correlations for U-Pb Geochronology Using 205pb-235u-(233u)-

Spiked Isotope Dilution Thermal Ionization Mass Spectrometric Data: Geochemistry, Geophysics, Geosystems, v. 8, p. 1-20.

Sclater, J. G., and Christie, P., 1980, Continental Stretching: An Explanation of the Post Mid-Cretaceous Subsidence of the Central North Sea Basin: Journal of Geophysical Research: Solid Earth (1978–2012), v. 85, p. 3711-3739.

Scotese, C., Boucot, A., and McKerrow, W., 1999, Gondwanan Palaeogeography and Palaeclimatology: Journal of African Earth Sciences, v. 28, p. 99-114.

Scotese, C. R., 2001, Paleomap Project: http://www.scotese.com. Date accessed 26/10/2015.

Scott, S., Anderson, B., Crosdale, P., Dingwall, J., and Leblang, G., 2004, Revised Geology and Coal Seam Gas Characteristics of the Walloon Subgroup, Surat Basin, Queensland: In Boult, P.J., Johns, P.R., & Lang, S.C. (eds) PESA Eastern Australian Basins Symposium II, p. 19-22.

Scott, S., Anderson, B., Crosdale, P., Dingwall, J., and Leblang, G., 2007, Coal Petrology and Coal Seam Gas Contents of the Walloon Subgroup, Surat Basin, Queensland, Australia: International Journal of Coal Geology, v. 70, p. 209-222.

Scott, S. G., 2008, The Geology, Stratigraphy and Coal Seam Gas Characteristics of the Walloon Subgroup - Northeastern Surat Basin: PhD thesis, James Cook University, Townsville, Australia, pp. 313.

Scott, S. G., Beeston, J. W., and Carr, A. F., 1995, Galilee Basin: Geology of Australian Coal Basins, Ward, CR, Harrington, HJ, Mallett, CW, Beeston, JW (eds). Geological Society of Australia Incorporated, Coal Geology Group, Special Publication, v. 1, p. 341-352.

Selden, P. A., and Beattie, R. G., 2013, A Spider Fossil from the Jurassic Talbragar Fossil Fish Bed of New South Wales: Alcheringa: An Australasian Journal of Palaeontology, v. 37, p. 203-208.

Sellwood, B. W., and Valdes, P. J., 1997, Geological Evaluation of Climate General Circulation Models and Model Implications for Mesozoic Cloud Cover: Terra Nova, v. 9, p. 75-78.

Shanley, K. W., and McCabe, P. J., 1993, Alluvial Architecture in a Sequence Stratigraphic Framework: A Case History from the Upper Cretaceous of Southern Utah, USA, *in* S. Flint and I. Bryant, eds., Quantitative Modeling of

Clastic Hydrocarbon Reservoirs and Outcrop Analogues, Special Publication, v. 15: Gent, Belgium, International Association of Sedimentologists, p. 21-56.

Shanley, K. W., and McCabe, P. J., 1994, Perspective on the Sequence Stratigraphy of Continental Strata: AAPG Bulletin (American Association of Petroleum Geologists);(United States), v. 78, p. 544-568.

Shanley, K. W., and McCabe, P. J., 1998, Relative Role of Eustasy, Climate, and Tectonism in Continental Rocks, v. 9: Tulsa, Oklahoma, , SEPM (Society for Sedimentary Petrology), pp. 234.

Shanmugam, G., Poffenberger, M., and Alava, J. T., 2000, Tide-Dominated Estuarine Facies in the Hollin and Napo Formations (Cretaceous), Sacha Field, Oriente Basin, Ecuador: AAPG Bulletin, v. 84, p. 652-682.

Shen, J. J. T., 1991, The Source and Reservoir Potential of the Late Jurassic Polda Formation, Sa: Honours thesis, University of Adelaide, Adelaide, Australia, pp. 96.

Shepherd, M., 2009a, Meandering Fluvial Reservoirs, *in* M. Shepherd, ed., Oil Field Production Geology, v. AAPG Memoir 91, p. 161-272.

Shepherd, M., 2009b, The Reservoir Framework, *in* M. Shepherd, ed., Oil Field Production Geology, v. AAPG Memoir 91, p. 81-92.

Shields, D., Bianchi, V., and Esterle, J., 2017, A Seismic Investigation into the Geometry and Controls Upon Alluvial Architecture in the Walloon Subgroup, Surat Basin, Queensland: Australian Journal of Earth Sciences, v. 64, p. 455-469.

Shields, D., and Esterle, J., 2015, Regional Insights into the Sedimentary Organisation of the Walloon Subgroup, Surat Basin, Queensland.: Australian Journal of Earth Sciences, v. 62, p. 949-967.

Sisulak, C. F., and Dashtgard, S. E., 2012, Seasonal Controls on the Development and Character of Inclined Heterolithic Stratification in a Tide-Influenced, Fluvially Dominated Channel: Fraser River, Canada: Journal of Sedimentary Research, v. 82, p. 244-257.

Sláma, J., Košler, J., Condon, D. J., Crowley, J. L., Gerdes, A., Hanchar, J. M., Horstwood, M. S., Morris, G. A., Nasdala, L., and Norberg, N., 2008, Plešovice Zircon—a New Natural Reference Material for U–Pb and Hf Isotopic Microanalysis: Chemical Geology, v. 249, p. 1-35.

Smelror, M., Key, R. M., Smith, R. A., and Njange, F., 2008, Late Jurassic and Cretaceous Palynostratigraphy of the Onshore Rovuma Basin, Northern Mozambique: Palynology, v. 32, p. 63-76.

Smith, D. G., 1986, Anastomosing River Deposits, Sedimentation Rates and Basin Subsidence, Magdalena River, Northwestern Colombia, South America: Sedimentary Geology, v. 46, p. 177-196.

Smith, N. D., 1971, Transverse Bars and Braiding in the Lower Platte River, Nebraska: Geological Society of America Bulletin, v. 82, p. 3407-3420.

Smith, N. D., McCarthy, T. S., Ellery, W., Merry, C. L., and Rüther, H., 1997, Avulsion and Anastomosis in the Panhandle Region of the Okavango Fan, Botswana: Geomorphology, v. 20, p. 49-65.

Smith, N. D., and Perez-Arlucea, M., 1994, Fine-Grained Splay Deposition in the Avulsion Belt of the Lower Saskatchewan River, Canada: Journal of Sedimentary Research, v. B64, p. 159–168.

Spicer, R., and Chapman, J., 1990, Climate Change and the Evolution of High-Latitude Terrestrial Vegetation and Floras: Trends in Ecology & Evolution, v. 5, p. 279-284.

Spicer, R. A., 1990, Reconstructing High-Latitude Cretaceous Vegetation and Climate: Arctic and Antarctic Compared, *in* T. Taylor and E. Taylor, eds., Antarctic Paleobiology: Its Role in the Reconstruction of Gondwana: New York, New York, Springer, p. 27-36.

Spicer, R. A., and Parrish, J. T., 1986, Paleobotanical Evidence for Cool North Polar Climates in Middle Cretaceous (Albian-Cenomanian) Time: Geology, v. 14, p. 703-706.

Spicer, R. A., Parrish, J. T., and Grant, P. R., 1992, Evolution of Vegetation and Coal-Forming Environments in the Late Cretaceous of the North Slope of Alaska: Geological Society of America Special Papers, v. 267, p. 177-192.

Srivastava, S. K., 1968, Fungal Elements from the Edmonton Formation (Maestrichtian), Alberta, Canada: Canadian Journal of Botany, v. 46, p. 1115-1118.

Stacey, J., and Kramers, J., 1975, Approximation of Terrestrial Lead Isotope Evolution by a Two-Stage Model: Earth and Planetary Science Letters, v. 26, p. 207-221.

Stach, E., Mackowsky, M.-T., Teichmüller, M., Taylor, G., Chandra, D., and Teichmüller, R., 1982, Coal Petrology: Gebrüder Borntraeger, Berlin, p. 1-535.

Staines, H., Falkner, A., and Thornton, M., 1995, Ipswich Coalfield: Geology of Australian Coal Basins, Geological Society of Australia Coal Geology Group Special Publication, v. 1, p. 455-464.

Stancliffe, R., 1990, Acritarchs and Other Non-Dinophycean Marine Palynomorphs from the Oxfordian (Upper Jurassic) of Skye, Western Scotland and Dorset, Southern England: Palynology, v. 14, p. 175-192.

Stasiuk, L., Goodarzi, F., and Bagheri-Sadeghi, H., 2006, Petrology, Rank and Evidence for Petroleum Generation, Upper Triassic to Middle Jurassic Coals, Central Alborz Region, Northern Iran: International Journal of Coal geology, v. 67, p. 249-258.

Stevens, G. R., 2004, Hettangian-Sinemurian (Early Jurassic) Ammonites of New Zealand, *in* G. R. Stevens, ed., Institute of Geological and Nuclear Sciences, Monograph, v. 23: Wellington, New Zealand, Institute of Geological & Nuclear Sciences Limited, p. 1-107.

Stewart, J. R., and Alder, D., 1995, New South Wales Petroleum Potential: Sydney, Australia NSW Department of Mineral Resources, pp. 188.

Strong, P., Wood, G., Lang, S. C., Jollands, A., Karalaus, E., and Kassan, J., 2002, High Resolution Palaeogeographic Mapping of the Fluvial-Lacustrine Patchawarra Formation in the Cooper Basin, South Australia: APPEA Journal, v. 42, p. 65-81.

Struckmeyer, H. I., and Totterdell, J. M., 1990, Australia: Evolution of a Continent: Canberra, Australia, Australian Government Publishing Service, pp. 97.

Stuart, J. Y., 2015, Subsurface Architecture of Fluvial-Deltaic Deposits in High- and Low-Accommodation Settings: PhD thesis, University of Leeds, Leeds, UK, pp. 327.

Swarbrick, C., 1973, Stratigraphy and Economic Potential of the Injune Creek Group in the Surat Basin: Queensland Government Mining Journal, p. 1-40.

Swarbrick, C., Gray, A., and Exon, N., 1973, Injune Creek Group—Amendments and an Addition to Stratigraphic Nomenclature in the Surat Basin: Queensland Government Mining Journal, v. 74, p. 57-63.

Tchoumatchenco, P., Rabrenović, D., Radulović, B., and Radulović, V., 2006, Trans-Border (South-East Serbia/West Bulgaria) Correlations of the Jurassic Sediments: Infra-Getic Unit: Geološki anali Balkanskoga poluostrva, p. 19-33.

Teichmuller, M., 1989, The Genesis of Coal from the Viewpoint of Coal Petrology: International Journal of Coal Geology, v. 12, p. 1-87.

Thomas, L., 2012, Coal Geology: Chichester, UK, John Wiley & Sons

pp. 379.

Thomas, M. A., and Anderson, J. B., 1994, Sea-Level Controls on the Facies Architecture of the Trinity/Sabine Incised-Valley System, Texas Continental Shelf, *in* R. W. Dalrymple, R. Boyd and B. A. Zaitlin, eds., Incised-Valley Systems: Origin and Sedimentary Sequences: Sepm Special Publication, v. 51: Tulsa, Oklahoma, SEPM, p. 63-82.

Thomas, R. G., Smith, D. G., Wood, J. M., Visser, J., Calverley-Range, E. A., and Koster, E. H., 1987, Inclined Heterolithic Stratification—Terminology, Description, Interpretation and Significance: Sedimentary Geology, v. 53, p. 123-179.

Tooth, S., and McCarthy, T., 2004, Controls on the Transition from Meandering to Straight Channels in the Wetlands of the Okavango Delta, Botswana: Earth surface processes and landforms, v. 29, p. 1627-1649.

Totterdell, J., Moloney, J., Korsch, R., and Krassay, A., 2009, Sequence Stratigraphy of the Bowen–Gunnedah and Surat Basins in New South Wales: Australian Journal of Earth Sciences, v. 56, p. 433-459.

Towler, B., Firouzi, M., Underschultz, J., Rifkin, W., Garnett, A., Schultz, H., Esterle, J., Tyson, S., and Witt, K., 2016, An Overview of the Coal Seam Gas Developments in Queensland: Journal of Natural Gas Science and Engineering, v. 31, p. 249-271.

Townshend, G., 1993, Distribution, Chemistry, Isotopic Compostion and Origin of Diagenetic Carbonates; Namur Sandstone, Copper-Eromanga Basin, South Australia, University of Melbourne, Melbourne, pp. 120.

Traverse, A., 2007, Paleopalynology, v. 28: Crows Nest, Australia, Unwin Hyman, pp. 600.

Triplehorn, D., and Bohor, B., 1986, Volcanic Ash Layers in Coal: Origin, Distribution, Composition and Significance: Mineral Matter and Ash in Coal, v. 301, p. 90-98.

Tucker, R. T., Roberts, E. M., Henderson, R. A., and Kemp, A. I., 2016, Large Igneous Province or Long-Lived Magmatic Arc Along the Eastern Margin of Australia During the Cretaceous? Insights from the Sedimentary Record: Geological Society of America Bulletin, v. 128, p. 1461-1480.

Turner, S., Bean, L. B., Dettmann, M., McKellar, J. L., McLoughlin, S., and Thulborn, T., 2009, Australian Jurassic Sedimentary and Fossil Successions: Current Work and Future Prospects for Marine and Non-Marine Correlation: GFF, v. 131, p. 49-70.

Vail, P., Hardenbol, J., and Todd, R., 1984, Jurassic Unconformities, Chronostratigraphy, and Sea-Level Changes from Seismic Stratigraphy and Biostratigraphy, *in* J. Schlee, ed., Interregional Unconformities and Hydrocarbon Accumulation, Aapg Memoir, v. 36, p. 129-144.

Valdes, P., Sellwood, B., and Price, G., 1995, Modelling Late Jurassic Milankovitch Climate Variations, *in* M. R. House and A. S. Gale, eds., Orbital Forcing Timescales and Cyclostratigraphy, v. 85: London, UK, Geological Society, London, Special Publications, p. 115-132.

Veevers, J., Powell, C. M., and Roots, S., 1991, Review of Seafloor Spreading around Australia. I. Synthesis of the Patterns of Spreading: Australian Journal of Earth Sciences, v. 38, p. 373-389.

Volkheimer, W., Rauhut, O. W., Quattrocchio, M. E., and Martinez, M. A., 2008, Jurassic Paleoclimates in Argentina, a Review: Revista de la Asociación Geológica Argentina, v. 63, p. 549-556.

Wadsworth, J., Boyd, R., Diessel, C., Leckie, D., and Zaitlin, B. A., 2002, Stratigraphic Style of Coal and Non-Marine Strata in a Tectonically Influenced Intermediate Accommodation Setting: The Mannville Group of the Western Canadian Sedimentary Basin, South-Central Alberta: Bulletin of Canadian Petroleum Geology, v. 50, p. 507-541.

Wainman, C. C., McCabe, P. J., and Crowley, J. L., 2017, Solving a Tuff Problem: A New Chronostratigraphic Framework for Middle to Upper Jurassic

Strata in Eastern Australia Using U-Pb Zircon Dates: AAPG Bulletin, v. 20, p. 1-28.

Wainman, C. C., McCabe, P. J., Crowley, J. L., and Nicoll, R. S., 2015, U–Pb Zircon Age of the Walloon Coal Measures in the Surat Basin, Southeast Queensland: Implications for Paleogeography and Basin Subsidence: Australian Journal of Earth Sciences, v. 62, p. 807-816.

Walter, B. P., and Heimann, M., 2000, A Process-Based, Climate-Sensitive Model to Derive Methane Emissions from Natural Wetlands: Application to Five Wetland Sites, Sensitivity to Model Parameters, and Climate: Global Biogeochemical Cycles, v. 14, p. 745-765.

Wang, Y., Mosbrugger, V., and Zhang, H., 2005, Early to Middle Jurassic Vegetation and Climatic Events in the Qaidam Basin, Northwest China: Palaeogeography, Palaeoclimatology, Palaeoecology, v. 224, p. 200-216.

Ward, C. R., 1995, Geology of Australian Coal Basins, v. 59: Sydney, Australia, Geological Society of Australia, Coal Geology Group, pp. 590.

Waschbusch, P., Korsch, R. J., and Beaumont, C., 2009, Geodynamic Modelling of Aspects of the Bowen, Gunnedah, Surat and Eromanga Basins from the Perspective of Convergent Margin Processes: Australian Journal of Earth Sciences, v. 56, p. 309-334.

Watson, E., Wark, D., and Thomas, J., 2006, Crystallization Thermometers for Zircon and Rutile: Contributions to Mineralogy and Petrology, v. 151, p. 413-433.

Watts, A. B., 2001, Isostasy and Flexure of the Lithosphere: Cambridge, UK, Cambridge University Press, pp. 458.

Watts, K., 1987, The Hutton Sandstone–Birkhead Formation Transition, Atp 269p (1), Eromanga Basin: The APEA Journal, v. 27, p. 215-229.

Weaver, J. N., Wood, G. H., and Fiscales, Y. C. 1994, Coal Map of South America: US Geological Survey Coal Investigations Map C-145.

Weissert, H., and Erba, E., 2004, Volcanism, Co2 and Palaeoclimate: A Late Jurassic–Early Cretaceous Carbon and Oxygen Isotope Record: Journal of the Geological Society, v. 161, p. 695-702.

Weissert, H., and Mohr, H., 1996, Late Jurassic Climate and Its Impact on Carbon Cycling: Palaeogeography, Palaeoclimatology, Palaeoecology, v. 122, p. 27-43.

Weissmann, G., Hartley, A., Nichols, G., Scuderi, L., Olson, M., Buehler, H., and Banteah, R., 2010, Fluvial Form in Modern Continental Sedimentary Basins: Distributive Fluvial Systems: Geology, v. 38, p. 39-42.

Wells, A., and O'Brien, P., 1994, Lithostratigraphic Framework of the Clarence-Moreton Basin: Bulletin of the Bureau of Mineral Resources Australia, v. 241, p. 4-47.

Wells, A., and O'Brien, P., 1994, Geology of the Clarence–Moreton Basin (1: 500 000 Scale Map): Australian Geological Survey Organisation: Canberra.

Wells, A. T., 1994, Geology and Petroleum Potential of the Clarence-Moreton Basin, New South Wales and Queensland, v. 241, Australian Government Publ. Service, pp. 47.

Wetzel, O., 1961, New Microfossils from Baltic Cretaceous Flintstones: Micropaleontology, v. 7, p. 337-350.

White, M., 1981, Revision of the Talbragar Fish Bed Flora (Jurassic) of New South Wales: Rec. Aust. Mus, v. 33, p. 695-721.

White, M. E., 1993, The Greening of Gondwana: Sydney, Australia, Reed, pp. 256.

Whitehouse, F. W., 1954, The Geology of the Queensland Portion of the Great Australian Artesian Basin, v. A-56: Brisbane, Australia, University of Queensland, Department of Geology, pp. 20.

Whitford, D., Hamilton, P., and Scot, J., 1994, Sedimentary Provenances Studies in Australian Basins Using Neodymium Model Ages: APEA Journal, v. 34, p. 320-329.

Willard, D. A., DiMichele, W. A., Eggert, D. L., Hower, J. C., Rexroad, C. B., and Scott, A. C., 1995, Paleoecology of the Springfield Coal Member (Desmoinesian, Illinois Basin) near the Leslie Cemetery Paleochannel, Southwestern Indiana: International Journal of Coal Geology, v. 27, p. 59-98.

Willard, D. A., Phillips, T. L., Lesnikowska, A. D., and DiMichele, W. A., 2007, Paleoecology of the Late Pennsylvanian-Age Calhoun Coal Bed and Implications for Long-Term Dynamics of Wetland Ecosystems: International Journal of Coal Geology

v. 69, p. 21-54.

Willis, A., 2000, Tectonic Control of Nested Sequence Architecture in the Sego Sandstone, Neslen Formation and Upper Castlegate Sandstone (Upper Cretaceous), Sevier Foreland Basin, Utah, USA: Sedimentary Geology, v. 136, p. 277-317.

Wilmsen, M., Fürsich, F. T., and Taheri, J., 2009, The Shemshak Group (Lower–Middle Jurassic) of the Binalud Mountains, Ne Iran: Stratigraphy, Depositional Environments and Geodynamic Implications: Geological Society, London, Special Publications, v. 312, p. 175-188.

Wiltshire, M., 1982, Revision of Eromanga Basin Limits: Eromanga Basin Symposium Summary Papers, p. 68-75

Wiltshire, M., 1989, Mesozoic Stratigraphy and Palaeogeography, Eastern Australia: The Cooper and Eromanga Basins, Australia: Proceedings of the Petroleum Exploration Society of Australia, Society of Petroleum Engineers, Australian Society of Exploration Geophysicists (SA Branches), Adelaide, p. 279-291.

Wing, S. L., Harrington, G. J., Smith, F. A., Bloch, J. I., Boyer, D. M., and Freeman, K. H., 2005, Transient Floral Change and Rapid Global Warming at the Paleocene-Eocene Boundary: Science, v. 310, p. 993-996.

Wood, G. D., Gabriel, A. M., and Lawson, J. C., 1996, Palynological Techniques - Processing and Microscopy, *in* J. Jansonius and D. C. McGregor, eds., Palynology, Principles and Applications, v. 1, American Association of Stratigraphic Palynologists Foundation, p. 29-50.

Woolley, J., 1941, Geological Report on the Area North-East of Tambo: Queensland. Department of Mines. Report C, v. 640, p. 15-21.

Yago, J., 1996a, Sedimentology of the Middle Jurassic Walloon Coal Measures in the Great Artesian Basin of Eastern Australia: Geological Society of Australia Abstracts v. 43, p. 574-574.

Yago, J. V., and Fielding, C., 2015, Depositional Environments and Sediment Dispersal Patterns of the Jurassic Walloon Subgroup in Eastern Australia, *in* W.

Lodwick, ed., Eastern Australasian Basins Symposium, a Powerhouse Emerges; Energy for the Next Fifty Years, Petroleum Exploration Society of Australia Special Publication: Perth, Australia, PESA, p. 141-150.

Yago, J. V. R., 1996b, Basin Analysis of the Middle Jurassic Walloon Coal Measures in the Great Artesian Basin, Australia: PhD thesis, University of Queensland, Brisbane, Australia, pp. 276.

Yoshida, S., 2000, Sequence and Facies Architecture of the Upper Blackhawk Formation and the Lower Castlegate Sandstone (Upper Cretaceous), Book Cliffs, Utah, USA: Sedimentary Geology, v. 136, p. 239-276.

Zachos, J. C., Dickens, G. R., and Zeebe, R. E., 2008, An Early Cenozoic Perspective on Greenhouse Warming and Carbon-Cycle Dynamics: Nature, v. 451, p. 279-283.

Zeiss, A., 2003, The Upper Jurassic of Europe: Its Subdivision and Correlation: Geological Survey of Denmark and Greenland Bulletin, v. 1, p. 75-114.

Zhao, W.-z., Zou, C.-n., Feng, Z.-q., Hu, S.-y., Zhang, Y., Li, M., Wang, Y.-h., Yang, T., and Yang, H., 2008, Geological Features and Evaluation Techniques of Deep-Seated Volcanics Gas Reservoirs, Songliao Basin: Petroleum Exploration and Development, v. 35, p. 129-142.

Zhou, F., Shields, D., Titheridge, D., Tyson, S., and Esterle, J., 2017, Understanding the Geometry and Distribution of Fluvial Channel Sandstones and Coal in the Walloon Coal Measures, Surat Basin, Australia: Marine and Petroleum Geology, v. 86, p. 573-586.

Ziegler, A., Raymond, A., Gierlowski, T., Horrell, M., Rowley, D., and Lottes, A., 1987, Coal, Climate and Terrestrial Productivity: The Present and Early Cretaceous Compared: Geological Society, London, Special Publications, v. 32, p. 25-49.

Zippi, P. A., 1998, Freshwater Algae from the Mattagami Formation (Albian), Ontario: Paleoecology, Botanical Affinities, and Systematic Taxonomy: Micropaleontology, v. 44, p. 1-78.

Zou, C., 2012, Unconventional Petroleum Geology: Amsterdam, Netherlands, Elsevier, pp. 482.

Appendices 1.

Analytical Methods

LA-ICPMS methods

Zircon grains were separated from rocks using standard techniques and annealed at 900° C for 60 hours in a muffle furnace. They were mounted in epoxy and polished until their centres were exposed. Cathodoluminescence (CL) images were obtained with a JEOL JSM-1300 scanning electron microscope and Gatan MiniCL. Zircon was analysed by laser ablation inductively coupled plasma mass spectrometry (LAICPMS) using a ThermoElectron X-Series II quadrupole ICPMS and New Wave Research UP-213 Nd:YAG UV (213 nm) laser ablation system. In-house analytical protocols, standard materials, and data reduction software were used for acquisition and calibration of U-Pb dates and a suite of high field strength elements (HFSE) and rare earth elements (REE). Zircon was ablated with a laser spot of 25 µm wide using fluence and pulse rates of 5 J/cm2 and 10 Hz, respectively, during a 45 second analysis (15 sec gas blank, 30 sec ablation) that excavated a pit ~25 µm deep. Ablated material was carried by a 1.2 L/min He gas stream to the nebuliser flow of the plasma. Dwell times were 5 ms for Si and Zr, 200 ms for ^{49}Ti and ^{207}Pb, 80 ms for ^{206}Pb, 40 ms for ^{202}Hg, ^{204}Pb, ^{208}Pb, ^{232}Th, and ^{238}U and 10 ms for all other HFSE and REE. Background count rates for each analyte were obtained prior to each spot analysis and subtracted from the raw count rate for each analyte. Ablations pits that appear to have intersected glass or mineral inclusions were identified based on Ti and P. U–Pb dates from these analyses are considered valid if the U–Pb ratios appear to have been unaffected by the inclusions. Analyses that appear contaminated by common Pb were rejected based on mass 204 being above baseline. For concentration calculations, background-subtracted count rates for each analyte were internally normalised to ^{29}Si and calibrated with respect to NIST SRM- 610 and -612 glasses as the primary standards. Temperature was calculated from the Ti-in-zircon thermometer (Watson et al. 2006). Because there are no constraints on the activity of TiO_2, an average value in crustal rocks of 0.8 was used.

Data were collected in one experiment in February 2015. For U–Pb and $^{207}Pb/^{206}Pb$ dates, instrumental fractionation of the background-subtracted ratios was corrected and dates were calibrated with respect to interspersed measurements of zircon standards and reference materials. The primary standard Plešovice zircon (Sláma et al. 2008) was used to monitor time-dependent instrumental fractionation based on two analyses for every 10 analyses of unknown zircon. A polynomial fit to the standard analyses yields each sample-specific fractionation factor.

Radiogenic isotope ratio and age error propagation for all analyses includes uncertainty contributions from counting statistics and background subtraction. For groups of analyses that are collectively interpreted from a weighted mean date (i.e., igneous zircon analyses), a weighted mean date is first calculated using Isoplot 3.0 (Ludwig 2003) using errors on individual dates that do not include a standard calibration uncertainty, and then a standard calibration uncertainty is propagated into the error on the weighted mean date. This uncertainty is the local standard deviation of the polynomial fit to the interspersed primary standard measurements versus time for the time-dependent, relatively larger U/Pb fractionation factor, and the standard error of the mean of the consistently time-invariant and smaller $^{207}Pb/^{206}Pb$ fractionation factor. This uncertainty is 2.24% (2σ) for $^{206}Pb/^{238}U$. Age interpretations are based on $^{206}Pb/^{238}U$ dates. Errors on the dates from individual analyses are given at 2σ, as are the errors on the weighted mean dates.

Two zircon secondary reference materials were treated as unknowns to assess accuracy, interspersed as groups of two analyses for every 20 unknown analyses. Weighted mean dates are calculated using Isoplot 3.0 (Ludwig 2003) from errors on individual dates that do not include the standard calibration uncertainties. However, errors on weighted mean dates include the standard calibration uncertainties within each experiment and are given at 2σ. Zirconia zircon (327 Ma from unpublished chemical abrasion thermal ionisation mass spectrometry (CA-TIMS) data, Boise State University) yielded a weighted mean $^{206}Pb/^{238}U$ date of 332 ± 9 Ma (MSWD=0.6, probability of fit = 0.80, n = 12). Seiland zircon (530 Ma from unpublished CA-TIMS data, Boise State University) yielded a weighted mean 206Pb/238U date of 522 ± 15 Ma (MSWD

= 0.7, probability of fit = 0.76, n =12). These results show that accurate $^{206}Pb/^{238}U$ dates were obtained.

CA-TIMS methods

U–Pb dates were obtained by the chemical abrasion isotope dilution thermal ionisation mass spectrometry (CA-TIMS) method from analyses composed of single zircon grains (Table 1). Zircon grains were separated from the rock sample using standard techniques and mounted in epoxy and polished until the centres of the grains were exposed. Cathodoluminescence (CL) images were obtained with a JEOL JSM-1300 scanning electron microscope and Gatan MiniCL. Zircon was then removed from the epoxy mounts and subjected to a modified version of the chemical abrasion method of Mattinson (2005), reflecting analysis of single grains. Grains were selected for dating based on CL images that appear to lack inherited cores.

Grains were placed in a muffle furnace at 900°C for 60 hours in quartz beakers. Single grains were transferred to 3 mL Teflon PFA beakers and loaded into 300 µL Teflon PFA microcapsules. Fifteen microcapsules were placed in a large-capacity Parr vessel, and the crystals partially dissolved in 120 µL of 29 M HF for 12 hours at 180°C. Contents of each microcapsule were returned to 3 mL Teflon PFA beakers, HF removed and residual grains immersed in 3.5 M HNO_3, ultrasonically cleaned for an hour, and fluxed on a hotplate at 80°C for an hour. The HNO_3 was removed and grains were rinsed twice in ultrapure H_2O before being reloaded into the same 300 µL Teflon PFA microcapsules (rinsed and fluxed in 6 M HCl during crystal sonication and washing) and spiked with the EARTHTIME mixed ^{233}U–^{235}U–^{205}Pb tracer solution (ET535). These chemically abraded grains were dissolved in Parr vessels in 120 µL of 29 M HF with a trace of 3.5 M HNO_3 at 220°C for 48 hours, dried to fluorides, and then redissolved in 6 M HCl at 180°C overnight. U and Pb were separated from the zircon matrix using an HCl-based anion-exchange chromatographic procedure (Krogh 1973) eluted together and dried with 2 µL of 0.05 N H_3PO_4.

Pb and U were loaded on a single outgassed Re filament in 5 µL of a silica gel/phosphoric acid mixture (Gerstenberger & Haase 1997), and U and Pb isotopic measurements made on a GV Isoprobe-T multicollector thermal ionisation mass spectrometer equipped with an ion-counting Daly detector. Pb isotopes were measured by peak-jumping all isotopes on the Daly detector for

160 cycles. Pb mass fractionation was corrected using the known $^{202}Pb/^{205}Pb$ ratio of the ET2535 tracer solution that was recently measured on other samples. Transitory isobaric interferences due to high-molecular weight organics, particularly on ^{204}Pb and ^{207}Pb, disappeared within approximately 30 cycles, while ionisation efficiency averaged 104 cps/pg of each Pb isotope. Linearity (to ≥1.4 x 106 cps) and the associated deadtime correction of the Daly detector were monitored by repeated analyses of NBS982, and have been constant since installation. Uranium was analysed as UO_2+ ions in static Faraday mode on 1012 ohm resistors for 250 cycles, and corrected for isobaric interference of $^{233}U^{18}O^{16}O$ on $^{235}U^{16}O^{16}O$ with an $^{18}O/^{16}O$ of 0.00206. Ionisation efficiency averaged 200 mV/ng of each U isotope. U mass fractionation was corrected using the known $^{233}U/^{235}U$ ratio of the ET535 tracer solution.

CA-TIMS U–Pb dates and uncertainties were calculated using the algorithms of (Schmitz and Schoene 2007), ET535 tracer solution (Condon et al. 2015; McLean et al. 2015) with calibration of $^{235}U/^{205}Pb$ = 100.233, $^{233}U/^{235}U$ = 0.99506, and $^{205}Pb/^{204}Pb$ = 1196, and U decay constants recommended by Jaffey et al. (1971). $^{206}Pb/^{238}U$ ratios and dates were corrected for initial ^{230}Th disequilibrium using a Th/U[magma] = 3.0 ± 0.3 using the algorithms of Crowley et al. (2007), resulting in an increase in the $^{206}Pb/^{238}U$ dates of ca 0.09 Ma. Common Pb in analyses was assigned to the zircon with a composition determined by Stacey and Kramers (1975), except for 0.3 pg that was assigned to laboratory blank and subtracted based on the measured laboratory Pb isotopic composition and associated uncertainty. U blanks are difficult to precisely measure, but are estimated at 0.075 pg.

Weighted mean $^{206}Pb/^{238}U$ dates were calculated from equivalent dates using Isoplot 3.0 (Ludwig 2003). Errors given below are presented as ± x / y / z. Error x is the 2σ internal error based on analytical uncertainties only, including counting statistics, subtraction of tracer solution, and blank and initial common Pb subtraction. It should be considered when comparing our dates with $^{206}Pb/^{238}U$ dates from other laboratories that used the same EARTHTIME tracer solution or a tracer solution that was cross calibrated using EARTHTIME gravimetric standards. Error y includes the tracer calibration uncertainty propagated in quadrature. It should be considered when comparing our dates

with those derived from other geochronological methods using the U–Pb decay scheme (e.g. laser ablation ICPMS). Error z includes the ^{238}U decay constant uncertainty (Jaffey et al. 1971). It should be considered when comparing our dates with those derived from other decay schemes (e.g. $^{40}Ar/^{39}Ar$, $^{187}Re–^{187}Os$).

Results

Six zircon grains from a tuff at 182.84 to 183.04 m yielded equivalent CA-TIMS $^{206}Pb/^{238}U$ dates with a weighted mean of 158.86 ± 0.04 / 0.09 / 0.19 Ma (MSWD = 1.5, probability of fit = 0.18). This is the interpreted age of ash deposition. Thirty-one of thirty-two LA-ICPMS analyses yielded equivalent $^{206}Pb/^{238}U$ dates with a weighted mean of 163 ± 4 Ma (MSWD = 1.2, probability of fit = 0.20). Seven zircon grains from a tuff at 396.41 to 396.46 m yielded equivalent CA-TIMS $^{206}Pb/^{238}U$ dates with a weighted mean of 162.55 ± 0.05 / 0.09 / 0.20 Ma (MSWD = 0.6, probability of fit = 0.74). This is the interpreted age of ash deposition. Three other grains yielded dates of 162.8 ± 0.1, 169.9 ± 0.2 and 171.2 ± 0.2 Ma. Twenty four of twenty-seven LA-ICPMS analyses yielded equivalent $^{206}Pb/^{238}U$ dates with a weighted mean of 166 ± 5 Ma (MSWD = 1.0, probability of fit = 0.43). Three other LA-ICPMS analyses yielded equivalent $^{206}Pb/^{238}U$ dates with a weighted mean of 184 ± 11 Ma (MSWD = 0.6, probability of fit = 0.83).

Table 1. U-Pb isotopic CA-TIMS data. Avaliable as supplementary material in the Australian Journal of Earth Sciences http://www.tandfonline.com/doi/full/10.1080/08120099.2015.1106975, or on the USB associated with this thesis.

Table 2. U-Pb geochronologic analyses and trace element concentrations. supplementary material in the Australian Journal of Earth Sciences http://www.tandfonline.com/doi/full/10.1080/08120099.2015.1106975, or on the USB associated with this thesis.

Figure 1. Cathodoluminescence (CL) images of selected zircons extracted from the two tuff samples from Stratheden 4. Grains dated by CA-TIMS and spot analysed by LA-ICPMS are shown.

Wainman et al. 2015. Australian Journal of Earth Sciences 62/7
http://dx.doi.org/10.1080/08120099.2015.1106975

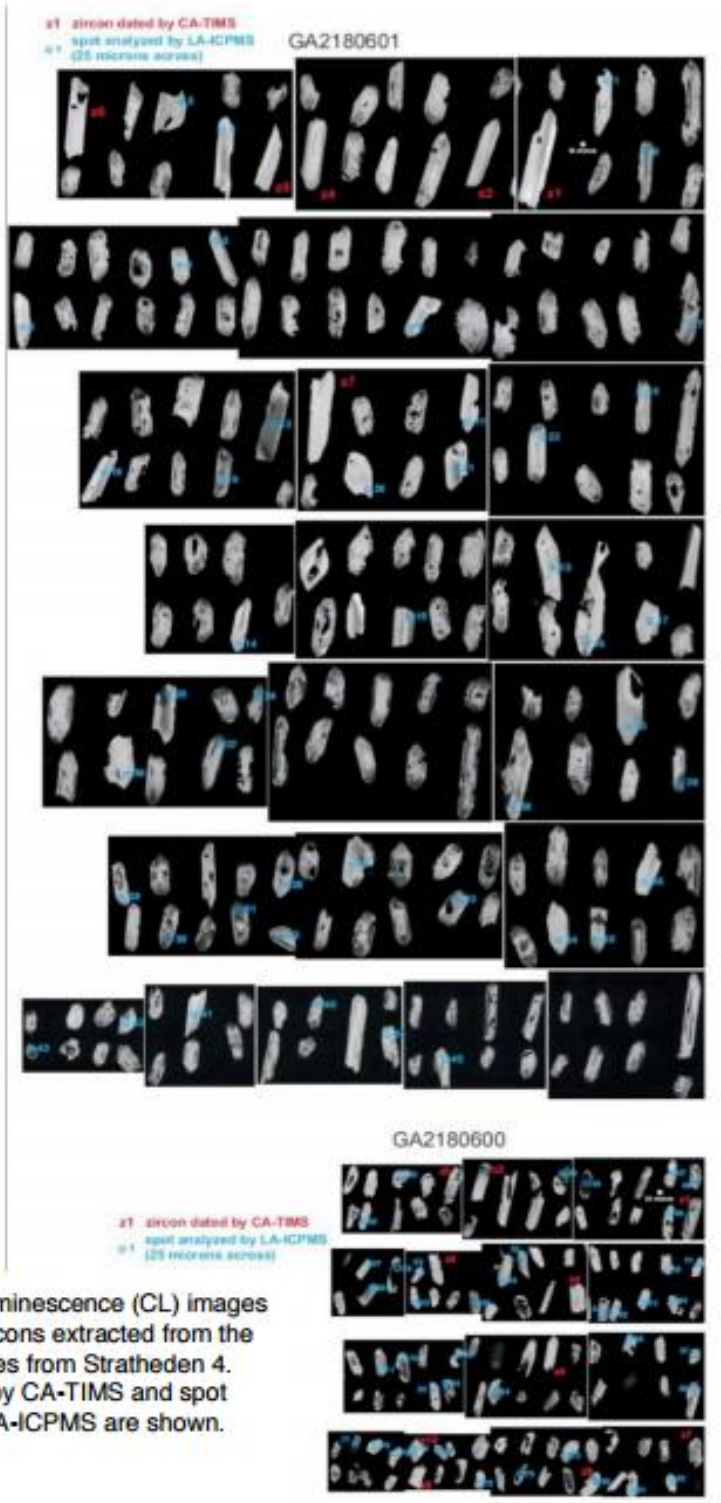

Figure 1 Cathodoluminescence (CL) images of selected zircons extracted from the two tuff samples from Stratheden 4. Grains dated by CA-TIMS and spot analysed by LA-ICPMS are shown.

Appendices 2.

LA-ICPMS methods

Zircon from ten samples of tuff were separated using standard techniques and annealed at 900^{o}C for 60 hours in a muffle furnace. Zircon from ten samples were analysed by LA-ICPMS. In two samples, sharply faceted and round grains were mounted separately. Grains were mounted in epoxy and polished until their centers were exposed. Cathodoluminescence (CL) images were obtained with a JEOL JSM-1300 scanning electron microscope and Gatan MiniCL. Zircon was analysed by laser ablation inductively coupled plasma mass spectrometry (LA-ICPMS) using a ThermoElectron X-Series II quadrupole ICPMS and New Wave Research UP-213 Nd:YAG UV (213 nm) laser ablation system. In-house analytical protocols, standard materials, and data reduction software were used for acquisition and calibration of U-Pb dates and a suite of high field strength elements (HFSE) and rare earth elements (REE). Zircon was ablated with a laser spot of 25 µm wide using fluence and pulse rates of 5 J/cm^2 and 10 Hz, respectively, during a 45 second analysis (15 sec gas blank, 30 sec ablation) that excavated a pit ~25 µm deep. Ablated material was carried by a 1.2 L/min He gas stream to the nebulizer flow of the plasma. Dwell times were 5 ms for Si and Zr, 200 ms for ^{49}Ti and ^{207}Pb, 80 ms for ^{206}Pb, 40 ms for ^{202}Hg, ^{204}Pb, ^{208}Pb, ^{232}Th, and ^{238}U and 10 ms for all other HFSE and REE. Background count rates for each analyte were obtained prior to each spot analysis and subtracted from the raw count rate for each analyte. Ablations pits that appear to have intersected glass or mineral inclusions were identified based on Ti and P. U-Pb dates from these analyses are considered valid if the U-Pb ratios appear to have been unaffected by the inclusions. Analyses that appear contaminated by common Pb were rejected based on mass 204 being above baseline. For concentration calculations, background-subtracted count rates for each analyte were internally normalised to ^{29}Si and calibrated with respect to NIST SRM-610 and -612 glasses as the primary standards. Temperature was calculated from the Ti-in-zircon thermometer (Watson et al. 2006). Because there are no constraints on the activity of TiO_2, an average value in crustal rocks of 0.8 was used.

Data were collected in five experiments from February 2015 to August 2016 (Table 1). For U-Pb and $^{207}Pb/^{206}Pb$ dates, instrumental fractionation of the background-subtracted ratios was corrected and dates were calibrated with respect to interspersed measurements of zircon standards and reference materials. The primary standard Plešovice zircon (Sláma et al. 2008) was used to monitor time-dependent instrumental fractionation based on two analyses for every 10 analyses of unknown zircon. A secondary correction to the $^{206}Pb/^{238}U$ dates was made based on results from the zircon standards Seiland (530 Ma, unpublished data, Boise State University) and Zirconia (327 Ma, unpublished data, Boise State University), which were treated as unknowns and measured once for every 10 analyses of unknown zircon. These results showed a linear age bias of up to 2% that is related to the ^{206}Pb count rate. The secondary correction is thought to mitigate matrix-dependent variations due to contrasting compositions and ablation characteristics between the Plešovice zircon and other standards (and unknowns).

Radiogenic isotope ratio and age error propagation for all analyses includes uncertainty contributions from counting statistics and background subtraction. Weighted mean $^{206}Pb/^{238}U$ dates are calculated from equivalent dates (i.e., probability of fit >0.05) that are at the young end of age spectra. A weighted mean date is first calculated using Isoplot 3.0 (Ludwig 2003) using errors on individual dates that do not include a standard calibration uncertainty, and then a standard calibration uncertainty is propagated into the error on the weighted mean date. This uncertainty is the local standard deviation of the polynomial fit to the interspersed primary standard measurements versus time for the time-dependent, relatively larger U/Pb fractionation factor, and the standard error of the mean of the consistently time-invariant and smaller $^{207}Pb/^{206}Pb$ fractionation factor. These uncertainties are 1.1-2.2% (2□) for $^{206}Pb/^{238}U$ and 0.3-1.5% (2□) for $^{207}Pb/^{206}Pb$. Age interpretations are based on $^{207}Pb/^{206}Pb$ dates for >1000 Ma zircon. The $^{206}Pb/^{238}U$ dates are used for <1000 Ma zircon. Errors on the $^{207}Pb/^{206}Pb$ and $^{206}Pb/^{238}U$ dates from individual analyses are given at 2□, as are the errors on the weighted mean dates.

CA-TIMS methods

U-Pb dates were obtained by the chemical abrasion isotope dilution thermal ionization mass spectrometry (CA-TIMS) method from analyses composed of single zircon grains (Table 2), modified after Mattinson (2005). Zircon was separated from 32 tuff samples using standard techniques. Only sharply faceted grains were selected for CA-TIMS dating. Grains were large enough in 20 samples to be mounted in epoxy and polished until the centers of the grains were exposed. Cathodoluminescence (CL) images were obtained with a JEOL JSM-1300 scanning electron microscope and Gatan MiniCL. Zircon in ten samples was analysed by LA-ICPMS. Eight were removed from the epoxy mounts for CA-TIMS dating based on the LA-ICPMS dates. For the 14 samples without LA-ICPMS data, the grains were removed from the epoxy mounts for CA-TIMS dating based CL images. Grains with homogeneous CL images from a dominant population were preferentially selected. For the ten samples without CL images, sharply faceted grains were randomly selected.

Zircon was placed in a muffle furnace at 900°C for 60 hours in quartz beakers. Single grains were then transferred to 3 ml Teflon PFA beakers and loaded into 300 □l Teflon PFA microcapsules. Fifteen microcapsules were placed in a large-capacity Parr vessel and the grains partially dissolved in 120 □l of 29 M HF for 12 hours at 180°C. The contents of the microcapsules were returned to 3 ml Teflon PFA beakers, HF removed, and the residual grains immersed in 3.5 M HNO_3, ultrasonically cleaned for an hour, and fluxed on a hotplate at 80°C for an hour. The HNO_3 was removed and grains were rinsed twice in ultrapure H_2O before being reloaded into the 300 □l Teflon PFA microcapsules (rinsed and fluxed in 6 M HCl during sonication and washing of the grains) and spiked with the EARTHTIME mixed ^{233}U-^{235}U-^{205}Pb tracer solution. Zircon was dissolved in Parr vessels in 120 □l of 29 M HF with a trace of 3.5 M HNO_3 at 220°C for 48 hours, dried to fluorides, and re-dissolved in 6 M HCl at 180°C overnight. U and Pb were separated from the zircon matrix using an HCl-based anion-exchange chromatographic procedure (Krogh 1973) eluted together and dried with 2 µl of 0.05 N H_3PO_4.

Pb and U were loaded on a single outgassed Re filament in 5 µl of a silica-gel/phosphoric acid mixture (Gerstenberger and Haase 1997) and U and Pb isotopic measurements made on a GV Isoprobe-T multicollector thermal ionization mass spectrometer equipped with an ion-counting Daly detector. Pb isotopes were measured by peak-jumping all isotopes on the Daly detector for 160 cycles, and corrected for 0.16 ± 0.03%/a.m.u. (1 sigma error) mass fractionation. Transitory isobaric interferences due to high-molecular weight organics, particularly on ^{204}Pb and ^{207}Pb, disappeared within approximately 30 cycles, while ionization efficiency averaged 10^4 cps/pg of each Pb isotope. Linearity (to ≥1.4 x 10^6 cps) and the associated deadtime correction of the Daly detector were monitored by repeated analyses of NBS982, and have been constant since installation. Uranium was analyzed as UO_2^+ ions in static Faraday mode on 10^{12} ohm resistors for 300 cycles, and corrected for isobaric interference of $^{233}U^{18}O^{16}O$ on $^{235}U^{16}O^{16}O$ with an $^{18}O/^{16}O$ of 0.00206. Ionization efficiency averaged 20 mV/ng of each U isotope. U mass fractionation was corrected using the known $^{233}U/^{235}U$ ratio of the EARTHTIME tracer solution.

CA-TIMS U-Pb dates and uncertainties were calculated using the algorithms of Schmitz and Schoene (2007), EARTHTIME ET535 tracer solution with calibration of $^{235}U/^{205}Pb$ = 100.233, $^{233}U/^{235}U$ = 0.99506, and $^{205}Pb/^{204}Pb$ = 11268, and U decay constants recommended by Jaffey et al. (1971). $^{206}Pb/^{238}U$ ratios and dates were corrected for initial ^{230}Th disequilibrium using a Th/U[magma] = 3.0 ± 0.3 using the algorithms of Crowley et al. (2007), resulting in an increase in the $^{206}Pb/^{238}U$ dates of ~0.09 Ma. All common Pb in analyses was attributed to laboratory blank and subtracted based on the measured laboratory Pb isotopic composition and associated uncertainty. U blanks are estimated at 0.02 pg.

An average of 7.8 grains per tuff were analyzed, with the age of tuff deposition being interpreted from an average of 5.0 grains per sample. In eight of the 30 tuffs, all analyzed grains yielded equivalent dates (i.e., probability of fit >0.05). For these samples, weighted mean $^{206}Pb/^{238}U$ dates were calculated from all dates using Isoplot 3.0 (Ludwig 2003) and interpreted as the ages of tuff deposition. For 21 of the other 22 samples, ages of tuff deposition are interpreted from weighted mean $^{206}Pb/^{238}U$ dates from equivalent dates (i.e., probability of fit >0.05) that are at the young end of age spectra. The older

dates are interpreted as being from detrital grains that were incorporated into the tuff after deposition or grains with extended residence histories in the magma chamber or were inherited in the magma chamber. For the one sample in which there are no equivalent dates, the youngest analysis is considered the maximum age of deposition.

Errors on the weighted mean dates are given as ± x / y / z, where x is the internal error based on analytical uncertainties only, including counting statistics, subtraction of tracer solution, and blank and initial common Pb subtraction, y includes the tracer calibration uncertainty propagated in quadrature, and z includes the ^{238}U decay constant uncertainty propagated in quadrature. Internal errors should be considered when comparing our dates with ^{206}Pb/^{238}U dates from other laboratories that used the same EARTHTIME tracer solution or a tracer solution that was cross-calibrated using EARTHTIME gravimetric standards. Errors including the uncertainty in the tracer calibration should be considered when comparing our dates with those derived from other geochronological methods using the U-Pb decay scheme (e.g., laser ablation ICPMS). Errors including uncertainties in the tracer calibration and ^{238}U decay constant (Jaffey et al. 1971) should be considered when comparing our dates with those derived from other decay schemes (e.g., ^{40}Ar/^{39}Ar, ^{187}Re-^{187}Os). Errors for weighted mean dates and dates from individual grains are given at 2□.

U-Pb geochronology results

Data are presented by well and location, from east to west. Zircon from all samples were mounted for CL imaging (Appendices Figures 1 to 23b), except where noted that the grains were too small for mounting. Plots of ^{206}Pb/^{238}U CA-TIMS dates are shown in Figure 24.

Mt. Lindesay 1

Six zircon grains from a tuff at 151.23 to 151.30 m (2389974) were analyzed. The five youngest yielded equivalent CA-TIMS dates with a weighted mean of 155.38 ± 0.07 / 0.11 / 0.20 Ma (MSWD = 1.4, probability of fit = 0.23). This is the interpreted age of ash deposition. An older date is 155.88 ± 0.16 Ma.

Kalbar 1

Ten zircon grains from a tuff at 400.50 to 400.67 m (2233282) were analyzed. Grains were too small for mounting and CL imaging. The four youngest yielded equivalent CA-TIMS dates with a weighted mean of 167.56 ± 0.06 / 0.10 / 0.21 Ma (MSWD = 2.2, probability of fit = 0.08). This is the interpreted age of ash deposition. Older dates are 167.84 ± 0.14 to 168.28 ± 0.15 Ma.

Turallin 1

Six zircon grains from a tuff at 185.37 to 185.66 m (2254136) yielded equivalent CA-TIMS dates with a weighted mean of 164.74 ± 0.04 / 0.09 / 0.20 Ma (MSWD = 0.3, probability of fit = 0.91). This is the interpreted age of ash deposition.

Stratheden 4

Seven zircon grains from a tuff at 396.41 to 396.46 m (2180600) were analyzed by Wainman et al. (2015). The seven youngest yielded equivalent CA-TIMS dates with a weighted mean of 162.54 ± 0.05 / 0.09 / 0.20 Ma (MSWD = 0.6, probability of fit = 0.74). This is the interpreted age of ash deposition. Older dates are 162.81 ± 0.14 to 171.18 ± 0.21 Ma. Thirty-two zircon grains were analyzed by LA-ICPMS. The youngest 24 analyses yielded equivalent dates with a weighted mean of 160.8 ± 4.3 Ma (MSWD = 0.7, probability of fit = 0.90). Older dates are 171.5 ± 16.8 to 182.2 ± 13.1 Ma.

Six zircon grains from a tuff at 209.62 to 209.87 m (2231585) yielded equivalent CA-TIMS dates with a weighted mean of 159.69 ± 0.04 / 0.09 / 0.19 Ma (MSWD = 1.0, probability of fit = 0.41). This is the interpreted age of ash deposition.

Six zircon grains from a tuff at 182.84 to 183.04 m (2180601) were analyzed by Wainman et al. (2015). All grains yielded equivalent CA-TIMS dates with a weighted mean of 158.86 ± 0.04 / 0.09 / 0.19 Ma (MSWD = 1.5, probability of fit = 0.18). This is the interpreted age of ash deposition. Twenty-seven zircon grains were analyzed by LA-ICPMS. The youngest 18 analyses yielded

equivalent dates with a weighted mean of 163.0 ± 4.7 Ma (MSWD = 0.6, probability of fit = 0.93). Older dates are 173.0 ± 14.3 to 183.8 ± 17.5 Ma.

Stratheden 60

Twelve zircon grains from a tuff at 477.64 to 477.70 m (2231590) were analyzed. The three youngest yielded equivalent CA-TIMS dates with a weighted mean of 168.07 ± 0.07 / 0.11 / 0.21 Ma (MSWD = 1.7, probability of fit = 0.18). This is the interpreted age of ash deposition. Older dates are 168.32 ± 0.14 to 172.97 ± 0.12 Ma. Twenty-eight zircon grains were analyzed by LA-ICPMS. The youngest 15 analyses yielded equivalent dates with a weighted mean of 171.1 ± 3.4 Ma (MSWD = 1.3, probability of fit = 0.21). Older dates are 185.8 ± 9.0 to 3392 ± 21 Ma.

Nine zircon grains from a tuff at 324.24 to 324.31 m (2231589) were analyzed. The five youngest yielded equivalent CA-TIMS dates with a weighted mean of 162.18 ± 0.06 / 0.10 / 0.20 Ma (MSWD = 1.1, probability of fit = 0.37). This is the interpreted age of ash deposition. Older dates are 162.43 ± 0.12 to 162.69 ± 0.13 Ma. Forty-six zircon grains were analyzed by LA-ICPMS. The youngest 44 analyses yielded equivalent dates with a weighted mean of 161.4 ± 2.9 Ma (MSWD = 0.9, probability of fit = 0.56). Older dates are 177.6 ± 11.7 and 183.1 ± 12.1 Ma.

Nine zircon grains from a tuff at 247.61 to 247.66 m (2231588) were analyzed. Grains were too small for mounting and CL imaging. The two youngest yielded equivalent CA-TIMS dates with a weighted mean of 160.54 ± 0.12 / 0.14 / 0.22 Ma (MSWD = 1.3, probability of fit = 0.25). This is the interpreted age of ash deposition. Older dates are 161.03 ± 0.19 to 343.27 ± 6.05 Ma.

Nine zircon grains from a tuff at 212.50 to 212.50 m (2254143) were analyzed. The seven youngest yielded equivalent CA-TIMS dates with a weighted mean of 160.45 ± 0.05 / 0.09 / 0.19 Ma (MSWD = 1.5, probability of fit = 0.18). This is the interpreted age of ash deposition. Older dates are 160.65 ± 0.13 and 160.90 ± 0.11 Ma.

Six zircon grains from a tuff at 135.86 to 136.11 m (2254141) yielded equivalent CA-TIMS dates with a weighted mean of 159.02 ± 0.04 / 0.09 / 0.19 Ma (MSWD = 1.8, probability of fit = 0.10). This is the interpreted age of ash deposition.

Wyalla 3

Ten zircon grains from a tuff at 345.54 to 354.60 m (2254151) were analyzed. The four youngest yielded equivalent CA-TIMS dates with a weighted mean of 163.16 ± 0.06 / 0.10 / 0.20 Ma (MSWD = 0.4, probability of fit = 0.72). This is the interpreted age of ash deposition. Older dates are 163.38 ± 0.10 to 166.13 ± 0.18 Ma.

Six zircon grains from a tuff at 127.3 to 127.4 m (2254147) yielded equivalent CA-TIMS dates with a weighted mean of 159.67 ± 0.04 / 0.09 / 0.19 Ma (MSWD = 2.2, probability of fit = 0.05). This is the interpreted age of ash deposition.

Alderley 1

Nine zircon grains from a tuff at 402.68 to 402.76 m (2254165) were analyzed. The six youngest yielded equivalent CA-TIMS dates with a weighted mean of 163.08 ± 0.05 / 0.09 / 0.20 Ma (MSWD = 0.5, probability of fit = 0.78). This is the interpreted age of ash deposition. Older dates are 163.44 ± 0.11 to 163.52 ± 0.13 Ma.

Ten zircon grains from a tuff at 156.13 to 156.17 m (2254160) were analyzed. The five youngest yielded equivalent CA-TIMS dates with a weighted mean of 157.55 ± 0.05 / 0.09 / 0.19 Ma (MSWD = 1.8, probability of fit = 0.13). This is the interpreted age of ash deposition. Older dates are 157.71 ± 0.14 to 160.02 ± 0.25 Ma. Thirty zircon grains were analyzed by LA-ICPMS. The youngest 25 analyses yielded equivalent dates with a weighted mean of 154.9 ± 3.2 Ma (MSWD = 1.2, probability of fit = 0.24). Older dates are 164.0 ± 8.4 to 167.8 ± 9.2 Ma.

Ten zircon grains from a tuff at 135.29 to 135.24 m (2254159) were analyzed. The three youngest yielded equivalent CA-TIMS dates with a

weighted mean of 152.99 ± 0.06 / 0.10 / 0.19 Ma (MSWD = 0.6, probability of fit = 0.55). This is the interpreted age of ash deposition. Older dates are 154.04 ± 0.11 to 181.35 ± 0.12 Ma. Forty-two zircon grains were analyzed by LA-ICPMS. The youngest 15 analyses yielded equivalent dates with a weighted mean of 150.9 ± 2.1 Ma (MSWD = 1.1, probability of fit = 0.32). Older dates are 156.1 ± 4.8 to 285.0 ± 6.7 Ma.

Guluguba 2

Nine zircon grains from a tuff at 509.40 to 509.43 m (2233310) were analyzed. The six youngest yielded equivalent CA-TIMS dates with a weighted mean of 165.93 ± 0.05 / 0.09 / 0.20 Ma (MSWD = 1.6, probability of fit = 0.17). This is the interpreted age of ash deposition. Older dates are 169.40 ± 0.12 to 519.20 ± 1.55 Ma.

Six zircon grains from a tuff at 428.51 to 428.57 m (2233308) were analyzed. The five youngest yielded equivalent CA-TIMS dates with a weighted mean of 163.05 ± 0.05 / 0.09 / 0.20 Ma (MSWD = 0.9, probability of fit = 0.46). This is the interpreted age of ash deposition. An older date is 163.37 ± 0.11 Ma.

Eight zircon grains from a tuff at 404.16 to 404.23 m (2233302) were analyzed. Grains were too small for mounting and CL imaging. The six youngest yielded equivalent CA-TIMS dates with a weighted mean of 162.40 ± 0.04 / 0.09 / 0.20 Ma (MSWD = 1.5, probability of fit = 0.19). This is the interpreted age of ash deposition. Older dates are 162.71 ± 0.12 to 162.86 ± 0.12 Ma.

Seven zircon grains from a tuff at 279.11 to 279.15 m (2233298) were analyzed. Grains were too small for mounting and CL imaging. The four youngest yielded equivalent CA-TIMS dates with a weighted mean of 159.92 ± 0.06 / 0.10 / 0.20 Ma (MSWD = 1.4, probability of fit = 0.23). This is the interpreted age of ash deposition. Older dates are 160.09 ± 0.12 to 160.15 ± 0.11 Ma.

Thirteen zircon grains from a tuff at 162.03 to 162.10 m (2233290) were analyzed. Grains were too small for mounting and CL imaging. The four youngest yielded equivalent CA-TIMS dates with a weighted mean of 157.97 ±

0.08 / 0.11 / 0.20 Ma (MSWD = 2.1, probability of fit = 0.10). This is the interpreted age of ash deposition. Older dates are 158.30 ± 0.12 to 678.64 ± 2.45 Ma.

Cameron 1

Five zircon grains from a tuff at 221.3 to 221.4 m (2389991) yielded equivalent CA-TIMS dates with a weighted mean of 157.70 ± 0.05 / 0.09 / 0.19 Ma (MSWD = 0.3, probability of fit = 0.88). This is the interpreted age of ash deposition.

Pleasant Hills 25

Five zircon grains from a tuff at 512.07 to 512.20 m (2390012) were analyzed. Grains were too small for mounting and CL imaging. The CA-TIMS dates are 151.39 ± 0.12 to 197.89 ± 0.34 Ma and none equivalent. The interpreted maximum age of ash deposition 151.39 ± 0.12 Ma.

Eight zircon grains from a tuff at 335.00 to 335.08 m (2390007) were analyzed. The seven youngest yielded equivalent CA-TIMS dates with a weighted mean of 150.79 ± 0.06 / 0.10 / 0.19 Ma (MSWD = 2.0, probability of fit = 0.06). This is the interpreted age of ash deposition. An older date is 151.10 ± 0.15 Ma.

Indy 4

Six zircon grains from a tuff at 201.59 to 202.00 m (2233272) were analyzed. The four youngest yielded equivalent CA-TIMS dates with a weighted mean of 152.90 ± 0.07 / 0.10 / 0.19 Ma (MSWD = 1.8, probability of fit = 0.14). This is the interpreted age of ash deposition. Older dates are 157.38 ± 0.41 to 188.06 ± 0.16 Ma.

Indy 3

Five zircon grains from a tuff at 159.57 to 159.76 m (2254172) yielded equivalent CA-TIMS dates with a weighted mean of 150.11 ± 0.04 / 0.09 / 0.18 Ma (MSWD = 1.2, probability of fit = 0.31). This is the interpreted age of ash deposition.

Eight zircon grains from a tuff at 139.97 to 140.38 m (2254170) were analyzed. Grains were too small for mounting and CL imaging. The seven youngest yielded equivalent CA-TIMS dates with a weighted mean of 149.78 ± 0.06 / 0.10 / 0.19 Ma (MSWD = 1.0, probability of fit = 0.41). This is the interpreted age of ash deposition. Older dates are 160.83 ± 0.39 and 190.05 ± 0.43 Ma.

Six zircon grains from a tuff at 104.40 to 140.62 m (2254169) yielded equivalent CA-TIMS dates with a weighted mean of 149.08 ± 0.06 / 0.09 / 0.18 Ma (MSWD = 1.1, probability of fit = 0.36). This is the interpreted age of ash deposition.

Zeus 7

Seven zircon grains from a tuff at 1677.31 to 1677.51 m (2550367) were analyzed. The three youngest yielded equivalent CA-TIMS dates with a weighted mean of 162.39 ± 0.06 / 0.10 / 0.20 Ma (MSWD = 2.5, probability of fit = 0.08). This is the interpreted age of ash deposition. Older dates are 162.57 ± 0.10 to 169.83 ± 0.11 Ma. Fifty-seven zircon grains were analyzed by LA-ICPMS. Thirty-one grains are sharply faceted and others are round. Ten of the youngest 11 analyses are from sharply faceted grains. These 11 analyses yielded equivalent dates with a weighted mean of 163.8 ± 2.2 Ma (MSWD = 1.5, probability of fit = 0.12). Older dates are 178.0 ± 7.3 to 2769 ± 29 Ma.

Eight zircon grains from a tuff at 1659.03 to 1659.31 m (2550364) were analyzed. The four youngest yielded equivalent CA-TIMS dates with a weighted mean of 161.11 ± 0.05 / 0.10 / 0.20 Ma (MSWD = 0.8, probability of fit = 0.47). This is the interpreted age of ash deposition. Older dates are 162.23 ± 0.09 to 166.36 ± 0.13 Ma. Fifty-eight zircon grains were analyzed by LA-ICPMS. Thirty-five grains are sharply faceted and others are round. Fourteen of the youngest 15 analyses are from sharply faceted grains. These 15 analyses yielded equivalent dates with a weighted mean of 160.7 ± 1.8 Ma (MSWD = 0.8, probability of fit = 0.73). Older dates are 174.1 ± 8.5 to 2692 ± 28 Ma.

Appendices

Table 1. LA-ICPMS isotopic U-Pb and trace element concentration data. Avaliable in AAPG Datashare 79 (online), or on the USB associated with this thesis.

Table 2. U-Pb CA-TIMS isotopic data. Avaliable in AAPG Datashare 79 (online), or on the USB associated with this thesis.

Figure 1. Cathodoluminescence (CL) images of selected zircons extracted from Mount Lindesay 1, 151.30 m (2389974). Grains dated by CA-TIMS are shown.

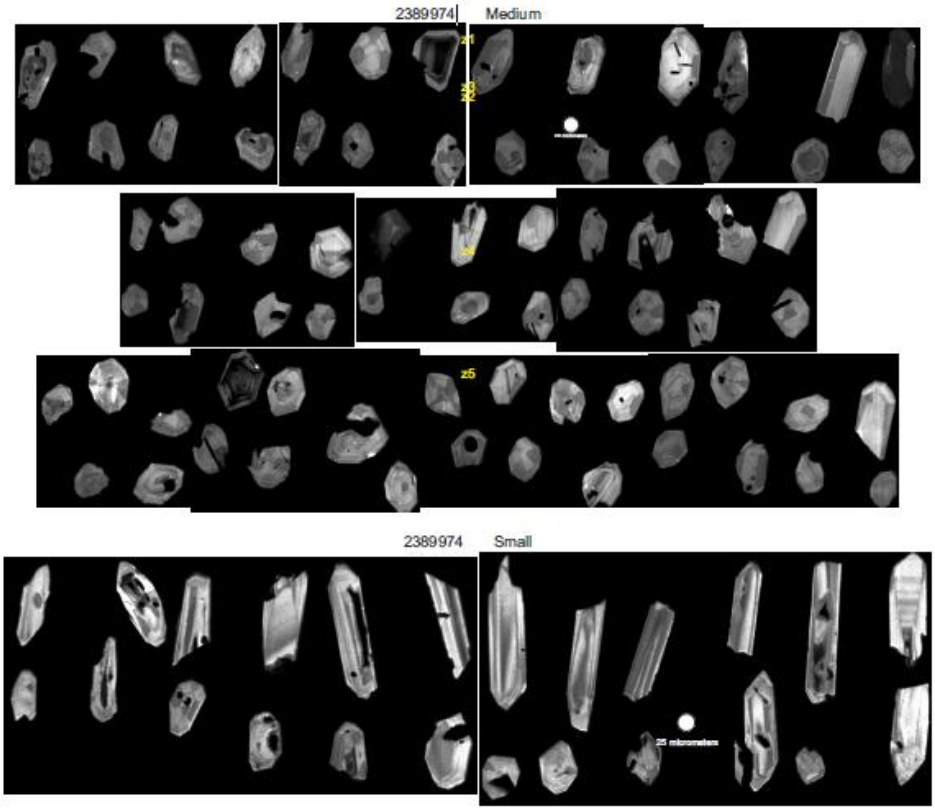

Figure 2. Cathodoluminescence (CL) images of selected zircons extracted from Turallin 1, 185.37 m (2254136). Grains dated by CA-TIMS are shown.

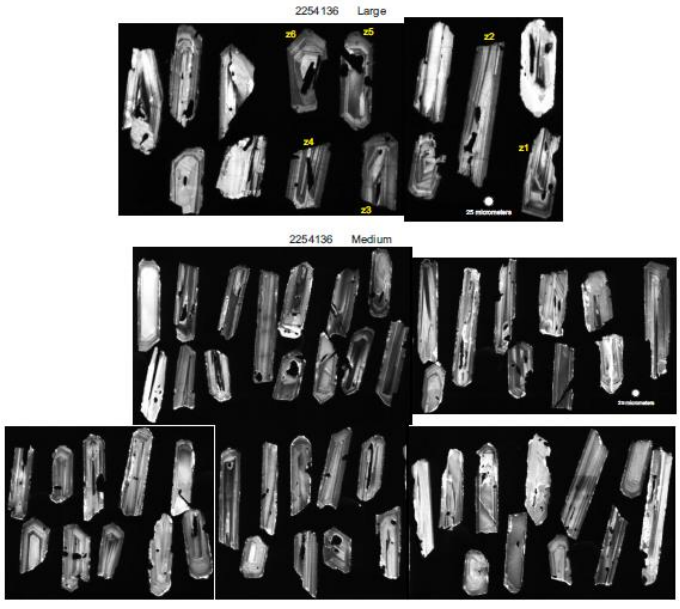

Figure 3. Cathodoluminescence (CL) images of selected zircons extracted from Stratheden 4, 209.87 m (2231585) from the study by Wainman et al. (2015). Grains dated by CA-TIMS are shown.

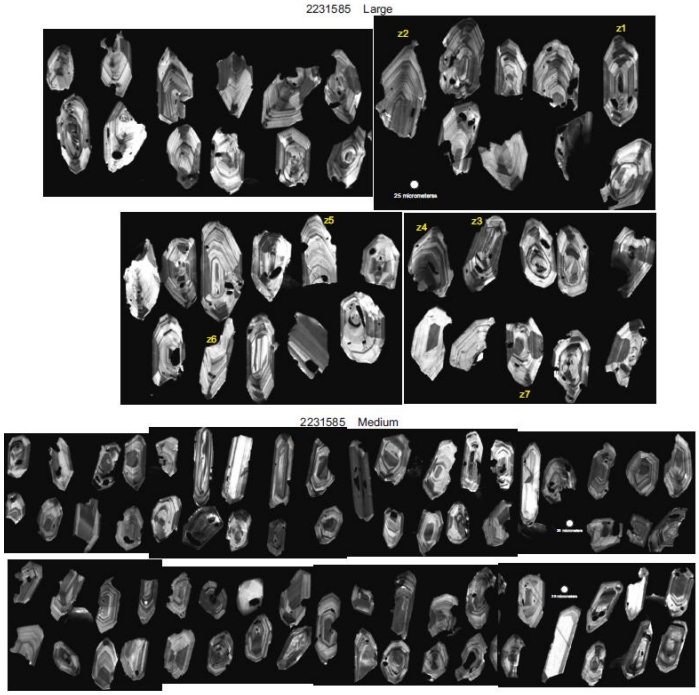

Figure 4. Cathodoluminescence (CL) images of selected zircons extracted from Stratheden 60, 477.70 m (2231590). Grains dated by CA-TIMS and spot analysed by LA-ICPMS are shown.

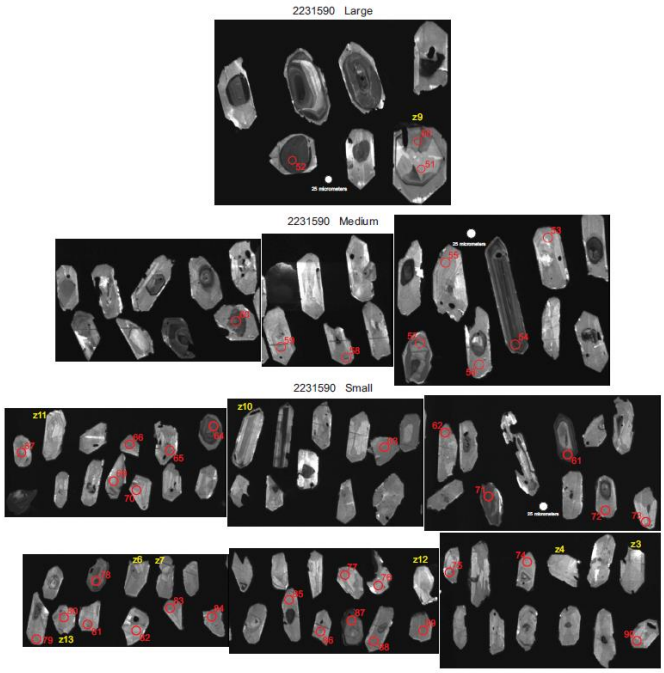

Figure 5. Cathodoluminescence (CL) images of selected zircons extracted from Stratheden 60, 342.24 m (2231589). Grains dated by CA-TIMS and spot analysed by LA-ICPMS are shown.

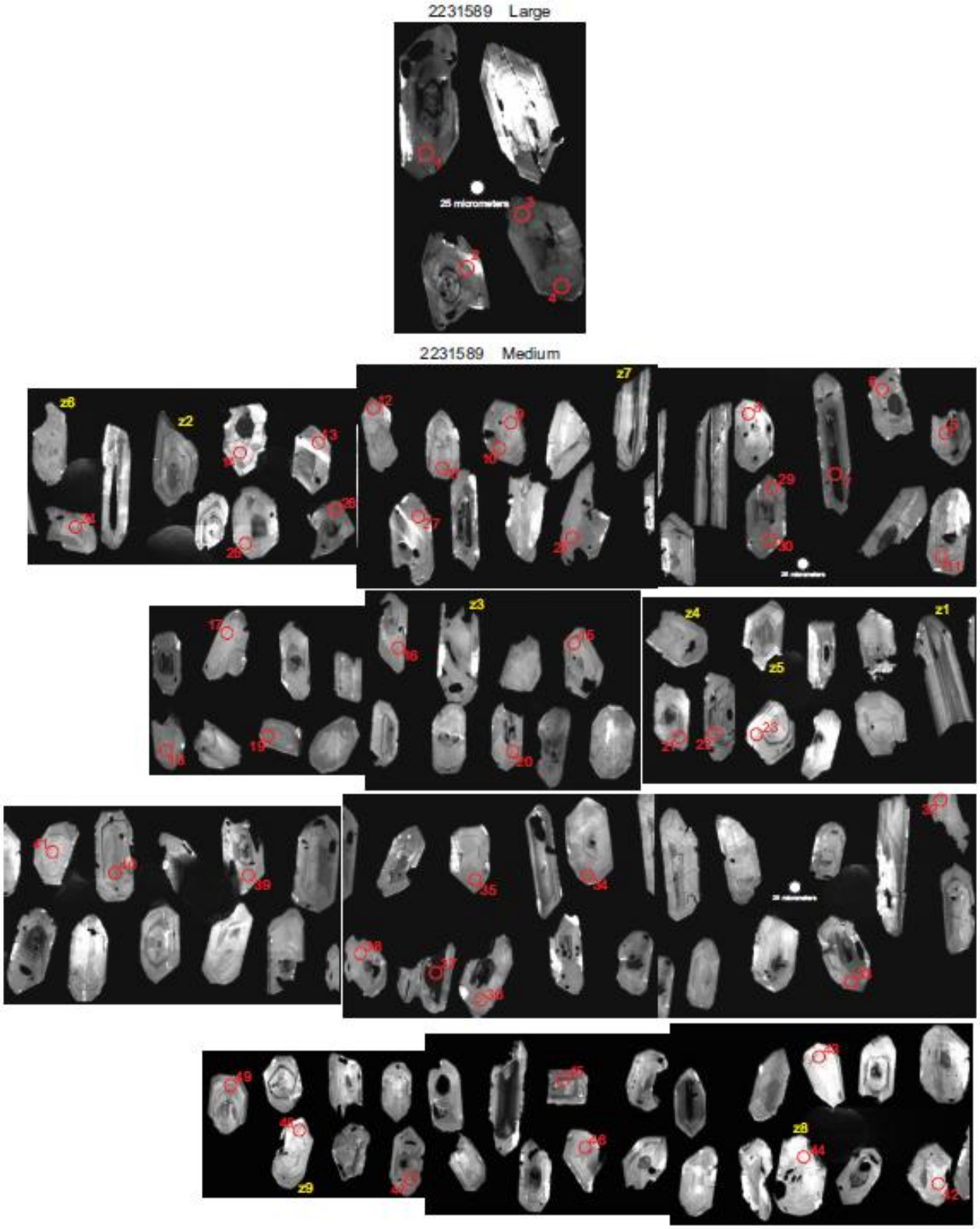

Figure 6. Cathodoluminescence (CL) images of selected zircons extracted from Stratheden 60, 212.50 m (2254143). Grains dated by CA-TIMS are shown.

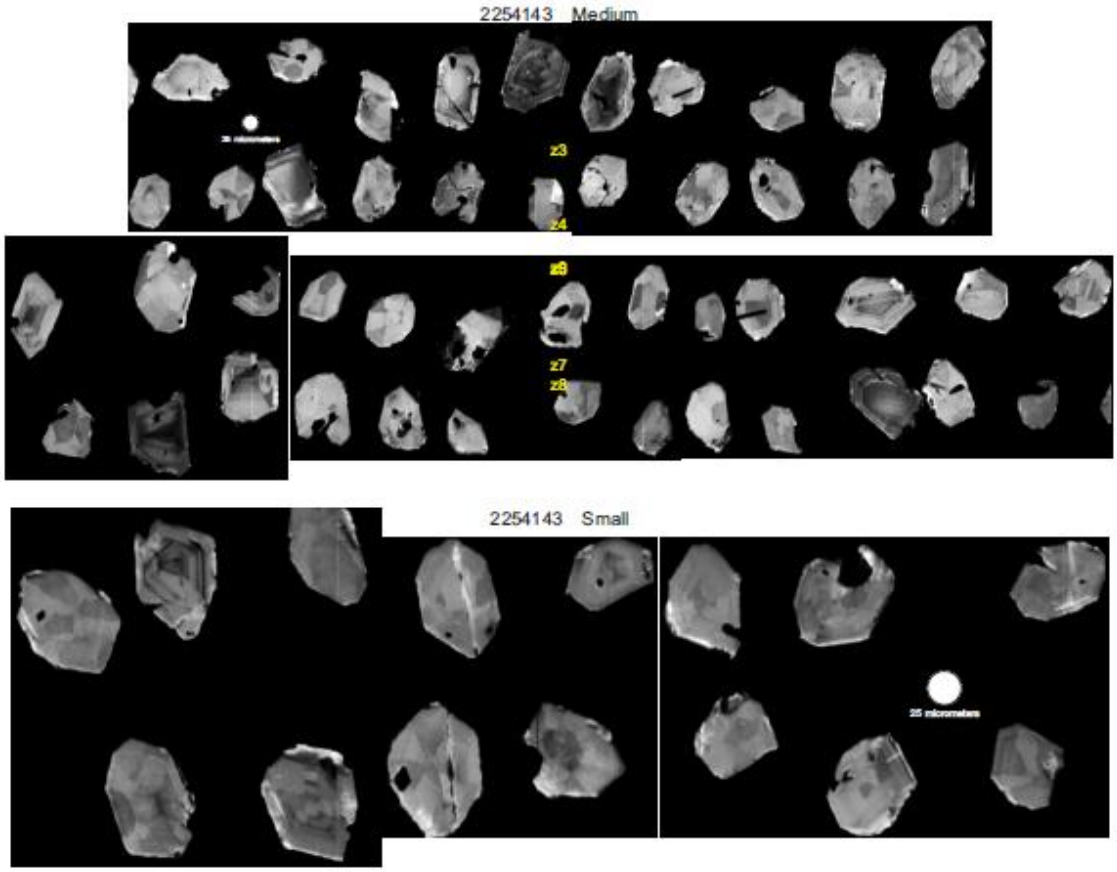

Figure 7. Cathodoluminescence (CL) images of selected zircons extracted from Stratheden 60, 136.86 m (2254141). Grains dated by CA-TIMS are shown.

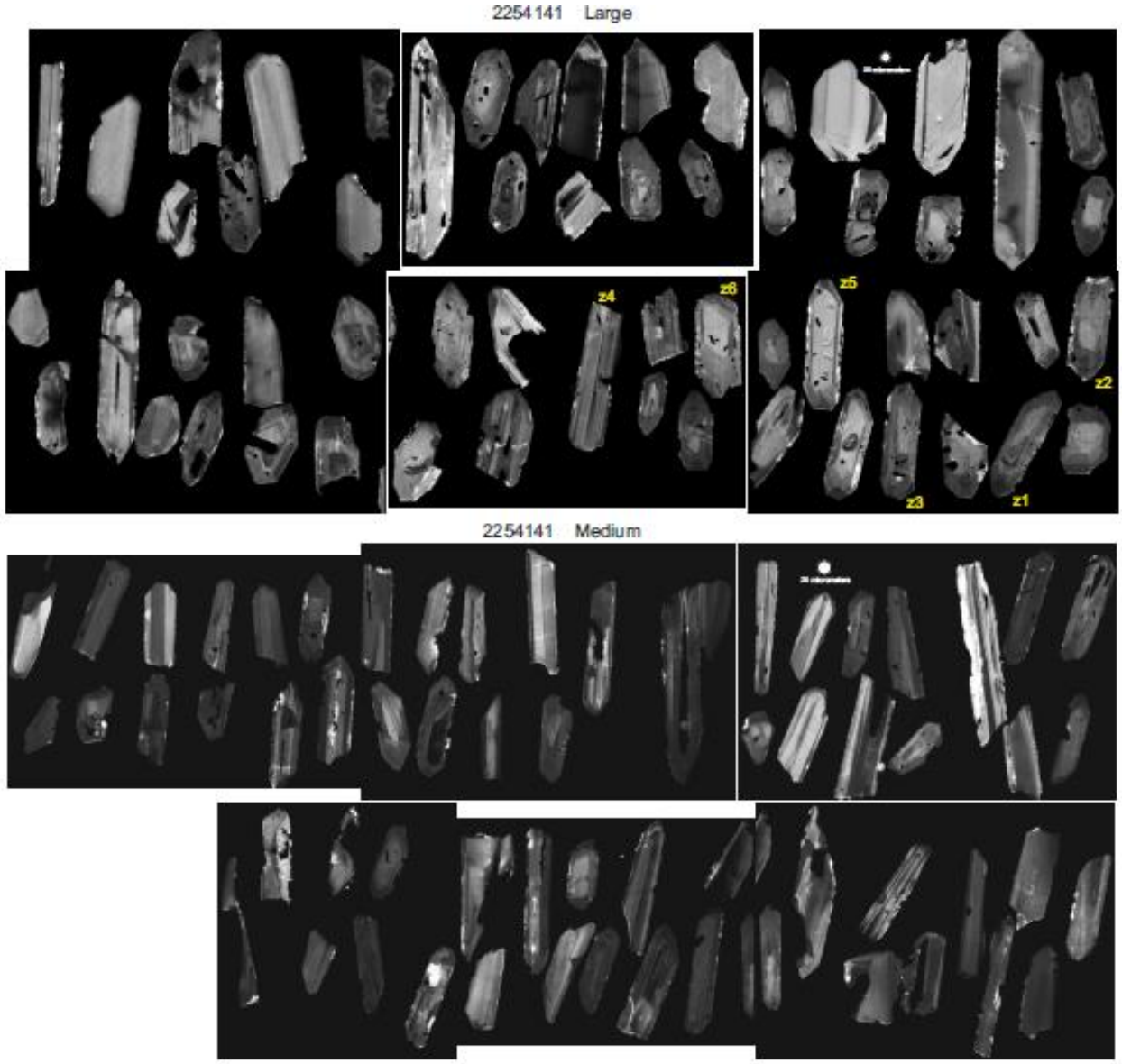

Figure 8. Cathodoluminescence (CL) images of selected zircons extracted from Wyalla 3, 345.60 m (2254151). Grains dated by CA-TIMS are shown.

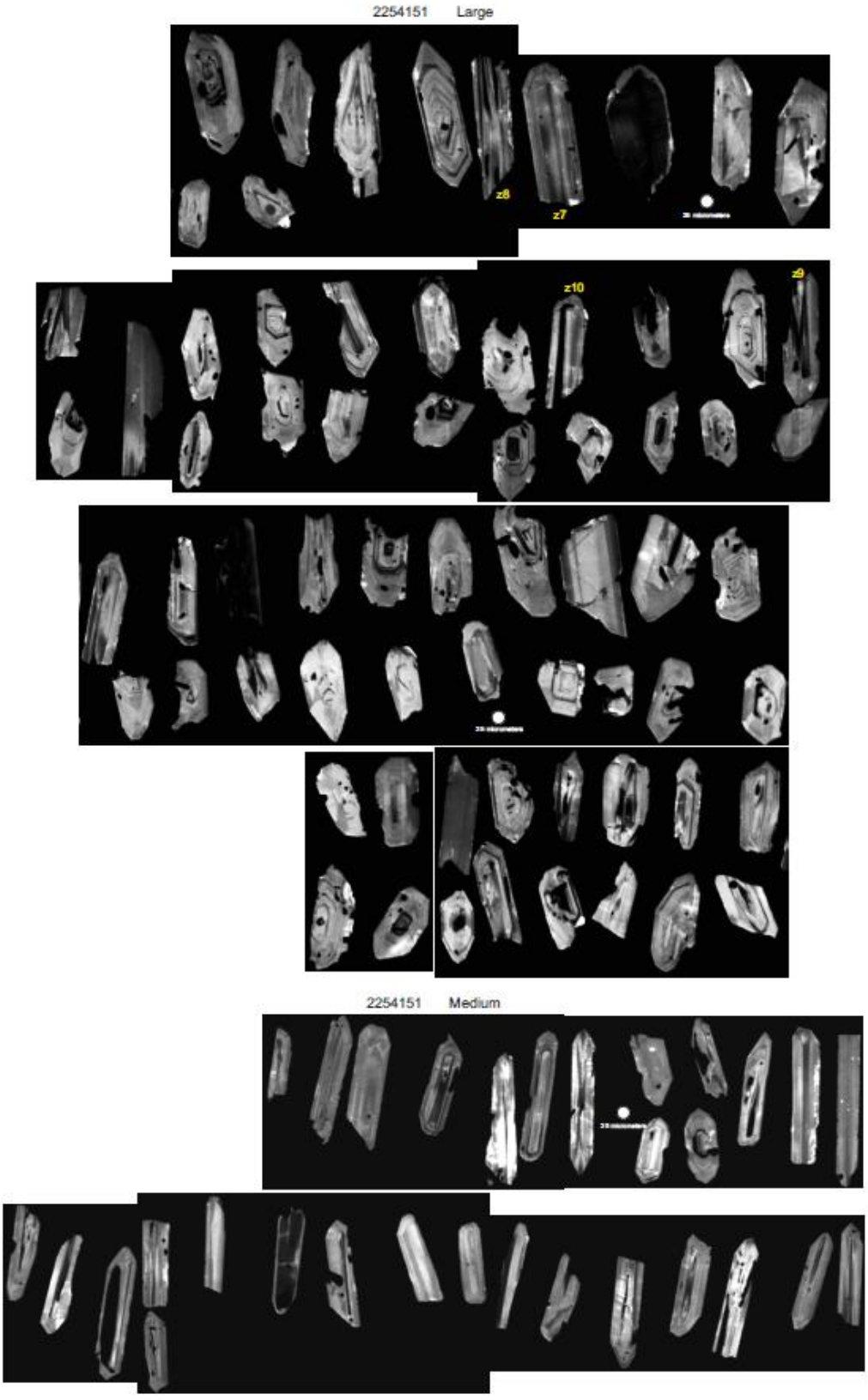

Figure 10. Cathodoluminescence (CL) images of selected zircons extracted from Wyalla 3, 127.40 m (2254147). Grains dated by CA-TIMS are shown.

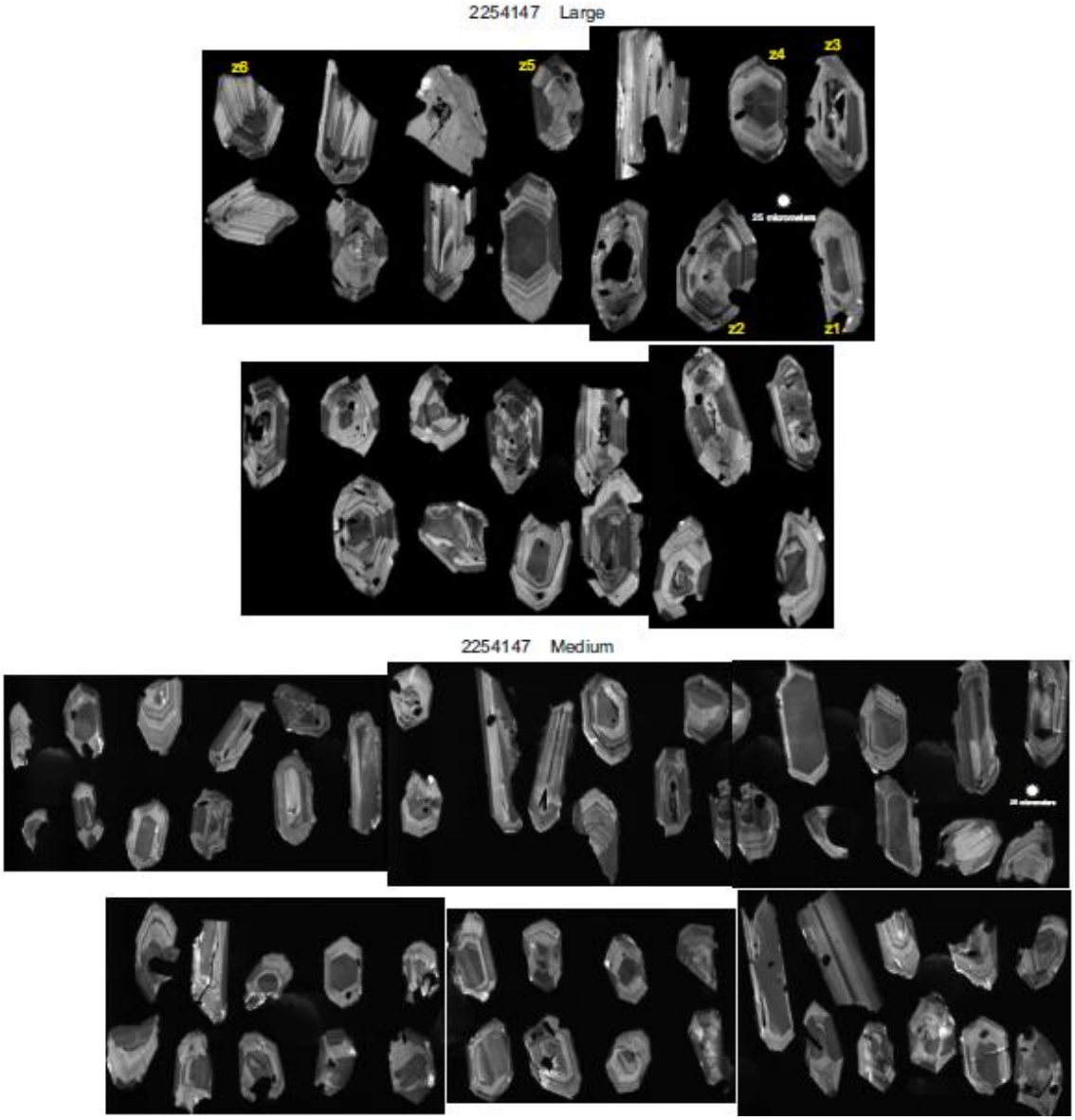

Figure 11. Cathodoluminescence (CL) images of selected zircons extracted from Alderley 1, 402.76 m (2254165). Grains dated by CA-TIMS are shown.

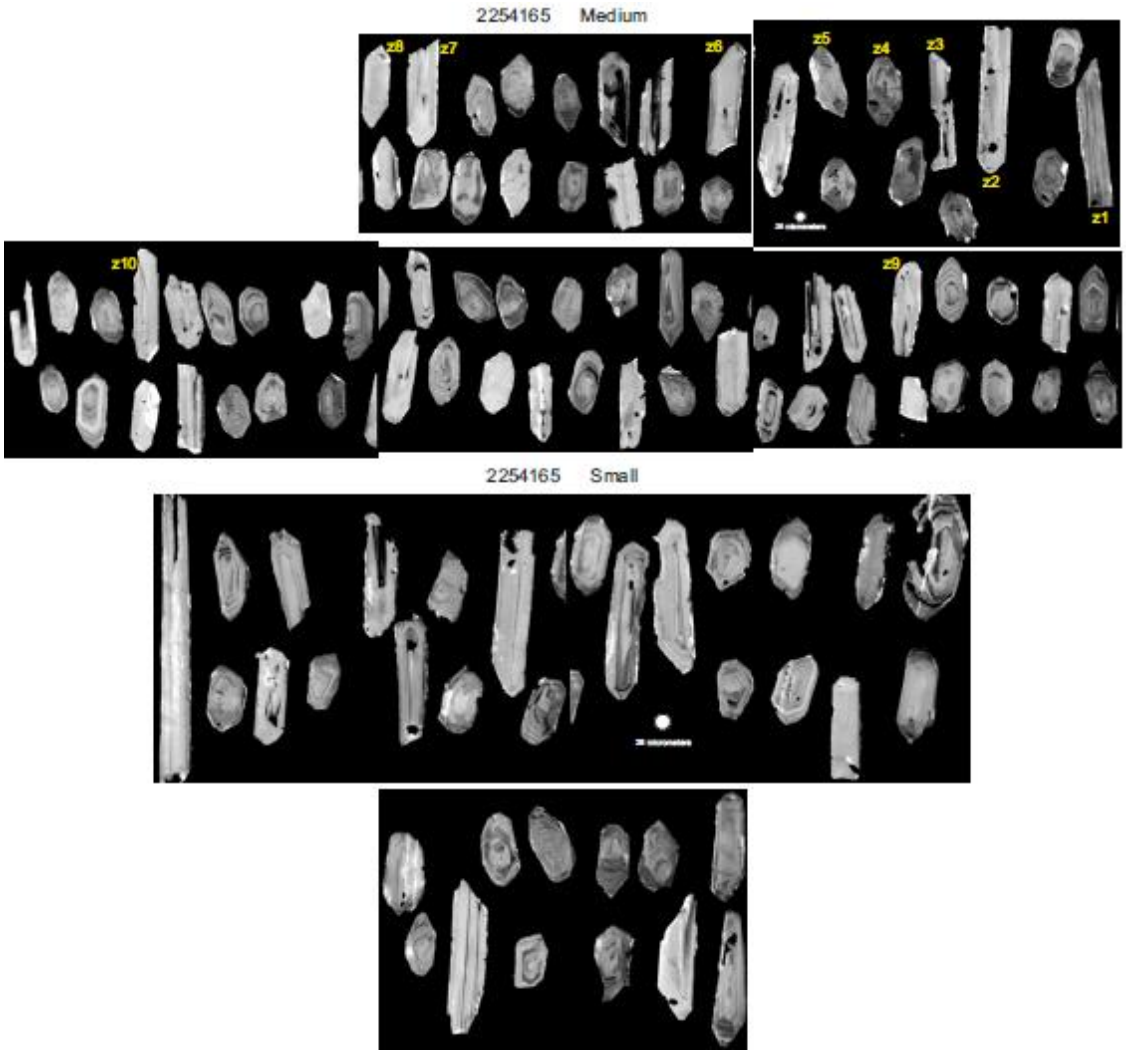

Figure 12. Cathodoluminescence (CL) images of selected zircons extracted from Alderley 1, 156.17 m (224160). Grains dated by CA-TIMS and spot analysed by LA-ICPMS are shown.

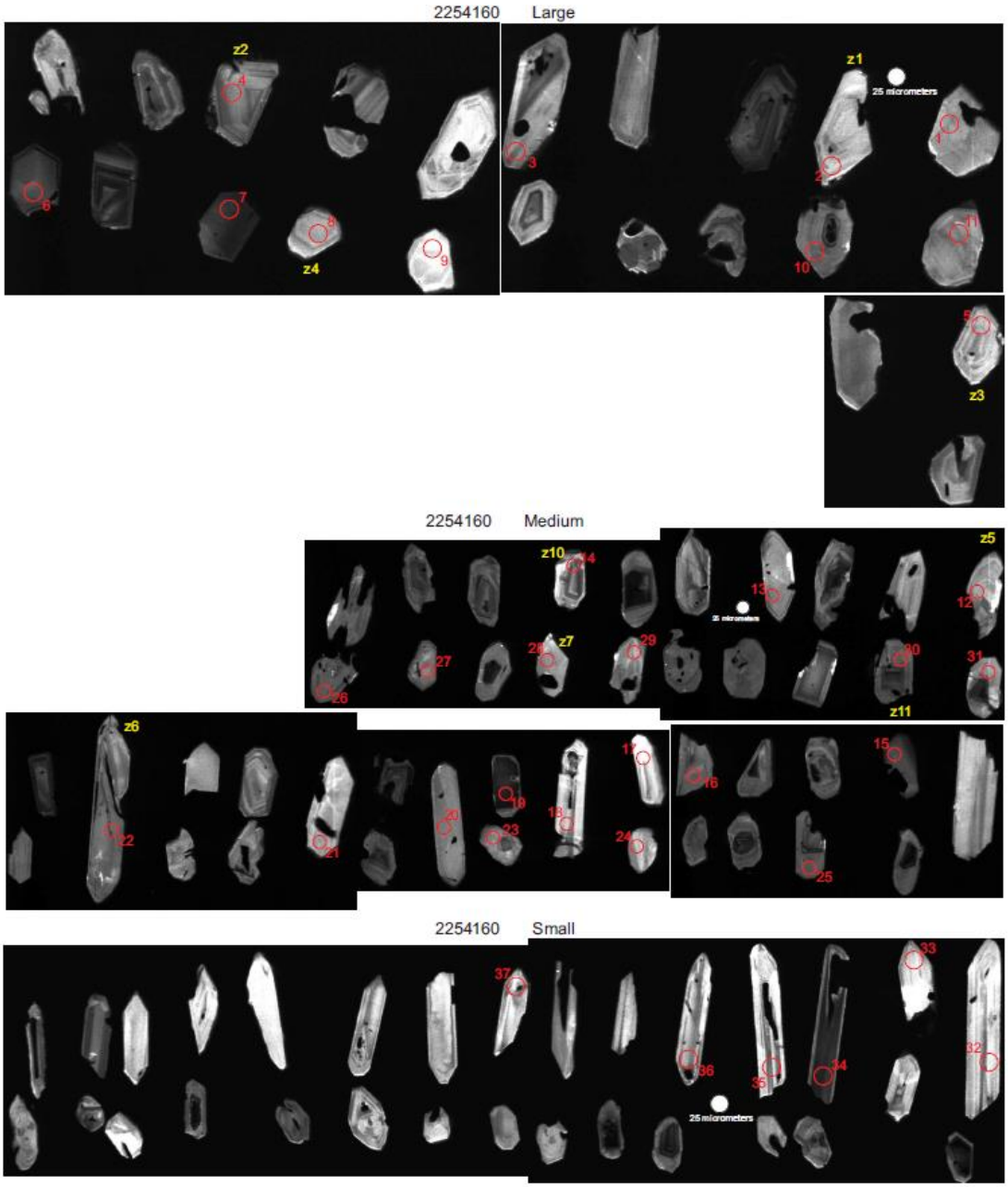

Figure 13. Cathodoluminescence (CL) images of selected zircons extracted from Alderley 1, 135.29 m (2251459). Grains dated by CA-TIMS and spot analysed by LA-ICPMS are shown.

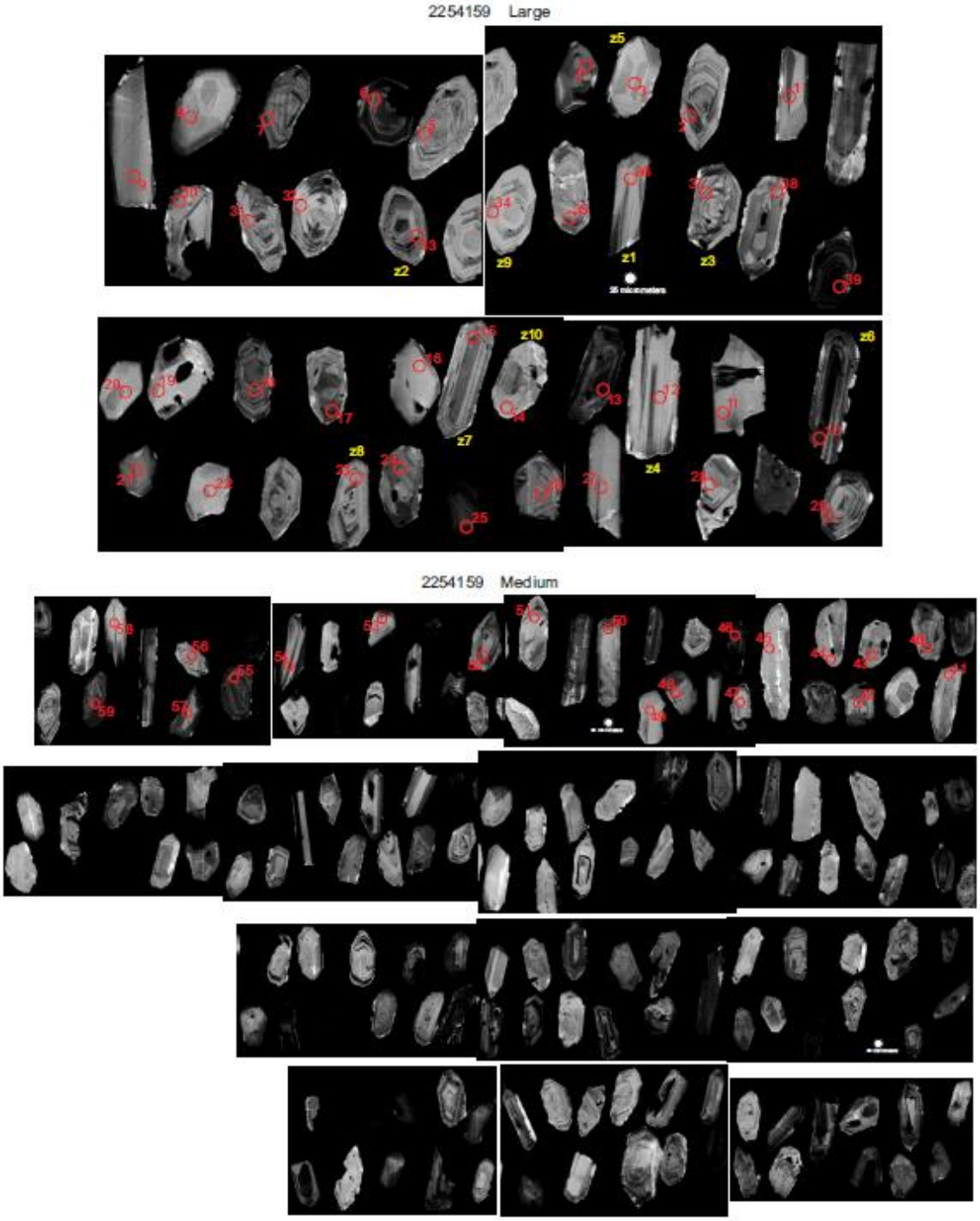

Figure 14. Cathodoluminescence (CL) images of selected zircons extracted from Guluguba 2, 509.43 m (2233310). Grains dated by CA-TIMS are shown.

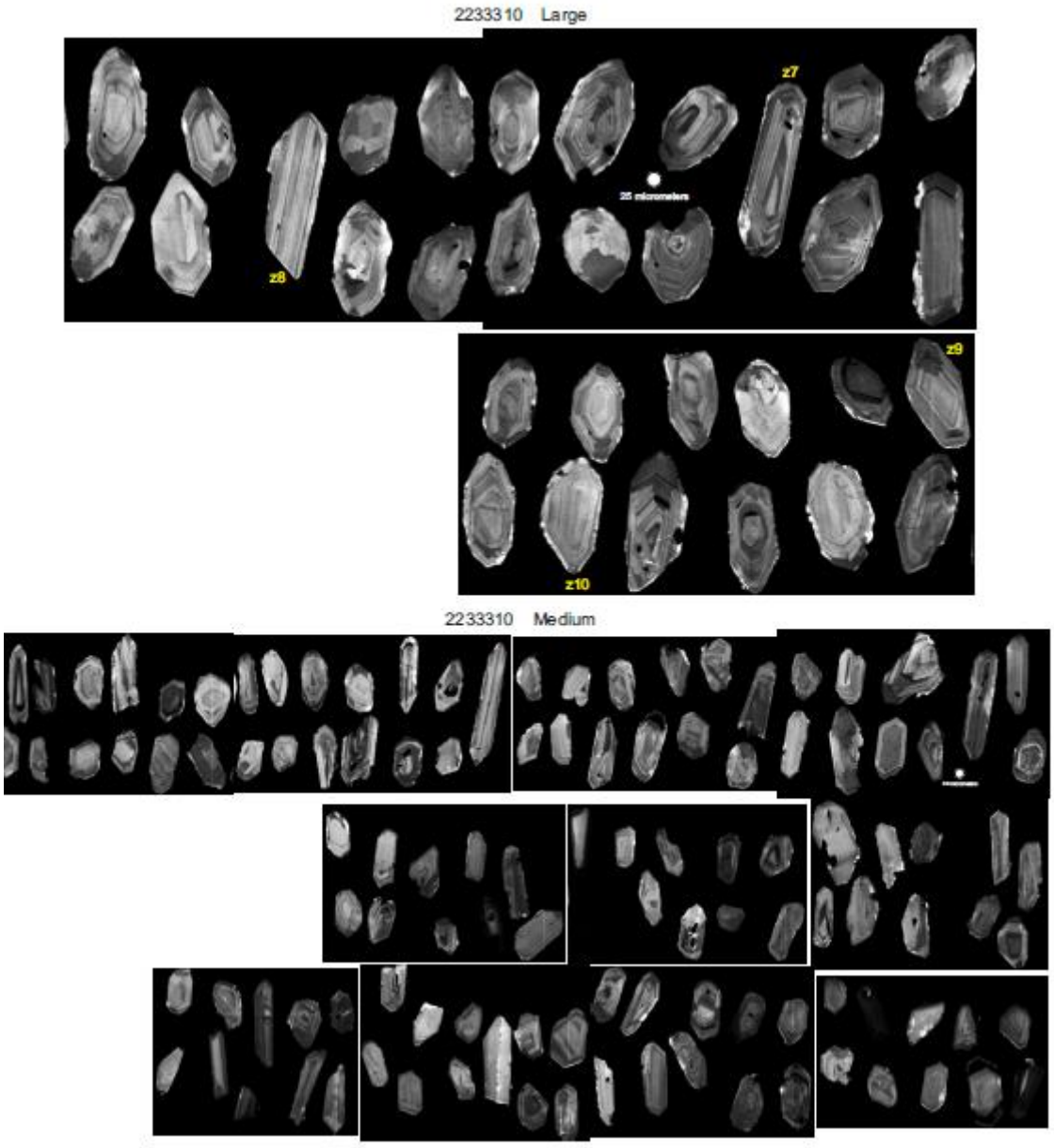

Figure 15. Cathodoluminescence (CL) images of selected zircons extracted from Guluguba 2, 428.57 m (2233308). Grains dated by CA-TIMS are shown.

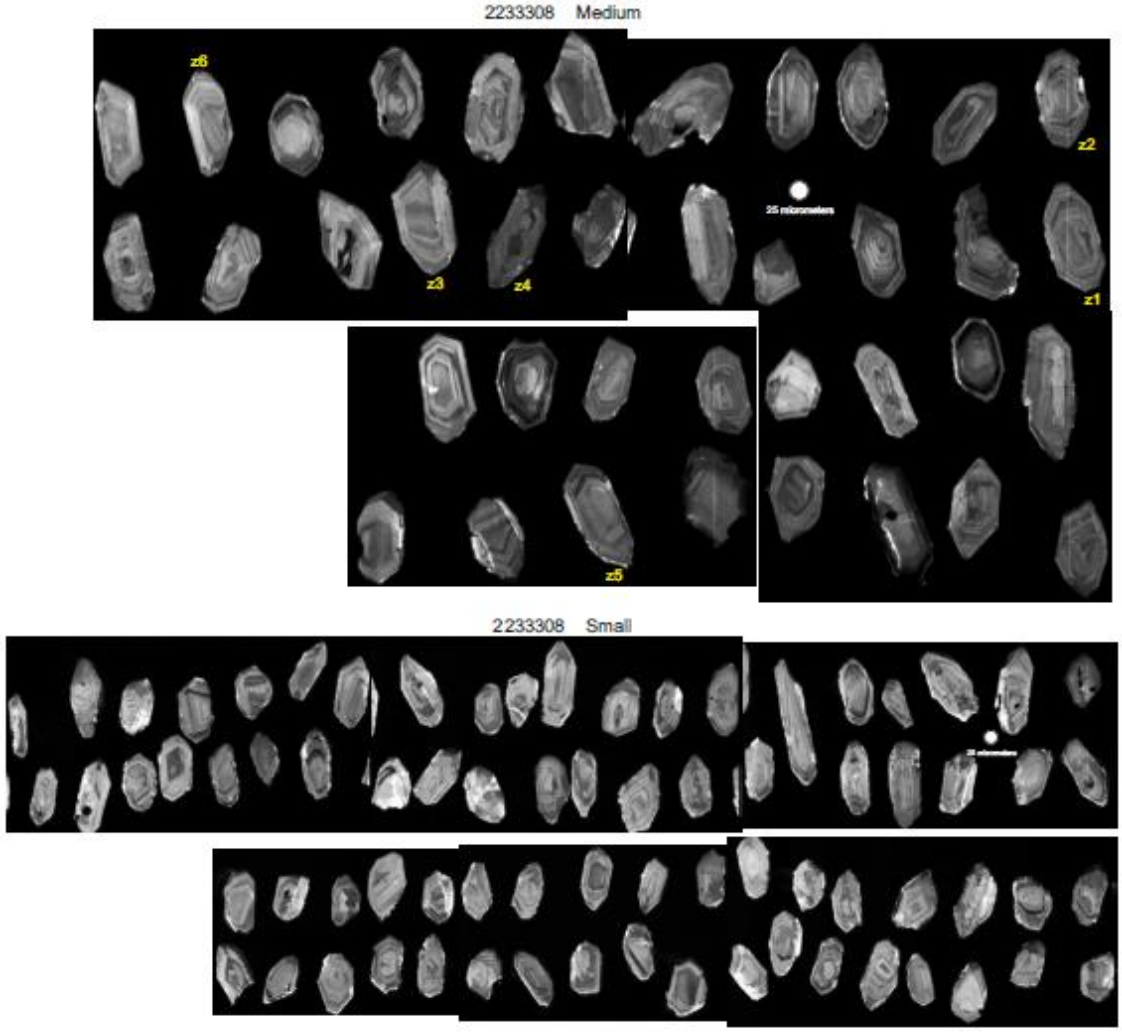

Figure 16. Cathodoluminescence (CL) images of selected zircons extracted from Cameron 1, 221.40 m (2389997). Grains dated by CA-TIMS are shown.

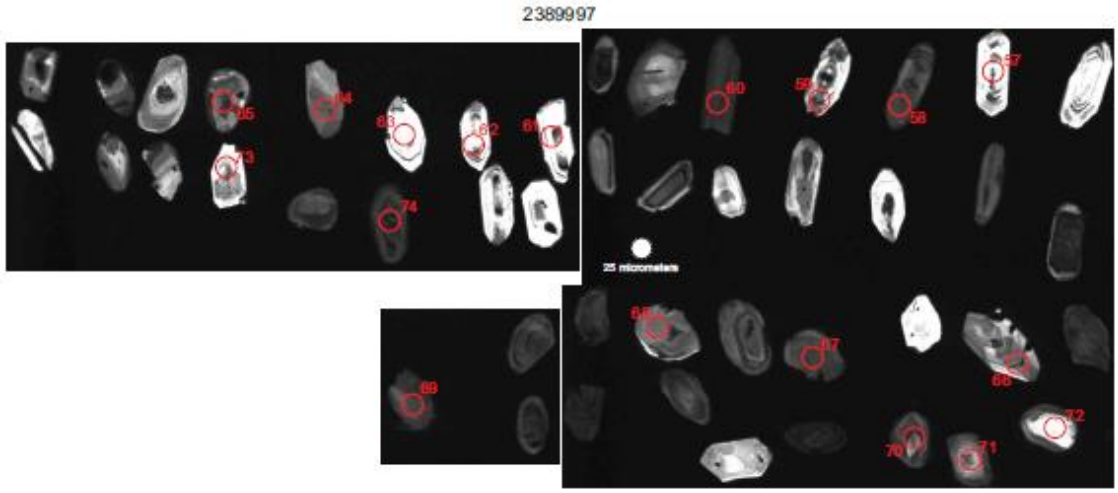

Figure 17. Cathodoluminescence (CL) images of selected zircons extracted from Pleasant Hills 25, 335.08 m (2390007). Grains dated by CA-TIMS are shown.

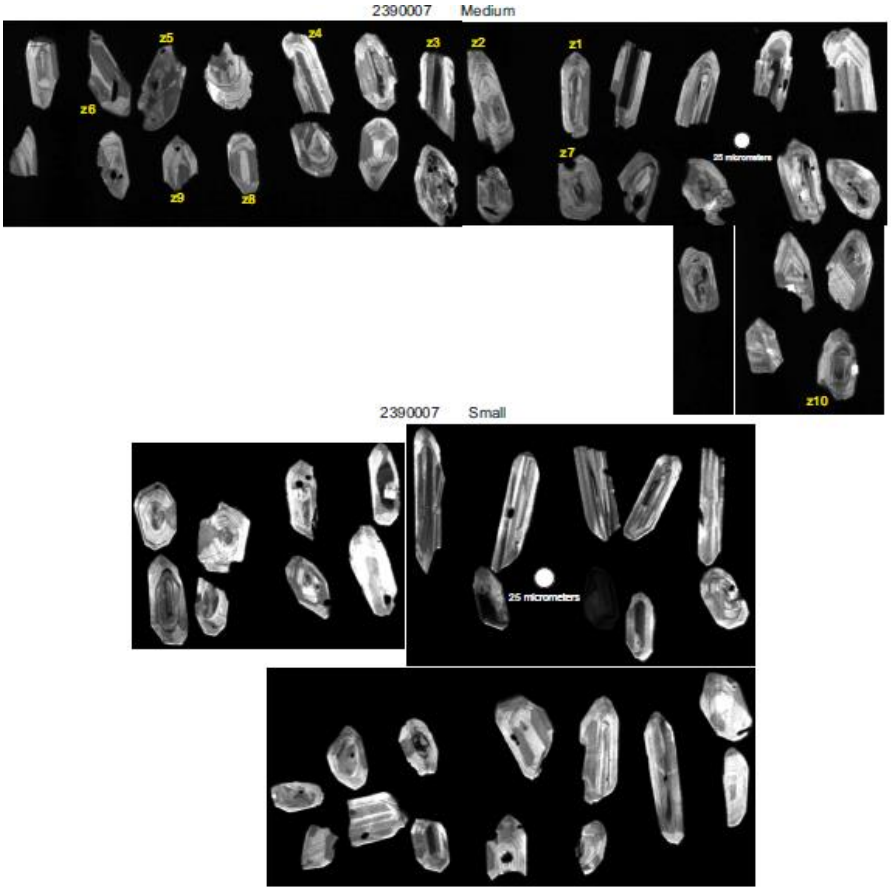

Figure 18. Cathodoluminescence (CL) images of selected zircons extracted from Indy 4, 202.00 m (2233272). Grains dated by CA-TIMS are shown.

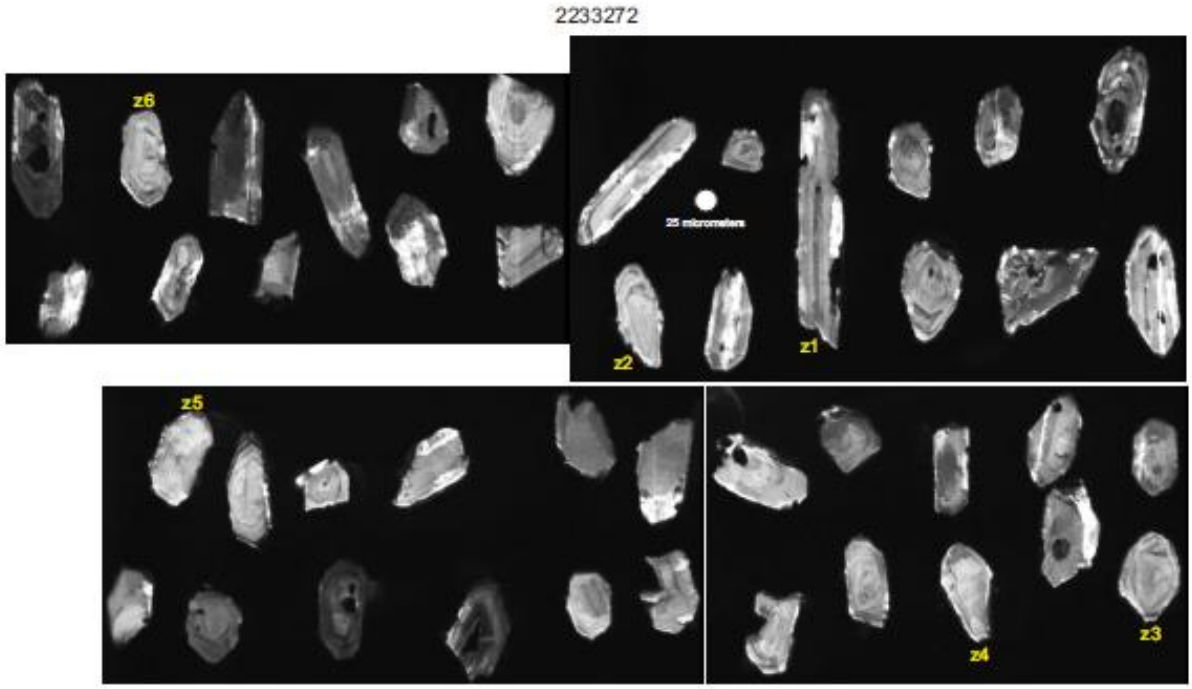

Figure 19. Cathodoluminescence (CL) images of selected zircons extracted from Indy 3, 159.76m (2254172). Grains dated by CA-TIMS are shown.

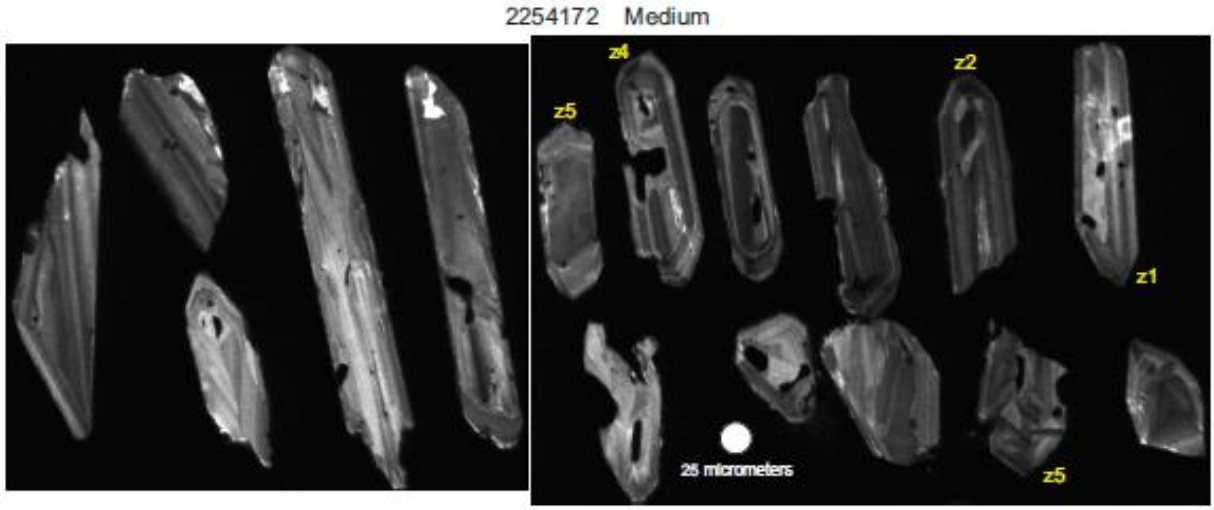

Figure 20. Cathodoluminescence (CL) images of selected zircons extracted from Indy 3, 104.62 m (2254169). Grains dated by CA-TIMS are shown.

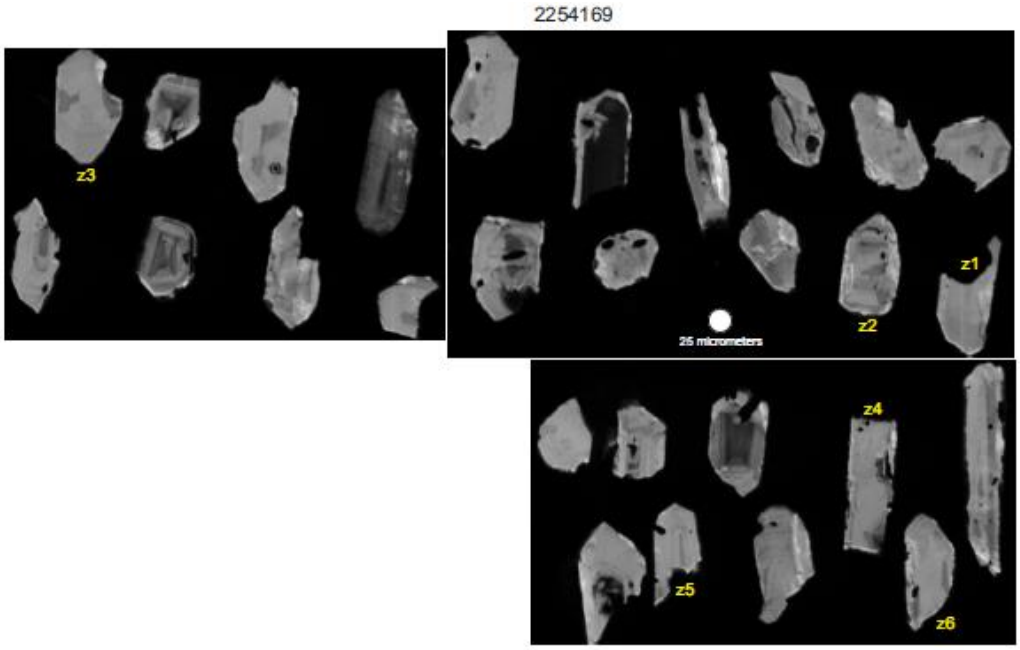

Figure 21a. Cathodoluminescence (CL) images of selected angular zircons extracted from Zeus 7, 1677.51 m (2550367). Grains dated by CA-TIMS and spot analysed by LA-ICPMS are shown.

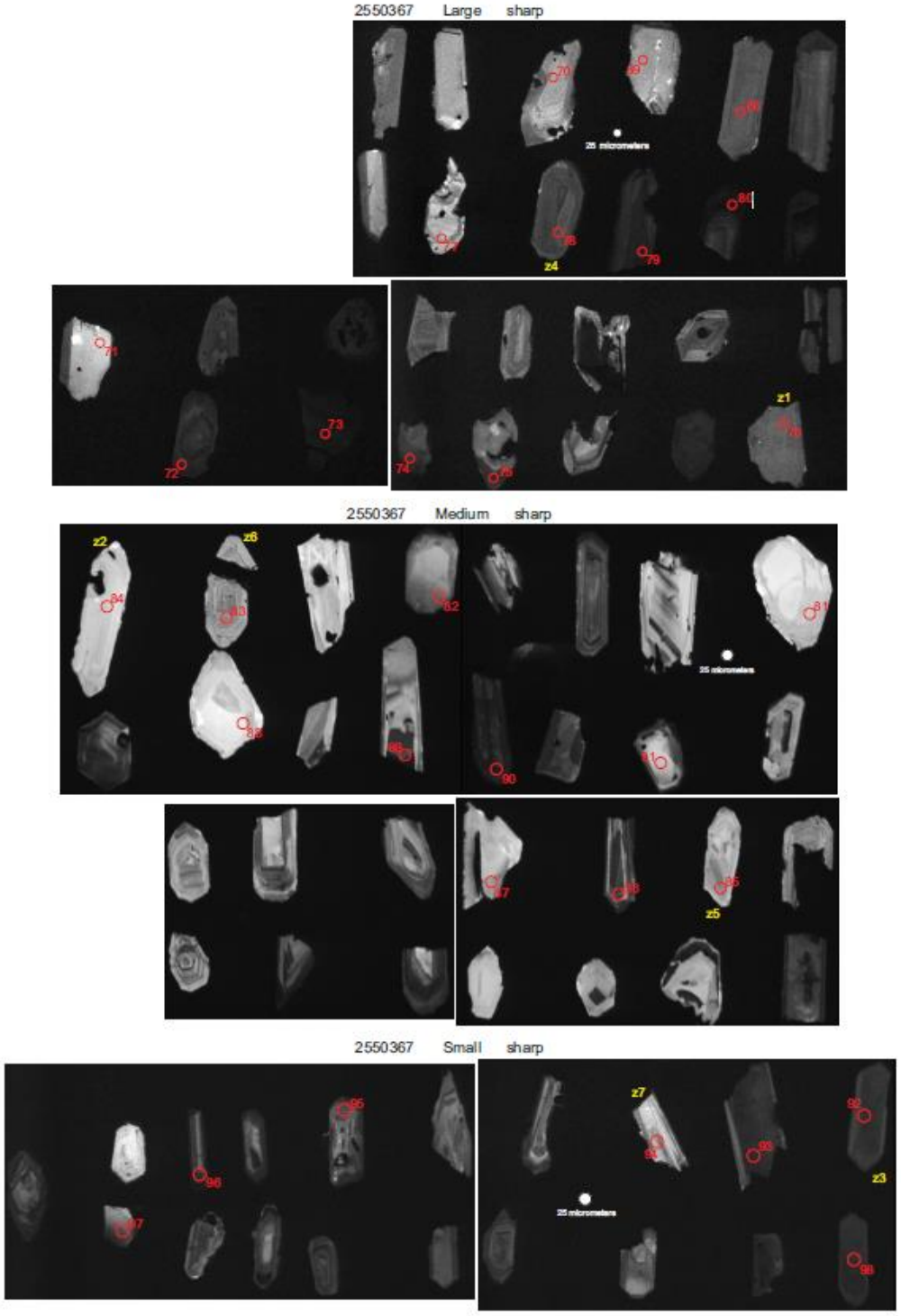

Figure 21b. Cathodoluminescence (CL) images of selected rounded zircons extracted from Zeus 7, 1677.51 m (2550367). Grains dated by CA-TIMS and spot analysed by LA-ICPMS are shown.

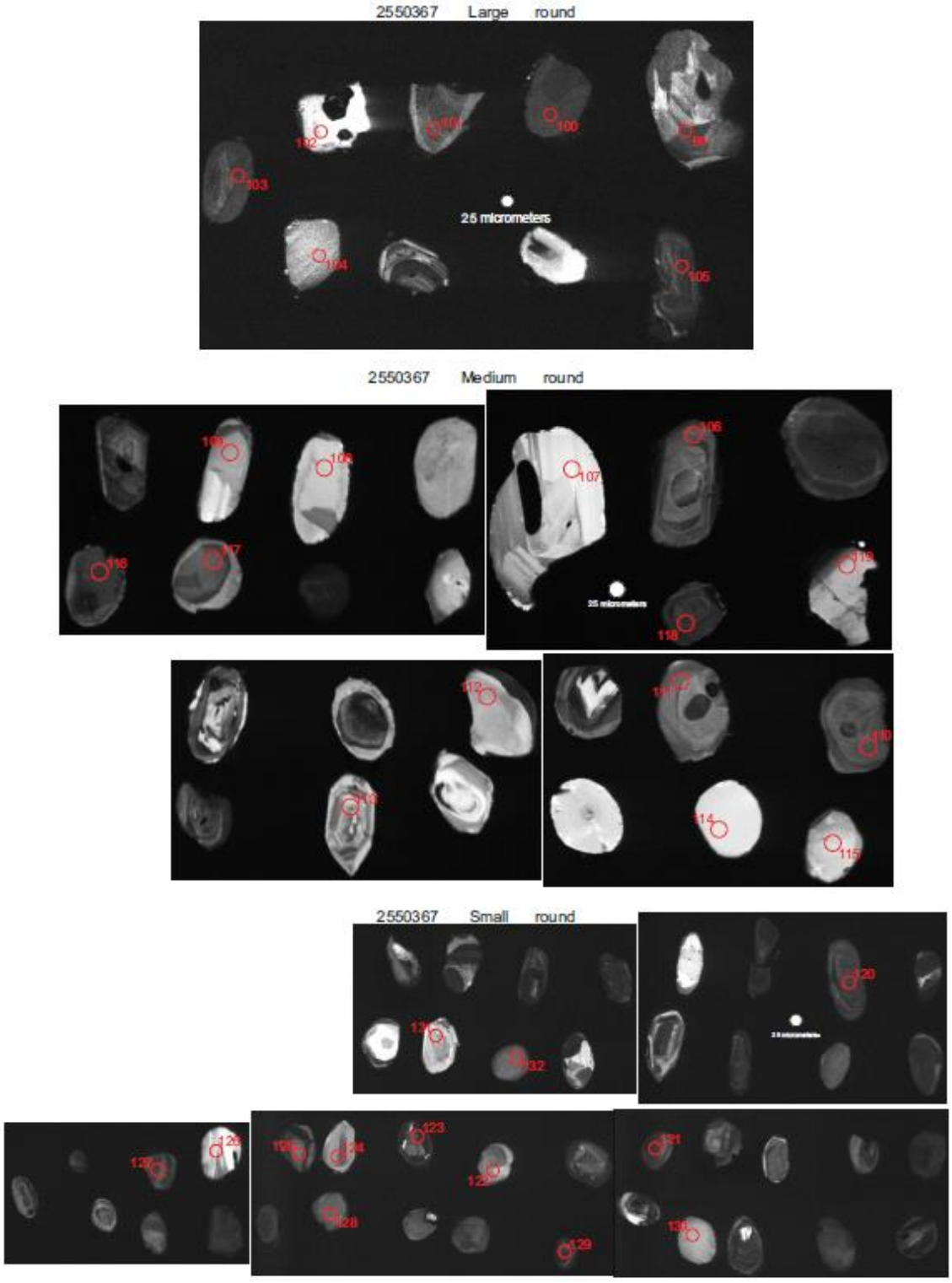

Figure 22a. Cathodoluminescence (CL) images of selected angular zircons extracted from Zeus 7, 1659.31 m (2550364). Grains dated by CA-TIMS and spot analysed by LA-ICPMS are shown.

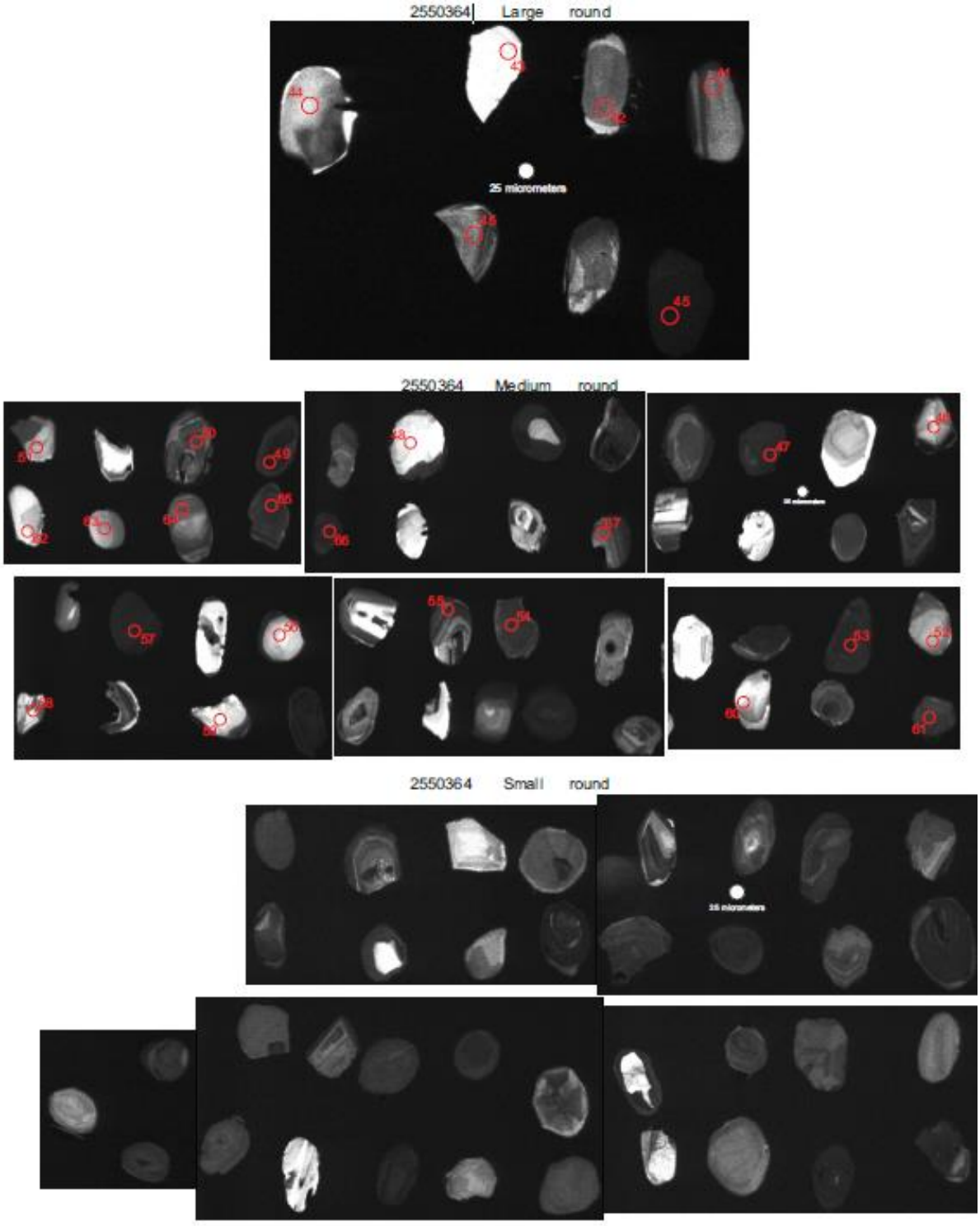

Figure 22b. Cathodoluminescence (CL) images of selected rounded zircons extracted from Zeus 7, 1659.31 m (2550364). Grains dated by CA-TIMS and spot analysed by LA-ICPMS are shown.

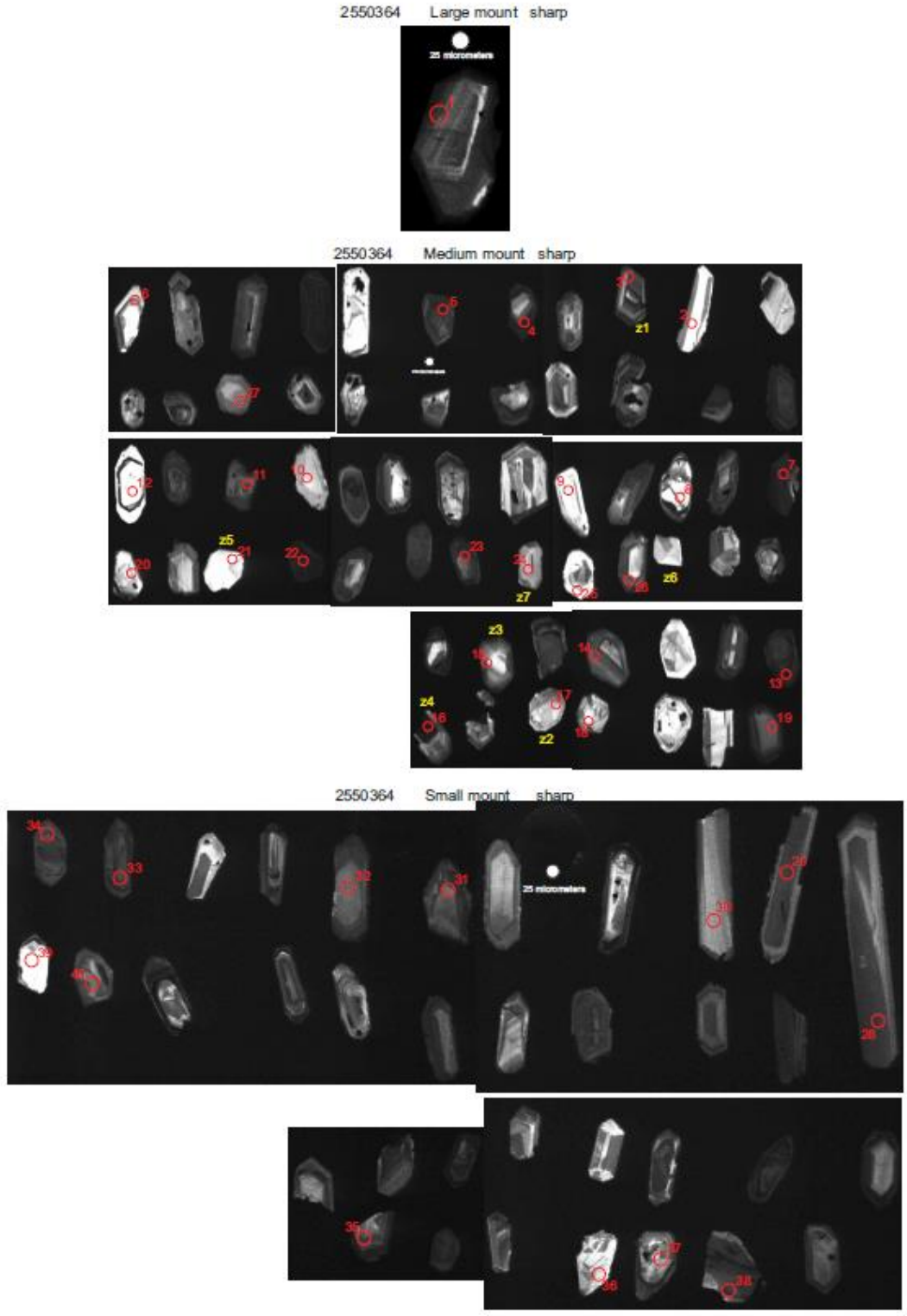

Appendices 3.

Figure 1. A measured section (including tuff and palynological sample locations) from the Turallin 1 well spanning the upper Hutton Sandstone (310 to 280 m), the Eurombah Formation (280 to 210 m?), and the Walloon Coal Measures (210 to 60 m?).

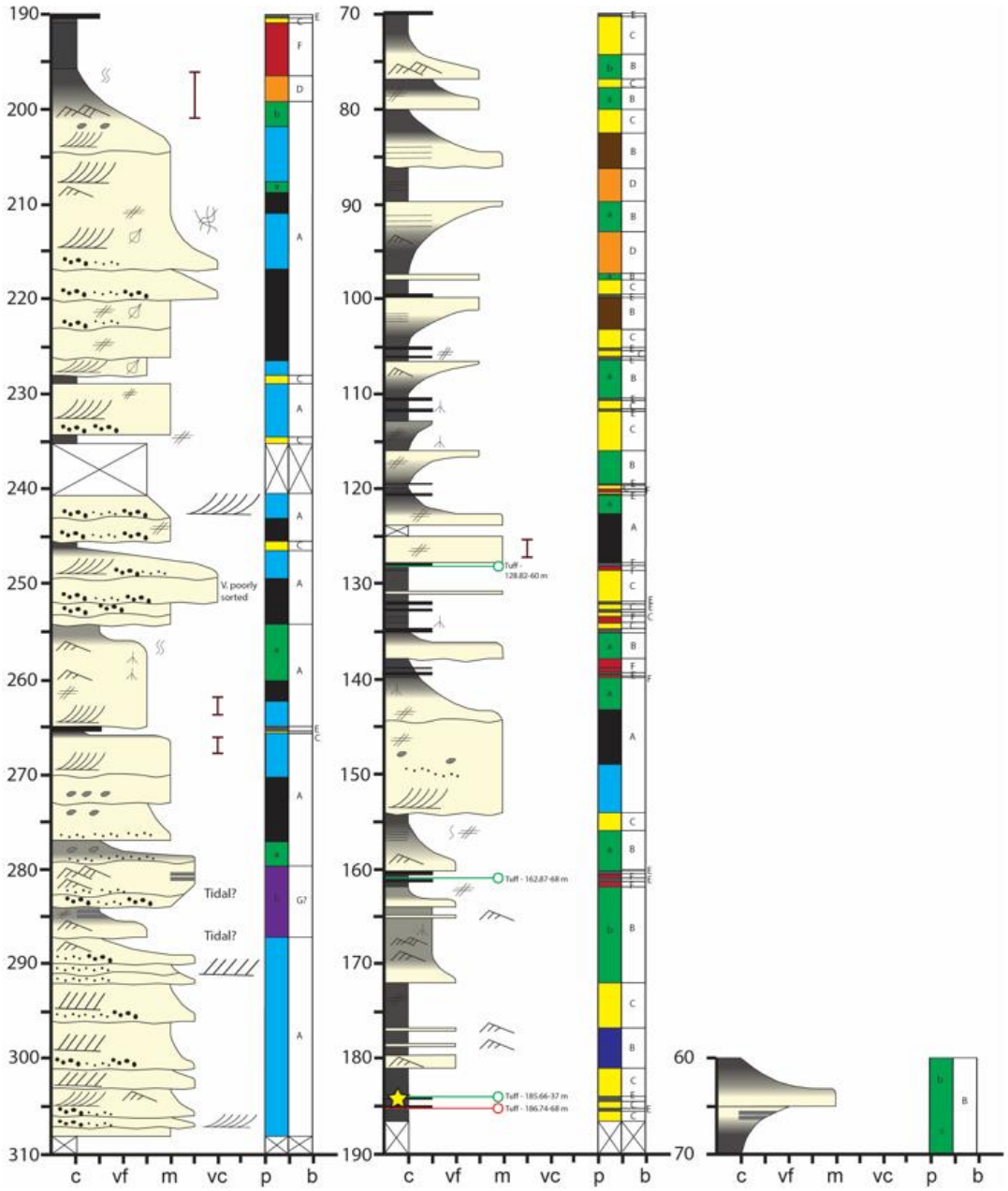

Figure 2. A measured section (including tuff and palynological sample locations) from the Stratheden 4 well spanning the Walloon Coal Measures adapted from Wainman et al. (2015).

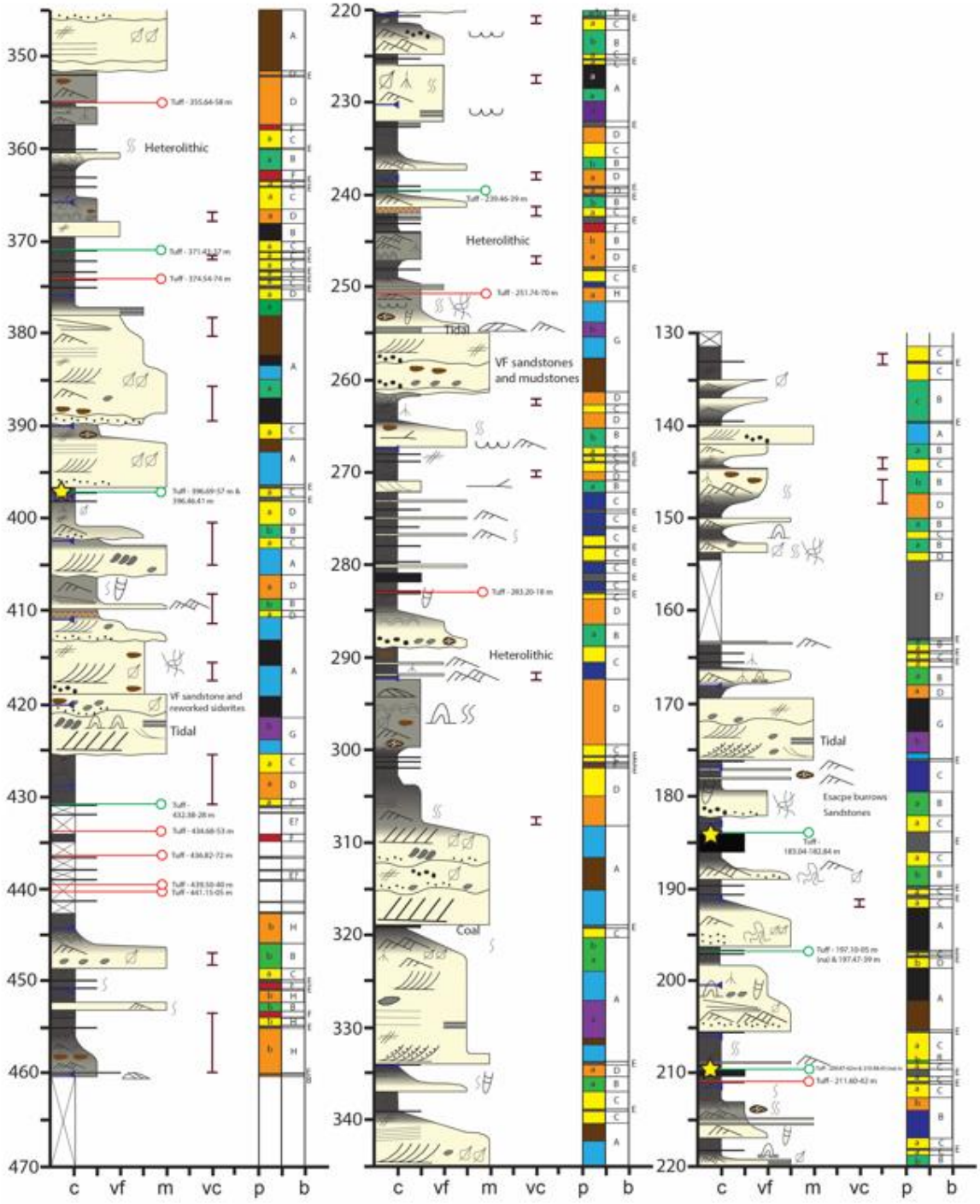

Figure 3. A measured section from the Wyalla 3 well spanning the Eurombah Formation (490 ? to 408 m) and the Walloon Coal Measures (408 to 110 m).

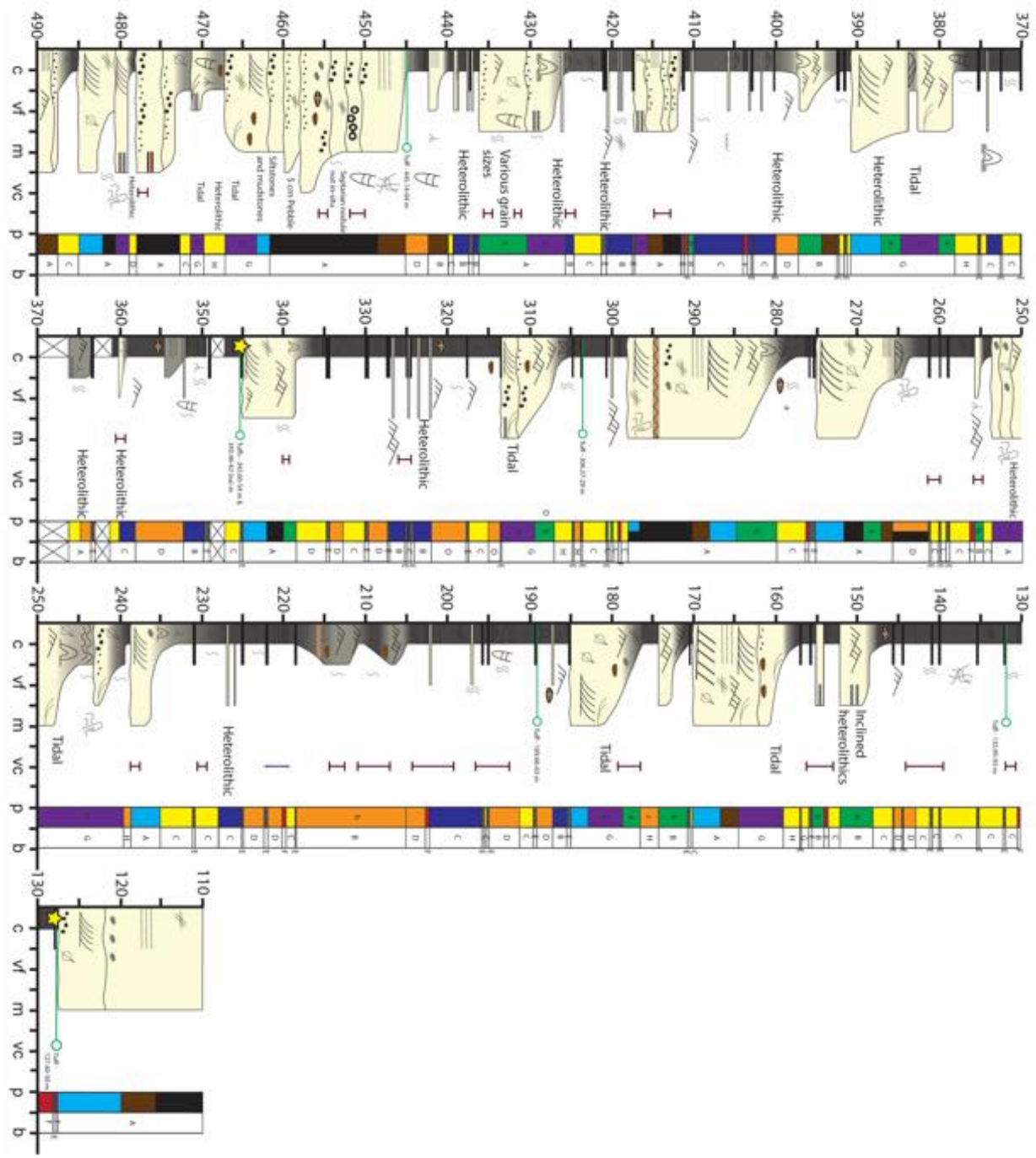

Figure 4. A measured section (including tuff and palynological sample locations) from the Alderley 1 well spanning the Eurombah Formation (540 ? to 494 m) and the Walloon Coal Measures (494 to 120 m).

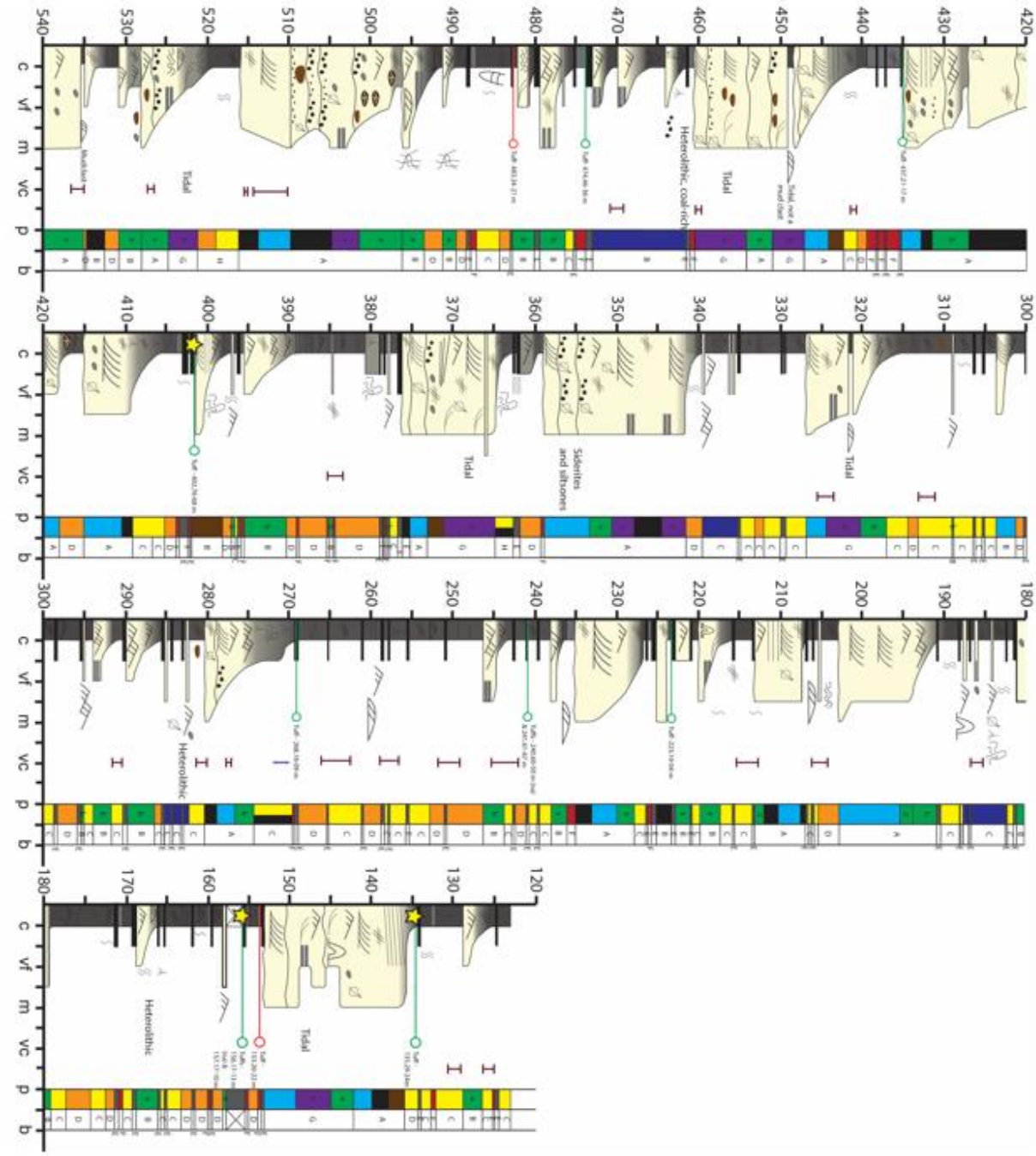

Figure 5. A measured section (including tuff and palynological sample locations) from the Pleasant Hills 25 well spanning the upper the Eurombah Formation (630 m to 596 m), the Walloon Coal Measures (596 to 371 m), the Springbok Sandstone (371 to 281 m) and the Westbourne Formation (281 to 260 m).

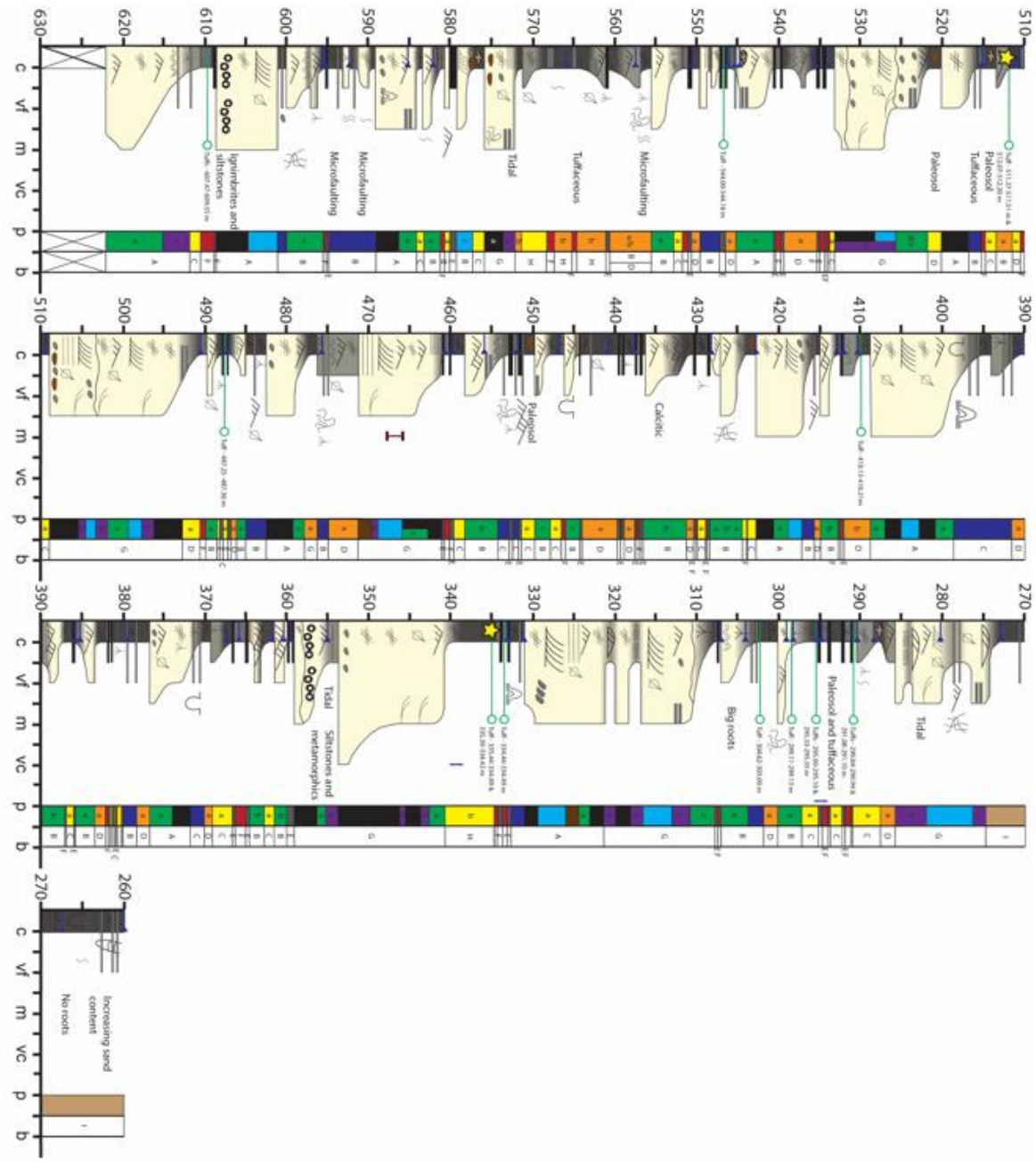

Figure 6. A measured section (including tuff and palynological sample locations) from the Kato 3 well spanning the Walloon Coal Measures (360 to 165 m) and the Springbok Sandstone (165 to 80 m).

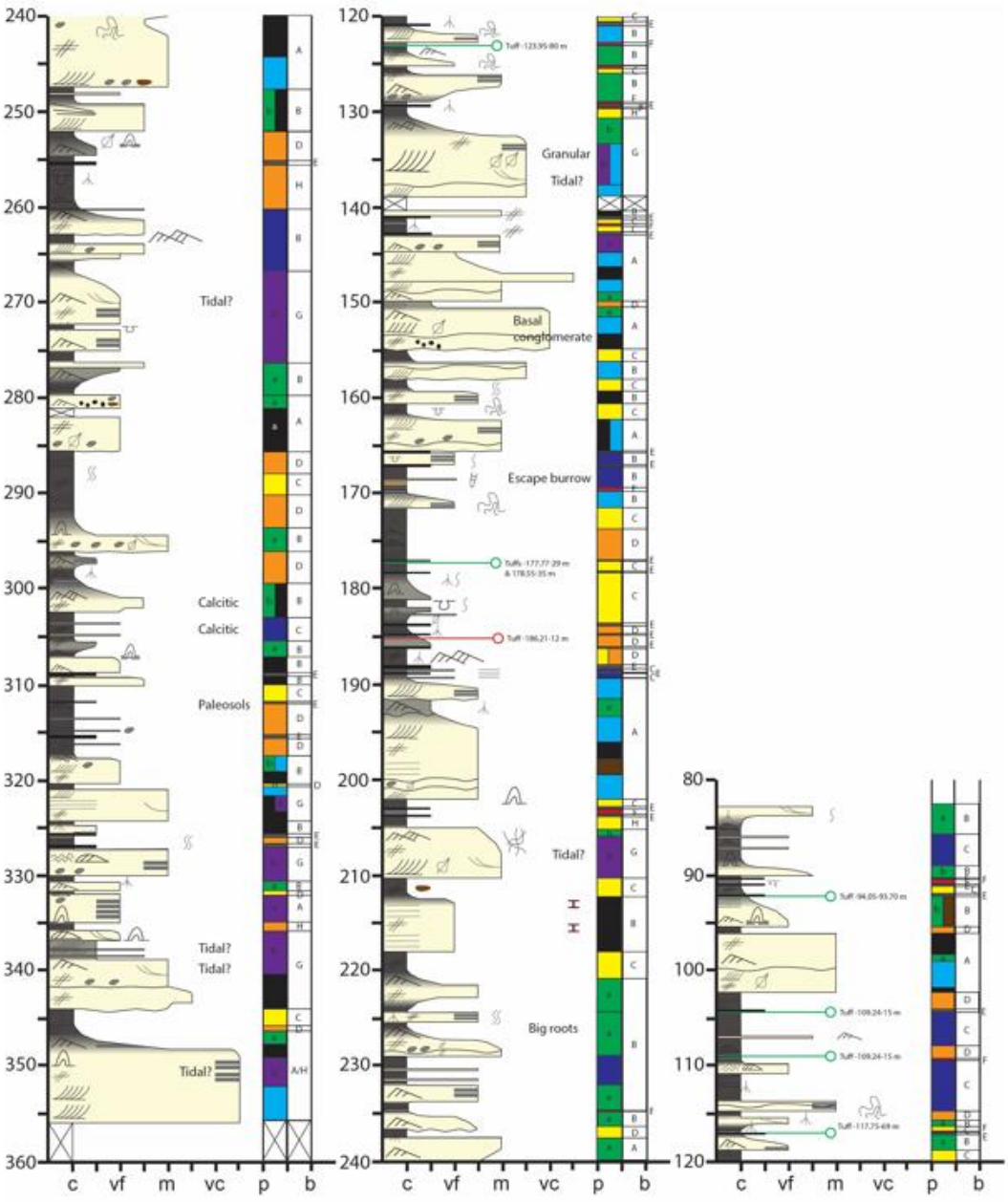

Figure 7. Surface, interval thickness, channel assemblage percentage and organic-rich assemblage percentage maps from the 162.18 to 160.54 Ma time slice.

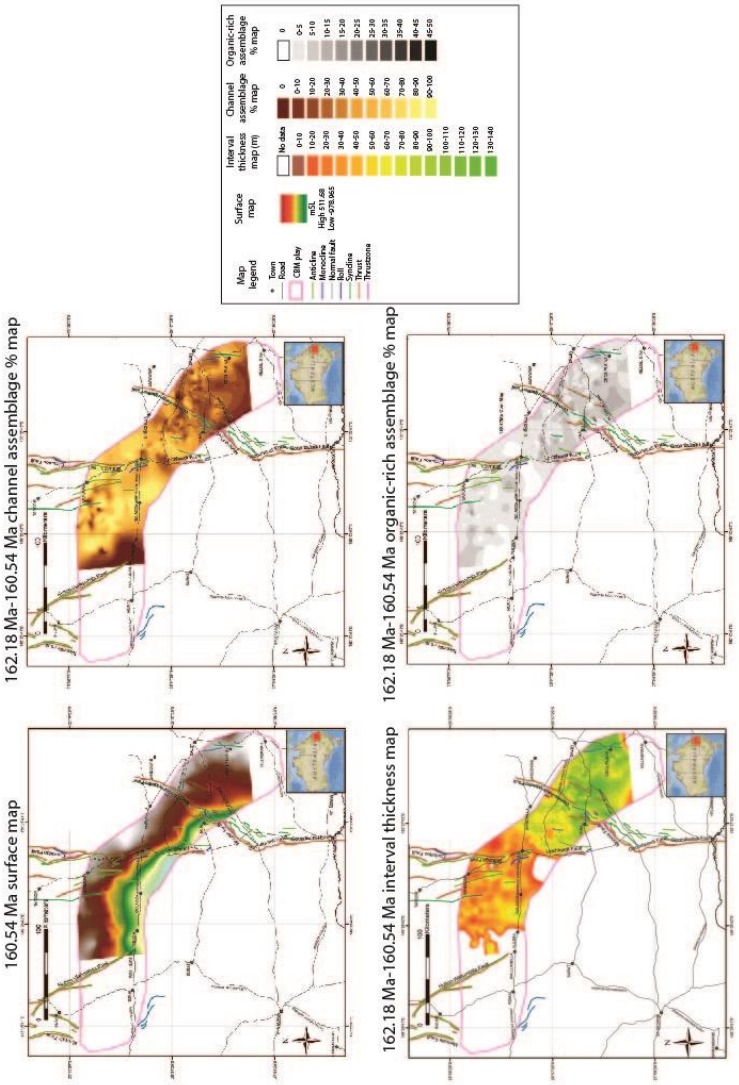

Figure 8. Surface, interval thickness, channel assemblage percentage and organic-rich assemblage percentage maps from the 160.54 to 160.45 Ma time slice.

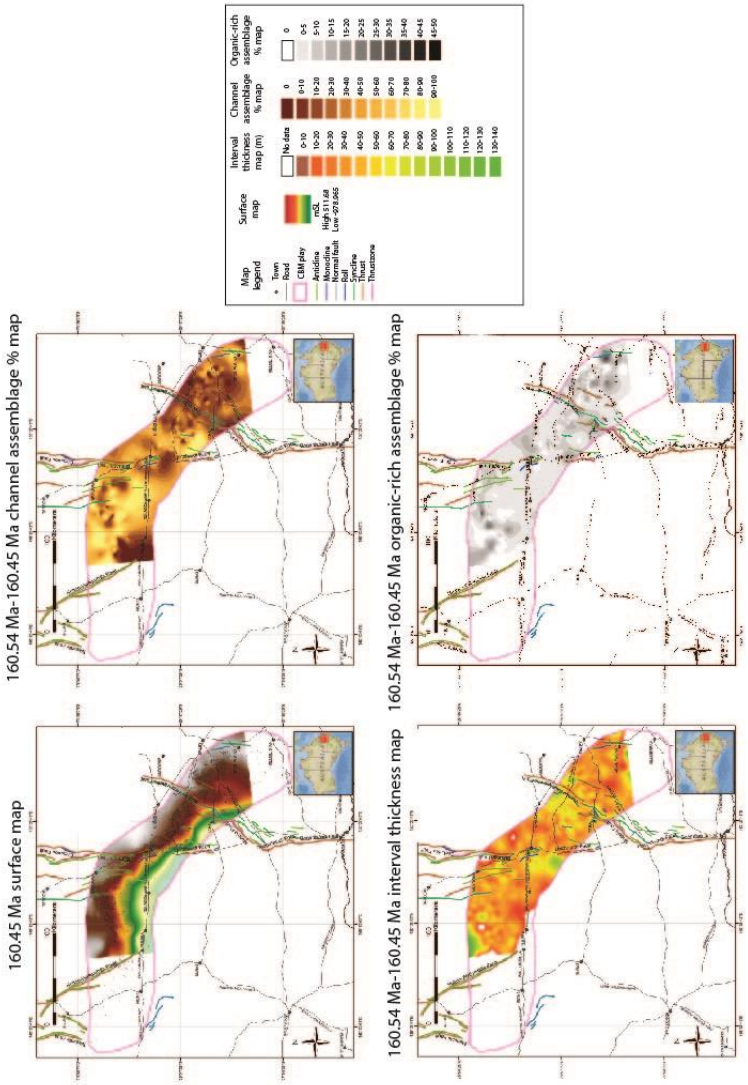

Figure 9. Surface, interval thickness, channel assemblage percentage and organic-rich assemblage percentage maps from the 160.45 to 159.69 Ma time slice.

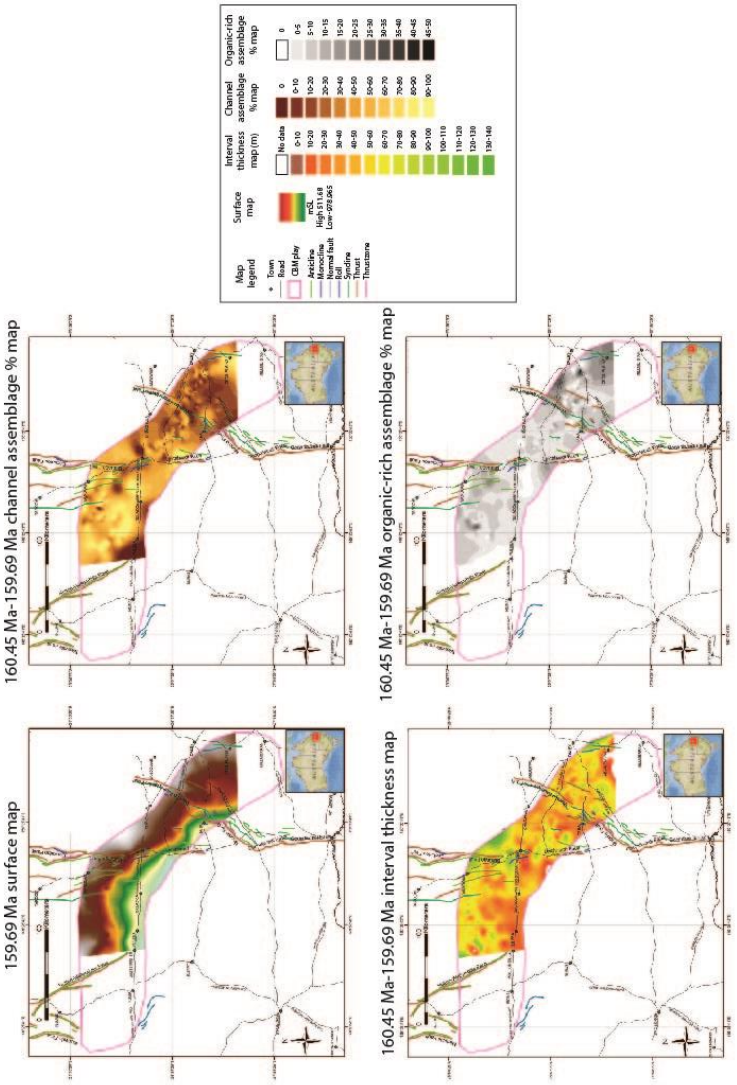

Figure 10. Surface, interval thickness, channel assemblage percentage and organic-rich assemblage percentage maps from the 159.69 to 158.86 time slice.

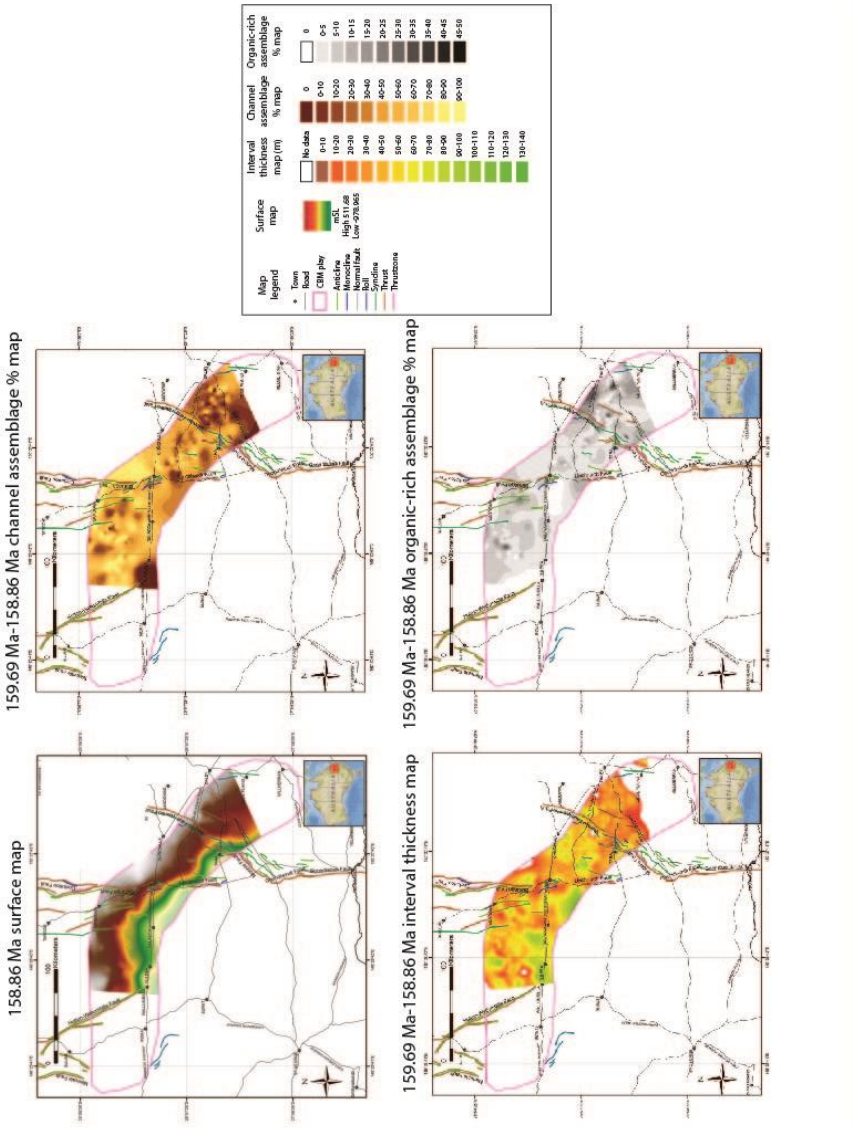

Figure 11. Surface, interval thickness, channel assemblage percentage and organic-rich assemblage percentage maps from the 158.86 to 157.55 Ma time slice.

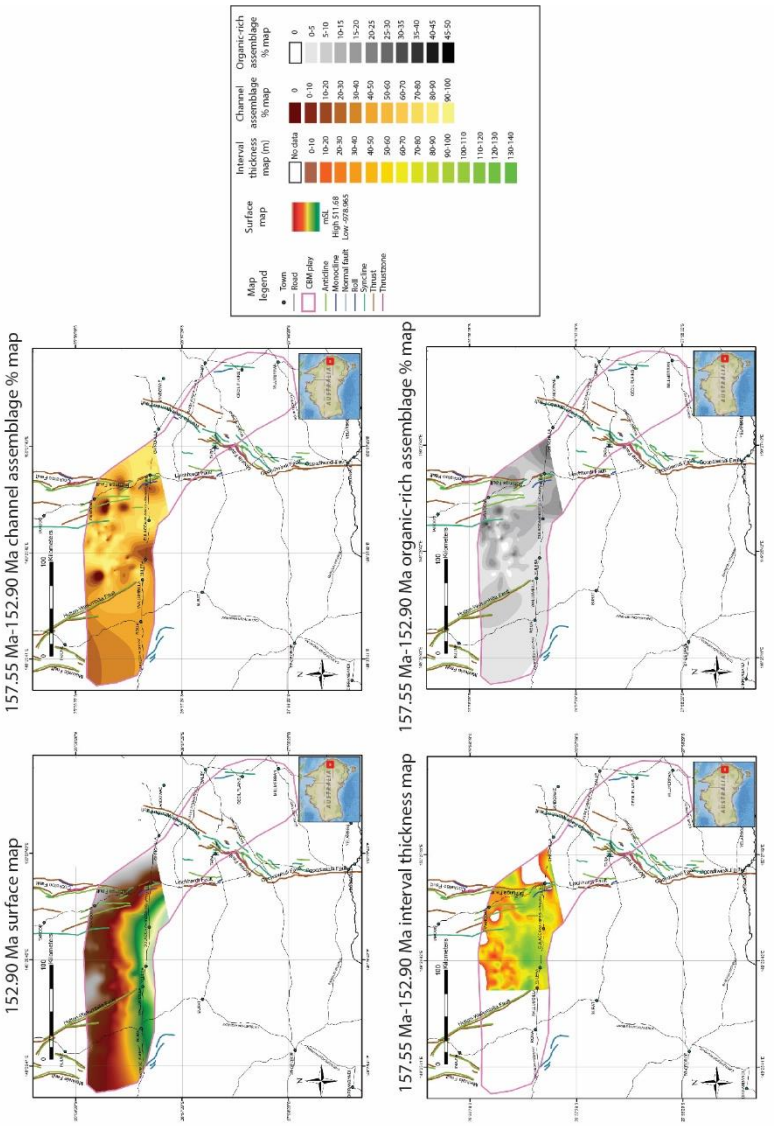

Figure 12. Surface, interval thickness, channel assemblage percentage and organic-rich assemblage percentage maps from the 157.55 to 152.90 Ma time slice.

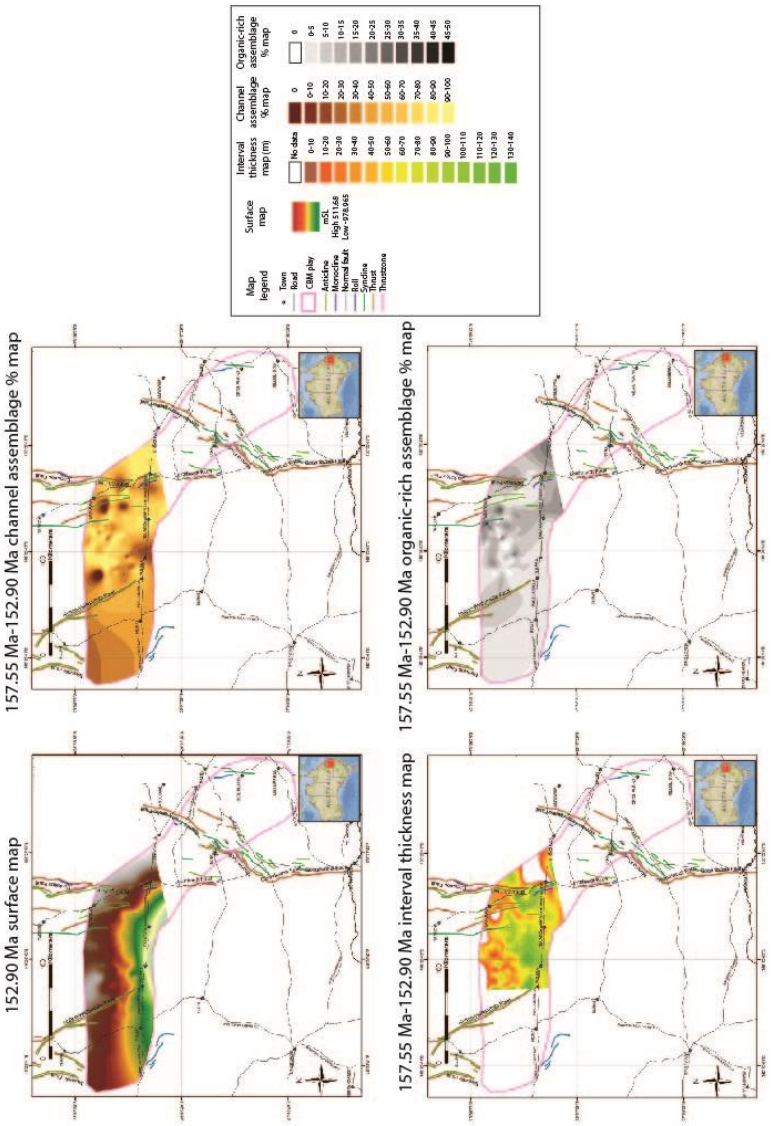

Figure 13. Surface, interval thickness, channel assemblage percentage and organic-rich assemblage percentage maps from the 152.90 to 151.39 Ma time slice.

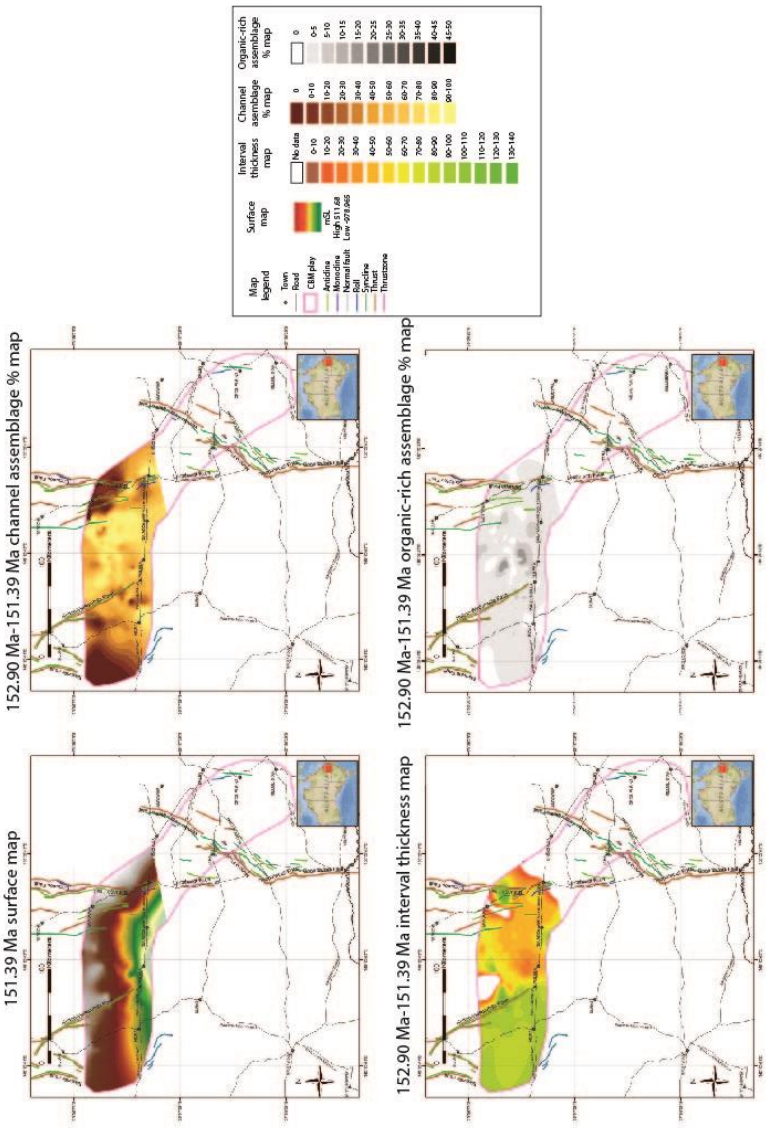

Figure 14. Surface, interval thickness, channel assemblage percentage and organic-rich assemblage percentage maps from the 151.39 to 150.77 Ma time slice.

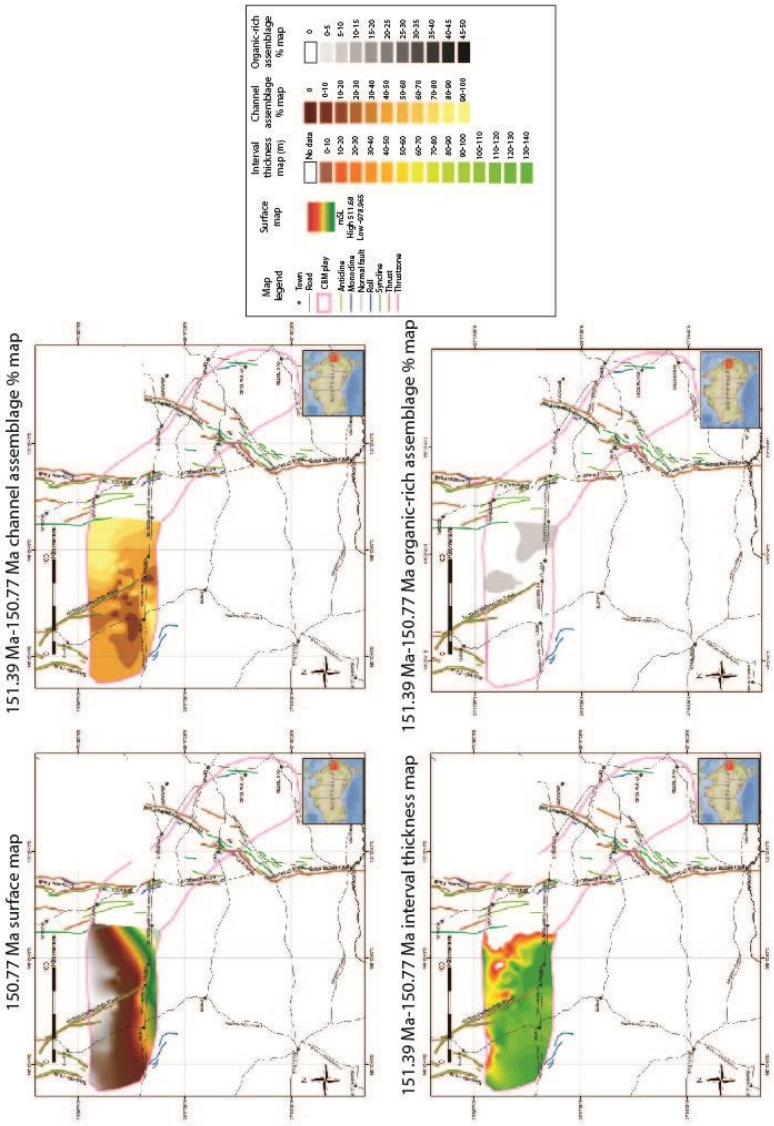

Figure 15. Surface, interval thickness, channel assemblage percentage and organic-rich assemblage percentage maps from the 150.77 to 150.11 Ma time slice.

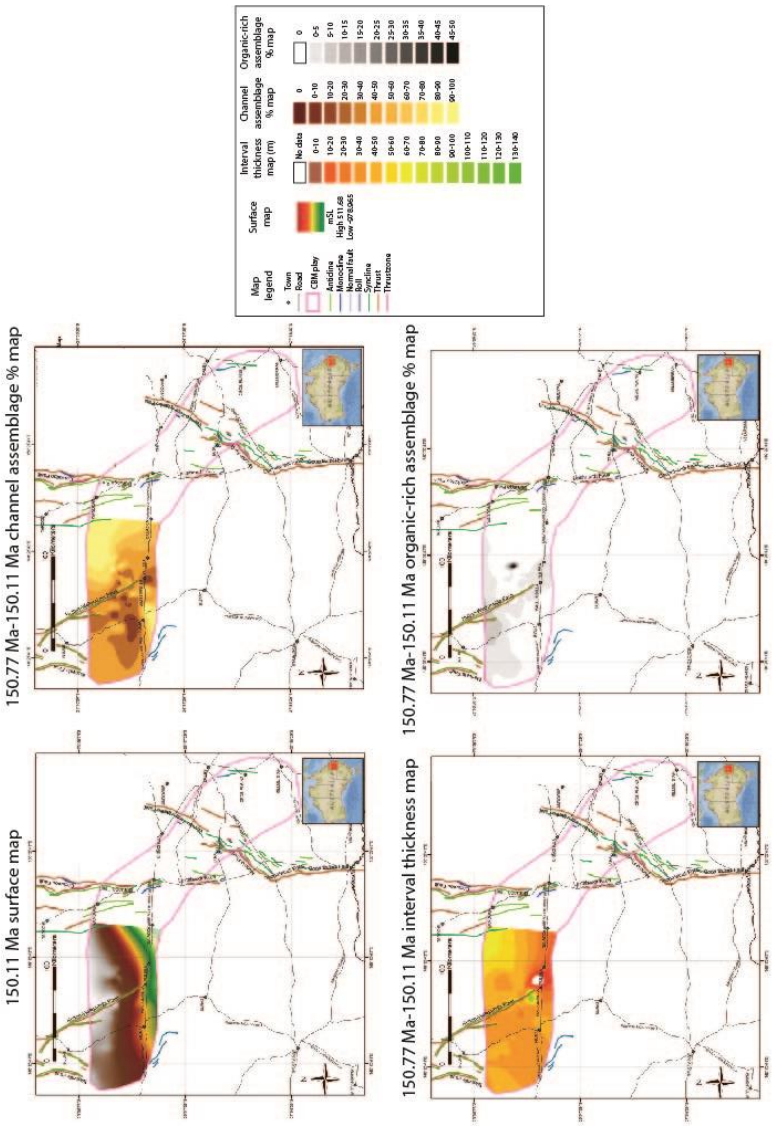

Figure 16. Surface, interval thickness, channel assemblage percentage and organic-rich assemblage percentage maps from the 150.11 to 149.78 Ma time slice.

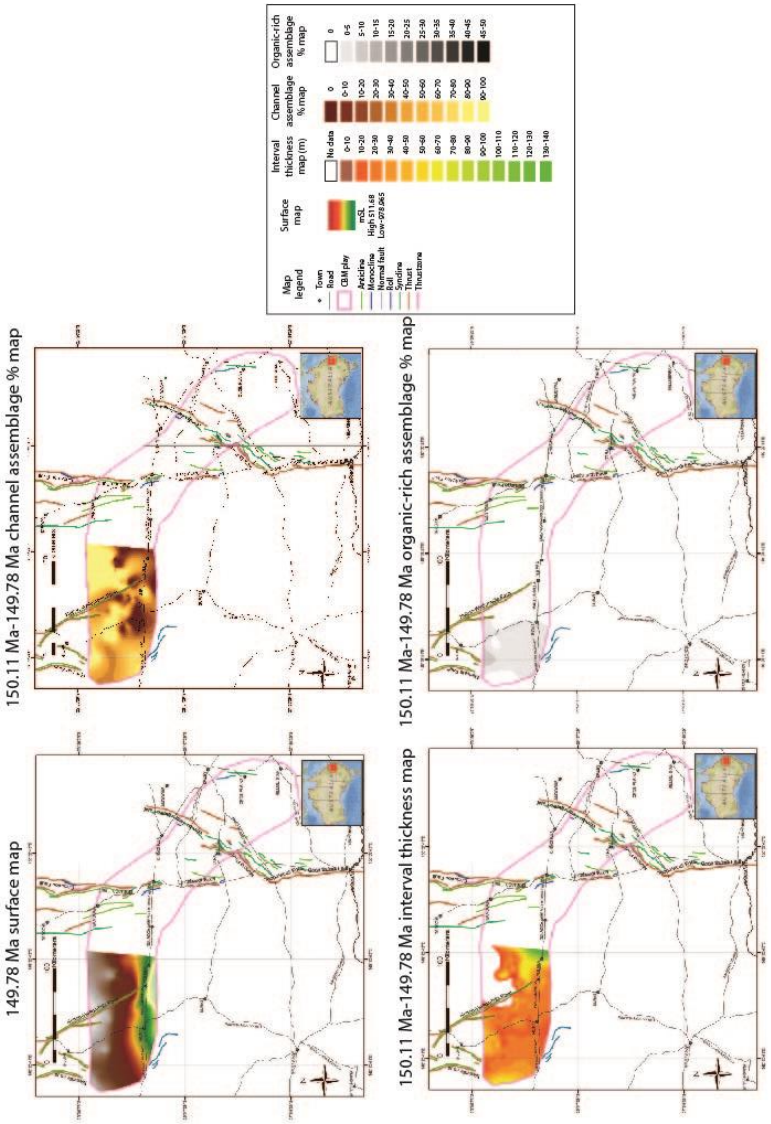

Appendices 4.

Figure 1. Normalised palynological counts (percent) for the Stratheden 4 well.

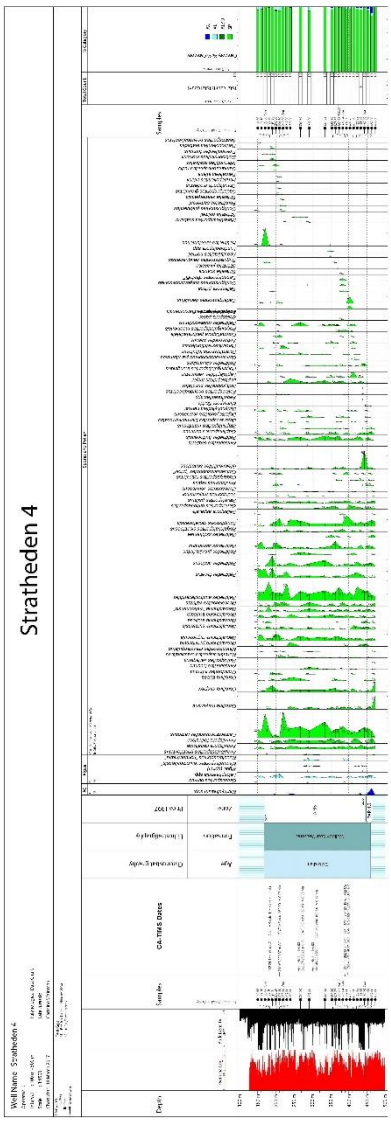

Figure 2. Normalised palynological counts (percent) for the Stratheden 60 well.

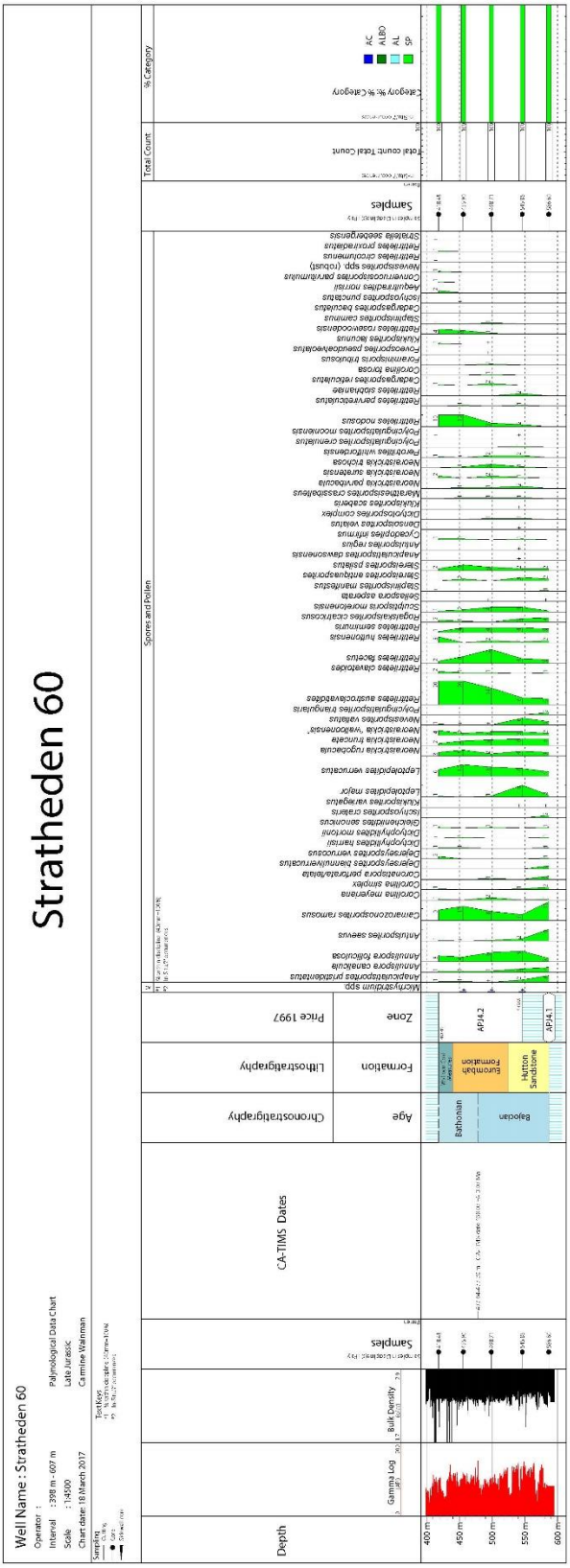

Figure 3. Normalized palynological counts (percent) for the Guluguba 2 well.

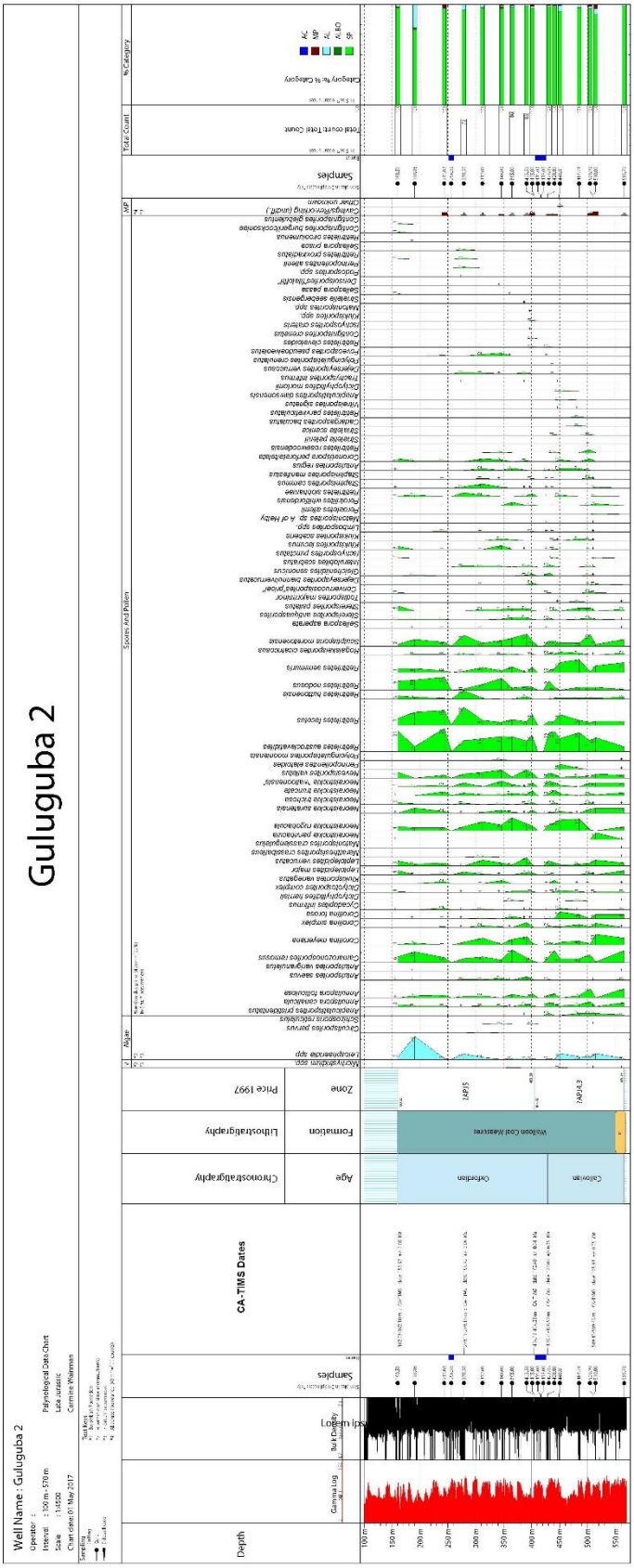

Figure 4. Normalised palynological counts (percent) for the Pleasant Hills 25 well.

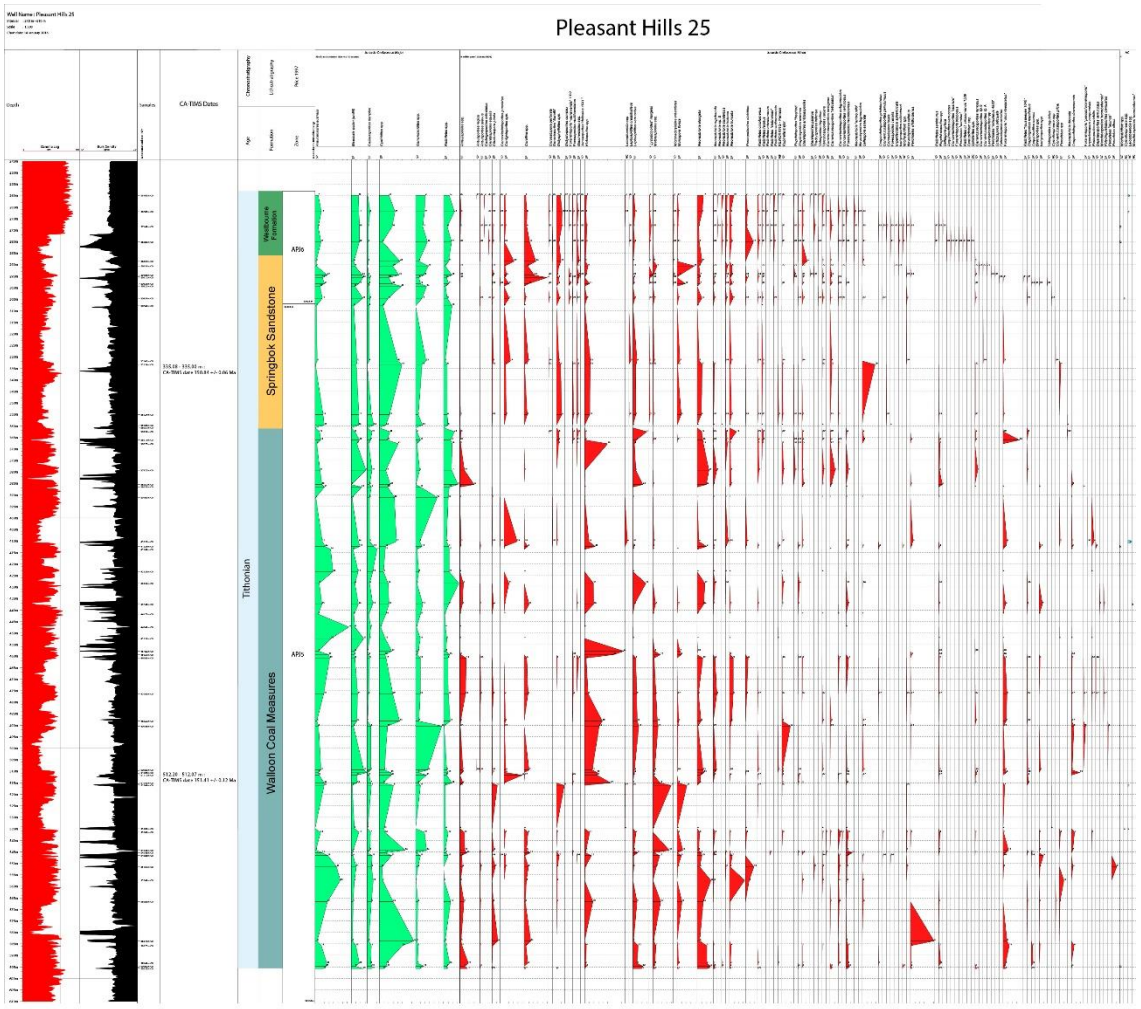

Figure 5. Normalised palynological counts (percent) for the Indy 3 well.

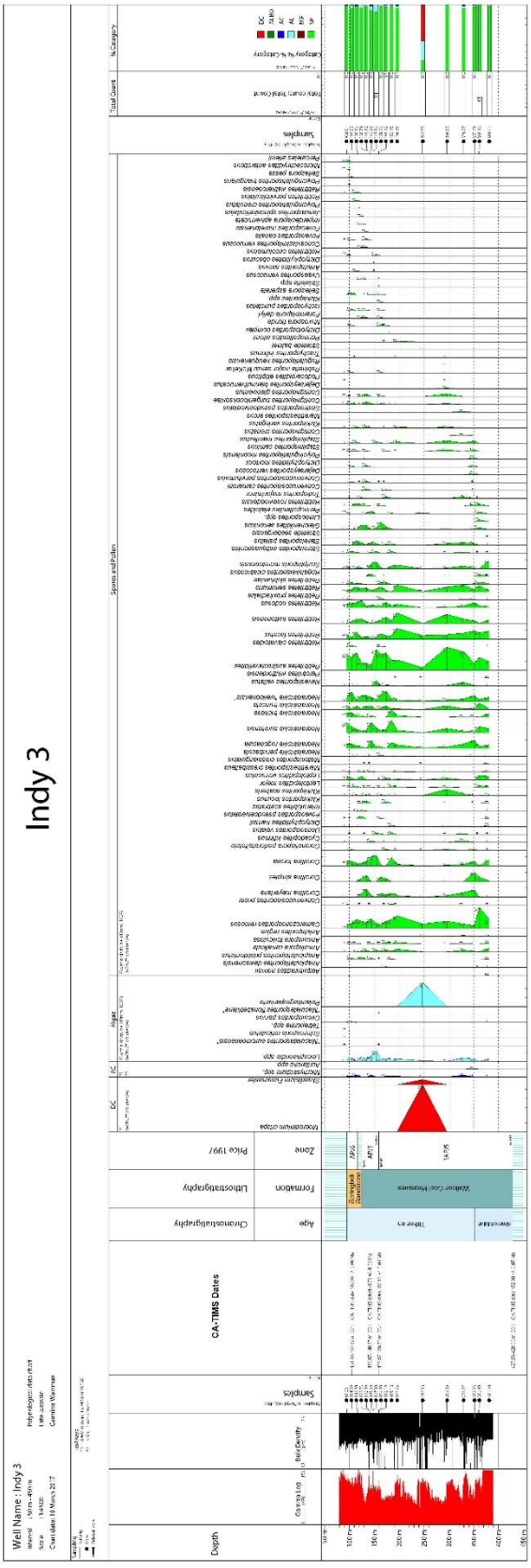

Appendices 5.

Figure 1. Common (300 counts) Stratabugs plot for the Indy 3 well.

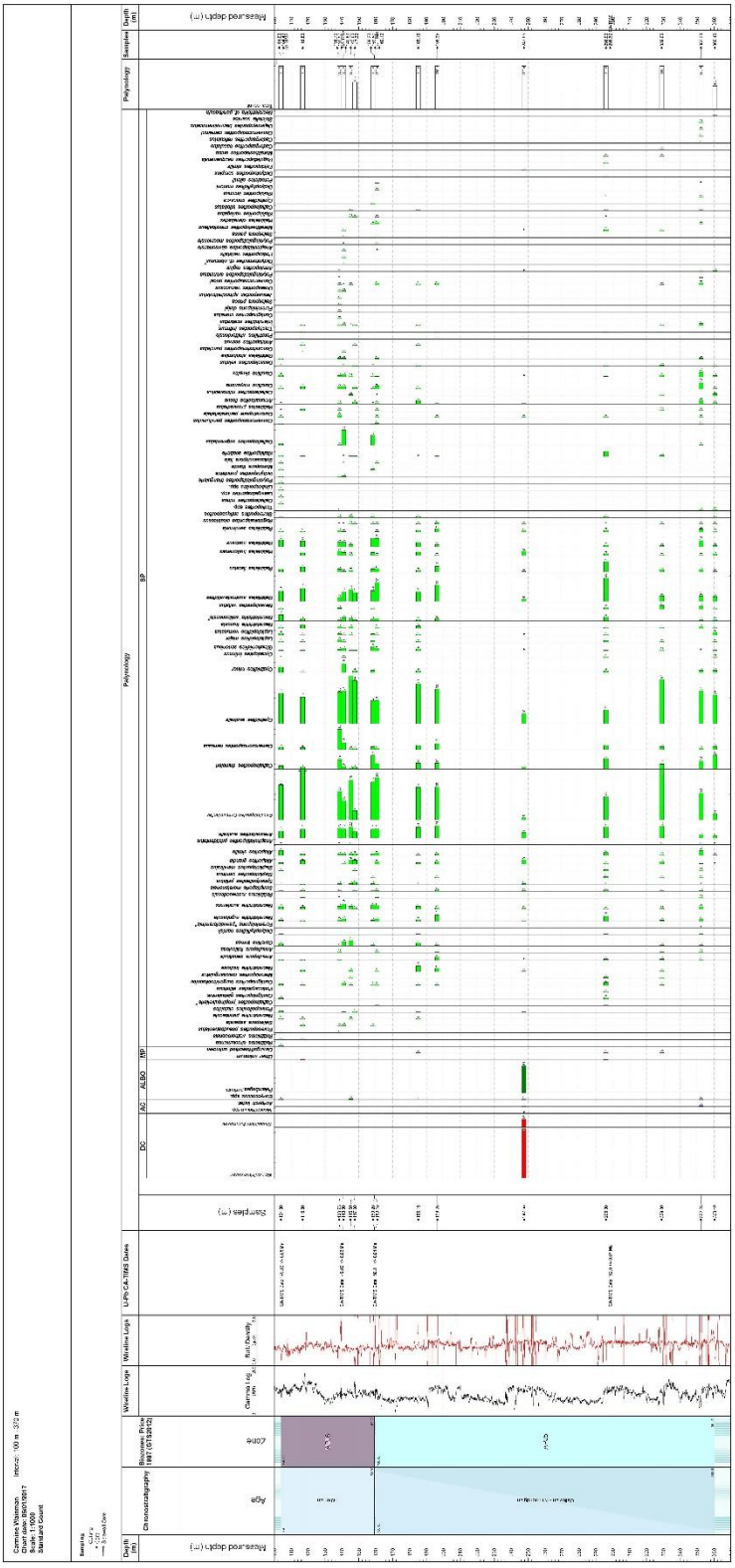

Table 1. Register of figured specimens. All slides are deposited with the Commonwealth Palaeontological Collection (CPC) at Geoscience Australia, Canberra, ACT, Australia. Slide coordinates of those of a standard England Finder.

Well	Sample depth (m)	Slide number	Plate	Plate figure number	Specimen	EF co-ordinates	CPC number
Indy 3	247.55	3	1	1	*Moorodinium crispa*	U41/1	43715
Indy 3	247.55	3	1	2	*Moorodinium crispa*	W47/3	43716
Indy 3	247.55	3	1	3	*Moorodinium crispa*	U23/0	43717
Indy 3	247.55	3	1	4	*Moorodinium crispa*	C41/4	43718
Indy 3	247.55	3	1	5a	*Moorodinium crispa*	S40/4	43719
Indy 3	247.55	3	1	5b	*Moorodinium crispa*	S40/4	43719
Indy 3	247.55	3	1	6a	*Moorodinium crispa*	U41/2	4372
Indy 3	247.55	3	1	6b	*Moorodinium crispa*	U41/2	43720
Indy 3	247.55	3	1	7	*Moorodinium crispa*	S40/4	43721
Indy 3	247.55	3	1	8	*Moorodinium crispa*	C38/2	43722
Indy 3	247.55	3	1	9	*Moorodinium crispa*	R26/3	43723
Indy 3	247.55	3	1	10	*Moorodinium crispa*	N19/2	43724
Indy 3	247.55	3	1	11a	*Moorodinium crispa*	J42/1	43725
Indy 3	247.55	3	1	11b	*Moorodinium crispa*	J42/1	43725
Indy 3	247.55	3	1	12	*Moorodinium crispa*	L44/0	43726
Indy 3	247.55	3	1	13	*Moorodinium crispa*	L45/3	43727
Indy 3	247.55	3	1	14	*Moorodinium crispa*	Q19/3	43728
Indy 3	247.55	3	1	15	*Moorodinium crispa*	J19/4	43729
Indy 3	247.55	3	1	16a	*Moorodinium crispa*	F30/3	43730
Indy 3	247.55	3	1	16b	*Moorodinium crispa*	F30/3	43730
Indy 3	247.55	3	2	1	*Skuadinium fusumaster*	S44/1	43731
Indy 3	247.55	3	2	2a	*Skuadinium fusumaster*	Q43/0	43732
Indy 3	247.55	3	2	2b	*Skuadinium fusumaster*	Q43/0	43732
Indy 3	247.55	3	2	3	*Skuadinium fusumaster*	X19/3	43733
Indy 3	247.55	3	2	4	*Skuadinium fusumaster*	U12/4	43734
Indy 3	247.55	3	2	5	*Skuadinium fusumaster*	S44/1	43735
Indy 3	247.55	3	2	6	*Skuadinium fusumaster*	M20/2	43736
Indy 3	247.55	3	2	7	*Skuadinium fusumaster*	H31/2	43737
Indy 3	247.55	3	2	8	*Palambages pariunta*	M20/2	43738
Indy 3	247.55	3	2	9	*Palambages pariunta*	V16/2	43739
Indy 3	247.55	3	2	10	*Palambages pariunta*	T17/4	43740
Indy 3	247.55	3	2	11a	*Palambages pariunta*	Q42/3	43741
Indy 3	247.55	3	2	11b	*Palambages pariunta*	Q42/3	43741
Indy 3	247.55	3	2	12a	*Palambages pariunta*	X15/2	43742
Indy 3	247.55	3	2	12b	*Palambages pariunta*	X15/2	43742
Indy 3	247.55	3	2	13a	*Palambages pariunta*	X44/2	43743
Indy 3	247.55	3	2	13b	*Palambages pariunta*	X44/2	43743
Indy 3	247.55	3	2	14a	*Palambages pariunta*	S33/1	43744
Indy 3	247.55	3	2	14b	*Palambages pariunta*	S33/1	43744